Brain Heart

PART 4 of the
PROCEEDINGS
of the FOURTH INTERNATIONAL
CONGRESS on RHEOLOGY

BROWN UNIVERSITY, PROVIDENCE
RHODE ISLAND, AUGUST 26-30, 1963

SYMPOSIUM on BIORHEOLOGY

EDITOR:
ALFRED L. COPLEY
NEW YORK MEDICAL COLLEGE

FACILITY FORM 602
N67 14561 (ACCESSION NUMBER)
656 (PAGES)
CR-80888 (NASA CR OR TMX OR AD NUMBER)
N67 14608 (THRU)
1 (CODE)
04 (CATEGORY)

Proceedings of the Fourth International Congress on Rheology

BROWN UNIVERSITY, PROVIDENCE, RHODE ISLAND

August 26–30, 1963

Part 4

SYMPOSIUM ON BIORHEOLOGY

EDITOR

ALFRED L. COPLEY

New York Medical College

Interscience Publishers

a division of John Wiley & Sons

NEW YORK • LONDON • SYDNEY

Copyright © 1965 by
John Wiley & Sons, Inc.

Library of Congress Catalog Card Number 50-19776

Printed in the United States of America

Proceedings of the Fourth International Congress on Rheology

PART 4

SYMPOSIUM ON BIORHEOLOGY

Dedicated to

Professor Robin Fåhraeus

Pioneer and Nestor of Contemporary Hemorheology

Preface

I am indebted to Doctor R. S. Marvin, Professor R. S. Rivlin, and Professor E. H. Lee of the Fourth International Congress on Rheology for encouraging and supporting this Symposium on Biorheology as part of the Congress. The participants in the Symposium wish to express their gratitude to Brown University for their generous hospitality.

My thanks are due to the Chairmen of the Symposium's eleven sessions and to the colleagues who read papers for those contributors who were unable to attend. I already expressed my gratitude to the financial sponsors in the Opening Address. Miss Catherine Mayhew was generous in providing secretarial services in the preparation of the Symposium.

It was the policy of the Organizing Committee of the Congress not to have contributions refereed and to exclude discussion remarks from the printed proceedings. A synopsis of the discussions at each session appeared together with the abstracts of the papers in *Biorheol.*, **1**, 261–329 (1963); **2**, 64 (1964). A report on a round table discussion on hemorheology was published in *Biorheol.*, **2**, 55–59 (1964).

I thank Pergamon Press, Oxford and New York, the publishers of *Biorheology*, for granting permission to print an abstract which was not contained in the volume of abstracts issued by the Congress. I express my appreciation to our publishers for encouraging the speedy production of this book.

Finally, I am grateful to Mrs. Robin Fåhraeus for the photograph which appears as Frontispiece in this volume dedicated to Professor Robin Fåhraeus. When this dedication was announced in the Opening Address, the participants gave a standing ovation to Professor Fåhraeus who accepted the honor bestowed on him.

A. L. COPLEY

New York, June 19, 1964

Editorial Note

The contents of the book are arranged in conformity with the sessions of the Symposium.

Of the fifty-five contributions presented at the Symposium, forty-seven are printed in full while eight papers appear as abstracts. One paper in the final program of the Congress was withdrawn by its author prior to the Symposium; its abstract is not included.

An asterisk behind a name denotes that its author had been invited to contribute the paper to the Symposium.

Contents

GENERAL SESSION

Chairmen: A. KATCHALSKY, G. L. BROOKS, S. OKA

A. L. COPLEY. Opening Address: On the Validity of Classical Fluid Mechanics in Biorheology 3
R. FÅHRAEUS. Archaic Hemorheology. The Early Historical Significance of Blood Sedimentation 11
K. WEISSENBERG. Research in Hemorheology. Introductory Lecture 19
G. W. SCOTT BLAIR. Some Aspects of Rheological Theory as Applied to Biological Systems 35
M. JOLY. Agrégation Provoquée par l'Ecoulement dans les Solutions de Macromolécules d'Origine Biologique 45
R. L. WHITMORE. An Application of Particle/Fluid Mechanics to Blood Flow 69

LAMINAR FLOW OF BIOLOGICAL FLUIDS

Chairmen: K. WEISSENBERG, A. M. FREUDENTHAL

H. L. GOLDSMITH AND S. G. MASON. Physical Aspects of the Flow of Biological Suspensions through Tubes 85
S. OKA. Theoretical Considerations on the Flow of Blood through a Capillary 89
G. SEGRÉ. Necklace-like Formations in the Poiseuille Flow of a Suspension of Spheres 103
A. SILBERBERG. Hydrodynamic Interaction between Particles in Suspension 119
E. A. FOX AND E. SAIBEL. A Formulation of the Problem of Flow through Tubes 125
E. W. MERRILL, W. G. MARGETTS, G. R. COKELET, AND E. R. GILLILAND. The Casson Equation and Rheology of Blood Near Zero Shear 135

CYTOPLASMIC STREAMING. HEMOLYSIS. SAP MOVEMENT

Chairmen: N. KAMIYA, D. DANON

S. ABE. The Viscoelasticity of Slime Mold Protoplasm.... 147
N. KAMIYA AND K. KURODA. Rotational Protoplasmic Streaming in *Nitella* and Some Physical Properties of the Endoplasm.... 157
R. D. ALLEN. Rheological Properties of Slime Mold Endoplasm (Abstract).... 173
E. W. TAYLOR. Brownian and Saltatory Movements of Cytoplasmic Granules and the Movement of Anaphase Chromosomes.... 175
J. A. KOCHEN. Flow Properties of Hemoglobin in the Hemolysing Red Cell.... 193
M. H. ZIMMERMANN. Sap Movements in Trees (Abstract).. 201

HEMORHEOLOGY OF PULSATILE FLOW

Chairmen: R. L. WHITMORE, H. HARDERS

D. A. MCDONALD. The Flow Properties of Blood as a Factor in the Stability of Pulsatile Flow.... 205
A. H. SACKS, K. R. RAMAN, AND J. A. BURNELL. A Study of Auscultatory Blood Pressures in Simulated Arteries.... 215
W. MCCOMIS, S. CHARM, AND G. KURLAND. Dimensional Analysis of Pulsating Blood Flow—An Introduction.... 231

BLOOD FLOW IN BRANCHING AND TAPERED TUBES

Chairmen: L-E. GELIN, S. D. CARLILL

A. A. PALMER. Plasma Skimming in Human Blood Flowing through Branching Glass Capillary Channels.... 245
C. SONG, S. CHARM, AND G. KURLAND. Energy Losses for Blood Flowing through Tapered Tubes and Curved Tubes (Abstract).... 255
W. G. FRASHER, JR., H. WAYLAND, AND S. S. SOBIN. Viscoelastic Behavior of the Main Pulmonary Artery Segment (Abstract).... 257

BIORHEOLOGICAL MEASUREMENTS AND OBSERVATIONS

Chairmen: M. REINER, H. WAYLAND

K. WEISSENBERG. Development of Instrumentation for the Testing of Extracorporeal Flow and Deformation of Biological Materials 261
R. B. WHITTINGTON AND J. HARKNESS. A New Capillary-Type Viscometer 267
H. KAWAI, E. FUKADA, T. IBE, AND H. SHONO. A New Capillary Viscometer for Measuring the Viscosity of Small Amounts of Blood 281
L-E. GELIN. Rheological Disturbances Following Tissue Injury 299
H. WAYLAND AND M. INTAGLIETTA. Streaming Birefringence Study of the Interaction of Submicroscopic Rods and Spheres 317

HEMORHEOLOGY OF RED CELL SUSPENSIONS

Chairmen: R. FÅHRAEUS, S. G. MASON

S. CHARM, W. MCCOMIS, AND G. KURLAND. Rheology and Structure of Red Cell Suspensions (Abstract) 335
H. A. COX, JR., AND G.-J. SU. The Influence of Electrokinetic Charge on the Rheological Properties of Red Blood Cell Suspensions 337
G. BUGLIARELLO, C. KAPUR, AND G. HSIAO. The Profile Viscosity and Other Characteristics of Blood Flow in a Non-uniform Shear Field 351
S. ROWLANDS, A. C. GROOM, AND H. W. THOMAS. The Difference in Circulation Times Between Erythrocytes and Plasma *in vivo* 371
H. W. THOMAS, R. J. FRENCH, A. C. GROOM, AND S. ROWLANDS. The Flow of Red Cell Suspensions through Narrow Tubes: The (Extracorporeal) Determination of the Difference in Mean Velocities of Red Cells and Their Suspending Phase 381

MEDICAL BIORHEOLOGY

Chairmen: H. HARTERT, R. E. WELLS, JR.

S. E. CHARM, G. S. KURLAND, C. TEJADA, AND W. MCCOMIS. The Effect of Dietary Fat on Whole Blood and Plasma Viscosity (Abstract) 395

B. ZEDERFELDT. Rheological Disturbances and Their Treatment in Clinical Surgery 397

C-M. RUDENSTAM. Rheologic Disturbances and Tumor Spread (Abstract) 409

IN VIVO HEMORHEOLOGY IN MAN AND ANIMALS

Chairmen: E. DAVIS, S. ROWLANDS

H. HARDERS. Hemorheological Investigations in the "Arterial Spiders" of the Human Skin 413

J. W. IRWIN AND D. C. ALCAIDE. Biological Reactions Interfering with Flow through the Microcirculation 425

R. E. WELLS, JR. The Effects of Plasma Proteins upon the Rheology of Blood in the Microcirculation 431

P. A. G. MONRO. Visual Particle Velocity Measurement in Fluid Streams 439

S. WITTE. Flow Pattern Pertaining to Vascular Permeability as Observed by Fluorescence Vital Microscopy 451

P. I. BRÅNEMARK. Intracapillary Rheological Phenomena .. 459

BIORHEOLOGY OF TISSUE MATERIALS

Chairmen: R. D. HARKNESS, G. VEJLENS

R. D. HARKNESS AND M. L. R. HARKNESS. Some Mechanical Properties of Collagenous Frameworks and Their Functional Significance 477

L. DINTENFASS. Rheology of Synovial Fluid and Its Role in Joint Lubrication 489

W. PIGMAN, G. MATSUMURA, AND A. HERP. Factors Affecting the Rheological Behavior of Hyaluronic Acid 505

B. J. RIGBY AND P. MASON. Structural Transitions in Native Collagen and Their Physiological Significance 521

H. Corey. The Subsidence of Muscle Fiber Dispersions (Abstract) 533
H. H. Pfeiffer. Polarisationsoptik aus dem Glaskörper tierischer Augen gesponnener Fäden als Ausdruck ihres biorheologischen Verhaltens 535

BLOOD CLOTTING AND LOW SHEAR HEMORHEOLOGY

Chairmen: M. Joly, K. M. Brinkhous

M. E. Leroux. La Propriété Thrombodynamique du Caillot: Propriété Hémorhéologique Spécifique Explorée par le Thrombélastographe (La fonction thrombodynamique des plaquettes, de la fibrine et de certaines facteurs du plasma et de sérum) 549
H. Hartert. Clot Retraction. Kinetics and Correlation with the Clotting Process 571
S-E. Bergentz. Fat Embolism—a Hemorheological Disturbance 581
L. Dintenfass. A Study in Rheology of Blood Clotting in Human Subjects 593
E. W. Merrill, W. G. Margetts, G. R. Cokelet, A. Britten, E. W. Salzman, R. B. Pennell, and M. Melin. Influence of Plasma Proteins on the Rheology of Human Blood 601
M. Gregersen, B. Peric, S. Chien, D. Sinclair, C. Chang, and H. Taylor. Viscosity of Blood at Low Shear Rates: Observations on Its Relation to Volume Concentration and Size of the Red Cells 613

Author Index 629
Subject Index 631

GENERAL SESSION

N67 14562

Opening Address
On the Validity of Classical Fluid Mechanics in Biorheology

A. L. COPLEY, *Department of Physiology and Pharmacology, New York Medical College, New York, New York*

I

It gives me great pleasure to open this Symposium and to welcome you all, in particular those who have come from far away and from different lands. It is my hope that our gatherings, within the sessions of the Symposium and the entire Congress, will be scientifically profitable. I trust that everyone will go back to his place of work, stimulated to seek any further knowledge in this new science branch, biorheology, and enriched by personal experiences, which are, in general, the raison d'être for international conferences such as this one, the first of its kind in the United States.

This Symposium was rather a late birth. It was not even conceived a year ago and had the magic incubation time of man's nine months up to its birth at this very moment. It so happened that last September, during my three days' stopover in New York between two international congresses in Mexico City and in Pavia, Italy, I received a phone call from Washington from the Congress Co-Chairman, Dr. Marvin. He and Professor Rivlin had just returned from sabbatical visits to Japan and Italy, and found some requests for a biorheology session at this Congress. Dr. Marvin asked me to organize such a session to which I replied that I could not promise. After having helped in the organization of two meetings on biorheology, one at London University* in 1958 and the other at Oxford University† in 1959, my answer may have been prompted

* G. W. Scott Blair, *Nature*, **182,** 90 (1958).

† G. W. Scott Blair, *Nature*, **184,** 1539 (1959).

by some kind of memories that perhaps a little work might be involved in such an undertaking. Dr. Marvin then asked me to be "at least an active consultant" and to find out in Pavia from the participants in the *European Conference on Microcirculation*, and from other colleagues during my subsequent travels in western Europe, whether sufficient interest could be found for one or possibly two sessions on biorheology. In Pavia and other places, I found a great deal of enthusiasm for such sessions, and on my return from Europe, I told Dr. Marvin about it. A meeting then took place last November in New York with Dr. Marvin, Dr. Rivlin, and Dr. Lee, at which, because of the enthusiastic response I had found in Europe, not merely one or two sessions on biorheology were planned, but this Symposium was conceived.

I have lived for more than half a century, but have not yet learned how and when to say, "No." This seems to be a conditioned protective property of the opposite sex at an early age. My inability to say No is probably responsible for the presence of most of the participants at this Symposium, now gathered providentially and happily here in Providence.

This is not the whole story. The organization of the Symposium needed financial support, and we were lucky enough to find it. Our special thanks go to the Office of Naval Research, U. S. Navy, in particular to Mr. Ralph Cooper, Dr. Silberstein, and Mr. Morton Cooper of the Fluid Mechanics Branch, to Dr. Galler and Dr. Helen Hayes of the Biology Branch, and to Dr. Libber of the Physiology Branch. The National Aeronautic and Space Administration has also helped us with a grant. We thank Dr. Pickering of the Jet Propulsion Laboratory at Pasadena, Dr. Eugene Konneci of the Office of Biotechnology and Human Research, and Mr. Greene, research program administrator of the National Aeronautic and Space Administration in Washington. Finally, I should like to thank the Hon. Edward T. Kennedy, Senator from Massachusetts, for his private contribution.

The program of this Symposium, unfortunately, does not cover all the biological sciences and I regret that biorheological work in the botanical sciences is represented by only four papers. In this connection, I trust that everyone here will listen next Friday morning to Professor Kamiya's paper on the rheology of cytoplasmic streaming yet the program of the Symposium mirrors the scope and

extent of biorheological research as it is being practiced presently. Most studies appear to be made in hemorheology, and I can assure you that it is not by design, or because of my special interest, that this field dominates the Symposium. But then, I trust, you will consider with me that blood vessels have very special variable structures with relevant functions, that blood is a very special fluid, and that as long as it keeps moving in our intricate circulations it keeps us moving in intricate ways.

It is unfortunate that the vast majority of biological fields has not yet become accessible to rheological treatments, including genetics, where certain phenomena exist and many processes occur which are rheological in nature. I hope that the outcome of this Symposium will change the situation.

Since the Symposium is a part of the Congress, only four afternoons were available to hold eleven sessions. This has the obvious disadvantage that none of us can listen simultaneously to two or three papers which may be of equal interest. This I do regret. However, I rescued this afternoon for the one single general session for everyone to participate in, and also to listen to the two reports by Professor Fåhraeus and Professor Weissenberg. We are honored by their presence. We all regret the absence of Dr. Scott Blair who has contributed so much to biorheology.

Many of us will be familiar with the investigations of Professor Fåhraeus, one of the great pioneers of modern hemorheology. I think it is high time that we all pay tribute to him as the Nestor among us students of biorheology. I hope he will accept the dedication to him of the planned volume of the proceedings of this Symposium as a sign of our gratitude.

II

Professor Fåhraeus will take us back in a little while to the humoral pathology of more than two thousands years ago. Before I talk on the rather contemporary topic of this Opening Address, I should like to take you briefly on a flight, not like Professor Fåhraeus' medical or biological excursion, but, like him, I shall take you to ancient Greece. Let us meet there some of those pre-Socratic thinkers who are the true founders of the natural sciences and whose powerful insights into nature have also a direct bearing on modern rheology.

Anaximander of Miletus (in his prime about 560 B.C.) dealt with the Non-Limited, which is indestructible, as the original material of existing things.[1]

Empedocles of Acragas (about 450 B.C.), in his poem "On Nature"[1] addressed to his pupil Pausanias, says: "There is no creation of substance in any one of mortal existences, nor any end in execrable death, but only mixing and exchange of what has been mixed; and the name 'substance' (Physis, 'nature') is applied to them by mankind. . . In so far as they (the elements) have the power to grow into One out of Many, and again, when the One grows apart and Many are formed, in this sense they come into being and have no stable life; but insofar as they never cease their continuous exchange, in this sense they remain always unmoved (unaltered) as they follow the cyclic process."

Heraclitus of Ephesus (about 500 B.C.) is known to rheologists with his thought that the world, not created in time but existing in all eternity, is ever in flux. παντα ρει, written on the cover of the program, is the motto of this Congress But Heraclitus[1] said something which is, by far, more profound: "It is not possible to step twice into the same river." In another citation, he said: "The 'mixed drink' (Kykeôn: mixture of wine, grated cheese and barley meal) also separates if it is not stirred."

It is spiritually refreshing to take this and other drinks from these pre-Socratic or pre-Platonic thinkers. They inspire us to keep asking questions anew about being, about nature, and about human relations on this troubled globe. The thoughts of these thinkers on the origin of matter kindle our quest to advance knowledge. I am convinced that from our pursuits in the different sciences and from pioneering in biorheology, the practice of healing will ultimately benefit. I believe it will be in good measure the science of biorheology which will contribute some pertinent answers to the perennial question: What is life?

Now let us descend from the flight to the more pedestrian part of this address.

III

It is occasionally assumed among rheologists that rheology is a discipline different from fluid mechanics, insofar as rheology concentrates on the study of flow of complex fluids, while fluid mechanics is concerned with the flow of idealized simple media. Nevertheless,

equations which have been formulated for such a simple medium as a linear viscous fluid are used in the interpretation of rheological measurements as if there were no difference between the two fields. An example is the use of the Poiseuille equation[2] for the interpretation of measurements with the capillary tube viscometer. It appears, therefore, that rheology is not different from fluid mechanics but is, in fact, the mechanics of flow of fluids that are less simple than those usually dealt with in classical fluid mechanics. This means that rheology should be considered as a fluid mechanics of higher complexity and, within rheology, the rheology of biological fluids would again still present an even higher level of intricacy. Fundamentally, however, the study of all flow phenomena, whether of simple or complex fluids, must be based on a certain number of axioms or assumptions, the number of which will be the smaller, the simpler the behavior of the fluid. Thus, in classical hydrodynamics of the incompressible fluid, the principle of conservation of mass in conjunction with Newton's laws[3] are sufficient for the construction of the complete theory.

The introduction of linear or Newtonian viscosity as a characteristic property of fluid, complicates the theory quite extensively and requires the introduction of additional assumptions. It is obvious that any further complication of the behavior of the fluid, such as non-Newtonian viscosity or the existence of a yield stress or the consideration of the flow of suspensions, where the suspended particles themselves may have certain characteristics, will lead to certain severe complications in the theoretical formulations. Adequate solutions to quite simple problems, such as laminar flow in a capillary, may then no longer be obtainable, a fact which may make a rational interpretation and analysis of rheological experiments practically impossible. In the absence of such solutions, workers in rheology have frequently no alternative but to fall back on simple equations. The validity of these equations is, to say the least, problematic. As a result, such evasive terms as "apparent viscosity" have permeated the literature.

It may, therefore, not be out of place, at the beginning of a symposium on biorheology, to point out some of the phenomena in which an apparent deviation from the principles of classical fluid mechanics exists. Choosing phenomena from my own sphere of interest, I would point, first, to the existence of the so-called "plasmatic zone," a layer free of red and white blood cells in the circulation, and, second, to our observations that the apparent viscosity in capillary viscom-

eters can be affected by coating the glass surface with different substances. The various possible explanations of the plasmatic zone have just been reviewed by Whitmore,[4] in a survey published in the current (August) issue of *Biorheology*.

It may be interesting to note that classical fluid mechanics itself provides a plausible explanation for this phenomenon in the principle of minimum energy dissipation in laminar viscous flow. This principle was already published in 1882 by Helmholtz,[5] and applied to suspensions in 1922 by Jeffery.[6] Since the viscosity of a suspension increases with increasing concentration of the particles, flow with minimum energy dissipation would require a concentration of the layers of highest viscosity in the range of the lowest shears. This means a concentration of the particles away from the wall along which the shears have the highest values. In this case, therefore, there does not seem to be any contradiction with classical fluid mechanics.

But the effect of different coatings on apparent viscosity is quite a different matter. This phenomenon which produces a rate of flow through a capillary tube dependent on the character of the coating has been demonstrated for water,[7] as well as for blood systems.[8–11] A possible explanation could be the existence of slip along the wall of a magnitude depending on the characteristics of the coating. This explanation would require the replacement of the Poiseuille equation by an extended equation due to Helmholtz[12] published in 1868. The assumption of slip at the wall, however, is at present definitely rejected in classical fluid mechanics, apparently on sufficient evidence.[13]

The observed difference in the thickness of the immobile layer as a function of the characteristics of the wall coatings may provide an alternative explanation of the effect of coatings on apparent viscosity. It is surmised that, if there is wall adherence, there is no slip at the wall.

Let us consider the phenomenon of different wall adherence of a given fluid, i.e., blood or plasma, on various surfaces. The relation to classical fluid mechanics could be re-established, if it could be considered in flow with wall adherence that the principle of conservation of mass was no longer valid, since the adhering portions of the fluid would remain immobile; the necessary corrections to the basic equations arising from this fact would then have to be introduced. The existence of wall adherence has only been established on

the basis of an index of blood systems bordering air surfaces and traveling in a capillary tube.[8–11] If wall adherence can be demonstrated in a closed system, it may then be also compatible with Poiseuille's concept of an immobile layer,[14] for which some evidence has recently been found in the living microcirculation in the hamster's cheek pouch.[15] Slip on the immobile layer as an assumption would still be compatible with the assumption of zero velocity at the wall. The examples given illustrate, I trust, a close relation of classical fluid mechanics and rheology rather than a contradiction between them.

There is the possibility, however, that entirely new approaches in physics other than classical fluid mechanics could be applied to our problems in biorheology, and I would not be surprised if in a little while Professor Weissenberg opened to us new vistas.

In biorheology, we should not lose sight of and should be aware of still another possibility, namely, in the living system as well as in extracorporeal biological materials, mechano-chemical interactions may occur which will invalidate the purely mechanical approach as exemplified in fluid mechanics. I suppose we may hear more on these realities from Professor Katchalsky in his lecture on mechanochemistry.

On this note, I hand the Chair over to Professor Katchalsky of the Weizmann Institute of Science and the other two Chairmen of this General Session: Professor Oka of Tokyo Metropolitan University and Professor Brooks of Brown University, our host.

I am very grateful to my friend, Professor A. M. Freudenthal of Columbia University, New York, for many helpful discussions. Part of the work described was aided by Grant HE-4793, National Institutes of Health, U. S. Public Health Service, Bethesda 14, Maryland.

References

1. Freeman, K., *Ancilla to The Pre-Socratic Philosophers.* A complete translation of the Fragments in Diels, *Fragmente der Vorsokratiker.* Harvard Univ. Press, Cambridge, Mass., 1956.

2. Poiseuille, J. L. M., *Compt. rend.*, **15,** 1167 (1842); *Ann. Chim.*, **7,** 50 (1843); *Poggendorff's Ann. Physik Chem.*, **58,** 424 (1843); Mémoires présentés par divers Savants à l'Académie Royale des Sciences de l'Institut de France. *Sci. math. phys.*, **9,** 433 (1846), Paris.

3. Newton, I., *Principia,* Libro II, London, 1687, Sec. IX. See I. Newton, "Principia," F. Cajori, ed., *Sir Isaac Newton's Mathematical Principles of Natural Philosophy and His System of the World,* Univ. California Press, Berkeley, California, 1947.

4. Whitmore, R. L., *Biorheol.*, **1**, 201 (1963).
5. Helmholtz, H. v., *Wiss. Abhandl. Leipzig*, **1**, 223 (1882).
6. Jeffery, G. B., *Proc. Roy. Soc. (London)*, **A102**, 161 (1922).
7. Traube, J., and S. H. Whang, *Z. Physik. Chem.*, **138**, 102 (1928).
8. Copley, A. L., *Nature*, **181**, 551 (1938).
9. Copley, A. L., and G. W. Scott Blair, *Rheol. Acta* Suppl. *Kolloid-Z.*, **1**, 170 (1958); **1**, 665 (1960).
10. Copley, A. L., in, *Flow Properties of Blood and Other Biological Systems*, A. L. Copley and G. Stainsby, eds., Pergamon Press, New York, 1960, p. 97.
11. Copley, A. L., G. W. Scott Blair, F. A. Glover, and R. S. Thorley, *Kolloid-Z.*, **168**, 101 (1960).
12. Helmholtz, H. v., *Berlin. Monatsber.*, 215 (1868); *Phil. Mag.*, **36**, 337 (1868).
13. Whetham, W. C. D., *Trans. Roy. Soc. (London)*, **A181**, 559 (1890).
14. Poiseuille, J. L. M., Recherches sur les causes du movement du sang dans les vaisseaux capillaires, Tome VII des Savants étrangers, Paris, Impr Royale, 1839.
15. Copley, A. L., and P. H. Staple, *Biorheol.* **1**, 3 (1962); *Federation Proc.*, **18**, 30 (1959).

Synopsis

14562

The Opening Address consists of three parts. The first part is a brief survey of the events pertaining to the organization of the Symposium on Biorheology as part of the 4th International Congress on Rheology. The second part refers to Heraclitus and other pre-Platonic thinkers, the founders of the natural sciences, and their insights into nature as related to modern rheology. In the third part, which deals with the topic of the Address, phenomena, in which an apparent deviation of fluid mechanics exists, are mentioned to point out the complexity of the rheology of certain biological fluids *in vivo* and *extra vivo*. Examples are the plasmatic zone, free of red and white blood cells, in the living circulation and the observations that the apparent viscosity of blood systems in capillary viscometers can be altered by coating the glass surface with different substances. A possible explanation for the latter phenomenon could be the existence of slip along the wall, an assumption which is rejected in classical fluid mechanics. As an alternative explanation, it is surmised that no slip exists, if there is wall adherence in a closed system. However, wall adherence has only been established on the basis of an index of blood systems bordering air surfaces and traveling in a capillary tube. The immobile layer of the plasmatic zone, proposed by Poiseuille, and recently found by Copley and Staple to exist to some extent in the living microcirculation of the hamster's cheek pouch, could then be related to wall adherence, if the latter can be found in a closed system. Then, as an assumption, slip on the immobile layer would be compatible with the assumption of zero velocity at the wall. Such an example would thus demonstrate that no contradiction but a close relation between classical fluid mechanics and rheology exists. However, in biorheology, mechano-chemical interactions may occur which will invalidate the purely mechanical approach in fluid mechanics. Still another possibility may exist in hitherto unknown, entirely new approaches in physics other than classical fluid mechanics.

author

N67 14563

Archaic Hemorheology. The Early Historical Significance of Blood Sedimentation

ROBIN FÅHRAEUS,* *University of Uppsala, Uppsala, Sweden*

One of the first important observations in the history of medical art bears upon the property of the blood. Even for the most primitive observer it was evident that the liquid content of the venous system was not a uniform fluid, but a mixture—a complex of different parts which separated from each other when the blood was exposed to the cooling influence outside the body.

In this mixture the Greek physician could easily distinguish four different fluids. First, there was one component almost black; that was the black bile, *melancholia.* Secondly, there was a light-red part of the mixture which seemed to rise to the surface of the caked blood; that was the blood in the limited, scientific sense of the word, in Greek *haima,* later in Latin *sanguis.* Thirdly, the serum, the yellow bile, *cholera* separated more or less from the clot by itself. In normal blood the fourth part of the mixture did not appear to the eyes, but the Greeks knew that it was present in the caked blood. The Hippocratic author mentions that by shaking blood a thread-shaped substance is obtained. That was the fibrinogen-fibrin, what the Greeks called the *phlegm.* When this had been removed, the mixture of the three other fluids lost the property to coagulate.

The division of the vascular contents in four different parts was considered in a peculiar way to correspond to the four elements of Empedocles and Aristotle and the adopted physical characteristics of these elements were transferred to the four parts of the vascular contents. Thus the black bile was like the earth, cold and dry; the "blood" in the limited sense of the word like the air, warm and humid; the yellow bile like the fire, warm and dry; and finally, the phlegm corresponded to the water and was like this element, cold and humid.

The theoretical consequences of these suppositions for the general

physiology and pathology are concentrated in the following sentences in the most celebrated of the Hippocratic writings, "On the Human Nature."

"The human body contains blood, phlegm, yellow bile, and black bile which constitute the body and is the cause of disease and health. The human being is healthiest when these elements with respect to combination, strength, and quantity stand in well-proportioned relationship to each other and are as much as possible intimately mixed, whereas she suffers when any one of these parts is present in too small or too great quantity or has separated and is not combined with all the rest."

Thus, theoretically, each one of the four fluids through increase or decrease could give rise to disease, but practically speaking it was only one of them which entirely dominated the pathology of the Greeks. Because of two almost equally important causes this was the phlegm.

The letted blood in almost all diseases had a different appearance than the blood from a healthy person. The difference consisted in the behavior of the phlegm. This fluid was, as already stated, invisible in the normal coagulated blood, but appeared in diseases as a more or less thick yellowish white layer at the top of the blood cake. That was the buffy coat, in the history of medical art known under many other names as buff, size, inflammatory pellicle. The blood was called buffy or sizy. The Germans spoke about *Speckhaut, Faserstoffhaut, Faserhaut, Lederhaut,* and *Entzündungshaut.* Blood with a thick crust was called *"zerfallenes Blut."* In French it was *couenne du sang* and *caillot blanche.* The blood was called *couenneux.* In Latin it was *crusta pseudomembranacea, lardacea, adiposa, pellea,* and *alba.* Probably the most used term in the classical language was *crusta inflammatoria.* The generally very thick crust in pulmonary diseases was called *crusta pleuritica.* This phenomenon does not exist in modern medicine and has consequently no name.

The cause of the buffy coat is increased blood sedimentation. The red corpuscles sink so fast in most diseases that they have time to sediment before the blood coagulates. Consequently, the upper part of the blood consists only of plasma after the coagulation of serum and fibrin. The increased sedimentation rate of the red cells depends upon their increased aggregation, so-called "rouleaux formation." The increased rouleaux formation again is generally due to an in-

creased concentration of fibrinogen in the plasma. The Greek physicians were thus in reality right when they believed that the phlegm (our fibrinogen-fibrin) increased in the vascular system in almost all diseases. They further found that there existed a direct relation between the seriousness of the disease and the thickness of the buffy coat.

The deplorable fact was now that the most common change in the blood was the observed increase of the phlegm, which alone of the four fluids had the ominous property to congeal. It is probably not by mere chance that the phlegm corresponded to water and ice among the four elements. Cold made the phlegm stiff, warmth melted it.

There was a misconception about the movement of blood in the venous system until Harvey, but evidently the Greeks were convinced that blood under normal conditions was liquid and that consequently its coagulation was of great pathogenetic importance.

It seems very probable to the author that the Greeks had made post-mortem examinations and that the presence of fibrin clots in the heart and the great vessels had contributed to founding their pathology. If this has not been the case, one must admit, however, that the contents of the vessels in the dead body after most diseases have that particular appearance, which the Greek physicians supposed to be the case. It is not necessary to mention that the rouleaux formation and the sedimentation rate of the red cells on the whole are the same in the blood vessels, after circulation has stopped, as in the glass tube (see Fig. 1).

Each of the four fluids was considered to have its particular "home" in the body. Thus the spleen was in the special service of the black bile, the heart of the blood, the liver of the yellow bile, and the brain of the phlegm. The latter implied a constant risk for the upright human being. The peril was that the phlegm leaked from the brain and then sank down in the lower parts of the body. This occurred in spite of the fact that nature had created two protections against a superabundance of phlegm in the head. One was the spinal cord, which transported the cold and humid fluid to the sexual organs. This made, especially for the man, sexual intercourse salubrious in all diseases dependent upon too much phlegm. The other protection was the nasal catarrh which freed one from too much cold and humid fluid. The nose was an ingenious safety valve placed just under the

broad frontal part of the brain. This idea lives on in the French expression "*rhume de cerveau.*"

Another complication of too much phlegm was combined with pregnancy. Already Empedocles of Akragas had in the sixty-eighth fragment of his preserved writings declared that the blood of the pregnant woman is altered to a *white beast,* an observation that without doubt alludes to the fact that the blood during the greater part of pregnancy shows a buffy coat. This alteration is also here the consequence of an increased blood sedimentation.

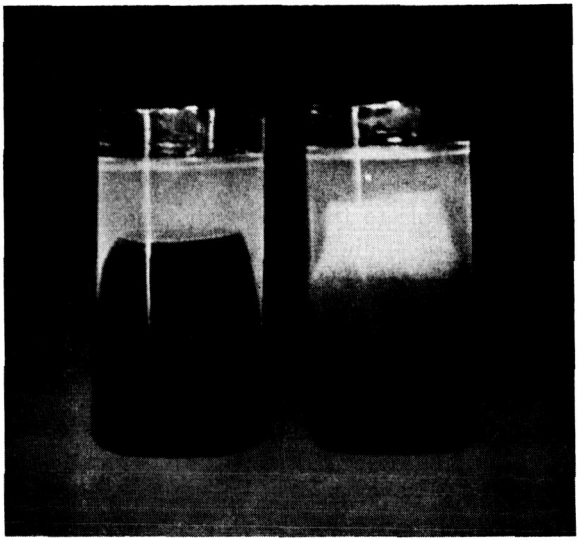

Fig. 1. Normal and pneumonic blood spontaneously coagulated.

If we, for a moment, accept the Greek pathology, important aetiological and clinical facts receive a natural explanation.

Catching cold was a sign that the low temperature of the surrounding air or water made the phlegm master of the three other fluids in the vascular content. Separated from them the phlegm had a tendency to congeal, which explained the fits of shivering, the clinical symptom of the struggle between the phlegm and the three other loyal fluids.

Throat catarrh arises when during the winter or spring an abundant flow of a viscous substance from the brain streams to the jugular veins.

When this cold and humid afflux fills up the channels for the blood and the air, it causes nearby parts to congeal and creates obstacles for the flow of the blood.

The great illness (epilepsy) is according to the Greek author not of any more divine origin than other diseases. All of its symptoms are explained by the behavior of the phlegm. When this cold and humid fluid overflows and arrives at the heart and lungs, the blood is cooled and the heart palpitates. The patient cannot get as much air as he needs. Generally, however, the phlegm is conquered and mixed with the remaining warm contents of the veins. For small children, however, the disease is dangerous because the narrow veins are not able to absorb the viscous phlegm. Therefore the blood is cooled and coagulates, which causes the death of the child.

One of the great thoughts in the Greek medical art was that many symptoms of disease were an expression of the organism to counteract the pathological development, in other words, to reduce the injurious influence of the phlegm. From this viewpoint the fever was easily explained as nature's own remedy to neutralize the harmful effects of the cold and humid fluid. The increased warmth of the body melted the phlegm in the same way as ice is dissolved by warmth, and lets it pass through the skin. That was the explanation of the fever sweat.

Another form of melted phlegm was pus. In cases of pneumonia, for instance, the fever melted the coagulated phlegm masses in the lungs, which made it possible for the patient to cough them up. Earache was treated with warm compresses, which melted the phlegm and expelled it from the head and the pain stopped.

But there was one cure which threw all other treatment into shadow. That was bloodletting. Since there was every sign that the phlegm was the great villain in the drama, it was theoretically well grounded to remove as much phlegm as possible from the diseased body. The Greek physicians lived in the erroneous conception that blood could be of different composition in different parts of the venous system. It was consequently possible to release the patient from bad blood and retain the good blood. Naturally, this idea made local diagnosis most important. The physician opens the spleen vein when the left lung is affected and the hepatic vein when the right lung is the seat of inflammation.

To understand the common, often excessive, bloodletting in most of the history of medical art, one should remember that venesection

seemed to fulfill the desired results. The fact is that the buffy coat is reduced and completely disappears after profuse and repeated bloodletting. This effect is caused by the reduction of blood sedimentation. Extensive bleedings stimulate the bone marrow to intensify the production of red corpuscles which in unripe condition join the blood. These young red cells, the so-called "reticulocytes" do not aggregate, consequently sink slowly, and hereby prevent the formation of a buffy coat. These facts are of great historical interest. The *crusta inflammatoria* created the theoretical foundation for great bloodletting, its disappearance, on the other hand, determined a limit for the most horrible abuse of heavy blood losses.

There were two categories of beings who became special victims of probably the greatest mistake in the history of therapeutics. One was pregnant women who had buffy blood because of increased blood sedimentation. The consequence was that a well-managed gravidity in the upper classes was combined with great losses of blood which, in combination with the delivery, was deadly perilous.

The other unhappy category was horses. The blood of these animals has normally a very intensive rouleaux formation and consequently a great sedimentation rate of red cells. A little more than 100 years ago horses belonging to the Swedish army were drawn together to bleed meetings.

During the first half of the last century the great French physicians Broussais and Bouillaud broke the record as to blood therapy. The last-named author prescribed, for instance, in cases of pneumonia daily and copious bloodletting. The patient lost about $2^1/_2$ liters of blood during the first week after arriving at the celebrated *Hopital de la Charité*. This was the final outcome in the use of a most drastic remedy.

To understand the unique position of bloodletting in the history of therapeutics it is necessary to remember an additional fact: The immediate effect of venesection in pneumonia, for instance, was most promising for the patient and for the physician, but improvement was of short duration and tripled the rate of mortality compared with the mortality in a group of patients who only obtained homeopathic treatment.

Venesection was without doubt a gigantic mistake and interpretations of blood changes in disease and pregnancy were erroneous. The observations of the Greek physicians of the blood were right,

however, and thus represent the first steps in the direction of scientific hematology.

It has been said: "To one small people it was given to create the principle of progress. That people was the Greek. Except the blind forces of nature nothing moves in this world, which is not Greek in its origin." This is at least true for the modern study of blood sedimentation.

Synopsis

14563

Pathology of the ancient Greeks was founded on observations of the blood. The contents of the venous system seemed to be a mixture of four fluids, which separated more or less when the mixture had left the warm body. One could thus distinguish the black bile, the yellow bile, the "blood" (in the limited sense of the word), and the phlegm. The properties of the last-named fluid had the greatest influence on the conception of diseases. In normal blood the phlegm was invisible but served as the connecting substance in the caked blood. In diseases, on the contrary, the phlegm formed a more or less thick layer at the top of the caked blood. This phenomenon was a consequence of increased blood sedimentation but was taken by the Greeks as proof that the phlegm had increased in amount, a change of the contents in the veins much more ominous, as the phlegm in contradistinction to the other three fluids had the property to congeal and make the contents of the vessels immovable. The fever was nature's means of counteracting this tendency. Venesection was considered by the physicians as the most effective way of reducing the predominance of phlegm.

Author

Research in Hemorheology
Introductory Lecture

N67 14564

K. WEISSENBERG,* *The Royal Institution, London, England*

The Chairman of this Symposium, Dr. A. L. Copley, has kindly invited me to give at this Session an address about the modern ways in which mathematical physics attacks the problems of research in hemorheology. I am deeply grateful to him for giving me this opportunity, and it gives me great pleasure to acknowledge my indebtedness to him and to other pioneers in hemorheology, including Drs. Knisely, Harders, Gelin, Davis, and Landau, who acted as my teachers and friends, and introduced me to the wide scope of the research projects here involved.

INTRODUCTION

Research in hemorheology may be traced back to the year 1686 when Marcello Malpighi discovered the micro-circulatory flow of blood in the living body. Since then it has been necessary to extend research over wider and wider ranges of materials and conditions in the living body and outside of it, i.e., *in vivo* and *ex vivo*. The extension was needed for a variety of reasons. It was recognized that blood already represented a whole group of materials with consistencies which varied from fluid to solid in accordance with the normal or pathological conditions of the body. Many more groups of materials were involved covering the whole range of consistencies—solid, liquid, gaseous, and intermediate—when one took into account that the *in vivo* blood flow was in constant interaction with the walls of the blood vessels, and that the interaction spread through these walls to all constituents of the body, including the muscles and tissues surrounding the vessel walls, and all the various body fluids which intercommunicated with the blood through semipermeable membranes. The interactions reached out even to the *ex vivo* environment of the body through the intake of food, drink, and air and the discard of excretions.

The research into the flow of blood *in vivo* had to be extended to *ex vivo* conditions, although the results obtained in the two types of research are not directly comparable. The extension was needed in order to study under controlled conditions various features of the flow not directly observable *in vivo*, and also in order to develop the many therapeutic techniques of deliberate medical *ex vivo* interference with the *in vivo* blood flow by way of injections and transfusions and by the use of heart and lung machines, etc. Thus, altogether, hemorheological research had to cover a vast territory and attempt to control the blood flow in all its various interactions with the body constituents and the body environment necessitating a study of the mechanics of materials of consistencies of the most varied and complex kinds. To demonstrate the consistencies of various groups of materials consider the fact that some groups, e.g., bones and teeth are hard and brittle like ceramics, others, such as muscles and thrombi are elastically extensible and tough like rubbers, still others are plastic and viscous like ordinary putties. Finally, there are some groups which are like silicone putties in that they exhibit different properties under different mechanical actions being soft, plastic, and viscous under slow deformation and hard, brittle, and elastic under fast deformations. Blood itself can have any and all the consistencies mentioned above according to the conditions under which it is observed, and it will exhibit under various pathological conditions all the diverse phenomena of flow which, for ease of demonstration, will be shown on different biological and technological materials.

The immense variety and complexity of behavior provide the scientist with a great challenge, and Poiseuille was probably the first to respond to it. However, his magnificent work could not be developed much further until the whole scheme had changed from the one adopted by classical physics to that of modern rheology.

The scheme of classical physics was generally accepted at the time when Poiseuille investigated the flow of blood in 1835. One did not doubt then the validity of the assumption underlying the classical scheme because it appeared to provide for many observed phenomena adequate explanations in terms of causes and effect linked to one another in the simplest possible manner by the functions of a mechanical model which could be clearly visualized in space and time, and which operated in accordance with fundamental principles so easily understandable as to be regarded as self-evident and neither in need

of proof nor capable of being proved. For classical mechanics in particular it was assumed that movements and forces were related by linear laws with constant coefficients which characterized the flow properties of the material. It was further assumed that one could approximate the macroscopic flow of materials by that of a continuous medium which was either an "ideally elastic solid" obeying Hooke's law of elasticity or "ideally viscous fluids (liquid or gas)" obeying Newton's law of viscosity. From these assumptions Poiseuille deduced his formula for the blood flow through capillaries *in vivo* and *ex vivo* by regarding blood as a liquid obeying Newton's law of viscosity and by idealizing the capillaries in various ways. When experimental tests were made one found at first some support for Poiseuille's formula and the classical assumptions and laws in general. In further tests, however, one became aware of an ever growing number of deviations as many important technological and biological materials, including blood, were neither ideally elastic solids nor ideally viscous fluids but had consistencies (as demonstrated earlier in this paper) in which elastic and viscous flow properties were mixed in various ratios and combined with other properties in an infinite variety and complexity of manner to which no simple linear law with constant coefficients could be fitted.

For the blood flow there is a nonlinear effect noticeable in that the flow resistance (apparent viscosity) varies with the rate of shear. For demonstrating this effect the author arranged a race in which one could compare at various rates of shear the flow of blood with that of a standard fluid (glycerol-water) obeying a linear law with a constant flow resistance. Experiments were made showing that in the outflow from similar tubes the blood first overtakes the glycerol water only to be overtaken by that fluid at a later stage and losing the race.

Other nonlinear effects can be observed in work hardening and or work softening occurring in time even at constant rates of shear. The work hardening may be either of an irreversible type as seen in the stirring of cream till it becomes a solid lump of butter, or it may be of a reversible type as demonstrated in the stirring of a fluid made up as a mixture of borax solution with polyvinyl alcohol. This fluid solidifies under stirring but regains its original fluidity after a period of rest.

In spite of all the deviations attempts were made to save the

classical scheme by a convention which outlawed all deviations as "abnormal" and recognized as "normal" only such phenomena which complied with linear laws of the scheme. This, however, was unsatisfactory because it led to a description of the flow phenomena in terms of a nomenclature which became more and more confusing as different investigators used the same name for different deviations and different names for the same deviations. Moreover, no amount of nomenclature could for long hide the fact that the classical theory gave results which were completely contradicted by all the experimental data obtained for the phenomena which had been outlawed as abnormal. The difficulties were by no means confined to the theory of classical mechanics but involved the theories of all classical physics and, to a certain degree, of all classical branches of natural science. There were apparently irreconcilable conflicts which separated the various branches of natural science from one another, and which were of such a profound nature that they affected the fundamental classical assumptions about the geometry of space and time, the particle and wave structure of matter and energy, and the relationship between the movement and force, etc. Progress was held up until the turn of the century when Einstein inaugurated the modern era of scientific research by his vision of an all-embracing natural science which would unite the various branches of mathematics, physics, chemistry, and biology on the basis of a new scheme for the study of movement through space and time free from certain crippling assumptions and laws which had led to the conflicts in the classical theory. Thus, a new science emerged which, with reference to the Greek saying, "παγτα ρει" (i.e., flow is universal) may be termed rheology in the widest sense of the word, suggesting the universality of the science of movement.

MODERN IDEAS AND CONCEPTS ON RESEARCH

Einstein's concept of an all-embracing natural science allows rheology as well as hemorheology to admit materials of all kinds and degrees of consistencies (such as demonstrated earlier in this paper) and places no restrictions as to linearity or nonlinearity on the laws governing the behavior of materials. However, he found it necessary to impose on the new science one important limitation to its domain by postulating that it should be restricted to a merely factual descrip-

tion in terms of quantitative data which the experimentalist would provide by taking measurements, and which the theoretician would interconnect by laws formulated in terms of mathematical equations. It would then be the aim of research to establish in the domain of quantitative data, and over the widest possible range of phenomena, a perfect fit between experiment and theory as between lock and key, the perfection of the fit being assessed by the degree of accuracy achieved and by the ease of the handling of the essentially abstract mathematical equations from which the experimental data are theoretically precalculated. Here the classical methods of research—though welcome wherever possible—are now extraneous and merely accidental, since the perfection of the fit is the same whether or not one can find explanations and mechanical models for the mathematical equations, and whether or not these equations are simple and self-evident or complicated and apparently paradoxical.* In any case one can no longer regard the tracing of the lines of cause and effect as a guide to modern research because in the factual description in terms of mathematical equations any one parameter can be calculated as a function of the others, irrespective of whether or not there is a causal interrelation. While, e.g., one regarded in classical research the forces as the causes and the movements as the effects, one may now choose arbitrarily either the forces as given and calculate the movements, or the movements as given and calculate the forces, without implying that either should be regarded as the cause or the effect of the other.

According to Einstein, the development of methods of research which would lead to the best fit between theory and experiment should be the responsibility of the mathematical physicist because his training in both mathematics and physics should enable him to coordinate the requirements of the theoretician with those of the experimentalist in the formulation of the principles, design of instrumentation, selection of the variables to be measured, choice of the calibration laws for the scale divisions of the measuring instruments, and last but not least in critically reviewing the evidence offered by the data obtained from quantitative observations.

* In many of the modern theories of relativistic and wave and quantum mechanics one has achieved a remarkably good fit over very wide ranges of conditions in spite of the fact that one could find no explanations, construct no mechanical models, nor formulate fundamental laws in a manner that could be regarded as simple and self-evident.

INSTRUMENTATION

The first task in research which the mathematical physicist ought to face is to find a complete metrical system of reference, i.e., a complete set of diverse measuring instruments (yardsticks, clocks, pressure gages, etc.) with calibrated scales which would allow quantitative observations to be made of all the variables, and then to define in terms of these variables all the parameters under consideration. Unless and until this task is completed, progress in research is blocked because the experimentalist cannot make quantitative observations, and any laws and mathematical equations which the theoretician may write down will not have any physical significance because it can neither be proved nor disproved by experiments.

The application of these considerations to rheology in general, and to hemorheology in particular, not only showed up the total inadequacy of the available instrumentation but also stimulated the more exact formulation of the ideal requirements and the development of new types of instruments which progressively approximated to the ideal. One of these new types of instruments, termed "rheogoniometer," is capable of taking goniometric measurements of movement and force in all three dimensions of space in a thoroughly comprehensive manner which had previously not even been attempted, and which now is capable of measuring in every material the elastic as well as the viscous properties over a wide range of conditions. These properties were exactly defined by the fundamental principles of thermodynamics and mechanics and related to one another by Maxwell's theory. In the definition the two properties were associated, respectively, with the two parts of the external work, one (elastic) which was reversibly stored, and the other (viscous) which was irreversibly dissipated as heat. A relation between the two properties was established by Maxwell's conception that all interatomic and intermolecular forces in a material are elastic bonds representing force fields which could reversibly store energy, and that the viscous properties are only due to a decay in time of the elastically stored energy due to the breaking and making of bonds. Accordingly, the viscosity modulus could always be resolved into the product of an elasticity modulus and a decay time, even under conditions in which the flow through capillary viscometers appear to conform to the Newton-Poiseuille laws. This resolution (which has been fully confirmed by the modern wave-mechanical theories of interatomic and intermolecular bonds) is

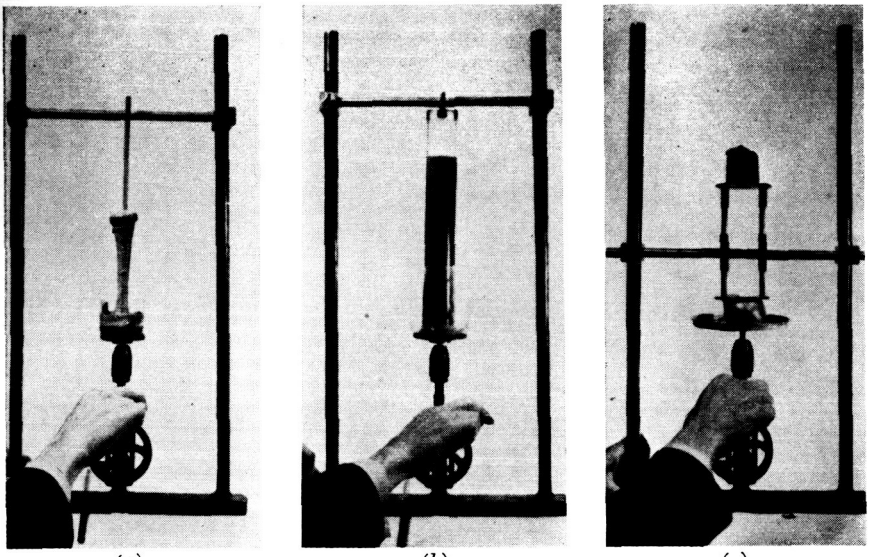

(*a*) (*b*) (*c*)

Fig. 1. Development of a positive normal pressure in (*a*) the climbing of the material on a stirring rod, (*b*) the mounting of the material in an inner cylinder, and (*c*) the pushing up of a weight by the material.

of particular importance to hemorheology where the structural interpretation of the blood flow in the Newton-Poiseuille region has so far been one-sided and entirely based on the apparent modulus of viscosity, while one ought to have measured the elasticity as well, and so obtained information about the strength of the bonds in the material and of the decay time for the breaking and making of the bonds. One may illustrate this resolution by way of a molecular model of the flowing fluid. The model consists of two brushes pushed together so that their bristles overlap. The elastic bristles represent a simplified version of the force fields and molecules of the fluid under consideration, and when one brush is tangentially moved against the other the stick-slip contacts between the bristles simulated the making and breaking of the bonds in the molecular entanglement, thereby showing how the viscous resistance of the movement is compounded from the elastically stored energy in the deformed bristles (force fields and molecules) and the time for making and breaking the contacts (bonds).

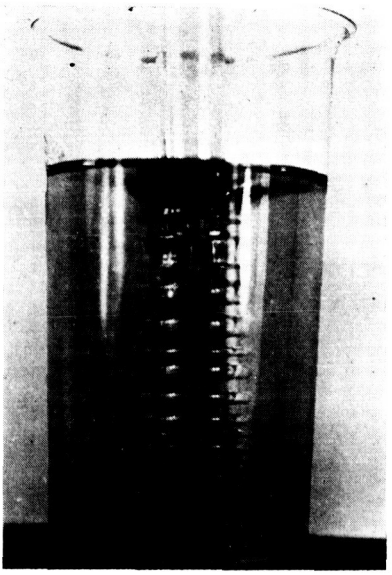

Fig. 2. The development of negative pressure and the descent of the material on a rotating tubular cylinder.

It follows from the above considerations that the flow behavior of every material will always be viscoelastic, and that in order to control it over a wide range of conditions one will have to use an instrument capable of measuring the viscosity modulus as well as the elasticity modulus of the material. However, the viscoelasticity will not always be apparent, and the material will appear to be purely viscous if the conditions of test are so chosen that the rate of shear is negligibly small compared with the reciprocal decay time of the elastic energy. The following are examples where the flow behavior for apparently purely viscous conditions is contrasted with that under apparently viscoelastic conditions. In either case the flow behavior will appear paradoxical but was in fact predicted from the author's theory and from the viscoelastic properties of the material as measured in the rheogoniometer.

In the first example the flow behavior of materials is examined when they are subjected to the action of rotating stirring rod.

Figure 1 corresponds to a material under apparently viscoelastic conditions, and shows in accordance with the development of a

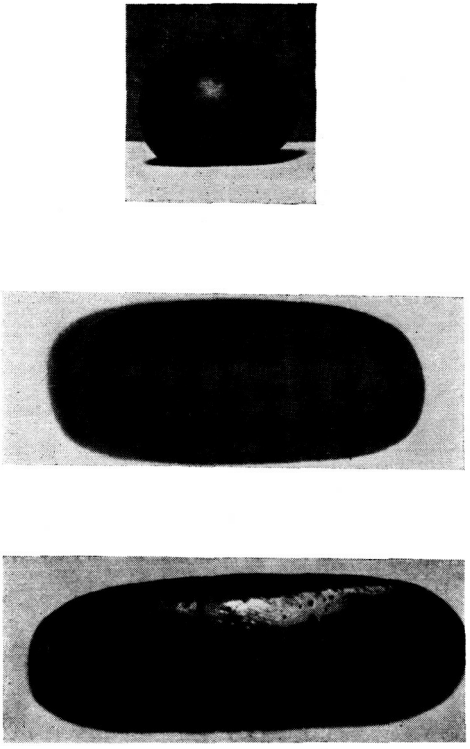

Fig. 3. The production of an elongated cylindrical form with convex ends according to a positive normal pressure.

positive normal pressure (Figs. 1*a*, 1*b*, and 1*c*) the climbing of the material on a stirring rod, the mounting of the material in an inner cylinder, and the pushing up of a weight by the material.

Figure 2 corresponds to a material under apparently purely viscous conditions and shows in accordance with the development of negative pressure (suction) the descent of the material on a rotating tubular cylinder. The rings appearing around this cylinder consist of air that has been sucked in, and the parabolic meniscus visible inside the cylinder shows the depression of the material there.

In the second example the flow behavior of materials is examined when a sphere is rolled out between two parallel plates.

Figure 3 corresponds to a material under apparently viscoelastic conditions and shows the production of an elongated cylindrical form with convex ends according to a positive normal pressure there.

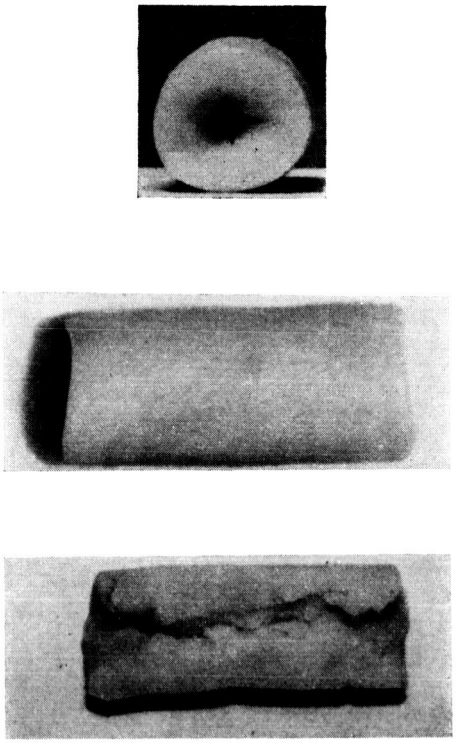

Fig. 4. The production of an elongated tubular form with the hole along the axis corresponding to the negative pressure at the ends.

Figure 4 corresponds to a material under apparently purely viscous conditions and shows the production of an elongated tubular form with the hole along the axis corresponding to the negative pressure at the ends.

UNCERTAINTY AND RELATIVITY OF QUANTITATIVE OBSERVATIONS

Once the instrumentation has been established one can make quantitative observations but their evidence has to be critically reviewed before they can be incorporated into a theory. The review revealed

that one could no longer accept the classical point of view according to which the system under consideration was observed undisturbed, and in isolation, and that therefore the observed data had the significance of exact and absolute characteristics. Instead one had to recognize that every quantitative observation was the result of an interaction between the system to be observed and the observing one and that it referred only to the relation between the two systems at the very moment when the disturbing interaction took place. Hence, however carefully the experiments may be conducted, the observation will inevitably bring about some disturbance, and with it a certain degree of uncertainty and inaccuracy which will have to be dealt with by statistical methods. In addition, the relation of the observed data to the observing system will introduce a considerable amount of arbitrariness because this system can be chosen in any way one likes with respect to its position in space and time, its units of measurements, and its scale functions which indicate how the scales of the measuring instruments are divided, subdivided, and associated with the numerical values of the variables. The inevitable interaction between the system to be observed and the observing one, and the associated uncertainty and relativity of all the observed data, have already been fully recognized as basic conceptions in all the modern theories of physics,* and it is important that this recognition should be extended throughout all the natural sciences, including chemistry, biology, and last but not least hemorheology where the interaction between living systems and the instruments used for observation has not always fully been taken into consideration and may then have given entirely misleading results. The question now arises of how one can possibly arrive at a theory for any given system under observation from experimental data which contain some amount of uncertainty and arbitrariness. It is in answering that question that under the inspired leadership of Einstein, Heisenberg, and Dirac the most powerful theoretical research tool of modern science was developed which not only accounted for the many experimental data already observed in various branches of natural science but also opened up vast unexplored regions, the very existence of which had not previously been even suspected.

* See, e.g., W. Heisenberg's *Uncertainty Principle in Wave and Quantum Mechanics, Naturwiss,* **14,** 989 (1926), and A. Einstein's *Relativity Principle in the Special and General Theories of Relativistic Mechanics,* J. A. Barth, Leipzig, 1916.

THEORETICAL EVALUATION OF EXPERIMENTAL DATA

In order to deal with the difficulties which arise from the interaction between the observed system and the observing one, it was necessary to use statistics to account for the uncertainty of observations and to introduce new methods specifically designed for the elimination of the arbitrariness.

The new methods were based on the group theory of transformations which allowed to derive from all the variables considered certain parameters and relations so constructed as to be increasingly free from arbitrariness by being invariant against wider and wider groups of transformations of the observing system of reference, and changes in the material and conditions.*

Amongst the invariants so constructed the quantities of matter and energy play a prominent part, so that the development of a useful theoretical scheme requires the rendering of an exact account of the movements through space and time of each particle of matter and each portion of energy. Another invariant, known as the "geodetic"† then serves as a guide to the path through space and time taken by the matter and energy, however complicated this path may be because of the presence of forces of various kinds. This is necessary for application to hemorheology as well as tracing the flow of matter and energy in the living body from the intake of food, drink, and air to the discard of excretions via an extremely elaborate transport system designed to maintain and coordinate the metabolism throughout all the cells of the body according to the local requirements on which depend the health and disease, and ultimately the life and death of the body as a whole and each of its cells. In following the lines of transport step by step one finds that matter and energy are carried into each cell and out of it by an intricate network of streams of body fluids of various compositions which all communicate with one another and with the blood stream. All the said streams, including that of the blood, are joined, separated, channeled, divided, and subdivided and filtered by an ordered assembly of semipermeable mem-

* Some particularly simple special cases of this method were already known in classical physics as, e.g. the model technique based on parameters which are dimensionless and thus invariant against all changes of the units of measurement used in the observing system of reference.

† The path along a geodetic line has an extreme length (shortest or longest) compared with all neighboring pathways.

branes, forming the walls of the compartments of the cells, organs, and blood vessels. The whole arrangement is such that oxygen and nutrients are carried into each cell and carbon dioxide and toxic waste out of it in accordance with the local metabolic requirements of irrigation, drainage, temperature, pressure, etc. Watching in particular the movements in and around the tubular walls of the blood vessels, one can observe that streams of matter and energy are constantly flowing in various directions, since some are united in the blood stream and flow along with it inside the tubular vessels, while others, including lymph, flow as crosscurrents in a perpendicular direction through the vessel walls and carry various components of blood in and out of the blood stream. These crosscurrents are in quantity as well as in biological significance at least comparable to the blood stream itself, as they alone maintain and coordinate the metabolism of the vessel walls and of all cells outside these walls.

The research into the *in vivo* blood flow will therefore have to consider all the above-mentioned currents and crosscurrents of the flow of matter and energy, in all the complexity of their interactions with one another, and with the tissues with which they are in contact, in accordance to the mechanical and electrodynamical and osmotical forces present. As a result one will have to investigate diverse flow patterns which vary in the body from one part to another and which in each part are different for the blood as a whole and for each of its various constituent components, such as water, oxygen, carbon dioxide, metal and hydrogen ions, serum, red and white cells, and platelets. Great progress has been made in the development of instrumentation for the disentanglement of the diverse flow patterns, and the measurement of the various blood components. However, much further development is required, and this may well be a fruitful field for cooperation between biologist, chemist, physicist, and mathematician. Such a cooperation would also be required when the research is extended to the field of *ex vivo* blood flow, since without it one could not choose the conditions of the *ex vivo* experiments in a way which would allow conclusions to be drawn for the blood flow under *in vivo* conditions.

Although it would be extremely difficult to develop an exact theory which would account for the whole maze of movements encountered in hemorheology, it seems likely that the tracing of geodetic pathways is a step in the right direction.

In the evaluation of experimental results one has to take into account certain essential differences between the flow of technological materials and that of blood. In particular it has been customary in macroscopic rheology to approximate a technological material by a continuous medium which preserves its continuity and coherence throughout all its movements. This approximation was justified because most materials of technological importance have a constitution such that all the flow patterns of the various structural components coincide in the statistical averages of macroscopic observations. However, there is no such coincidence in macroscopic hemorheology as there is already in the *ex vivo* flow a visible separation of the flow pattern of the serum from that of the red and white cells, the platelets, etc., and this separation becomes even more pronounced in the *in vivo* flow in view of the crosscurrents which carry selectively some of the blood components through the membranes of the vessel walls and cells. A more elaborate continuum theory would here be required in which blood is approximated by a number of different interpenetrating continua which move relative to one another when the blood is in a state of flow. Making due allowance for the separation in the flow of various structural components of blood one may still be able to make good use of the experience gained in the flow of technological materials. It may well be, e.g., that the phenomena of aggregation and agglutination in blood are related to the "dilatency" phenomena which can be observed in almost all technological suspensions (with a solid content of 30% or more) and also in granulated materials, and other structures of solids, and which present effects of the most paradoxical appearance, some of which shall be demonstrated herein.

The dilatancy phenomena have first been noticed by Reynolds in walking on wet sand, i.e., on a highly concentrated sand-water suspension. He observed that the sand around his footprints appeared to dry out, indicating that the sand particles had in the average moved further apart from each other, thereby increasing the apparent volume occupied by the particles (dilatancy) and allowing the water to vanish from the surface and to seep down into the interstices of the structure. He explained the dilationary movement of the sand particles on the assumption that prior to putting down his foot the sand particles had been in closest packing so that any movement could only increase the apparent volume. This explanation was so plausible that it was

generally accepted. However, it was shown later that dilatency occurred not only subsequent to closest packing but also when the packing was quite loose and nowhere near to the closest. One found further that there was a paradoxical effect associated with the dilatency in that, in spite of the solid particles moving further apart, the material work hardened, solidified, and became more brittle. Moreover the same material which exhibited a positive dilatency, with an increase in apparent volume, work hardening, and solidifying under certain mechanical actions, exhibited under different mechanical actions negative dilatancy, with a decrease in apparent volume, work softening, and fluidification.

Synopsis

14564

Research in hemorheology can form an integral part of Einstein's concept of research in an all-embracing natural science. In that science one aims to fit experiment and theory to one another as closely as possible and over the widest possible range of conditions, while one takes fully into account the inevitable uncertainty and arbitrariness of all experimental data. The theory here eliminates the defects of the experimental data for wider and wider changes of materials, conditions, and modes of observation by way of the group theory of transformations and invariants, and thereby makes it possible to approach step by step to the ideal of obtaining a perfect fit between experiment and theory as between lock and key.

Author

N67 14565

Some Aspects of Rheological Theory as Applied to Biological Systems

G. W. SCOTT BLAIR,* *National Institute for Research in Dairying, University of Reading, Reading, England*

First, it is important to emphasize that nothing in the present paper is to be taken to imply that biological systems, whether *in vitro* or *in vivo*, fail to obey the ordinary laws of physics. No suggestion of biorheological vitalism is made; only that there are certain modes of behavior, characteristic of biological systems, which are more amenable to particular types of mathematical and theoretical treatment than are those of most systems of nonbiological origin.

Some eight or ten years ago, an elderly British philosopher fell out of an airplane into the sea. Fortunately he was rescued and, although now ninety years old, his activities still arouse much controversy. Suppose that a piece of baggage had also fallen out of the plane at the same time. Exactly the same laws of motion† would have been applicable to the two falling objects; and yet a study of Bertrand Russell's behavior, based entirely on the laws of falling bodies would arouse little interest; because, unlike the baggage, his subsequent activities have so much more of interest that may be studied by other techniques for which the laws of physiology and psychology are better suited.

Before proceeding to consider the special mechanical characteristics of biorheological phenomena, the author will take the liberty of repeating an argument which he expressed at a meeting on biorheology and microcirculation held in Jerusalem, Israel, two years ago, since he believes that the proceedings of this very interesting symposium were never published in full.‡

† Subject, of course, to aerodynamic corrections to allow for differences of shape, orientation, etc.

‡ For a brief summary of the rheological aspects see Scott Blair.[1]

PRECEDING PAGE BLANK NOT FILMED.

It is an interesting historical fact that rheological milestones have closely paralleled the development of thermodynamic theory, though often anticipating it. Probably the first quantitative rheological measurements, were those made by Hooke (published 1676) who stretched long metal wires and coiled springs and found that "as the extension, so is the force." This illustrates the first law of thermodynamics in that the energy stored in the stretched wire is almost entirely restored when the atoms are allowed to resume their positions representing the natural balance between attractive and repulsive forces. Newton's law (1687) "that the resistance which arises from the lack of slipperiness of the parts of the liquid, other things being equal, is proportional to the velocity with which the parts of the liquid are separated from one another"* also includes the concept of the second law, in that the applied energy is irreversibly dissipated as heat: cooling a capillary viscometer after a run will not cause the liquid to flow backwards through the viscometer.

The third main group of rheological materials to be studied constitutes the rubberlike substances, and in this case the theory consciously introduces the concept of entropy since by the time it was developed the laws of classical thermodynamics were already well known. When the load on a stretched rubber band is released, it retracts because of the much greater "probability" (i.e., number of possible complexions) of coiled up configurations than of extended ones.

The fourth fundamental stage is the study of living things. These

* Translation taken from Reiner.[2] If Aristotle had not confused density with viscosity he could have claimed priority over Newton. Indeed this very confusion brought him near to discovering Stokes' law. He wrote: "Now the medium causes a difference because it impedes the moving thing most of all if it is moving in the opposite direction, but in a secondary degree even if it is at rest; and especially a medium that is not easily divided; i.e., a medium that is somewhat dense. A, then, will move through B in time C and through D, which is thinner, in time E (if the length of B is equal to D) in proportion to the density of the hindering body. For let B be water and D air; then by so much as air is thinner and more incorporeal than water, A will move through D faster than through B. Let the speed have the same ratio to the speed, then, that air has to water. Then if air is twice as thin, the body will traverse B in twice the time that it does D, and the time C will be twice the time E. And always, by so much as the medium is more incorporeal and less resistant and more easily divided, the faster will be the movement." (Quoted from W. D. Ross, *Aristotle*, 5th ed., London, 1949, p. 227.)

maintain themselves, as Schrödinger[3] so clearly pointed out, by absorbing negative entropy: "When is a piece of matter said to be alive? When it goes on 'doing something' moving, *exchanging material with its environment*, and so forth and that for a much longer period than we would expect an inanimate piece of matter to 'keep going' under similar circumstances.... What an organism feeds on is negative entropy." (Author's italics.)

All this suggests that just as classical thermodynamics proved to be the "key treatment" in the last principal stage of rheological development (i.e., that of high polymers) so the new science of irreversible thermodynamics will be of great benefit to those studying the flow and deformation of living systems (see especially de Groot and Mazur[4] and Katchalsky and Kedem[5]).

But to proceed to the main theme: what the author wishes to show is that in biorheology, especially for studies *in vivo*, one must generally look for different types of invariant from those which characterize nonbiological materials. This is because living processes never repeat themselves precisely.

There are, of course, special cases where the classical theory may well be applied. Wood is a material of biological origin and its behavior under stress is well described in terms of tensor notation. Hearmon[6] has shown that of the 21 possible elastic coefficients for an anisotropic material under small strains, wood has nine independent constants. To determine these "properties," which are vectorial in character, use is made of the fourth-rank tensor product of two second-rank tensors. The principal variables of classical rheology—stress, strain, and strain-rate—are all second-rank tensors. The principal properties of isotropic bodies such as viscosities and shear moduli are scalars and those of anisotropic bodies have vectorial characteristics. Since scalars may be regarded as tensors of zero order and vectors as of first order, all these entities are tensorial in character.

In the human or animal body one material, bone, which is essentially structural, can be profitably studied as an engineering material and this has been most effectively done by Bell[7] and his colleagues in Scotland. But bone is exceptional. Most biological systems and, to a lesser extent, many nonbiological colloidal systems, have entirely different characteristics. Some plastics come very near to Schrödinger's description of the behavior of living things.

The popular work of Eddington[8] and others has firmly rooted in

our minds certain principles which should underlie all the concepts of "exact science," but further consideration will show that much valuable scientific work lies outside the category of taking pointer readings on a scale requiring the use only of one color-blind eye. Moreover, although scientific experiments must be repeatable in such a way as to give invariant results independent of observer, time, and place, many highly valuable data cannot be reproduced by a mere reversal of the experiment; i.e., experiments cannot always be repeated on the same sample, only on replicate samples. Thus when we say that "physical laws" must be invariant under space inversion and independent of time; or that lengths and times should not appear explicitly in fundamental physical equations, we are really defining a very special type of physical law. As Bunge[9,10] has very ably pointed out, we are here making laws about laws (which he calls "meta-laws"*).

These are rules—injunctions—not propositions, as he puts it, and it is perhaps a pity that he uses the word "law" rather than "rule." Meta-laws are not laws of nature. A law of nature is a generalization derived from or tested by inductive experience. In the United States there is a "law" that traffic keeps to the right of the road. Such laws are very necessary, but in the present sense they are really *rules*, not laws of nature. In England and in Sweden, traffic equally successfully keeps to the left.

The meta-laws of classical physics are well established, though they have had to be modified from time to time. Thus it is no longer possible to insist, as it used to be, that the process of making a physical measurement must not interfere with the value of the measured quantity.

It is the author's purpose to show that most biological processes cannot be adequately studied by the use of the classical meta-laws, and that the experimental situation has much more in common with quantum phenomena than with the Newton-Einstein type of physics whose culmination in the general theory of relativity would hardly have been possible without tensor theory.

The analogy between biological and quantum-level processes has been made before but is generally regarded as superficial. The prin-

* In fact, the specific type of statements to be discussed here, Bunge would call "metanomological statements," but this term seems needlessly cumbersome and the more general term "meta-law" will be used in the present paper.

ciple of complimentarity does not depend, we are told, merely on the fact that it is impossible to measure conjugate variables such as position and momentum without changing what one is measuring by the act of measurement. There is a much more fundamental sense in which simultaneous precision with respect to certain pairs of entities is meaningless.

All this Bunge denies. The author is not competent to judge between Bunge, Bohr, Dirac, and the rest, he can only recommend biorheologists to read Bunge's articles with extreme care. It is also Bunge's main contention that "linearity is not an absolute and ultimate quality of nature but only an approximation of our knowledge of it" (Bunge,[9] p. 12). (The author feels sure that Einstein would have agreed with many of Bunge's ideas.)

If Bunge is right, the analogy between biorheological and quantum problems is fundamental and intimate: if Bunge is wrong, it is still sufficiently striking to warrant our attention since, even in the latter case, it is possible that similar mathematical tools might prove useful in both fields.

Bergson long ago attempted to argue that sensations were, in their very nature, unmeasurable because every increment of sensation differs not only in quantity but in quality. This is essentially invoking a meta-law. Yet few scientists today would deny objectivity to the work of S. S. Stevens and many others (see West Churchman and Ratoosh[11]) who "measure" sensations with very considerable success. The distinction between quantity and quality is less clear than was formerly believed.

In the case of biorheological phenomena, this means that our most useful invariants (not the only possible ones) will probably prove to be measures of change under certain experimental conditions and that our principal mathematical tool will not be the three-dimensional classical tensor theory of elasticity but something much more like the mathematics of quantum mechanics. The author's personal limitations as a mathematician will allow him to go no further with this suggestion which he gladly passes on, for what it is worth, to those more familiar with matrix algebra and mechanics and with group theory than he is.

But he would like to illustrate these ideas with an example taken from a branch of biorheology with which he has had some experience: the flow of blood through narrow tubes. When blood is

forced, under pressure to flow along a narrow cylindrical tube,* its physical condition is changed. There is a redistribution of the corpuscles in their positions relative to the wall and changes take place in their relative concentration (see many papers in the present Symposium). If we use the term "physical property" in the classical sense, these "properties" cannot be accurately measured, since we change them as a result of the measuring processes. It is possible, of course, to minimize the effect by using very special apparatus and very small strains, e.g., that of Birnboim and Ferry[12] and, because no quantum is involved, there is no sharp limit to the possible accuracy. Herein lies the one essential difference between biorheological and quantum experimentation, but even so there are certainly cases where we have phenomena very reminiscent of quanta, e.g., in the method of transmission of nerve impulses. When a sense organ is stimulated by touching the skin, a series of impulses passes up the sensory fibers. All the action currents are of the same magnitude, independent of the stimulus strength. It is the frequency that depends on the strength of the stimulus, and this may vary over a wide range.

To return to blood, we cannot express its behavior in terms of any one viscosity, even for a single capillary and the fourth-power law of Poiseuille does not hold when the capillary radius is changed.

It is possible, however, to describe shear rate-stress relations in a single tube by two parameters, since straight lines are obtained for very many sets of data for different species and rates of shear when the square roots of shear rate and of stress are plotted against one another. These parameters may then themselves be plotted against functions of tube radius.

This square-root plot was originally proposed by Casson[13,14] for varnishes and has since been found to hold for many materials. Working at very low rates of shear, Merrill et al.[15] confirmed Casson's equation for blood and conclude that this "implies reversible aggregation of red cells in rouleaux." Sometime previously, however, the author examined data from various sources, including bovine blood which does not form rouleaux (Scott Blair[16]) at quite high rates of shear and got excellent Casson curves. Thus, we cannot take Merrill's conclusion (which he derived from Casson's original treatment)

* The word "capillary" has a physiological significance. What is said here would not apply to the case when the corpuscles are large compared with the diameter of the tube.

as conclusive. When the author first used Casson's equation, A. Katchalsky[17] pointed out that it has an interesting property. Suppose we cause the blood to flow from left to right in a horizontal capillary viscometer, we may define the pressure and the rate of flow which we measure as positive. But if we reverse the direction of flow by exerting a suction they become negative and the data from which the parameters of the straight lines are calculated assume imaginary values. We are quite used to imaginary numbers in rheology, e.g., the "viscous" part of the complex modulus; but surely the measured variables from which the same "properties" of a material are derived should not be "real" when the experiment is carried out in one direction and "imaginary" when the direction is reversed.

The author has already quoted Bunge at some length and it is only fair to cite also an article by Dirac[18] which gives, in semipopular terms, the more orthodox viewpoint. In this paper, Dirac discusses the three fundamental quantities: c, the speed of light; e, the charge on the electron; and $h/2\pi$, the famous quantum constant. Since the ratio hc/e^2 is a numeric, he points out that only two of these will ultimately prove to be independently fundamental and, unwilling to question the fundamental nature of c, he proposes that it is $h/2\pi$ that will finally be explained in terms of e^2, "since square roots do not occur in basic equations." Here again we have a meta-law qualifying "basic equations."

In the case of flowing blood, the difficulty may be met by pointing out that blood which has been sheared from left to right in a capillary starts as a different physical system if at the end of the process we reverse the sign and direction of the flow, and the author feels sure that we should not get the same flow curve on the return journey. This has obvious implications when we study pulsatile flow.

How close an analogy have we here to the recently discovered failure of the conservation of parity for weak interactions? Bunge has pointed out that the failure of the conservation of parity is in many ways analogous to the replacement of a real by a complex variable, i.e., on the failure of the conservation of "reality." According to Bunge, parity and reality are comparable concepts. For electrons, parity depends on the sum of the azimuthal quantum numbers expressed in units of $h/2\pi$, which, as we have seen, introduces a square root in the fundamental expression, which Dirac believes "should not occur in basic equations."

In general, the principle of parity implies that the laws of nature are invariant under space reflection, i.e., that if an object exists its mirror image can also exist. Ulbricht,[19] who gives a very interesting discussion on the failure of conservation of parity in general, makes the tentative suggestion that if we assume that optical activity was required for the origin of life on the earth, this may have come about as a result of lack of parity. He quotes Havinga[20,21] as having shown experimentally that unequal quantities of *dextro-* and *laevo*-isomers may be obtained during crystallization of certain easily racemized materials. Lack of "parity" between optical isomers is, of course, characteristic of biological materials.

To return to Bunge's point, it is possible that there is at least a formal resemblance between the failure of (electron) parity and the lack of symmetry in the Casson equation.

To conclude, we must not overgeneralize the validity of our meta-laws. The author long ago proposed that if we want to compare complex rheological parameters with statistically determined reports of subjective sensations through handling materials the best mathematical approach would be through the use of fractional differential equations (Scott Blair[22]). These are difficult to define precisely, and those who have followed up the author's suggestion have generally inverted the idea and used fractional integrals, which are easier to handle (e.g., Graham[23]). But they have not generally applied these to psychophysical problems, and the connection is not so obvious.

The author will not again presume to advise the use of any specified mathematical tool but he does suggest that in treating biorheological data experiments be made, especially with those techniques which have proved fruitful in the field of quantum mechanics, even when there is no quantum involved. He also suggests that the exclusive use of three-dimensional tensors of the elasticity type is slightly reminiscent of the application of Newton's laws of falling bodies to study the philosophy of Russell: correct within very narrow limits of time and space but ultimately not very profitable. (It has been pointed out that the author's criticism of tensors in this connection might be taken to imply that the quantities involved in the mathematics of quantum theory are all nontensorial. This is not so. When referring in this paper to "tensors" the author is thinking only of the three-dimensional tensors of stress, strain, and rate of change of strain and of their products and components.) Against this idea, it will

be argued that our parameters will be too much dependent on experimental conditions. This is true, but it is inherent in the nature of biological systems and in this respect we must follow nature where she leads us. It is true that the wider the invariance, the more fundamental the concept, but on the other hand Occam's principle is worth remembering and what we gain in the range of our invariance, we generally lose in the increasing number of "properties" which have to be measured.

The author is very much indebted to Professor M. Reiner and Dr. P. White for helpful criticisms and discussions.

References

1. Scott Blair, G. W., *Nature*, **183**, 613 (1959).
2. Reiner, M., *Deformation, Strain and Flow*, 2nd ed., Lewis, London, 1960.
3. Schrödinger, E., *What is Life?*, Macmillan, New York, 1946.
4. Groot, de, S. R., and P. Mazur, *Non-equilibrium Thermodynamics*, North Holland Publishing Co., Amsterdam, 1962.
5. Katchalsky, A., and O. Kedem, *Biophys. J.*, **2**, 53 (1962).
6. Hearmon, R. F. S., *Proc. Phys. Soc. (London)*, **55**, 67 (1943).
7. Bell, G. H., in *The Biochemistry and Physiology of Bone*," G. H. Bourne, ed., Academic Press, New York, 1956, ch. 2.
8. Eddington, A. S., *New Pathways of Science*, Cambridge Univ. Press, New York, 1935.
9. Bunge, M., *Brit. J. Phil. Sci.*, **6**, 1, 141 (1955).
10. Bunge, M., *Am. J. Phys.*, **29**, 518 (1961).
11. West Churchman, C., and P. Ratoosh, eds., *Measurement: Definitions and Theories*, Wiley, New York, 1959.
12. Birnboim, M. H., and J. D. Ferry, *J. Appl. Phys.*, **32**, 2305 (1961).
13. Casson, N., *Brit. Soc. Rheol. Bull.*, No. 52, 5 (1957).
14. Casson, N., in *Rheology of Disperse Systems*, C. C. Mill, ed., Pergamon, New York–London, 1959.
15. Merrill, E. W., E. R. Gilliland, G. Cokelet, H. Shin, A. Britten, adn R. E. Wells, *Biophys. J.*, **3**, 199 (1963).
16. Scott Blair, G. W., *Nature*, **191**, 757 (1961).
17. Katchalsky, A., private communication.
18. Dirac, P. A. M., *Sci. Am.*, **208**, 45 (1963).
19. Ulbricht, T. L. V., *Quart. Rev. Chem. Soc.*, **13**, 48 (1959).
20. Havinga, E., *Chem. Weekblad*, **38**, 642 (1941).
21. Havinga, E., *Biochem. Biophys. Acta*, **13**, 171 (1954).
22. Scott Blair, G. W., *Measurements of Mind and Matter*, Dobson, London, 1950, and Philosophical Library, New York, 1956.
23. Graham, A., *Research*, **6**, 92 (1953).

Author's note: Since writing this paper, the author's attention has been drawn to an article entitled "Quantum Mechanics and Biology" by H. C. Longuet-Higgins [*Biophys. J.*, **2**, 207 (1962)]. This does not deal with rheological problems but should interest readers of the present paper.

Synopsis

14565

Although the same fundamental mechanical laws apply to all rheological systems, certain treatments are more appropriate than others for studying biological phenomena. Following the parallel growths of rheology and thermodynamics, it is suggested that the new irreversible thermodynamics will be of special value for studying processes *in vivo*. Classical elasticity theory, though useful enough for a few structural materials such as bone, is hardly suited, even as extended by recent workers, to most biological systems. It is proposed that the mathematics of quantum theory, leading to a new type of invariant, concerned rather with processes than with properties, would be worth careful consideration.

author

N67 14566

Agrégation Provoquée par l'Ecoulement dans les Solutions de Macromolecules d'Origine Biologique

M. JOLY,* *Service de Biophysique, Institut Pasteur, Paris, France*

I. INTRODUCTION

Il est bien connu des chimistes, en particulier depuis les observations de Paine[1] sur la floculation des sols d'hydroxyde cuivrique, que l'état de dispersion de nombreuses substances est grandement influencé par l'agitation de leurs suspensions. Plus récemment les recherches sur la déformation en écoulement des molécules de hauts polymères dissous[2-4] ont attiré l'attention sur les possibilités de rupture des macromolécules sous l'effet de forces de cisaillement, principalement dans le cas de grosses molécules d'origine biologique.[5-12] Par contre, l'agrégation provoquée par l'écoulement laminaire, quoique fréquente et apparaissant souvent dès les faibles vitesses de cisaillement, a été relativement peu étudiée en elle-même bien que dès 1918 Smoluchowski[13] en eût donné le principe en montrant que l'écoulement laminaire d'une suspension entraine une augmentation de la fréquence des collisions entre particules. Toutefois, quelques études expérimentales précises ont été faites sur des systèmes aussi divers que des suspensions de fibres de cellulose[14-16] ou de virus de la mosaïque du tabac,[5,6] des solutions de complexes cuivre-cystine[17] ou de protéines dénaturées.[18,19] En ce qui concerne les études théoriques, le problème de la fréquence de collision entre les particules d'une suspension en écoulement a été traité complètement par Mason et coll.[20,21] dans le cas des particules sphériques sans interaction.

Nous avons repris cette question de l'agrégation provoquée dans le cas plus général de particules géométriquement assimilables à des sphères ou à des ellipsoïdes allongés, porteuses de charges électriques et entre lesquelles les énergies d'interaction dues aux forces de Van der Waals ne sont pas négligeables devant l'énergie moyenne

d'agitation thermique.[22–24] Nous allons rappeler les principaux résultats obtenus, et nous montrerons sur des exemples dans quelle mesure ils sont compatibles avec les données expérimentales. En effet, les mesures de biréfringence d'écoulement[19] et de rhéoturbidité[25] permettent de déterminer, avec une assez bonne précision, les dimensions des particules d'une suspension en écoulement, ou tout au moins celles de particules fictives, sphériques ou ellipsoïdales pour lesquelles l'angle d'extinction ou la turbidité seraient les mêmes que pour les particules du système réel.[24,26]

II. CINETIQUE D'AGREGATION

Soit un ensemble de particules ou de molécules, toutes identiques, en nombre n_0 par cm^3, et distribuées en une dispersion d'agrégats constitués par l'association d'un nombre variable de ces particules. Désignons par n_s le nombre par cm^3 à l'instant t d'agrégats contenant s particules ou molécules constitutives. On admet que sous l'effet de conditions convenables chaque agrégat de la suspension peut se dissocier en agrégats plus petits ou s'associer à d'autres agrégats; les associations et dissociations multiples sont considérées comme des successions d'associations simples et de dissociations simples.

On appelle fréquence d'association d'un agrégat de i particules avec un agrégat de j particules la grandeur A_{ij} telle que le nombre par seconde et par cm^3 de collisions d'agrégats de i et j particules donnant naissance à un agrégat de $i + j$ particules soit égal à $A_{ij}\, n_i\, n_j$. La fréquence de dissociation d'un agrégat de i particules est B_i tel que le nombre par cm^3 et par seconde d'agrégats de i particules qui se dissocient soit $B_i\, n_i$. Les valeurs de A_{ij} et B_i ont été calculées précédemment[23,27] en fonction de la vitesse de cisaillement g. Rappelons-les brièvement.

Notations

m_0 masse d'une particule constitutive de diamètre a_0 (particule sphérique) ou de longueur l_0 (particule ellipsoïdale); m_i, a_i, l_i les grandeurs correspondantes pour un agrégat formé de i particules constitutives; U_0 barrière de potentiel séparant 2 particules constitutives chargées dans l'état de dispersion totale; U_{ij} la barrière de potentiel séparant 2 agrégats de i et j particules; $F(U)$ la fonction

$$1 - \frac{2}{\sqrt{\pi}} (kT)^{-3/2} \int_0^U \exp\{-z/kT\} \sqrt{z}\, dz$$

dont les valeurs numériques ont été calculées précédemment[27]; W l'énergie d'interaction entre une particule constitutive et l'ensemble de ses voisines dans un agrégat: η viscosité du solvant.

Expression de A_{ij}

Agrégats globulaires de particules sphériques

$$A_{ij} = \frac{2}{3}\,[(kT)/(\pi\eta)]F(U_{ij}) + X_{ij} \tag{1}$$

$X_{ij} = 0$ pour $g < g_c$, valeur seuil de la vitesse de cisaillement au-dessous de laquelle seules les collisions spontanées se produisent sous l'effet de l'agitation thermique, la vitesse de cisaillement étant trop faible pour communiquer aux agrégats une énergie cinétique suffisante pour vaincre les répulsions électriques. On a

$$g_c = \frac{4}{a_i + a_j}\sqrt{\frac{U_{ij}}{m_i + m_j}} \tag{2}$$

Pour $g > g_c$

$$X_{ij} = \frac{1}{12}\,(a_i + a_j)^2\left[(a_i + a_j)g - 4\sqrt{\frac{U_{ij}}{m_i + m_j}}\right] \tag{3}$$

A_{ij} est alors fonction linéaire de g.

Agrégats allongés de particules ellipsoïdales

$$A_{ij} = [(2kT)/(\pi\eta)]F(U_{ij}) + X_{ij} \tag{4}$$

$X_{ij} = 0$ pour $g < g_c$ avec

$$g_c = \frac{4}{l_i + l_j}\sqrt{\frac{U_{ij}}{m_i + m_j}} \tag{5}$$

Soit

$$g_p = \frac{275kT}{\pi\eta(l_i + l_j)^3} \tag{6}$$

g_p est une valeur seuil de la vitesse de cisaillement au-dessus de laquelle l'orientation des agrégats sous l'effet de l'écoulement entraîne

une diminution relative de la fréquence de collision. Pour $g_c < g < g_p$

$$X_{ij} = 0{,}06(l_i + l_j)^2\left[(l_i + l_j)g - 4\sqrt{\frac{U_{ij}}{m_i + m_j}}\right] \tag{7}$$

Pour $g_c < g_p < g$

$$X_{ij} = \frac{16kT}{\pi\eta}\left[1 - \frac{4}{g(l_i + l_j)}\sqrt{\frac{U_{ij}}{m_i + m_j}}\right] \tag{8}$$

Expressions de B_i

Agrégats globulaires de particules sphériques

$$B_i = \frac{1}{a_0}\sqrt{\frac{kT}{2\pi m_0}}\exp\left\{-\frac{W}{kT} + Y_i\right\} \tag{9}$$

Soit

$$g_r = \frac{8W}{\pi\eta a_0^2 a_i} \tag{10}$$

g_r est une valeur seuil de la vitesse de cisaillement au-dessus de laquelle les forces de cisaillement sont suffisamment grandes pour provoquer la rupture des agrégats tandis qu'au-dessous de g_r seule l'agitation thermique intervient dans la dissociation des agrégats. Pour $g < g_r$, $Y_i = 0$; et pour $g > g_r$

$$Y_i = \frac{\pi\eta a_0^2 a_i g}{8W} - 1 \tag{11}$$

Agrégats allongés de particules ellipsoïdales

$$B_i = \frac{1}{l_0}\sqrt{\frac{2kT}{\pi m_0}}\exp\left\{-\frac{W}{kT} + Y_i\right\} \tag{12}$$

et

$$g_r = \frac{128W}{\pi\eta l_0^2 l_i} \tag{13}$$

Pour $g < g_r$, $Y_i = 0$; et pour $g > g_r$

$$Y_i = \frac{\pi\eta l_0^2 l_i g}{128} - 1 \tag{14}$$

Nombre et taille moyenne des agrégats

Si on considère les divers processus pouvant conduire à la formation ou à la disparition d'un agrégat contenant s particules constitutives, on trouve[23,24,27] que la variation en fonction du temps du nombre de ces agrégats est

$$\frac{dn_s}{dt} = \frac{1}{2}\sum_{i=1}^{i=s-1} A_{i,s-i}n_i n_{s-i} - n_s \sum_{i=1}^{i=\lambda} A_{i,s}n_i - B_s(s-1)\, n_s + 2\sum_{i=s-1}^{i=\lambda} B_i n_i \quad (15)$$

avec λ défini par $\sum_{i=1}^{i=\lambda} in_i = n_0$. Si les A_{ij} et B_i sont, avec une approximation suffisante, indépendants de i et j, (15) se réduit à

$$dn_s/dt = A\left[\frac{1}{2}\sum_{i=1}^{i=s-1} n_i n_{i-s} - n_s\sum_{i=1}^{i=\lambda} n_i\right] - B\left[(s-1)n_s - 2\sum_{i=s+1}^{i=\lambda} n_i\right]$$

et le système correspondant est intégrable.[28] Soit x le nombre moyen de particules constitutives par agrégat:

$$x = \frac{\sum_1^\lambda sn_s}{\sum_1^\lambda n_s}$$

Lorsque $B \ll n_0 A$, condition nécessaire pour qu'il y ait une agrégation appréciable, la variation de x en fonction de la durée d'écoulement, pour une valeur de g maintenue constante, est donnée par

$$x(t) = \frac{1 + \sqrt{\frac{2B}{n_0 A}}\coth\sqrt{\frac{n_0 AB}{2}}\, t}{\sqrt{\frac{2B}{n_0 A}}\coth\sqrt{\frac{n_0 AB}{2}}\, t}$$

et lorsque l'état stationnaire est atteint

$$x = \sqrt{\frac{n_0 A}{2B}} \quad (16)$$

Les expression de A_{ij} et B_i données plus haut montrent que l'hypothèse selon laquelle les fréquences d'association et de dissociation

des agrégats sont indépendantes du nombre de particules qu'ils contiennent correspond à une approximation assez grossière. Toutefois, si au cours de l'évolution d'une suspension initialement peu polydispersée, l'amplitude des changements de taille des agrégats demeure relativement limitée, on ne commet pas une erreur excessive en prenant pour A et B les valeurs moyennes obtenues en remplaçant dans A_{ij} et B_i les grandeurs caractéristiques de chaque type d'agrégat par leurs valeurs moyennes, m, a ou l, U, etc. On peut donc, dans ces conditions, obtenir à partir de (16) des relations entre x et g qui ne dépendent plus, avec une approximation satisfaisante, que de m_0, U_0, a_0 ou l_0.

III. DIVERS COMPORTEMENTS DES SUSPENSIONS EN ECOULEMENT

Nous avons vu que les expressions de A et B sont différentes selon que g est plus grand ou plus petit que certaines valeurs particulières de la vitesse de cisaillement, g_c, g_p, g_r. Il faut donc s'attendre à une série de comportements différents des suspensions lorsqu'on

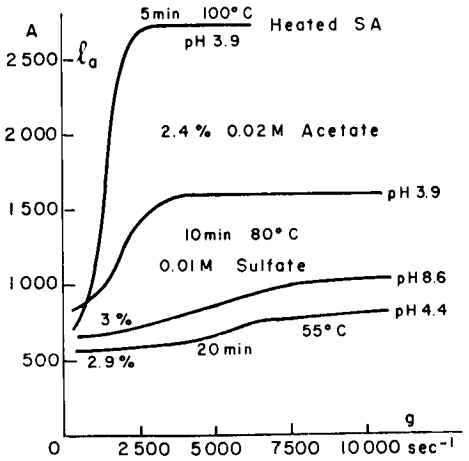

Fig. 1. Variation, en fonction de la vitesse de cisaillement, de la longueur apparente moyenne (déterminée par biréfringence d'écoulement) d'agrégats de serum albumine de cheval dénaturée par chauffage, dans diverses conditions de température, durée de chauffage, concentration, pH et force ionique. Agrégation par écoulement.

passe d'un domaine de variation de g à un autre, et à ce que, par suite, la variation de la taille moyenne des agrégats ne soit pas simple lorsque les variations de g sont de grande amplitude. Les figures 1 à 3 en donnent des exemples.

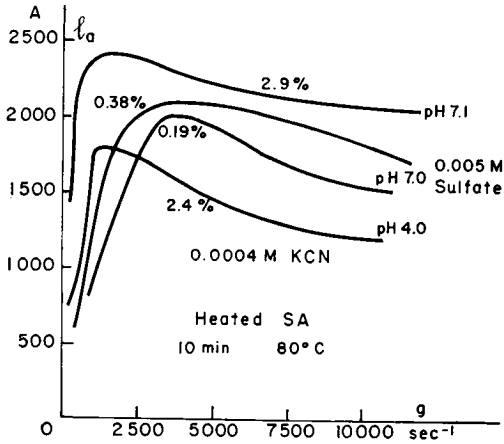

Fig. 2. Variation, en fonction de la vitesse de cisaillement, de la longueur apparente moyenne (déterminée par biréfringence d'écoulement) d'agrégats de serum albumine de cheval dénaturée par 10 mn de chauffage a 80°C dans diverses conditions de concentration, pH et force ionique. Agrégation et dissociation par écoulement.

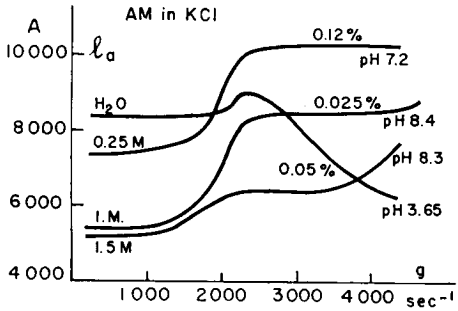

Fig. 3. Variation, en fonction de la vitesse de cisaillement, de la longueur apparente moyenne (déterminée par biréfringence d'écoulement) d'actomyosine en présence de KCl dans différentes conditions de concentration, pH et force ionique. Agrégation et dissociation par écoulement.

TABLEAU I

(1) Concentration SA, %	(2) pH	(3) a_0 × 10^6	(4) g_c × 10^{-2}	(5) g_r × 10^{-2}	(6) g_m × 10^{-2}	(7) a_r × 10^6	(8) a_m × 10^6	(9) g_α × 10^{-3}	(10) g_β × 10^{-3}	(11) a_α × 10^6	(12) a_β × 10^6	(13) $\frac{g_\beta - g_\alpha}{g_r}$	(14) 2,3 log $\frac{x_\alpha g_\beta}{n_\beta g_\alpha}$	(15) W × 10^{16}
1[a]	6,9	3,8	2	6	6,5	6,5	9,6	1	3	9,5	5,5	3,3	2,8	1,9
—	7,4	6,2	1,5	6	6,5	12	12,5	1	3	11,5	7	3,3	2,6	10,9
1,2[b]	6,3	5	1	5,5	6	7,5	8,5	1	3	8,35	4,75	3,6	2,8	4,15
1,66[c]	4,35	5,4	2	8,9	9,7	8,5	9,5	2	4	9,15	7	2,25	1,55	7,6
—	4,4	7	1,5	8,8	15,2	15,1	16,4							25,2
—	4,45	9,2	1	7,5	10	29	30,5							57

[a] Solution de 4% comprimée 1 heure à 8.000 kg./cm.².
[b] Solution de 6,9% comprimée 16 heures à 10.000 kg./cm.².
[c] Solution de 8,3% comprimée 16 heures à 10.000 kg./cm.².

TABLEAU II

Concentration SA, %	Concentration $AlCl_3$, 10^{-4}M	pH	a_0 × 10^7	a_s × 10^7	x_0	g_c	g × 10^{-2}	a × 10^7	x	K^{-1}
0,8	2,85	4,75	5,35	9,15	5	45	1,45	9,9	6,3	49
—	—	—	—	—	—	—	2,9	10,9	8,5	47
—	—	4,5	—	9,6	5,8	10	1,45	10,1	6,9	70
—	—	—	—	—	—	—	2,9	10,8	8,3	68
—	—	—	—	—	—	—	5,6	11,8	10,8	71

Les courbes expérimentales sont évidemment continues alors que pour les différents domaines de variation de g les fonctions $x(g)$ sont très différentes les unes des autres. Les valeurs de g_c, g_p ou g_r sont d'ailleurs difficiles à déterminer expérimentalement avec exactitude car, dans les zones de raccordement entre les différents domaines, il y a en fait superposition de plusieurs régimes. Dans ces régions de transition, les phénomènes ne se prêtent pas à une représentation analytique commode. Par contre, à l'intérieur de chaque domaine mais suffisamment loin de ses frontières les expressions $x(g)$ sont relativement simples et, comme nous le verrons, rendent compte de façon satisfaisante des résultats expérimentaux. Nous allons examiner certains des cas qui se présentent le plus fréquemment.

1. Suspension de particules globulaires sans agrégation spontanée

Pour U_0 suffisamment grand ($F(U_0)\#0$) et W suffisamment petit pour qu'il n'y ait pas d'agrégation spontanée, l'écoulement est sans action sur l'état de dispersion de la solution tant que $g < g_c$ avec, d'après (2)

$$g_c = \frac{1}{a_0}\sqrt{\frac{2U_0}{m_0}} \tag{17}$$

Par contre, dès que $g > g_c$ l'écoulement entraîne la formation d'agrégats.

(a) $g_c < g < g_r$

En portant (1), (3) et (9) dans (16) il vient

$$x = 0{,}835 n_0 a_0^4 \sqrt{\frac{m_0}{kT}}\,(g - 0{,}45\sqrt[6]{x}g_c)\exp\{W/kT\} \tag{18}$$

Le taux d'agrégation moyen est fonction linéaire de la vitesse de cisaillement. Il résulte de (10) que

$$g_i \leq \frac{8W}{\pi\eta a_0^3}$$

Comme U_0 est grand et W petit, le domaine $g_c - g_r$ est relativement étroit (il peut même dans certains cas disparaître: $g_r \leq g_c$); par suite le régime décrit par (18)ne s'observe que rarement.

(b) $g > g_r$

En portant (1), (3), et (9) dans (16) il vient

$$x = 0{,}835 n_0 a_0^4 \sqrt{\frac{m_0}{kT}} (g - 0{,}45\sqrt[6]{x g_c}) \exp\left\{\frac{W}{kT} + 1 - \frac{g_r}{g}\right\} \quad (19)$$

avec

$$g_r = \frac{8W}{\pi\eta a_0^2 a_r} \quad (20)$$

et comme $x \# (a/a_0)^3$, a passe par un maximum a_M pour une valeur g_M de g puis décroît plus ou moins rapidement selon les valeurs de W, lorsque g continue à augmenter, par suite de la compétition entre la formation et la rupture des agrégats sous l'effet des forces de cisaillement. La détermination de g_r et a_r à partir des changements de courbure de la courbe $a(g)$ est imprécise mais g_M et a_M en donnent une limite supérieure. Tant que les valeurs de x ne sont pas trop élevées, on a, sur la partie décroissante de $a(g)$, pour 2 valeurs quelconques de g, g_α et g_β, grandes devant g_c, la relation

$$\frac{g_\alpha - g_\beta}{g_r} \# 2{,}3 \log \frac{g_\beta x_\alpha}{g_\alpha x_\beta} \quad (21)$$

Quoiqu'assez peu fréquent, ce comportement s'observe dans le cas de très grosses particules chargées. Par exemple, lorsqu'une solution relativement concentrée de serumalbumine de cheval, à 37°C, est soumise à de très fortes pressions, il apparaît des globules submicroscopiques[27,29] dont l'agrégation spontanée est négligeable mais dont les suspensions, après dilution à température ordinaire, se comportent comme il vient d'être dit.[19] Le tableau I en donne des exemples. La comparaison des colonnes 13 et 14 montre le degré de vérification de (21), donc de validité de (19). Compte tenu des erreurs expérimentales et des simplifications introduites dans les calculs, l'accord peut être considéré comme assez satisfaisant.

2. Suspension de particules globulaires avec faible agrégation spontanée

(a) $g < g_c$ et g_r

Si U_0 et W sont tels que les particules puissent s'agréger spontanément, on déduit de (1), (9) et (16) que le taux stationnaire d'agrégation spontanée x_0 est donné par

$$x_0^2 = 0{,}265 \frac{n_0 a_0}{\eta} \sqrt{m_0 kT} F(V_0) \exp\{W/kT\} \tag{22}$$

avec

$$V_0 \# 0{,}2 x_0^2 U_0 \tag{23}$$

Le diamètre moyen des agrégats ainsi formés est $a_s \# a_0 \sqrt[3]{x_0}$.

(*b*) $g_r < g < g_c$

Dans ce cas relativement rare, compte tenu de (11), il vient

$$x^2 \# x_0^2 \exp\left\{1 - \frac{g}{g_r}\right\} \tag{24}$$

où x_0^2, donné par (22), correspond à l'état d'agrégation atteint spontanément en absence d'écoulement.

(*c*) $g_c < g < g_r$

Comme précédemment, g_c est défini par (17) et g_r par (20). Il y a simultanément agrégation spontanée et agrégation provoquée, et il résulte de (1), (3), (9) et (16) que

$$x^2 = 0{,}265 \frac{n_0 a_0}{\eta} \sqrt{m_0 kT} F(V) \exp\{W/kT\} + 0{,}835 n_0 x a_0^4 \sqrt{\frac{m_0}{kT}} (g - 0{,}45 \sqrt[6]{x} g_c) \exp\{W/kT\}$$

c'est-à-dire, puisque $V \# V_0$,

$$x^2 \# x_0^2 + 0{,}835 n_0 x a_0^4 \sqrt{\frac{m_0}{kT}} (g - 0{,}45 \sqrt[6]{x} g_c) \exp\{W/kT\}$$

On a donc dans ce domaine de g

$$\frac{x^2 - x_0^2}{x} \# K(g - 0{,}45 \sqrt[6]{x} g_c) \tag{25}$$

où K est une constante pour un système donné. Cette relation est bien vérifiée par l'expérience. Le tableau II en donne des exemples relatifs à de la sérum albumine de boeuf en solution aqueuse de chlorure d'aluminium.

(*d*) g_c *et* $g_r < g$

La destruction des agrégats sous l'influence des forces de cisaillement intervient et, comme en absence d'agrégation spontanée, $a(g)$

présente un maximum a_M pour la valeur g_M de g. Par suite de (1), (3), (9), (11) et (16) il vient

$$x^2\#\left[x_0^2 + 0{,}835 n_0 x a_0^4 \sqrt{\frac{m_0}{kT}}\,(g - 0{,}45\sqrt[6]{x}g_c)\,\exp\{W/kT\}\right] \times \exp\{1 - g/g_r\}$$

3. Suspension de particules globulaires avec forte agrégation spontanée

Lorsque U_0 et W sont tels qu'il y a une forte tendance à l'agrégation spontanée, celle-ci est pratiquement totale dès le début de l'écoulement et l'agrégation provoquée par celui-ci se produit entre des agrégats primaires de diamètre a_s et d'énergie d'interaction W_s. On a alors

$$g_c = \frac{\sqrt[6]{x_0}}{a_0}\sqrt{\frac{2U_0}{m_0}} \text{ et } g_r = \frac{8W_s}{\pi\eta a_s^2 a_r} \tag{26}$$

(a) $g < g_c$ et g_r(défini par (20))

x_0 reste, comme précédemment, défini par (22).

(b) g_r (défini par (24)) $< g < g_c$

L'équation (24) reste valable.

(c) $g_c < g < g_r$ (défini par (26))

En appelant x_1 le nombre moyen d'agrégats primaires spontanés contenus dans un agrégat secondaire provoqué par l'écoulement, on a, par transposition de (18)

$$x_1 = 0{,}835 n_s a_s^4 \sqrt{\frac{m_s}{kT}}\,(g - 0{,}45\sqrt[6]{x_1}g_c)\,\exp\{W_s/kT\}$$

qui, puisque

$$n_s = n_0 x_0^{-1} \tag{27}$$

et

$$m_s = x_0 m_0 \tag{28}$$

Concentration SA, %	Concentration électrolyte (10^{-4} M)	pH	$a_0 \times 10^7$	$a_s \times 10^5$	x_0	g_c	$g_r \times 10^{-2}$	$g_M \times 10^{-2}$	$a_r \times 10^5$	$a_M \times 10^5$	$g_\alpha \times 10^{-3}$	$g_\beta \times 10^{-3}$	$a_\alpha \times 10^5$	$a_\beta \times 10^5$	$\frac{g_\beta - g_\alpha}{g_r}$	$\frac{2,3 \log x_\alpha g_\beta}{n_\beta g_\alpha}$	W_s
0,6	4-$AlCl_3$	6,9	5,35	1,35	16,2	50	9	10	3,2	3,3	2	4	2,95	2,10	2,2	1,75	1,5
2,4	2-$FeCl_3$	6,2	—	1,36	16,4	25	7	7,5	3,05	3,15	—	—	3,05	1,9	2,85	2,1	1,1

TABLEAU IV

Concentration SA, %		Concentration électrolyte, 10^{-3}M	pH	Traitement, mn °C	$l_0 \times 10^6$	$g_c \times 10^{-2}$	$g \times 10^{-2}$	$l \times 10^6$	x	$\frac{g - 0,45\sqrt[6]{x}g_c}{x}$	W/kT
1	Boeuf	50-SO_4Na_2	6,8	10 mn 80°	4,6	0,5	1,45	6,8	3,25	37	15,8
							2,9	8,45	6,2	41	15,3
	—	8,35-$CaCl_2$	4,3	—	7,2	0,2	0,4	8,25	1,5	20	14,6
							1,5	12,9	5,7	23	14,3
2	—	4-NO_3Na	6,1	—	3,5	2,5	2,9	4,2	1,7	96	14,1
							5,6	6,2	5,5	75	14,6
2,4	Cheval	20-acétate	3,9	—	8,5	4	13	11	2,2	500	8,5
							25	14	4,5	495	
							37	16	6,7	515	
	—	20-acétate	3,9	5 mn 100°	6,5	5	10	15,5	13,5	48	12,25
							14	18,5	23	43	
							25	22,5	42	50	
2,5	—	H_2O	4,4	10 mn 100°	6,5	3	13	10,5	4,2	270	9,75
							25	13	8	288	
							37	14	10	350	
3	—	10-Na_2SO_4	8,6	10 mn 80°	6,5	22	38	8	1,85	1460	7,95
							55	9,5	3,1	1380	
							75	10,5	4,25	1470	

peut aussi s'écrire

$$x_1 = 0{,}835 n_0 a_0^4 x_0^{5/6} \sqrt{\frac{m_0}{kT}} \, (g - 0{,}45\sqrt[6]{x_1} g_c) \exp\{W_s/kT\}$$

$$(d) \quad g_c \; et \; g_r < g$$

De la même façon (19) est remplacé par

$$x_1 = 0{,}835 n_0 a_0^4 x_0^{5/6} \sqrt{\frac{m_0}{kT}} \, (g - 0{,}45\sqrt[6]{x_1} g_c) \exp\left\{\frac{W_s}{kT} + 1 - \frac{g_r}{g}\right\}$$

$a(g)$ passe par un maximum et, dans la partie descendante de la courbe, (21) reste valable. Le tableau III relatif à de la sérum albumine de cheval en présence de cations trivalents en donne des exemples. On voit que (21) est vérifié avec une bonne approximation.

4. Suspensions de particules allongées sans agrégation spontanée

Dans le cas des particules allongées les comportements sont analogues à ceux des particules globulaires sauf en ce qui concerne la complication supplémentaire due à l'orientation des particules dans l'écoulement. Le diverses valeurs seuils de g sont les suivantes: d'après (5), (6) et (13)

$$g_c = \frac{1}{l_0} \sqrt{\frac{2U_0}{m_0}} \tag{29}$$

$$g_p = \frac{34{,}5kT}{\pi\eta l_p^3} \text{ et } g_r = \frac{128W}{\pi\eta l_0^2 l_r} \tag{30}$$

$$(a) \quad g_c < g < g_p \; et \; g_r$$

Il résulte de (4), (7), (12) et (16) que

$$x = 0{,}3 n_0 l_0^4 \sqrt{\frac{m_0}{kT}} \, (g - 0{,}45\sqrt[6]{x} g_c) \exp\{W/kT\} \tag{31}$$

Le taux moyen d'agrégation, du moins tant qu'il demeure relativement petit, est en première approximation fonction linéaire de g. Le tableau IV donne des exemples de ce comportement observé dans des solutions de sérum albumine de boeuf ou de cheval dénaturée

TABLEAU V

Concentration AM, %	Concentration electrolyte, M	pH	l_0 $\times 10^5$	g_c $\times 10^{-3}$	g_α $\times 10^{-3}$	g_β 10^{-3}	x_α	x_β	$(x_\alpha/x_\beta)^2$	$f(g_\alpha, g_\beta)$	W/kT
0,05	H_2O	4	8,8	1,8	2,5	4	1,3	1,48	0,77	0,84	11,8
—	0,5-KCl	8,2	6,3	1,5	2,5	4	2,07	2,3	0,81	0,86	10
—	2-KCl	6,95	5	1,5	2,5	4	2,6	2,95	0,78	0,86	10,65

TABLEAU VI

Concentration AM, %	Concentration électrolyte, 10^{-4}M	pH	l_0 $\times 10^5$	g_c $\times 10^{-3}$	g_r $\times 10^{-3}$	g_M $\times 10^{-3}$	l_r $\times 10^5$	l_M $\times 10^5$	g_α $\times 10^{-3}$	g_β $\times 10^{-3}$	l_α $\times 10^5$	l_β $\times 10^5$	$\frac{g_\beta - g_\alpha}{g_r}$	$13,8 \log \frac{l_\alpha}{l_\beta}$	W/kT
0,05	H_2O	3,65	8,5	1,7	1,8	2,2	8,7	9,3	2,7	4	8	7	0,72	0,8	6,8–7,9
0,05	1-KCl	8,6	6,5	1,4	2	2,2	7,9	8,1	2,5	3,5	7,8	7,2	0,5	0,47	4,1–5,5
0,12	0,5-KCl	7,2	8,4	1,5	2,2	2,3	9,3	9,5	2,5	3,5	9,4	8,8	0,45	0,39	8,7–8,9

par chauffage en présence d'électrolytes. On sait que la dénaturation thermique ménagée de la sérum albumine donne naissance dans ces conditions à des agrégats en forme de chapelets (27) stables au repos mais susceptibles de s'agréger lorsqu'ils sont soumis à un écoulement laminaire. L'équation (31) est également assez bien vérifiée avec des suspensions très diluées de virus de la mosaïque du tabac en présence de fortes concentrations en KCl.

$$(b)\ g_c \text{ et } g_p < g < g_r$$

D'après (4), (8), (12) et (16) on a

$$x^2 = 3{,}2\,\frac{n_0 l_0}{\eta}\sqrt{m_0 kT}\left(1 - 0{,}45\sqrt[6]{x}\,\frac{g_c}{g}\right)\exp\{W/kT\} \qquad (32)$$

Il en résulte que pour deux valeurs quelconques g_α et g_β de g on a

$$\left(\frac{l_\alpha}{l_\beta}\right)^6 \# \left(\frac{x_\alpha}{x_\beta}\right)^2 = \left(1 - 0{,}45\sqrt[6]{x_\alpha}\,\frac{g_c}{g_\alpha}\right)\left(1 - 0{,}45\sqrt[6]{x_\beta}\,\frac{g_c}{g_\beta}\right)^{-1}$$
$$= f(g_\alpha, g_\beta) \qquad (33)$$

Le tableau V donne des exemples de ce comportement manifesté par des solutions d'actomyosine de lapin.

$$(c)\ g_c \text{ et } g_p < g_r < g$$

Compte tenu de (4), (8), (12), (14) et (16) le taux moyen d'agrégation est donné par

$$x^2 = 3{,}2\,\frac{n_0 l_0}{\eta}\sqrt{m_0 kT}\left(1 - 0{,}45\sqrt[6]{x}\,\frac{g_c}{g}\right)\exp\left\{\frac{W}{kT} + 1 - \frac{g_r}{g}\right\} \qquad (34)$$

l passe par un maximum l_M pour la valeur g_M de g et, dans la partie descendante de la courbe, si les valeurs de x ne sont pas trop grandes, on an en première approximation

$$\frac{g_\beta - g_\alpha}{g_r} \# 4{,}6 \log \frac{x_\alpha}{x_\beta} \# 13{,}8 \log \frac{l_\alpha}{l_\beta} \qquad (35)$$

Le tableau VI donne des exemples de ce comportement dans le cas de solutions d'actomyosine de lapin.

(*d*) g_c *et* $g_r < g < g_p$

Dans ce cas qui est relativement fréquent, il découle de (4), (7), (12), (14) et (16) que

$$x = 0{,}3 n_0 l_0^4 \sqrt{\frac{m_0}{kT}} (g - 0{,}45\sqrt[6]{x}\, g_c) \exp\{W/kT + 1 - g/g_r\} \quad (36)$$

$l(g)$ passe par un maximum l_M pour $g = g_M$ et dans la partie descendante de la courbe, tant que x n'est pas trop élevé, on a pour g_α et g_β grands devant g_c la relation approchée

$$\frac{g_\alpha - g_\beta}{g_r} \# 2{,}3 \log \frac{g_\beta x_\alpha}{g_\alpha x_\beta} \quad (37)$$

Le tableau VII donne des exemples de ce comportement observé avec des suspensions de sérum albumine dénaturée par chauffage.

5. Suspension de particules allongées avec faible agrégation spontanée

Comme dans le cas de particules globulaires, lorsque l'énergie de cohésion W est suffisamment grande et la répulsion électrique U_0/m_0 suffisamment petite pour qu'il y ait possibilité d'agrégation spontanée; les relations se compliquent.

(*a*) $g < g_c$ *et* g_r

D'après (4), (12) et (16), l'état stationnaire de l'agrégation spontanée est donné par

$$x_0^2 = 0{,}4 \frac{n_0 l_0}{\eta} \sqrt{m_0 kT} F(V_0) \exp\{W/kT\} \quad (38)$$

avec V_0 exprimé par (23).

(*b*) $g_r < g < g_c$

Compte tenu de (14) l'équation (24) s'applique avec pour x_0 la valeur donnée par (38).

(*c*) $g_c < g < g_p$ *et* g_r

TABLEAU VII

Concentration SA, %	Concentration electrolyte 10^{-3}M	pH	Traitement, °C. 10 mn	l_0 × 10^6	g_c × 10^{-2}	g_r × 10^{-3}	g_M × 10^{-3}	l_r × 10^5	l_M × 10^5	g_α × 10^{-3}	g_β × 10^{-3}	l_α × 10^5	l_β × 10^5	$\frac{g_\alpha - g_\beta}{g_r}$	2,3 log $\frac{x_\alpha g_\beta}{x_\beta g_\alpha}$	W/kT × 10^2
0,19	5-SO_4Na_2	7	80	7,5	8	3,5	3,7	1,9	2	5	10	1,85	1,6	1,45	1,15	2,5
—	—	—	100	8	7	3	3,4	2,1	2,3	5	10	2,2	1,85	1,65	1,25	2,4
0,38	—	—	80	7,5	6	3,75	3,6	1,95	2,1	5	10	2,05	1,75	1,55	1,15	2,2
0,6	20-acétate	4,15	100	15	2	0,85	0,9	1,75	1,85	2,5	5	1,8	1,4	2,9	1,45	1,9
1,5	2-NO_3Na	7	80	9	4	2,2	2,5	1,5	1,55	5	7,5	1,5	1,3	1,15	0,85	1,7
1,6	100-$CaCl_2$	4,4	60	11,5	2	1,7	1,9	2,1	2,2	4	8	2,1	1,5	2,35	1,7	2,8
2,9	H_2O	4,1	80	7	0,5	1,2	1,3	2,02	2,05	2,5	7,5	1,95	1,3	4,15	2,35	0,8
—	—	7,1	—	12,5	1	1,3	1,4	2,55	2,6	2,5	7,5	2,55	1,9	3,85	2,05	2,9
3,1	—	4	—	7	1	1,1	1,2	2,05	2,15	2,5	5	2,05	1,65	2,25	1,35	0,7
—	1,7-NaCl	—	—	6	1	1,1	1,4	2,3	2,35	2,5	4	2,2	1,7	1,35	1,25	0,6
—	2-LiCl	—	—	18	3	1,2	1,3	2,05	2,1	2,5	5	2,05	1,7	2,1	1,25	4,5
—	0,8-NaCl	7	—	4,75	2	1,2	1,3	1,85	1,9	2,5	5	1,85	1,5	2,1	1,35	0,35
—	1,7 —	—	—	5,5	2	1,2	1,3	2	2,05	2,5	4	1,95	1,65	1,25	0,95	0,4
—	3,33 —	—	—	18,5	3	1,3	1,4	2,1	2,2	2,5	5	2,1	1,8	1,95	1,15	5,7

La simultanéité de l'agrégation spontanée et de l'agrégation provoquée par l'écoulement conduit à remplacer (31) par

$$x^2 \# x_0^2 + 0{,}3 n_0 l_0^4 x \sqrt{\frac{n_0}{kT}} (g - 0{,}45 \sqrt[6]{x}\, g_c) \exp\{W/kT\} \quad (39)$$

où x_0^2 est donné par (38). La relation (32) est donc vérifiée comme dans le cans des particules globulaires.

$$(d) \quad g_c \text{ et } g_p < g < g_r$$

(32) est remplacé par

$$x^2 \# x_0^2 + 3{,}2 \frac{n_0 l_0}{\eta} \sqrt{m_0 k T} \left(1 - 0{,}45 \sqrt[6]{x} \frac{g_c}{g}\right) \exp\{W/kT\} \quad (40)$$

d'où

$$x^2 - x_0^2 = K\left(1 - 0{,}45 \sqrt[6]{x} \frac{g_c}{g}\right)$$

avec K constant pour un système donné.

$$(e) \quad g_c \text{ et } g_p < g_r < g$$

La relation (34) est à remplacer par une expression qui se déduit de (40) en en multipliant tout le second membre par exp $\{1 - (g/g_r)\}$.

$$(f) \quad g_c \text{ et } g_r < g < g_p$$

Il faut substituer à l'équation (36) une relation déduite de (39) en multipliant également son second membre par exp $\{1 - (g/g_r)\}$.

Dans ces deux derniers cas $x(g)$ passe par un maximum x_M pour la valeur g_M de g, mais la forme des courbes n'est pas simple dès que x_0 et x atteignent des valeurs un peu élevées.

6. Suspension de particules allongées avec forte agrégation spontanée

On peut admettre que dans ce cas l'agrégation spontanée est totale dès le début de l'écoulement et que l'agrégation provoquée est une agrégation secondaire d'agrégats primaires formés spontanément. Il en résulte que les équations correspondantes sont les

TABLEAU

Concentration AM, %	Concentration electrolyte, M	pH	$l_0 \times 10^5$	$l_s \times 10^5$	$g_c \times 10^{-2}$	$g_r \times 10^{-2}$	$g_r' \times 10^{-2}$	$g_M \times 10^{-2}$
0,11	1-KCl	6,7	2,1	9	0,5	1,5	5	2
—	—	6,8	—	7,2	1	5	12,5	6

mêmes que celles du paragraphe 4 à condition d'y remplacer x par x_1, m_0 par m_s, l_0 par l_s et W par W_s tels qu'ils ont été définis au paragraphe 3, et de substituer à (29) et (30) les relations

$$g_c = \frac{\sqrt[6]{x_0}}{l_0}\sqrt{\frac{2U_0}{m_0}} \quad \text{et} \quad g_r = \frac{128W_s}{\pi\eta l_0^2 l_r} \tag{41}$$

(*a*) $g < g_c$ *et* g_r (*défini par* (30))

x_0 est comme précédemment donné par (38)

(*b*) g_r (*défini par* (30)) $< g < g_c$

L'équation (24) reste valable pour x avec x_0 tiré de (38).

(*c*) $g_c < g < g_p$ *et* g_r

Compte tenu de (27) et (28), (31) prend la forme

$$x_1 = \frac{x}{x_0} = 0{,}3 n_0 l_0^4 x_0^{5/6}\sqrt{\frac{m_0}{kT}}\,(g - 0{,}45\sqrt{x_1}\,g_c)\exp\{W_s/kT\} \tag{42}$$

(*d*) g_c *et* $g_p < g < g_r$

Les mêmes substitutions effectuées sur (32) conduisent à

$$x_1^2 = \left(\frac{x}{x_0}\right)^2 = 3{,}2\frac{n_0 l_0}{\eta}x_0^{-1/6}\sqrt{m_0 kT}\left(1 - 0{,}45\sqrt[6]{x_1}\,\frac{g_c}{g}\right)\exp\{W_s/kT\} \tag{43}$$

et la relation (33) reste valable.

(*e*) g_c *et* $g_p < g_r < g$

VIII

l_r × 10^5	l_r' × 10^5	g_α × 10^{-3}	g_β × 10^{-3}	l_α × 10^5	l_β × 10^5	$\frac{g_\beta - g_\alpha}{g_r'}$	$2{,}3 \log \frac{g_\beta x_\alpha}{g_\alpha x_\beta}$	W × 10^{15}	W_s × 10^{14}
9,5	8	1	3	5,9	2,7	4	3,45	4,3	2,8
9,5	6,2	2	6	4,9	2,9	3,2	2,75	8,4	6

L'équation (34) se transforme en une relation qui se déduit de (43) par multiplication du second membre par $\exp\{1 - (g/g_r)\}$:

$$x_1^2 = 3{,}2\frac{n_0 l_0}{\eta} x_0^{-1/6}\sqrt{m_0 kT}\left(1 - 0{,}45\sqrt[6]{x_1}\,\frac{g_c}{g}\right)\exp\left\{\frac{W_s}{kT} + 1 - \frac{g}{g_r}\right\} \tag{44}$$

l'équation (35) demeure applicable.

$$(f)\quad g_c \text{ et } g_r < g < g_p$$

(36) est remplacé par une équation déduite de (42) en en multipliant le second membre par $\exp\{1 - (g/g_r)\}$:

$$x_1 = 0{,}3 n_0 l_0^4 x_0^{5/6}\sqrt{\frac{m_0}{kT}}\,(g - 0{,}45\sqrt{x_1}g_c)\exp\left\{\frac{W_s}{kT} + 1 - \frac{g}{g_r}\right\} \tag{45}$$

et la relation (37) est encore valable.

IV. DISCUSSION ET CONCLUSION

La série d'équations qui vient d'être donnée montre l'extrême diversité des comportements que peuvent présenter les solutions de macromolécules d'origine biologique lorsque varient les conditions de concentration, pH, force ionique et nature des électrolytes. D'autres complications peuvent apparaître. Ainsi, de même que l'écoulement provoque l'association en agrégats secondaires d'agrégats primaires formés spontanément au repos (paragraphes 3 et 6 de la troisième partie), il n'est pas rare que ces agrégats secondaires, à partir d'une certaine valeur g_c' de g s'associent à leur tour en très gros agrégats tertiaires, ce qui se manifeste sur les courbes $a(g)$ou $l(g)$ par des paliers et des remontées successifs. Ceci s'observe en particulier avec des solutions très diluées d'actomyosine en présence

de fortes concentrations de KCl et à pH élevé.[27] Par contre, pour des solutions plus concentrées mais à pH plus faible, lorsque g augmente, les agrégats secondaires sont dissociés en agrégats primaires à partir de $g = g_r$, puis à partir d'une valeur $g_r' > g_r$ il y a dissociation des agrégats primaires spontanés en leurs particules constitutives. Le phénomène est donc successivement décrit par (44) ou (45) puis (34) ou (36). Le tableau VIII en donne des exemples.

La complexité de ces comportements est la conséquence du gr nd nombre de paramètres dont ils dépendent. Dans les conditions de l'expérience g varie entre 0 et 8.10^3 sec.$^{-1}$. Or, les valeurs de g qui séparent les divers types de comportement: g_c, g_r, g_r', g_p, sont, ainsi qu'on l'a vu, fonction de a_0, l_0, m_0, U_0, W, x_1 et W_s, les quatre derniers dépendant eux-mêmes, pour une substance donnée, des concentrations, du pH, de la force ionique et de la nature des ions tandis que les trois premiers sont caractéristiques des macromolécules étudiées. Il en résulte qu'un faible changement des conditions d'environnement peut suffire pour faire passer, pour un même domaine de variation de la vitesse de cisaillement, d'un type de comportement à un autre.

Il découle des diverses équations données plus haut que la connaissance des courbes expérimentales $a(g)$ou $l(g)$ relatives aux états stationnaires permet de déterminer les valeurs des énergies d'interaction entre les particules constitutives des agrégats.[30] Nous avons donné à titre d'exemple quelques valeurs de ces énergies de cohésion dans les divers tableaux du présent article. En particulier il est aisé de déduire une valeur approchée de W et W_s de la valeur approximative de g_r au moyen de (20), (26), (30) ou (41). De même, dans le cas des courbes présentant un maximum et pour lesquelles la variation de x est d'assez faible amplitude, on a en première approximation

$$W \# 0{,}4\eta a_0^2 a_M (g_M - 0{,}45\sqrt[6]{x_M} g_e)$$

ou

$$W \# 0{,}15\eta l_0^2 l_M (g_M - 0.45\sqrt[6]{x_M} g_e)$$

lorsque g_M g_p.

Parmi les conséquences de l'effet de l'écoulement sur l'état de dispersion des suspensions, on peut citer le cas extrême où un écoulement prolongé, à une vitesse de cisaillement convenable, peut con-

duire jusqu'à la précipitation totale et définitive des macromolécules dissoutes. Dans le cas extrême opposé on observe une réversibilité totale de l'agrégation en fonction de la vitesse de cissaillement.[25]

Cette facilité d'agrégation par écoulement est une cause d'erreurs importantes dans les déterminations des grandeurs moléculaires des substances macromoléculaires en solution. En effet, il peut y avoir formation d'agrégats irréversibles au cours des pipettages et des filtrations pendant la préparation des solutions, ainsi que formation ou dissociation d'agrégats pendant les mesures elles-mêmes. Ceci explique certaines divergences entre les valeurs des dimensions ou des poids moléculaires trouvées dans la littérature, et c'est probablement la raison de la difficulté qu'il y a souvent à obtenir une bonne reproductibilité dans les mesures effectuées sur les macromolécules biologiques.

Par ailleurs, le caractère de généralité des faits que nous venons de décrire incite à penser que de tels phénomènes doivent jouer un grand rôle dans la circulation des liquides biologiques et des éléments, substances dissoutes, cellules ou corpuscules divers, qu'ils contiennent. D'autre part, on est en droit de se demander dans quelle mesure certaines structures cytologiques ne sont pas conditionnées par l'état de mouvement du protoplasme lors de leur élaboration et si, par suite, l'organisation submicroscopique de la matière vivante n'est pas dans certains cas la manifestation d'un comportement très général des systèmes colloidaux en phase aqueuse, à savoir la corrélation écoulement-structure.[31-33]

Bibliographie

1. Paine, H. H., *Kolloid-Z.*, **2**, 115 (1912); *Kolloidchem. Beih.*, **4**, 24 (1912).
2. Kuhn, W., *Z. Phys. Chem.*, **161A**, 1,447 (1932); *Kolloid-Z.*, **62**, 269 (1933).
3. Tsvetkov, V. N., et E. Frisman, *Acta Phys. Chim. URSS*, **20**, 61 (1945).
4. Bestul, A. B., *J. Appl. Phys.*, **25**, 1069 (1954).
5. Joly, M., *Bull. Soc. Chim. Biol.*, **30**, 409 (1948); **31**, 108 (1949).
6. Joly, M., *Biochim. Biophys. Acta*, **8**, 134, 245 (1952).
7. Barbu, E., et M. Joly, *Bull. Soc. Chim. Belges*, **65**, 17 (1956).
8. Cavalieri, L. F., *J. Am. Chem. Soc.*, **79**, 5319 (1957).
9. Barbu, E., et M. Joly, *J. Chim. Phys.*, **55**, 799 (1958).
10. Cavalieri, L. F., et B. H. Rosenberg, *J. Am. Chem. Soc.*, **81**, 5136 (1959).
11. Rosenkranz, H. S., et A. Bendich, *J. Am. Chem. Soc.*, **82**, 3198 (1960).
12. Levinthal, C., et P. F. Davison, *J. Chim. Phys.*, **58**, 882 (1961).
13. Smoluchowski, M., *Z. Phys. Chem.*, **92**, 129 (1918).
14. Mason, S. G., *Pulp Paper Mag. Can.*, **49**, 99 (1948).

15. Mason, S. G., *TAPPI*, **33**, 440 (1950).
16. Hubley, C. E., A. A. Robertson, et S. G. Mason, *Can. J. Research*, **B28**, 70 (1950).
17. Kahler, H., B. J. Lloyd, et M. Eden, *J. Phys. Chem.*, **56**, 768 (1952).
18. Joly, M., et E. Barbu, *Bull. Soc. Chim. Biol.*, **31**, 1642 (1949); **32**, 908 (1950).
19. Joly, M., *Discussions Faraday Soc.*, **25**, 150 (1958).
20. Trevelyan, B. J., et S. G. Mason, *J. Colloid Sci.*, **6**, 354 (1951).
21. Manley, R. S., et S. G. Mason, *J. Colloid Sci.*, **7**, 354 (1952).
22. Joly, M., *Kolloid-Z.*, **145**, 65 (1956).
23. Joly, M., *Rheol. Acta*, **1**, 180 (1958).
24. Joly, M., *J. Chim. Phys.*, **59**, 249 (1962).
25. Joly, M., *Kolloid-Z.*, **182**, 133 (1962).
26. Joly, M., *Trans. Faraday Soc.*, **48**, 279 (1952).
27. Barbu, E., et M. Joly, *Discussions Faraday Soc.*, **13**, 77 (1953).
28. Blatz, P. J., et A. V. Tobolsky, *J. Phys. Chem.*, **49**, 77 (1945).
29. Barbu, E., J. Basset, et M. Joly, *Bull. Soc. Chim. Biol.*, **36**, 323 (1954).
30. Joly, M., *J. Chim. Phys.*, **56**, 897 (1959).
31. Bourgoin, D., *Materialprüfung*, **1**, 391 (1959).
32. Bourgoin, D., *Cahier Groupe Franç. Etudes Rheol.*, **4**, 33 (1959).
33. Bourgoin, D., *J. Chim. Phys.*, **60**, 902, 911, 923 (1963).

Résumé

14566

On rappelle les principes généraux de la cinétique d'agrégation en écoulement et on décrit les comportements caractéristiques de suspensions de particules indéformables globulaires ou ellipsoïdales. Ces comportements dépendent des valeurs relatives des vitesses de cisaillement, des dimensions des particules initiales et des énergies d'interaction entre celles-ci. Il en résulte que, pour un système donné (dimensions et énergies d'interaction des particules de valeurs définies), il existe des domaines successifs de vitesse de cisaillement pour chacun desquels l'effet de l'écoulement sur l'état de dispersion des particules en suspension est d'un type distinct. On en donne des exemples et on montre que, malgré le caractère schématique des modèles utilisés, il y a accord satisfaisant entre les résultats expérimentaux et les expressions théoriques de la variation de la grosseur moyenne des agrégats en fonction de la vitesse de cisaillement. On indique quelques application à la détermination des énergies d'interaction.

author

N67 14567

An Application of Particle/Fluid Mechanics to Blood Flow

R. L. WHITMORE,* *University of Nottingham, Nottingham, England*

INTRODUCTION

During the last few years evidence has been accumulating that, under certain circumstances, neutrally buoyant particles can migrate from the walls of a tube down which they are being carried by a liquid. The evidence in some cases comes from direct observation of the particles,[1–4] and in others it is deduced from changes in the viscosity,[5,6] concentration,[7,8] or opacity of the flowing mass,[9] but the existence of a particle-free layer adjacent to the tube walls is not always confirmed. When the particles consist of red blood cells the problems of direct measurement *in vitro* are extremely great because of optical distortion adjacent to the wall[10,11] so that deductive methods of determining the presence of a cell-free layer have generally been necessary.[12–20] Moreover the results can be interpreted in various ways, according to different theories, to give different pictures of the flow conditions prevailing in the tube.[21]

Existing theories of the radial displacement of bodies when flowing down a capillary tube have considered the forces exerted on a single body in the vicinity of the wall.[2–4,8,10,11,19,20] Although such theories might be applicable to suspensions at low concentration they are unlikely to apply to normal blood where the volume occupied by red cells may be 0.4 or more of the total. It has been shown[22] that when a mass of spheres undergoes shear, a pressure is developed at right angles to the direction of shear which increases rapidly in magnitude as the concentration of spheres is raised. When a certain rate of shear is exceeded blood behaves very similarly to a suspension of dispersed particles,[23,24] and it is unrealistic not to assume that it too will develop a dispersive pressure in opposition to any inwardly directed force exerted by the individual cells. In this paper the rela-

tive magnitude of the inwardly and outwardly directed forces are considered for a suspension of spheres, and the results are applied to blood.

THEORY

It has long been recognized that when a closely packed mass of static grains is sheared there is a tendency for it to dilate, and the expansion of the mass can only be resisted by the application of a compressive stress during shear. Bagnold has shown that this phenomenon has its counterpart "in the dynamic case of continuing shear strain when the limit of static dilation has been far exceeded and the grain mass has become a dispersion."[22] He considered two cases, depending on whether grain inertia or fluid viscosity predominated. At the shear rates involved in the flow of blood and fine suspensions in capillary tubes, Bagnold's flow parameter confirms the normal Reynolds number criterion for single-phase flow that viscosity forces are dominant. For a sheared neutral-density suspension of hard, equisized spheres,

$$\text{Dispersive pressure} = 1.3(1 + \lambda)(1 + {}^1/_2\lambda)(dU/dy)\eta_F \quad (1)$$

where

$$\lambda = \frac{\text{Particle diameter}}{\text{Mean free dispersion distance}}$$

$$= 1/[(C_0/C)^{1/3} - 1]$$

where C is the volume concentration of spheres, C_0 is the maximum possible static volume concentration (0.74 for spheres), dU/dy is the rate of shear of the particles (assumed equal to that of the suspending fluid), and η_F is the viscosity of the suspending fluid.

Suppose that a suspension of the spheres of radius a and volume concentration C' flows from a reservoir down a straight, smooth, cylindrical tube of radius R. As they enter the tube, some spheres will be displaced from their transporting streamlines by the mechanical interference of the converging walls, leading to a reduction in the mean concentration of spheres at any cross section of the tube.[7,16,23–25] The new concentration C is given by

$$C = C'[1 - K(a/R)] \quad (2)$$

where

$$K = 1.42 \pm 0.1^{16}$$

In the present paper K is assumed equal to 1.5.

Now suppose that as the spheres are carried down the tube they are drawn into an axial core. Particles situated on the outside edge of the core will experience an outwardly directed pressure generated by the shearing of suspension nearer the tube axis. In the limiting case when the peripheral spheres of the core are just touching the tube wall,

$$\text{Outward pressure} = 1.3[(1 + \lambda)(1 + {}^1/_2\lambda) - 1]D \cdot \eta_F \qquad (3)$$

where D is the rate of shear at distance $R - a$ from the tube axis.

Assuming that the velocity distribution across the tube is parabolic and that the concentration of particles is uniform,

Outward pressure =

$$\frac{2.6[(1 + \lambda)(1 + {}^1/_2\lambda) - 1]Re \cdot \eta_F \cdot \eta_S \cdot [1 - (a/R)]}{\rho \cdot R^2} \qquad (4)$$

where Re is the tube Reynolds number $= [(2V_m \cdot R \cdot \rho)/(\eta_S)]$, V_m is the mean velocity of the suspension in the tube, ρ is the density of the suspension, and η_s is the viscosity of the suspension. It is given by

$$\eta_S = (\eta_F)/(1 - 2{\cdot}5C) \text{ for } C < 0.3^* \qquad (5)$$

If V_m, or the shear stress at distance $R - a$ from the axis, is known it is obvious that some simplification is possible in eq. (4).

The outward pressure exerted on a peripheral sphere is opposed by an inward force developed apparently from its rotation in the sheared fluid. The exact origin and nature of this force is still open to discussion,[2] but in general terms it is of the form:

$$\text{Inward force} = \frac{K' V_m^2 \rho \cdot a^{n+1} r}{R^n} \qquad (6)$$

where r is the distance of sphere center from tube axis and n and K' are constants.

The equation is strictly applicable only to a single sphere, unhindered by the presence of other bodies. When the concentration

* See Oliver and Ward, ref. 26.

of particles in a suspension increases, interference between particles could affect the inward force and a reduction in their angular velocity might increase the inward force,[4] but possibilities of this type will be ignored. From eq. (6), the inward pressure experienced by a sphere at the wall of the tube is given by

$$\text{Inward pressure} = \frac{K''\mathrm{Re}^2\eta_s{}^2a^{n-1}[1 - (a/R)]}{\rho \cdot R^{n+1}} \tag{7}$$

where K'' is a constant.

We have now to assign values to n and K''. Classical theories which make no allowance for the presence of the tube walls lead to a value of 4 for n.[2] However, Oliver[4] has shown experimentally that the effect of the walls cannot be neglected and Segré and Silberberg concluded from their experiments[2] that n is likely to be nearer 3 than 4. A value of 3 is accepted in the present paper, but the selection of other values for n between 2 and 4 makes no significant difference to the general conclusions reached in this paper. No reliable value of K'' has been deduced from first principles and so it was obtained empirically from eqs. (4) and (7) and the experiments of Segré and Silberberg.[2] They found that at the lowest flow rates no concentration changes were detectable across the tube down which a low concentration of spheres was flowing. The relevant data are summarized in Table I.

TABLE I
Experiments of Segré and Silberberg (ref. 2)

Test No.	Sphere radius, cm.	Tube radius, cm.	Feed vol. concn. × 100 ×−0±	Reynolds No.	Pressure, dynes cm.$^{-2}$		K'' for bal. of pressures
					Inward[a]	Outward[b]	
7	0.04	0.56	0.026	3.7	$2.66K''$	41.2	15.5
13,15	0.0605	0.56	0.18	3.3	$3.54K''$	54.3	15.4

[a] From eq. (7) with $n = 3$.
[b] From eq. (4).

Assuming that in tests Nos. 7, 13, and 15 a very slight inward resultant pressure was, in fact, present K'' can be taken as approximately 16. A weakness of the derivation is that the volume concen-

trations are much lower than those used by Bagnold in obtaining the constant in eq. (4), but unfortunately no better data are available.

So eq. (7) becomes

$$\text{Inward pressure} = 16\left[\frac{\text{Re}\cdot\eta_s(a/R)}{R}\right]^2 \frac{1-(a/R)}{\rho} \tag{8}$$

In some cases it is convenient to consider the relative magnitudes of the inward and outward pressures, rather than their absolute values.

$$\frac{\text{Inward pressure}}{\text{Outward pressure}} = \frac{6.2\text{Re}\cdot\eta_r(a/R)^2}{(1+\lambda)(1+{}^1/_2\lambda)-1} \tag{9}$$

where η_r is the viscosity of the suspension relative to that of the suspending fluid.

It is evident from eqs. (4), (8), and (9) that the direction of the resultant pressure is dependent upon the Reynolds number, the concentration of particles, and the ratio of their radius to the radius of the tube. That is, for a given suspension flowing in a given tube, the resultant radial pressure at the tube wall may be outwardly directed at low rates of flow but inwardly directed at high flow rates. In the former case the formation of a core of particles cannot be expected. In the latter, a movement of particles from the wall of the tube might reasonably be anticipated.

SUSPENSIONS OF SPHERES

Direct visual evidence of radial movements in a suspension of neutral-density spheres when being carried down a tube by the suspended fluid is remarkably scarce. Other than the work of Segré and Silberberg[2] mentioned above, the only quantitative data which the author has been able to trace are those of Schultz-Grunow.[9] He used a tube of rectangular cross section, 1 by 0.5 cm., in order to reduce distortion when observing the particles. He photographed sphere-free zones at the tube walls under conditions summarized in Table II. It is not immediately obvious what alterations to the theory given above are required in order to deal with the geometry of Schultz-Grunow's system but if the distance between the closest spaced pair of walls is taken as the tube diameter, the pressures experienced by his spheres of average size in the tube are as given in

TABLE II

Pressures on Spheres at a Tube Wall from Visual Observations

Investigator	Sphere radius, cm.	Tube radius, cm.	Feed vol. concn.	Reynolds No	Pressure, dynes cm.$^{-2}$			Inward pressure/ outward pressure
					Inward	Outward	Resultant[a]	
Schultz-Grunow[9]	0.0085	0.5	0.006	1250[b]	6.1	1.1	+5	5.5
	0.0085	0.5	0.10	1250[b]	10.7	7.5	+3.2	1.4
Segré and Silberberg[2] (test 41)	0.0805	0.56	0.0025	3.95	164	82	+82	2.0

[a] Positive pressure is directed radially inward.

[b] Method of calculating Reynolds number for a rectangular cross section not stated in paper.

TABLE III

Pressures on Spheres at a Tube Wall from Concentration and Viscosity Data

Investigator	Sphere radius, cm.	Tube radius, cm.	Feed vol. concn.	Reynolds No.	Pressure, dynes cm.$^{-2}$			Inward pressure/ outward pressure	Tube length/ tube radius
					Inward	Out-ward	Resultant[a]		
Starkey et al.[8]	0.017	0.1	0.015	485	3100	20	+3080	155	1530
Maude and Whitmore[7]	0.0048	0.094	0.17	207	198	120	+78	1.6	635
Higginbotham et al.[5]	0.0165	0.15	0.03	533	4430	90	+4340	49	300

[a] Positive pressure is directed radially inward.

Table II. A resultant inward pressure is, in fact, obtained but it is rather small when compared, for example, with that obtained from Segré and Silberberg's experiments when some inward movement was clearly observable at the wall (Table II). If, however, the ratio of the inward to the outward pressures is considered [eq. (9)], the results become comparable.

Indirect evidence of the inward migration of spheres should be obtainable from changes in the mean concentration of particles in the tube. Moreover, as concentration is related to viscosity by eq. (5), the radial migration of particles should show up as a viscosity change in the suspension. When a suspension enters a tube a fall in concentration occurs automatically according to eq. (2), but in Table III the conditions under which Starkey et al.[8] were just able to detect a velocity-dependent change in mean concentration (a reduction of $1^1/_2\%$) is shown. Maude and Whitmore, by measuring concentration changes,[7] and Higginbotham et al.,[5] from viscosity measurements, were unable to find any velocity dependence in their results. In the former case this was probably because the forces involved were very small compared with those found by Starkey et al. (Table III). This explanation is not satisfactory, however, in the case of Higginbotham et al. and other reasons probably obtained. First, the highest pressures were developed at the lowest concentration of particles (3% by volume). The viscosities were, therefore, small and changes in them difficult to detect. Second, although the formation of a core of particles is probably progressive down a tube, concentration and viscosity changes give a mean value over the whole tube length. If the tube is short, the influence of core formation on mean concentration may be immeasurable, compared with the automatic concentration change at the inlet. In Table III, it will be seen that the length/radius ratio for the tube used by Starkey et al.[8] was appreciably greater than that used by Higginbotham et al.[5]

A comparison of Tables II and III indicates that if axial migration of spheres is to be detected from changes in concentration or viscosity, the resultant inward pressure and the ratio of the inward to outward pressures must be very high, compared with those necessary for detection by direct visual means.

So far the necessity for making an allowance for the length of tube required for entrance turbulence to die away and a stable velocity profile to develop has not been considered; Smith's criterion[27] can be

applied, if desired, but as it is uncertain to what extent it applies to suspensions, it will not be considered further in this paper.

APPLICATION OF THEORY TO BLOOD

A primary problem in extending the theory to the flow of blood is that blood does not behave as a Newtonian liquid and the suspended cells are not hard spheres. Fortunately the deviation of plasma and serum from Newtonian behavior is small and is insignificant at flow rates corresponding to shear rates at the tube wall greater than about 250 sec.$^{-1}$.[24] Whole blood, and red cells suspended in serum or other fluids, also become Newtonian if the rate of shear at the tube walls exceeds about 250 sec^{-1} [24] so that experimental results at low rates of flow may be inapplicable and are not analyzed in this paper.

The effect of red cell distortion and flexibility is difficult to resolve. If the erythrocytes distort under shear into soft spheres they might be treated as emulsion droplets but it is more likely that they flex rather than distort bodily. Rigid discs at low concentration, where interparticle collisions are rare, spend most of their time with their flat faces roughly parallel to the streamlines, flipping over periodically.[28] During this movement, the flexing of red cells would be most likely to occur. From the space required for a red cell to rotate, the equivalent of the diameter of a sphere should therefore be the diameter of the cell, reduced a little by flexing. At higher concentrations the interlocking of rigid discs during rotation would probably lead to greater interference than for spheres, but the flexing of erythrocytes might reduce this effect. Oliver has shown[4] that, for spheres, rotation reduces their rate of movement from a tube wall so that if in the theory we treat the cells as spheres of diameter equal to the cell diameter, rotating at the same rate as spheres, we should obtain a fair approximation to the inward force likely to be experienced by a red cell compared with a sphere. There is no evidence that the flexibility of a disclike element in itself assists transverse movement, experimental verification being available only for rods and liquid droplets[29] at present.

Before applying the theory to blood it can be tested against the experiments of Müller who studied the flow of suspensions of neutral-density, India-rubber discs, 3 mm. in diameter by 0.55 mm. in thick-

TABLE IV

Flow of Flexible Discs and Blood Cells

Investigator	Suspended phase	Tube radius, cm.	Haemat-ocrit[a]	Reynolds No.	Pressure, dyne cm.$^{-2}$ Inward	Outward	Resultant[b]	Inward pressure/ outward pressure	Measure-ment
Müller[31]	India-rubber discs	0.375	0.15	106	695	8.3	+687	83.7	Visual, viscosity
	Blood cells								
Haynes and Burton[14]	Human	0.01847	0.088	4.70	0.62	30.8	−30.2	0.020	Viscosity
Copley[19]	Human	0.05	0.30	23.1	0.39	92.7	−92.3	0.004	Viscosity
Taylor[11]	Human	0.0095	0.17	16	30	360	−330	0.083	Visual
Fahraeus and Lindqvist[18]	Human	0.002	0.40	0.18	6.4	422	−416	0.015	Viscosity
Kümin[13]	Bovine	0.00145	0.40	0.26	23	486	−463	0.047	Viscosity
Thomas[15]	Human	0.01	0.37	3.76	4.6	469	−464	0.010	Concentration
Bayliss[20]	Canine	0.048	0.25	379	30	668	−638	0.044	Viscosity
Müller[12]	Bovine	0.05	0.40	129	15	1310	−1295	0.011	Viscosity
Charm and Kurland[17]	Canine	0.0044	0.40	6.30	370	4490	−4120	0.082	Viscosity
Coulter and Pappenheimer[34]	Bovine	0.126	0.44	2000	120	4960	−4840	0.024	Electrical resistance
Cerny, Cook, and Walker[35]	Canine	0.01174[c]	0.015–0.44[d]	—	—	—	—	—	Viscosity

[a] Assuming hematocrit is equal to volume concentration of suspended phase.

[b] Positive pressure is directed radially inward.

[c] High shear-rate viscometer.

[d] Uncertain which suspensions were tested in viscometer specified. At lowest hematocrit, inward resultant pressure is developed but relative viscosity is so small that concentration changes would be immeasurable. At normal concentration no inward movement would be expected.

ness, in tubes.[30] From visual and viscometric evidence he concluded that the particles formed a core in the tube whose diameter was dependent upon the concentration of the particles, the velocity of flow, and the tube radius. This finding is in qualitative agreement with the theory developed in the present paper. Using a typical particle concentration and a minimum flow rate,[31] the inward and outward pressures at the tube wall can be calculated from eqs. (4), (8), and (9) and are shown in Table IV. An inward movement of the discs would be expected which, by comparison with Tables II and III, should certainly be visible and might just be detected by viscosity measurements. With increasing flow velocity the inward pressure rises faster than the outward pressure so that in Müller's experiments a clear indication of the presence of an axial core of particles should have been obtained from visual or viscosity data. This is in satisfactory agreement with his experimental findings.

In Table IV the published data of a variety of workers have been used to calculate the radial pressures present when blood flows down capillary tubes. The cell diameter has in all cases been taken as 8 μ, although this is rather large for some of the bloods used, and a value of C_0 of 0.74 assumed. The suspending fluid varied from worker to worker, but in each case the test has been chosen which gives the maximum inward and minimum outward pressure at flow rates sufficiently high for non-Newtonian behavior to be insignificant. This is the most likely hemodynamic condition for the formation of an axial stream of cells. In every case the resultant pressure is outwardly directed, and the inward pressure would need to be increased by a factor of at least 15 before visual movement of cells from the wall could be observed under ideal conditions. For detecting the movement of cells from the wall by viscometric measurements, the inward pressure would have to increase by a factor of at least 100 under the most favorable detecting conditions. Thus it appears either that in the blood flow experiments in capillary tubes which were examined the presence of a cell-free zone adjacent to the wall was unlikely, or that the above theory is seriously at fault by a large factor. A major problem in the theory is to assign a reliable value to K'' and the tentative nature of the value of 16 used in the paper must be stressed. The possibility that cell flexure also influences the radial force must not be overlooked, although it is not considered further in the present paper.

DISCUSSION

The problem of testing the theory against experimental demonstrations of the presence of a cell-free zone adjacent to the tube wall must now be considered. The detection methods which have been used depend upon the measurement of viscosity or concentration changes in the blood or on direct visual or photoelectric observation of the region near the walls. The first two methods are influenced by the purely mechanical change in distribution of peripheral cells which occurs as the blood enters the tube[7,16,23–25] giving rise to the Fåhraeus-Lindqvist[18] or Sigma effect[32] of a decreasing measured viscosity and concentration with decreasing tube diameter. The phenomenon is substantially independent of the velocity of flow in the tube but may be influenced to some extent by the concentration of erythrocytes.[16,21] In addition, deductions from viscosity data suffer from the difficulty that at low rates of flow blood is non-Newtonian and shows an inherent fall in viscosity with rate of shear.[24,33] Unless the shear rate at the wall exceeds about 250 sec.$^{-1}$ this behavior is likely to mask any velocity-dependent viscosity changes arising from a radial redistribution of cells. However, as the pressures in Table IV were all calculated for experiments made at wall shear rates exceeding 250 sec.$^{-1}$, and as the resultant pressures are all outwardly directed, it is unlikely that simple hydrodynamic forces of the type considered in this paper could lead to a cell-free zone in the non-Newtonian flow region. At shear rates at the wall exceeding 250 sec.$^{-1}$ and until turbulence develops, a radial redistribution of the cells in a given blood might be detectable as a systematic fall in viscosity with increasing velocity of flow in a given tube. Unfortunately this region has only been thoroughly explored at its lower end because of the high pressures required to drive the blood along narrow tubes. It is true that the average velocity of flow, the Reynolds number, and the shear rate at the wall can be increased by using a larger diameter tube and the same driving pressure, but the corresponding reduction in the ratio of cell to tube diameter offsets any velocity advantage gained. This is clearly shown by the results of Coulter and Pappenheimer[34] in Table IV. In the experiments of Cerny et al.[35] it is possible that if the highest shear rate had been employed with the lowest hematocrit an inwardly directed pressure could have developed, but unfortunately the published data are not sufficiently detailed to tell whether such conditions were tried (Table IV).

Direct evidence of a radial redistribution of cells (but not necessarily of a cell-free layer at the tube wall) can be gained from measurements of concentration changes. Experiments of this type have been made by Fåhraeus and Lindqvist[18] but their reliability is doubtful,[16] and the most precise technique so far described is probably that of Thomas.[15] It is significant that of the 8% change in red cell concentration which he detected with his equipment, 6% must be attributed to the automatic, mechanical redistribution of cells at the inlet, leaving only 2% as a possible result of radial redistribution.

The primary problem in making a direct, visual measurement of a cell-free zone is that of optical distortion adjacent to the curved inner wall of the tube. Bayliss[10] has concluded that if any discontinuity is present it must be less than 5 μ wide because this is the region which cannot be accurately observed. He was unable to confirm Taylor's optical measurements of a cell-free zone,[11] and it is significant that Taylor's results do not show a dependence of zone thickness on Reynolds number as would be anticipated. As expected, Table IV indicates that the resultant radial pressure should discourage the movement of cells from the tube wall. Charm and Kurland[17] recently claim to have detected a cell-free layer from 3 to 5 μ wide at the walls of a tube 0.0883 mm. in diameter, but the precautions used to overcome optical distortion are not described. They made their measurements at a low (but unspecified) velocity, and so the possibility should not be overlooked that the blood was behaving as a non-Newtonian fluid through cell aggregation,[23,24] and that intercell attraction caused the formation of a plasmatic layer at the wall. A similar effect has been observed in a rotating-cylinder viscometer but only when the rate of shear was less than 1 sec.$^{-1}$.[33]

It is of interest to consider very briefly the possible result of an outwardly directed pressure at the wall of a capillary on the radial movement of erythrocytes flowing down the tube. Along the tube axis there should be no pressure originating from the shear of the suspending fluid or from rotation of the cells so that a radial pressure gradient should develop in the tube. This might lead to some radial redistribution of the cells as the blood flowed along the tube in order to eliminate the gradient, and thus to changes in concentration and viscosity. However, the forces which the available pressure could exert would be extremely small and might be modified by the radial forces discovered by Segré and Silberberg.[2] An estimate of the mag-

nitude of these effects in the case of blood is beyond the scope of the present paper, but a qualitative prediction is that they could lead to a reduction in concentration at the walls but never to a cell-free layer.

CONCLUSIONS

From a consideration of the dynamics of a suspension flowing in a tube it appears unlikely that the red cells in full blood when passing down a capillary tube under pressures normally available in the laboratory form themselves into an axial core, leaving an annulus of plasma (or other suspending medium) at the walls. This is because the dispersion pressure which is developed by a sheared suspension exceeds the inwardly directed pressure which is caused by the presence of the walls and the rotation of the cells. The possibility of additional forces developing from red cell flexibility are neglected in this conclusion because of the absence of data, but further work in this field is vital. The reason for the presence of a plasmatic layer which can be seen at the walls of small blood vessels in living bodies is still a mystery but by analogy with flow in glass capillaries it is unlikely to be explicable in simple, hydrodynamic terms. A similar conclusion has been reached before but on different experimental evidence and for different reasons from these given in this paper.[36]

References

1. Segré, G., and A. Silberberg, *Nature*, **189**, 209 (1961).
2. Segré, G., and A. Silberberg, *J. Fluid Mech.*, **14**, 136 (1962).
3. Starkey, T. V., *Brit. J. Appl. Phys.*, **7**, 52 (1956).
4. Oliver, D. R., *Nature*, **194**, 1269 (1962).
5. Higginbotham, G. H., D. R. Oliver, and S. G. Ward, *Brit. J. Appl. Phys.*, **9**, 372 (1958).
6. Vand, V., *J. Phys. Colloid Chem.*, **52**, 300 (1948).
7. Maude, A. D., and R. L. Whitmore, *Brit. J. Appl. Phys.*, **7**, 98 (1956).
8. Starkey, T. V., V. A. Hewlett, J. H. A. Roberts, and R. E. James, *Brit. J. Appl. Phys.*, **12**, 545 (1961).
9. Schultz-Grunow, F., *Chem.-Ing.-Tech.*, **34**, 223 (1962).
10. Bayliss, L. E., *J. Physiol.*, **149**, 593 (1959).
11. Taylor, M., *Aust. J. Exptl. Biol.*, **33**, 1 (1955).
12. Müller, A., *Helv. Physiol. Pharmacol. Acta*, **6**, 181 (1948).
13. Kümin, K., Inaugural dissertation, Univ. of Bern, 1949; quoted by ref. 16.
14. Haynes, R. H., and A. C. Burton, *Am. J. Physiol.*, **197**, 943 (1959).
15. Thomas, H. W., *Lab. Pract.*, **10**, 771 (1961).
16. Thomas, H. W., *Biorheol.*, **1**, 41 (1962).
17. Charm, S., and G. S. Kurland, *Am. J. Physiol.*, **203**, 417 (1962).
18. Fåhraeus, R., and T. Lindqvist, *Am. J. Physiol.*, **96**, 562 (1931).

19. Copley, A. L., in *Flow Properties of Blood and other Biological Systems*, A. L. Copley and G. Stainsby, eds., Pergamon Press, New York–Oxford, 1960, p. 97.
20. Bayliss, L. E., in *Flow Properties of Blood and Other Biological Systems*, A. L. Copley and G. Stainsby, eds., Pergamon Press, New York–Oxford, 1960, p. 29.
21. Haynes, R. H., *Am. J. Physiol.*, **198,** 1193 (1960).
22. Bagnold, R. A., *Proc. Roy. Soc. (London)*, **A225,** 49 (1954).
23. Maude, A. D., and R. L. Whitmore, *Am. J. Appl. Physiol.*, **12,** 105 (1958).
24. Whitmore, R. L., *Biorheol.*, **1,** 201 (1963).
25. Whitmore, R. L., *Rheology of Disperse Systems*, C. C. Mill, ed., Pergamon Press, New York–London, 1959, p. 49.
26. Oliver, D. R., and S. G. Ward, *Nature*, **171,** 397 (1953).
27. Smith, A. M. O., *J. Fluid Mech.*, **7,** 565 (1960).
28. Goldsmith, H. L., and S. G. Mason, *J. Fluid Mech.*, **12,** 88 (1962).
29. Goldsmith, H. L., and S. G. Mason, *Nature*, **190,** 1095 (1961).
30. Müller, A., *Arch. Kreisl.*, **8,** 245 (1941).
31. Müller, A., *Arch. Kreisl.*, **8,** 269 (1941), Table 7.
32. Dix, F. J., and G. W. Scott Blair, *J. Appl. Phys.*, **11,** 574 (1940).
33. Cokelet, G. R., E. W. Merrill, E. R. Gilliland, H. Shin, A. Britten and R. E. Wells, Jr., *Trans. Soc. Rheology*, **7,** 303 (1963).
34. Coulter, N. A., Jr., and J. R. Pappenheimer, *Am. J. Physiol.*, **159,** 401 (1949).
35. Cerny, L. C., F. B. Cook, and C. C. Walker, *Am. J. Physiol.*, **202,** 1188 (1962).
36. Whitmore, R. L., in *Flow Properties of Blood and other Biological Systems*, A. L. Copley and G. Stainsby, eds., Pergamon Press, New York–Oxford, 1960, p. 63.

Synopsis

14567

The observed fall in blood viscosity and erythrocyte concentration, when the diameter of a glass capillary down which the blood is flowing is decreased, is frequently attributed to the presence of a cell-free layer at the tube wall. Experiments show that under suitable conditions individual particles, flowing near a wall, may move away from it but when a mass of particles is present an opposing dispersive pressure is also developed. From published results on the flow of suspensions of spheres in tubes the parameters indicating the conditions for spheres to leave the wall are derived. On applying them to data on the flow of blood in glass capillaries it is shown that normally the outwardly directed dispersive pressure is many times greater than the inward pressure developed by the erythrocytes. Thus the existence of a "plasmatic layer" at the wall of a capillary tube down which blood is flowing is unlikely, and the layer which is observed *in vivo* must be the product of some other interaction or force.

Author

LAMINAR FLOW OF BIOLOGICAL FLUIDS

N67 14568

Physical Aspects of the Flow of Biological Suspensions through Tubes

H. L. GOLDSMITH* and S. G. MASON,* *Chemistry Department, McGill University, Montreal, Canada*

This paper summarizes the results of a series of recent investigations[1–6] on the flow behavior of liquid suspensions of various rigid and deformable particles such as spheres, discs, and rods. The purpose in undertaking the work was to try to establish the basic physical phenomena involved and to relate the results, where possible, to the flow of blood and other biological suspensions through small and large vessels. The experiments refer to steady laminar flow in straight rigid tubes at low Reynolds numbers for particles which are (*1*) small, and (*2*) large compared to the tube width. In each case the behavior of single particles was studied first, followed by particle interactions in dilute suspensions and finally by studies on the flow of concentrated suspensions.

The particle motions in the tube were observed directly by means of a traveling microscope[1] and recorded where necessary by the use of still- and cine-photomicrography.

PARTICLE SIZE SMALL COMPARED TO TUBE WIDTH

Single Particles[1,4,5]

At particle Reynolds numbers[7] below 10^{-6} single rigid spheres rotated with steady angular velocity, rigid discs, and rods with variable angular velocity in spherical elliptical orbits as predicted by the theory of Jeffery,[8] *without the particles migrating radially.* However, single liquid drops which were deformed into prolate spheroids[9,10] *migrated toward the tube axis during flow,* the rate of migration increasing with increasing drop radius, flow rate, and radial distance from the tube axis. The observed difference between rigid and deformable

PRECEDING PAGE BLANK NOT FILMED.

particles could be accounted for by a theory of radial migration based on the variation of the velocity gradient across the ends of the particles and their deformation.

The existence of the "tubular pinch effect"[11,12] at particle Reynolds numbers $> 10^{-3}$, whereby particles initially situated close to the tube axis migrate toward the tube wall while those initially close to the tube wall migrate toward the tube axis, was confirmed with single rigid spheres, discs, and rods.[4,5] The rate of migration was found to increase with increasing flow rate and radial distance from the equilibrium position approximately halfway between the axis and the wall of the tube. However, deformable drops in systems of viscosity ratio suspended phase/suspending phase less than 10 always migrated to the tube axis.

Dilute Suspensions[4,6]

Two-body collisions between rigid spheres were found to be symmetrical, as previously described for Couette flow,[13] the particles regaining their radial positions and translational velocities before collision. With fluid spheres, however, the collisions were unsymmetrical resulting in an appreciable radial migration toward the axis of the particle moving with the greater velocity, and in a smaller migration toward the wall of the particle moving with the lower velocity.

Concentrated Suspensions[4,6]

Experiments conducted with flowing transparent suspensions of rigid spheres containing visible tracer spheres showed that at volume concentrations below 15% the velocity profiles approximated those of Poiseuille flow. At higher concentrations the profiles became blunted, the velocity gradients near the wall being greater, and those in the central portion of the tube smaller than those in Poiseuille flow, decreasing to zero at a concentration of 40%.

PARTICLE SIZE LARGE COMPARED TO TUBE WIDTH

Single Flowing Bubbles[3]

The flow and deformation of large liquid bubbles suspended in wetting liquids undergoing Poiseuille flow was studied. It was

shown that the bubbles traveled axisymmetrically through the tube surrounded by a film of liquid of constant thickness between the spheroidal bubble ends. The thickness of the film and the velocity profiles in bubble and film were measured as a function of the tube radius, bubble velocity, and the ratio of bubble to suspending liquid viscosity. The results were in good agreement with a theory based on parallel creeping motion in the film between the bubble ends.

At negligibly small values of the viscosity ratio there was no flow in the film of constant thickness surrounding the bubble. With increasing viscosity ratio velocity gradients developed in the film and within the bubble. At high viscosity ratios the system approximated plug flow with all parts of the bubble moving with the bubble velocity.

At high bubble speeds the rear ends developed re-entrant cavities of suspending liquid, and in systems of high viscosity ratio these penetrated far into the body of the bubble.

Train of Flowing Bubbles: "Bolus Flow"[4]

When several bubbles followed each other down the tube, it was observed that within an axial core of the liquid between the rear end of one bubble and the leading end of the following bubble, circulation patterns were set up similar to those previously described.[14] The effect of such flow is that a bolus of suspending liquid between the bubbles is carried down the tube with the bubble velocity.

This work was supported by Research Grant H-5911 from the National Heart Institute of the U. S. Public Health Service.

References

1. Goldsmith, H. L., and S. G. Mason, *J. Colloid Sci.*, **17**, 447 (1962).
2. Goldsmith, H. L., and S. G. Mason, *J. Fluid Mech.*, **14**, 42 (1962).
3. Goldsmith, H. L., and S. G. Mason, *J. Colloid Sci.*, **18**, 237 (1963).
4. Goldsmith, H. L., and S. G. Mason, Second European Conference on Microcirculation, Pavia, 1962, *Bibliotheca Anatomica*, Vol. 4, S. Karger, Basel-New York, 1964, p. 462.
5. Karnis, A., H. L. Goldsmith, and S. G. Mason, to be published.
6. Goldsmith, H. L., and S. G. Mason, *Nature*, **200**, 159 (1963).
7. Segré, G., and A. Silberberg, *Nature*, **189**, 209 (1961).
8. Jeffery, G. B., *Proc. Roy. Soc. (London)*, **A102**, 161 (1922).
9. Taylor, G. I., *Proc. Roy. Soc. (London)*, **A146**, 501 (1934).
10. Cerf, R., *J. Chim. Phys.*, **48**, 59 (1951).
11. Segré, G., and A. Silberberg, *J. Fluid Mech.*, **14**, 115 (1962).

12. Oliver, D. R., *Nature*, **194**, 1269 (1962).
13. Manley, R. St. J., and S. G. Mason, *J. Colloid Sci.*, **7**, 354 (1952).
14. Prothero, J., and A. C. Burton, *Biophys. J.*, **1**, 565 (1961).

Synopsis

14568

The steady laminar flow of liquid suspensions of rigid and deformable particles through rigid tubes has been investigated by direct observations of the particle motions through a travelling microscope. The phenomena studied in the first part of the work included the rotation of single small rigid spheres, rods, and discs; the radial migration of rigid and deformable spheres; and particle interactions in dilute and concentrated suspensions. The second part describes the flow and deformation of large liquid bubbles suspended in wetting liquids undergoing Poiseuille flow.

Author

N67 14569

Theoretical Considerations on the Flow of Blood through a Capillary

SYOTEN OKA,* *Tokyo Metropolitan University, Setagaya-ku, Tokyo, Japan*

FLOW OF A LIQUID OBEYING CASSON'S EQUATION THROUGH A CAPILLARY

Casson[1] has proposed an equation for the flow of varnishes relating the shear stress F to the rate of shear D. This relation has the form

$$F^{1/2} = k_0 + k_1 D^{1/2} \tag{1}$$

k_0 and k_1 being constants whose values depend on the properties of the suspension. Equation (1) is called Casson's equation, and has been applied by Steiner to molten chocolate. Scott Blair[2] has shown that Casson's equation applies to blood on both glass and fibrin surfaces.

In the following, the shear stress and the rate of shear are denoted by τ and $\dot{\gamma}$, respectively. Casson's eq. (1) may then be written in the form

$$\begin{aligned} \dot{\gamma} &= 1/(\eta^{1/2})\ (\tau^{1/2} - f^{1/2}), && \tau > f \\ &= 0, && \tau < f \end{aligned} \tag{2}$$

η and f being material constants. Here f has the dimensions of a stress, corresponding to the yield value of Bingham solids, and η has the dimensions of a coefficient of viscosity, corresponding to the plastic viscosity of Bingham solids. The relation between $\dot{\gamma}^{1/2}$ and $\tau^{1/2}$ is as in Figure 1.

Consider the flow of a liquid obeying Casson's equation through a straight circular tube of uniform radius R and length L under pressure difference P. The following assumptions are made regarding the motion of the liquid: (*1*) the liquid is incompressible; (*2*) the motion of the liquid is laminar; (*3*) the streamlines are parallel to the axis of

the tube, that is, the liquid is "telescoping" through the tube; (*4*) the motion is steady; and (*5*) there is no relative motion at liquid-wall interfaces.

As is well known, Stokes' relation

$$\tau = Pr/2L \tag{3}$$

can be obtained by using the above assumptions.

The rheological behavior of liquids is specified generally by the flow equation

$$\dot{\gamma} = \varphi(\tau) \tag{4}$$

We denote the velocity of the liquid at a distance r from the axis of the tube by $v(r)$. Integration of the equation $-dv/dr = \varphi(\tau)$ leads to the distribution of the velocity

$$v = R/\tau_R \int_{\tau}^{\tau_R} \varphi(\tau) d\tau \tag{5}$$

where

$$\tau_R = PR/2L \tag{6}$$

denotes the shear stress at the wall.

Two cases may be distinguished: (*1*) $\tau_R < f$. In this case $\tau < f$ and there is no flow. (*2*) $\tau_R > f$.

When $\tau < f$. In this case $v(r)$ is given by

$$v = R/\tau_R \int_{f}^{\tau_R} \varphi(\tau) d\tau \tag{7}$$

Substitution of the functional form of φ defined by eq. (2) leads to the result

$$\begin{aligned} v &= \frac{P}{4\eta L} \left(R^2 - \frac{8}{3} r_c^{1/2} R^{3/2} + 2r_c R - \frac{1}{3} r_c^2\right) \\ &= \frac{P}{4\eta L} (R^{1/2} - r_c^{1/2})^3 (3R^{1/2} + r_c)^{1/2} \end{aligned} \tag{8}$$

where r_c is given by

$$r_c = 2fL/P \tag{9}$$

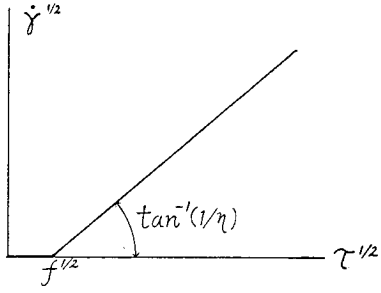

Fig. 1. $\dot{\gamma}^{1/2}$ versus $\tau^{1/2}$.

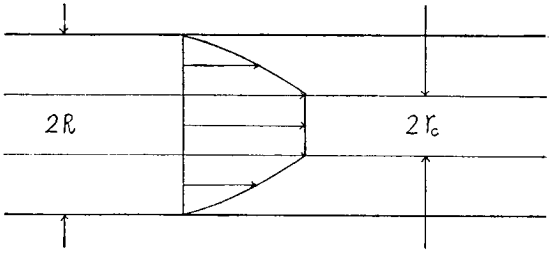

Fig. 2. Plug flow in a circular tube.

When $\tau < f$ we have $r < r_c$. Thus the velocity is constant and independent of r for values of r not exceeding the critical radius r_c.

When $\tau > f$, that is, $r > r_c$, we obtain from eq. (5) and eq. (2)

$$v = \frac{P}{4\eta L}\left[(R^2 - r^2) - \frac{8}{3} r_c^{1/2}(R^{3/2} - r^{3/2}) + 2r_c(R - r)\right] \quad (10)$$

From the above calculations, it can be seen that the type of flow is plug flow. The cylindrical portion of radius r_c moves as if it were rigid. The distribution of velocity is as in Figure 2.

We now consider the volume of flow per unit time

$$Q = \int_0^R 2\pi r v(r) dr = \frac{R^3}{\tau_R{}^3} \int_0^{\tau_R} \varphi(\tau)\tau^2 d\tau \quad (11)$$

Substitution of the functional form φ into eq. (11) leads to the result

$$Q = \frac{\pi R^4}{8\eta L}\left(P - \frac{16}{7} p^{1/2} P^{1/2} + \frac{4}{3} p - \frac{1}{21}\frac{p^4}{p^3}\right) \quad (12)$$

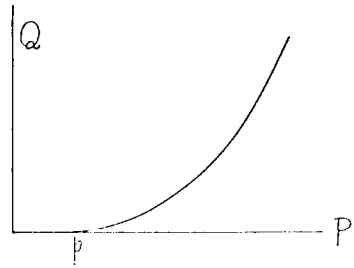

Fig. 3. Volume of flow Q per unit time versus the pressure difference P.

This equation corresponds to the Buckingham-Reiner equation for Bingham solids. Here p is defined by

$$p = 2Lf/R \tag{13}$$

When $\tau_R < f$, $P < p$ and Q vanishes. Equation (12) holds for $P > p$. The relation between Q and P is as in Figure 3.

Equation (12) shows the deviation from the Poiseuille equation. In order to discuss the non-Newtonian behavior of a liquid obeying Casson's equation we introduce the apparent viscosity η_a by means of the relation

$$Q = \frac{\pi R^4 P}{8\eta_a L} \tag{14}$$

Then we have from eqs. (12) and (14)

$$\eta_a = \eta/F(\xi) \tag{15}$$

where

$$F(\xi) = 1 - \frac{16}{7}\xi^{1/2} + \frac{4}{3}\xi - \frac{1}{21}\xi^4$$

$$= (1 - \xi^{1/2})^3\left(1 + \frac{5}{7}\xi^{1/2} + \frac{10}{21}\xi + \frac{2}{7}\xi^{3/2} + \frac{1}{7}\xi^2 + \frac{1}{21}\xi^{5/2}\right) \tag{16}$$

and

$$\xi = \frac{p}{P} = 2\frac{L}{P}\frac{f}{R} \tag{17}$$

Thus, we can see that the apparent viscosity η_a is a function of the pressure gradient P/L and f/R. For a particular value of R, eq. (15) exhibits a non-Newtonian behavior. It has been shown experimentally for blood that the yield value f varies with the radius R of the capillaries.[3] Thus, for a given pressure gradient, eq. (15) exhibits the sigma effect, i.e., a decrease of the apparent viscosity with a decrease of the tube diameter.

Equation (12) may be written in the form

$$Q = \frac{\pi R^4}{8\eta L}\left(1 - \frac{16}{7}\xi^{1/2} + \frac{4}{3}\xi - \frac{1}{21}\xi^4\right) \tag{18}$$

When P is close to p, we put

$$\xi = 1 - \delta \tag{19}$$

δ being a small quantity. Thus, we have

$$Q = \frac{\pi R^4 P}{8\eta L} \cdot \frac{2}{35}\delta^3 \tag{20}$$

This shows that the deviation from Poiseuille's law is very remarkable in this case.

NORMAL FORCE AS A CAUSE OF THE AXIAL ACCUMULATION OF SUSPENDED PARTICLES

When blood and certain other suspensions of particles in Newtonian fluids flow through small tubes, the suspended particles tend to become concentrated in the axial portion of the stream being surrounded by a narrow annulus of fluid containing few, if any, particles. This phenomenon of axial accumulation shows that a suspended particle must experience a force normal to the direction of flow.

From observations of injected graphite particles and blood platelets in plasma-skimmed vessels, Copley and Staple[4] have demonstrated experimentally that a plasmatic zone results from the action of axially directed forces on suspended particles. From a theoretical point of view, it should be mentioned specially that a rigid spherical particle is acted upon by a component of force normal to the direction of flow.

The red blood cells are often thought to be biconcave discs which have a fairly constant diameter and thickness in a given species.

However, Brånemark and Lindström[5] have shown by close examination that the individual red blood cells assume a wide variety of shapes as they pass through the capillaries. The red cell is the most deformable type among the three main types of corpuscular elements in the blood, erythrocytes, leucocytes, and platelets. Strictly speaking, the dispersion medium of blood should be regarded as a non-Newtonian fluid because it is a concentrated protein solution.

Although it is desirable that all these factors—shape, deformability, and non-Newtonian viscosity—be taken into consideration in the explanation of the normal force causing the axial accumulation, it is a very difficult problem, and no satisfactory theory has yet been proposed. Thus, an important theoretical problem at the present state of understanding is to show that a free rigid spherical particle in a Poiseuille flow experiences a force normal to the direction of flow.

Insofar as the author is aware, such a calculation has not yet been carried out. Brenner and Happel[6] presented a theoretical treatment for the slow flow of a viscous fluid through a cylindrical container within which a small spherical particle is confined. The sphere is situated in an arbitrary position within the cylinder and moves at a given constant velocity parallel to the wall. Their treatment is based on the Stokes equations of motion and fails to reveal the presence of a normal force tending to move the sphere toward the tube center. This lack of a normal force is a characteristic failing of the Stokes equations of motion and stems from a neglect of fluid inertia in the original Navier-Stokes equations of motion. Brenner[7] has also discussed the effect of finite boundaries on the Stokes resistance of an arbitrary particle. It was shown by Lorentz[8] that no lift is predicted for the case of a sphere moving with low speed parallel to the wall in a semi-infinite viscous quiescent fluid bounded by a plane wall.

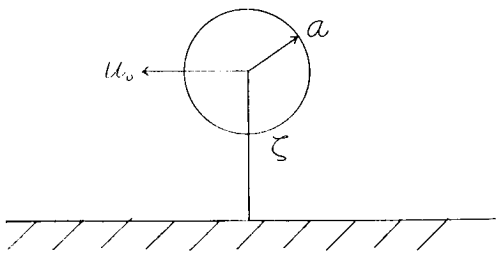

Fig. 4. A sphere moving parallel to a plane wall in a semi-infinite viscous fluid.

The failure to predict a normal force on the basis of Stokes' equations of motion has also been shown for two-dimensional cases by Takaisi and Wakiya. Takaisi[9] has treated the steady slow motion of a circular cylinder in a semi-infinite viscous fluid bounded by a plane wall on the basis of Stokes' equations of motion and has shown that no lift is predicted in this case. Wakiya[10] has discussed the effect of an elliptic cylinder in a slow viscous flow in a similar way.

However, the author is of the opinion that a normal force might be explained from the standpoint of classical fluid mechanics if the calculations were based on the Navier-Stokes equations of motion without neglecting the inertia terms.

In this connection Faxén's work[11] should be considered. By means of Oseen's equations, he has calculated the lift L on a sphere moving with low speed parallel to the wall in a semi-infinite viscous fluid bounded by a plane wall (see Fig. 4). The result is

$$L = \frac{9}{8}\pi\eta a u_0 \cdot \sigma a \frac{\psi(\sigma\zeta)}{1 - \frac{27}{16}\frac{a}{\zeta} + \frac{1459}{384}\frac{a^2}{\zeta^2} + \cdots} \tag{21}$$

$$\psi(x) = 1 - \frac{11}{8}x^2 + \frac{8}{3}x^3 - \frac{137}{288}x^4 - \frac{8}{5}x^5 + \cdots + \left(\frac{175}{96}x^4 + \cdots\right)\log\frac{\gamma q}{2} \tag{22}$$

where a is the radius of the sphere, ζ is the distance of the center of the sphere from the wall, u_0 is the translational velocity of the sphere, η is the coefficient of viscosity of the fluid, $\sigma = \rho u/2\eta$, ρ is the density of the fluid and γ is Euler's constant. The ratio a/ζ is assumed to be very small and its higher order terms are neglected. It can be seen from eq. (21) that the lift vanishes when the conditions of the Stokes approximation are imposed, i.e., terms of order u_0^2 are negligible. If the sphere can move freely about its center, it rotates with an angular velocity

$$\omega = \frac{3u_0}{32a}\cdot\frac{a^4}{\zeta^4}\left(1 - \frac{3}{8}\frac{a}{\zeta}\right) \tag{23}$$

The direction of rotation of the sphere is the same as when it is in contact with the wall.

Similar calculations have been carried out by Takaisi[12] for a two-dimensional case. He treated the steady slow motion of a circular cylinder in a semi-infinite viscous fluid bounded by a plane wall by the use of Oseen's equations of motion, assuming that the cylinder is moving parallel to the bounding wall. He obtained for a special case an approximate formula for the lift

$$L = 2\pi\eta u_0 \cdot \sigma a \frac{\zeta/a}{(1/2 - \log 2\zeta/a)^2 - 1/4} \tag{24}$$

which is valid for sufficiently small values of σa and $\sigma\zeta$. The notation is the same as in eq. (21). He plotted the lift coefficient $L/\eta u_0$ for three values of the Reynolds number $R = 4\sigma a$ against the ratio ζ/a for the range 2 to 50. According to his results, the cylinder experiences a repulsive force from the bounding plane wall, just as in the case of a sphere in a semi-infinite viscous fluid along its bounding plane wall. In a separate paper, Takaisi[13] also discussed the effect of the wall upon the forces experienced by an inclined elliptic cylinder in a viscous fluid, and obtained a formula for the lift.

In the above we have referred only to the lift on a sphere or cylinder moving with low speed in a quiescent fluid and did not consider the lift on a sphere moving freely in a Poiseuille flow. Happel and Byrne[14] have discussed the motion of a sphere and fluid in a cylindrical tube by the use of the Stokes equations of motion, and have given a relation for the "slip" at the axis of the tube

$$[(u - u_0)/u]_{r=0} = \frac{2}{3}(a/R)^2 \tag{25}$$

where u_0 is the translational velocity of the sphere, u is the streamline velocity at the center of the tube given by Poiseuille's equation, a and R are the radius of the sphere and the tube, respectively. Goldsmith and Mason[15] plotted $[(u - u_0)/u][^2/_3(a/R)^2]$ against r/R and obtained a monotonically increasing curve (see Fig. 5).

Brenner and Happel[6] discussed the slow viscous flow past a sphere in a cylindrical tube on the basis of the Stokes equations of motion and showed that the translational velocity u_0 of the sphere is always less than the local fluid velocity u at the center of the sphere when no external force acts on the sphere.

If we take into consideration the fact that there is a difference between the translational velocity and the local fluid velocity, and

that a finite lift is experienced by a sphere or a cylinder, as has been shown by Faxén and Takaisi, it seems very probable that a normal force can be adequately explained from the standpoint of classical fluid mechanics. In this connection it should be mentioned that Oseen's equations of motion are not suitable for the treatment of the normal force, because the undisturbed velocity of the fluid varies with the distance from the wall. It should also be mentioned that the Brownian motion of the particles must be taken into consideration in the explanation of the mechanism of axial accumulation in suspensions.

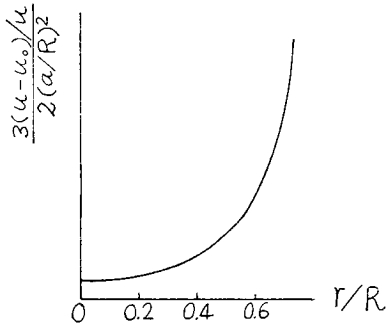

Fig. 5. A plot of $[(u - u_0)/u][^2/_3(a/R)^2]$ against r/R.

The theoretical studies of the mechanism of axial accumulation which have been reported in the literature may be roughly classified into two categories: one is hydrodynamical, the other thermodynamical. The latter is based on the principle of minimum dissipation of energy in an irreversible process.[16-18] According to his principle a particle initially situated at a point in a velocity field at which the gradient is not zero is expected to move with a velocity component normal to the direction of flow toward the region of lower velocity gradient.

Fundamentally speaking, the principle of minimum dissipation of energy will hold only for the flow of a viscous fluid with fixed boundaries. It is not clear whether the principle will hold or not when the boundaries are free to move through the fluid. Hence, the author is of the opinion that the mechanism of axial accumulation should be sought from the standpoint of fluid mechanics.

INTERACTION OF SUSPENDED PARTICLES

It is very important to consider the interaction of particles in the flow of blood and other suspensions. From a theoretical point of view the problem of the interaction of two spheres is a most fundamental one. When two spheres move through a viscous fluid, the flow of fluid in the neighborhood of one sphere depends not only on the motion of that sphere but also on the motion of the other sphere. Consequently, the force experienced by one sphere is influenced by the motion of the other sphere through the medium of the fluid. Such forces are important in the study of colloids.

The interaction of two spheres in a uniform flow has been discussed on the basis of Stokes' equations of motion by Smoluchowski[19] and Faxén.[20] Faxén[21] and Stimson and Jeffery[22] have discussed the drag on the spheres for the special case when they move in the direction of the central line. Wakiya[23] has investigated the forces on the spheres placed in general configuration in a uniform flow on the basis of Stokes' equations of motion.

Insofar as the author is aware, the interaction of two spheres has not been discussed on the basis of Oseen's equations of motion. How-

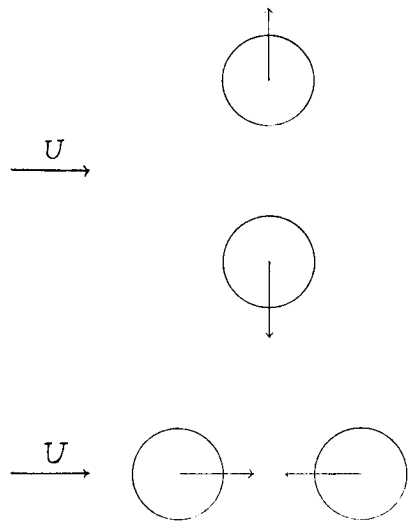

Fig. 6. The mutual interaction of the two circular cylinders in a uniform viscous flow U.

ever, Kuwabara[24] has investigated the forces experienced by two parallel circular cylinders placed in general configuration in a uniform flow at small Reynolds numbers on the basis of Oseen's equations of motion. He calculated the drag and lift coefficients of one of the two circular cylinders. The qualitative results obtained from the calculations are as follows: (*1*) the drag coefficients for one of the two cylinders is smaller than that for a single cylinder at the same Reynolds numbers; and (*2*) the mutual interaction is attractive when the central line is parallel to the uniform flow and is repulsive when it is perpendicular.

These tendencies are opposite to those occurring in an ideal fluid. It should be mentioned that no attractive force between two spheres is predicted when the calculations are based on Stokes' equations of motion, as is seen from Wakiya's paper. In a separate paper, Kuwabara[25] also discussed the forces experienced by two parallel elliptic cylinders in a uniform flow at small Reynolds numbers using the same method and obtained the drag and lift coefficients for one of the two cylinders (see Fig. 6).

The above-mentioned qualitative results obtained by Kuwabara will be valid for the case of two spheres. If the results are applied to the sedimentation of a suspension, vertical aggregates of suspended particles may be expected. Thus the mechanism of sedimentation will differ throughout the course of the process.

The behavior of suspended particles in the flow of suspensions through a tube is also interesting. If we consider collectively the works of Happel and Byrne, Brenner and Happel, and Kuwabara, it may be expected that the distribution of the particles will not be random, but rather that there will be a tendency to form aggregates of particles in the direction of flow. Of course, this tendency is hindered by the Brownian motion of the particles and therefore this effect should be also taken into consideration.

SUMMARY

(*1*) The flow of a liquid obeying Casson's equation through a straight circular tube of uniform radius R under a given pressure gradient has been treated theoretically. The distribution of velocity is calculated and it is shown that the type of flow is plug flow. The volume of flow per unit time is also calculated, and an equation corresponding to the Buckingham-Reiner equation for Bingham solids

has been obtained. A formula for the apparent viscosity is obtained as a function of the pressure gradient and f/R, where f is a material constant of the liquid corresponding to the yield value of Bingham solids. For a particular value of R, the formula exhibits a non-Newtonian behavior, while for a given pressure gradient it exhibits the sigma effect. When the pressure is close to a critical value, the deviation from Poiseuille's law is very remarkable.

(*2*) When blood and certain other suspensions of particles flow through small tubes, axial accumulation occurs, showing that a suspended particle must experience a force normal to the direction of flow. Theoretical considerations have been given concerning the normal force from the standpoint of fluid mechanics. The failure to predict the normal force stems from a neglect of fluid inertia in the original Navier-Stokes equations of motion. It is pointed out that no theory has yet been proposed which reveals the presence of a normal force. However, if we take into consideration the fact that there is a difference between the translational velocity and the local fluid velocity, and that a finite lift is experienced by a sphere or a cyclinder, as has been shown by Faxén and Takaisi, it seems very probable that a normal force can be adequately explained from the standpoint of fluid mechanics.

Since it is not clear whether the principle of minimum dissipation of energy holds or not when the boundaries are free to move, the mechanism of axial accumulation should be sought from the standpoint of fluid mechanics.

(*3*) It is important to consider the interaction of particles in the flow and sedimentation of blood and other suspensions. From a theoretical point of view the problem of the interaction of two spheres in a uniform flow is a most fundamental one. It is pointed out that all the theories hitherto appearing in the literature are based on the Stokes equations of motion. However, Kuwabara has investigated the forces experienced by two parallel circular cylinders placed in general configuration in a uniform flow at small Reynolds numbers on the basis of Oseen's equations of motion and has shown that the mutual interaction is attractive when the central line is parallel to the uniform flow and is repulsive when it is perpendicular. The qualitative results obtained by Kuwabara will be valid for the case of two spheres. If the results are applied to the sedimentation of a suspension, vertical aggregates of suspended particles may be ex-

pected. Thus the mechanism of sedimentation will differ throughout the course of the process. The behavior of suspended particles in the flow of suspensions through a tube is also considered. It may be expected that the distribution of the particles will not be random, but rather that there will be a tendency to form aggregates of particles in the direction of flow. The effect of the Brownian motion of the particles should also be taken into consideration.

The author wishes to express his sincere thanks to Professor S. Wakiya, Professor Y. Takaisi, Dr. S. Kuwabara, and Dr. James M. Kendall for their invaluable advice and discussions. The present investigation has partly been supported by the Medical Affairs Bureau of the Ministry of Health and Welfare and by the fund of the Ministry of Education in Aid of Scientific Researches.

References

1. Casson, N., in *Rheology of Disperse Systems*, C. C. Mill, ed., Pergamon Press, New York, 1959, p. 84.
2. Scott Blair, G. W., *Nature*, **183**, 613 (1959).
3. Copley, A. L., and G. Stainsby, eds., *Flow Properties of Blood and Other Biological Systems*, Pergamon Press, New York–Oxford, 1960, p. 106.
4. Copley, A. L., and P. H. Staple, *Biorheol.*, **1**, 3 (1962).
5. Brânemark, P.-I., and J. Lindström, *Biorheol.*, **1**, 139 (1963).
6. Brenner, H., J. Happel, *J. Fluid Mech.*, **4**, 195 (1958).
7. Brenner, H., *J. Fluid Mech.*, **12**, 35 (1962).
8. Lorentz, H. A., *Abhandl. theoret. Phys., Leipzig*, **1**, 23 (1907).
9. Takaisi, Y., *J. Phys. Soc. Japan*, **11**, 1004 (1956).
10. Wakiya, S., *Res. Repts. Fac. Eng. Niigata Univ., Japan*, **6**, 31 (1959) (in Japanese).
11. Faxén, H., dissertation Uppsala, 1921.
12. Takaisi, Y., *J. Phys. Soc. Japan*, **10**, 407 (1955).
13. Takaisi, Y., *J. Phys. Soc. Japan*, **13**, 496 (1958).
14. Happel, J., and B. J. Byrne, *Ind. Eng. Chem.*, **46**, 1181 (1954).
15. Goldsmith, H. L., and S. G. Mason, *J. Colloid Sci.*, **17**, 448 (1962).
16. Jeffery, G. B., *Proc. Roy. Soc. (London)*, **A102**, 161 (1922).
17. Starkey, T. V., and R. E. James, *Nature*, **178**, 207 (1956).
18. Yamamoto, M., and S. Ohki, *Busseiron Kenkyu*, **2**, 641 (1959) (in Japanese).
19. Smoluchowski, M., *Bull. intern. Acad. Sci. Cracovie*, **1A** (1911).
20. Faxén, H., *Z. Angew. Math. Mech.*, **7** (1927).
21. Faxén, H., *Arkiv. Mat. Astr. Fys.*, **19A** (1925).
22. Stimson, M., and G. M. Jeffery, *Proc. Roy. Soc. (London)*, **A111** (1926).
23. Wakiya, S., *Res. Rept. Fac. Eng. Niigata Univ., Japan*, **6**, 155 (1957).
24. Kuwabara, S., *J. Phys. Soc. Japan*, **12**, 291 (1957).
25. Kuwabara, S., *J. Phys. Soc. Japan*, **13**, 506 (1958).

Synopsis

14569

Scott Blair has shown that an equation proposed by Casson for varnishes and which was later applied by Steiner to molten chocolate, gives excellent straight lines for bovine, rabbit, and human blood, on both glass and fibrin surfaces. Following this equation, straight lines are obtained when the square root of the shear rate is plotted against the square root of the shear stress. On the assumption that Casson's equation is applicable to blood, we treated theoretically the rheological behavior of blood flowing in a capillary. We have obtained both the velocity distribution across the capillary and the volume of flow in unit time as a function of pressure difference. The result was compared with the rheological behavior of a Bingham system and other non-Newtonian systems.

Author

N67 14570

Necklace-like Formations in the Poiseuille Flow of a Suspension of Spheres

GIORGIO SEGRÉ,*† *Cartiera Vita Mayer e C., Sezione Ricerche, Milan, Italy*

INTRODUCTION

Studies of the flow of suspensions derive their interest from the importance such systems have in technology and biology. As theoretical investigations are confronted with tremendous mathematical difficulties, such studies present a challenge for the experimentalist, who may frequently go further in this field and show the way to the theoretician.

In this research we are limiting ourselves to the Poiseuille flow of suspensions of spheres, that is, to nonturbulent flow in a tube of a system composed of an ideally viscous liquid and a number of identical, rigid, spherical particles. Apart from mechanical or hydrodynamic interaction, no other interaction is assumed to take place, either between the particles or between the particles and the tube wall.

Most theoretical studies refer to the isolated particles or to extremely dilute suspensions in which the suspended particles are assumed to behave independently of each other, and the effects are additive (see for instance, the calculation of viscosity by Einstein[1]). Even in this simple case the integration of the Navier-Stokes equations of motion is possible only on neglect of higher order terms in the velocity, that is, by neglecting accelerations and inertia forces. These so-called "creeping motion solutions" (Simha,[2] Vand,[3] Happel and Brenner,[4] Happel and Byrne[5]) tell us of the existence of a "slip velocity" that is about a particle velocity somewhat smaller than that of the undisturbed fluid at the position of the particle center.

† Present address: Istituto Chimico dell' Universitá, Naples, Italy.

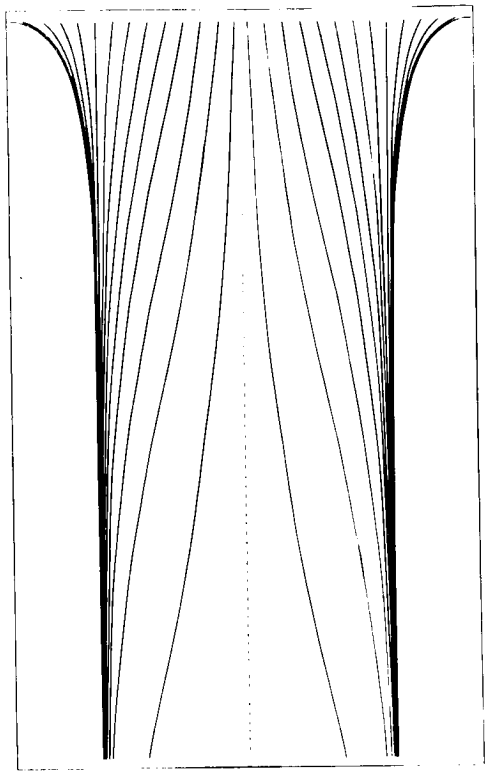

Fig. 1. Trajectories of suspended particles (tubular pinch effect). The tube diameter is expanded and its length compressed in comparison with most experimental conditions.

Apart from this relative longitudinal motion no transverse displacement is predicted at very low Reynolds numbers.

Radial displacements arising from the mechanical interaction between the particles and the tube wall have been observed however and were studied by Whitmore and Maude[6] and others.[7,8] More recently Segré and Silberberg[9] have shown experimentally that radial rearrangements of the particles, of purely hydrodynamic origin, take place at Reynolds numbers where inertia effects can no longer be neglected. Working at dilutions such that the particles still behave independently, the suspended particles were observed to follow trajectories of the type shown in Figure 1. They thus tend to reach a

Fig. 2. Some pairs of stereoscopic pictures of the flowing suspension.

radial position at about two-thirds of the tube radius, in the limit of low Reynolds numbers, while at Reynolds numbers in excess of about 30 the equilibrium radial distance increases with Reynolds number. These displacements give rise to the so-called "tubular pinch effect" which is intended to describe the local increase of concentration occurring at the equilibrium radial position at points in the tube a sufficient length from its mouth. Particles which were initially dispersed homogeneously in the liquid are found to be concentrated in a thin cylindrical layer, all moving with the same velocity. When this situation is reached, it is easy to follow, visually, the motion of con-

stellations of particles, which progress along the tube without changing relative position.

At the initial particle concentration usually employed this steady state is only apparent, however. If the observation is carried sufficiently far along the tube, evolutions in these constellations shapes are noted, which are clearly due to particle-particle interaction. Two particles which happen to move along the same line start attracting each other, until they reach a minimum (not touching) distance. Then repulsion predominates, till by damped oscillations an equilibrium distance is found, and the particles form a stable pair. If the two particles were not initially aligned, a transverse displacement concomitant with this longitudinal rocking motion brings the particles into the same final configuration. This, too, however is final only if no other particle is found nearby; otherwise this also tends to align itself with the first two, and a group of three, equidistant particles is formed. And the process goes on, by capture of isolated spheres or by fusion of already formed groups, till all the suspension is nothing more than a collection of nice, regular, long necklaces (Fig. 2).

This phenomenon, without any speculations about the theoretical reasons for its occurrence, invites quantitative analysis and description. This is the purpose and scope of the present communication.

EXPERIMENTAL METHOD

The flow system was practically the same as that employed in the tubular pinch experiment;[9] its aim was once again to feed the flow tube with a homogeneous suspension at a controlled velocity. The flow tube itself should allow the observation of the necklaces without too much distortion and consisted of a Plexiglas tube whose external surface was milled, brought to a square section, and polished. This shape permitted good illumination and a clear view of the interior perpendicular to the prism faces. Such an arrangement is not ideally suited to measuring all the coordinates of the particles, but it is good enough to examine their alignment and determine their separation in a direction parallel to the tube axis.

The observation was carried on by taking photographic pictures during the flow: the particles were sufficiently opaque to give good contrast in rear illumination. A distant electronic flash and an opaline glass diffusor, placed just behind the flow tube, were employed

for this purpose. Besides the direct picture, an image in the transverse direction was taken with the help of two mirrors. Two stereoscopic pictures are necessary in order to check on the true linearity of the groups of particles. Two flow tubes were used, their internal diameter being, respectively, $2R = 11.59 \pm 0.02$ mm. and 8.42 ± 0.02 mm. (average values obtained by the weighing of distilled water columns). The total tube length was 180 cm., but, apart from some control experiments, only its last 25 to 50 cm. were photographed. The camera was placed at distances varying from 50 to 110 cm.; for every setting a length scale calibration was performed by taking pictures of a transparent rule immersed in the tube. In this way it was also checked that no appreciable linear distortion was present at the edge of the picture.

The suspensions were made up of polymethyl methacrylate spheres in media of equal density ($\rho_{34^0} = 1.178$) and different viscosities (20 to 200 cp.) prepared by mixing glycerine, 1,3-butanediol and water in various proportions. The particles were closely matched in diameter by passing them through a "sieve" composed of a slit whose gap could be accurately adjusted. Fractions characterized by mean particle diameters $2a = 0.80$, 1.00, 1.21, and 1.71 mm. were employed. Concentration C_0 ranged from 0.5 to 2 particles/cm.^{3} of liquid. By changing the viscosity of the liquid η and its flow velocity V_m, a range of tube Reynolds numbers from 30 to 1000 has been obtained. Errors in these Re values, arising primarily from calibration errors in the viscosity factor, were unfortunately rather large (from 5 to 10%). The concentrations and other flow variables chosen were such that the development of the tubular pinch occurred as an "independent particle" phenomenon in the very first part of the tube, while the concentrations built up at the equilibrium radial position were sufficient for the occurrence of interaction phenomena in the remaining part of the tube.

For every set of experimental conditions (which in the following shall be called an experiment), 40 to 80 pictures were taken. The negatives were examined under a low magnification microscope, groups of spheres were classified according to the number of particles they contained, and for every well-formed "necklace" all the center-to-center distances d of adjacent particles were measured. For all group of i particles ($i = 2, 3, 4, \ldots$), and for given experimental conditions, an average $\langle d_i \rangle$, a standard deviation σ_i, and a standard

error of the average were computed. As long groups were rare, the results for these were pooled together, giving a value $\langle d_{>j} \rangle$ with better statistics.

RESULTS

(a) Tendency to Group Formation

Observations were carried out at a fixed distance from the tube inlet, and therefore represent comparable stages in the formation of the groups. Every experiment represents a moment in the building up of the necklaces. The number and the average length of these necklaces depend both on the bulk concentration of the suspension and on the range of the force of interaction between the particles. Concentration dependence is exemplified in Table I, where pairs of

TABLE I
Concentration Dependence of Group Distribution

Expt. No.	C_0, particle/cm.^{3}	Re	Number of groups of i particles							Isolated particles fraction, f
			$i = 2$	3	4	5	6	7	>7	
E2	0.5	177	44	8	1	2	—	—	—	0.628
E3	1	177	234	98	29	10	2	—	1	0.416
E5	0.5	293	115	47	8	4	—	—	—	0.540
E6	1	295	195	94	39	9	5	3	—	0.353
E7	0.5	392	68	26	12	4	—	—	—	0.435
E8	1	394	265	141	73	28	8	6	—	0.291
F6	0.5	271	139	57	16	8	2	1	—	0.436
F7	1	280	195	124	80	30	12	9	5	0.258
F10	0.5	420	119	47	34	13	5	2	—	0.440
F11	1	435	199	128	79	34	20	7	4	0.351

experiments made under the same geometric and hydrodynamic conditions but at concentrations, of 0.5 and 1 particle/cm.^{3} respectively, are listed. Note the shift toward larger groups at the larger concentration, and the corresponding decrease of the relative frequency f of isolated particles.

Dependence on tube Reynolds number, on particle diameter, and concentration is shown in Figure 3. The frequency of all grouped particles for experiments made with two particles fractions under various flow conditions has been plotted. The tendency to group is

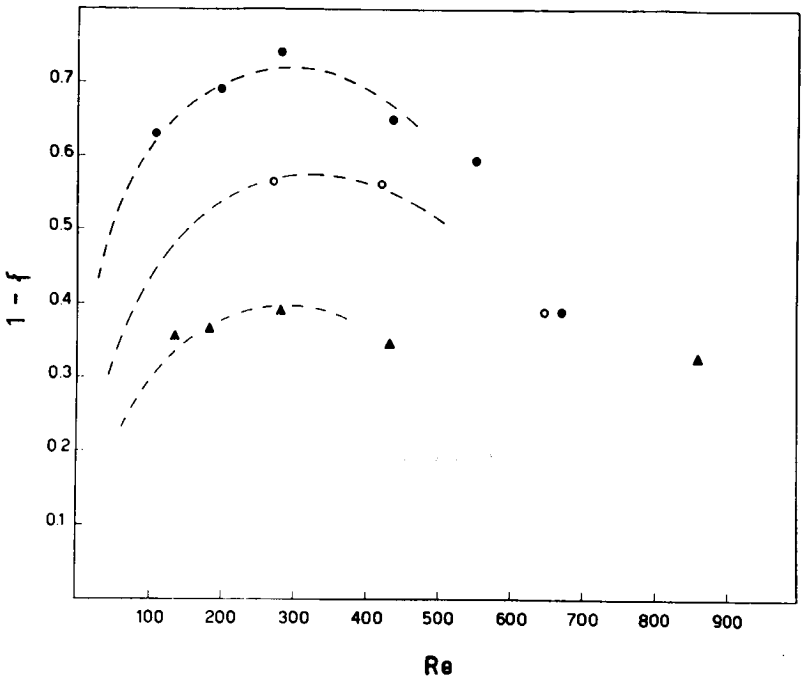

Fig. 3. Tendency to group formation as a function of Reynolds number, for different concentrations and for two particle diameters: (●) experiments of series F, concentration 1 particle/cm.^{3}; (○) experiments of series F, concentration 0.5 particle/cm.^{3}; and (▲) experiments of series C, concentration 0.8 particle/cm.^{3}

an increasing function of the particle dimensions and concentration. As a function of the Reynolds number the grouping tendency initially increases, reaches a maximum, and then decreases. If, however, one looks at the regularity within the groups (which finds its quantitative expression in the reciprocal of the standard deviation σ_i of the distribution of particles distances), one sees that $1/\sigma_i$ increases monotonically with Re. It is natural to conclude, therefore, that the decrease of the number of grouped particles at large Reynolds number is due not to a decrease of the strength and range of interaction, but to the disturbing action of local turbulence (arising mainly from other particles passing nearby) which counteracts the tendency to form stable groups.

TABLE II
Average $\langle d_i \rangle$ for Groups of i Particles

No. of particles/ group, i	Average distance between particles $\langle d_i \rangle$, mm.					
	C4	C6	C8	D2	D3	D5
2	4.14 ± 0.06	3.44 ± 0.04	2.79 ± 0.05	3.73 ± 0.05	3.30 ± 0.06	3.07 ± 0.04
3	3.74 ± 0.04	3.16 ± 0.03	2.61 ± 0.02	3.41 ± 0.04	3.18 ± 0.04	2.83 ± 0.04
4	3.60 ± 0.04	2.99 ± 0.04	2.47 ± 0.02	3.17 ± 0.06	2.98 ± 0.05	2.76 ± 0.06
5	3.45 ± 0.05	2.89 ± 0.04	2.44 ± 0.04	3.12 ± 0.09	2.90 ± 0.05	2.49 ± 0.09
6	3.09 ± 0.06	3.00 ± 0.06	2.41 ± 0.03			
7		2.91 ± 0.05	2.60 ± 0.05	2.90 ± 0.10	3.12 ± 0.09	2.52 ± 0.06
	3.19 ± 0.07					
>7		2.86 ± 0.06	2.54 ± 0.05			

TABLE III. Series of Experiments Listed in Order of Increasing $\alpha = a/R$[a]

Expt. No.	Re	$2a$, mm.	$2R$, mm.	$\langle d \rangle$, mm.	$\delta - \alpha$	Expt. No.	Re	$2a$, mm.	$2R$, mm.	$\langle d \rangle$, mm.	$\delta - \alpha$
A1	334	0.80	11.59	3.35	0.220	E4	240	1.21	8.42	3.49	0.270
A2	425	0.80	11.59	3.16	0.204	E5	293	1.21	8.42	3.26	0.243
B1	191	0.80	8.42	3.29	0.296	E6	295	1.21	8.42	3.20	0.236
B2	205	0.80	8.42	3.24	0.290	E7	392	1.21	8.42	2.80	0.189
B3	247	0.80	8.42	2.86	0.244	E8	394	1.21	8.42	2.86	0.196
B4	324	0.80	8.42	2.82	0.240	F1	78.5	1.71	11.59	5.70	0.344
B5	342	0.80	8.42	2.65	0.220	F2	99.5	1.71	11.59	5.51	0.328
B6	343	0.80	8.42	2.73	0.229	F3	107.5	1.71	11.59	5.48	0.325
C1	133	1.21	11.59	5.18	0.342	F4	197	1.71	11.59	4.71	0.259
C2	181	1.21	11.59	4.45	0.280	F5	206	1.71	11.59	4.81	0.268
C3	280	1.21	11.59	4.07	0.247	F6	271	1.71	11.59	4.38	0.230
C4	325	1.21	11.59	3.83	0.226	F7	280	1.71	11.59	4.25	0.219
C5	430	1.21	11.59	3.30	0.180	F8	297	1.71	11.59	4.05	0.202
C6	500	1.21	11.59	3.20	0.172	F9	306	1.71	11.59	3.95	0.193
C7	860	1.21	11.59	2.36	0.099	F10	420	1.71	11.59	3.85	0.185
C8	1000	1.21	11.59	2.62	0.122	F11	435	1.71	11.59	3.65	0.167
D1	133	1.00	8.42	4.16	0.375	F12	470	1.71	11.59	3.58	0.161
D2	195	1.00	8.42	3.44	0.290	F13	550	1.71	11.59	3.21	0.129
D3	270	1.00	8.42	3.15	0.255	F14	646	1.71	11.59	3.10	0.120
D4	295	1.21	8.42	3.16	0.256	F15	670	1.71	11.59	2.92	0.104
D5	341	1.21	8.42	2.87	0.222	F16	940	1.71	11.59	2.70	0.085
D6	458	1.00	8.42	2.63	0.193	G1	114	1.71	8.42	4.32	0.310
E1	110	1.21	8.42	4.27	0.363	G2	122	1.71	8.42	4.29	0.306
E2	177	1.21	8.42	Poor statistics		G3	185	1.71	8.42	3.75	0.242
E3	177	1.21	8.42	3.90	0.319	G4	299	1.71	8.42	3.13	0.169

[a] Concentrations in particles/cm.^{3} are: 2 in series A, B, and D; 0.8 in experiments C1, C2, C3, C5, and C7; 1.6 in experiments C4, C6, and C8; 0.5 in experiments E2, E5, E7, F6, F10, and F14; and 1 in all other experiments.

(b) Group Configuration

Assuming that the lifetime of an individual group has been sufficiently long to have allowed it to reach the equilibrium configuration, we now shift our attention to the distance between the particles.

Table II gives the average $\langle d_i \rangle$ for groups of i particles for some typical experiments. Note that $\langle d_i \rangle$ decreases regularly as one passes from groups of two to three and four particles. It is not easy to say if for larger groups a constant value is approached: large groups are rare and their configuration is not, in general, as regular as that of smaller groups. Both these facts tend to increase the statistical error of the measured $\langle d_i \rangle$ values.

In order to characterize each experiment by a single magnitude a typical distance was defined as $\langle d \rangle = {}^1/_3(\langle d_2 \rangle + \langle d_3 \rangle + \langle d_4 \rangle)$. Table III gives the value of $\langle d \rangle$ for all experiments as well as other relevant information about the experimental conditions.

One sees immediately that, for given particles and tube diameters, $\langle d \rangle$ is a decreasing function of Reynolds number. Plotting $\langle d \rangle$ against Re for the different groups of experiments one finds a family of similar curves, from which one could possibly derive a law stating the dependence of $\langle d \rangle$ on the particle diameter. This point will be discussed later. Observe, however, that while this dependence is close to linear, $\langle d \rangle$ is undoubtedly not proportional directly to a, as one might have been tempted to expect.

DISCUSSION OF RESULTS

(a) Concentration Dependence

It is clear that the effects we are observing are due to some kind of interaction between the particles. Thus, consider the dependence on concentration.

The occurrence in the first part of the tube of the tubular pinch effect will bring all the particles, which entered the tube with a uniform concentration C_0 (in particles per unit volume) and with an average velocity V_m, to a radial position r^* where the velocity is $V(r^*) = 2V_m(R^2 - r^{*2})/R^2$.

The number of particles per unit length of tube, after radial equilibrium has been reached, is therefore

$$N = C_0\pi R^2 V_m / V(r^*) = \pi C_0 R^4 / 2(R^2 - r^{*2}) \qquad (1)$$

At this point interaction begins to play a role. We introduce a simplification which is probably not too drastic. We shall assume that a necklace will be formed from particles which move along streamlines being within a narrow arc of aperture γ, and treat them as if they were already moving along the same streamline. This allows us to study the problem as a unidimensional queuing process.

As the distribution of the particles at the inlet is random, so the particles which we are now considering will be distributed at random along the streamline, and the distance g of one particle from the next will satisfy the *negative exponential distribution:*

$$dp(g) = n \exp \{-ng\} dg \tag{2}$$

where $dp(g)$ is the probability that the distance has a value between g and $g + dg$, and

$$n = N\gamma/2\pi \tag{3}$$

is the mean number of particles per unit length.

By only considering nearest neighbor interaction, we assume that two particles shall be observed as grouped at the end of a length L of tube if, and only if, initially, they were closer than a critical distance g_c, which is a function of the strength of interaction and of the tube length L. An individual particle, however, may interact both with the particle preceding it (at distance g_1) and with that following it (at distance g_2), and it will be observed at the end of the tube as an isolated particle if both

$$g_1 > g_c \text{ and } g_2 > g_c \tag{4}$$

The probability of observing the sequence g_1, g_2 is

$$dp(g_1, g_2) = n^2 \exp \{-n(g_1 + g_2)\} dg_1 dg_2 \tag{5}$$

and the expected number of particles satisfying conditions in eq. (4) is readily obtained by integration. The result is that the fraction of particles which, at the end of the tube, are still isolated is

$$f = \int_{gc}^{\infty} \int_{gc}^{\infty} dp(g_1, g_2) = \exp \{-2ng_c\} \tag{6}$$

Since we ignore the value of γ in eq. (3), we cannot use this result to calculate the range g_c from observations of f. However eqs. (3) and (6) give us the law for the concentration dependence of f, and this

may be checked experimentally. It is easy to see, for instance, that doubling the concentration C_0 should reduce f to its square. This is confirmed very well in experiments E2 and E3, for which f has the values 0.628 and 0.416, respectively (see Table I). For other pairs of experiments the check is worse, and deviations are larger the higher the Reynolds number. This agrees with the fact already noted that at increasing values the tendency to group is contrasted by the disturbing action of other particles, and it is not surprising that this effect be larger the higher the concentration.

(b) The Frequency Distribution of Groups

The expected frequency of particles occurring in groups of length i, in a given experiment, may be calculated by an extension of the above method. Consider a sequence $g_1, g_2, \ldots g_i, g_{i+1}$ which will give rise to a necklace of just i particles if, and only if,

$$g_1 > g_c,\ g_2 < g_c,\ \ldots\ g_i < g_c \text{ and } g_{i+1} > g_c \tag{7}$$

The result is that the probability of a particle being in a group of length i is

$$f_i = i \int_{gc}^{\infty} \int_{0}^{gc} \cdots \int_{0}^{gc} \int_{gc}^{\infty} n^{i+1} \exp\left\{- n \sum_{1}^{i+1} g_j\right\} dg \ldots dg_{i+1}$$
$$= if(1 - f^{1/2})^{i-1} \tag{8}$$

TABLE IV

Observed and Expected Frequencies f_i of Particles in Groups of Length i

Expt. No.		f	f_2	f_3	f_4	f_5	f_6	f_7	f_8
E2	obs.	0.628	0.260	0.071	0.012	0.030	—	—	—
	calc.		0.261	0.081	0.023	0.006	0.001		
E3	obs.	0.416	0.288	0.181	0.071	0.031	0.007	—	0.005
	calc.		0.295	0.157	0.074	0.033	0.017	0.007	0.003
E7	obs.	0.435	0.273	0.156	0.096	0.040	—	—	—
	calc.		0.297	0.152	0.069	0.029	0.012	0.005	0.002
E8	obs.	0.291	0.254	0.203	0.140	0.067	0.023	0.020	—
	calc.		0.268	0.185	0.114	0.066	0.036	0.020	0.010
F10	obs.	0.441	0.210	0.133	0.120	0.057	0.026	0.013	—
	calc.		0.297	0.150	0.067	0.028	0.011	0.004	0.002
F11	obs.	0.351	0.175	0.169	0.139	0.075	0.053	0.022	0.014
	calc.		0.286	0.175	0.095	0.049	0.024	0.011	0.005

The frequency distributions thus obtained are compared in Table IV (where f is the observed frequency of isolated particles) with experimental frequencies for some typical experiments. Agreement in all cases is satisfactory. There is, however, definite evidence that nearest neighbor interaction is insufficient to describe the process of formation of large groups at high Reynolds numbers. The observed ratios f_4/f_2, f_5/f_2, etc., tend in fact, in these cases, to be larger than the expected ratios, showing that the process of aggregation of small groups into larger ones is more frequent than required by the theory outlined above.

(c) The Equilibrium Configuration

Identification of $\langle d_i \rangle$ with the equilibrium distance is subject to doubt. In fact it is known that, if equilibrium is reached by damped oscillations and if there is a good chance that a photograph has been taken before equilibrium is established, the distribution of distances d_i will be very different from a normal distribution, and therefore any justification for taking the arithmetical mean is lacking. For present purposes, however, we are interested in finding a simple statistical parameter to characterize the particle behavior. For this reason also the variable $\langle d \rangle$ was devised instead of choosing a $\langle d_i \rangle$ value for, say, $i = 2$ or for $i \to \infty$.

It has already been noted that there is good correlation between the values of $\langle d \rangle$ and the Reynolds number for given particle and tube diameters. Before looking for other correlations, the choice of non-dimensional variables should be completed. In addition to $\mathrm{Re} = 2R\rho V_m/\eta$, the variables $\alpha = a/R$ and $\delta = \langle d \rangle/2R$ which correspond to taking the tube diameter as unit of length shall be used.

In the range of concentration used, δ appears to be independent of concentration; see, for instance in Table III the pairs of experiments E5–E6 and E7–E8.

It is noted[9] that the "particle Reynolds number" and the "limiting radial position" are only functions of Re and α. Therefore, the parameter δ as well can only be a function of α and Re. A plot of $\delta - \alpha$ against Re (Fig. 4) shows that good correlation is found in reduced variables between the "gap" (the free space left between the particles) and the Reynolds number. It is noted in particular that $\delta - \alpha$ is practically independent of α, i.e., the ratio between tube and

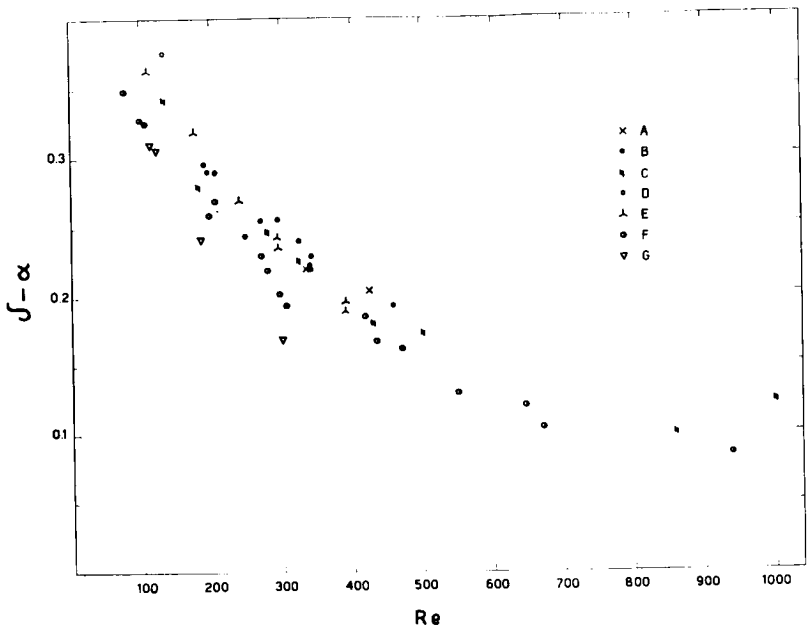

Fig. 4. The correlation between the reduced gap $\delta - \alpha$ and the Reynolds number. For experimental conditions see Table III.

particle diameters, although a certain trend may be present. Much more precise experiments would be needed to test this further.

It would be of great interest to observe the spinning motion of the particles, which has a very important role in all these types of phenomena[10] and for which a cinematographic method would recommend itself.

QUALITATIVE THEORETICAL CONSIDERATIONS

The phenomenon described has some superficial resemblance to vortex systems of which the von Kármán-Street is a well-known example.[11,12] Von Kármán's studies apply to inviscid fluids, whereas, in Poiseuille flow, viscosity and the rotational character of the undisturbed flow are basic. In inviscid fluids a single row of vortices is unstable, and only a special double row of vortices, the above-mentioned von Kármán-Street, is stable. Here we have something which is certainly not a double row, but which is stable and could be

considered a system of localized vortices. It is thus of interest to compare the results of von Kármán's theory with the author's case. One of the conditions of stability is given by the expression[13]

$$\kappa = 2\sqrt{2}dU_s$$

where κ is the strength of a vortex, d is the spacing along a row, and U_s is the velocity of displacement of the vortices relative to the undisturbed fluid. If we identify this velocity with the slip velocity of the particles[14]

$$U_s = {}^4/_3 V_m(a/R)^2$$

and κ with the circulation along the equator of the spinning sphere

$$\kappa = 2\pi a^2\Omega$$

(where $\Omega = 2V_m r^*/R^2$ is the angular velocity assumed to equal that of the isolated particle placed at a distance r^* from the axis), we find

$$\delta = d/2R = 3\pi r^*/4\sqrt{2}R = 1.66r^*/R \qquad (4)$$

which bears no resemblance to what we already know about δ. It is sufficient to remember that δ decreases with increasing Reynolds numbers, while r^* increases under the same conditions.[15]

References

1. Einstein, A., *Ann. Physik*, **19**, 289 (1906); **34**, 591 (1911).
2. Simha, R., *Kolloid-Z.*, **76**, 16 (1936).
3. Vand, V., *J. Phys. Chem.*, **52**, 277 (1948).
4. Happel, J., and H. Brenner, *J. Fluid Mech.*, **4**, 195 (1958).
5. Happel, J., and B. J. Byrne, *Ind. Eng. Chem.*, **46**, 1181 (1954).
6. Whitmore, R. L., and A. D. Maude, *Brit. J. Appl. Phys.*, **7**, 98 (1956).
7. Higginbotham, G., Ph.D. thesis, Univ. of Birmingham, 1951, as quoted by Whitmore, ref. 6.
8. Oliver, R. D., Ph.D. thesis, Univ. of Birmingham, 1954, as quoted by Whitmore, ref. 6.
9. Segré, G., and A. Silberberg, *J. Fluid Mech.*, **14**, 136 (1962).
10. Oliver, R. D., *Nature*, **194**, 1269 (1962).
11. Lamb, H., *Hydrodynamics*, Dover, New York, 1945, p. 228.
12. Goldstein, S., *Modern Developments in Fluid Dynamics*, Clarendon Press, Oxford, 1938, p. 556.
13. Goldstein, S., *Modern Developments in Fluid Dynamics*, Clarendon Press, Oxford, 1938, p. 563.
14. Segré, G., and A. Silberberg, *J. Fluid Mech.*, **14**, 155 (1962).
15. Segré, G., and A. Silberberg, *J. Fluid Mech.*, **14**, 152 (1962).

Synopsis

14570

Experiments on the rearrangement of spherical particles carried in a dilute suspension in Poiseuille flow are presented. The tendency of the particles to form regular groups (necklaces) aligned parallel to the tube axis is established and is analyzed photographically. It is shown that this tendency increases with the particle diameter, and that the observed distribution of groups agrees with an interpretation based on nearest neighbor hydrodynamic interaction. In the stable configurations the gap between the particles is a function of the number of particles in the group, independent of the particle diameter, and strongly correlated with the Reynolds number. A comparison with von Kármán's theory on vortex systems is made, but no correlation results.

Author

N67 14571

Hydrodynamic Interaction between Particles in Suspension

A. SILBERBERG,* *Weizmann Institute of Science, Rehovot, Israel*

INTRODUCTION

Rheology has two main applications in the study of biology. The first of these is the characterization and study, under physiologically defined conditions, of biological processes which involve flow or deformation. In this way an understanding of the functions is to be reached which such processes are intended to fulfill; in particular how the rheological properties, which measurements allow one to determine, predicate the biological aspects. Often it is only the nature of the rheological behavior which allows one to understand the physiological phenomenon and to evaluate pathological deviations. Ideally this could lead to suggestions for remedies of such conditions, but for this to be done effectively the molecular structural and chemical basis of the rheological phenomena under discussion must be understood.

This approaches the second motivation for introducing rheology into the biological sciences. The biochemist or biophysicist often isolates and purifies material, sometimes colloidally, sometimes molecularly disperse, which he seeks to define and describe in terms of the size and shape adopted by the particle in solution under certain well-defined environmental conditions. To find his answers he turns to rheological techniques.

In this respect the questions of the biologist become no different from those of the researcher in colloid chemistry in general, but very often the biologist has to understand molecular structures which are considerably more complex and peculiar than the class of colloidal particles commonly dealt with in polymer physics.

Thus problems are continually arising in biorheology which, though fundamentally the same as those of macromolecular physics, require the researcher to find new solutions and send him back to the fundamentals in the search for theoretical explanation and understanding.

The biorheologist has to be content with morphological descriptions and has turned to molecular theories and models. A well chosen set of instruments and rheological techniques is no longer enough. One also needs an adequate theoretical apparatus which will allow one to reduce data into parameter descriptions which are both informative and convenient.

It is to the question of these theoretical tools or models to which the present discussion is turned.

One finds that the armory available at present is very small and that one is really very far yet from attempting to deal with complicated problems exactly. What can be done is to reduce the complicated structures to assemblies of much simpler bodies for which exact solutions have been worked out. The complicated structure is then replaced by the assembly of simpler ones when the interactions between the composite parts are taken into account.

It has been found adequate for many purposes, when dealing with complex liquid systems, to replace the particulate matter by assemblies of rigid spheres dispersed in a continuous phase consisting of an hydrodynamic fluid of shear independent viscosity η_0. The intricate rheological behavior of a large number of different systems is remarkably well represented by such models when the hydrodynamic interactions between the spheres are taken into account.

THE OSEEN HYDRODYNAMIC INTERACTION TENSOR

Stokes has dealt with the problem of a sphere moving slowly through an infinite medium at rest, and Einstein has solved the case of a sphere embedded in a fluid in laminar shear flow. In the solutions of these problems it is assumed that inertial effects may be neglected, that the fluid moves with the velocity of the sphere at the boundary of the sphere, and that at sufficiently large distances the velocity of the fluid approaches that which would prevail were the sphere not present.

Due to these boundary conditions the sphere in the Stokes case is under a force which is directly proportional to the velocity difference between the sphere and the fluid in the absence of the sphere. In terms of this force, the velocity disturbance set up by the sphere is found not to depend on the sphere radius in the leading term in an expansion in increasing powers of the radius a. By allowing the volume of the sphere to shrink to zero it is thus possible to find the disturb-

ance in the velocity set up by a force acting at a point in the fluid. In the case of a sphere in a laminar field of flow of constant gradient, the sphere in the limit of zero volume may be replaced by a force couple which rotates with the same angular velocity. Each force in the couple may be equated, in the velocity disturbance it sets up, to the Stokes force just discussed. The small separation of the forces in the couple has the effect, however, of effectively changing the angular dependence of the disturbance to that of the derivative of the disturbance in the Stokes case. This was the technique used by Burgers.[1]

For his calculations Burgers used formulas derived from a treatment by Oseen[2] which was designed to allow for a much more complex situation in which inertial effects were not neglected. In the approximation used by Burgers, and by almost everybody since, Oseen's formulas are so simplified as to reduce to the Stokes case for vanishing sphere volume. Despite this, the disturbance tensor so calculated is traditionally termed the Oseen hydrodynamic interaction tensor and may be written as follows:

$$\mathbf{T}(\mathbf{R}) = (1/8\pi\eta_0 R)\{\mathbf{1} + (\mathbf{R})(\mathbf{R})/R^2\} \tag{1}$$

Here $\mathbf{R}$ is the vector distance from the center of the sphere to the point of interest, $\mathbf{1}$ is unit tensor and the second tensor in the above expression has been put in dyadic form. The tensor $\mathbf{T}$ relates the forces which are acting to the velocity disturbances they produce, e.g., if there is a force $\mathbf{F}$ acting at $\mathbf{R}$ the velocity disturbance at the origin is given by

$$\mathbf{v}'(\mathbf{R}) = \mathbf{T}(\mathbf{R}) \cdot \mathbf{F} \tag{2}$$

Notable problems which have been treated by this expression are the intrinsic viscosity of rigid sphere suspensions (Burgers[1]), the intrinsic viscosity of linear flexible macromolecules (Kirkwood and Riseman[3]), and the relaxation time spectrum of dilute solutions of macromolecules (Zimm[4]).

THE INTRINSIC VISCOSITY OF SPHERES AND PARTICLES COMPOSED OF AN ASSEMBLY OF SPHERES

In Burgers' treatment of a suspension of spheres in a fluid undergoing laminar shear in the x-y plane, he finds that the disturbance set up at the origin by a sphere at $\mathbf{R}$ is given by

$$\mathbf{v}'(\mathbf{R}) = (3/4\pi)(c[\eta]/\nu)\ \dot{\epsilon}\ (\mathbf{R}\cdot\mathbf{e}_x)(\mathbf{R}\cdot\mathbf{e}_y)\mathbf{R}/R^5 + \ldots \qquad (3)$$

where $[\eta]$ is the intrinsic viscosity in (grams per 100 ml.)$^{-1}$, c is the concentration in grams per 100 ml., ν is the concentration in particles per unit volume, $\dot{\epsilon}$ is the rate of shear of the laminar flow, and $\mathbf{e}_i$ is unit vector into the i direction.

If the origin of coordinates is placed at the wall of the viscometer and the velocity distribution [eq. (3)] is averaged over all positions $\mathbf{R}$ accessible to the particle between the (assumed) infinite parallel walls of the viscometer, it is found that a certain retardation in velocity is experienced, but that only the term written out explicitly in eq. (3) contributes to the integral. Higher terms average to zero. When the rate of shear [i.e., the shear stress contribution at the viscometer wall as derived from eq. (3)] is averaged, this contribution too vanishes. The only effect of the presence of the sphere is thus the retardation already mentioned. Expressing this as an effective increase in the viscosity from η_0 to η, one can calculate the intrinsic viscosity

$$[\eta] = \operatorname*{Lim}_{c \to 0} \frac{\eta - \eta_0}{\eta_0 c} \qquad (4)$$

and find on the basis of eq. (3) and the boundary conditions on the wall a result in agreement with the Einstein computation performed in an entirely different way.

Kirkwood and Riseman,[3] in dealing with a flexible macromolecule, replaced the molecular chain by an assembly of spherical beads and arrived at a result for the velocity disturbance identical in its leading term to eq. (3). In the case of macromolecules however $\mathbf{v}'$ is an average taken over all configurations, positions, and orientations of the assembly. It can be shown that such a result necessarily follows from the form of the Oseen tensor $\mathbf{T}$ and that the result will be the same for any particle built up of spheres which is not preferentially orientated in the flow. The peculiarities of the correlations between the spheres are contained in $[\eta]$ which can be shown to be an expression for the average torque acting on the macromolecule.

VISCOSITY AT FINITE CONCENTRATIONS OF PARTICLES

Although the above cases are well understood, the concentration dependence of the viscosity of suspensions has given rise to a large and conflicting literature.[5–7] One is concerned here primarily with a theory for the Huggins coefficient k' in the expression

$$(\eta/\eta_0) = 1 + [\eta]\, c + k'\, [\eta]^2 c^2 + \ldots \qquad (5)$$

As most determinations are performed at finite concentration and it is often impossible to effect sufficient dilution in biological systems, a theory for the Huggins coefficient is of great importance. In general the Huggins coefficient is characteristic of the interparticle correlation function. Here we shall be concerned only with the simplest case of hard sphere exclusion and uniform distribution of a set of noninteracting particles possessing spherical symmetry. It will be our purpose to show that in these cases the Huggins coefficient should be the same for all systems where the dispersed species may be represented by an assembly of spheres and the disturbance in consequence takes the form eq. (3).

In the case of a sphere suspension one makes allowance for the hydrodynamic interaction between spheres by calculating the change in gradient induced at the site of one sphere by the presence of the others. Following the procedure of Saito[5] and integrating over all spheres assuming a uniform distribution, one finds an integral analogous to that which lead to $[\eta]c$ in the noninteracting case. Hence, a correction term proportional to $[\eta]c$ results when the rate of shear $\dot{\epsilon}$ in eq. (3) is replaced by the effective rate of shear calculated. Since one is dealing with an integral over a derivative of eq. (3), however, the numerical coefficient is different and turns out to be $k' = 0.4$.

Applying this to an assembly of spheres, say to the Kirkwood-Riseman model,[3] and considering all interactions between spheres leads to a long algebraic computation but the same Huggins coefficient results. This is in disagreement with Riseman and Ullman[6] who set up this problem but chose the wrong integration domain.

As only the symmetry but not the specific nature of the sphere distribution function was used, the final result is independent of it and hence applies to all such distributions. Why this should be so is obvious. As long as no specific pairing of particles occurs and there are no distribution changes within the assembly of spheres the hydrodynamic interparticle interaction must lead to the same factors as in the intrinsic viscosity calculations.

The Huggins coefficient is thus an expression of the dependence of $\mathbf{v}'$ and its derivative on $\mathbf{R}$, and this, in the first approximation, does not depend upon how many spheres constitute the assembly and how these spheres are distributed within it.

Peterson and Fixman[8] have recently discussed this and conclude that the correction of the velocity gradient change induced by the other spheres at the site of the reference sphere is not simply a linear superposition of the unaltered contributions resulting from eq. (3). The changed gradient will in turn change the disturbance, and the true correction is obtained only by solving this mutual interaction problem simultaneously. By doing this a Huggins coefficient of 0.6909 is found by Peterson and Fixman. This new value should, however, again be independent of the type of sphere assemblies considered.

One may conclude therefore that, taking the rigid sphere suspension Huggins parameter as reference, deviations from it in a case of more complex systems are due to inter- and intra-molecular rearrangements and aggregate formation, resulting in the main from particle interaction of a nonhydrodynamic character. Much more work remains to be done to handle the results for more complex cases effectively. The approach of Peterson and Fixman,[8] in which they consider the possibility of dumbbell formation as a contributory cause in the viscosity rise, does seem very promising in this connection. Note finally that the considerations advanced apply only to particles subject to a very high degree of Brownian motion.

References

1. Burgers, J. M., *Second Report on Viscosity and Plasticity*, North Holland Publishing Co., Amsterdam, 1938.

2. Oseen, C. W., *Hydrodynamik*, Akademische Verlagsgesellschaft, Leipzig, 1927.

3. Kirkwood, J. G., and J. Riseman, *J. Chem. Phys.*, **16**, 565 (1948).

4. Zimm, B. H., *J. Chem. Phys.*, **24**, 269 (1956).

5. Saito, N., *J. Phys. Soc. Japan*, **5**, 4 (1950); **7**, 447 (1952).

6. Riseman, J., and R. Ullman, *J. Chem. Phys.*, **19**, 578 (1951).

7. Guth, E., and R. Simha, *Kolloid-Z.*, **74**, 266 (1936); Simha, R., *J. Research Natl. Bur. Standards*, **42**, 409 (1949); *J. Appl. Phys.*, **23**, 1020 (1952).

8. Peterson, J. M., and M. Fixman, *Dilute Solutions Symposium*, Mellon Institute, Pittsburgh, Aug. 1963.

Synopsis

The importance of theoretical models for the understanding of biorheological phenomena was stressed, and the central position of the hydrodynamic interaction tensor in these considerations underscored. The use of this tensor for studies of the concentration dependence of specific viscosity was examined, and it could be shown that the Huggins coefficient for a class of models based on statistical assemblies of connected spheres should be identical with that of the hard sphere case. Deviations can be interpreted as due to specific interactions.

14571

Author

N67 14572

A Formulation of the Problem of Flow through Tubes

E. A. FOX* and EDWARD SAIBEL,* *Department of Mechanics, Rensselaer Polytechnic Institute, Troy, New York*

INTRODUCTION

It is the object of the present paper to formulate in a general manner the equations of motion of a fluid in a deformable tube; further, to put these equations in a form suitable for calculation, with particular reference to the flow of blood in arterial systems; and finally, to suggest experiments crucial to the formulation of the problem and its solution.

From the outset it is evident that the problem is far too complex to yield "closed solutions" and that the eventual use of digital or analog-digital calculating machines will be necessary..

It also becomes apparent that simplifications in the equations are necessary, but that in order to get meaningful results these must be carefully and consistently made. Even in the case of a Newtonian fluid flowing in a rigid circular tube of constant cross section, the equations have proved to be, so far, intractable. In fact just to show existence and uniqueness of a solution of this simple problem, one must be able to specify the entire velocity field initially, which is impossible in the blood flow problem.

Consequently, in the present work the equations have been averaged over the cross section. Thus, although the detailed velocity field is not forthcoming, quantities are obtained which it is hoped will yield information of physiological interest and which are functions of other measurable quantities.

The present formulation though does allow for a general type of fluid, inertia and time effects, a general type of distensible wall, general boundary conditions between wall and fluid including slip or no-

slip, leakage through the wall or not, variable cross section of the wall, and inclusion of body forces.

The last has great significance in that it allows for variation in position of tube, horizontal, vertical, etc.; as well as arbitrary rigid body motions of the tube. Thus blood flow can be calculated under dynamic conditions at rest in any position under any gravitational conditions or in motion on the earth or in space.

The equations may be derived by using the integral statements of the balance of mass and momentum applied to a volume element consisting of a piece of the tube cut by two planes a differential distance apart[1] or by integrating the differential equation across the cross section. Each method has distinct advantages in giving understanding to the coupling of fluid and wall. The authors have preferred the latter method.

EQUATIONS OF MOTION

The equation of continuity is

$$d\rho/dt + \rho \nabla \cdot \bar{u} = 0 \text{ or } \partial\rho/\partial t + \nabla \cdot (\rho \bar{u}) = 0 \tag{1}$$

The equations of linear momentum are

$$\nabla \cdot [\bar{\bar{\sigma}} - \rho \bar{u} \bar{u}] = \partial/\partial t (\rho \bar{u}) - \rho \bar{F} \tag{2}$$

where ρ is density, t is time, $\bar{u}$ is the velocity vector, $\bar{\bar{\sigma}}$ is the stress tensor, $\bar{F}$ is the body force vector, and ∇ is the customary vector operator.

The equation of angular momentum yields simply

$$\bar{\bar{\sigma}} = \bar{\bar{\sigma}}_c \tag{3}$$

which expresses the symmetry of the stress tensor, it being assumed that internal stress couples are absent.

Let

$$\nabla = \bar{k} (\partial/\partial_z) + \nabla_1 \tag{4}$$

where

$$\nabla_1 = \bar{i} (\partial/\partial x) + \bar{j} (\partial/\partial y)$$

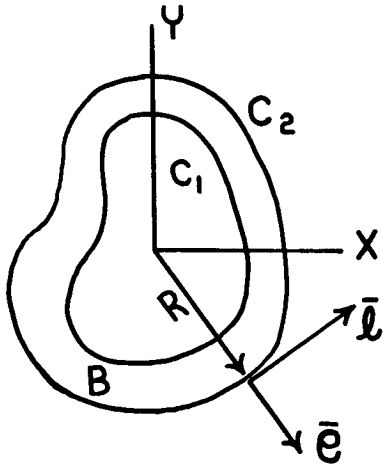

Figure 1.

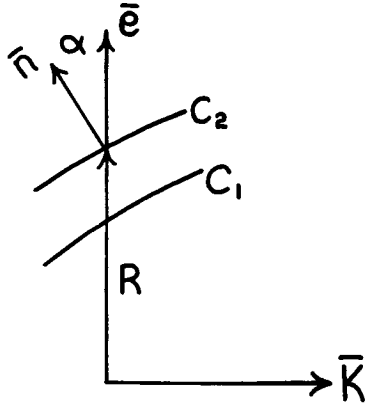

Figure 2.

Substituting eq. (4) into eq. (2), integrating over domain B (see Fig. 1), and applying the two-dimensional divergence theorem results in

$$\int_B \left\{ \frac{\partial}{\partial z} (\bar{T}_z - \rho \bar{u}_z \bar{u}) - \frac{\partial}{\partial t} (\rho \bar{u}) + \rho \bar{F} \right\} dB = - \oint_{c_1+c_2} (\bar{\bar{\sigma}} - \rho \bar{u}\, \bar{u}) \cdot \bar{e} dl \quad (5)$$

where $\bar{T}_z = \bar{k} \cdot \bar{\bar{\sigma}} = \bar{\bar{\sigma}} \cdot \bar{k}$ and $u_z = \bar{k} \cdot \bar{u}$.

Similarly, eq. (1) yields

$$\int_B \left\{ \frac{\partial \rho}{\partial t} + \frac{\partial}{\partial z} (\rho u_z) \right\} dB = - \oint_{c_1+c_2} \rho \bar{u} \cdot \bar{e} dl \tag{6}$$

Now (see Fig. 2)

$$\tan \alpha = \partial R / \partial z \tag{7}$$

$$\bar{n} = \bar{e} \cos \alpha - \bar{k} \sin \alpha \tag{8}$$

Hence,

$$\bar{c} = \bar{n} \sec \alpha + \bar{k} (\partial R / \partial z) \tag{9}$$

Further,

$$\begin{aligned} \int_B \frac{\partial}{\partial z} (\bar{T}_z - \rho u_z \bar{u}) dB &= \int_0^{2\pi} d\theta \int_{R_1(\theta,z,t)}^{R_2(\theta,z,t)} \frac{\partial}{\partial z} (\bar{T}_z - \rho u_z \bar{u}) r \, dr \\ &= \int_0^{2\pi} \left\{ \frac{\partial}{\partial z} \int_{R_1}^{R_2} (\bar{T}_z - \rho u_z \bar{u}) r \, dr - \right. \\ &\qquad \left. \left[(\bar{T}_z - \rho u_z \bar{u}) R \frac{\partial R}{\partial z} \right]_{R_1}^{R_2} \right\} d\theta \\ &= \frac{\partial}{\partial z} \int_B (\bar{T}_z - \rho u_z \bar{u}) dB - \oint_{c_1+c_2} \\ &\qquad (\bar{T}_z - \rho u_z \bar{u}) \frac{\partial R}{\partial z} dl \end{aligned} \tag{10}$$

Similarly

$$\int_B \frac{\partial}{\partial t} (\rho \bar{u}) dB = \frac{\partial}{\partial t} \int_B \rho \bar{u} \, dB - \oint_{c_1+c_2} \rho \bar{u} \frac{\partial R}{\partial t} dl \tag{11}$$

Equations (5), (9), and (10) yield

$$\begin{aligned} &\frac{\partial}{\partial z} \int_B (\bar{T}_z - \rho u_z \bar{u}) dB - \frac{\partial}{\partial t} \int_B \rho \bar{u} \, dB + \int_B \rho \bar{F} \, dB \\ &\quad = - \oint_{c_1+c_2} (\bar{\sigma} - \rho \bar{u} \, \bar{u}) \cdot \bar{n} \sec \alpha \, dl - \oint_{c_1+c_2} \rho \bar{u} \frac{\partial R}{\partial t} dl \end{aligned} \tag{12}$$

Similarly, eq. (6) becomes

$$\int_B \frac{\partial \rho}{\partial t}\, dB + \frac{\partial}{\partial z}\int_B \rho u_z\, dB = -\oint_{c_1+c_2} \rho \bar{u}\cdot\bar{n}\sec\alpha\, dl \quad (13)$$

We can write similar equations for the fluid in the hole A where now c_1 is the outer boundary and there is no inner boundary.

We shall now let the wall material B be denoted by primes and the fluid material A be unprimed. Further we shall consider the wall as solid so that the convective acceleration terms may be neglected. Then eq. (12) for the wall becomes

$$\frac{\partial}{\partial z}\int_B \bar{T}'_z\, dB - \frac{\partial}{\partial t}\int_B \rho'\bar{u}'\, dB + \int_B \rho'\bar{F}'\, dB = -\oint_{c_1+c_2} \bar{\bar{\sigma}}'\cdot\bar{n}\sec\alpha\, dl - \oint_{c_1+c_2} \rho'\bar{u}'\frac{\partial R}{\partial t}\, dl \quad (14)$$

while for the fluid eq. (12) becomes

$$\frac{\partial}{\partial z}\int_A (\bar{T}_z - \rho u_z\bar{u})dA - \frac{\partial}{\partial t}\int_A \rho\bar{u}\, dA + \int_A \rho\bar{F}\, dA = -\oint_{c_1} (\bar{\bar{\sigma}} - \rho\bar{u}\,\bar{u})\cdot\bar{n}\sec\alpha\, dl - \oint_{c_1} \rho\bar{u}\frac{\partial R}{\partial t}\, dl \quad (15)$$

At the interface c_1

$$[\bar{\bar{\sigma}}\cdot\bar{n} = \bar{\sigma}'\cdot\bar{n}]_{c_1} \quad (16)$$

noting that

$$\oint_{A\,c_1} = -\oint_{B\,c_1}$$

and if there is no transport between A and B then

$$[\bar{u}\cdot\bar{n} = \bar{u}'\cdot\bar{n}]_{c_1}$$

which follows from the requirement that the interface C_1, satisfy the surface condition[2]

$$\frac{d}{dt}[r - R(\theta.z.t)] = 0$$

Thus on C_1

$$u_r = \frac{\partial R}{\partial t} + u_z \frac{\partial R}{\partial z} + \frac{u_\theta}{R} \frac{\partial R}{\partial \theta}$$

$$u_r' = \frac{\partial R}{\partial t} + u_z' \frac{\partial R}{\partial z} + \frac{u_\theta'}{R} \frac{\partial R}{\partial \theta} \tag{17}$$

Thus eqs. (16) and (17) couple eqs. (14) and (15) which are completely general under the assumption of a nonpolar continuum and of no transport between A and B. However $\bar{F}$ and $\bar{F}'$ must be specified as well as the conditions on c_2.

Important special cases are covered by the following assumptions

$$\bar{F} = 0,\ \rho = \text{constant},\ \rho' = 0, \text{ and } [\bar{\bar{\sigma}}' \cdot \bar{n}]_{c_2} = 0$$

which express the following: no body forces, fluid of constant density, neglect of mass of the wall, and traction free outer wall surface, respectively.

Under these assumptions eqs. (14), (15), (16), become

$$-\frac{\partial}{\partial z}\int_A \rho u_z \bar{u}\, dA + \frac{\partial}{\partial z}\int_A \bar{T}_z\, dA + \frac{\partial}{\partial z}\int_B \bar{T}'_z\, dB - \frac{\partial}{\partial t}\int_A \rho \bar{u}\, dA = \oint_{c_1} \bar{u}\left[\bar{u} \cdot \bar{n} \sec \alpha - \frac{\partial R}{\partial t}\right] dl \tag{18}$$

and eqs. (13) applied to the fluid yields

$$\frac{\partial Q}{\partial z} = \frac{\partial}{\partial z}\int_A \rho u_z dA = -\oint_{c_1} \rho \bar{u} \cdot \bar{n} \sec \alpha\, dl \tag{19}$$

where Q is the flow.

All of the foregoing has been valid for any cross section. Let us now consider the case of axisymmetry. We note that eq. (18) is a vector equation and that upon integration over A or B there results

$$\int_A f(r)\, \bar{e}_r\, dA = 0 \text{ and } \int_A g(r)\, \bar{e}_\theta\, dA = 0$$

Thus the only nonvanishing component of eq. (18) is along the axis.

Dropping the unit vector $\bar{k}$, eq. (18) then becomes

$$-2\pi \frac{\partial}{\partial z} \int_0^R \rho u_z^2 \, r \, dr + 2\pi \frac{\partial}{\partial z} \int_0^R \sigma_{zz} \, r \, dr + 2\pi \frac{\partial}{\partial z} \int_R^{R + h \sec \alpha} \sigma'_{zz} \, r \, dr - 2\pi \frac{\partial}{\partial t} \int_0^R \rho u_z \, r \, dr = 2\pi\rho \left[u_z \left(\bar{u}' \cdot \bar{n} \sec \alpha - \frac{\partial R}{\partial t} \right) R \right]_R \quad (20)$$

Introducing the notation $P_z = 2\pi \int_0^R \sigma_{zz} \, r \, dr$, the axial force in the fluid, and $P_z' = 2\pi \int_R^{R + h \sec \alpha} \sigma_{zz}' \, r \, dr$, the axial force in the wall, and noting $u_r' \big|_R = \partial R / \partial t$ then using eq. (9) and (17), eq. (20) becomes

$$-2\pi \frac{\partial}{\partial z} \int_0^R \rho u_z^2 \, r \, dr + \frac{\partial P_z}{\partial z} + \frac{\partial P_z'}{\partial z} - \frac{\partial Q}{\partial t} \quad (21)$$

Let N be the meridional stress resultant and V the shear stress resultant (see Fig. 3). Then

$$P_z' = 2\pi R [N \cos \alpha + V \sin \alpha]$$

If we now assume $V = 0$, eq. (21) becomes

$$\frac{\partial Q}{\partial t} - \frac{\partial P_z}{\partial z} - 2\pi \frac{\partial}{\partial z} [RN \cos \alpha] + 2\pi \frac{\partial}{\partial z} \int_0^R \rho u_z^2 \, r \, dr = 0 \quad (22)$$

Assuming ρ is constant, eqs. (19) and (8) yield with (17)

$$\frac{\partial Q}{\partial z} = 2\pi\rho R \left[- \frac{\partial R}{\partial t} \right] = \rho \left[- \frac{\partial A}{\partial t} \right] \quad (23)$$

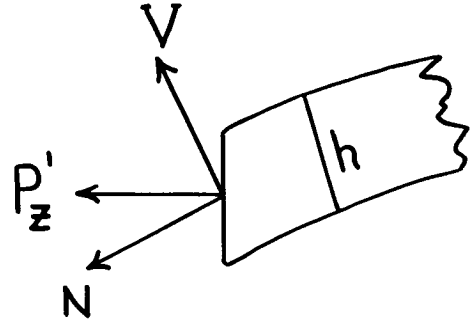

Figure 3.

Thus, eqs. (22) and (23) relate the flow, the axial force, and the wall motion. It is interesting to note that the integral in eq. (22) is set equal to zero (or never appears) in linearized theory. However by Schwarz' inequality

$$Q^2 = \left[2\pi\rho \int_0^R u_z\, r\, dr\right]^2 = \left[\int_0^R (\sqrt{2\pi\rho r})\,(u_z \sqrt{2\pi\rho r})dr\right]^2$$

$$\leq \rho A\, 2\pi\, \rho \int_0^R u_z^2\, r\, dr \quad (24)$$

This may be expressed

$$2\pi\rho \int_0^R u_z^2\, r\, dr = \beta(Q^2/\rho A) \quad (25)$$

where $\beta = \beta(z,t) \geq 1$.

If the velocity profile is flat, $\beta = 1$. As pointed out above, in linearized theory, $\beta = 0$. Lambert[3] arbitrarily sets $\beta = 1$. In other hydraulic applications β is determined experimentally.

If we now rewrite eqs. (21) and (23) making use of eq. (25),

$$\frac{\partial Q}{\partial t} + \frac{\partial}{\partial z}\left(\beta \frac{Q^2}{\rho A}\right) - \frac{\partial P_z}{\partial z} - 2\pi \frac{\partial}{\partial z}(RN \cos\alpha) = 0 \quad (26)$$

$$\frac{\partial Q}{\partial z} = \rho\left[-\frac{\partial A}{\partial t}\right] \quad (27)$$

The equations are valid for any type of fluid and any type of wall. So far no constitutive equation has been used for either fluid or wall. These equations represent balances of mass and momentum and are two equations in the unknowns Q, A, β, N, and P_z; R and α are known functions of A.

The parameter β in hydraulic applications is of the order of 1.03 to 1.1 for turbulent pipe flow and 1.33 for laminar flow. In biological systems this must be determined by experiment.

A constitutive relation for the wall, relating N and A must be determined. This may not be a simple rheological model, for the system may be active rather than passive, as in a servo or cybernatic system. In the arterial system in living creatures the cross-sectional area A is changed not only by mechanical interactions but possibly by internal chemical and electrical activity as well.

It is possible to take such activity into account by hypothecating various relationships, putting them in the above equations, solving, and checking with observed phenomena to establish indirectly the laws governing the behavior. It would seem at this time that direct experimentation is not feasible.

The constitutive equation for the liquid will introduce a new variable, namely, the spherical part of the stress tensor, sometimes called "pressure." This quantity is never measured in pressure sensing devices except in the static case. What is measured by these devices is difficult to correlate with the variables of continuum mechanics unless the problem of the flow in these devices is solved, a problem generally as difficult as the problem under study.[4] It is for this reason that the introduction of a constitutive equation for the fluid adds nothing to this formulation. It would be essential, however, if a detailed knowledge of the velocity field were desired. Hence, the authors believe that the net axial force P_z should be computed from the equations developed. It is this quantity that may have physiological significance, rather than the so-called "pressure."

The equations indicate that the proper transducer is the arterial wall itself. Wall motion measured on the intact organism at pressure points or other accessible places will permit Q and P_z to be computed at these stations. These are the quantities that may well correlate with physiological and clinical information.

References

1. Ginzburg, I. P., *Applied Fluid Dynamics*, Leningrad, 1958; translated as National Aeronautics and Space Administration Report NASATT F-94.
2. Lamb, H., *Hydrodynamics*, Cambridge, 1932, p. 7.
3. Lambert, S. W., *J. Franklin Inst.*, **266**, 83 (1958).
4. Truesdell, C., *J. Rat. Mech. Anal.*, **1**, 125 (1952).

Synopsis

14572

The equations of motion of a general fluid in an extensible tube are put in a form suitable for calculating flow from quantities which may reasonably be measured. These are the cross-sectional area of the tube, its time derivative and the derivative along its length. From these quantities, information regarding the flow rate and the axial force can be obtained. The equations are developed in terms of net axial force and thus obviate a fluid constitutive equation. Before meaningful calculations can be made the constitutive relations in the wall must be determined by experiment *in vivo*. The equations lend themselves to such experiments. The equations developed include inertia and body forces and are suitable for calculations of flow in deformable tubes.

Author

N67 14573

The Casson Equation and Rheology of Blood Near Zero Shear

E. W. MERRILL, W. G. MARGETTS, G. R. COKELET, and E. R. GILLILAND
Department of Chemical Engineering, Massachusetts Institute of Technology, Cambridge, Massachusetts

ALGEBRAIC ASPECTS OF THE CASSON EQUATION

Casson[1] has developed an equation relating the rheological properties of a suspension composed of particles which are capable of aggregating into rodlike clusters. His physical model thus suggests rodlike rouleaux such as encountered with human blood, and good correlation has been found between the rheological data taken on human blood with the Casson equation.[2,3] The Casson equation is of the form

$$\tau^{1/2} = S\dot{\gamma}^{1/2} + b \tag{1}$$

where

$$S = \left(\frac{\eta_0}{(1 - H)^{a\alpha - 1}}\right)^{1/2} \tag{2}$$

$$b = \frac{a\beta}{a\alpha - 1}\left[\left(\frac{1}{1 - H}\right)^{(a\alpha - 1)/2} - 1\right] \tag{3}$$

and τ is the shear stress in dynes/cm.^{2}, $\dot{\gamma}$ the shear rate in sec.$^{-1}$, η_0 the viscosity of the suspending medium in poise, H the hematocrit (volume fraction red cells), α a length factor, β a length factor, and a the orientation constant.

As can be seen from eq. (1) there is a square root-square root dependence between the shear stress and shear rate. In addition the equation predicts a yield shear stress although Casson's physical model does not predict a yield shear stress as such, due to the as-

PRECEDING PAGE BLANK NOT FILMED.

sumptions in his derivation that there are no interactions between the rodlike aggregates. The yield shear stress would be b^2.

Since the axial ratio is dependent on the shear rate, Casson makes the assumption that the axial ratio of the rodlike aggregate is inversely proportional to the square root of the shear rate as shown in eq. (4),

$$J = \alpha + \beta[(1)/(\eta_0\dot{\gamma})]^{1/2} \tag{4}$$

where J is the axial ratio of the rodlike aggregates. Equation (5),

$$J = [(9F_A)/(48\eta_0\dot{\gamma}_a)]^{1/2} \tag{5}$$

also a prediction of the axial ratio as a function of the shear rate, is derived by obtaining that axial ratio which will exist at the rod orientation which causes the maximum tension in the rod. Here F_A is the cohesive force per unit cross-sectional area of a rouleaux or rodlike aggregate in dynes/cm.[2]

By eqs. (4) and (5) an expression,

$$F_A{}^{1/2} = (48a/9)^{1/2}[\beta + \alpha(\eta_0\dot{\gamma})^{1/2}] \tag{6}$$

may be obtained for the cohesive force between the individual particles in the rodlike aggregates.

Considering the assumptions made by Casson, especially that there are no rod-rod interactions, it is interesting that the low shear rheological data taken on human blood should correlate so well with the Casson equations.

EXPERIMENTAL DATA

The constants α and β in eqs. (2) and (3) were determined from experimental rheological data obtained with the a Couette viscometer[3] by determining the shear stress as a function of the shear rate at different volume fractions of red cells. Following the equations of Casson, it is possible to obtain the extrapolated value of the yield shear stress as a function of the hematocrit or volume fraction red cells. Initially, shear stress-shear rate curves are plotted at different hematocrits as shown in Figure 1. The value of the shear stress at zero shear rate is designated by τ_y or the yield shear stress. In Figure 2 the slopes of the $\tau^{1/2}$ versus $\dot{\gamma}^{1/2}$ curves at low shear rates are graphed versus the function $(1 - H)$ on a log-log plot. The slope of this plot

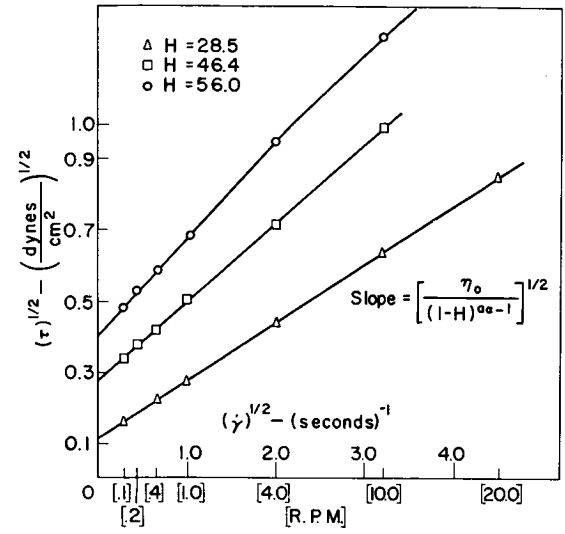

Fig. 1. Rheological properties of normal whole blood—Casson plot (K-4782).

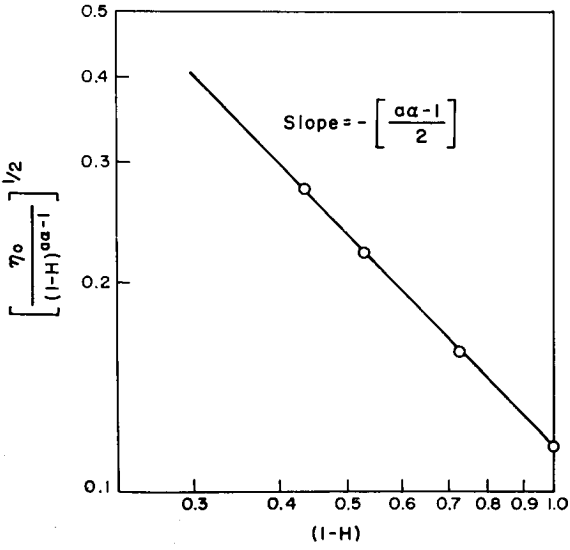

Fig. 2. Casson plot of normal blood (K-4782).

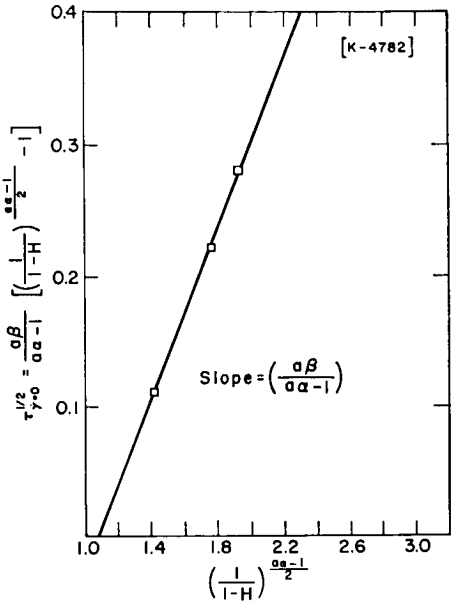

Fig. 3. Yield shear stress as a function of hematocrit.

is equal to parameter $-[(a\alpha - 1)/2]$. Following Casson's method in Figure 3, $\tau_y^{1/2}$ is plotted against function $[(1)/(1 - H)]^{[(a\alpha-1)/2]}$. The slope of the straight line thus obtained (Fig. 3) is $a\beta/(a\alpha - 1)$. For the purpose of evaluating α and β the orientation constant a is arbitrarily assumed to be $2^{-1/2}$ corresponding to alignment of the rod-like aggregates at an angle of 45° to the direction of flow—the alignment angle at which maximum tension in the rod should exist in consequence of viscous drag of the continuous medium.

Several samples of normal human blood have been analyzed in this manner to determine the effects of innate fibrinogen concentration[9] on the constants α and β. The results are shown in Table I and Figure 4.

It is found that α is substantially independent of fibrinogen concentration. On the other hand, β—which must be zero at zero fibrinogen concentration in accordance with the experimental finding that b (cf. eq. 3) is zero under this condition—gradually increases over the range of fibrinogen concentrations (0.2 to 0.5 g./100 ml.) found in normal human blood (Fig. 4).

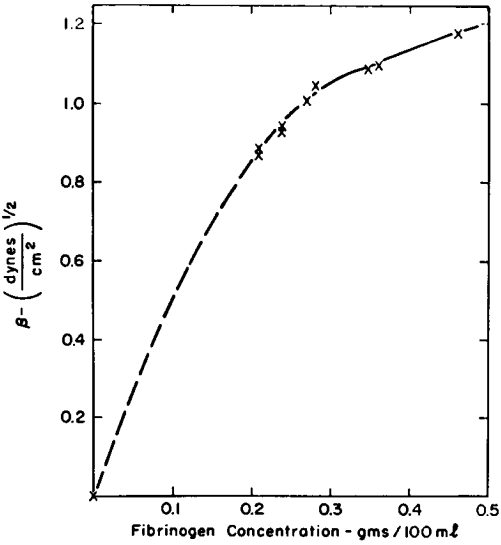

Fig. 4. Rheological properties of natural blood.

TABLE I
Effect of Fibrinogen on Casson Constants

Sample No.	$\frac{a\alpha - 1}{2}$	$\frac{a\beta}{a\alpha - 1}$	α	β	Fibrinogen concn., g./100 ml. (plasma + ACD soln.)
K-6005	1.05	0.301	4.39	0.894	0.21
K-6804	0.98	0.315	4.19	0.875	0.21
K-4782	1.05	0.317	4.39	0.940	0.24
K-1265	0.95	0.346	4.10	0.930	0.24
N-2380	0.98	0.364	4.19	1.01	0.27
N-8492	0.97	0.385	4.17	1.05	0.28
K-6237	1.00	0.385	4.25	1.10	0.36
K-5834	0.96	0.400	4.14	1.09	0.35
K-4370	0.92	0.454	4.03	1.18	0.46

Without reference to any theoretical significance, the technique of plotting rheological data as illustrated in Figures 1, 2, and 3 using appropriate values of α and β serves as a useful means of interpolation or extrapolation of shear stress-shear rate data and of estimating the

yield shear stress in the absence of direct experimental data, provided (*1*) that the only variables be hematocrit level H and the innate concentration of fibrinogen (in contradistinction to concentration of fibrinogen wholly or partly produced by the addition of the fractionated protein) and that (*2*) the blood be normal human, i.e., clinically administerable.

In the total absence of fibrinogen, or in plasma containing abnormally low concentrations of fibrinogen, the double square root plot of the experimental data leads to marked curvature and an intercept near, or coinciding with, the origin.

Figure 5 shows the rheological curves for a normal sample of blood and for the same red cells washed and suspended in various protein fractions. There was not an extrapolated yield shear stress for any of the protein fractions which did not contain fibrinogen.

Additionally, red cell suspensions have been prepared by adding washed red cells to saline solutions of varying fibrinogen concentration.[8] The correlation between the shear stress and the shear rate when graphed as square root vs. square root is quite good, as shown

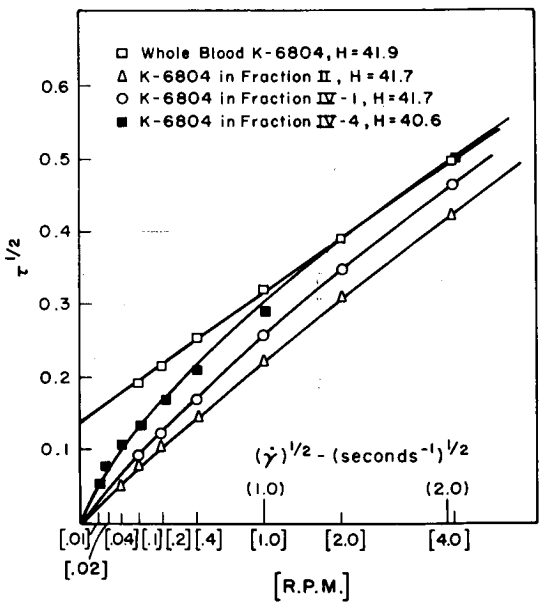

Fig. 5. Red cells suspended in protien fractions.

in Figure 6. In addition the correlation between the values of yield shear stress and the square of the fibrinogen concentration has been found to be linear.[8]

The values of yield shear stress obtained from red cells suspended in high molecular weight Dextran have also been shown to correlate with the concentration of Dextran. In fact, rheological data taken on all of the blood samples studied which contained fibrinogen or which were altered so as to cause aggregation have followed the square root-square root linearity of which Figure 1 is typical.

RELEVANCE OF THE CASSON MODEL TO BLOOD

Casson assumes that the axial ratio of the rodlike aggregates varies inversely with the square root of the shear rate as indicated in eq. (4). For the case of red blood cells aligning and bonding into rouleaux, such a relationship is arbitrary. In addition, the prediction that the axial ratio of the rodlike aggregate approaches infinity when the shear rate approaches zero is basically not valid. Normally, for

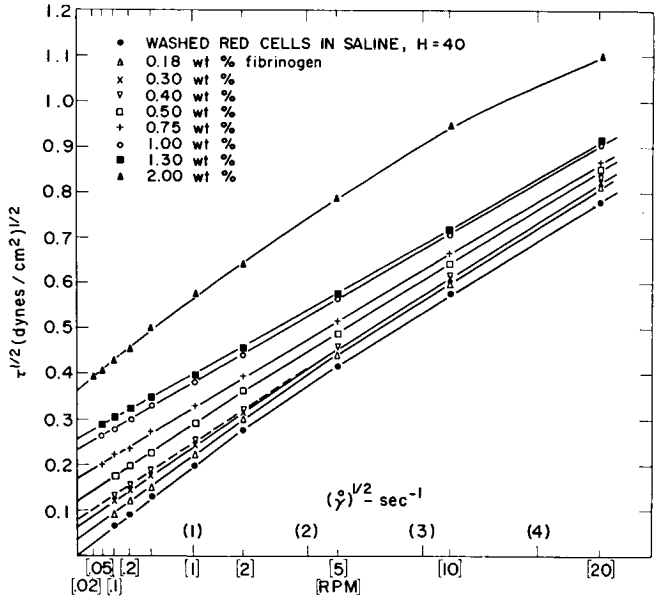

Fig. 6. Red cells suspended in fibrinogen solution.

the case of normal rouleaux formation, the axial ratio of the rouleaux cannot go to infinity as there are not an infinite number of primary particles or red blood cells. Also there are a number of nucleating sites (i.e., rouleaux ends), which are in competition for fundamental particles. It can be proposed that at exceedingly low shear rates the rouleaux are entangled and that substantially all of the red cells are in one large aggregate. However, this physical picture contradicts the mathematical and physical model used by Casson as he does not allow for any interaction between the rodlike aggregates.

Actually, in the shear rate range attainable experimentally (20 to 0.01 sec.$^{-1}$) the rouleaux occurring in the shear field would perhaps have from two to fifteen red blood cells, this observation based on microscopic work and the realization that rouleaux-rouleaux interactions and disentanglement will not allow a very large axial ratio once the system is undergoing shear.

In determining the axial ratio of the rodlike aggregates and the cohesive force between red cells, Casson makes use of that orientation which will produce the maximum tension in the rod caused by the shearing forces of the suspending liquid. This procedure enables the parameter β in eq. (3) to be calculated. Again, this tension in the rod is assumed to result only from shear forces caused by the suspending medium, and not by interactions between the rouleaux.

The largest discrepancy in the Casson model is that the effect of rod interactions on the rheological properties is not considered. If one considers cylinders or rouleaux with an axial ratio of J, uniformly suspended in a fluid and rotating in a plane parallel to the velocity gradient in a shear field, they will define an area of rotation such that the maximum volume fraction of rods possible without having collisions would be $\pi/(4J^2)$. Thus for $J = 2$ the maximum volume fraction is about 0.19, and for $J = 4$ about 0.05. This is the key problem to the Casson analogy, because the limits of maximum concentration imposed by tension in the rod and the equilibrium axial ratio by Casson's method prevent its theoretical application to any blood samples except those with a very low hematocrit.

Thus, the physical model set forth by Casson seems applicable only to very dilute suspensions of red cells in plasma. One must conclude that the model is inapplicable to suspensions of red cells of volume fraction (e.g., 40%) ordinarily found. On the other hand, the mathematical form of the Casson equation turns out to be an excel-

lent means, of correlating the shear stress against shear rate near zero shear, for red cells suspended in media containing fibrinogen or in media which promote aggregation (e.g., high molecular weight Dextran). It is inapplicable for suspended red cells which do not aggregate near zero shear rate.

This study was supported in major part by Public Health Service Grant HE-06423 from the National Heart Institute, U.S. Public Health Service.

References

1. Casson, N., *Rheology of Disperse Systems*, C. C. Mill, ed., Pergamon Press, New York-London, 1959, Ch. 5.

2. Merrill, E. W., C. R. Cokelet, E. R. Gilliland, and H. Shin, *Biophys. J.*, **3** (1963).

3. Cokelet, G. R., E. W. Merrill, E. R. Gilliland, H. Shin, A. Britten, and R. E. Wells, Jr., *Trans. Soc. Rheology*, **7**, 303 (1963).

4. Merrill, E. W., E. R. Gilliland, G. R. Cokelet, H. Shin, A. Britten, and R. E. Wells, Jr., *J. Appl. Physiol.*, **18**, 225 (1963).

5. Gilinson, P. J., Jr., C. R. Dauwalter, and E. W. Merrill, *Trans. Soc. Rheology*, **7**, 319 (1963).

6. Fahaeus, R., *Acta Med. Scand.*, **161**, 151 (1958).

7. Thorsen, G., and H. Hint, *Acta Chir. Scand., Suppl.* **154** (1950).

8. Margetts, W. G., E. W. Merrill, E. R. Gilliland, A. Britten, and E. W. Salzman, *Circulation Res.*, to be published.

9. Merrill, E. W., W. G. Margetts, G. R. Cokelet, et al., in *Proceedings of the Fourth International Congress on Rheology, Part 4*, Interscience, New York, 1965, p. 601.

Synopsis

14573

As a continuation of previous studies this paper is concerned with assessing the relevance to blood rheology of the model upon which N. Casson derived the equation

$$\tau^{1/2} = S\dot{\gamma}^{1/2} + b$$

where $S = [\eta_0/(1 - H)^{a\alpha - 1}]^{1/2}$; $b = [(a\beta)/(a\alpha - 1)][(1 - H)^{1 - a\alpha/2} - 1]$; τ is the shear stress, $\dot{\gamma}$ the shear rate, η_0 the viscosity of suspending medium, H the volume fraction of dispersed particles, a the factor depending on average orientation of aggregate, and α,β the constants. On the one hand, the *form* of the equation serves well in correlating the low shear rate data on blood near and at zero shear. On the other hand, the model on which the equation is based does not allow for attraction between, or three-dimensional structural organization of, the rodlike aggregates (rouleaux). The applicability of the Casson equations to the rheology of human blood is discussed.

author

CYTOPLASMIC STREAMING, HEMOLYSIS, SAP MOVEMENT

N67 14574

The Viscoelasticity of Slime Mold Protoplasm

SHIGEMI ABE,* *Department of Biology, Faculty of Science, Osaka University, Osaka, Japan*

INTRODUCTION

Estimation of the viscosity of living protoplasm has hitherto been attempted by a number of researchers through various methods. Whether or not protoplasm is elastic was once a subject of intensive discussion. Elasticity as an intrinsic attribute of the normal protoplasm was stressed especially by Seifriz a few decades ago.[1] It is now common knowledge that living protoplasm has both elasticity and viscosity, i.e., it is viscoelastic in nature. Quantitative aspects of viscoelasticity of living protoplasm were first dealt with by Crick and Hughes in cultured chick embryo cells through the application of a magnet-particle method.[2]

Since the plasmodium of the slime mold grows as an enormous mass of naked protoplasm, it is considered to be one of the most suitable materials for the study of rheological properties of living protoplasm. The plasmodium forms smooth strands which sometimes amount to 900 μ in diameter under favorable conditions. Viscoelasticity of the plasmodial strand was investigated by applying certain torques around its axis. This method was adopted because torsion around the longitudinal axis of a cylinder brings about practically no changes both in its length and in diameter.

EXPERIMENTAL

Smooth strands of the plasmodium of *Physarum polycephalum* from 500 to 750 μ in diameter and from 6 to 20 mm. in length were cut off from culture and were used as materials throughout the present investigation.

Length and diameter of the plasmodial strands were measured by a traveling microscope equipped with an ocular micrometer.

PRECEDING PAGE BLANK NOT FILMED.

Since there is a possibility that thickness and form of the plasmodial strands vary with time spontaneously, all experiments were made in a short period after the measurement of the diameter. These two values were checked before and after each experiment.

As reported by Kamiya and Seifriz,[3] the free end of the plasmodial strand hanging vertically in the moist air rotates alternately right and left with a nearly constant period with no external torque. Although this characteristic is of an obstructive nature for the present investigation, this spontaneous twisting of the strand is usually weak or scarcely observed within one hour after the preparation has been made. Consequently, in the present investigation all experiments were made within the period.

Investigation was made by the two methods. Setups for them are diagrammatically illustrated in Figure 1.

Method *A* and Results Obtained

A piece of plasmodium was put on the lower surface of an agar gel block *a* and kept in a moist chamber *c* to prevent from drying. After the plasmodium spread over the agar surface, one end of a plasmodial strand *s* was attached to the plasmodium on the agar and the other end was hung freely in the moist air. In 10 to 15 min. the two portions fused into one plasmodium. Thereafter a fine glass handle of a tiny weight *w* was attached to the lower free end of the strand. This weight, whose moment of inertia was known, was equipped with a minute mirror *m* working as an optical lever. In order to prevent the weight from slipping, it was held by a micromanipulator until adhesion between the protoplasm and the glass handle became strong enough to support the weight. Such a system worked as a torsion pendulum and showed a remarkable damped oscillation if a torque was applied and released for a brief period of time by slightly turning the cover of the moist chamber. Records were made photographically by means of the optical lever. Figure 2 shows one of the photographic registrations of the damped oscillation shown by this system.

Strong adhesion of the protoplasm with glass is a prerequisite for this experiment, because if a slip should occur between the protoplasm and glass handle the result obtained from the following measurements might deal with the properties of slip itself. However, this is not likely if a certain period of time has elapsed after

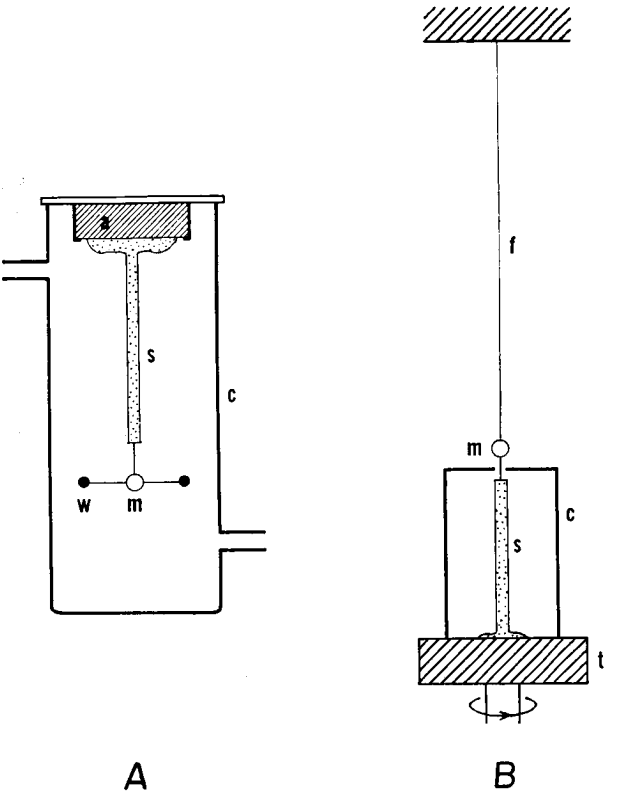

Fig. 1. Diagrams illustrating two setups for measuring the viscoelasticity of slime mold protoplasm.

attachment, since no sign of slip whatever was detected even when carefully observed.

Determination of the elasticity and viscosity values of the strand was made through the following formulas:

$$\gamma = \frac{2l}{\pi a^4} I \left[\left(\frac{2\pi}{T} \right)^2 + \left(\frac{\delta}{T} \right)^2 \right] \tag{1}$$

$$\eta = \frac{2l}{\pi a^4} 2I \frac{\delta}{T} \tag{2}$$

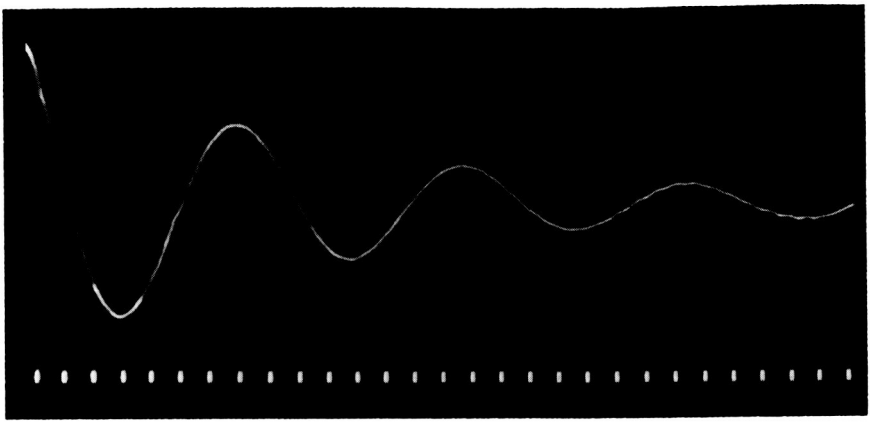

Fig. 2. Damped oscillation shown by the system illustrated in Fig. 1*A*. The length and diameter of the plasmodial strand used were 14 mm. and 650 μ, respectively. Time interval, $^1/_2$ sec.; temperature, 30°C.

In these formulas, l represents the length and a the radius of the plasmodial strand, T is the period of damped oscillation shown by the system, δ represents logarithmic decrement of the damped oscillation, γ is the modulus of rigidity, and η is the coefficient of viscosity of the strand. All of these values are experimentally determinable.

Some of the data determined by method *A* are shown in Table I.

TABLE I

Elasticity and Viscosity Values Obtained by Method *A*

Expt. No.	I, g. × cm.^{2}	l, cm.	a, cm.	T, sec.	δ	γ, dynes/cm.^{2}	η, poise
1	3.5×10^{-3}	2.7	3 × 10^{-2}	2.7	1.26	2.8×10^4	4.7×10^3
2	4.5×10^{-3}	1.7	3.4×10^{-2}	2.4	1.33	2.6×10^4	4 × 10^3
3	3.5×10^{-3}	1.3	4 × 10^{-2}	1.4	1.13	2.4×10^4	2.2×10^3
4	5.7×10^{-3}	0.9	2.7×10^{-2}	2.7	1.11	3.5×10^4	5.1×10^3
Av. value of γ and viscosity:						2.8×10^4	4 × 10^3

Though values of moduli of rigidity and viscosity thus obtained vary to some extent, they are nevertheless all in the same order. Average value of γ is 2.8×10^4 dynes/cm.^{2} and that of viscosity is 4×10^3 poise.

Method *B* and Results Obtained

In this experiment fine fibers of hard glass from 130 to 140 mm. in length and from 15 to 50 μ in diameter were previously prepared. One end of a glass fiber *f* was fixed with a metal chuck and hung freely right above the center of a turntable *t*. A circular protractor was attached to the turntable and the rotating angle of the table could be measured accurately. One end of a plasmodial strand was attached to the lower end of the glass fiber *f* and the other end to the center of the turntable *t*. Under such a setup, when the table was turned, the plasmodial strand was twisted. Concomitantly the glass fiber was also slightly twisted in the same direction. The twist angles of the fiber were measured by means of the ordinary lamp and scale method. Deflection of a light beam reflected at mirror *m* attached to the glass fiber was a measure of the torque applied to the strand. The twist of the glass fiber being exceedingly small, usually less than 0.4% of the twist angle of the strand, the rotating angle of the turntable can be regarded as the torsion of the strand. Thus

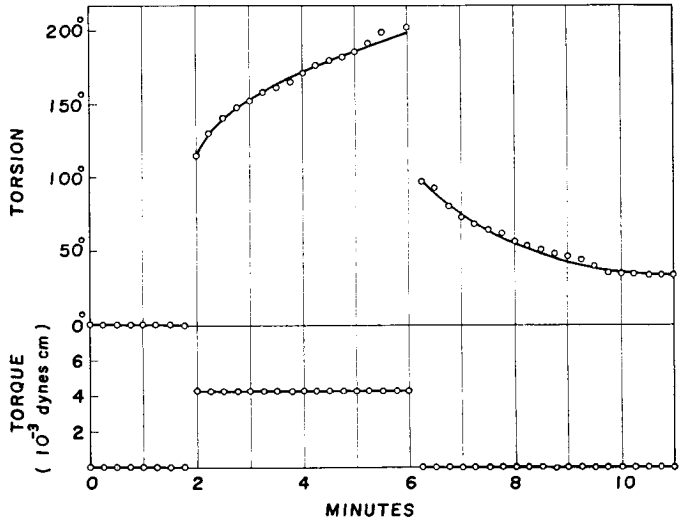

Fig. 3. Time course of the change in twist angle of a plasmodial strand on application and release of a torque (4.3×10^{-3} dynes $\times$ cm.). The length and diameter of the plasmodial strand used were 8 mm. and 380 μ, respectively. Temperature, 30°C.

stress-strain relationship in a plasmodial strand can be obtained. Measurements were made every 10 or 15 sec. Figure 3 shows one of the representative results obtained by this method when a constant torque was applied and released. As can be seen in the figure there was an instantaneous elastic deformation on application of a torque, which was followed by a nearly exponential creep. When the torque was removed, instantaneous elastic recovery was again observed, which was followed by an approximately exponential creep recovery. This type of behavior of slime mold protoplasm can be represented in terms of a four-element model.

Based on the foregoing experiment we are now in a position to determine each of the elasticity and viscosity values of the four elements, γ_1, γ_2, η_1, and η_2 in Figure 4.

Some examples of the values obtained by this means are shown in Table II.

TABLE II
Elasticity and Viscosity Values of the Four Elements Shown in Figure 4

Expt. No.	Plasmodial length, cm.,	Strand radius, cm., $\times 10^{-2}$	Torque appld., dynes cm. $\times 10^{-3}$	γ_1, dynes cm.^{2} $\times 10^4$	γ_2, dynes cm.^{2} $\times 10^4$	η_1, poise $\times 10^6$	η_2, poise $\times 10^6$
1	0.8	1.9	4.3	1	2.5	2	5.2
2	0.8	1.1	1.6	5	6.6	2.2	12

In the next place, a torque was applied on a plasmodial strand alternately in opposite directions. A time course of the change in twist angle of a plasmodial strand under such a treatment is shown in Figure 5. In this figure, it is noticed that the strain corresponding to each torque increases progressively. This fact indicates that the slime mold protoplasm is thixotropic in nature.

DISCUSSION

Regarding elasticity of slime mold protoplasm, Norris investigated stress-strain relationship of the plasmodial strands by pulling them, and found that its Young's modulus was about 9×10^4 dynes/cm.^{2}.[4] If the modulus of rigidity is calculated from the Norris Young's

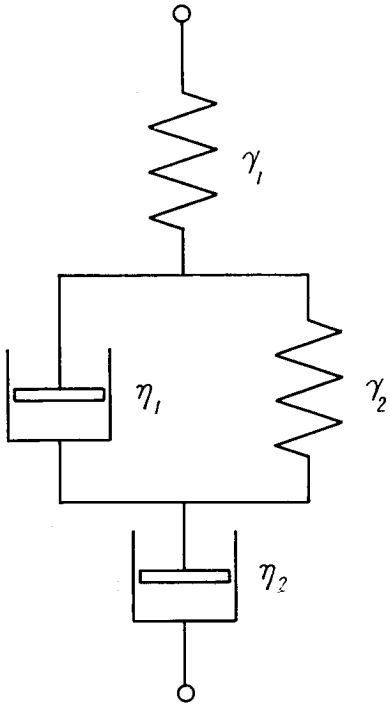

Fig. 4. A four-element model representing the viscoelasticity of the slime mold strand.

modulus with the assumption that the Poisson's ratio of the protoplasm is 0.5, it is known to be about 3×10^4 dynes/cm.^{2}. This value coincides neatly with those obtained by the above methods.

It is to be noticed, however, that the viscosity values obtained by the two foregoing methods are all much larger than the values hitherto obtained by previous authors in various materials by different methods. For instance, it was reported that in sea urchin eggs and amoeba the viscosity is only several times that of water.[5] Crick and Hughes estimated the order of the moduli of rigidity and viscosity of the cytoplasm of cultured chick embryo cells *in vitro* to be of the order of 10^2 dynes/cm.^{2} and 10 poises respectively.[2] The reason why the author's results show such high values both in moduli of rigidity and viscosity is probably because the material used in the present experiments was the plasmodial strand, a considerable part of which

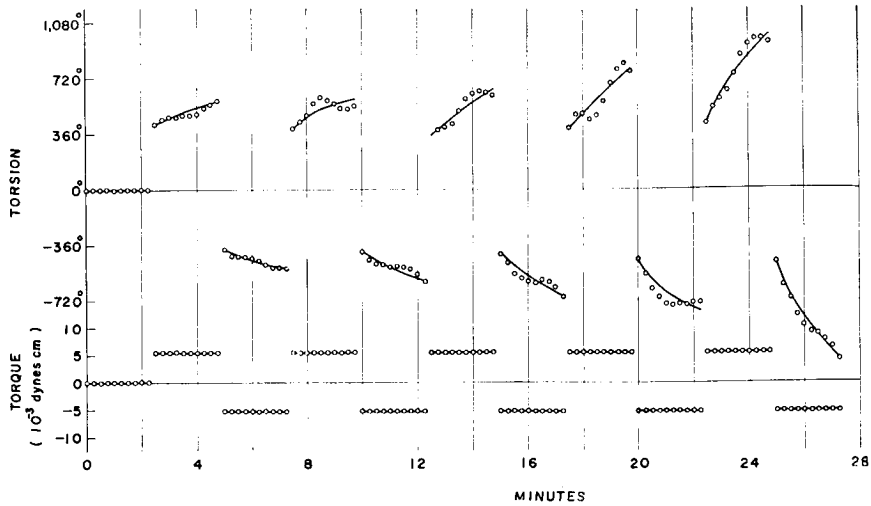

Fig. 5. Time course of the change in twist angle of a plasmodial strand under alternate application of a torque (5.4×10^{-3} dynes $\times$ cm.) in opposite directions. The length and diameter of the plasmodial strand were 11.8 mm. and 380 μ, respectively. Temperature, 25.7°C.

is made of gel ectoplasm, far surpassing the sol endoplasm, in both moduli. It is noticed that the values of the modulus of rigidity obtained by the two different methods used coincide very well, but those of viscosity are exceedingly different. Though the author is unable to explain this discrepancy, he believes it is because one is concerned with dynamic viscosity and the other with static viscosity. In other words, it may again reflect the thixotropic nature of the living matter such as demonstrated in the foregoing experiment.

The above methods give a unique opportunity to measure viscosity of the living gel cytoplasm for which there has been no known method of measurement. It is hoped that a further precise rheological analysis of viscoelastic system of the living protoplasm will be made possible by taking advantage of the technique used.

The author wishes to express his thanks to Professor N. Kamiya of Osaka University for his continued help during the course of the work.

References

1. Seifriz, W., *The Structure of Protoplasm*, W. Seifriz, ed., Iowa State College Press, Iowa, 1942.
2. Crick, F. H. C., and A. F. W. Hughes, *Exptl. Cell Res.*, **1**, 37 (1950).
3. Kamiya, N., and W. Seifriz, *Exptl. Cell Res.*, **6**, 1 (1954).
4. Norris, C. H., *J. Cell. Comp. Physiol.*, **16**, 313 (1940).
5. Heilbrunn, L. V., *An Outline of General Physiology*, Saunders, Philadelphia, 1952.

Synopsis

14574

(*1*) By analyzing a damped oscillation shown by the plasmodial strands, elasticity and viscosity values of the slime mold protoplasm were determined independently of each other. (*2*) On the basis of the type of deformation caused by the application and release of a torque, it is found that rheological behavior of the slime mold protoplasm can be well represented in terms of a four-element model. Each of these elasticity and viscosity values were determined. (*3*) When a torque was applied on a plasmodial strand repeatedly at short intervals, it was observed that the strain corresponding to each torque increased progressively indicating that the slime mold protoplasm is thixotropic in nature.

author

N67 14575

Rotational Protoplasmic Streaming in *Nitella* and Some Physical Properties of the Endoplasm

NOBURO KAMIYA* and KIYOKO KURODA, *Department of Biology, Faculty of Science, Osaka University, Osaka, Japan and Department of Biology, Princeton University, Princeton, New Jersey*

INTRODUCTION

Among various types of cytoplasmic flow, rotational streaming in the stonewort *Nitella* was the subject of extensive study for a long time. It is in this group of plants that protoplasmic streaming was discovered for the first time nearly two centuries ago. This paper is concerned with the streaming and some rheological properties of the endoplasm in this material.

This plant has cells several centimeters long with a continuous band of cytoplasm constantly rotating around its periphery.

INTRACELLULAR VELOCITY DISTRIBUTION[1-3]

Figure 1 represents the velocity distribution of endoplasmic streaming in a rhizoid cell of *Nitella flexilis*.[4] Here it can be seen that the small particles found on the transverse section YY' at an arbitrary time reach the points marked by open circles 1 sec. later. This figure shows that the protoplasm in different layers moves with nearly the same speed. Therefore, the endoplasmic layer is, as it were, sliding as a complete unit inside the cortical gel layer.

Next, the authors tried to make a cell having no vacuole, that is, with the whole cell space filled solely with the endoplasm to see how such a cell's protoplasm behaved. Of course no such cells exist in nature, but making a cell artificially is not impossible by an appropriate operation combining centrifugation and subsequent ligation.[4]

Figure 2 shows how it was done. Figure 2*a* represents a part of the normal internodal cell of *Nitella*. Here protoplasm streams along

PRECEDING PAGE BLANK NOT FILMED.

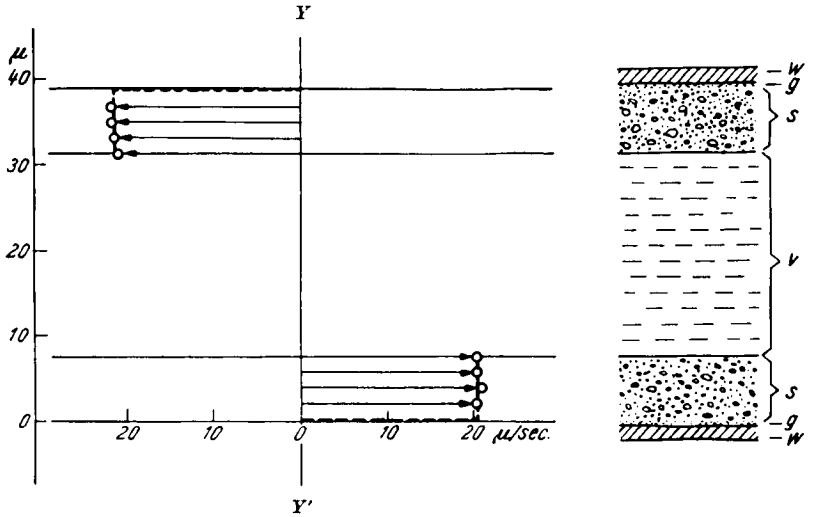

Fig. 1. Velocity distribution of the endoplasmic streaming in a rhizoid cell of *Nitella flexilis*. A part of the rhizoid cell as seen under the microscope is shown on the right: *w*, cell wall; *g*, plasmagel (ectoplasm); *s*, plasmasol (endoplasm); and *v*, vacuole (see ref. 4).

the cell wall. When the cell is centrifuged, the endoplasm is accumulated at the centrifugal end of the cell as shown in Figure 2*b*. Now, if the cell is tied off quickly with a strip of fine silk thread as shown in Figure 2*c*, we get two fragments of an internodal cell, one larger and poor in protoplasm and the other smaller and replete throughout its whole space with the endoplasm. The larger one does not survive long, but the smaller fragment filled with endoplasm can live practically for an indefinite period of time forming new vacuoles subsequently. What draws one's attention here is whether or not protoplasm can flow in such a cell.

Figure 3 shows that even in such a cell a rather vigorous streaming of endoplasm takes place. The right side shows a part of the plasm-filled cell fragment. There are thin cortical gel layers replete with chloroplasts. The main central space is filled with the endoplasmic sol. To the left is shown how the rate of the endoplasmic flow is distributed in the optical section through the axis of the cell. From this figure it can be seen that the rate is the highest in the direct proximity of the cortical gel layer and decreases as the center is

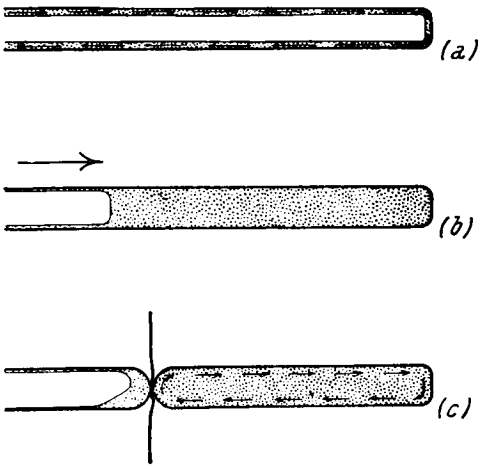

Fig. 2. The procedure for obtaining a plasm-filled cell fragment. (*a*) One end of an internodal cell of *Nitella* under natural condition. Chloroplasts in the cortical layer are not shown. (*b*) One end of the cell at which the endoplasm is collected under the influence of centrifugal force. Arrow indicates the direction of centrifugation. (*c*) A plasm-filled cell fragment produced through ligation from the centrifuged cell (see ref. 4).

approached. Though the authors will not go into details of analysis of this profile, this figure has a significant implication in that the endoplasm is driven, in this case, by the parallel shifting force generated at the boundary between the stationary cortical gel and the outer edge of the endoplasm.[4] It is this mechanical energy generated at this boundary that becomes the motive force of the protoplasmic streaming occurring in the cell of *Nitella*.

ISOLATION OF ENDOPLASM *IN VITRO*

Next, the internodal cell of *Nitella* was cut and only the endoplasm taken from it to observe what kind of behavior it manifested when it was out of the cell. The question here was how the cell was to be cut. In order to avoid collapsing the cell when cutting it, the authors made a glass vessel as shown in Figure 4.[5]

The cell *c* was placed in the tube *A* vertically in order to have the lower end of the cell reach out of the tube. In the glass tube *A*, as well as in the vessel *B* placed under it, was an isotonic balanced solu-

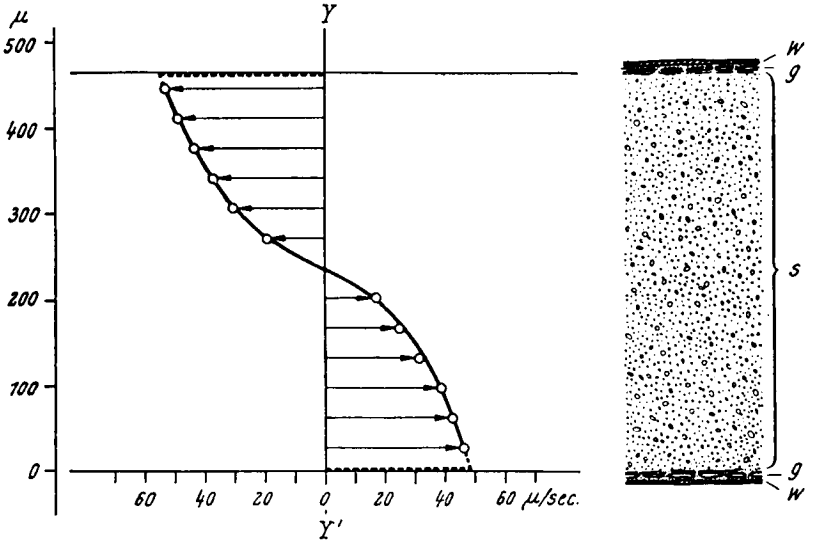

Fig. 3. Velocity distribution of the endoplasmic streaming in an internodal cell of *Nitella*, the entire space of which is filled with endoplasm. A part of the cell as seen under the microscope is shown on the right: *w*, cell wall; *g*, plasmagel layer in which chloroplasts are imbedded; and *s*, plasmasol (endoplasm). No vacuole is visible. The rate of protoplasmic streaming in an intact internodal cell was 78 μ/sec. Temperature, 28°C. (see ref. 4).

tion [0.08*M* KNO_3 + 0.05*M* NaCl + 0.004*M* $Ca(NO_3)_2$],whose cationic constitution was similar to that of the natural cell sap. The cell was then cut at the broken line while a negative pressure was given to *A*. The protoplasmic streaming was still kept going quite normally within the cell above the opening, but when the endoplasm, carried along by the streaming, came as far as the opening, it effused of its own accord out of the cell into the solution in vessel *B* (Fig. 5).

Such effusion of endoplasm lasts for 30 min. or longer. When the endoplasm in the cell is nearly exhausted, it ceases to make a continuous column but forms pendant drops continually.

The cytoplasm which comes out of the cell through such a procedure consists almost purely of the endoplasm, for the cortical layer remains completely within the cell except at the very limited part where it was injured at the opening. In such an isolated drop of endoplasm containing no ectoplasm there can be seen Brownian

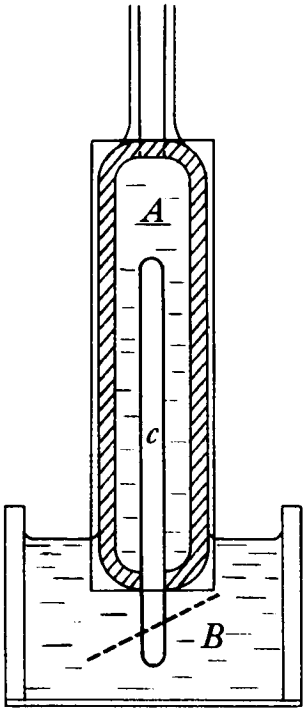

Fig. 4. The setup for cutting the *Nitella* cell while applying negative hydrostatic pressure. *A*, pressure chamber; *B*, vessel; and *c*, internodal cell of *Nitella*. Broken line indicates the locus where amputation is to be conducted (see ref. 5).

movement of minute particles, but there is no longer any sign of mass streaming of the endoplasm itself. This is a further confirmation of the conclusions arrived at before by the authors, to the effect that the rotational cytoplasmic streaming within the cell is caused by the active shearing force generated at the boundary between the cortical gel layer and the outer edge of the endoplasm and that the endoplasm is passively carried along.

At any rate by the method mentioned above, one can get *in vitro* enormous endoplasmic drops which survive in the artificial medium whose cationic constitution is similar to the natural cell sap for usually 24 hr. With an incubation medium containing glucose and proper growth substances the isolated endoplasmic

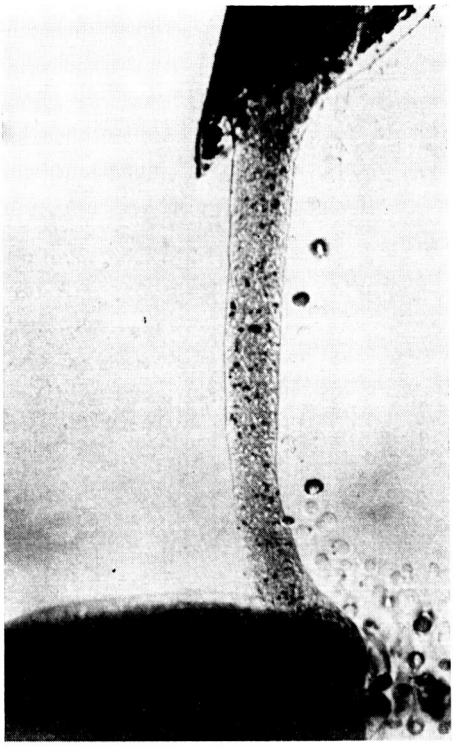

Fig. 5. Effusion of the endoplasm in the form of a continuous strand from the lower opening of the internodal cell of *Nitella flexilis*. On the bottom of the cuvette is seen a large drop of the naked endoplasm (taken about 30 min. after amputation) (see ref. 5).

drops can survive about three days outside the cell.[6] This can be confirmed by an active rotation of chloroplasts included in the drops.

DENSITY AND TENSION AT THE SURFACE OF AN ISOLATED ENDOPLASMIC DROP

Endoplasmic drops thus isolated give a unique opportunity to test its physical properties.

So far, density and tension at the surface were measured. The density of this endoplasmic drop was known to be from 1.014 to 1.015 g./cm.^{3} by the falling sphere method as well as the density gradient method.[7]

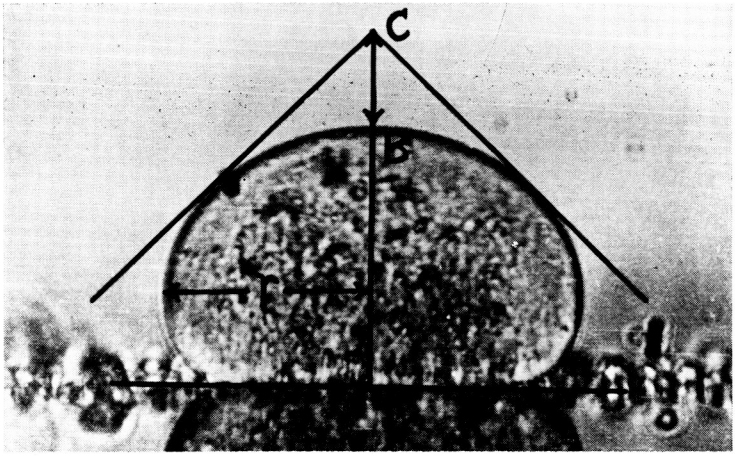

Fig. 6. The profile of a flattened sessile drop of endoplasm on the bottom of the cuvette (see ref. 8).

The profile of the naked drop of endoplasm fallen on the bottom of the vessel, when seen through a horizontal microscope, looks like that of a mercury drop (Fig. 6). When this drop forms a pendant drop at the opening of the cell it takes a form as shown in Figure 7.

Tension at the surface of the naked endoplasmic drop was calculated through the analysis of the profiles of both sessile and pendant drops. The values obtained from the two different methods coincide well. They are found mostly in the range of 0.002 to 0.004 dyne/cm.[8]

RHEOLOGICAL PROPERTIES OF THE ENDOPLASM

Next some rheological properties of the endoplasm thus isolated were studied.

Generally it is not possible to measure the viscosity of protoplasm by forcing it to flow through a minute glass capillary. One reason for this is that there has been no technique which enabled the authors to collect a sufficient amount of uninjured endoplasm permitting this kind of experiment. Another reason for this is that the living protoplasm often clots when it is forced to flow through an artificial

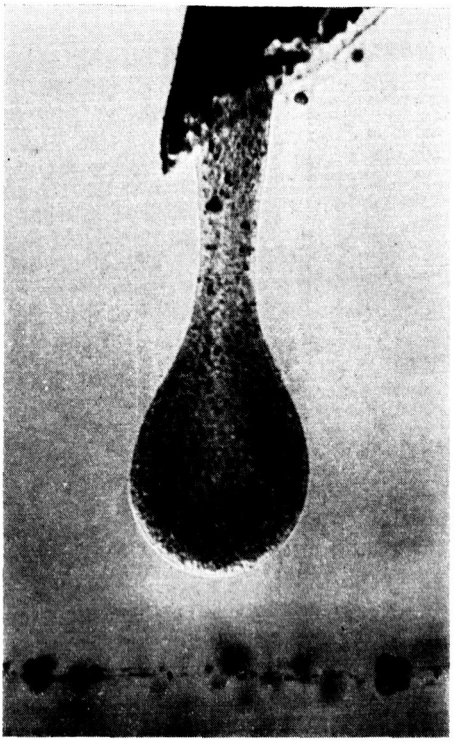

Fig. 7. A pendant drop of the endoplasm at the opening of the *Nitella* cell (see ref. 5).

capillary. Fortunately, however, this is not the case in isolated endoplasm of *Nitella* if a proper technique is applied.

In their experiment the authors tried to separate an endoplasmic drop into two chambers which were connected with a minute capillary and to induce the endoplasm to flow through it under moderate pressure gradient. *Nitella megacarpa* was used for this experiment.

Figure 8 shows a diagram of the experimental setup used. The endoplasmic drop was separated into two blobs *a* and *b* but they were connected with each other through the capillary penetrating the agar wall. By moving the vessel V_2 up and down by means of a

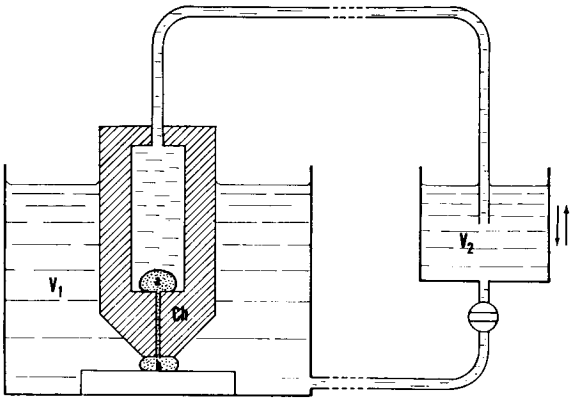

Fig. 8. A diagram of the experimental setup to induce the isolated endoplasm to flow through an agar capillary: *a* and *b*, blobs of endoplasm connected with a capillary; *Ch*, agar chamber; V_1, a vessel to which the lower blob of the dumbbell-shaped endoplasmic drop was exposed; and V_2, a vessel whose height can be adjusted by a microscrew.

microscrew, a hydrostatic pressure difference could be adjusted between the interior and exterior of the chamber very exactly.

The chamber was made of 4% agar dissolved in the artificial cell sap [0.08*M* KNO_3 + 0.05*M* NaCl + 0.004*M* $Ca(NO_3)_2$]. Agar capillary has a distingusihed advantage over glass, because it not only keeps endoplasm in a more favorable condition but further, in virtue of its refractive index extremely close to that of the endoplasm, it enables analysis of the velocity profile of the endoplasm when it flows under pressure gradient.

The agar chamber was made according to the technique developed by Kamiya for measuring the motive force of endoplasmic streaming in ameba.[9] Figure 9 shows how such a chamber was made, where F_1 and F_2 are the Lucite frames placed on a glass slide. Inside glass tubing *T* there is a glass capillary the lower end of which was fire-polished and ground off slightly so that a small hole was made just big enough to allow a glass fiber *f* of an appropriate diameter to penetrate it. This central glass fiber also penetrated a small hole made in frame F_2. Under this setup, the authors were then ready to pour molten agar throughout the circular and other narrow free spaces. While agar was still in a sol state a glass cover was placed on the top. After the poured agar had set, first the central fiber

was pulled, next the glass capillary; then the glass cover on the top, Lucite frame F_2 and finally the glass slide at the bottom of the frame were removed. What was left behind was a small agar chamber with a tiny capillary at its pointed end.

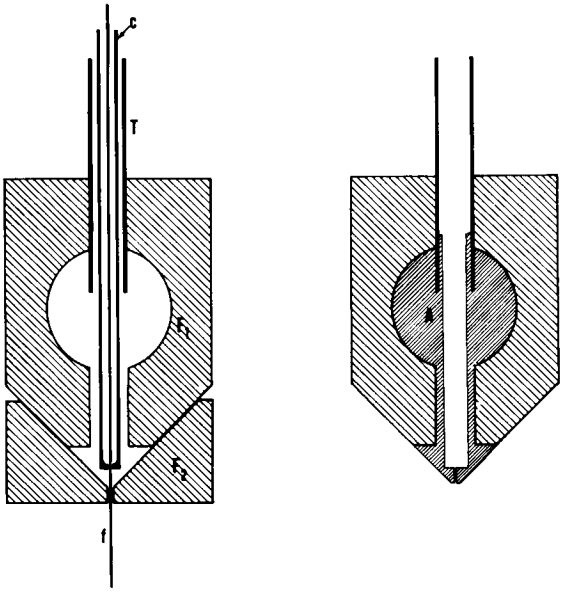

Fig. 9. A diagram showing the method of making an agar chamber with a tiny capillary at its lower end: F_1 and F_2, Lucite frames; T, glass tubing affixed to the frame F_1; c, glass capillary with a tiny hole at the lower end; f, glass fiber; and A, agar gel.

This whole system was then ready to be immersed in a vessel containing endoplasmic drops on the bottom. By bringing the orifice of the agar capillary in contract with the top of an endoplasmic drop, and by applying a weak negative pressure to the interior of the agar chamber, the endoplasm can be sucked up into the agar capillary in the form of a continuous column and be transported from the bottom of the vessel V_1 into the chamber Ch.

The flow of endoplasm between a and b was very sensitive to the difference in water level between V_1 and V_2. Pressure difference appropriate to the experiment was found to be less than 2 mm. of

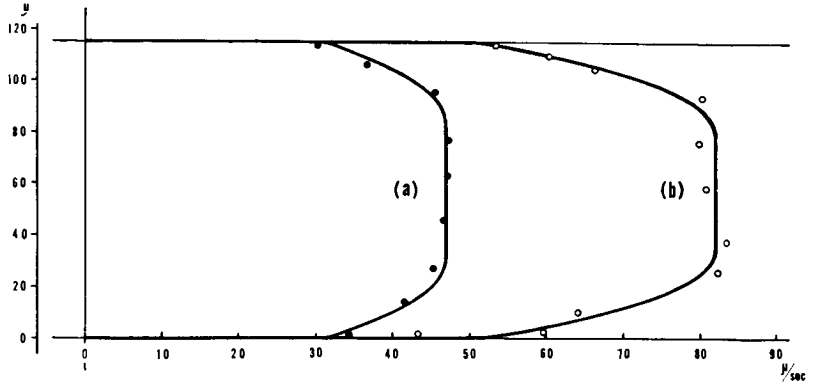

Fig. 10. Velocity profiles of the flow of endoplasm through an agar capillary 1 mm. long under pressure difference of (*a*) 1 mm. and (*b*) 1.5 mm. water column.

hydrostatic head.* A suitable diameter of the capillary is around 100 μ. The length of the capillary was from 1 to 1.5 mm. A longer capillary was not used simply because of the limited amount of the endoplasm which was about 0.02 mm.^{3}.

In order to obtain the velocity profile of the endoplasm passing through the capillary under known pressure gradient, the image of the flowing endoplasm was taken with a motion picture camera and the flow velocities measured at different strata through frame by frame analysis. Induced flow of the endoplasm did not seem to give harmful effect since the experiment could be repeated many times without clotting or without any sign of abnormal changes in plasm morphology.

Figure 10 shows one of the representative results thus obtained. The measurement was done at the middle region between the two openings of a 1 mm. long capillary. Curve *a* shows the velocity profile of the flow induced by the pressure of 1 mm. water column. Curve *b* is the velocity distribution under 1.5 mm. water column. From these profiles, one notices first of all that there is a considerable

* Pressure difference between the interiors of the two blobs may not be the same as the level difference between V_1 and V_2 due to the tension at the surface of the endoplasmic drop (0.002 to 0.004 dyne/cm.) and that of the difference in density between the endoplasm (1.015 g./cm.^{3}) and the external medium (1.007 g./cm.^{3}). But the error caused by these factors was less than 1% of the pressure applied and hence no correction was made for them.

slip between the agar wall and the surface of the endoplasm, but there is also a flow of the endoplasm. Except at the axial region where the endoplasm is likely to be moved as a plug, there is a distinct shear zone near the periphery. Without taking the slip into account, this type of flow is a good indication of the fact that the endoplasm is non-Newtonian.

As is well known, the shear stress τ in a fluid passing through a circular tube under a stationary state is given by

$$\tau = rP/2L \tag{1}$$

where r is the radius of a cylindrical element of the fluid, and P the pressure difference between the two ends of the capillary of the length L. Since

$$\tau = -\eta_a (dv/dr) \tag{2}$$

where η_a is the apparent viscosity, we get from eqs. (1) and (2):

$$\eta_a = -\frac{rP}{2L\,(dv/dr)} \tag{3}$$

Some of the numerical values obtained from tangents of the velocity profiles at the peripheral region of the intracapillary flow are shown in Table I. The data of experiments 2 and 3 were obtained from Figure 10.

TABLE I

Experimental Data of the Flow of Isolated Endoplasm through an Agar Capillary (temperature 24°C.)

Expt. No.	L, cm.	r, cm.	P, dyne/cm.^{2}	τ, dyne/cm.^{2}	dv/dr, sec.$^{-1}$	η_a, dyne/sec·cm.^{2}
1	0.1	0.0058	−69	−2	0.2	10
2	0.1	0.0058	98	2.8	−0.9	3.2
3	0.1	0.0058	−147	−4.3	1.7	2.5

From these data it was found that the apparent viscosity of the endoplasm becomes the higher the less the shear rate. Obviously the apparent viscosity is very different according to the shear stress τ applied. At a higher shear range, it is 2.5 poises or 250 cp.

Once the velocity profile of the endoplasmic flow under known pressure gradient is obtained it is possible to replot shear rate at each point in the radius against the shear stress which is linearly proportional to the radius as is indicated in formula (1). Such shear rate–shear stress diagrams, an example of which is shown in Figure 11, are always concave toward higher shear rate. As is seen in Figure 11, which was obtained from slopes of curve *b* in Figure 10, there seems to be the minimum shear stress τ_y causing the flow, that is, the yield value ("the lower yield value"[10]) of the endoplasm. It is around 1.5 dyne/cm.^{2}.

It is to be noted in this connection that the present experiments were all carried out rapidly in a very short period of time; the velocity profiles were determined from strips of cinematographic film covering 3 sec. As a matter of fact, in such a short term test, the endoplasm behaves as if it had a yield value. This, however, should not be taken too strictly, since the limited accuracy of the measurement does not allow one to decide whether the velocity profile at the plug region is perfectly truncate or only flattened. It is probable that the living endoplasm might behave somewhat differently were it possible for the authors to conduct a test of a longer term. What can

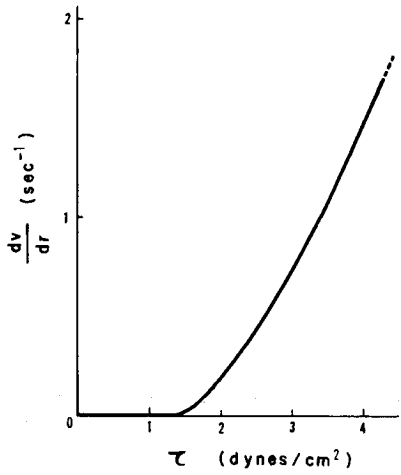

Fig. 11. Shear rate-shear stress diagram of the endoplasm constructed from fat line *b* in Fig. 10.

safely be said at present is that the apparent viscosity becomes exceedingly high when the shearing stress becomes smaller than 1.5 dyne/cm.^{2}.

In many of the previous papers dealing with the consistency of living cytoplasm the data of the absolute shear stress were not available. The present results show that the magnitude of applied shear stress, on which apparent viscosity is extensively dependent, is extremely important when discussing the consistency of cytoplasm.

CONCLUSIONS

The above rheological data were obtained from an endoplasmic system as a whole which contains a great many cytological organelles and inclusions of microscopical dimensions such as nuclei, vacuoles, etc. This is the reason why too thin a capillary was not used for the above experiments. At any rate, the rheological properties measured were those of a heterogeneous structure and not its matrix, or what is called ground cytoplasm. Yet these data explain that the endoplasmic layer in a living cell moves as a unit inside the cortical layer, there being scarcely any shear inside (cf. Fig. 1).

From these rheological data alone, however, the authors are still not in a position to answer the important question of why cytoplasm streams with the power generated in the cell itself. As stated before, what has been made clear so far is that the motive force responsible for this streaming is an active shearing force, or parallel shifting force, generated at the boundary between the cortical cytoplasmic gel layer and the outer edge of the endoplasm. The bulk of endoplasm is thought to be dragged by this shearing force generated in an entirely unknown manner. The crucial point of the mechanism of rotational streaming is, therefore, to elucidate how the tangential force is produced at the peripheral region of the cell.

A part of the present work was carried out during the author's sojourn at Princeton University, where they enjoyed the privileges of the laboratory through the courtesy of Professor R. D. Allen. This work was partly supported by a grant-in-aid from the Japanese Ministry of Education and partly by a research grant (RG8691) from the Institute of General Medical Science, U. S. Public Health Service administered by Professor R. D. Allen.

References

1. Kamiya, N., *Protoplasmatologia*, **8**, 3a (1959).
2. Kamiya, N., *Ann. Rev. Plant Physiol.*, **11**, 323 (1960).
3. Kamiya, N., *Handbuch Pflanzenphysiol.*, **17/2**, 979 (1962).
4. Kamiya, N., and K. Kuroda, *Botan. Mag. (Tokyo)*, **69**, 544 (1956).
5. Kamiya, N., and K. Kuroda, *Proc. Japan Acad.*, **33**, 149 (1957).
6. Kuroda, K., in *Primitive Motile Systems in Cell Biology*, R. D. Allen and N. Kamiya, eds., Academic Press, New York–London, 1964, p. 31.
7. Kamiya, N., and K. Kuroda, *Proc. Japan Acad.*, **33**, 403 (1957).
8. Kamiya, N., and K. Kuroda, *Proc. Japan Acad.*, **34**, 435 (1958).
9. Kamiya, N., in *Primitive Motile Systems in Cell Biology*, R. D. Allen and N. Kamiya, eds., Academic Press, New York–London, 1964, p. 257.
10. Houwink, R., *Elasticity, Plasticity and Structure of Matter*, Cambridge Univ. Press, New York, 1937.

Synopsis

14575

(*1*) From the velocity distribution of rotational streaming in the *Nitella* cell it was concluded that this type of streaming is driven by an active shearing force generated at the endoplasm-ectoplasm boundary. (*2*) By means of a suitable technique the endoplasm can be isolated out of the cell in comparatively large drops which can survive more than 24 hr. *in vitro*. (*3*) The density of the naked endoplasmic drops is from 1.014 to 1.015 g./cm.^{3}; tension at the surface is from 0.002 to 0.004 dyne/cm. (*4*) The isolated endoplasm can flow under an adequate pressure gradient if it is properly introduced into an agar capillary. (*5*) There is no indication that artificially induced flow under pressure gives rise to any harmful effect. (*6*) The velocity profile of the endoplasm in a circular capillary represents a plug flow. (*7*) From the velocity gradient of the intracapillary flow of endoplasm apparent viscosity of the endoplasm was measured under different shear stresses; it is 250 cp. when shear stress is 4.3 dyne/cm.^{2}. (*8*) Apparent viscosity increases rapidly as the shear stress becomes smaller than 1.5 dyne/cm.^{2}.

author

Abstract

Rheological Properties of Slime Mold Endoplasm

ROBERT D. ALLEN,* *Department of Biology, Princeton University, Princeton, New Jersey*

Before the advent of the electron microscope, biologists interested in the general problem of cytoplasmic structure often resorted to centrifugation, quantitative analysis of Brownian motion, and other procedures to measure "protoplasmic viscosity." While the techniques for studying the rheological properties of cytoplasm have not improved very much in recent years, modern rheology has made biologists aware that a great deal more information than "apparent viscosity" is required to characterize the rheological properties of cytoplasm. Early studies of "protoplasmic viscosity" were misleading in two important respects. First, the internal shearing forces in cells were greatly underestimated, so that some of the very low apparent viscosities measured were for shearing forces at which cytoplasmic structure had been destroyed, and second, cells subjected to centrifugation or to compression for some Brownian motion studies were not in a normal state when studied.

Plasmodia of the acellular slime mold, *Physarum polycephalum*, contain cytoplasm in at least two states: gelated channel wall material, which was the subject of Dr. Abe's paper, and more fluid endoplasmic material which streams back and forth with a characteristic periodicity. In some recent, incomplete experiments done in collaboration with Stephen Cox and Jonathan Belcher, an attempt has been made to determine some of the rheological properties of the endoplasm *in vivo*, under as normal conditions as possible. Iron spheres 3–8 in. diameter were injected into plasmodial blobs in a Kamiya double-chamber mounted on the rotating stage of a horizontal microscope. After resumption of normal streaming, some of the iron spheres were seen to pass along the channel connecting the blobs.

PRECEDING PAGE BLANK NOT FILMED.

When a suitable sphere appeared in view, a balance pressure was applied to one of the chambers and changed continuously so that the cytoplasm was prevented from streaming and the spheres kept in view. By rotating the stage, spheres of various sizes could be made to fall either across the endoplasmic stream or parallel to its axis at any point along the diameter in such a way that their displacements were recorded cinematographically.

It was invariably found that the iron spheres slowed down to 50–80% of their initial velocity when they reached approximately the central third of the channel. In the axial region of the endoplasm, the fall was discontinuous (or "bumpy") as though interrupted by obstacles. After passing through this region, the spheres again fell more rapidly. The same regional difference in resistance to fall was found when the spheres fell parallel to the axis of the channel. The variability in velocities in orthogonal directions and variability in the apparent viscosities calculated from Stokes' law for data on spheres of different diameters was such that it was not possible to establish a force-flow curve or determine whether the endoplasm was structurally anisotropic. Apparent viscosity values (calculated from Stokes' law with suitable corrections for channel dimensions) ranged from 0.2 to 1.5 poise, with very great variability between serial determinations. It was quite clear from these simple observations that streaming endoplasm of *Physarum* could in no way be considered to be a "watery" fluid, but rather a complex fluid in a highly unstable state and partially structured. Present rheological techniques which can be applied *in vivo* do not offer much hope of further analyzing this structure.

In a separate study to be reported elsewhere, Dr. Hiromichi Nakajima and I have examined slime mold plasmodia in polarized light. The ectoplasm contains positively birefringent fibrillar structures similar to those demonstrated electron microscopically by Wohlfarth-Bottermann, as well as diffuse birefringence due to unresolved structures. An unexpected finding, however, was a negative birefringence in the endoplasm which remains whether or not streaming is taking place. This finding emphasizes the dilemma that while the ground cytoplasm is sufficiently structured to be birefringent even during cytoplasmic streaming, the birefringence observed is not the immediate result of flow, as is the flow birefringence of solutions.

N67 14576

Brownian and Saltatory Movements of Cytoplasmic Granules and the Movement of Anaphase Chromosomes

EDWIN W. TAYLOR,* *University of Chicago, Chicago, Illinois*

INTRODUCTION

The cytoplasm in many types of cells contains particles ranging in size from a few microns down to the limit of resolution of the light microscope. Brownian motion of the particles is readily apparent in time lapse movies even though it may be hardly visible when the cell is examined under the microscope. In order to study the mechanics of the movement of chromosomes and other subcellular particles it is necessary to know the intracellular viscosity. An approximate value can be obtained from measurements of Brownian movement although the numbers must be employed with caution because of the non-Newtonian flow properties of the cytoplasm and the possible effects of the boundaries.

A study was made of particle movements in cultured cells of the newt (*Triturus viridescens*).[1] Most of the measurements were made on films of mitosis from the collection of Dr. R. E. Zirkle and Dr. W. Bloom. The methods of culture and photography have been described by these authors.[2] It was noted that occasionally particles executed a rapid, often rectilinear movement of as much as 20 μ in a few seconds. These large jumps were superimposed on a general random movement attributable to Brownian motion.

Similar movements have been described in a variety of plant and animal cells.[3–7] When the author's observations were made he regarded these movements as an uncontrollable source of experimental error which raised doubts about the validity of measurements of Brownian movement. These movements have since been studied in more detail by Rebhun[4–6] who has given them the name saltatory

particle movements. Therefore, a movement of this type shall be referred to as a saltation.

Measurements of Brownian movement excluding saltation are used to estimate the cytoplasmic viscosity which gives us a basis on which to discuss semiquantitatively the energetics of saltatory and chromosomal movements. A consideration of possible mechanisms of saltation suggests that the motive force is not generated by the particles but arises through association of the particles with (presumably) fibrous elements of the cytoplasm. Rebhun has arrived at an essentially similar conclusion.[5,6]

BROWNIAN MOVEMENT AND CYTOPLASMIC VISCOSITY

The viscosity of a Newtonian fluid can be computed from Brownian movement using the Einstein equation

$$\bar{X}^2 = (kTt)/(3\pi\eta a)$$

where $\bar{X}^2$ is the mean square particle displacement for successive equal time intervals t. The Boltzmann constant, absolute temperature, viscosity, and particle radius are k, T, η, a, respectively. Some measurements were made using the equation in this form but it was more convenient to employ the method of Fürth.[8] The equation can be rewritten

$$\eta = (kTt)/(3\pi aL^2n)$$

where t is the time for n first passages of the particle across a series of grid lines of spacing L.

In applying this method to the cell a number of sources of error must be considered:

1. Because of the large viscosity the passage times are large. It was necessary to determine whether other movements introduced by mechanical vibrations or thermal gradients would obscure the Brownian movement. For this purpose measurements were made on glycerol-water mixtures of known viscosity containing a low concentration of mastic particles. In the range from 1 to 300 cp. the error in the calculated viscosity obtained from one hundred passages was never larger than 30% and averaged about 12%. The error did not increase with increasing viscosity.

2. Wall effects. When a particle moves close to a wall Stokes' law must be modified.[9] The correction is appreciable when the distance to the wall is a few times the diameter of the particle. It was noted that viscosities computed from particles moving near the nuclear membrane were somewhat lower. Measurements on particles several diameters from the membrane often gave lower viscosity values for movements parallel to the membrane than perpendicular to it. Whenever possible particles for measurement were selected some distance from the membrane or spindle.

3. Heterogeneity. Some variations may be expected in different regions of the cell, but because of wall effects the measurements were made, as far as possible, on particles in the body of the cytoplasm. Thus although we assign an average viscosity to a given cell there may be variations near the nuclear or plasma membrane. The possible occurrence of viscosity "holes" is discussed under saltatory movement.

4. Non-Newtonian properties. The viscosity will probably depend on the shear gradient used in measuring it. The apparent viscosity of a dilute solution of asymmetric macromolecules increases with decreasing shear until the ratio of shear gradient to rotatory diffusion constant becomes small compared to unity. At very low shear gradients the behavior is approximately Newtonian.[10] At high concentration or if gel structures are present the viscosity may become very large as the shear approaches zero. The gel shows a yield point so that the stress must exceed some finite value before flow occurs. At very high shear gradients the viscosity may increase again because of relaxation processes and elastic effects may be evident (i.e., if the driving force is removed a particle may oscillate). The work of Crick and Hughes[11] has shown that elastic effects can be neglected in animal cells.

The steady motion of a sphere of diameter 1 μ and velocity 1 μ/sec. produces a maximum shear gradient close to the surface of the order of a few reciprocal seconds.[9] This is sufficient to cause some orientation of very long molecules. Thus the estimated viscosity may be expected to be somewhat less than the viscosity at zero shear gradient. We wish to use the viscosities obtained from Brownian movement to investigate saltatory and chromosomal movements. Ideally, the viscosity should be determined in the same shear gradient range as occurs in these movements. This

condition is not quite fulfilled since the shear gradient for saltations would be perhaps ten times higher than for Brownian movement. We therefore expect that any calculation based on the apparent viscosities would not be correct to better than a factor of two or three.

Subject to these reservations the apparent viscosities obtained for 22 cells in mitosis are shown in Table I. The average viscosity of a

TABLE I
Cell Viscosity during Division

Cell serial	Viscosity, cp.		
	Prophase	Metaphase	Anaphase
10-4	501	529	366
N-47	178	476	492
N-81	115	186	210
N-37	32	23	17
N-95	270	302	200
N-77	1000	1350	870
N-102	128	428	180
N-105	246	264	211
N-107	485	497	296
N-140	290	441	242
N-139	220	158	120
N-127	348	411	304
N-130	212	351	325
N-136	157	103	78
N-149	210	106	67
N-151	281	214	212
N-162	121	295	178
N-171	102	542	318
N-180	86	196	144
N-185	77	92	97
N-193	314	307	253
N-197	336	402	222
Av. viscosity	260	350	240

number of cells in interphase did not differ significantly from prophase values. The average passage time for one hundred passages of a group of particles was used except during anaphase where the time and the number of suitable particles available were not sufficient. Many of the films examined had to be rejected because the movements

were evidently not random. The cells (presumably fibroblasts) are capable of movement and when the cell drifted in the field the measurements had to be rejected unless a correction could be made by referring the displacements to a fixed point in the cell. If in a fixed cell displacements tended to carry the particle in a particular direction the measurements were rejected. This could arise from local currents but also from a viscosity gradient. Thus if there are local changes in viscosity the measurements will not show them and this may bias the average values reported here. The reproducibility of viscosities calculated from the movements of different sets of particles in the same cell was about 20%. It has been pointed out by Mysels[12] that if the motion of particles is caused by Brownian movement the root mean square path length should increase in proportion to the square root of the time interval. In the Fürth method the corresponding criterion is that the average first passage time should be proportional to the square of the grid spacing. This condition was satisfied since the value of the viscosity did not depend on the magnitude of the grid spacing.

The viscosity varied considerably from cell to cell covering a range of about a factor of ten. Differences in the intensity of particle movements were readily apparent when the films were screened. The average viscosity at metaphase is from 30 to 40% higher than in prophase or anaphase. The difference in the means is significant, well below the 1% level on the basis of Student's t test. A decrease in viscosity at anaphase derived from qualitative observations of Brownian movement has also been reported by Carlson.[13] Since the change is small and might arise in a number of ways this point will not be stressed.

SALTATORY MOVEMENTS

Occasionally a particle was seen to execute a translation which appeared to belong in a different class from the Brownian movements since the displacement was several times the average value of all other movements of the given particle. The average translation in a 4-sec. interval (the time between frames) of a particle 1 μ in diameter in a medium of viscosity 300 cp. is 0.35 μ. In a number of cases, displacements of 4 to 6 μ were recorded on successive frames. The probability of the saltatory movement occurring by Brownian motion

can be calculated from the root mean square displacement of the particle excluding the saltation.[14] A number of saltations were tested, and the probabilities were found to be about 10^{-6}.

Therefore, the saltations cannot be caused by Brownian movement in a medium having the average viscosity of the cell. However, the high apparent viscosity is probably attributable to lamellar or gel elements, and one must consider the possibility of "holes" filled with cell sap which could have viscosities one hundred times smaller. On this basis many of the saltations could arise by Brownian movement, although the largest ones involving velocities of 10 μ/sec. still could not be explained. The occurrence of large regions of low viscosity persisting for a few seconds appears improbable, but the physical evidence alone does not allow one to entirely discount this mechanism. Rebhun[5] has noted a radial arrangement of the endoplasmic reticulum about the centrosome region where saltations occur most frequently. Although radial channels may facilitate saltations, it is unlikely that the movement can be accounted for in this way. In particular, it does not explain why the particles accumulate in the asters.

CHROMOSOME AND CENTROSOME MOVEMENTS

Anaphase movements can be divided into two parts: (*1*) the motion of the chromosome from the equator to the poles of the spindle for which a plot of chromosome to pole distance versus time is roughly exponential; (*2*) the separation of the poles which proceeds at constant velocity.

The velocities are of the order of a few microns per minute.

In a representative newt cell the chromosome to pole movement occurs at an average velocity of 4 μ/min. over a distance of 10 μ in a medium of viscosity 300 cp. If the chromosome is represented by a cylinder of radius 1 μ and length 10 μ moving with the long axis perpendicular to the direction of motion the work done is 1.2×10^{-11} dyne cm. per chromosome or about 60×10^{-11} dyne cm. for the chromosome set. This figure was obtained using the formula given by Lamb[9] for the drag on a cylinder.

The spindle elongation step can be represented by the motion of two spheres of radius 5 μ moving at a velocity of 2 μ/min. The work done is approximately 20×10^{-11} dyne cm. Therefore, the

total work done is approximately 10^{-9} dyne cm. These figures can be taken only as order of magnitude estimates. The important point is that the numbers are very small relative to the energy available to the cell. By comparison the energy required to synthesize the protein of the mitotic apparatus allowing one molecule of ATP per peptide bond, and a free energy of 7 kcal./mole for ATP is about 2×10^{-11} kcal. The mechanical work is equal to 2×10^{-20} kcal.

This point may be illustrated in another way. A muscle of cylindrical shape and the same volume as the mitotic spindle could perform work equal to 2×10^{-3} dyne cm. in contracting to 60% of rest length under a load of 2 kg./cm.^{2}. This is 10^6 times greater than the mechanical work done by the mitotic apparatus.

The small quantity of mechanical work performed suggests that the rate of chromosome motion is not determined by energy dissipation in overcoming viscous drag. To illustrate this point the velocities of chromosome and pole movements were measured in cells for which viscosity data were available. The Reynolds number, which is the ratio of the inertial to viscous forces is the order of 10^{-6}. Therefore inertial effects can be completely ignored, and hence one expects that in cells of different viscosity ηv should tend to be constant at corresponding points in the movement. The velocity decreases as the chromosomes approach the poles, so to compare different cells one must select a velocity at some reference point such as the initial velocity. This is difficult to measure so one compares instead the values of $t_{1/2}$, the time to travel half the initial distance to the poles. The plot of chromosome-pole distance versus time

TABLE II
Motion of Chromosomes to Poles

Cell serial No.	$t_{1/2}$, min.	Viscosity η, cp.	$\eta/t_{1/2}$[a]
37	2	17	9
130	2.3	325	140
149	2.5	67	27
55	2.8	527	190
47	3.5	492	140
185	3.5	97	28
151	3.7	212	57

[a] Here $t_{1/2}$ is the time necessary to travel one-half the original distance to the pole.

can be fitted by an exponential function; therefore, it can easily be shown that $t_{1/2}$ is inversely proportional to the initial velocity. Hence if the viscous drag determines the velocity, $\eta/t_{1/2}$ should be constant in cells with different viscosities. (There is some variation in spindle length from cell to cell, but if there is an increased initial velocity for longer spindles this will be partially canceled by comparing values of $t_{1/2}$ rather than initial velocities.) The data in Table II show no correlation between $t_{1/2}$ and viscosity.

Similarly, for the separation of the poles which occurs at a constant rate, ηv should be a constant while the data in Table III show no such relationship.

TABLE III
Spindle Elongation

Cell serial No.	Velocity v, μ/min.	Viscosity η, cp.	$v\eta$
127	0.85	304	260
47	0.89	492	440
77	1.16	870	1000
151	1.35	212	290
149	1.36	67	90
185	1.75	97	170

The results of our attempt to analyze chromosomal and pole motions are essentially negative. However, certain conclusions of a limited nature may be drawn.

The lack of dependence of the velocity of movement on the viscosity of the medium and the very small amount of mechanical work done on the chromosomes suggest that the energy requirement is largely a matter of the internal structure of the spindle. Chromosome movements have often been described in terms of a contractile system moving a weight through a viscous medium, and analogies have been drawn to muscle contraction. Since it has been shown that varying the load by a factor of more than ten (through the differences in viscosity) did not effect the chromosome velocity, one should at best compare the spindle with an unloaded muscle. If the velocities of twitch contractions were measured over a range of vanishingly small loads it would be found that the velocity of contraction was independent of load. In this case the velocity of shortening would be determined by the internal resistance of the

muscle itself. Furthermore, the external work done in contracting a distance x would not be a measure of the energy expended since almost all of the energy would be accounted for by the activation heat and the heat of shortening a distance x. Therefore, the external work done in chromosome movements may be orders of magnitude smaller than the total energy expended by the mitotic apparatus. For example, a muscle of the same dimensions would produce 10^{-14} kcal. in shortening heat, while the external work done on the chromosomes was found to be only 10^{-20} kcal. (The thermal data refer to frog sartorius muscle.[15])

MECHANISM OF SALTATORY MOVEMENT

The properties of saltatory movement have been discussed in detail by Rebhun[5] based on observations of eggs of the surf clam, *Spisula solidissima*, the annelid, *Pectinaria*, and melanocytes of the minnow, *Fundulus*.

A number of different kinds of granules are involved in saltatory movement: β granules in *Spisula*, melanin granules in *Fundulus*, echinochrome granules in the sea urchin *Arbacia*, and unidentified particles in newt fibroblasts.

Rebhun has stated that the characteristics of the motion are: (*a*) uniform velocity uninfluenced by the proximity of other particles (although the particles of a group are sometimes observed to move together), (*b*) only one or two types of granules are involved, and (*c*) no change in form or size of the particle is observed.

The motion occurs occasionally during interphase but is most intense during prophase and metaphase. The granules appear to be attracted by the aster and partly also by the mitotic spindle surface and undergo motions which tend to be radial to the center of the aster or parallel to the surface of the spindle.

The author's observations on newt fibroblasts in tissue culture are essentially in agreement with *a* and *c*. The main differences are the following:

1. No special type of granule has been implicated in the movement. The particles have simply been referred to as lipid granules. The multivesiculate β granules of Rebhun have not been observed in electron micrographs of these cells although a specific search has not been made.

2. The saltatory movement is not always as striking as in the eggs described by Rebhun, but a few cells do show marked association of granules with the asters and the mitotic spindle.

The mechanism of saltations is unknown and since the work done in these movements is small both in absolute magnitude and relative to other energy requiring processes in the cell it is necessary to give at least a preliminary hearing to a variety of theories. Similar comments apply to anaphase movements.

Two general criteria can be applied to decide whether a particular mechanism is feasible. First, we have the general character of the movement. Particles travel large distances at relatively constant velocities which do not seem to correlate with the size of the particles. The movements lead to an accumulation of particles around the asters and to some extent along the spindle surface. This behavior is strong evidence against field theories in which the particles are moved by a force generated in the centrosome or near the plasma membrane. Such theories, as discussed below, lead to inverse power law forces which are usually dependent in magnitude on the particle volume. The small dimensions of the cell and the presence of many particles will lead to reflections or distortions which prevent any simple spacial dependence of the field strength. This also suggests that a translation covering a moderate fraction of the cell dimensions would be difficult to explain. Theories which require a special structure for the particles, such as a jet propulsion theory, are extremely improbable since the movement is exhibited by a variety of particles, which do not have common structural features.

Secondly, one may give an order of magnitude calculation on the forces which could arise from a particular mechanism using reasonable values for the parameters. In many cases this will show that the mechanism cannot generate the required forces.

Theories in which heat produced in local regions by metabolism produces flow or supplies energy for a jet can be dismissed. The high thermal conductivity reduces the efficiency of such mechanisms to extremely small values. The rate of production of heat cannot produce thermal convection in an object the size of the cell since the critical Rayleigh number for the onset of convection[16] is orders of magnitude larger than values calculated for the cell.

A number of field theories require brief consideration. Particle

movements could be attributed to (*a*) electric fields, (*b*) hydrodynamic fields (Bierknes pulsating sphere theory,[17] and (*c*) diffusion fields (Rashevsky-Landahl diffusion drag theory[18]).

We consider as a representative particle a sphere of diameter 0.5 μ moving with a velocity of 5 μ/sec. in a fluid of viscosity 100 cp. The applied force from Stokes' law is 2.5×10^{-8} dyne and the power output is 10^{-10} dyne cm./sec. It is worth noting that the work done in a saltation is the same order of magnitude as that done on a chromosome during anaphase. Since the asters appear to be involved in both types of movement the mechanisms may be similar.

Electric Fields

Electrostatic forces have been proposed as an explanation of chromosome movements, but simple considerations show that the theory is untenable. The cell is a relatively good conductor, thus if two oppositely charged bodies are placed in the cell a counter ion atmosphere will form around them producing a double layer distribution. At an ionic strength of 0.1 the Debye radius (the distance over which the field decreases to $1/e$ or about 1/3 of its initial value) is 10 A. Therefore, a field can be maintained over moderate distances only through continuous current flow. The system as a whole must remain electrically neutral which requires both a source and sink of current.

In any chemical reaction the net charge is unchanged; thus, it is very difficult to conceive of any mechanism by which a continuous current could be produced. In any case a calculation shows that the strength of the current source would have to be prohibitively large to move granules or chromosomes at the required velocities. Since the charge on the objects to be moved will be screened by the counter ions, the velocity will be determined by the zeta potential.[19] Although its value could be estimated, the electrophoretic mobility of the granules (and therefore the velocity) can be obtained from known values for biological particles (bacteria, red cells, etc.) in aqueous solutions.[20] The field strength necessary for saltations in a medium of viscosity 100 cp. is the order of 100 v./cm. At a distance of 10 μ from a spherical source the current strength of the source necessary to maintain this field strength is 10^{-10} g. equivalents per second. (The conductivity was taken as 0.01 mho/cm. corresponding to 0.1M KCl or axoplasm,[21] and the charge change was

taken as one unit.) Since the charge is to be produced by a chemical reaction, if we take the molecular weight of a reactant as 100, the mass of material reacting per second exceeds the dry mass of the cell.

Hydrodynamic Fields

It was suggested by Lamb[22] in 1907 that the separation of the poles might be accomplished by the force of repulsion of pulsating or oscillating spheres located in the centrosomes. The idea was based on the hydrodynamic studies of Bierknes.[17] The hypothesis was further extended by Cannon[23] to the chromosomes, since according to Bierknes a body of different density from the surrounding fluid would move in the field of two pulsating or oscillating spheres. Succeeding authors (e.g., Schrader[24]) have continued to refer to the theory, and it has also been discussed (and dismissed) by Rebhun[6] as a possible driving force for saltations.

The requirements of the theory do not seem to have been critically examined possibly because Bierknes' work is described in two large volumes. (A treatment of the pulsating sphere problem has also been given by Hicks.[25]) The work of Bierknes, which was intended as a hydrodynamic analog of electric forces, applies to a nonviscous, incompressible fluid. In a real fluid a small pulsating sphere (a sphere which undergoes cyclic volume changes) is a simple sound source, while an oscillating sphere acts as a dipole source.[26] The author's remarks will be confined to a pulsating sphere since the field of an oscillating sphere is smaller.

The problems to be considered are the interaction of two point sources of sound and the motion of a sphere in a sound field. Even at a frequency of 1 Mc. the wavelength of sound in a liquid is the order of millimeters. Thus the Bierknes force cannot depend on a pattern of standing waves in the cell as was supposed by Rebhun.[6])

First consider the motion of a sphere in the sound field of a spherical source of radius 1 μ pulsating with an amplitude of one-tenth the radius. Clearly the power utilized in saltations cannot exceed the power output of the source. The power output in a medium of density one is $\pi f^2 Q_0^2/2v$ where f is the frequency, v is the velocity of sound (1.5×10^5 cm./sec.) and Q_0 is the source strength (the maximum radial flow velocity at the surface of the sphere[26]). Where

a is the average radius of the sphere and αa is the amplitude of pulsation, $Q_0 = 8\pi^2 f \alpha a^3$. To achieve a power output of 10^{-10} dyne cm./sec., f must be about 20,000 cycles/sec. In addition, the energy removed from the field by scattering of the wave by a sphere a micron in diameter will be very small, since it depends on the fourth power of the ratio of particle dimension to wavelength. Therefore the source must pulsate at frequencies greater than 10^5 cycles/sec. which is clearly out of the question.

Two spherical particles in a sound field will attract each other if they are unable to follow the oscillation of the field. This problem has been treated by Heuter and Bolt,[27] but the force is orders of magnitude too small at the sound intensities available from the pulsating sphere.

The force between two pulsating spheres given by the formula of Hicks[25] can be used since the viscous damping is small in the dimensions considered and the wavelength is large compared to the separation of the spheres. Again we arrive at frequencies in excess of 10^5 cycles/sec. to account either for saltations or separation of the poles.

Diffusion Drag Forces

In this theory we consider some region such as the centrosome as the source of a reaction product which diffuses outward. The force on a sphere of volume V in a steady-state diffusion gradient is

$$F = \frac{-3}{2} \frac{RT}{M} \alpha V \text{ grad } c$$

where M is the molecular weight of the substance diffusing, c the concentration, R the gas constant, and T the absolute temperature; α is a parameter occurring in the theory which was calculated to be approximately 0.7.

If we allow the gradient to be 10^{-4} g./cm.^{4} at a distance of 10 μ from the source, the force on the standard particle would produce a velocity of 0.01 μ/sec., which is two orders of magnitude too small. The gradient chosen corresponds to a source strength of 6×10^{-15} g./sec. If the strength is increased 100 times to account for the velocity a source of diameter 2 μ would have to react 10% of its mass per second. This would require unreasonable rate constants for the enzymes of the source.

The diffusion drag theory does not account for saltations, but since the force increases with the volume of the particle it becomes a feasible mechanism for larger objects. It must be remembered that the theory has not been experimentally verified and that the value of α depends on an involved kinetic theory calculation based on the assumption that the solvent may be treated as a very dense gas.

CYTOPLASMIC INTERACTION THEORIES

A critical consideration of mechanisms based on thermal, hydrodynamic, diffusion, or electrical gradients shows that they are inadequate to explain saltations. (The same conclusion can be drawn regarding chromosomal movements.) We are forced back on a theory which is essentially unsatisfactory, namely, that saltations arise through interaction with (presumably) filamentous elements in the cytoplasm. The filaments have not been observed in the cells examined by Rebhun and the author. Weak and rather indirect evidence is provided by the occurrence of more intense saltatory movements during mitosis which tends to be found in the region around the asters or to a lesser extent, along the mitotic spindle. Direct evidence for the occurrence of motile filaments is provided by the studies of Kamiya[28] and Jarosch.[3] In extruded cytoplasm of Nitella, filaments are found which undergo either parallel translation or rotation when the ends are joined. A case has been documented by Jarosch[3] in which a particle was translated along the length of a filament in a direction opposite to the movement of the filament itself. The action of these filaments has been suggested as an explanation for the rotation of nuclei and chloroplasts in extruded Nitella cytoplasm. A significant observation is the presence of a countercurrent stream which accompanies the rotation of filaments, nuclei, and chloroplasts (i.e., the fluid boundary layer streams in the opposite sense to the filament motion).

Although motile filaments provide a convenient solution to the saltation problem, little real progress has been made unless we can explain the action of the filaments.

The author suggests that the behavior of a filament is in some respects similar to that of a sperm tail. The hydrodynamic problem of sperm propulsion has been treated by Taylor[29, 30] and Hancock,[31] and quantitative agreement has been obtained with the velocity of

P. miliaris sperm.[32] The motion depends on the propagation of a transverse wave in the opposite direction to the motion of the sperm.

The motion of a cylinder parallel to its axis drags the adjacent fluid in the direction of motion of the cylinder, while the active filaments produce a stream in the opposite direction. This suggests that the solution to the problem be sought in terms of wave propagation along the cylinder of a type which could account for the counter streaming.

The wave theory can only be regarded as an untested hypothesis until it can be determined whether or not solutions of the required type exist for the hydrodynamic problem. However, it raises certain interesting questions. The centrosome is involved in the formation of flagella and sperm tails as well as the mitotic spindle and astral rays. The separation of the poles of the spindle which is difficult to explain on the basis of contraction theories might arise by wave propagation along continuous filaments. There are a number of other movements (chromosome to pole movements, streaming in Nitella, and even muscle contraction) in which the propagation of waves along fibrous elements might play a role. Jarosch has also proposed a mechanism involving the propagation of torsional waves as an explanation for various cell movements.[33] Since a quantitative solution to the hydrodynamic problem has not been given, it is not as yet clear whether this theory will account for the counter stream.

The author wishes to express his appreciation to Dr. L. Rebhun for interesting discussion and for making available unpublished material. This work was supported by a grant from U. S. Public Health Service, GM-10992.

References

1. Taylor, E. W., Ph.D. dissertation, Univ. of Chicago, Illinois, 1957.
2. Bloom, W., R. E. Zirkel, and R. B. Uretz, *Ann. N. Y. Acad. Sci.*, **59**, 503 (1955).
3. Jarosch, R., *Phyton (Buenos Aires)*, **6**, 87 (1956).
4. Rebhun, L., *Ann. N. Y. Acad. Sci.*, **90**, 357 (1960).
5. Rebhun, L., in *The Cell in Mitosis*, L. Levine, ed., Academic Press, New York.
6. Rebhun, L., in *Symposium on Cell Movements*, R. D. Allen, ed., in press.
7. Parpart, A. K., in *Symposium on Cell Movements*, R. D. Allen, ed., in press.
8. Fürth, R., *Ann. Physik*, **53**, 177 (1917).

9. Lamb, Sir H., *Hydrodynamics*, 6th ed., Dover, New York, 1955.
10. Yang, J. T., in *Advances in Protein Chemistry*, Vol. 16, C. B. Anfinsen M. L. Anson, K. Bailey, and J. T. Edsall, eds., Academic Press, New York, 1961.
11. Crick, F. H. C., and A. F. W. Hughes, *Exptl. Cell Res.*, **1**, 37 (1950).
12. Mysels, K. J., *Introduction to Colloid Chemistry*, Interscience, New York, 1959.
13. Carlson, J. G., *Biol. Bull.*, **90**, 109 (1946).
14. Feller, W., *An Introduction to Probability Theory*, Vol. 1, 2nd ed., Wiley, 1957.
15. Hill, A. V., *Proc. Roy. Soc.* (*London*), **B136**, 195 (1949).
16. Chandrasekhar, S., *Hydrodynamic and Hydromagnetic Stability*, Clarendon Press, Oxford, 1961.
17. Bjerknes, V., *Hydrodynamische Fernkräfte*, Vols. 1 and 2, J. A. Barth, Leipzig, 1902.
18. Rashevsky, N., *Mathematical Biophysics*, Univ. of Chicago Press, Illinois, 1948.
19. Overbeck, J. Th. G., and J. Lijklema, in *Electrophoresis*, M. Bier, ed., Academic Press, New York, 1959.
20. Brinton, C. C., and M. A. Lauffer, in *Electrophoresis*, M. Bier, ed., Academic Press, New York, 1959.
21. Hodgkin, A. L., and W. A. H. Rushton, *Proc. Roy. Soc.* (*London*), **B133**, 444 (1946).
22. Lamb, A. B., *J. Exptl. Zool.*, **5**, 27 (1907).
23. Cannon, H. G., *J. Genet.*, **13**, 47 (1923).
24. Schrader, F., *Mitosis*, 2nd ed., Columbia Univ. Press, New York, 1953.
25. Hicks, W. M., *Proc. Camb. Phil. Soc.*, **3**, 276 (1879); **4**, 29 (1880).
26. Morse, P. M., *Vibrations and Sound*, McGraw-Hill, New York, 1955.
27. Heuter, T. F., and R. H. Bolt, *Sonics*, Wiley, New York, 1955.
28. Kamiya, N., *Protoplasmatologia*, **8**, No. 3a, 1 (1959).
29. Taylor, Sir G., *Proc. Roy. Soc.* (*London*), **A209**, 447 (1951).
30. Taylor, Sir G., *Proc. Roy. Soc.* (*London*), **A211**, 225 (1952).
31. Hancock, G. J., *Proc. Roy. Soc.* (*London*), **A217**, 96 (1953).
32. Grey, J., and G. J. Hancock, *J. Exptl. Biol.*, **32**, 802 (1955).
33. Jarosch, R., *Protoplasma*, **57**, 448 (1963).

Synopsis

14576

The viscosity of cytoplasm in cultured cells of the newt (*Triturus viridescens*) was estimated from measurements of Brownian motion of granular components. The average viscosity was about 300 cp., but it varied considerably from cell to cell. In addition to Brownian movement granules were occasionally seen to undergo saltatory displacements of several microns in a few seconds. These displacements cannot be accounted for as Brownian movements unless they occur in local regions with a viscosity at least one hundred times smaller than the average. From a knowledge of the viscosity, the mechanical work in saltatory and chromosomal movements was estimated. Neither type of movement appeared to depend on particle size or cell viscosity. From considerations of the general character of

the movements and approximate calculations of the power that can be generated it is concluded that the movements cannot be produced by thermal, electrical, hydrodynamic, or diffusion fields. It is suggested that saltatory movements arise from interaction with motile cytoplasmic filaments. The mechanism of filament movements and the presence of a countercurrent stream in the fluid adjacent to the filaments is discussed in terms of the propagation of waves along the filaments.

Author

N67 14577

Flow Properties of Hemoglobin in the Hemolysing Red Cell

JOSEPH A. KOCHEN,* *Department of Pediatrics, Albert Einstein College of Medicine, New York, New York*

The term hemolysis implies the escape of a considerable portion of the intracellular contents of the red cell into the surrounding medium. A clear understanding of this process has been limited by the absence of direct evidence of a flow of hemoglobin through holes, pores, or other permeable areas in the red cell membrane. The present consideration of the hemolytic process is based on a recent study which concluded that hemolysis due to a sudden decrease in the ionic strength of the surrounding medium is associated with an outward flow of hemoglobin through a single microscopic defect in the red cell membrane.[1,2]

By utilizing an equation based on Fricke's theoretical treatment of hemolysis[3] which relates the size of the membrane defect to the critical red cell volume, fading time, and proportional hemoglobin loss, it was possible to compute the diffusion coefficient of hemoglobin in the lysing red cell. A comparison with existing values for the diffusion coefficient of hemoglobin solutions at various concentrations[4,5] permitted a consideration of the physical state of hemoglobin in the lysing red cell and the mechanism of its escape during hemolysis.

Fricke's eq. (1) for the rate of escape of hemoglobin from the hemolysing red cell is derived from Fick's law and is an expression of the statement that the decrease in hemoglobin within the red cell is equal to the amount which has diffused through the membrane.

$$^4/_3\pi r^3\, dC = \mu_H C 4\pi r^2\, dt \qquad (1)$$

from which

$$\mu_H = \frac{r \log_e (C_0/C)}{3t} \qquad (2)$$

PRECEDING PAGE BLANK NOT FILMED.

where μ_H refers to the permeability of the membrane to hemoglobin and is defined as the amount of hemoglobin passing through unit area of membrane, in unit time, per unit difference in concentration; r is the radius of the swollen prelytic red cell; C_0 is the concentration of hemoglobin in the red cell; C is the concentration of hemoglobin in the red cell ghost; and t is the fading time or the time for the concentration of hemoglobin to decrease from C_0 to C.

In view of the statement by Ponder[6] that hemoglobin may leave the red cell through one or more holes in the membrane, Fricke suggested eq. (3)

$$\mu_H = \frac{0.96\ dND}{4\pi r^2} \tag{3}$$

for the number (N) of holes of diameter (d), through which the escape of hemoglobin would occur at a rate corresponding to various values of μ_H. The term D refers to the diffusion coefficient of hemoglobin in the lysing red cell. It was not possible to solve eq. (3) since the number and diameters of the membrane defects in the hemolysing red cell were not known.

Recently a method was developed which permitted the determination of the number and apparent sizes of the hemolytic membrane defects.[1,2,7] This was accomplished by precipitating and thereby visualizing the emerging intracellular material at the site of membrane breakdown. Alizarin Red S (sodium 1,2 dihydroxyanthraquinone 3-sulfonate), an anionic dye which interacts with hemoglobin to form an insoluble dye-protein complex on the acid side of the iso-electric point of hemoglobin, was used as the precipitating agent. Under appropriate isotonic conditions this dye did not itself cause lysis or appreciable alteration of the osmotic fragility or morphologic appearance of red cells. However, sudden osmotic hemolysis in the presence of this dye resulted in the appearance of a single steadily lengthening stream of precipitated extruded intracellular material. This stream, which emerged with sufficient force to propel the lysing red cell in the reverse direction, was in each cell relatively constant in cross-sectional diameter and remained attached to the red cell ghost at the site of membrane breakdown. Variation in the pH of the solution in which the red cells were suspended prior to lysis was found to have a significant effect on the length and diameters of these streams. Thus, hemolysing red cells previously suspended in isotonic saline

buffered at pH 5.2 extruded streams of intracellular material which were of smaller diameter and considerably greater length (Fig. 1a) than those extruded by cells suspended at pH 7 (Fig. 1b).

By determining the number and diameters of the extruded streams of hemoglobin and by assuming that these were essentially the same as the number and diameters of the membrane defects, it became possible to solve Fricke's equations and to compute the diffusion coefficient of hemoglobin in the lysing red cell. Equations (2) and (3) were combined by eliminating μ_H and solving for D. This yielded eq. (4).

$$D = \frac{4\pi r^3 \log_e(C_0/C)}{3t\ 0.96\ dN} \tag{4}$$

Since the expression $^4/_3\pi r^3$ corresponds to the critical red cell volume (V_c) and the difference between the numerical factor 0.96 and unity is within the range of experimental error, eq. (5) follows:

$$D = \frac{V_c \log_e (C_0/C)}{tdN} \tag{5}$$

In the present study, which will be reported in greater detail elsewhere,[7] values for the terms in eq. (5) were experimentally determined over a range of hemoglobin stream diameters by varying the

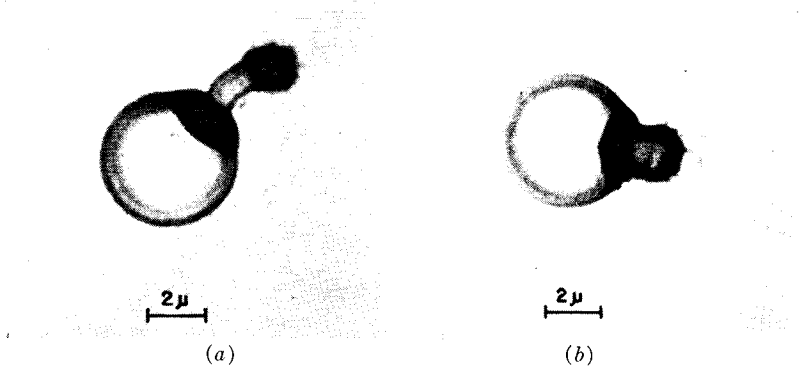

Fig. 1. Human red blood cells which have undergone sudden osmotic hemolysis in the presence of Alizarin Red S following incubation at (*a*) pH 5.2 and (*b*) pH 7. These microphotographs demonstrate the effect of pH variation on the cross-sectional diameter and length of the emerging stream of hemoglobin.

pH of normal human red cell suspensions prior to sudden osmotic hemolysis.

The frequency distribution and modal volumes of red cells suspended in saline solutions at isotonicity and at the critical tonicity at which maximal swelling (V_c) occurred, were determined with a Model B Coulter Counter.[8] The mean red cell hemoglobin (C_0) and mean ghost hemoglobin (C) values were determined by a modification of the benzidine reaction.[9] The fading times (t) were determined by phase-contrast microcinematography of lysing red cells. The onset of lysis was detected by an abrupt propulsive movement of the red cell and the termination of lysis by the cessation of further changes in the optical density of the cell. The diameters of the membrane defects (d) were determined by microphotography and measurement of the cross-sectional diameters of extruded streams of hemoglobin visualized with Alizarin Red S. Hemolysis under these conditions resulted in the extrusion of a single stream of hemoglobin from each red cell ($N = 1$).

Calculation of the diffusion coefficient of hemoglobin by the use of eq. (5) yielded values which ranged from 1.9 to 3.1 $\times 10^{-7}$ cm.^{2}/sec. (Table I). Polson[4] showed by direct measurement that the diffusion coefficient of hemoglobin in dilute solutions up to the 4% range is 6.9 $\times 10^{-7}$ cm.^{2}/sec. Roughton,[5] from his analysis of the uptake of oxygen by thin films of hemoglobin, concluded that Polson's value was approximately correct up to a concentration of about 25%. Above 25% the viscosity of hemoglobin solutions increases rapidly and is probably accompanied by a sharp fall in the diffusion coefficient. From measurements on the rate of diffusion of gases in hemoglobin solutions of 31 to 34%, Roughton computed the upper limits of the diffusion coefficient of hemoglobin at these concentrations to be less than 0.2 $\times 10^{-7}$ cm.^{2}/sec.

The finding that the diffusion coefficient of hemoglobin in the lysing red cell corresponds to that of a hemoglobin solution in the less than 25% concentration range suggests that a significant portion of the hemoglobin in the lysing red cell is in the form of a similar solution in the less than 25% concentration range. This conclusion is consistent with the finding that red cells with an initial hemoglobin concentration in the 30% range, undergo a volume increase of 42 to 69% before hemolysing.[7] This finding indicates that the proportional increase in cell volume represents the amount by which the hemoglobin

TABLE I

pH of red cell suspension prior to hemolysis	Diameter of hemoglobin stream[a] $\times 10^{-4}$ cm.	Diffusion coefficient of hemoglobin $\times 10^{-7}$ cm.^{2} sec.$^{-1}$
5.2	0.6	3.1
5.2	0.8	2.7
7	1.9	1.9
7	2.0	2.2

[a] Mean value of ten determinations.

content of the red cell is diluted by an influx of extracellular fluid before hemolysing.

The swelling of the red cell is presumably accompanied by the development of localized stresses in the red cell membrane.[10] These ultimately lead to the formation of a single region of membrane breakdown through which the outward flow of hemoglobin occurs. The plausible magnitude of the experimentally derived values for the diffusion coefficient suggests that this flow occurs predominantly by a process of free passive diffusion across the resulting concentration gradient, and implies that the hemolytic membrane defect represents a region of complete membrane breakdown which does not impede the diffusion of hemoglobin. This conclusion is in accord with Danon's[11] recent demonstration by electron-microscopy that sudden osmotic hemolysis may result in the formation of a single large hole in the red cell membrane.

An alternative and less likely interpretation of these findings is that an impedance to free passive diffusion of hemoglobin exists in the interior of the red cell or at the membrane defect. This is compensated by a more active extrusion process which yields apparent values for the diffusion coefficient of hemoglobin which only coincidentally correspond to that of a hemoglobin solution in the less than 25% concentration range.

Of particular interest is the finding that a larger diffusion coefficient may be associated with a narrower stream of hemoglobin and presumably the occurrence of a smaller membrane defect (Table I). The Stokes-Einstein relation predicts that the diffusion coefficient will increase with a decrease in viscosity. If this relation holds in the 25% concentration range, then this finding indicates that hemoglobin flow through a smaller membrane defect results in an apparent

decrease in the relative viscosity of hemoglobin. Since flow through a smaller defect is presumably associated with a greater shearing stress, it may be concluded that the apparent decrease in hemoglobin viscosity is a thixotropic phenomenon. This conclusion suggests that the intracellular content of the red cell is in the form of a non-newtonian fluid whose viscosity may vary according to changing internal and external conditions.

The thixotropic character of the red cell interior implies that it may be capable of undergoing reversible sol-gel transformations. This may offer an explanation of the mechanism whereby the red cell is capable of undergoing marked deformation under a variety of mechanical stresses and then resume its original shape on relaxation of these stresses. This type of red cell deformation is known to occur in the capillaries[12] and may also be of importance in the rapid exchange of respiratory gases. The shearing which the thixotropic interior of the red cell undergoes during flow in the axial stream of a very narrow tube presumably results in a reduction in intracellular viscosity. This reduction in viscosity may facilitate oxygen transfer by permitting the diffusion of oxygenated hemoglobin within the red cell.

The evidence presented in this study indicates that sudden osmotic hemolysis is preceded by an influx of extracellular fluid into the red cell. This results in a swelling of the cell and a corresponding dilution of its hemoglobin content, which at the time of lysis is predominantly in the form of a thixotropic solution. The increase in red cell volume is presumably accompanied by the development of stresses in the cell membrane leading to the formation of a single localized region of complete membrane breakdown. It is through this microscopic defect in the red cell membrane and across the resulting concentration gradient that the outward flow of a considerable portion of the intracellular hemoglobin occurs by a process of free passive diffusion.

This investigation was supported by U. S. Public Health Service research grant H 7234; research grant U 1283 from the Health Research Council of the City of New York; and a grant from the National Cystic Fibrosis Research Foundation.

References

1. Kochen, J. A., *Am. J. Diseases Children*, **104**, 537 (1962).
2. Kochen, J. A., *Proc. IX Congr. Intern. Soc. Hematology*, 1962, in press.
3. Fricke, H., *J. Gen. Physiol.*, **18**, 103 (1934).

4. Polson, O., *Kolloid-Z.*, **87**, 149 (1939).

5. Roughton, F. J. W., *Progr. Biophys. Biophys. Chem.*, **9**, 55 (1959).

6. Ponder, E., *Protoplasma-Monographien*, Gebruder Borntraeger, Berlin, Vol. 6, 1934.

7. Kochen, J. A., in preparation.

8. Mattern, C. F. T., F. S. Brackett, and B. J. Olson, *J. Appl. Physiol.*, **10**, 56 (1957).

9. Crosby, W. H., and F. W. Furth, *Blood*, **11**, 380 (1956).

10. Katchalsky, A., O. Kedem, C. Klibansky, and A. DeVries, *Flow Properties of Blood and Other Biological Systems*, A. L. Copley and G. Stainsby, eds., Pergamon, Oxford–New York, 1960, p. 155.

11. Danon, D., *J. Cell. Comp. Physiol.*, **57**, 111 (1961).

12. Guest, M. M., T. P. Bond, R. G. Cooper, and J. R. Derrick, *Science*, **142**, 1319 (1963).

Synopsis

14577

Conflicting evidence exists on the mechanism of hemoglobin loss during osmotic hemolysis. In order to visualize the outward flow of hemoglobin from individual lysing red cells, the emerging hemoglobin was complexed with Alizarin Red S. This resulted in the formation of steadily lengthening streams of precipitated extruded intracellular material which remained attached to the red cell ghosts at the sites of membrane breakdown. Under these conditions, hypotonic hemolysis induced by a sudden decrease in the ionic strength of the surrounding medium resulted in the extrusion of a single stream of hemoglobin from each lysing red cell. The length and cross-sectional diameters of these streams differed markedly with variation in the pH of the solution in which the red cells were suspended prior to lysis.

By assuming that the diameters of the extruded streams of hemoglobin were essentially the same as the diameters of the membrane defects through which the hemoglobin emerged, and by relating these values to the critical red cell volumes, fading times and proportional hemoglobin loss, it was possible to compute the diffusion coefficient of hemoglobin in the lysing red cell. This was found to yield values which varied from 1.9 to 3.1 $\times$ 10^{-7} cm.^{2} sec.$^{-1}$ depending on the size of the membrane defect. These values correspond to previously reported values for hemoglobin solutions in the less than 25% concentration range.

These studies suggest that sudden osmotic hemolysis is preceded by an influx of extracellular fluid which results in swelling of the red cell and a corresponding dilution of its hemoglobin content. The increase in red cell volume leads to the formation of a single microscopic region ot complete membrane breakdown through which the intracellular hemoglobin escapes by a process of free passive diffusion.

Author

Abstract

Sap Movements in Trees

MARTIN H. ZIMMERMANN,* *Maria Moors Cabot Foundation for Botanical Research, Petersham, Massachusetts*

The most spectacular movements of liquids found anywhere in the animal or plant kingdom are sap movements in trees and lianas. Water and mineral nutrients are taken up by the roots and ascend via xylem (the wood) into the leaves, where most of the water is lost by transpiration. Transpiration from leaves pulls up the water; movement is presumably along a gradient of negative pressure (tensions). The conductive tissues are uniquely adapted to negative pressures. They contain rigid tubes which acquire a strong cellulose and lignin reinforced wall during growth. These cells die before they become functional. The whole water-conduction tissue is continuous throughout the plant, rapid movement takes place through xylem tubes, slow movement through walls of all the cells, even living ones. The transpiration stream is very low in concentration, it usually contains less than 0.5% solutes. However, the rapid rate of movement (up to around 50 m./hr.), and loss of water by transpiration from leaves, carry sufficient quantities of mineral nutrients into the leaves.

Most of the plant material is made of carbohydrates which are formed in green parts (leaves) by photosynthesis. Growth of branches, stem and roots can only take place if building materials (photosynthetic products) are translocated from leaves downward. This type of long-distance movement is quite different from the one described above. It takes place in the phloem (the inner bark); the conducting channels are living but enucleate cells. Velocities of translocation are slower (ca. 1 m./hr.), the concentration of the moving solution is higher (10–20%, mostly sugars), and the pressures are positive. During recent years entomologists have developed an effective new method for sampling this descending nutrient stream of

plants. Aphids, feeding on these channels, are anaesthetized and cut from their mouth parts. The high pressure within the phloem keeps exudation from the mouth parts going for many days, and the exudate can be collected from the stylet stump for analysis.

HEMORHEOLOGY OF PULSATILE FLOW

N67 14578

The Flow Properties of Blood as a Factor in the Stability of Pulsatile Flow

D. A. McDONALD,*† *Department of Physiology, Medical College of St. Bartholomew's Hospital, London, England*

In the study of pulsatile flow in the vascular system, which is very active at the present time, the approach is almost exclusively that of classical hydrodynamics. Indeed, the hydrodynamics of simple systems is all that our analyses have managed to cope with so far. However, progress has been such that it is now becoming necessary, as Attinger[1] has pointed out in his detailed investigation of pulmonary hydrodynamics, for "secondary" effects to be taken into consideration. While there is a multitude of these of a purely hydrodynamic nature, this seems to be a good opportunity to consider possible rheological effects due to the structure of blood. It is possible that the points suggested here will prove to be negligible—indeed, it is hoped so, for those of us who work on pulsatile flow do not wish to add to the factors already necessary to consider. That the effects will be small is certain, and some may regard it as an over-optimistic act to bring them up at this time.

In referring to the stability of flow the maintenance of laminar flow is meant, and its importance lies in the fact that it is the only type of flow that can easily be treated by hydrodynamic theory. This problem was considered briefly by the author.[2] In steady flow (i.e., where flow velocity does not vary with time) the important parameter is that of the Reynolds number, Re. For a liquid of kinematic viscosity ν stokes, flowing in a pipe of diameter D cm., with an average velocity across the pipe of $\bar{V}$ cm./sec. the Reynolds number (which is dimensionless) is defined as

$$\mathrm{Re} = \bar{V} \cdot D/\nu$$

† Present address: Research Institute, Presbyterian Hospital, Philadelphia, Pennsylvania.

PRECEDING PAGE BLANK NOT FILMED.

For steady established flow the "lower critical value" is 2000, and above this value flow will be turbulent under normal circumstances. (Taking very special precautions laminar flow can be maintained at very much higher Reynolds numbers.)

Below this value marked instability of the flow can easily be caused by factors such as irregularity of the wall, but these will tend to die out away from the site of origin.

When we consider nonsteady (pulsatile) flow it can easily be argued that the concept of the Reynolds number has no validity. Nevertheless, until it is replaced by some other agreed parameter it has its uses as a yardstick. In the vascular system of man it is interesting to note that in all vessels where flow may be regarded as "steady" the Re is probably always well below 2000, but this only comprises veins which are well away from the thorax and the most distal arterioles and capillaries (Helps and McDonald[3]). In the proximal arteries peak Reynolds numbers of up to 40,000 or so may be attained momentarily during systole, but disturbances created then will tend to die out during diastole, when flow rates are very low (McDonald[4]). Thus, some workers only regard pulsatile flow as turbulent if this is maintained continuously throughout the cycle. With this criterion Cotton[5] studied models in which the flow oscillated with simple harmonic motion and derived an empirical formula relating the peak Re and the parameter $\alpha = R(\omega/\nu)^{1/2}$, where α is the circular frequency (radians/sec.), R the tube radius, and as before ν is the kinematic viscosity. Like the Reynolds number, α is also dimensionless and is an important determinant of the characteristics of oscillatory.

This formula makes it appear that the critical value for nonsteady flow is much higher than for steady flow, but it must be emphasized that this is only applicable for *sustained* turbulence throughout the cycle. When one considers *sustained* laminar flow the situation is quite different for oscillatory flow easily becomes unstable and shows transient disturbances. The times in the cycle at which this is apt to occur and (*a*) when flow velocity is at its greatest, and (*b*) when reversal of flow occurs.

The type of unstability under (*a*) is presumably explained by the same mechanisms as the onset of turbulence in steady flow, but they may occur at relatively low values of Re; e.g., McDonald[6] filmed the breakup of laminar flow pattern in the abdominal aorta of the rabbit

with Re below 1000. The presence of branches makes for even greater instability as was shown in the same films at the bifurcation of the aorta. The type of instability under (*b*) is probably due to inflections in the velocity profile which occur predominantly near the wall during reversal of flow and which may be seen in Figure 1.

Lord Rayleigh long ago postulated theoretically that re-entrant angles in the velocity profile would be important points of instability. This was later shown to be the case by Tollmein (see Prandtl[7]) and has been emphasized again more recently by Attinger.[8] Indeed, it is easy to show them in a model with quite low rates of flow, using dye as an indicator. When a well-marked parabolic profile is established the flow is gradually reversed by lowering the supply reservoir and the profile appears as though it is turning inside out, rather like the finger of a rubber glove when it is pulled off the hand. The reversal starts at the wall where the velocity gradient is steep and hence the first inflections to form are sharply angled. Circular vortices can usually be seen forming at the apex of such inflections, but at low rates of flow they soon die away as the more axial regions of the flowing liquid reverse direction. Circular vortices of this type were seen by Helps and McDonald[3] when inflation of the lungs caused reversal of flow in the thoracic inferior vena cava of the rabbit.

When considering the effects of the rheological properties of blood on its flow stability it may be useful to categories (*a*) and (*b*) separately, Prandtl[7] had suggested that the initiation of turbulence in steady flow is due to the formation of inflections in the profile due to minute irregularities in the wall, and Evans[9] developed Theodorsen's suggestion that the first stage of turbulence was in vortices similar to those described. The standard estimation of the critical value of the Reynolds number in blood is that of Coulter and Pappenheimer.[10] Using the discontinuity in the pressure gradient/flow relation they obtained a value of 1960 ± 160, which is not significantly different from the value of 2000 taken for Newtonian fluids. However, on the basis of measurements of the longitudinal electrical impedance they postulated that there was a continuing stability of the red cells which had moved axially away from the wall and maintained a constant orientation ("floating like a log in a stream"). While this picturesque analogy is clearly not intended to be taken too literally, it does show that the effect of the red cells on the flow pattern of the more axial regions of flowing blood needs to be investigated more

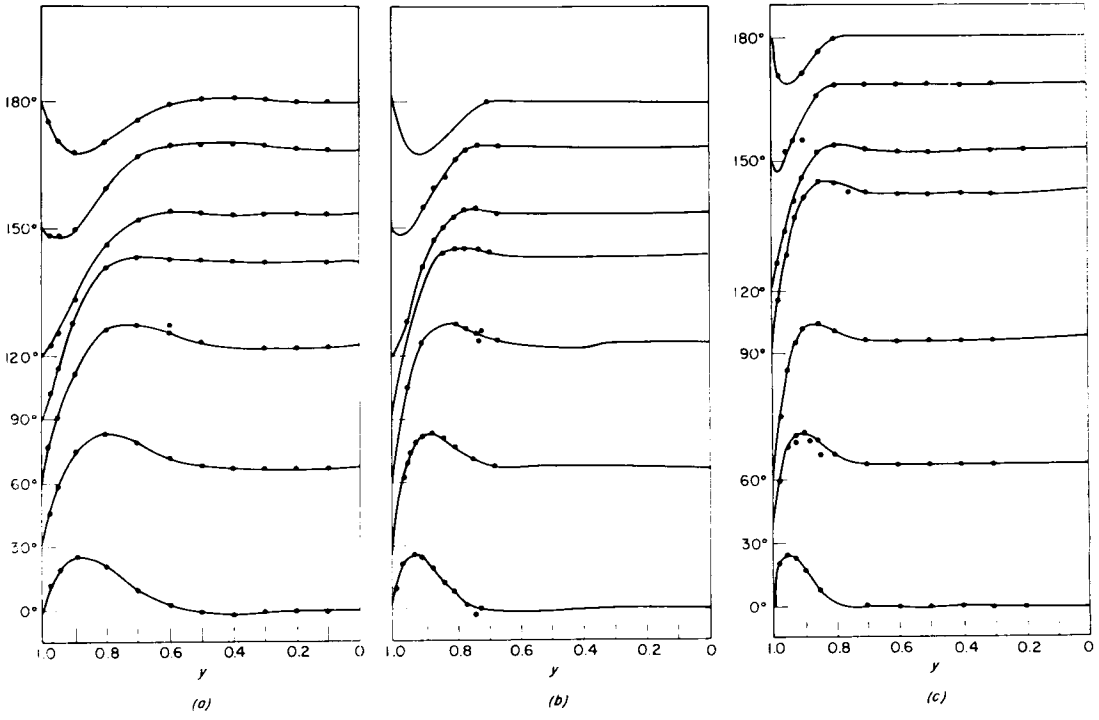

Fig. 1. Velocity profiles of oscillatory flow in a cylindrical tube created by a pressure gradient of the form $M \cos t$. Profiles are shown for half the tube at intervals of 30° for a half-cycle (after which they repeat in inverse form cp. profiles at 0° and 180°). (*a*) When $\alpha = R(\omega/\nu) = 10$, (*b*) $\alpha = 15$, and (*c*) $\alpha = 20$. The amplitude effect due to increasing seen in the profiles of Hale et al. (ref. 21) has been eliminated for clarity. Abscissa, the fractional radius, $y = r/R$.

fully. For example, Hess[11] found that dye injected in a solution of the same viscosity as blood remained relatively unmixed through the aorta in a large dog, and Ralston et al.[12] obtained similar results in the cat.

The anomalous viscous behavior of blood is well known to rheologists in that the apparent viscosity is lower in small tubes than in large ones. This effect is only marked in tubes of less than 0.5 mm. diam. and is attributed to the axial accumulation of cells creating a cell-free zone of lower viscosity close to the wall. Also, at low rate of shear the viscosity of blood increases markedly. Bayliss[13] has given a full review of these topics. Because it was thought that pulsatile flow was probably damped out by the time the smallest arteries were reached, the "small-tube" effect has not been much considered in arterial flow studies. Recent work reported at the *Symposium on Pulsatile Flow* (Attinger[14]) has shown that the pressure remains markedly pulsatile in vessels of arteriolar dimensions so that this assumption about flow in the minute vessels must be reconsidered. In the pulmonary circulation the flow is pulsatile through the capillaries and there is a marked transmission of pressure to the veins, especially of the lower frequencies (Caro and McDonald[15] and Attinger[1]).

In the larger arteries Taylor[16] showed that in regard to pressure flow relations an error of not more than 2% would be caused if the "asymptotic" viscosity of blood was used in the calculations. He showed that shear-dependent viscosity had less effect on oscillatory flow than on steady flow. The asymptotic viscosity is the constant value which is attained in a tube at high rates of shear, and the data he used were the very detailed ones of Kümin.[17] In addition, he studied the case where the flowing blood was considered as having a marginal annulus of reduced viscosity—a slip zone. This led to similar conclusions, and he also showed that the effect on wave velocity is negligible.

The presence of a cell-free zone at the wall has been described by many workers and various effects ascribed to it. Detailed measurements by Bayliss,[18] however, have cast serious doubt on whether there is any true cell-free zone and show that, if one exists, it is less than 2 to 5 μ wide. There is, however, a region of reduced optical density at the wall; the density increases for a distance to a maximum and then falls markedly in the axial region (Taylor[19] and Bayliss[18]).

While some of this effect is presumably due to changing cell density toward the boundary, and hence indicates a region of changing viscosity, much of it is probably due to increasing cell orientation—a factor which must be the reason for the low optical density in the axial zone. The region of reduced optical density near the wall may be considerable, e.g., Bayliss[18] found it to be from 5 to 20 μ wide in a capillary of 100 μ diam. With regard to the presence of a cell-free zone, Taylor[16] supports Bayliss' findings with the calculation that all the anomalous viscous effects reported can be accounted for by a cell-free zone of not more than 3 μ wide. These dimensions must be borne in mind when discussing the effect of radial variations of viscosity on the form of the velocity profile which, in turn, may modify the stability of the flow.

The form of the velocity profile during oscillatory flow of a Newtonian liquid can be calculated from the formulas of Womersley[20] and have been published (Hale et al.[21]) for selected values of α up to 6.67 (representing the first four harmonic components in a typical dog femoral artery).

In Figure 1 selected profiles for values of $\alpha = 10$, 15, and 20 are shown because they are more representative of conditions in the large vessels where flow conditions are the subject of a lot of study, namely, the proximal regions of the great vessels. For example, α for the pulse frequency (fundamental harmonic) in the ascending aorta of the dog is commonly about 10, and in that of the human being between 15 and 20; the values for the higher harmonics are, of course, correspondingly greater. From the illustration it can be seen that shear rates are confined to the regions near the wall, and this is more marked as α gets larger. This may be characterized by noting that the maximum flow velocity, which in steady flow is always in the axis, occurs at a fractional radius of 0.7 when $\alpha = 10$, and at a fractional radius of 0.85 (i.e., only 15% of the radius away from the wall) when $\alpha = 20$. In addition, the most marked inflections in the profiles occur near the wall; all the striking ones occur in the peripheral 10% of the tube.

The effect of diminished viscosity close to the wall due to reduced cell density would be expected to exaggerate rates of shear in the boundary regions and diminish them in the regions toward the axis. This may be made clearer by reference to Figure 2 which shows velocity profiles for steady flow if we make the assumption, used by

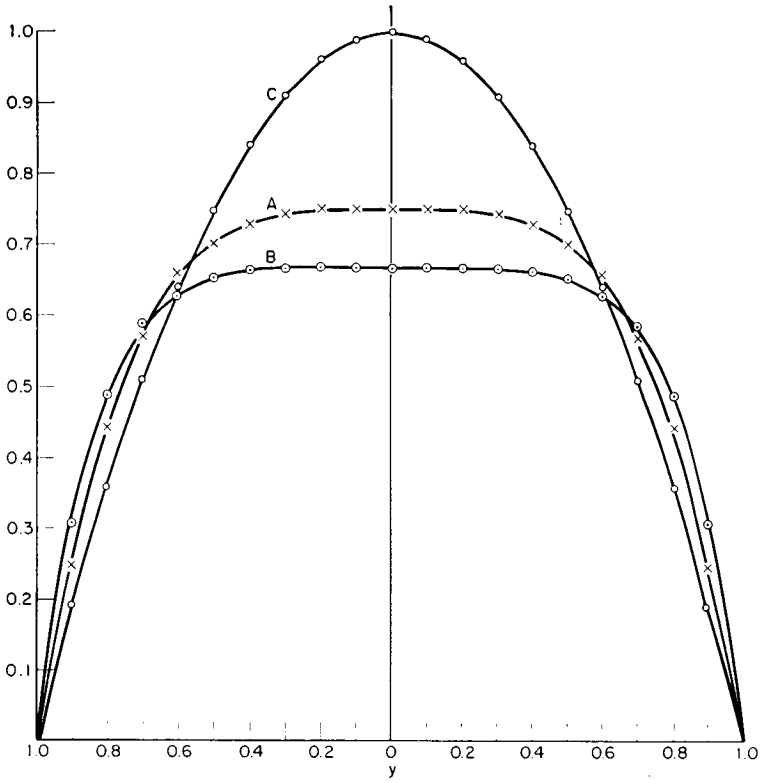

Fig. 2. Velocity profiles of steady flow when the viscosity varies as an inverse power of the fractional radius (see text). *A*: The power, $m = 2$. *B*: $m = 4$. *C*: A parabolic profile for comparison (after Womersley, ref. 22).

Womersley,[22] that the viscosity varies as an inverse power of the radius, i.e., the mean viscosity $\bar{\mu} = \mu(r/R)^{-m}$. There is, of course, no experimental justification for this assumption in this precise form, but it is tractable mathematically and does show the effects in a fluid when the viscosity diminishes rapidly close to the wall. The two curves, where $m = 2$ and $m = 4$, are shown in comparison with the normal parabolic profile of a Newtonian fluid. It can be seen that the velocity gradient is markedly increased close to the wall but is greatly reduced in the paraxial regions.

If the onset of turbulence occurs when a critical rate of shear is exceeded, as implied under (*a*) above, the anomalous viscous prop-

erties of blood would be expected to decrease its stability. With regard to the effect of the inflections considered under (*b*), the effect is not so easy to predict. If the critical ones are those very close to the wall, the marginal layer of lower viscosity might be expected to exaggerate them. Further into the stream the effect might, rather, be in the opposite direction. We also see that in oscillatory flow there are large regions of very low shear. Here the blood will show its other anomalous property of having a high viscosity, but it is difficult to see how this would have any important overall effect. The estimates of the cell-free zone quoted above indicate that it is extremely small, and the fact that the Reynolds number appears normal for blood in steady flow (Coulter and Pappenheimer[10]) may well mean that the behavior of blood in oscillatory flow is not appreciably different from that of a Newtonian fluid. It would, however, be most helpful to have experimental evidence on this point rather than speculations of the kind presented here.

The recent work of Meisner and Rushmer[23] and Attinger[24] using the flow of birefringent materials in models suggests a way in which this might be done. Physicists have used this method for the study of turbulence, e.g., Wayland[25] if such a solution could be made with non-Newtonian properties similar to that of blood this would be a very powerful technique in the elucidation of this problem. The physiologically orientated studies quoted above do, however, emphasize that the conformation of the vessels—the presence of branches, valves, and the arch of the aorta—are major causes of instability in blood flowing in the vascular system. Not only have models with pulsatile flow and distensible walls been used, but Meisner and Rushmer[26] have used the technique for a detailed quantitative analysis of the relation between flow patterns and the generation of wall vibrations. This would indicate that this technique could be used to provide a much more precise knowledge about the problems concerning the stability of oscillatory flows which have been discussed here.

References

1. Attinger, E. O., *Circulation Res.*, **12**, 623 (1963).
2. McDonald, D. A., in *Flow Properties of Blood and Other Biological Systems*, A. L. Copley and G. Stainsby, eds., Pergamon Press, Oxford-New York, 1960, p. 84.
3. Helps, E. P. W., and D. A. McDonald, *J. Physiol.*, **124**, 631 (1954).
4. McDonald, D. A., *Blood Flow in Arteries*, Arnold, London, 1960.
5. Cotton, K. L., Ph.D. thesis, Univ. of London, 1960.

6. McDonald, D. A., *J. Physiol.*, **118,** 340 (1952).
7. Prandtl, L., *Essentials of Fluid Dynamics*, Blackie and Son, London, 1952.
8. Attinger, E. O., in *Symposium on Pulsatile Flow*, Blakiston, New York, 1964, in press.
9. Evans, R. L., *Res. Bull. Purdue Exptl. Sta.*, **128,** 235 (1955).
10. Coulter, N. A., and J. R. Pappenheimer, *Am. J. Physiol.*, **159,** 401 (1949).
11. Hess, W. R., *Pflügers Arch.*, **168,** 439 (1917).
12. Ralston, J. H., A. N. Taylor, and H. W. Elliott, *Am. J. Physiol.*, **150,** 52 (1947).
13. Bayliss, L. E., in *Flow Properties of Blood and Other Biological Systems*, A. L. Copley and G. Stainsby, eds., Pergamon Press, Oxford-New York, 1960, p. 29.
14. Attinger, E. O., ed., *Symposium on Pulsatile Flow*, Blakiston, New York, 1964, in press.
15. Caro, C. G., and D. A. McDonald, *J. Physiol.*, **157,** 426 (1961).
16. Taylor, M. G., *Phys. Med. Biol.*, **3,** 273 (1959).
17. Kümin, K., Inaugural dissertation, Univ. of Bern, 1949, cited by Bayliss, ref. 13.
18. Bayliss, L. E., *J. Physiol.*, **149,** 593 (1960).
19. Taylor, M. G., *Aust. J. Exptl. Biol. Med. Sci.*, **33,** 1 (1955).
20. Womersley, J. R., *J. Physiol.*, **127,** 553 (1955).
21. Hale, J. F., D. A. McDonald, and J. R. Womersley, *J. Physiol.*, **128,** 629 (1955).
22. Womersley, J. R., *J. Physiol.*, **127,** 38P (1955).
23. Meisner, J. E., and R. F. Rushmer, *Circulation Res.*, **12,** 455 (1963).
24. Attinger, E. O., in *Symposium on Pulsatile Flow*, Blakiston, New York, 1964, in press.
25. Wayland, H., *J. Appl. Phys.*, **26,** 1197 (1955).
26. Meisner, J. E., and R. F. Rushmer, *Circulation Res.*, **12,** 651 (1963).

Synopsis

The applicability of concepts determining the transition from laminar to turbulent flow, which are based on studies of steady flow, is discussed in relation to the oscillatory flows found in the circulatory system. While transient breakdowns of laminar flow occur at relatively low Reynolds' numbers, there is some evidence that there may be increased stability with regard to sustained turbulence. The distribution of rates of shear and inflections in the velocity profiles that occur in pulsatile flow are considered in relation to this problem, together with probable changes due to the inhomogenous character of the blood.

N67 14579

A Study of Auscultatory Blood Pressures in Simulated Arteries

ALVIN H. SACKS,* K. R. RAMAN, and JACK A. BURNELL,
Vidya Division, Itek Corporation, Palo Alto, California

The work described herein is concerned with an engineering investigation of the precise meaning of the so-called systolic and diastolic blood pressures ordinarily measured by a physician using the auscultatory technique. In practice, these blood pressure measurements are made by applying a pneumatic cuff to the patient's upper arm and inflating the cuff by means of a hand pump until there is no pulse in the radial artery at the wrist. The physician then applies a stethoscope to the brachial artery just below the cuff and starts to decompress the cuff slowly. As he decompresses, at some pressure level, he begins to hear a faint tapping sound (first phase of the Korotkoff sounds) and at this point he records the pressure as the systolic pressure reading. As the cuff pressure is reduced further, the sound changes in character (second phase), becomes clearer and increases in intensity (third phase), then fades rather suddenly (fourth phase), and finally disappears altogether (fifth phase). The pressure corresponding to the cessation of sounds is customarily recorded by the physician as the diastolic pressure reading. Figure 1 shows a qualitative plot of the cuff pressure and the Korotkoff sound intensity (as heard in the stethoscope) as functions of time during the decompression of the cuff. Starting at the left, at zero time, is the occluding pressure, at which point there is no flow through the tube and hence, no sound is produced. Now, according to Erlanger,[1] at some point below the occluding pressure, a part of the fluid passes through the tube on each cycle and impacts on the downstream stationary fluid, thereby producing a water hammer and a consequent sound. In addition, however, the sound must radiate in the radial direction and is attenuated at a rate that

PRECEDING PAGE BLANK NOT FILMED.

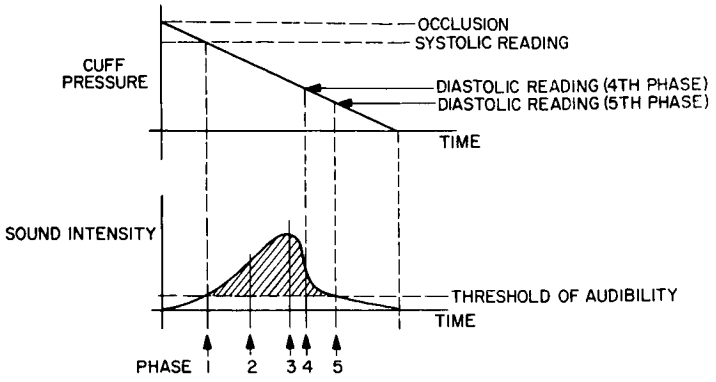

Fig. 1. Variation of intensity of Korotkoff sounds during cuff decompression.

depends on the viscosity of the fluid. The sound is then picked up by the arterial wall, which responds at its natural frequency, and it is a combination of these sounds which is heard in the stethoscope. Beyond the first phase, the sound then increases in intensity and, as shown on the lower diagram of the figure, it reaches a peak intensity after which a sudden drop-off occurs (the fourth phase), at which point some physicians take the diastolic reading. At a still lower pressure, the sounds disappear entirely, going below the threshold of audibility, and this is the fifth phase, which is usually taken as the diastolic pressure reading. (This point will be discussed later.) Since the arterial wall responds at its natural frequency, it seems clear that if the natural frequency of the arterial wall is below the audible level of about 20 cycles/sec., it will be difficult to hear the Korotkoff sounds. This is typical of young children and of patients in hypothermia.

The purpose of the present investigation is to determine the relationship (if any) between the blood pressure readings obtained by the auscultatory technique and the actual oscillatory intra-arterial pressures that existed in the vessel *before* the cuff was applied. According to the medical literature, the systolic pressure reading corresponds to the peak of this oscillatory pressure, and the diastolic pressure reading corresponds to the minimum of this oscillatory pressure.

Now, in order to understand the problem at hand, we must first attempt to determine the cuff pressure required to stop the oscillatory

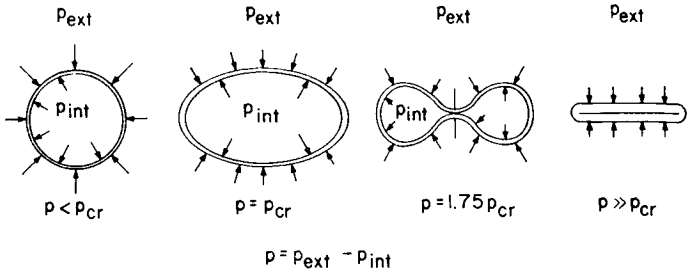

Fig. 2. Collapse of thin wall tube due to external pressure.

flow in the artery. As a first step, then, let us consider the pressure required to occlude the flexible tube with no flow in it at all. According to the theory of elastic stability[2] the critical pressure p_{cr} required (in excess of the internal pressure in the tube) for initial buckling of the tube is given by

$$p_{cr} = \{E/[4(1 - \sigma^2)]\} (h/R_0)^3$$

where E is the elastic modulus of the tube, h/R_0 is the wall thickness-to-radius ratio, and σ is Poisson's ratio for the tube material. However, a higher pressure is clearly required to bring the diametrically opposite sides of the tube together. The analysis of Halphen[3] and more recently of McIvor[4] indicate that this pressure is given by

$$p = 1.75 p_{cr}$$

and a still higher pressure, for which there is no theory at present, is required to collapse the tube entirely. The cross sections of the flexible tube at various applied external pressures are illustrated in Figure 2. For complete collapse, as shown at the extreme right, the classical theoretical method for solving such buckling problems fails because of the nonlinear character of the problem associated with large deformations and appreciable bending moments. Even the solution of this problem, however, would at best yield only the occluding pressure for a tube with no oscillatory flow in it. The theoretical determination of the auscultatory systolic and diastolic pressures is considerably more complicated, and no theoretical analysis has yet been attempted.

An experimental approach is pursued here by use of a simulated system in which control of each of the parameters can be accom-

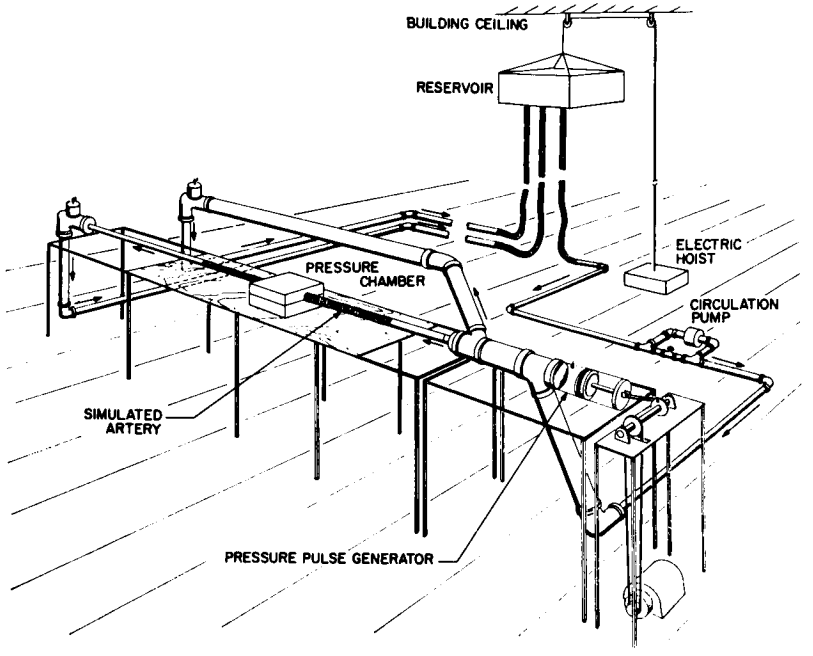

Fig. 3. Schematic sketch of experimental apparatus.

plished independently. Of course, in resorting to a simulated system, one must observe the rules of proper modeling or scaling of the system in order to obtain meaningful results. In other words, there should be dynamic similarity between the simulated system and the actual physiological system. For the present problem, this involves matching the Reynolds number based on mean flow, the Reynolds number based on frequency and the radius of the tube, the ratio of the mean pressure level to the elastic modulus of the tube, the ratio of the pulse pressure or pressure amplitude to the mean pressure, the wall thickness-to-radius ratio, the natural frequency of the tube, and Poisson's ratio for the tube material. In addition, if the material is viscoelastic, as we know natural arteries to be, then one should also match the dynamic elastic modulus compared with the static elastic modulus. Since most of the above parameters are not accurately known for the human brachial artery, the emphasis in the present investigation is on the variation of each of the nondimensional

parameters over a wide range covering the physiological range of interest insofar as it is known. For the idealized model studied here, gum rubber tubing is used to represent the artery, and the fluid initially is represented by a combination of water and glycerol at varying concentrations in order to vary the viscosity of the fluid and thereby the Reynolds numbers of the flow. Experiments using real blood will be discussed later.

The experimental apparatus is shown schematically in Figure 3. The apparatus is a closed loop system in which the test fluid is fed from the reservoir through the circulation pump to the pulse generator section. With the pulse generator operating, periodic pressure pulses are imparted to the test liquid which then divides into two branches. These two branches represent (*1*) the test artery and (*2*) that part of the human system that is not closed off when the oscillatory flow in the artery is cut off by application of the pressure cuff. In order to avoid mutual interference of the pressure waves in the two branches, the test section and the bypass have separate venous return lines that connect back to the reservoir. The gum rubber "artery" is 10 ft. long and has a nominal inside diameter of 1 in. and a wall thickness of $^1/_{16}$ in.

After the experimental apparatus had been assembled, the first futile attempts to produce the Korotkoff sounds by using a physician's pneumatic cuff led to a re-examination of Erlanger's work done in 1916.[1] From Erlanger's work, it became apparent that a large-volume pressure chamber, properly scaled up to our system, was required. The volume of air in the chamber must be above a certain minimum value relative to the size of the artery, and the diaphragms used in the chamber to compress the artery must be sufficiently flexible to permit a pressure pulse to pass through the artery. In addition, the pressure chamber must not impose any artificial constraints on the artery at the ends of the chamber.

An exploded view of the resulting pressure chamber is shown in Figure 4, where only the parts of the lower section of the chamber are identified since the upper and lower sections are identical. The top and bottom parts of the pressure chamber are essentially open hardwood boxes with outside dimensions 18 by 12 by 2 in. A rubber O-ring gasket is imbedded in the wall of the box to provide a seal, and a thin rubber diaphragm covers the opening of each box. A plastic frame 1 in. thick is placed over each diaphragm as shown in

the figure. The plastic frames have semicircular openings in their opposite ends to permit the artery to pass freely through the pressure chamber so that the chamber does not exert any artificial "end effects" on the artery.

Using this pressure chamber, Dr. David Bruns, our cardiovascular consultant, was able to hear the entire spectrum of Korotkoff sounds and obtain the associated systolic and diastolic pressure readings. It was noted that an auscultatory gap could be produced at either

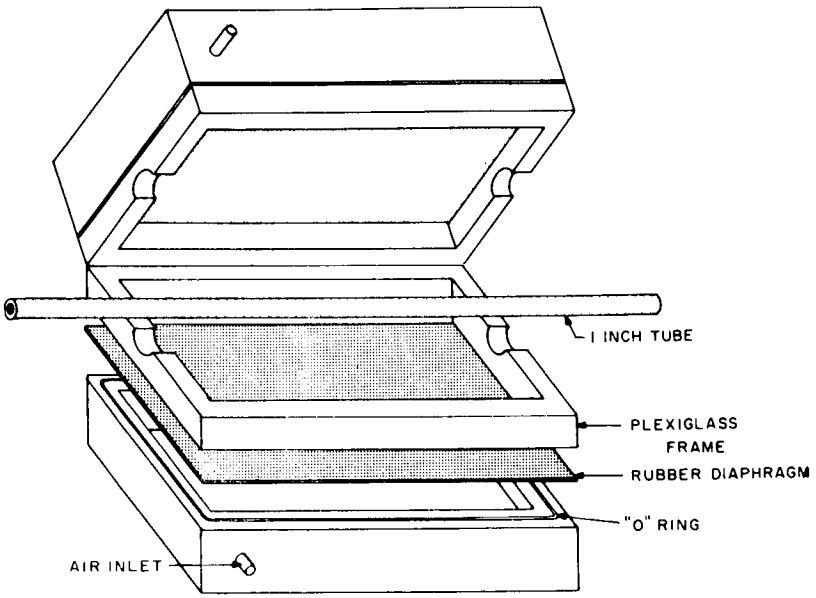

Fig. 4. Exploded view of pressure chamber used in present tests.

very high pulse rates and/or high mean pressure levels, and changes in quality and intensity of the Korotkoff sounds ordinarily associated with such clinical conditions as hypertension and aortic insufficiency could be produced by changes in the flow conditions or in the arterial wall. Now, since the auscultatory readings do depend to some degree upon the auditory acuity of the individual observer, each of the observers for the present experiments was trained by Dr. Bruns to recognize and distinguish the sounds at the onset of the Korotkoff sounds (systolic pressure) and at the fourth and fifth phases (diastolic

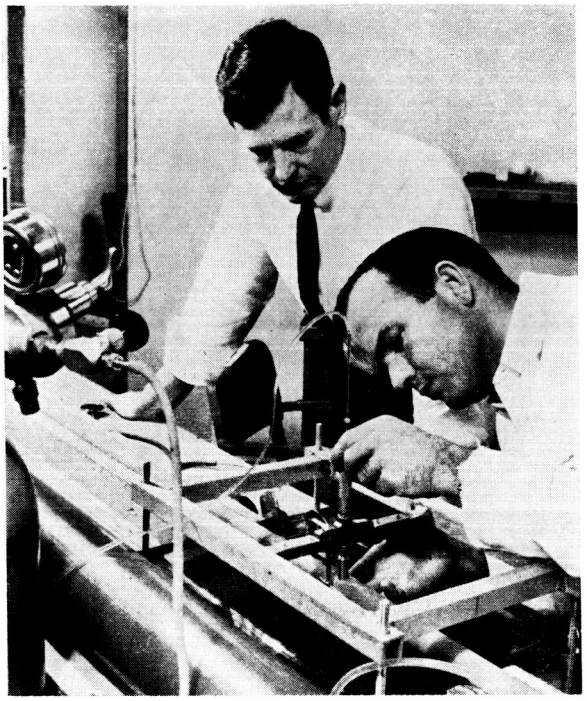

Fig. 5. Installation of pressure probe traverse mechanism on pressure chamber mounting.

pressure). All readings were made by at least two observers, and agreement within 5 mm. Hg was obtained in all cases.

Since the present investigation is made to compare the auscultatory pressure readings with direct pressure readings inside the artery, the instrumentation for determining the actual oscillatory pressure inside the tube becomes important. Figure 5 shows a pressure traverse mechanism which consists of a pressure probe mounted in such a way that it can be moved radially inside the test artery, by means of a micrometer adjustment, to any vertical location relative to the fixed table. The frame on which the probe is mounted is the same frame that clamps the pressure chamber into place (see Fig. 7) and insures that both measurements are made at the same axial location in the tube. The measurements made with this traverse mechanism indicated that there was no appreciable variation of pressure with radial

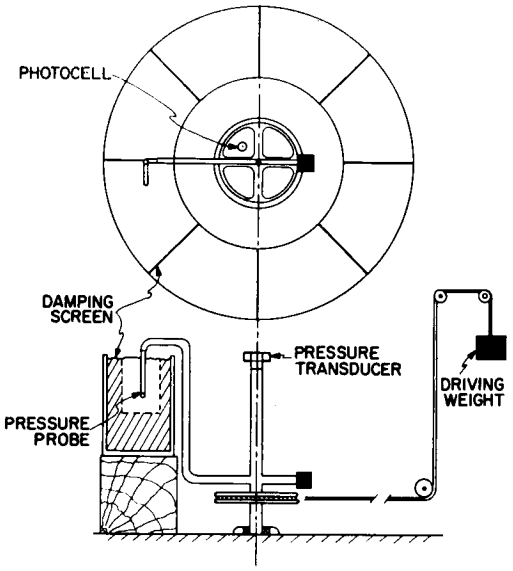

Fig. 6. Calibration rig for pressure probes.

position through the tube. Thus, a fixed probe installation was designed and used in all the tests. But, in order to make the measurements required to compare the auscultatory readings with direct readings, the pressure probes must be calibrated in their proper environment. For the present problem this is of no minor concern, since at very low Reynolds numbers an impact tube may not read the actual impact pressure, because of viscous dissipation ahead of the stagnation point. In addition, we have an oscillatory flow in which the probe may be subject to a time lag. And finally, over part of the cycle the probe will be operating in reverse flow, so that it will read the pressure in its own wake, which may be less than free-stream pressure. Therefore, in order to calibrate for all these effects, a special calibration rig (Fig. 6) was designed and constructed. A similar rig was originally used for steady flow by Hurd et al.[5] But for the present experiments, it has been adapted for unsteady effects and for reverse flow over the probe. This device is simply a rotating arm on which the probe to be used is mounted and is immersed in an annular tank containing the test fluid. The arm can be rotated at

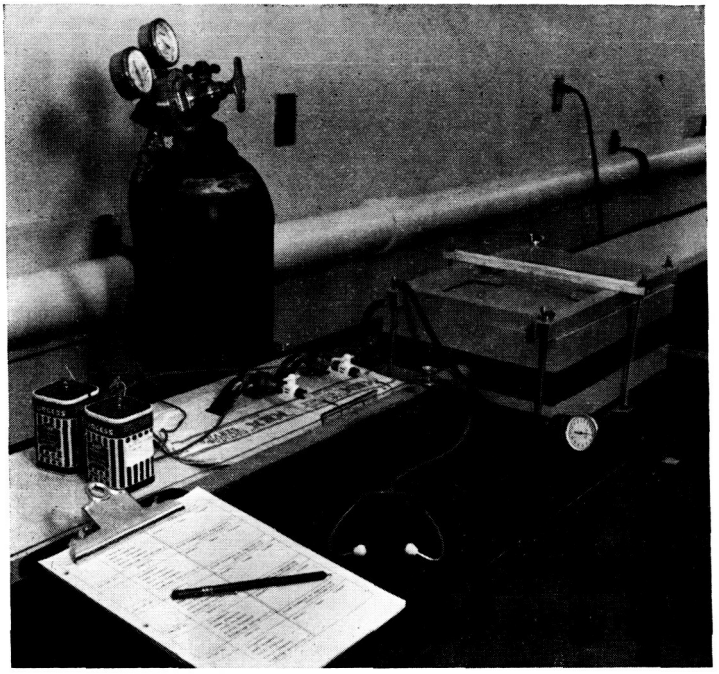

Fig. 7. Equipment used for auscultatory and direct blood pressure measurements on simulated artery.

variable speeds and accelerations by means of a falling weight. The instantaneous speed of rotation is recorded by monitoring the shadow of the spoke falling on a photocell, and from this record the velocities and accelerations can be calculated. The pressure reading from the probe is recorded simultaneously and is compared with the known pressure head given by the depth of the probe below the surface of liquid. These probe calibration tests for both viscous and acceleration effects indicated a maximum error of 2% for total pressure and 1% for static pressure over the range of the present tests. Hence, these errors were neglected and the measured probe readings were taken as correct within the accuracy with which the blood pressure readings could be made.

In the present tests, two pressure probes were mounted downstream from (i.e., distal to) the pressure chamber, as shown in Figure 7. One probe measures static (lateral) pressure and the other total

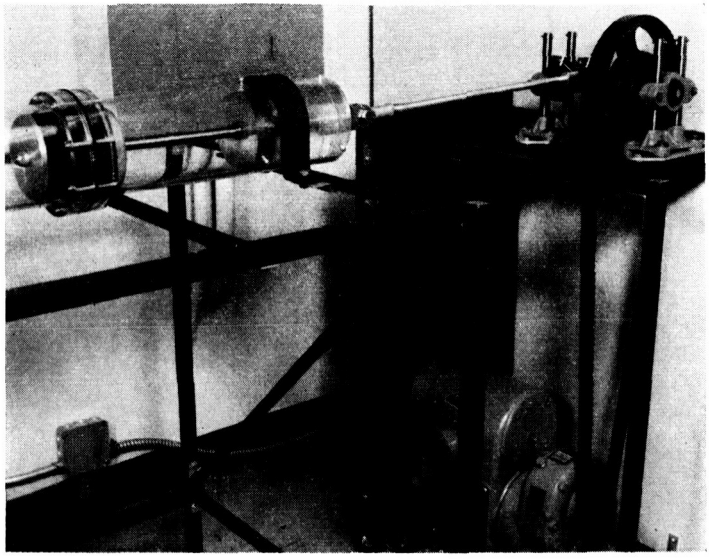

Fig. 8. Variable amplitude, variable frequency sinusoidal pulse generator.

(stagnation) pressure inside the tube as a function of time. These fixed probes were installed approximately on the axis of the test artery by inserting them from the bottom of the tube in order not to disturb the tube during pulsation. The pressure outputs from the probes are recorded on an oscillograph by the use of battery-powered transducers. A check of the pressure readings obtained with these probes against readings obtained at the location of the pressure chamber showed that the error in pressure level and pulse amplitude was less than 2%. There will, of course, also be a phase shift due to the downstream location of the probes, but this is of no concern for the present investigation.

The variable-stroke piston arrangement shown in Figure 8 is provided with an air chamber which separates the actual working fluid from the driving mechanism. The piston itself is mounted on a rolling diaphragm for quiet operation. The pressure in the chamber is adjusted to give a fine control on the volumetric displacement and the pulse pressure amplitude. The main purpose of this chamber is to provide a means of obtaining a large pulse pressure amplitude with a small volumetric displacement.

The actual experiments that were carried out can perhaps best be illustrated by a brief description of the test procedure. The reservoir height is first adjusted to give the required mean pressure level in the artery. Then the stroke of the piston is adjusted to obtain the desired pulse pressure amplitude, and the pulse generator apparatus is adjusted for motor speed to obtain the desired pulse rate. The pressure in the air chamber, which separates the actual test fluid from the pulse pump, is adjusted to give a finer control on the volumetric displacement and the pulse pressure amplitude and wave shape. It should be noted that all the experimental data presented here are for a sinusoidal pulse wave.

Analytical expressions relating the pulse wave velocity to the oscillatory pressure and wall displacements in flexible tubes have been derived using the theoretical work of Womersley[6] and Morgan and Kiely.[7] Therefore, in order to check these relationships, the pulse wave velocity was measured in the test artery by using two photocells to follow the wall displacement of the tube at two axial locations as functions of time. (The wave velocity is determined from the phase difference between the two photocell outputs.)

The auscultatory pressure measurements are made by trained engineers by pressurizing the pressure chamber with the gas bottle, applying the stethoscope snugly to the simulated artery just distal to the pressure cuff, and recording the pressures observed on the manometer when the first and fifth phases of the Korotkoff sounds occur. The oscillograph record consists of two photocell outputs (giving wall displacements), two pressure traces (for the intra-arterial pressures), and one timing pulse for frequency determinations. The viscosity of the test fluid and the radius of the artery as a function of the mean internal pressure are also determined just prior to the actual tests. From these inputs, the static and total pressures inside the artery are obtained as functions of time, the wave velocity is calculated, and the elastic properties of the vessel are determined.

The results of the experiments are shown, in part, in Figure 9 for a 1-in. diam., gum rubber simulated artery of $^1/_{16}$ in. wall thickness. This figure is a composite plot of the auscultatory systolic and diastolic pressure readings against the corresponding maximum or minimum of the oscillatory pressure which existed in the unobstructed vessel before the pressure chamber was activated. A 45° "line of perfect agreement" is shown for reference, as well as a line along which the

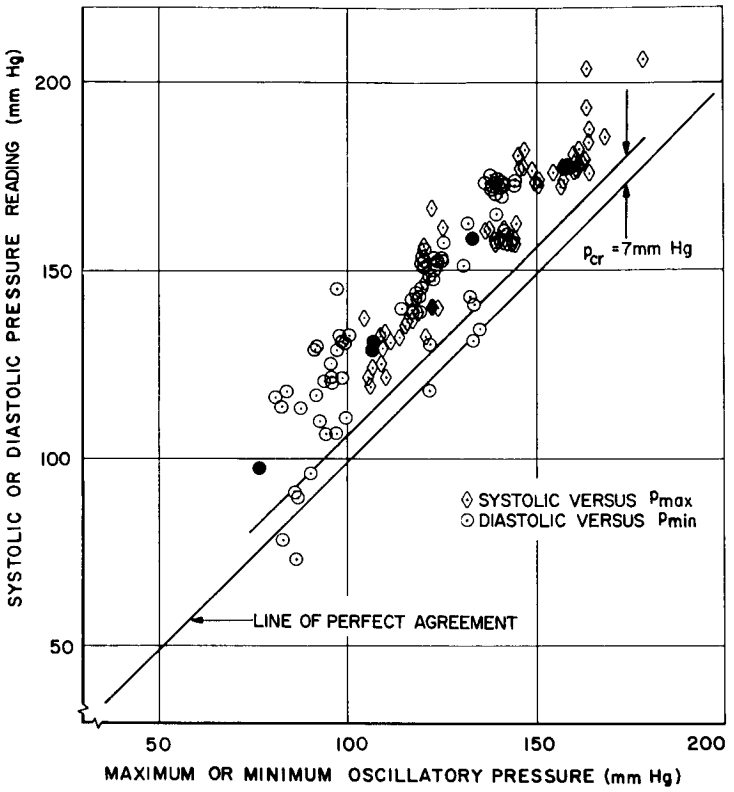

Fig. 9. Auscultatory versus direct pressure measurements for 1 in. diameter gum rubber simulated artery of $^1/_{16}$ in. wall thickness. (Note: Solid symbols are for steer blood.)

auscultatory readings would exceed the direct readings by the critical buckling pressure of the tube. The buckling pressure p_{cr} is calculated from the measured elastic properties of the particular vessel tested. The data points shown cover a range of pulse rates from about 60 to 150 beats/min., mean pressures from 100 to 150 mm. Hg, pulse pressures from 10 to 60 mm. Hg, and fluid viscosities from 1 to 12 times that of water. It can be seen that, with few exceptions, the auscultatory systolic and diastolic pressure readings exceed the corresponding direct pressure readings by an amount which is greater than the critical buckling pressure of the vessel in question.

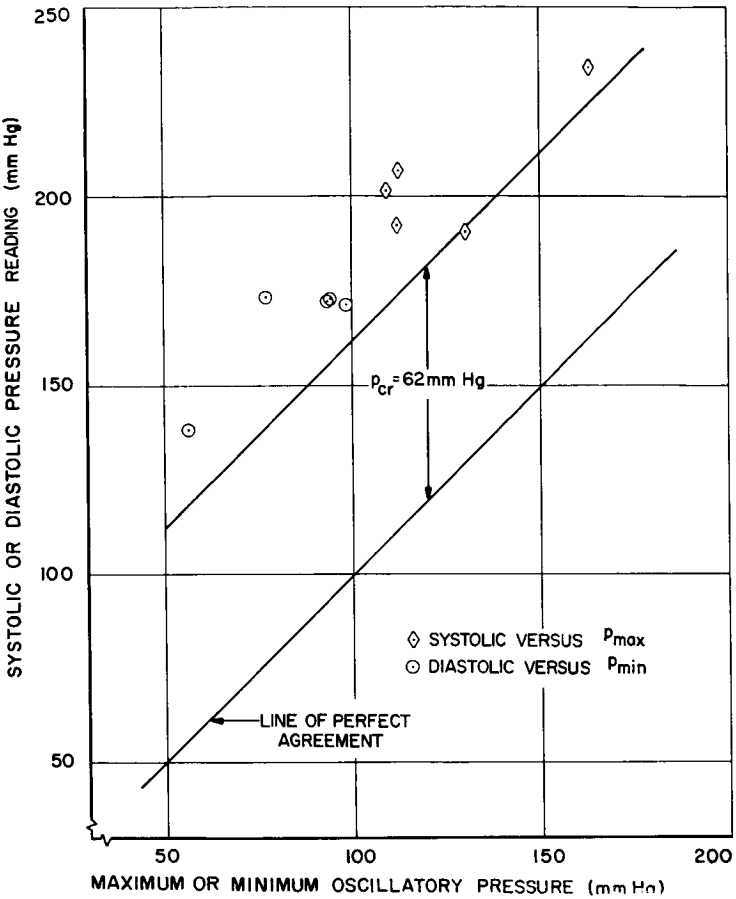

Fig. 10. Auscultatory versus direct pressure measurements for 1 in. diameter gum rubber simulated artery of $^1/_8$ in. wall thickness.

Since the critical buckling pressure of a thin-walled tube increases as the cube of the wall-thickness-to-radius ratio, we can expect that the auscultatory errors will increase rapidly with vessel wall thickness. Therefore, limited data were obtained on a 1-in. diameter gum rubber tube of $^1/_8$ in. wall thickness, and these results are shown in Figure 10. It can be seen that the auscultatory errors are indeed large for this vessel. Here again, the auscultatory readings exceed the corresponding direct readings by a relatively constant amount which is some-

what larger than the critical buckling pressure. Consequently, the errors would be aggravated by taking the fourth phase of the Korotkoff sounds as an indication of diastolic pressure, since this would further increase the auscultatory reading.

All in all, with few exceptions, it would appear from Figures 9 and 10 that both the auscultatory systolic and diastolic pressure readings generally exceed the corresponding maximum and minimum intra-arterial pressures, respectively, by an amount which depends primarily upon the elasticity and the wall thickness of the vessel itself. This would suggest that the critical buckling pressure of the vessel may be of primary importance in the production of the Korotkoff sounds during partial occlusion. This buckling pressure is the pressure difference (external minus internal) at which the tube initially buckles from a circular into an elliptical cross section. Once this happens to the arterial wall, the reduction in cross-sectional area of the vessel causes a reduction of the fluid pressure because of the increased velocity through the resulting orifice (the Bernoulli effect). This produces a further decrease in cross section, and the vessel collapses. The intermittent phenomenon which produces the Korotkoff sounds would then be initiated when the oncoming pressure wave becomes amplified ahead of the occlusion and forces the vessel to open. The pressure then drops again and the process repeats itself.

An obvious question in regard to the foregoing results is whether or not they are applicable to real blood. It is recalled that the test fluid was a combination of water and glycerol to provide a wide range of viscosity. In order to check the generality of these results, the possibility of modeling the red blood cells by means of plastic or glass beads was considered, but it was decided that these were not a satisfactory representation of the red cells for this problem, since the diffusion, reflection, and absorption of sound would be quite different for such solid particles than for the actual flexible red cells. Therefore, we resorted to the use of real blood. However, since our system requires 250 gallons of fluid, we were forced to confine the blood to the test section itself, and this was done by installing toy balloons at either end of the test section. On one side of the balloon is the blood and on the other side (and throughout the rest of the system) is water. Before this system was used in actual test runs, it was tested both with the same fluid and with two different fluids on the two sides, to insure that the presence of the balloons did not

affect the auscultatory readings. Specific cases were rerun using fresh steer blood in the simulated artery. Two medical technicians assisted in these tests, and fresh steer blood was obtained each morning. Then, at the end of each day, the system was sterilized in a special ultraviolet light chamber, after being thoroughly scrubbed with Haemosol and rinsed. Hematocrit readings and sedimentation rates were taken for the blood used, and we found essentially a zero sedimentation rate which is typical of steer blood, and which simplified the testing, since no stirring was required. The hematocrit averaged about 45%, and the specific gravity was 1.06.

Results for the real blood obtained in this manner are shown by the solid symbols in the plots of systolic and diastolic pressure ratios against unsteady Reynolds number (see Figs. 9 and 10). It is seen that the results for real blood are in essential agreement with those obtained using combinations of water and glycerol.

Results for the real blood obtained in this manner are shown by the solid symbols in Figure 9. It is seen that the results for real blood are in essential agreement with those obtained using combinations of water and glycerol.

The conclusions from this experimental investigation are as follows: (*1*) The auscultatory systolic and diastolic pressure readings generally exceed the corresponding maximum and minimum intra-arterial pressures, respectively, by an amount which depends primarily upon the thickness and stiffness of the arterial wall. (*2*) The magnitude of the error in both the systolic and diastolic readings is generally somewhat greater than the critical buckling pressure of the arterial wall and is relatively independent of either pulse rate or mean pressure level. (*3*) The error in diastolic reading is evidently aggravated by using the fourth phase rather than the fifth phase of the Korotkoff sounds for the diastolic reading. (*4*) The results using real steer blood are in good agreement with those obtained using water and glycerol to represent the blood fluid. Finally, it should be mentioned that the wave velocity and wall displacement measurements indicate fairly good agreement with the theoretical results of Womersley[6] and Morgan and Kiely,[7] except for the transient case in which the mean pressure level is changing with time.

In view of the importance of the elastic properties of the vessel being occluded, tests are now being conducted to determine the elastic behavior of the human brachial artery.

The work reported herein was originally supported by the U. S. Air Force Systems Command. More recently, funding has been continued by the Ames Research Center of NASA as part of a larger fundamental research program.

References

1. Erlanger, J., *Am. J. Physiol.*, **40**, 82 (1916).
2. Timoshenko, S., *Theory of Elastic Stability*, McGraw-Hill, New York, 1936, p. 216.
3. Halphen, G. H., *Treatise on Elliptic Functions*, Vol. 2, Gauthiers-Villars, Paris, 1888, ch. V.
4. McIvor, I. K., Ph.D. thesis, to be published.
5. Hurd, C. W., K. P. Chesky, and A. H. Shapiro, *J. Appl. Mech.*, 253 (1953).
6. Womersley, J. R., WADC Tech. Rept. 56-614, 1957.
7. Morgan, G. W., and J. P. Kiely, *J. Acoust. Soc. Am.*, **26**, 323 (1954).

Synopsis

14579

After considerable preliminary analysis of the pulsatile viscous flow in flexible tubes, a large-scale pulsating flow system has been constructed and various simulated arteries of 1 in. i.d. have been tested over wide ranges of pulse rate, pressure level, and pulse pressure using, first, various mixtures of water and glycerol and, finally, whole steer blood as the fluid. The oscillatory intra-arterial pressures were recorded by pressure transducers which were attached to both static and total pressure probes in the flow itself, and these are compared with measurements of the systolic and diastolic pressures which were obtained by the clinical auscultatory technique, using a stethoscope and a specially designed pressure chamber. In addition, simultaneous measurements were made of arterial wall displacements and the velocity of the pulse wave along the tube. The simulated system has exhibited many of the qualitative features of a living human subject, and the entire spectrum of characteristic Korotkoff sounds was produced in the artery.

The test results indicate that the auscultatory systolic and diastolic pressure readings are consistently higher than the corresponding maximum and minimum of the oscillatory intraarterial pressures by an amount which depends on the stiffness and thickness of the arterial wall. In fact, the error in both readings is evidently somewhat larger than the critical buckling pressure of the vessel in question and is relatively independent of frequency and pressure level. Consequently, the error in the diastolic reading is aggravated if one uses the fourth phase of the Korotkoff sounds (rather than the fifth) as an indication of diastolic pressure. The auscultatory readings with whole steer blood are in agreement with those using water and glycerol at the same conditions. Measured arterial wall displacements and wave velocities are in approximate agreement with theory except during transient changes in mean pressure level.

author

N67 14580

Dimensional Analysis of Pulsating Blood Flow—An Introduction

W. McCOMIS, *Massachusetts Institute of Technology, Department of Nutrition and Food Science, Cambridge, Massachusetts,* S. CHARM, *Tufts University School of Medicine, Boston, Massachusetts,* and G. KURLAND, *Beth Israel Hospital and Harvard Medical School, Cambridge, Massachusetts*

Many physiologists study the oscillatory flow of blood *in vivo* rather than *in vitro*. The early German workers attempted to analyze the circulatory system as a whole by the use of an analog model called the "Windkessel." More recently, investigators such as McDonald,[1] realizing the complexities, have chosen to isolate and analyze a segment of the system such as a single artery with the thought of synthesizing an analysis for the whole system from these segments. In either case, the investigator working *in vivo* must correct for or temporarily neglect the effects of such complicating factors as elasticity, tube taper, branching, and anomalous blood viscosity.

It is the authors' approach to take the further simplifying step of working first *in vitro*. In this way these factors may be isolated and the system treated as analytically as possible. Refinements may then be added in a stepwise fashion until an *in vivo* study may be more confidently attempted.

THEORETICAL

It is difficult to find in the literature a detailed development of the equations of motion for pulsatile flow of fluid through rigid cylindrical tubes. Too often one finds only condensed and simplified equations which apply only in specific cases. The approximations which lead to

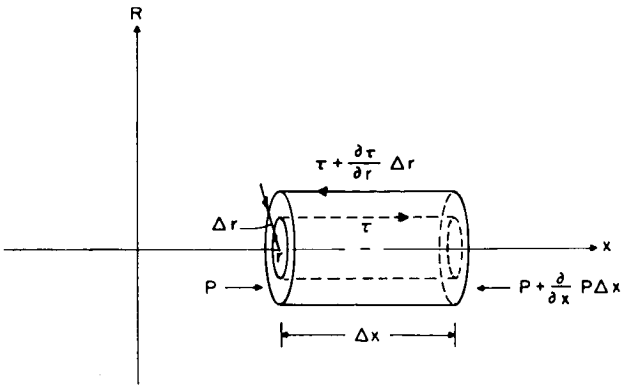

Fig. 1. Fluid control volume.

these simplified equations should be realized. The general method for developing such equations may be found in many mass transfer books.[2]

Consider a cylindrical shell of fluid of inside radius r, outside radius $r + \Delta r$, and length Δx as shown in Figure 1. A balance of forces in the x-direction gives:

$$P \cdot 2\pi r \Delta r - [P 2\pi r \Delta r + (\partial/\partial x)(P 2\pi r \Delta r)\Delta x] + \tau \cdot 2\pi r \Delta x - [\tau 2\pi r \Delta x + (\partial/\partial r)(\tau 2\pi r \Delta x)\Delta r]$$

which results in a net balance of forces in the x-direction of

$$-(\partial P/\partial x)\Delta x 2\pi r \Delta r - \partial/\partial r\,(\tau 2\pi r \Delta x)\Delta r \qquad (1)$$

where τ represents the shearing stress.

The x-direction momentum flux due to fluid motion in the x- and r-directions is considered next:

$$[(2\pi r \Delta r \rho) V_x] V_x - [(2\pi r \Delta r \rho)\ V_x^2 + (\partial/\partial x)(2\pi r \Delta r \rho\ V_x^2)\ \Delta x] + [(2\pi r \Delta x \rho) V_r] V_x - [(2\pi r \Delta x \rho) V_r V_x + (\partial/\partial r)(2\pi r \Delta x \rho V_r V_x)\Delta r]$$

where ρ is the fluid density, V_x the x-direction velocity, and V_r the r-direction velocity. The net x-direction momentum flux associated with fluid motion in the x- and r-directions is therefore:

$$\{[\partial(\rho V_x^2)]/(\partial x)\}\ \Delta x 2\pi r \Delta r - (\partial/\partial r)\ (\rho V_r V_x r) 2\pi \Delta x \Delta r \qquad (2)$$

Recalling that force may be expressed as rate of momentum change, e.g., $Fdt = dm$, eqs. (1) and (2) may be combined to give the net

change in the x-direction momentum of the fluid within the control volume for the period t to $(t + \Delta t)$:

$$- (\partial P/\partial x)\ \Delta x 2\pi r \Delta r \Delta t - (\partial/\partial r)\ (\tau 2\pi r \Delta x)\Delta r \Delta t$$
$$- (\partial/\partial x)\ (\rho V_x^2)\ \Delta x 2\pi r \Delta r \Delta t - (\partial/\partial r)\ (\rho V_r V_x r) 2\pi \Delta x \Delta r \Delta r \quad (3)$$

which must also equal

$$(\partial/\partial t)\ (\rho V_x) 2\pi r \Delta r \Delta x \Delta \quad (4)$$

Equating (3) and (4) gives:

$$- (\partial/\partial t)\ (\rho V_x) = (\partial P/\partial x) + (1/r)(\partial/\partial r)\ (\tau r)$$
$$+ (\partial/\partial x)\ (\rho V_x^2) + (1/r)(\partial/\partial r)\ (\rho V_x V_r t) \quad (5)$$

The first simplification usually made on this complete equation is to assume the fluid has constant density. This is a very reasonable assumption for liquids and means that the principle of continuity as expressed by eq. (6) may be used to cancel many of the terms in the expanded form of equation (5).

$$\partial V_r/\partial r + V_r/r + (1/r)(\partial V_\theta/\partial \phi) + \partial V_x/\partial x = 0 \quad (6)$$

Equation (7) is the final result of this manipulation.

$$-\rho(\partial V x/\partial t) = \partial P/\partial x + (1/r)\partial(\tau r)/\partial r$$
$$+ \rho V_r(\partial V_x/\partial r) + \rho V_x(\partial V_x/\partial x) \quad (7)$$

The next assumption which may be made is that the flow is fully developed in the sense that $V_r = 0$. Since $\partial V_\theta/\partial \theta$ is zero from symmetry, this assumption also makes $\partial V_x/\partial x = 0$ from eq. (6). Therefore, the last two terms of eq. (7) drop off to give:

$$-\rho(\partial V_x/\partial t) = \partial P/\partial x + (1/r)\ \partial(r\tau)/\partial r \quad (8)$$

The validity of this assumption will be discussed with the experimental results.

If the equation is to be developed further, τ must be expressed in terms of V and r. If the fluid in question is Newtonian, τ may be replaced by $-\mu(\partial V_x/\partial r)$, where μ is the constant viscosity. Equation (8) then expands to

$$\partial^2 V_x/\partial r^2 + 1/r(\partial V_x/\partial r) - 1/\nu(\partial V_x/\partial t) = 1/\mu\ (\partial P/\partial x) \quad (9)$$

where ν, the kinematic viscosity, equals μ/ρ.

This form of the equation of motion is usually taken as the starting point for analyzing the oscillatory flow of fluid through cylindrical tubes. The late J. R. Womersley in his classical analysis of blood flow in arteries begins with this equation.[3] His solution of this equation and its correlation with experimental data taken in the femoral artery of the dog is fully discussed by McDonald.[4]

A few points need to be emphasized. Womersley's solution of this simplified equation involves expressing the pressure curves in terms of a Fourier series and reconstructing the corresponding flow curves. This solution gives only the oscillatory components of the flow which have a mean value of zero. For this reason, a mean value must be added to the oscillatory terms. This mean value is taken as a Poiseuille flow calculated from the mean pressure gradient. Womersley's analysis is therefore as McDonald clearly explains, "of no practical application in the prediction of mean flow in an artery."

The second important point is that Womersley's equation for flow predicts that in small vessels Poiseuille's equation will hold. That is, although the pressure gradient pulses, the flow will vary linearly with it. Although Taylor[5] has shown theoretically why the anomalous viscosity of blood may not influence the oscillatory flow in large arteries, it is well known that the effect is important in small tubes in steady flow.[6] Until now no experimental evidence has been presented to determine the effect on energy losses of pulsating flow through small tubes.

Since at this time methods are not available for rigorously solving the partial differential equations which express the flow, the authors propose to investigate various parameters which may influence the pulsating flow of blood through small tubes. One method of organizing such parameters which will be tried is that of dimensional analysis. Such analysis has proved successful in characterizing steady flow of blood through small glass tubes.[7]

DIMENSIONAL ANALYSIS

It should be possible to describe the pulsatile flow of a power-law fluid using the following variables where ΔP is the mean pressure difference, V the mean velocity of flow, ρ the density of fluid, L the length of tube, D the diameter of tube, f the frequency of pressure pulse, b the power-law constant expressing the relationship between

shear stress and shear rate, s the dimensionless power-law constant, E the Young's modulus, and δ the tube thickness.

This choice of variables assumes a constant wave form, e.g., a sine wave. Using the methods described by Brown,[8] these variables may be assembled into the following dimensionless groups:

$$L/\delta,\ D/\delta,\ E/V^2\rho,\ s,\ E/\rho f^2\delta^2,\ [E(s - 2/2)b]/\rho^{s/2}\ \delta^3,\ \Delta P/E$$

These groups are not unique, but appear to be the easiest to manipulate experimentally. Only experimentation will tell whether the relationship between these groups is of such a nature to be expressed in a simple form.

EXPERIMENTAL

Figure 2 shows diagrammatically the equipment used in this investigation. The syringe, acting as an air piston, is driven by a governed speed motor. This provides a pulsating air pressure which may

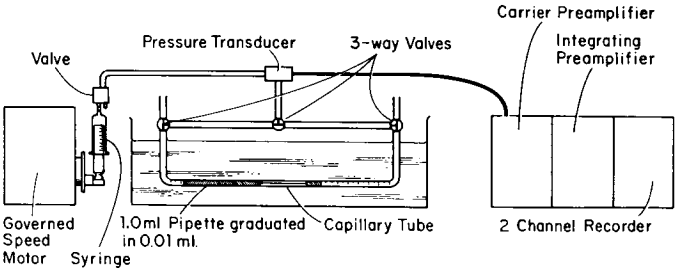

Fig. 2. Experimental apparatus.

be adjusted both in frequency and amplitude. The pulsating air pressure is the driving force which acts upon the fluid in the reservoir. The reservoir is a modified pipette of 1 ml. capacity graduated in 0.01 ml. The glass capillary tubing is positioned between two such reservoirs. By the use of three-way valves, the fluid may be forced through the capillary tube from either side while the other is open to the atmosphere.

A pressure transducer located in the air line is used to measure the oscillating pressure. The signal from the transducer is amplified and recorded on a two-channel recorder with a chart speed of 5 mm./sec.

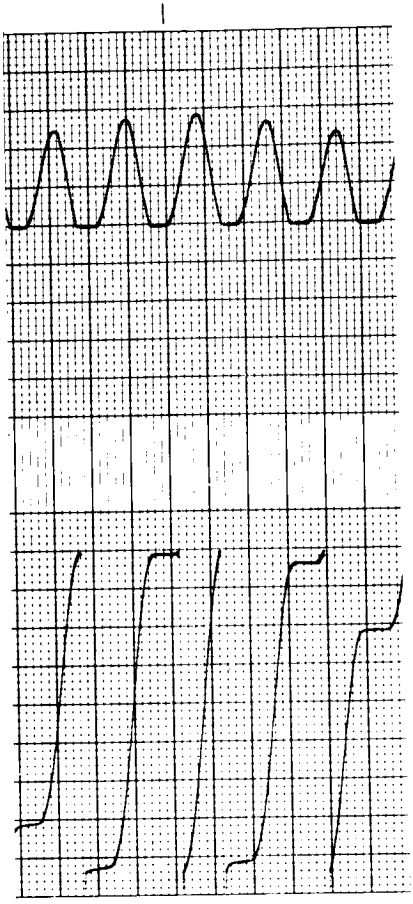

Fig. 3. Pressure recording.

The second channel is used to record the area under the pressure time curve. This time-pressure integration is accomplished by an integrating preamplifier. A typical recording is shown in Figure 3. To simplify the pressure pulse and prevent backflow, the air line contains a ball valve which opens to the atmosphere on the intake stroke. This allows air to enter, filling the space left by the displacement of the fluid through the capillary. In this way the pressure never goes below atmospheric.

The recorder has a timing device which is used to mark the pressure tape as the fluid flows through the capillary. The integral of Pdt is obtained as well as the time required for a specific volume of fluid to flow through the tube. By dividing $\int Pdt$ by Δt the mean ΔP is obtained.

All measurements were made in silicon-coated glass capillaries at 37°C.

RESULTS AND DISCUSSION

While this investigation is still in its primary stages, some interesting data have been taken.

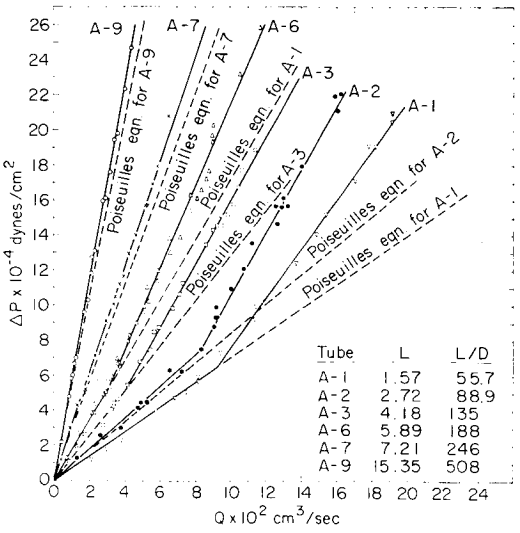

Fig. 4. Mean pressure drop vs. mean volumetric flow for distilled water.

Figure 4 shows the mean pressure drop ΔP in dynes/cm.^{2} plotted against the mean flow Q in cm.^{3}/sec. for six tubes. The fluid was distilled water. The tubes varied in length only, having a common diameter of approximately 0.3 mm. The dashed lines describe the ΔP vs. Q relationship for each tube as predicted by Poiseuille's equation.

The mean values of ΔP and Q follow Poiseuille's equation over a limited range of flows and then seem to deviate rather abruptly to an-

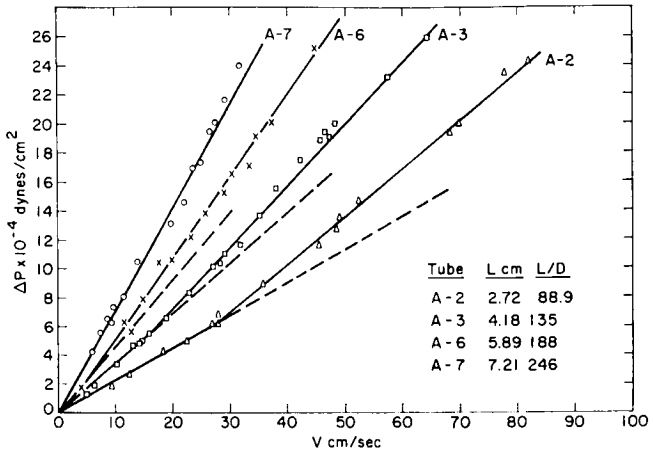

Fig. 5. Mean pressure drop vs. mass average velocity for citrated human blood.

other straight-line relationship. This deviation occurs at lower flows in the longer tubes but is much more pronounced in the shorter tubes.

Womersley's analysis predicts, as noted before, that flow in small tubes will follow Poiseuille's equation. That is, where α is less than 0.5 for the fundamental harmonic, the flow will follow the pressure gradient linearly. For the fundamental harmonic α was equal to $R\sqrt{(2\pi f\rho)/\mu}$, and under the experimental conditions was equal to 0.32. Yet the flow did not follow Poiseuille's line as predicted.

The fact that these energy losses occur with water at Reynold's numbers of 650 and much less, depending on the tube length, suggests that the development of gross turbulence is not the best explanation. Since the effect seems to be more pronounced in short tubes, the effect of entrance conditions may be important. Chang and Atabek[9] have shown that the velocity profile is continually changing over the initial portion of the tube and fully developed flow only occurs beyond what is called "the inlet length." Although this inlet length is independent of tube length, any energy losses which occur will be of a larger percentage of the total pressure drop for short tubes than for long at the same rate of flow. Thus the assumption that $V_r = 0$ may not necessarily hold for short tubes.

The deviation from Poiseuille's line at lower flow rates for the longer tubes can probably be attributed to larger inertial effects which occur

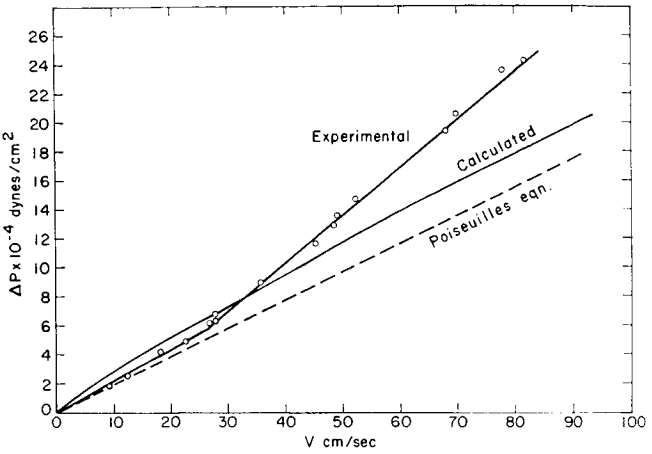

Fig. 6. Experimental and calculated lines for citrated human blood.

at higher pressures. If the pressure pulse is considered, it is noted that by holding the frequency constant and increasing the amplitude of the pulse, the rate of change of the pressure and therefore of the flow must increase, thus increasing the energy losses due to inertial effects. Since higher pressures are needed to give the same flow through long tubes as compared with short, this effect would be noted at lower flow rates in the long tubes.

Figure 5 shows similar curves for blood flow where ΔP has been plotted against the mass average velocity V in cm./sec. The same tendency is noted here for the pressure to increase more rapidly at higher flow rates. Again this increase tends to occur later but more markedly in the shorter tubes.

One of these curves was redrawn in Figure 6. Also appearing in this figure are two calculated lines. An apparent viscosity was measured in a capillary tube viscometer at a wall stress of 1680 dynes/cm.^{2}. This "asymptotic viscosity" was used in Poiseuille's equation. As with the water, the data approximate this line at low flows but not at high velocities. The second line was calculated using the equation of Charm et al.[7] as modified by Song et al.[10] This equation considers the fact that blood is not a Newtonian fluid and would have described the flow better than Poiseuille's equation at high flow rates if the experimental curve had continued straight.

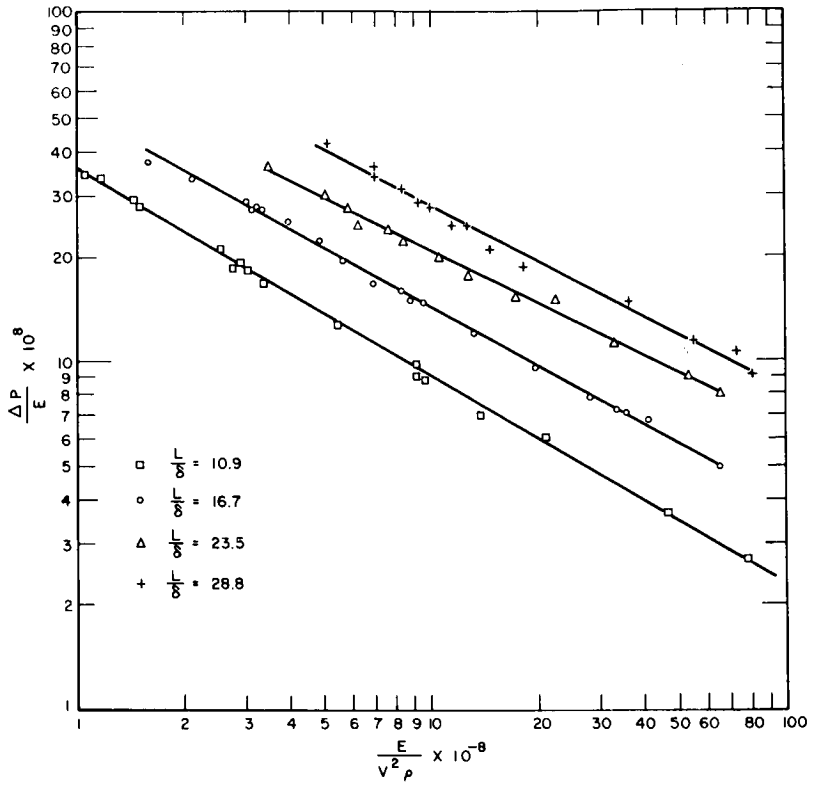

Fig. 7. Log $\Delta P/E$ vs. log $E/V^2\rho$.

As a first approach to applying dimensional analysis to the limited amount of data available at present, $\Delta P/E$ has been plotted against $E/V^2\rho$ on a log-log scale as shown in Figure 7. The effect of a third group, L/δ, is also shown in this figure. The relationship between log $\Delta P/E$ and log $E/V^2\rho$ appears to be linear. More data are needed to establish the slopes of these lines as a function of L/δ. From the data available, they do not appear to be constant.

SUMMARY

Until now no experimental work has been done to determine the effect of pulsating flow on energy losses for blood in small tubes. At

this time methods are not available for rigorously solving the partial differential equations which express the flow. However, it is possible to investigate the various parameters in pulsating flow through dimensional analysis. A similar approach in characterizing the steady flow in small tubes has been successful.

The tube diameters investigated are in the order of 100 to 300 μ. A pressure pulsing system permitted the delivery of pulsating air to the blood reservoir which pulsed the flowing blood. The shear stress-shear rate characteristics of the blood were measured in a Brookfield cone and plate viscometer.

In plots of pressure loss vs. mass average velocity, it is observed for both blood and water that a deviation in the curve occurs at a critical point. The deviation occurs at lower flow rates in longer tubes but is more marked in shorter tubes.

At the low flow rates (prior to the break in the curve), the flow of both blood and water appear to follow the equations expressing steady flow. However, after the critical conditions appear, the energy losses become considerably greater. This is apparently due to a type of induced turbulence, although the Reynolds numbers where this occurs with water are much less than 650.

Since the effect appears to be more pronounced in short tubes, the effect of entrance conditions may be important. The deviation from the steady flow equations at low flow rates in longer tubes can probably be attributed to larger inertial effects which occur at higher pressures.

It is noted that by holding the frequency constant and increasing the amplitude of the pulse, the rate of change of the pressure and therefore of the flow must increase, thus increasing the energy losses due to inertial effects.

Since higher pressures are needed to give the same flow through long tubes as compared with short tubes, this effect would be noted at lower flow rates. A dimensional analysis of the variables in the pulsating system yields a relationship between the variables. The variables in the system considered are: pressure loss, pulse frequency, average velocity, tube diameter, tube wall elastic modulus, tube wall thickness, tube length, fluid viscometry, diameter, and density.

References

1. McDonald, D. A., *J. Physiol.*, **127**, 533 (1955).
2. Rohsenow, W. M., and H. Choi, *Heat, Mass and Momentum Transfer*, Prentice Hall, New Jersey, 1961.
3. Womersley J. R., J. *Physiol.*, **127**, 553 (1955).
4. McDonald, D. A., *Blood Flow in Arteries*, Williams & Wilkins, Baltimore, Md., 1960.
5. Taylor, M. G., *Phys. Med. Biol.*, **3**, 273 (1959).
6. Charm, S., and G. S. Kurland, *Am. J. Physiol.*, **203**, 417 (1962).
7. Charm, S., W. McComis, and G. H. Kurland, in *2nd European Conf. Microcirculation, Pavia 1962*, ed. H. Harders, *Bibliotheca Anatomica*, **4**, 72 (1964), Karger, Basel-New York, 1964.
8. Brown, G. G., *Unit Operations*, Wiley, New York, 1960, p. 137.
9. Chang, C. C., and H. B. Atabek, *Phys. Med. Biol.*, **6**, 303 (1961).
10. Song, C., M.S. Thesis, M.I.T., 1964.

Synopsis

14580

A detailed consideration is made of the equations of motion for pulsatile flow of a non-Newtonian fluid through cylindrical tubes and the usual assumptions made in obtaining a solution. In view of the fact that the assumptions necessary to reduce the theoretical equations to a solvable form are unrealistic for flow of blood through small tubes, the authors suggest dimensional analysis as a method for obtaining equations which describe the pressure-velocity relationships.

author

BLOOD FLOW IN BRANCHING AND TAPERED TUBES

N67 14581

Plasma Skimming in Human Blood Flowing through Branching Glass Capillary Channels

A. A. PALMER,* *Research Department, Kanematsu Memorial Institute, Sydney Hospital, Sydney, Australia*

INTRODUCTION

The term "plasma skimming" was used by Krogh[1] in 1922 to denote an unequal distribution of plasma and cells in branching arterioles and capillaries, a phenomenon which he related to the axial drift of the red cells in blood flowing in small vessels. Although many observers have since commented on the occurrence of plasma skimming in the microcirculation, very few attempts at quantitative investigation have been made.

Some quantitative studies of axial streaming have been made by Fåhraeus,[2,3] Taylor,[4] and Bayliss.[5] A few direct measurements of plasma skimming *in vivo* are cited by Mchedlishvili.[6] Gelin[7] has made the only direct *in vitro* measurement of plasma skimming that the author has been able to find; he passed blood of high sedimentation rate through a metal tube with diametrically opposed side branches and showed that the hematocrit was lower in the blood from the side branches.

The present paper deals with some studies of the distribution of red cells when human blood flows through branching glass channels.

METHODS

In most of the experiments slitlike rectangular channels were used as they are much simpler to construct precisely than branching tubes of circular section, and at comparable shear rates they yield larger volumes for analysis. They were made from glass prisms separated at the edges with metal or glass strips of the required thickness (30, 100, and 200 μ); the channels were 50 mm. long and 6 or 25 mm. wide.

PRECEDING PAGE BLANK NOT FILMED.

Some experiments were done with circular glass tubes aligned and butted end to end so as to leave a small defect which acted as an encircling branch. Human blood was drawn freshly into a polyethylene bag containing acid citrate dextrose solution, heparin was then added and the blood with anticoagulants was filtered through a millipore filter of nominal pore size, 10 μ. A sample of the blood was made to flow through a transparent chamber 100 μ thick and watched with the microscope to exclude the presence of minute clots or platelet aggregates. The results were inconsistent if microscopic clots or aggregates were present. For this reason transfusion bank blood was unsatisfactory.

The channel led directly from the reservoir and was kept vertical so that sedimentation would not affect the distribution of the cells. Dead space in the tubes leading from the branches was kept as small as possible. The blood reservoir and channels were maintained at 37 °C. with a water jacket. Reservoir pressure could be regulated between 0 and 200 cm. of water. The ratio of the flow in the branches was regulated with micrometer screws on fine plastic tubes. The outflowing blood was collected in graduated pipets, mixed mechanically and the red cell volume concentration determined with the Hawksley microhematocrit apparatus.

RESULTS

Partial plasma skimming, that is, an unequal distribution of cells and plasma, was found consistently in branching, channels of dimension 200 μ or less in the plane of branching whenever the rate of flow from the branches was unequal or if the arrangement of the branches was such that unequal proportions of axial and peripheral blood entered them. Figure 1 illustrates diagrammatically how, with streamlined flow, there may be unequal distribution to branches of peripheral and axial parts of the stream. An unshaded arbitrary peripheral zone and a shaded axial zone are illustrated; it will be seen in Figure 1*a* that at a simple branch the proportion of peripheral and axial streams depends on the ratio of flow in the branches; in Figure 1*b* the arrangement is such that the through channel will receive a higher proportion of blood from the axial zone. These results will be independent of the angle of branching provided the flow remains streamlined and provided inertial effects do not cause

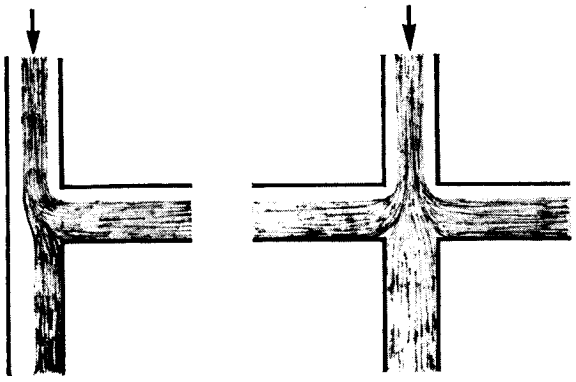

Fig. 1. Diagram to illustrate distribution of axial and peripheral parts of stream to branches when there is streamline flow: (*a*) the proportions depend on the ratio of the flow rates in the branches, (*b*) the through channel receives a greater proportion of blood from the axial zone. The channels used were rectangular in cross section and the dimension in the plane of the diagram (i.e., the plane of branching) was very small compared with the dimension at right angles to the plane of the diagram; the through channel can then be made to give an almost pure sample of axial blood and the width of the zone sampled can be regulated by the outflow ratios.

redistribution of suspended particles. No significant difference was found in the distribution of red cells with channels having different angles of branching.

The next two figures show the result of passing blood through branching channels corresponding firstly to the simple branch (Fig. 1*a*) and then to the diametrically opposed branching system (Fig. 1*b*).

Figure 2 shows the effect of the outflow ratio on skimming at a simple branch in a wide slitlike rectangular channel of cross section 30 by 25,000 μ. Difference in hematocrit of blood from the branches (ordinate) is plotted against outflow ratio (abscissa). The line drawn is $H_1 - H_0 = K\ [1 - (F_2/F_1)]$ where $K = 15$. It can be seen that most of the experimentally determined points fall close to this line. The reason for this relationship can be best explained by reference to the Figure 3 but before doing this it should be mentioned that at flow ratios greater than about 6 to 1 (or less than 0.17) the results became inconsistent and there is reason to believe from watching

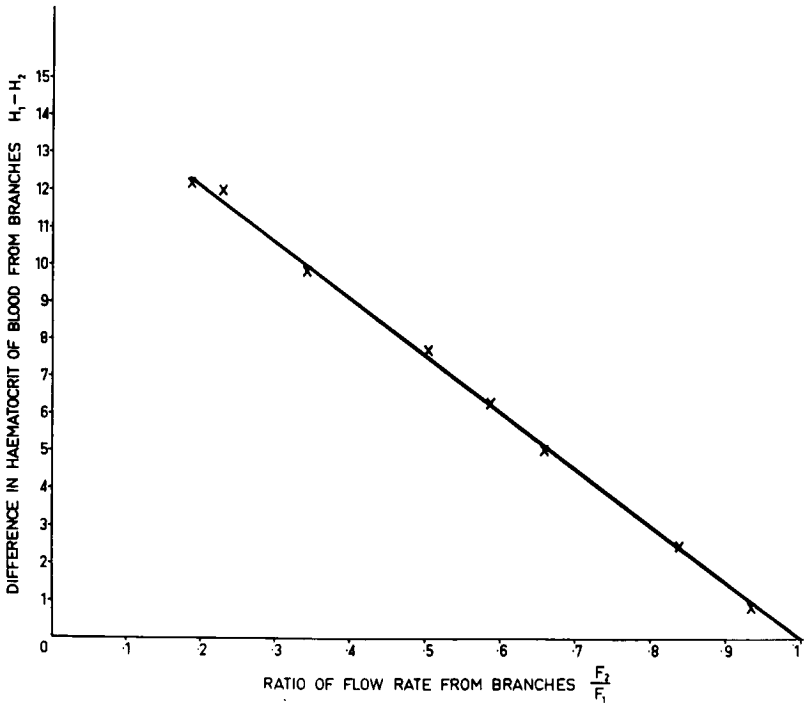

Fig. 2. The graph shows dependence of skimming at a simple branch on the outflow ratio. Difference in hematocrit of the blood from the branches is plotted against the ratio of the flow rates from the branches. The experimental points fall close to the line $H_1 - H_2 = K|1 - (F_2/F_1)|$ with $K = 15$.

flow in channels under the microscope that with high ratios an eddy may form in the branch entrance and disturb the laminar pattern.

Figure 3 shows the results with diametrically opposed branches, when varying proportions of the flow are taken from the center branch. The method of presentation needs some explanation; the vertical lines at each side correspond to the walls of the channel and the interrupted vertical line to the center of the channel. Ordinates are hematocrits and the abscissa now represents fractional increments of volume flow starting from the left wall, so that the distance to the center represents half the flow (0.5) and the distance to the other wall the total flow (1). Each of the points plotted represents the mean of a fairly wide zone and hence small local variations would not

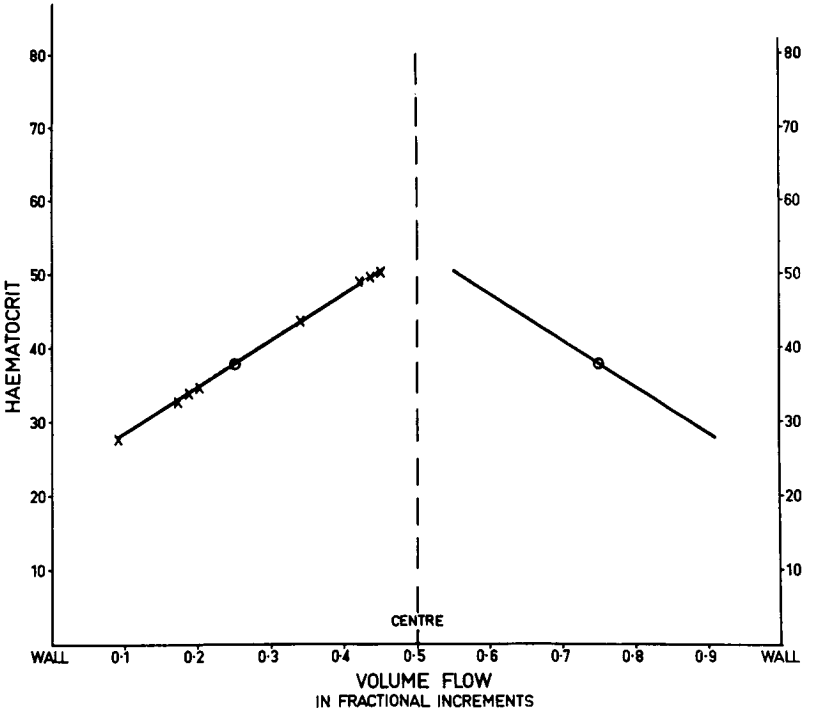

Fig. 3. Semidiagrammatic representation of the progressive increase in hematocrit from the wall to the center which would account for the experimental results. The experimental points plotted are from results using a channel which divided into three branches but the results from Fig. 2 with two branches are in equally good agreement. It must be noted that the distances along the abscissa do not correspond to distances from the wall but to fractional increments of volume flow from the wall. The line is semidiagrammatic because each of the points plotted represents the mean of a fairly wide zone and minor irregularities would be smoothed out. Each point is the mean of two or more experiments.

be evident. With this reservation it appears that in the region that can be tested there is a linear increase in hematocrit with each volume flow increment from the wall to the center. The curve shown in Figure 2, $H_1 - H_2 = K\ [1 - (F_2/F_1)]$ can be simply derived from this linear relationship provided the width of the channel is great compared with its thickness.

Only limited studies have been done on the influence of channel dimensions: in a channel of 30 μ dimension in the plane of branching

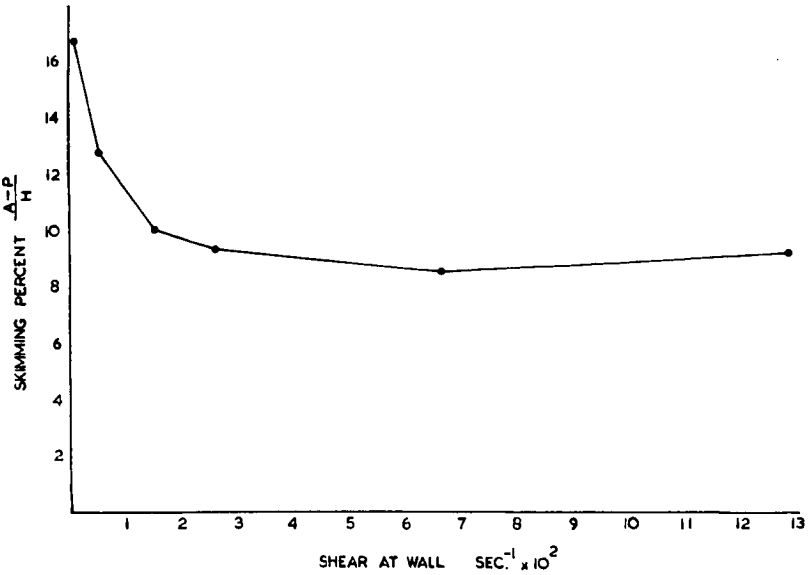

Fig. 4. The effect of varying absolute or total flow rate on skimming in a channel of cross section 100 by 6000 μ which divided into three branches. Mean per cent difference in hematocrit of blood from the central and side branches is plotted against flow rate expressed as apparent shear rate at the wall, calculated assuming that the velocity profile had been parabolic.

the difference in hematocrit between the samples from the branches was 3 to 4 times greater than in a channel of 100 μ, other parameters being equal.

Skimming was the same from two branches situated 25 and 50 mm., respectively, from the inlet along the 30-μ channel. This indicated that the distribution of red cells reaches equilibrium after 25 mm., but the minimum distance necessary for equilibrium has not been determined.

Figure 4 shows skimming plotted against absolute flow rate in a rectangular channel 100 by 6000 μ. Flow rate is expressed as apparent shear rate at the wall, calculated by assuming a parabolic velocity profile, although it is appreciated that the actual velocity profile will be somewhat flattened by the axial hematocrit gradient. Skimming did not vary significantly with absolute flow rates above an apparent shear rate at the wall of about 200 sec.$^{-1}$ but increased progressively as the apparent shear rate fell to 20 sec.$^{-1}$.

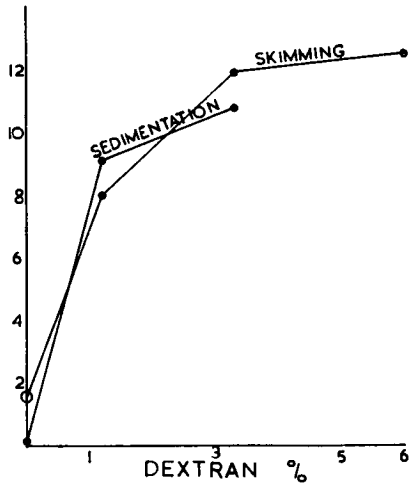

Fig. 5. The effect of addition of high molecular weight dextran on skimming and sedimentation rate. Skimming is expressed as per cent difference of hematocrit of blood from the branches, and sedimentation rate is measured in millimeters/hour.

Figure 5 shows the effect of the addition of high molecular weight dextran (B.D.H. grade A, molecular weight 200,000 to 275,000) to the blood-anticoagulant mixture. Skimming and sedimentation rate both increase with increasing concentration of Dextran in the ranges shown. The increased sedimentation rate is indicative of rouleau formation where red cells clump together like a pile of coins.

All the results presented are from experiments using rectangular channels but corresponding studies relating to shear rate and to Dextran addition were made with tubes of circular cross section, 200 μ in diameter. These results were in agreement with those from rectangular channels but the skimming was small, presumably because of the larger diameter, and technical difficulties have so far prevented the use of finer tubes.

DISCUSSION

The finding of a progressive increase in hematocrit from the wall to the axial plane of the channel was unexpected. Oliver[8] showed that suspended rigid spheres, free to rotate, drift during flow to a position

roughly midway between the wall and center of a tube, while spheres biased to prevent rotation drift to the center of the tube. Microscopic observation of the red cells in the present experiments shows that at least some of them rotate. Goldsmith and Mason[11] found axial migration only with particles which underwent shear deformation. Rat red cells undergo conspicuous shear deformation but human red cells, at least in the presence of anticoagulants, are less readily deformed. Taylor[4] considered that the flow in the axial stream could not be regarded as laminar and believed that rotation and collision would disperse and mix the particles. This dispersion no doubt opposes the tendency to axial drift but an equilibrium is apparently reached in which a concentration gradient is maintained.

The failure to demonstrate an increase in skimming with increase in shear rate is surprising in view of the findings of Fåhraeus,[2] Taylor,[4] and Bayliss[5] and further study is needed. Increased skimming at low rates of shear might be due to the persistence of rouleaux increasing the effective particle size. The author has often noticed increased plasma skimming when the flow slows in rat pancreatic capillaries (Palmer[10]) but had previously attributed this to successive plasma skimming at earlier branches; the present finding if applicable to living capillaries offers an alternative explanation.

The increase in skimming found after the addition of high molecular weight Dextran which increases rouleau formation and sedimentation rate is in accord with the findings of Fåhraeus,[2] Vejlens,[9] and Gelin.[7]

It would be premature to attempt to apply these limited *in vitro* results in detail to the living circulation. No study has been made of the influence of the chemical and physical properties of the material forming the walls of the channels or of the possible effects of the anticoagulants, and the analysis of the influence of the geometry of the channels needs much further elaboration. Furthermore complete plasma skimming such as can frequently be seen in the microcirculation has not been demonstrated *in vitro*.

The present studies are however relevant to investigations of the flow of blood through fine glass tubes, and studies are in progress to find to what extent the Fåhraeus-Lindqvist effect or sigma phenomenon can be accounted for by the present results.

The research was supported in part by The National Heart Foundation of Australia.

References

1. Krogh, A., *The Anatomy and Physiology of Capillaries*, Yale Univ. Press, New Haven, 1922.
2. Fåhraeus, R., *Physiol. Rev.*, **9**, 241 (1929).
3. Fåhraeus, R., *Deut. Med. Wochschr.*, **47**, 2266 (1961).
4. Taylor, M., *Aust. J. Exptl. Med. Sci.*, **33**, 1 (1955).
5. Bayliss, L. E., *J. Physiol.*, **149**, 593 (1959).
6. Mchedlishvili, G., *Capillary Circulation*, Georgian Academy Press, Tbilisi, U.S.S.R., 1958.
7. Gelin, L. E., *Acta. Chir. Scand.*, **122**, 287 (1961).
8. Oliver, D. R., *Nature*, **194**, 1269 (1962).
9. Vejlens, G., *Acta Pathol. Microbiol. Scand.*, Suppl. 33, 1 (1938).
10. Palmer, A. A., *Quart. J. Exptl. Physiol.*, **44**, 149 (1959).
11. Goldsmith, H. L., and S. G. Mason, *Nature*, **190**, 1095 (1961).

Synopsis

(*1*) Partial plasma skimming (i.e., unequal distribution of cells and plasma) was found consistently when human blood with anticoagulants flowed through branching glass channels, of dimension 200 μ or less in the plane of branching, whenever the rate of flow from the branches was unequal or if the arrangement of the branches was such that there was unequal distribution of axial and peripheral blood. (*2*) At a simple branch in a channel of rectangular cross section, when the ratio of the axes was large and the branch was in the plane of the minor axis, the difference between the hematocrits (H_1 and H_2) of the blood from the branches was related to the ratio of the flow rates (F_1 and F_2) from the branches as follows: $H_1 - H_2 = K[1 - (F_2/F_1)]$. It can be shown that this relationship follows it is assumed (*a*) that there is a linear increase in hematocrit for increments of volume flow from the wall to the major axis and (*b*) that the flow is laminar. Here K is the difference between axial and mean hematocrits. (*3*) Results with channels which divided into three branches were in good agreement with these assumptions; however, when less than about one-seventh of the total flow passed into any one branch the results became inconsistent probably because of eddy formation. Hence, although complete plasma skimming never occurred, the possibility that there was a narrow cell-free plasma zone near the wall cannot be excluded. (*4*) Partial plasma skimming was greatest at the lowest shear rate tested; it fell as the apparent shear rate at the wall as increased to about 200 sec.$^{-1}$ and thereafter remained at an almost constant level as the shear rate was further increased. (*5*) The addition of high molecular weight dextran to the blood greatly increased partial plasma skimming.

Abstract

Viscoelastic Behavior of the Main Pulmonary Artery Segment

WALLACE G. FRASHER, JR., *Loma Linda University, Los Angeles, California,* H. WAYLAND, *California Institute of Technology, Pasadena, California,* and SIDNEY S. SOBIN, *Loma Linda University, Los Angeles, California*

The main pulmonary artery segment has been studied in dogs maintained by extracorporeal perfusion and with circulation to the segment wall intact. Segment preparation resulted in a closed sac whose proximal end was attached to a rigid delivery tube. Initial contained volume was measured at a fixed reference pressure. Pressures generated in the specimen in response to known volume inputs were recorded both statically and with sinusoidal oscillations in the normal heart rate frequency (40–180 cycles/min.). The complex geometry of the interior of the specimen at varying levels of distention was preserved by preparing casts using known volumes of a silicone elastomer.

Results in 47 experiments may be summarized as follows: (*1*) At steady state, in the normal frequency and pressure range, pressure-volume response is linear. (*2*) From the unstressed state a viscous component results in a decrement of pressure from the initial input toward an asymptotic value at the steady state. The viscous term is a function of time in quasi-static loading and a function of the number of loadings in the dynamic state. (*3*) Pressure-volume responses measured directly differ from computed values derived from other dimensional changes. The most likely explanation is the unique geometry of the segment which can be described as progressing from an ellipsoidal toward a spherical configuration.

PRECEDING PAGE BLANK NOT FILMED.

Abstract

Energy Losses for Blood Flowing through Tapered Tubes and Curved Tubes†

C. SONG and S. CHARM, *Massachusetts Institute of Technology, Cambridge, Massachusetts,* and G. KURLAND, *Beth Israel Hospital, Brookline, Massachusetts*

The energy losses for blood flowing through straight tubes, tapered tubes, and curved tubes were investigated.

An equation for calculating the energy losses for blood flow through rigid glass capillary tubes was developed by applying dimensional analysis to the experimental data. The equation so developed was used to calculate the pressure drop across the tapered tubes and curved tubes.

The energy losses in tapered tubes were calculated by considering the tapered tubes to be composed of a number of incremental straight tubes with different diameters. The energy losses in curved tubes were computed by treating them as straight tubes of the same diameters and same lengths.

The calculated results obtained with curved tubes agreed with the experimentally measured pressure drops within the expected theoretical error. The calculated pressure drops for tapered tubes showed somewhat greater deviations when compared with the experimentally measured pressures. The larger deviations in the results from tapered tubes are attributed to the technical difficulties in the calibration of the diameters of the tapered tubes. In addition, since lower pressures were used with these tubes as compared to the other tubes, the manometric errors were greater.

† Submitted to *Biorheology.*

BIORHEOLOGICAL MEASUREMENTS AND OBSERVATIONS

PRECEDING PAGE BLANK NOT FILMED.

N67 14582

Development of Instrumentation for the Testing of Extracorporeal Flow and Deformation of Biological Materials

K. WEISSENBERG,* *The Royal Institution, London, England*

The science of flow and deformation, termed "rheology," aims at the development of theories and instrumentation which would allow to test materials in such manner that one can predetermine the macroscopic behavior of the materials under all applied mechanical actions from the experimental data obtained in the tests. When the materials are of a biological nature one speaks of "biorheology," and here one has to combine two types of testing, one inside the living body, and one outside of it, and use the combined data to predetermine the behavior in the living organism under all conditions of health and disease.

As a preliminary step to the more important but very much more complicated problem of the testing of biological material inside the living body the discussion here will be restricted to the theory and instrumentation of the extracorporeal testing and, for brevity, the terms "materials" and "testing" may be used whenever there is no need to emphasize the biological aspect.

At first the testing was based on the theoretical scheme of classical mechanics which assumed that materials could possess only three different types of consistencies, solid, liquid and gaseous, each governed by a simple linear law with constant coefficients, viz., Hooke's law of elasticity for solids and Newton's law of viscosity (or friction) for liquids and gases. Within the domain of validity of these laws the testing could be carried out satisfactorily by simple instruments of conventional design which measure the movements and forces in the material only in one dimension of space under static or stationary conditions in time. It was in this way, e.g., that Poiseuille carried out his magnificent pioneer work on the flow of blood through glass

PRECEDING PAGE BLANK NOT FILMED.

capillaries (with dimensions and forms approximating those found in arteries and veins) and deduced from Newton's law of viscosity the Poiseuille law for the volume of the flow. Subsequently, Copley, Scott Blair, Gelin, Kamiya, Bayliss, Mason, and many others developed to a fine art the testing by way of capillary instruments by making the capillaries conform closer and closer to the *in vivo* condition, with respect to branching, deformability, application of pulsating pressure, and chemical and colloidal constitution of the surface. The information obtained from the testing with simple instruments such as those of the capillary type, produced most valuable information but was in certain vital aspects unsatisfactory because one found that the rheological behavior of the materials in these testing instruments deviated considerably from the classical laws on which the evaluation of the experimental results was based. One found in particular that the volume of flow through capillaries often deviated from that predicted by Poiseuille's law, and that the Newtonian viscosity then lost its significance as the resistance to flow deviated from that predicted by Newton's law. Attempts to save the validity of the classical laws failed as one found deviations in ever increasing numbers in blood and in other biological materials as well as in most engineering material of technical importance including metals, plastics, glass, timer, and colloidal gels and sols of all kinds, and nothing could hide the fact that for all these materials the classical laws made wrong predictions, at variance with the experimental results. Thus, the introduction of a new scheme became inevitable.

The new scheme was based on the modern conception of rheology which admits materials of consistencies of all kinds, solid, liquid, gaseous, and materials intermediate between two or three of them, with an infinite variety and complexity of properties and associated rheological phenomena showing up in different rheological states ranging from a "ground state" in which a material is at rest and free from applied mechanical actions, to some "worked state" in which it may be in any movement and subjected to any actions. In the framework of the new scheme one derived from the fundamental principles of thermodynamics and mechanics a continuum theory which agreed with the experimental data, and which showed for every material that the energy supplied to it by the external work is always compounded of two parts, of which one is reversibly stored and gives rise to properties termed "elastic" while the other is irreversibly dissipated (as

2. They provide for every material data for an exact analysis of its mechanical properties into elastic and viscous ones, and this helps to relate the properties to the colloidal-chemical structure.

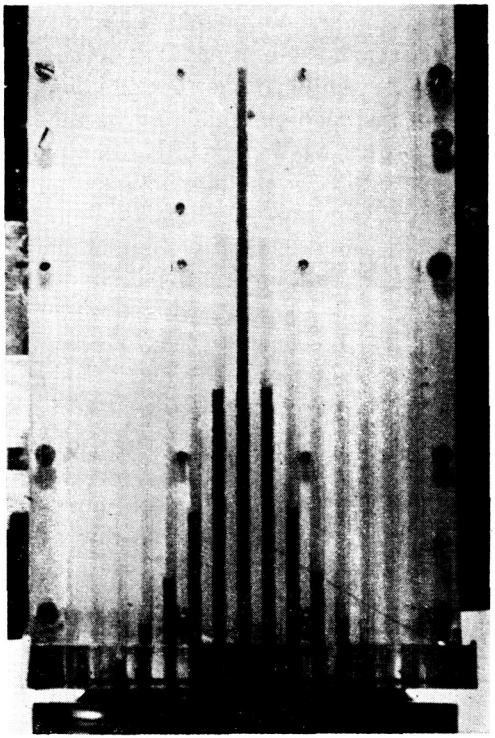

Fig. 1. The resultant pressure distribution when the cone (lower member) is rotated at a constant rate while the plate (upper member) is fixed. It is seen that the pressure distribution is in accordance with Weissenberg's theory[2] as at the free rim, the normal pressures in the axial and radial directions are equal to one another and equal to atmospheric pressure, while there is a tension (pull) along the lines of flow in the circumferential direction, causing a strangulation of the liquid in the gap and a corresponding increase of normal pressure towards the axis of rotation.

3. They can be superimposed on states with steady rates of shear, and so provide a common base for comparison of the elastic and viscous properties in the ground state with the corresponding properties in the various states of steady shear. Moreover, such a super-

position can be made to approximate the pulsating flow of blood and of other biological materials in the living organism.

4. They give results from which one can precalculate the elastic and viscous properties of the material under mechanical actions of any kind that can be built up (by way of the Fourier theorem) from a superposition of the harmonic vibrations used in the tests.

Altogether it may be said that the rheogoniometer provides for a fairly comprehensive testing of materials within the framework of the continuum theory[2] of rheology. It is intended to develop it further so as to allow, too, a study of the interaction between the material under test and the boundary surfaces, a study of the flow of one structural component of the material relative to another, a study of penetration of a structural component through a boundary surface, etc. Such further developments would be of particular interest also in extracorporeal testing of the flow of blood where phenomena of the types mentioned above are of great biological significance, as has been shown *in vivo* by the beautiful experiments of Knisely, Fåhraeus, Copley, Harders, Braenemark, Bayliss, Davis, Landau, and others.

The testing in the rheogoniometer is illustrated in Figure 1 by an example in which a viscoelastic liquid (polyisobutylene tetraline) is subjected to a torsional shear in a narrow gap between a cone and a flat circular plate which bears a series of capillary gages along a diameter.

References

1. Oka, S., *Biorheol.*, **1**, 57 (1962).
2. Weissenberg, K., *Proc. 2nd Int. Congr. Rheol., Holland*, **2**, 114 (1948).

Synopsis

The development of an instrument is discussed which allows testing of the mechanical shear properties of a material over wide ranges of conditions by taking goniometric measurements of the distributions of the movements and forces in space and time.

heat) and accounts for the properties termed "viscous." The laws of this continuum theory then allow to calculate for every material its elastic and viscous properties, as well as its macroscopic rheological behavior from experimental tests in which sufficiently comprehensive measurements are taken of the movements and forces which coexist at every point in the material and at every instant of time. The variety and complexity of the conditions encountered here could not be resolved by the use of the simple testing instruments of the capillary type which had sufficed in the classical scheme, and great progress was made through the development of instrumentation for the study of flow at various steady shear rates by Couette, Mooney, Wayland, Hartert, Philippoff, Scott Blair, Noda, Fukada, Merrill, and others. A review of the instruments was recently published by Oka.[1]

The above-named types of instruments allowed, however, neither singly nor in combination a sufficiently comprehensive testing, and this made it necessary to introduce a testing instrument of a new type. This instrument, termed "rheogoniometer," was conceived by Weissenberg first in its ideal form, and then developed in the form of various models approximating to the ideal thanks to the collaboration and help given by the Ministry of Supply represented by J. Roberts and by the manufacturers, Messrs. Farol Research Engineers Ltd., North Bersted, Bognor Regis, Sussex, England. The latest model was specifically designed to meet the requirement of technological as well as of biological research. In its ideal form the rheogoniometer achieved comprehensive testing by taking goniometric measurements of the movements and forces: (*1*) for all the various consistencies of the materials considered; (*2*) at every point in the material round the full solid angle of directions and in all kinds of development in time; (*3*) for the whole of the envisaged ranges of temperatures and of applied mechanical actions, static conditions, and unidirectional shears at various rates, as well as harmonical vibration of shears of various frequencies and amplitudes, and finally all superpositions of the unidirectional and vibrational shears.

In using a rheogoniometer model approaching the ideal, one can obtain through the testing of technological as well as biological materials an insight into the mechanical properties with features not readily available by other means. This may be appreciated by the

following considerations which illustrate the three points mentioned above, viz.:

The measurements have to be extended as indicated in (*1*) because they provide for all the materials considered a common basis for a comparison of their elastic and viscous properties. They may conveniently be applied to a series of materials in which one has systematically varied one parameter, such as the temperature, concentration, and molecular weight and wants to assess the influence of that parameter on the mechanical properties.

Measurements have to be taken as postulated in (*2*) because a material exhibits in general movements and/or forces in all three dimensions of space, even if the applied mechanical action were confined to only one or two dimensions, and there may also be noticeable various time effects such as work hardening or work softening under steady rates of shear, or persistence of movements and/or forces considerable time after the application of the mechanical action has been stopped.

The measurements have to be extended over various ranges as indicated in (*3*) because the applied mechanical action produces a change in the material from one rheological state to another accompanied in general by changes of temperature, structure, and properties. Considering first actions providing laminar shearing movements at various steady rates of shear one obtains here double the information available in a conventional viscometer, as one finds that the measurement of the tangential and normal forces as functions of the shear rate determine a non-Newtonian viscosity, as well as a non-Hookian elasticity, expressed in terms of shear dependent moduli of viscosity and elasticity. Still further information is obtained by actions providing harmonic vibrations, and these are particularly useful for the following reasons:

1. They can be applied with amplitudes so small as to cause only a minimum of disturbance to the colloidal-chemical structure of the material and so give the nearest approach to a characterization of the structure of the state in terms of mechanical properties, and such a characterization will be reproducible even in materials with a fragile or unstable structure which would be damaged by more vigorous actions. A subsequently applied series of tests with steadily increasing amplitudes will then reveal the changes of mechanical properties due to the increasing disturbance or damage of the structure.

N67 14583

A New Capillary-Type Viscometer

R. B. WHITTINGTON,* *Department of Civil Engineering, The University of Liverpool, England,* and
JOHN HARKNESS, *Department of Clinical Pathology, Musgrove Park Hospital, Taunton, Somerset, England*

SYMBOLS

η	Viscosity
η_0	Viscosity of solvent
ν	Kinematic viscosity (η/ρ)
ρ	Density
ρ_m	Density (Hg)
h_m	Suction head (Hg)
g	Acceleration due to gravity
v	Mean velocity
y	Displacement; y' and y'', time derivatives
Y	$e^{bt}\cdot y$ (t, general time)
d, D	Diameters
L	Length of capillary, length of liquid column
W	Weight
a	$(2g/L)^{1/2}$
b	$16\nu/d^2$
n^2	$\pm\ (a^2 - b^2)$
N_R	Reynolds number vd/ν
N_F	Froude number v^2/gd
ϵ	$\mathrm{Tan}^{-1}\ b/n$
m	$(D/d)^2$
C	$gd^4/L\nu^2$
K	Quadratic loss coefficient
T	Time of flow
R	Fall of liquid surface
Δ	Difference in surface levels

A, B Coefficients in calibration equations
V Transpired volume
c Concentration w/v
v_p Partial specific volume of solute molecules
H "Intrinsic viscosity," a specific volume
τ Shear stress (τ_0 at wall)

In one form or another Ostwald's U tube is the most widely used capillary viscometer. When introducing the new instrument, it was felt appropriate to compare it in all respects with the established one.

PHYSICAL BASIS OF THE OSTWALD VISCOMETER

Figure 1 shows the Ostwald U tube in its simplest form. In terms of the mean velocity v the Reynolds number $N_R = vd/\nu$, where $\nu = \eta/\rho$, the kinematic viscosity. The Froude number $N_F = v^2/gd$.

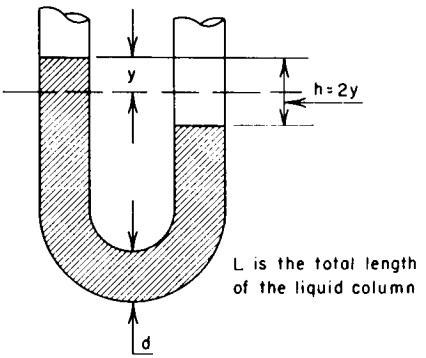

Fig. 1. The Ostwald U tube in its simplest form.

Dimensional Analysis

The physical behavior of the liquid results from the interplay of viscous and gravitational forces, which are respectively characterized by the numbers N_R and N_F.

The principle of dimensional homogeneity requires that

$$d/L = f(N_R, N_F) \tag{1}$$

The left side of the equation is constant, but the right side is in general time dependent since h (and hence v) are functions of time. However, both sides become independent of time if f is such that

$$d/L = C(N_R^2/N_F)^p \tag{2}$$

where p is arbitrary and C is constant.

Taking $p = -1$, then

$$C = (d/L)\,(N_R^2/N_F) = gd^4/Lv^2 = \text{constant} \tag{3}$$

This constant combination of the parameters pertaining to the liquid and to the apparatus is a highly significant one, for it will be shown that the motion is overdamped and unidirectional if $C < 128$.

Much thought has been expended in hydrodynamics upon the topic of theoretical critical values when one regime gives place to another. Here we have an actual example of a theoretical criterion of transition, from gradually decelerated "laminar" flow to an oscillatory motion (which can also be streamline, if the initial amplitude be small enough).

Dynamics (Viscous Losses Only)

Referring again to Figure 1, if $W = \pi d^2/L^4$ is the entire weight of the liquid, then $W/L(2y) = W/L(h)$ is the weight of the unbalanced column. The viscous drag force is

$$\frac{W}{L}\,\frac{(32vvL)}{gd^2}$$

and the net accelerating force is

$$(W/g)(a^2y + 2by') = -Wy''/g$$

where $a^2 = 2g/L$ and $b = 16v/d^2$. Here y' and y'' are the first and second time derivatives of y, and $y' = -v$. Hence the equation of motion is

$$y'' + 2by' + a^2y = 0 \tag{4}$$

Case 1. C [Equation (3)] < 128, Motion Unidirectional and Overdamped

$a < b$. Let $a^2 - b^2 = -n^2$ and let $y = Ye^{-bt}$. The equation of motion becomes

$$Y'' = -n^2Y = 0 \tag{5}$$

whose solution is

$$y = \alpha e^{-(b-n)t} + \beta e^{-(b+n)t} \tag{6}$$

The initial conditions $y = y_0$ and $y_0' = 0$ when $t = 0$ yield $\alpha, \beta = \{[(b \pm n)y_0]/(2b)\}$.

Equation (6) represents a unidirectional motion, since $y \to 0$ as $t \to \infty$. For heavy overdamping, the acceleration term in eq. (4) may be neglected, and

$$y' = -a^2 y/2b \tag{7}$$

If the liquid flows between the levels y_1 and y_2 in time $t_2 - t_1 = T$, then by integration of eq. (7)

$$\ln(y_1/y_2) = a^2 T/2b = gd^2/16\nu L$$

and

$$\nu = \frac{(gd^2)}{(16L \ln(y_1/y_2)} \cdot T = AT \tag{8}$$

where A is constant for a fixed run in a given instrument.

Thus the Ostwald viscometer basically measures the kinematic viscosity (η/ρ) and not η. This is a fact which, strangely enough, is often forgotten. The simple result $\nu = AT$ is, of course, only an approximation. It has been assumed that $a \ll b$ (heavy overdamping) and that all minor losses of energy are negligible.

Case 2. $C = 128$. Critical Damping. $a = b$

With the same definition of n as in case 1, and with the same initial conditions, $n = 0$, and the motion is described by

$$y/y_0 = (1 + bt)\, e^{-bt} \tag{9}$$

and is also unidirectional. For a given instrument, the motion is critical only for a unique value of the kinematic viscosity, and the case is therefore of little practical importance.

Case 3. $C > 128$, Oscillatory Motion. $a > b$

Setting $a^2 - b^2 = n^2$ and Y as in case 1, the equation of motion becomes

$$Y'' + n^2 Y = 0 \tag{10}$$

with the (damped) harmonic solution

$$y/y_0 = \frac{e^{-bt}}{\cos \epsilon} \cos (nt - \epsilon) \tag{11}$$

where $\tan \epsilon = b/n$. The initial conditions are as in case 1.

This oscillatory motion is shown in Figure 2 and gives rise to two possible uses of the tube as a viscometer.

Logarithmic Decrement of Amplitude

$$\ln(y_0/y_B) = 2b\ \pi/n \tag{12a}$$

where b and $1/n$ both increase with the kinematic viscosity. Thus the measurement of successive levels affords a sensitive measure of ν, but the problem of drainage errors is rather difficult.

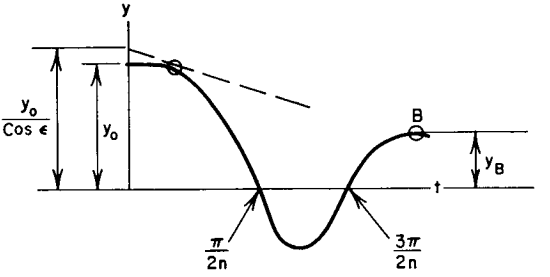

Fig. 2. Oscillatory motion. The dashed line is $y = y_0 e^{-bt}/\cos \epsilon$.

Time of Oscillation. This is given by $T = [(2\pi)/(n)] = \{(2\pi)/[(a^2 - b^2)^{1/2}]\}$, so that

$$\nu = (d/4)^2 \sqrt{(2g/L) - (2\pi/T)^2} \tag{12b}$$

Although great accuracy of timing is required, it should be well within the scope of modern electronic methods.

Dynamics (With Quadratic Losses)

To avoid the consequences of a bend in the capillary, the U tube in practice frequently takes the form idealized in Figure 3.

Let $m = (D/d)^2$ and let K equal the sum of the loss coefficients at the ends of the capillary, so that the total loss at the ends is $Kv^2/2g$. Let $E = 32\nu L/gd^2$.

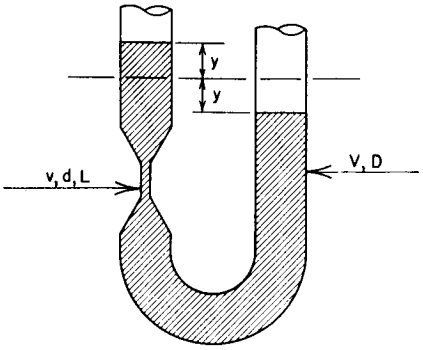

Fig. 3. Idealized form of U tube.

Neglecting viscous losses in the wide bore, then (following the energy equation between the two free surfaces) $2y = Ev + Kv^2/2g$. And since $y' = -v/m$, the equation of motion is

$$(y')^2 - [(2gE)/(mK)]\, y' - 4gy/m^2k = 0 \tag{13}$$

The solution to this equation is

$$T = v/A + mKR/Eg \tag{14}$$

Here $R = (y_1 - y_2)$, the total run of one surface, $T = (t_2 - t_1)$, and

$$A = \frac{gd^2}{16mL \ln(y_1/y_2)} \tag{15}$$

Now E is proportional to v, so that the final solution (for a heavily overdamped instrument) is

$$v = AT - B/T \tag{16}$$

where A is given by eq. (15) and

$$B = mKRd^2/32L \tag{17}$$

If the volume of the liquid transpired in time T is V,

$$B = KV/8\pi L \tag{18}$$

and A becomes $[(\pi d^4 g)/(128LV)]\{[2(y_1 - y_2)]/[\ln(y_1/y_2)]\}$ which may be written (in terms of the mean head $\bar{h}$) as

$$A = \{[\pi(d^4 g)]/(128LV)\}\bar{h} \tag{19}$$

provided that $(y_1 - y_2)$ is small, a condition usually achieved by the use of bulbs in the limbs.

For the single-bore instrument shown in Figure 1, where $m = 1$ and K is assumed zero, eqs. (15) and (16) together become identical with eq. (8).

In view of the practical indeterminacy of K and L, the instrument is usually calibrated with two or more liquids, so as to evaluate and check the coefficients A and B.

PRESSURIZED VISCOMETER

Idealized Instrument, With Constant Negative Driving Head h_m cm. H_g

In Figure 4 it will be assumed that $\rho_m h_m/\rho \gg \Delta$, where ρ is the density of the test liquid.

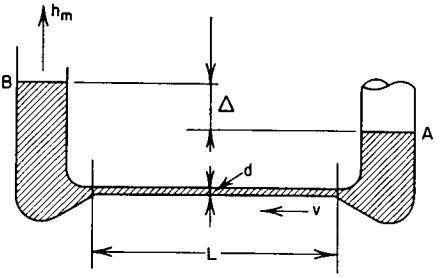

Fig. 4. Pressurized viscometer (idealized).

Quadratic Losses Neglected

The instrument is electrically timed for the transpiration of a fixed volume V. The viscous loss in the capillary will be $32\nu vL/gd^2$ cm. of test liquid. Neglecting viscous losses in the wide bore, and assuming the kinetic energies in the side limbs to be equal to one another,

$$h_m = [(32\eta vL)/(gd^2\rho_m)]$$

Eliminating v with $V = \pi d^2 vT/4$, then

$$\eta = AT \tag{20}$$

where

$$A = [(\pi h_m \rho_m g d^4)/(128LV)] \tag{21}$$

Thus the instrument, unlike the Ostwald, primarily measures η.

The Same, but with Energy Losses at the Ends of the Capillary

The conservation of energy between the interfaces at A and B requires that

$$h_m \rho_m / \rho = \Delta + 32\nu v L/gd^2 + Kv^2/2g$$

Neglecting Δ as before, and multiplying by ρ, then

$$h_m \rho_m = [(32\nu L)/(gd)^2] \cdot \eta + K\rho v^2/2g \tag{22}$$

Eliminating v in favor of the transpired volume V, then

$$= AT - B\rho/T \tag{23}$$

where A is as in eq. (21) and

$$B = KV/16\pi L \tag{24}$$

Thus, if the second term in eq. (23) is sufficiently small, the time of flow is approximately proportional to η. The second term, however, involves the density ρ of the test liquid.

The ratio of the second to the first term is $B\rho/AT^2$. In the viscometer illustrated in Figure 5, A and B are numerically of the same order, while the time of flow for water is roughly 20 sec. Thus theoretically, for water, the second term is of the order of 1/400 of the first term. This assumes, however, that there are no losses except in and at the ends of the capillary.

Uncertainty arises, even in this simplified case, not only from the indeterminate effective length L of the capillary but also from K. One would expect the entry loss (arising from the re-expansion of the entering jet) to be negligible, since the boundaries conform reasonably well with the streamlines. The exit loss (due to separation of flow from the solid boundaries) is probably less than the kinetic energy per unit weight of liquid. As this is $2(v^2)/2g$, the expected value of K would be less than 2. Various workers have found empirical values of K up to about 1.5. In the computation of B above, it is assumed that K is of this order.

Not shown are a small air pump, a Woulff bottle, and air leak, by means of which suction can be applied at C, L, or R as required. The electronic digital timer is a further component not shown.

The mercury reservoir A (into which a standard weight of mercury is introduced) and its tubular extension with the electrodes E_1 and E_2, serves as a manometer for indicating the suction head. Passage of

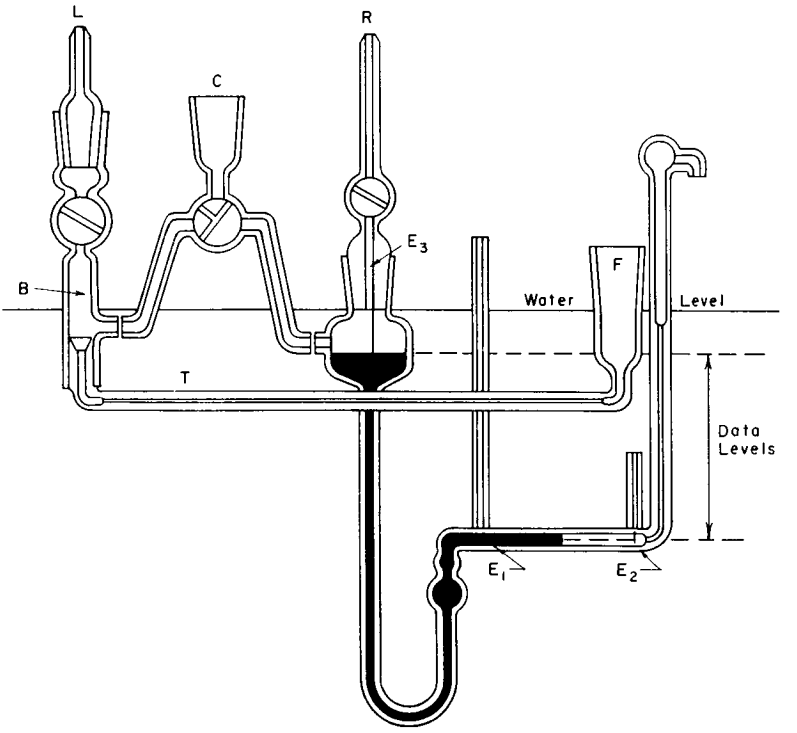

Fig. 5. Viscometer.

the mercury between these electrodes indicates the transpiration of a fixed volume of test liquid through the measuring capillary T, and also starts and stops the digital timer.

The instrument is first filled with "priming liquid," from the reservoirs F and C, through the capillary, the spaces A and B, and the connecting tubes, all air being removed and all stopcocks closed. Details of the necessary manipulations are omitted.

The reservoir F is now emptied by pipet, and the standard volume of test liquid is introduced into F. The remaining routine is: (*1*) the cock at C is opened (**T**); (*2*) the cock at L is opened to standard suction; (*3*) when the mercury is about 1 cm. to the left of E_1, the electronic timer is reset and the cock at L is closed; and (*4*) the standard negative pressure now pulls the test fluid through the capillary, and the passage of the standard volume is timed.

The instrument was primarily designed for routine measurements on blood plasma and to be suitable for use in a busy pathological laboratory. Thus the principal features aimed at were small volume of plasma required for each test, rapidity of operation, an accuracy of 1% or better.

In the instrument shown in Figure 5, the total test volume required is 0.5 ml., the transpired measured volume being 0.2 ml. The total time per test has been reduced to about 2 min. if the "bubble technique" is used instead of cleaning and drying the capillary between tests. The time of flow is displayed on the digital counter, and it remains visible until the dials are deliberately cleared. Constant attention to the instrument is thus not required.

The base of the reservoir F is coated with a water-repellent silicone. After the test the plasma is drawn into the tube at the base of the reservoir, so that when the next plasma is introduced an air bubble separates the samples. This bubble effectively scavenges the preceding plasma from the capillary walls, and eliminates the need for cleaning and drying between tests.

The priming fluid for use with plasma is 3.6% saline. When calibrating the instrument with water or with sucrose solutions, the instrument is primed with the test liquid.

The driving head falls slightly during the test, owing to the transpiration of mercury, and the mean mercury level is arranged to coincide with the mean test-liquid level in F. The small residual effect varying with the density of the priming fluid is therefore eliminated.

The smallest digit of the counter is 0.01 sec.

Some indeterminacies affecting the use of the viscometer as an absolute—as opposed to a calibrated—instrument are as follows:

1. Curvature. The measuring capillary is straight but the other tubes, by their curvature, will contribute a small, indeterminate amount to the B coefficient of eq. (23).

2. Viscous losses in connecting pipes and reservoirs. These will add an indeterminate fraction to the effective length of the capillary, the contribution varying with the priming liquid.

3. Flow of mercury in the timing section. There is a small loss of energy resulting in a further small increase in the effective length of the capillary.

Surface Tension. All capillary viscometers mingle a surface tension effect with the primary viscosity effect to a greater or lesser degree. The surface tension effect, not being readily separable, represents a residual source of *error.*

Use of the Pressurized Viscometer with Blood Plasma. Normal (Newtonian) liquids give the same results in all viscometers. The Newtonian equation for the shearing stress τ is

$$\tau = \eta \, dv/dr \text{ or } \eta \, dv/dy \tag{25}$$

When applied to normal liquids this yields a constant value of η for a given liquid at constant temperature. In non-Newtonian liquids, η is a function of τ, and the liquid is "shear sensitive." In the authors experience, blood plasma and serum are shear sensitive, the apparent viscosity diminishing as the rate of shear (velocity gradient) increases.

$$\partial\eta/\partial\tau < 0 \tag{26}$$

It would be presumptuous for the authors to attempt here a discussion of the many sources of liquid anomaly. An excellent recent introduction to the subject has been published by Wilkinson.[1]

However, a simple working concept of one relevant source of non-Newtonianism in sols containing some large molecules of significant aspect ratio is: it may be conceived that an initial random (thermal) orientation is increasingly ordered toward a selective reorientation in the direction of flow. This reorientation can be easily attributed to the action of couples set up by the velocity gradients.

Miesowicz[2] demonstrated the existence of three principal viscosity coefficients corresponding to the forced orientation of molecules along the three principal directions.

This information plunges us at once into a world in which the classical Navier-Stokes equations do not apply. In rheology, the term "viscosity" is used for want of a better one. It is an unfortunate fact that most practical interest in viscosity measurement is concentrated

upon shear-sensitive substances, whether in blood, paint, rubber, or textile technology.

However, we are measuring something which is partly a property of the liquid and partly a property of the viscometer, and consequently for the comparison of results it is necessary to specify the rate of shear or the shearing stress in some manner.

The shear stress at the wall is given by

$$\tau_0 = (dp/dL)d/4 \tag{27}$$

where dp/dL is the longitudinal pressure gradient. In the viscometer shown in Figure 5, dp/dL is sensibly constant, so that τ_0 measures a constant property of the instrument.

In the literature, reference is often made to "rate of shear," implying an average value of dv/dr. In a Newtonian velocity distribution this may be interpreted as

$$dv/dr = (dp/dL)d/8\eta \tag{28}$$

so that reference should be made both to η and to dv/dr in specifying the viscometer.

For the instrument shown in Figure 5, eq. (27) becomes

$$\tau_0 = g\rho_m h_m(d/4L) \tag{29}$$

It is a comparatively simple matter to insert capillaries of various L/d ratios, and this was tried with an earlier version[3] of the instrumentation in Figure 5. Three tubes whose L/d ratios were approximately 340, 660, and 1010 were used with each of three (normal and pathological) plasmas. The corresponding values of τ_0 were about 64, 33, and 22 dynes/sq. cm. In each case the apparent viscosity (at 25°C.) decreased with increasing shear stress. In this small series, the shear sensitivity varied, the value of $-\eta_{22} \cdot \partial\tau_0/\partial\eta$ lying between 400 and 700 dynes/sq. cm.

Intrinsic Viscosity. The term "intrinsic viscosity" appears to have been introduced by Kraemer[4] with a modified definition by Hess and Coburn,[5] who defined the intrinsic viscosity H as

$$H = \lim_{c \to 0} [(1/c) \ln(\eta/\eta_0)] \tag{30}$$

It is unfortunate that the term "intrinsic viscosity" has persisted since c, the concentration of macromolecules, is measured in g./100 ml.

H is therefore a specific volume. This fact was noted by Hess and Cobure, who base a physical concept upon it. This concept is that $(H - v_p)$ represents the increase of specific volume required in order that the molecules may flow in random orientation. The partial specific volume of the macromolecules is v_p, only about 0.75 ml./gm. for most proteins; but H varies from about 4 ml./gm. for albumin to about 25 ml./g. for fibrinogen. Thus there is a wide spread in H, for the demarcation of fractions, and H is computed from results at low concentrations at which anomalous effects would be expected to subside. These two facts suggest that H has great potentialities.

In practical estimations, it is sometimes assumed that $(1/c) \ln (\eta/\eta_0)$ is a linear function of the concentration, and H is determined by a straight line drawn through somewhat scattered points. On other occasions, curvature is accepted and H is determined by assuming, in effect, that

$$\lim_{c \to 0} \{d/dc \ [(1/c) \ln(\eta/\eta_0)]\} = 0 \tag{31}$$

These procedures are incompatible. In many cases the point is of little practical importance, but study of the variation (with c) of the derivative in eq. (31) might be valuable.

In some published studies of H, it will be found tacitly assumed that the B coefficient of the viscometer is zero, and in some instances even the fact that the Ostwald instrument measures ν and not η is overlooked.

References

1. Wilkinson, W. L., *Non-Newtonian Fluids*, Pergamon, New York-London, 1960.
2. Miesowicz, M., *Nature*, **B158**, 27 (1946).
3. Harkness, J., *Lancet*, **1963** (Aug. 10th) 280.
4. Kraemer, C. O., *Ind. Eng. Chem.*, **30**, 1200 (1938).
5. Hess, E. L., and A. Cobure, *J. Gen. Physiol.*, **33**, 511 (1949).

Synopsis

14583

The general U tube viscometer is analyzed, and the conditions for unidirectional or oscillatory flow are derived. Ostwald's viscometer, as a unidirectional instrument, is analyzed. A new pressurized instrument is compared with the Ostwald. The question of true "absolute" determination is discussed. There are some observations on non-Newtonian measurements and on "intrinsic viscosity."

author

N67 14584

A New Capillary Viscometer for Measuring the Viscosity of Small Amounts of Blood

HEIJI KAWAI, *Kobayashi Institute of Physical Research, Kokubunji, Tokyo,* EIICHI FUKADA, *The Institute of Physical and Chemical Research, Bunkyo-Ku, Tokyo, Japan,* and TAKAYOSHI IBE and HISAO SHONO, *Rion Co. Ltd., Kokubunji, Tokyo, Japan*

INTRODUCTION

The viscosity of blood has been studied by a number of different methods.[1] Rapid, accurate, and consistent measurements with small amounts of specimen are desirable.[2] Coagulation of blood is usually prevented by adding anticoagulant which would cause some alteration in the viscosity of blood. The measurement of viscosity of blood *in vivo* without adding any anticoagulant is most desirable. This paper describes a new capillary viscometer which requires about 0.3 ml. for volume of liquid specimen and about 5 sec. for measuring time. The viscometer has been used for measuring the viscosity of blood in the veins of living animals.

PRINCIPLE OF THE VISCOMETER

Figure 1 represents the schematic diagram of the new capillary viscometer. Two syringe needles A and B are connected to both ends of a graduated glass tube C, to which a hollow rubber ball D is joined at the upper side.

The instrument is held vertically and the lower needle B is immersed into the liquid to be tested by a fixed height h. When the rubber ball is pressed and released, the negative pressure is produced within the glass tube. Then both the air and the liquid is sucked into the tube through the upper and lower needles, respectively. The amount of liquid sucked in $\bar{V}_l$ is determined primarily by the dimensions of capillaries of two needles and the viscosity of air and liquid. Since

PRECEDING PAGE BLANK NOT FILMED.

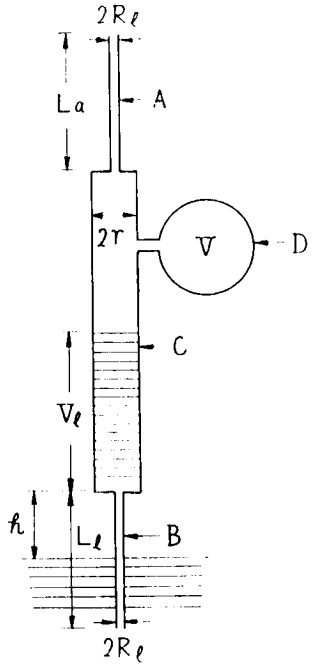

Fig. 1. Schematic diagram of a new capillary viscometer.

the quantities other than the viscosity of liquid are known or calibrated experimentally, the volume of liquid drawn in gives a measure of viscosity of liquid. The gravity proportional to the height of liquid works against the negative pressure. The liquid goes up to a certain height and then comes down gradually. From a practical point of view, the maximum height of liquid observed gives a good measure of viscosity.

According to the well-known Poiseuilles law, when the volume Γ of liquid flows for a time interval t through a capillary tube with a radius R and a length L under a pressure difference ΔP between two ends of the capillary tube, the viscosity η of the liquid is represented by the following relation:

$$\eta = K\Delta P \cdot t / \Gamma \tag{1}$$

where

$$K = \pi R^4 / 8L \tag{2}$$

In the present capillary viscometer pressure difference is counteracted by the gravitational force proportional to the height of liquid. The viscosity of liquid η_l is therefore given by the following formula:

$$\eta_l = K_l/\bar{V}_l \int (\Delta P - \rho g\{h + [(\bar{V}_l)/(\pi r^2)]\})dt \tag{3}$$

where K_l denotes the dimensional constant of the capillary of the lower needle, $\bar{V}_l$ the volume of liquid drawn in, ρ the density of liquid, and g the acceleration of gravity.

For air, the simpler formula holds:

$$\eta_a = K_a/\bar{V}_a \int \Delta P\, dt \tag{4}$$

where K_a is the dimensional constant of upper needle and $\bar{V}_a$ is the volume of air drawn in. If one takes the maximum values for $\bar{V}_l$ and $\bar{V}_a$, the sum of $\bar{V}_l$ and $\bar{V}_a$ should be equal to the inner volume of rubber ball $\bar{V}$.

$$\bar{V}_l + \bar{V}_a = \bar{V} \tag{5}$$

Combining eqs. (3) to (5), one obtains the viscosity of liquid η_l in the first approximation as follows:

$$\eta_l = \frac{\bar{V}}{\bar{V}_l}\left(\frac{K_l\eta_a}{K_a} - \frac{K_l\rho ghl}{V_a}\right) - \left(\frac{K_l\eta_a}{K_a} + \frac{K_l\rho gl}{\pi r^2}\right) \tag{6}$$

When $\bar{V}_l$, ρ, and t are measured, η_l can be calculated from eq. (6). But the actual procedure is much simpler. The calibration curves for a relation of η_l vs. $\bar{V}_l$ is easily obtained by the measurements for the liquids with known viscosity. In the present case several kinds of silicone oils whose viscosity has been determined by the ordinary Ostwald-type viscometer have been used in order to determine the calibration curve.

CALIBRATION OF VISCOMETER

The viscosity of blood is usually around a few centipoises at the high rate of shear such as those encountered in the capillary viscometer. The range of measurable viscosity can be adjusted to a large extent by choosing the suitable combination of two syringe needles with various length and radius. The detail for a viscometer specially

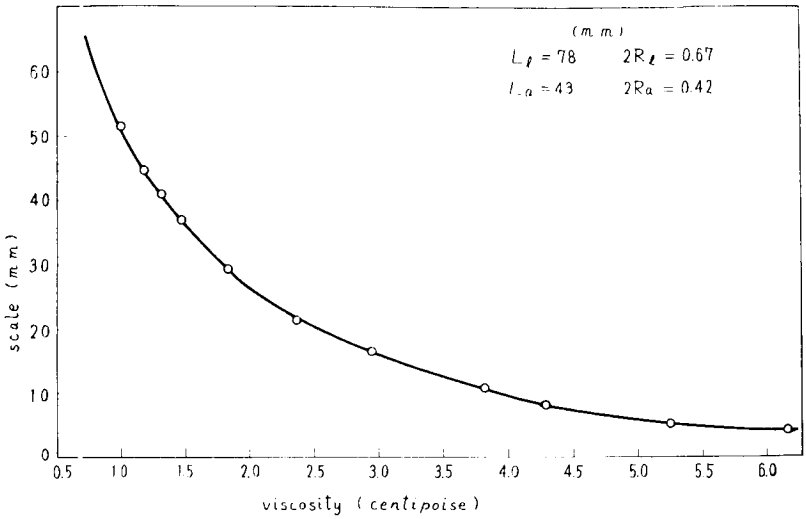

Fig. 2. A calibration curve representing the relation between scale of glass tube and viscosity of liquid.

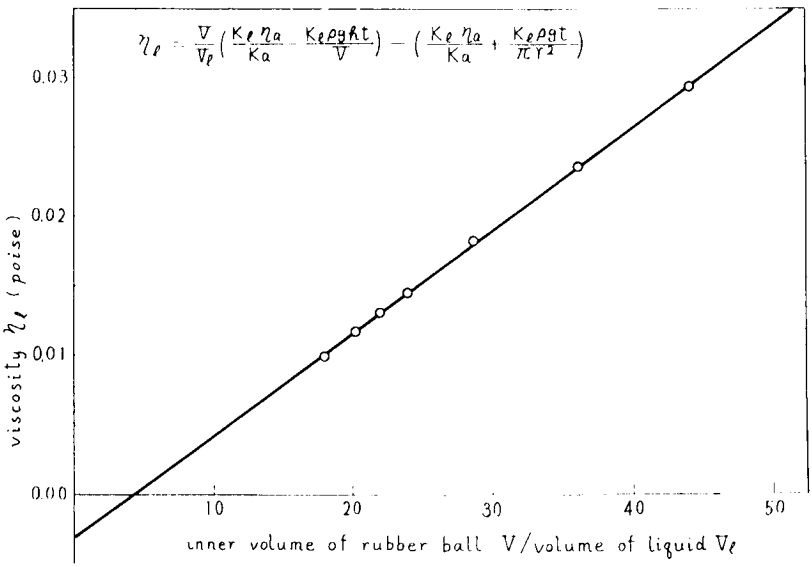

Fig 3. η_l vs. $\overline{V}/\overline{V}_l$ for silicone oils.

designed for the study of blood viscosity, which covers a range of viscosity from 0.6 to 6 cp., will be described below.

In this instrument $L_a = 43$ mm., $2R_a = 0.42$ mm., $L_l = 78$ mm., $2R_l = 0.67$ mm., $2r = 4.6$ mm., and length of the graduated glass tube is about 65 mm. The inner volume $\bar{V}$ of rubber ball is 18 cm.^{3}. Figure 2 illustrates the calibration curve for scale of glass tube against viscosity for this viscometer, which has been obtained by using the three kinds of silicone oils and different measuring temperatures. The immersion depth of the lower needle into the liquid is kept constant to be about 1 cm. for all the measurements.

Figure 3 illustrates the plot of η_l against $\bar{V}/\bar{V}_l$ for the silicone oils which have been used in calibration. The straight line obtained proves very well the validity of eq. (6). From the intersection with the vertical axis and the slope of line, the values of K_l and K_a can be derived using the values $\eta_a = 1.8 \times 10^{-4}$ poise, $\rho \simeq 0.8$ g./cm.^{3}, and $t \simeq 5$ sec. Taking the measured values of L_l and L_a, R_l and R_a have been calculated from these values, and are shown in Table I.

TABLE I

Dimensional Constants and Radii of Two Capillaries Obtained from Three Different Methods

	K_a, cm.^{3}	K_l, cm.^{3}	R_a, mm.	R_l, mm.
From $\eta_l \sim \bar{V}/\bar{V}_l$	1.67×10^{-8}	8.44×10^{-8}	0.21	0.36
From $\bar{V}_l \sim h$	1.64×10^{-8}	7.64×10^{-8}	0.20	0.35
Observation by microscope	1.77×10^{-8}	6.44×10^{-8}	0.21	0.34

The volume of liquid $\bar{V}_l$ also depends on the length h of lower needle which lies between the surface of liquid and the bottom of glass tube. The relation between $\bar{V}_l$ and h is derived from eq. (6) as follows:

$$\bar{V}_l = \left(\frac{K_l \eta_a \bar{V}}{K_a} - K_l \rho g t \cdot h\right) \Big/ \left(\eta_l + \frac{K_l \eta_a}{K_a} + \frac{K_l \rho g t}{\pi r^2}\right) \qquad (7)$$

Figure 4 illustrates the variation of $\bar{V}_l$ with h for silicone oils with different values of η_l. The intersection of the straight line with the vertical axis and the slope of line again calculate the values of K_l and K_a, hence R_l and R_a. Averaged values of R_l and R_a are given in Table I. In this table the values of R_l and R_a observed by a

microscope are also given, and the agreement among values derived from three different methods is fairly good.

When the viscometer is not standing vertically, the effect of gravity is reduced and causes the increase of $\bar{V}_l$. If the viscometer is in-

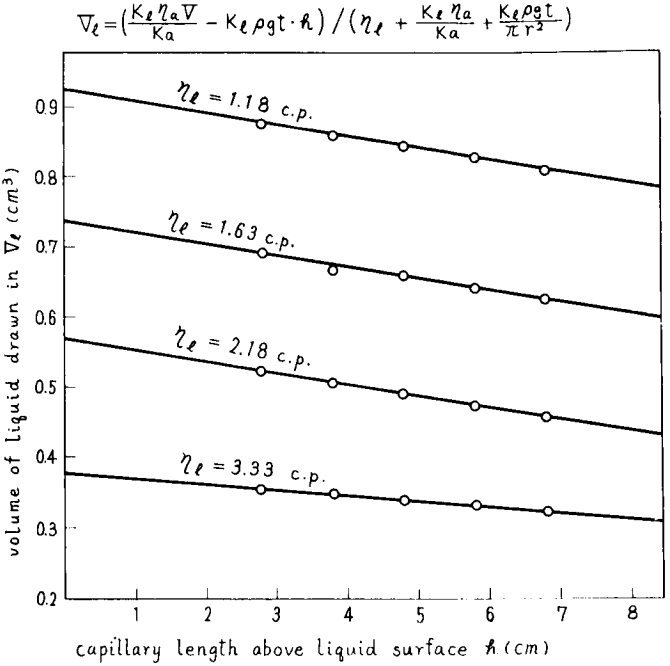

Fig. 4. $\bar{V}_l$ vs. h for silicone oils.

clined by the angle θ with the vertical line, the relation between $\bar{V}_l$ and $\cos\theta$ is derived from eq. (7) as follows:

$$\bar{V}_l = \left(\frac{K_l \eta_a \bar{V}}{K_a} - K_l \rho g t \cdot h \cos\theta\right) \Big/ \left(\eta_l + \frac{K_l \eta_a}{K_a} + \frac{K_l \rho g t}{\pi r^2} \cos\theta\right) \quad (8)$$

Experimental results for silicone oils with three different viscosity values are given in Figure 5. The points are the measured values and the solid lines are those calculated according to eq. (8) with the numerical constants derived already.

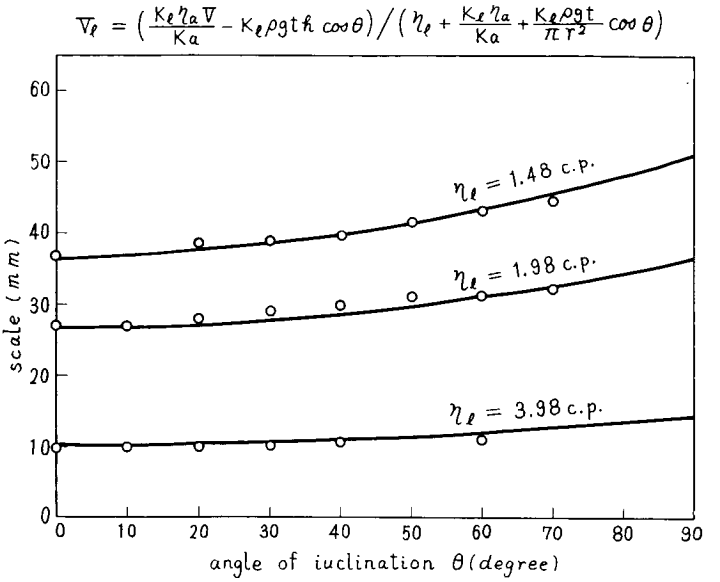

Fig. 5. The relation between scale and inclination angle.

From these considerations the validity of eq. (6) has been proved and the numerical constants involved in the equation have also been determined. Equation (6) can be altered to

$$\eta_l = \frac{K_l \eta_a}{K_a}\left(\frac{\bar{V}}{\bar{V}_l} - 1\right) - K_l \rho g t \left(\frac{h}{\bar{V}_l} + \frac{l}{\pi r^2}\right) \tag{9}$$

If one puts $\rho = 1$ g./cm.^{3}, $t = 5$ sec., $h = 6$ cm., and $\bar{V}_l = 0.5$ cm.^{3}, the second term containing the density of liquid ρ is evaluated as about 0.6 cp., which is 20% of the viscosity of blood 3 cp. Therefore the difference in density, $\Delta\rho = 0.2$, produces only about 4% difference in the value of viscosity η_l. The calibration curve in Figure 2 has been determined by the silicone oils with a density of 0.85 which differs about 0.2 from the density of blood 1.06. The viscosity of blood obtained is therefore about 4% higher than the true value.

The reproducibility of the present viscometer has been examined by measuring the viscosity of one specimen repeatedly. The standard error in the reading was around 1% for both silicone oil and blood. The rate of shear in the capillary wall is given by $4\bar{V}_l/\pi R_l^3 t$ and has

been found to be around 2×10^3 sec.$^{-1}$ which is the same order as that for the actual blood flow in vessels. When the rate of shear in liquid is large, the correction for the kinetic energy is usually required. The term $-\rho \bar{V}_l / 8\pi l t$ should be added to eq. (6) or (9). This is calculated to be about 0.08 cp., which is only 3% of the average viscosity of blood of 3 cp.

It is now seen that the precision of the present instrument is within about 4% even when the difference of density between the calibration oils and blood and the correction due to kinetic energy are ignored. The accuracy of measurements can be improved by taking into account these corrections, but it was thought unnecessary for the present study.

SOME EXPERIMENTAL RESULTS

The measurements of viscosity for the whole blood and the plasma taken from a number of patients in the hospital of Juntendo University have been carried out. Professors Kosakai, Hayashi, and Nakajima have given great help by permitting the authors to make the measurements in their laboratories. Blood has been drawn into the heparinized syringe in the amount of approximately 1 to 2 ml. By

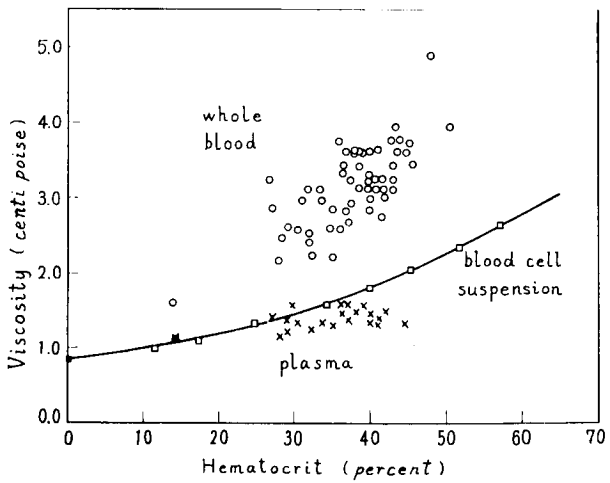

Fig. 6. The viscosity of (O) whole blood (×) plasma, and (—) suspension of red blood cells plotted against hematocrit, i.e., the volume fraction of red blood cells.

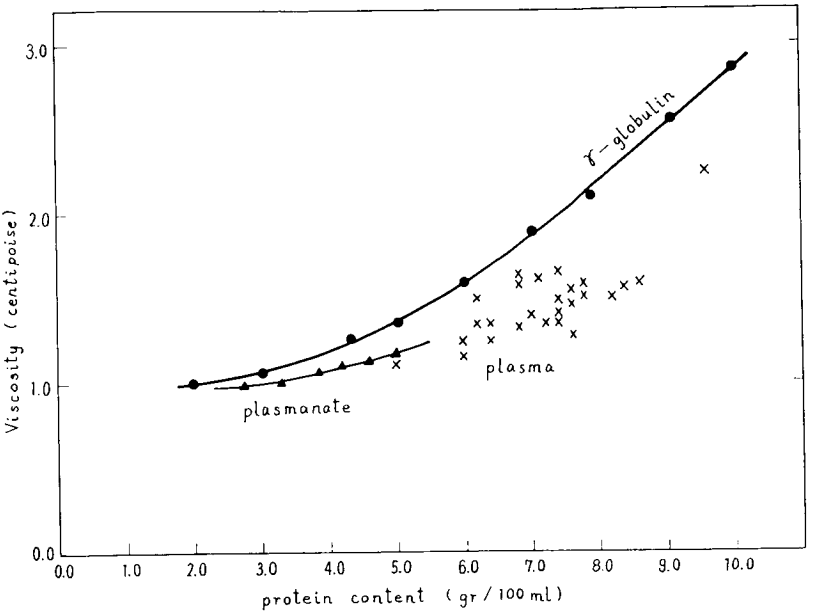

Fig. 8. The viscosity of plasma plotted against protein contents. Solid lines represent solutions of γ-globulin and plasmanate, respectively.

hematocrit, is seen to hold on the whole. At higher hematocrit, however, η_r increases more rapidly.

The quantitative determination of protein contents in plasma as well as globulin and albumin fractions have been made by a paper electrophoresis. In Figure 8 viscosity of plasma is plotted as cross points against total protein contents. The viscosity-concentration relations for aqueous solutions of γ-globulin with 0.1% citric acid and for similar solutions of plasmanate are also shown in the figure. The latter is the heat-treated human plasma containing albumin and α- and β-globulin.

The sedimentation of red blood cells is usually observed for the clinical purpose. In the ordinary Westergren method, the 3.8% aqueous solution of sodium citrate is mixed with blood in the proportion of 1 to 4 and the fall of suspension surface in 1 hr. is indicated as the rate of sedimentation. In Figure 9 the viscosities of whole blood and plasma used for sedimentation are plotted against the rate of sedimentation for about fifty specimens of human blood. These

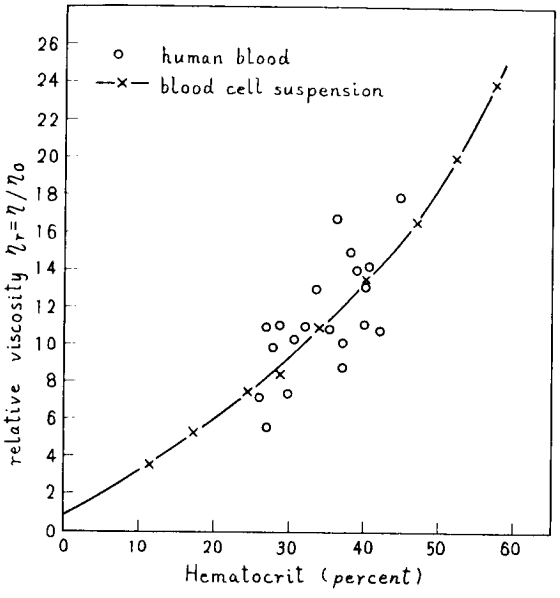

Fig. 7. The relation with hematocrit of relative viscosity η(whole blood)/η-(plasma) for circles or η(suspension)/η(medium) for solid line.

means of centrifugation the plasma and the blood cells were separated and from its volume ratio the hematocrit, i.e., the volume fraction of red blood cell was determined. All measurements have been performed at the temperature of 37°C. in a temperature regulated bath.

Figure 6 represents the results obtained. The viscosity of whole blood increases with the increase of hematocrit, whereas the viscosity of plasma is independent of hematocrit. The results of measurement for the floating suspensions of red blood cells in an aqueous solution of sodium citrate (0.22 g./100 ml.), citric acid (0.66 g./100 ml.), glucose (0.44 g./100 ml.), and sodium chloride (0.54 g./100 ml.) are also shown by the solid line in the figure.

When the relative viscosity η_r is defined as the ratio of η (whole blood) to η(plasma), η_r should be a function of hematocrit. Figure 7 illustrates the relation. The solid line represents the suspension of red cells where η_r is defined as the ratio of viscosity of blood cell suspension to the viscosity of suspending medium. At small hematocrit the well-known Einstein equation $\eta_r = 1 + 2.5\varphi$, where φ is the

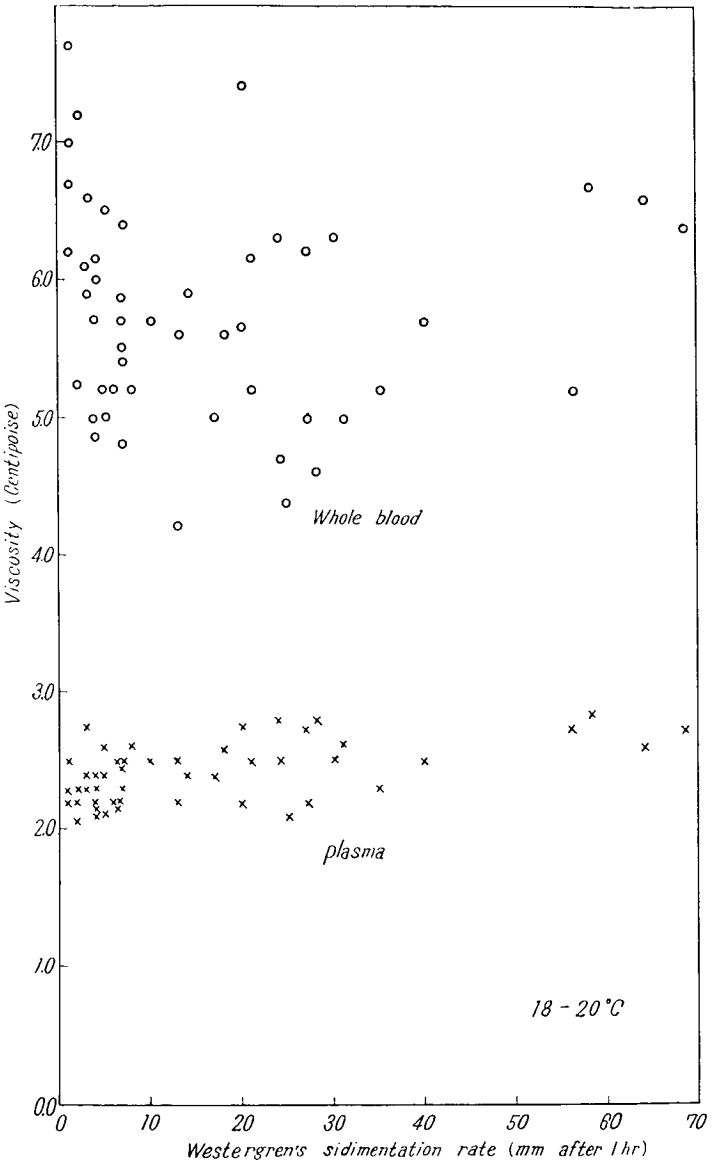

Fig. 9. The viscosity of whole blood and plasma plotted against the one-hour value of sedimentation rate of blood cell by Westergren's method.

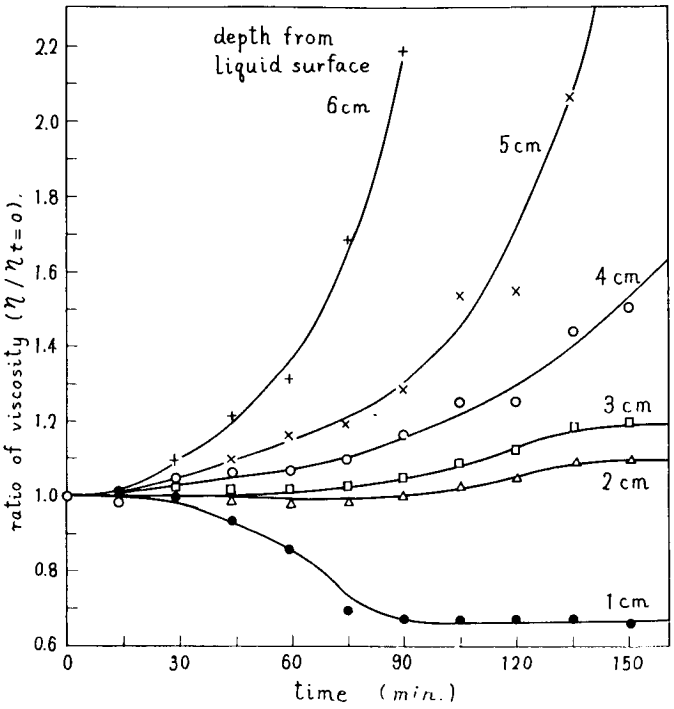

Fig. 10. The viscosity of blood at various depths during sedimentation of blood cells.

results have been obtained at room temperature of 18 to 20°C. Although no definite correlation is observed, it is generally seen that the rise of viscosity of plasma tends to increase the rate of sedimentation. It is known that the rouleaux formation in blood cells is enhanced by the increase of fraction of globulin and fibrinogen and causes the rise of sedimentation rate. The greater viscosity of plasma corresponds to the higher concentration of protein or globulin which favors the rouleaux formation.

The change of viscosity with time during sedimentation has been measured by inserting the needle of the viscometer into various depths from the surface of blood. About 100 ml. of heparinized human blood is poured into a glass tube with an inner diameter of 3.5 cm. and a length of 11.5 cm. The viscosity of blood at the depth of 1, 2,

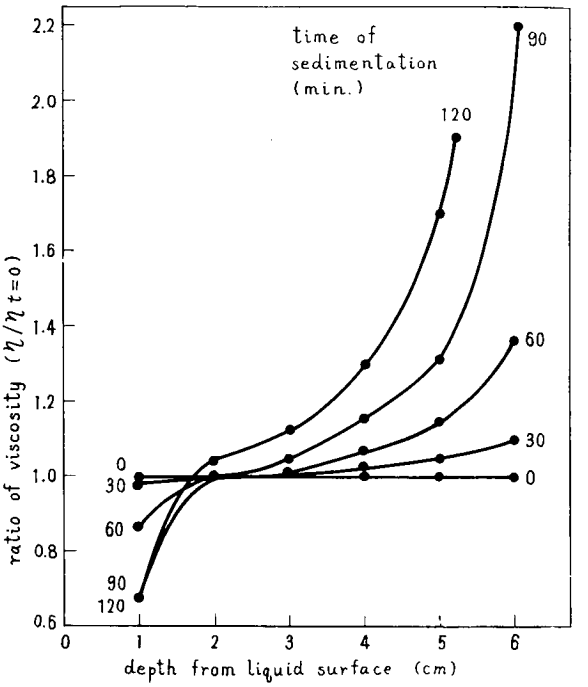

Fig. 11. Spatial distribution of viscosity of blood during sedimentation of blood cell.

3, 4, and 5 cm. from the liquid surface was measured at 15 min. intervals for about 3 hr. The amount of liquid sucked in at one time, left after each run of measurements, was less than 0.3 ml. The ratio of viscosity to the initial viscosity at the beginning of sedimentation is plotted against elapsed time in Figure 10. From the results in this figure the spatial distribution of relative viscosity is replotted in Figure 11. This would correspond to the distribution of concentration of cell or hematocrit in the sedimentation tube.

MEASUREMENTS OF VISCOSITY OF BLOOD *IN VIVO*

In the present viscometer the syringe needles are cut at the pointed ends and used as capillary tubes. When the needle with a pointed end is used as the capillary for liquid side, the end of the instrument

Fig. 12. The needle of the viscometer is being inserted into the external jugular vein of a dog.

is easily inserted into veins. It is possible, therefore, to measure the viscosity of blood in vessels *in situ* if the intravenous pressure is sufficiently low. Zero intravenous pressure is actually encountered in certain parts of the vein in animals. Through the courtesy of Professor Atsumi and Dr. Fujimori of Tokyo University the authors had an opportunity to make measurements of the viscosity of venous blood *in vivo* of an anesthetized dog.

The throat of the dog was opened and the external jugular veins were exposed. A catheter was introduced into one jugular and the intravenous pressure was measured with a water column manometer. The place with zero pressure was easily found by moving the open end of the catheter. The needle of the viscometer was inserted in another jugular in a place which corresponds to the point of the previous jugular where the intravenous pressure was measured. The measurements were made at the place where the pressure is about 3 cm. of

Fig. 13. The viscosity of blood *in vivo* being read.

water column. Figure 12 shows the needle tip of the viscometer with the compressed rubber ball being inserted into a jugular vein of the dog. Figure 13 shows that the viscometer is held vertically while the reading of liquid level is taken.

The blood pressure of 3 cm. water column is balanced by the gravitational force due to the height of liquid in the needle, about 5 cm., and hardly produces any disturbance. The viscosity of heparinized water was frequently observed during measurements in order to ascertain that the thrombus was not formed in the capillary and also that the sensitivity of the instrument was not altered.

Two measurements of the viscosity of intravenous blood gave 3.5 and 3.3 cp., respectively, the average being 3.4 cp. For the purpose of diluting blood the 5% aqueous solution of glucose was injected into the vein in the femoral region. The viscosity of glucose solution was 1.3 cp. The variation of viscosity in the intravenous blood with the injection of glucose solution up to 350 cu. cm. was followed by the same measurement procedure. The total volume of blood in the dog was estimated as about 850 cu. cm. from the body weight of 11 kg. The injection of glucose solution of 350 cu. cm. reduced the blood concentration to about 70%. Measurement results are shown in Figure 14. If the hematocrit of blood of the dog is assumed to be around 40%, the curve in Figure 14 resembles the relation between viscosity and hematocrit in human blood as shown in Figure 6.

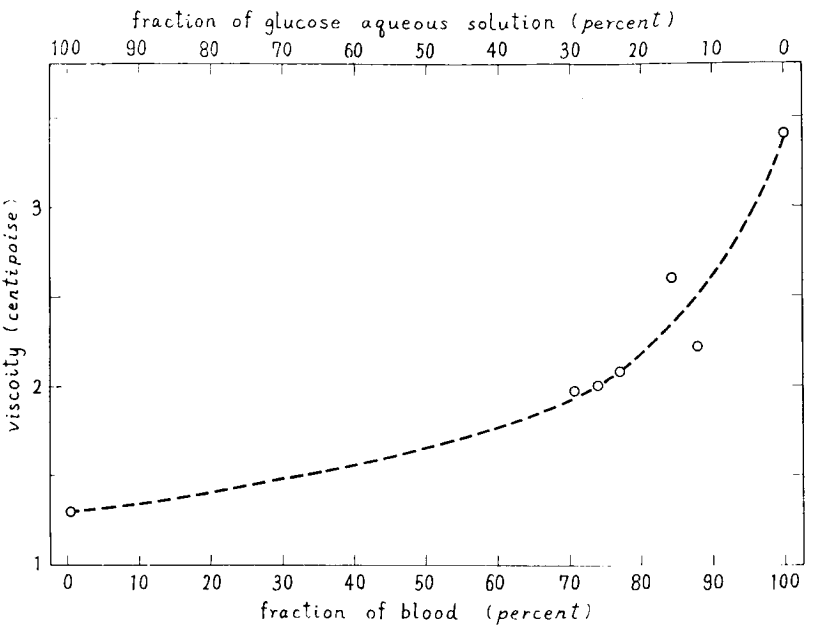

Fig. 14. The variation of viscosity for intravenous blood of a dog with the injection of aqueous solution of glucose.

CONCLUSION

The advantage of the new capillary viscometer is its ease in handling as well as the very small amount of liquid required for measurement. The ordinary time for one run of measurements is less than 10 sec. The measurement procedure requires only compressing and releasing the rubber ball and reading the height of liquid drawn in the glass tube. No particular practice is needed to get reliable results.

The amounts of liquid required for the instrument described in this paper is around 0.3 ml. If smaller amounts of liquid are desired, a glass tube of smaller diameter should be used. Actually, an instrument which needs only 0.1 ml. of liquid has been constructed and is shown to have comparable precision with that described above.

The overall precision of the viscometer lies within a few per cent even when no correction is taken into account. The viscometer promises to have wide use in viscosity studies not only of blood but also of a variety of solutions and suspensions.

Preliminary measurement of viscosity in the intravenous blood was carried out in the jugular vein of a dog. Similar measurement would be useful in particular cases such as blood transfusion or operation with artificial organs.

Insertion of the instrument into the vein is not always necessary. If the venous blood is drawn out by a syringe with a side-arm hole covered with a rubber cap such as that used by Swank and Roth,[2] the tip of the needle of the viscometer is inserted into blood in the syringe through the rubber cap, and the measurement of viscosity is quickly performed. The time required would be only approximately 10 to 20 sec. Coagulation of blood would not take place during this time.

The authors wish to express their sincerest gratitude to Professors N. Kosakai, Y. Hayashi, and A. Nakajima of Juntendo University and Professor K. Atsumi and Dr. Y. Fujimori of Tokyo University for their cooperation and helpful discussions. Without their aid the measurements on blood viscosity would not have been accomplished. The authors are also indebted to Mr. I. Kono for his generous assistance in carrying out the experiments.

References

1. Copley, A. L., and G. Stainsby, eds., *Flow Properties of Blood and Other Biological Systems*, Pergamon Press, New York-Oxford, 1960.
2. Swank, R. L., and J. G. Roth, *Rev. Sci. Instr.*, **25**, 1020 (1954).

Synopsis

14584

A graduated glass tube is closed at the top and bottom with two syringe needles and held in a vertical position. A negative pressure is produced within the glass tube by releasing a compressed rubber ball joined to the upper side of the tube. The air and liquid to be tested are drawn through the top and bottom capillaries, respectively, into the glass tube. Maximum height of liquid thus drawn in measures the value of viscosity within the accuracy of 4%. The volume of liquid required is only 0.3 ml., and the measuring time is less than 10 sec. The viscosity of whole blood as a function of hematocrit and the viscosity of plasma as a function of protein contents have been studied. The viscosity of venous blood in a dog has been measured *in vivo* by inserting the needle of the viscometer into the external jugular vein. Variation of viscosity with the injection of aqueous solution of glucose has been observed.

author

N67 14585

Rheological Disturbances Following Tissue Injury

LARS-ERIK GELIN,* *Surgical Department I, Sahlgrenska Sjukhuset, University of Gothenburg, Sweden*

INTRODUCTION

Tissue injury is known to produce an alteration of the microcirculatory flow pattern of blood. These alterations are induced locally but become generalized and act generally in the circulation. The most striking microcirculatory phenomena are aggregation and stasis of the formed elements of blood in the postcapillary venules.

Within a few seconds of local crush injury white masses are formed in those venules which drain the crushed tissue. Sometimes these masses can be seen to adhere to the venular endothelium, increase in size by taking up white material, and later release white emboli, which are swept away by the flow.

After about 1 hr., aggregation of the red cells is seen to develop in the veins draining the injured area. This aggregation increases with time and may occlude these venules. The microcirculatory alterations in an area distant to the injury does not show any aggregation of red cells until 2 to 4 hr. after a more severe injury. Then increasing with time there develops aggregation of cells, stasis of aggregated cells, and also occlusion of aggregated cells in the venules of the general circulation. In the precapillary arterioles there is an increased orientation of the cells toward the axis of the stream and a constriction of the arterioles. Arteriolovenular shunts will open, which allow blood to bypass true capillaries. About 2 to 3 days after injury these flow changes are less pronounced, but there is still aggregation and stasis of cells at least 2 to 3 weeks after a moderate injury such as a tibia fracture.

The most striking microcirculatory phenomenon in severe traumatic shock is the stagnation of aggregated cells in the venules and sinusoids. This stagnation may result in hypoxia, or anoxia and

PRECEDING PAGE BLANK NOT FILMED.

microthrombosis with deleterious effects on organ function. Such stagnation is produced by lowered perfusion pressure, arteriolar constriction, and such changes in the physical properties of blood that decrease its fluidity.

The purpose of this investigation was to draw attention to some factors which influence the fluidity of blood in the posttraumatic period.

METHOD

A Brookfield synchrolectric viscometer model LVT was used equipped with a special adapter for small blood samples. The determinations were made in a water bath at 37°. The samples were drawn into dry-heparinized bottles. The viscometer was calibrated against distilled water under identical conditions. The values obtained were plotted in a coordinate system.

RESULTS

Alterations in Viscosity of Whole Blood in Experimental Injury on Dogs

Twenty-five healthy mongrel dogs were anaesthetized and polyethylene catheters inserted into the femoral artery. Seven dogs were subjected to a severe contusion injury by 400 blows on both thighs with an unpadded hammer. In six of the dogs viscosity determinations were made 12 hr. after the contusion. One of the dogs was followed with repeated samples during three days after contusion. Eighteen dogs were subjected to a smaller surgical injury in form of neck dissection for exposure of the thoracic and cervical lymph ducts.

The results are summarized in Figures 1, 2, and 3.

The variations in the viscosity of whole blood and plasma at different time intervals after a contusion injury are shown in Figure 1. Two hours after the contusion the viscosity of whole blood and the hematocrit had increased (curve *B* compared with curve *A*). The increase in viscosity was most marked at low rates of shear. Sixteen hours after the contusion whole blood viscosity had dropped to about pre-experimental values (curve *C*). The hematocrit was, however, lower than pre-experimentally. Since a lowering of the hematocrit should result in a decreased viscosity of the whole blood,

the unchanged viscosity, despite a lowered hematocrit, indicates an alteration in the viscous properties of the blood. Three days after the contusion the viscosity of whole blood had decreased compared to the pre-experimental value. Now the hematocrit was very low.

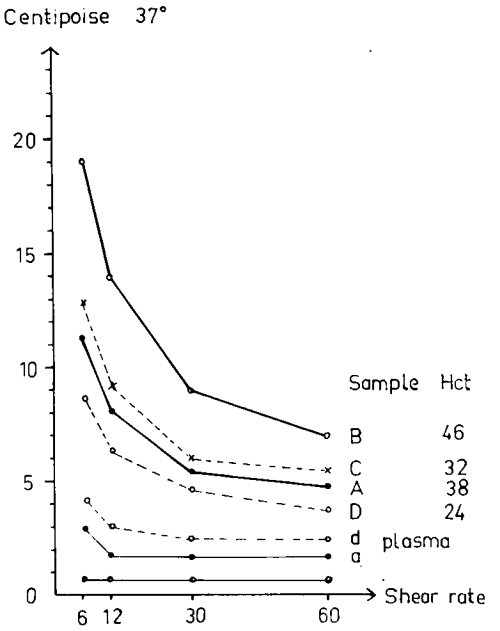

Fig. 1. Viscosity of whole blood and plasma at different time intervals after contusion injury. (Curve *A* before, curve *B* 2 hr. after, curve *C* 16 hr. after, and curve *D* 96 hr. after injury.) Shear rate of 6 corresponds to 23 sec.$^{-1}$, shear rate of 12 corresponds to 46 sec.$^{-1}$, shear rate of 30 corresponds to 115 sec.$^{-1}$, and shear rate of 60 corresponds to 230 sec.$^{-1}$. The same rates apply to all figures. The bottom curve is for distilled water.

The viscosity of the plasma was only slightly decreased 2 and 16 hr. after the contusion. Three days after the contusion the viscosity of plasma was significantly increased at any rate of shear. These changes indicate an altered distribution of the polymers in the plasma (compare curves *a* and *d*).

Figure 2 gives the mean values and error of the mean of whole blood viscosity from the uncontused and the contused dogs 12 hr. after the contusion. As apparent from the figure the contusion was

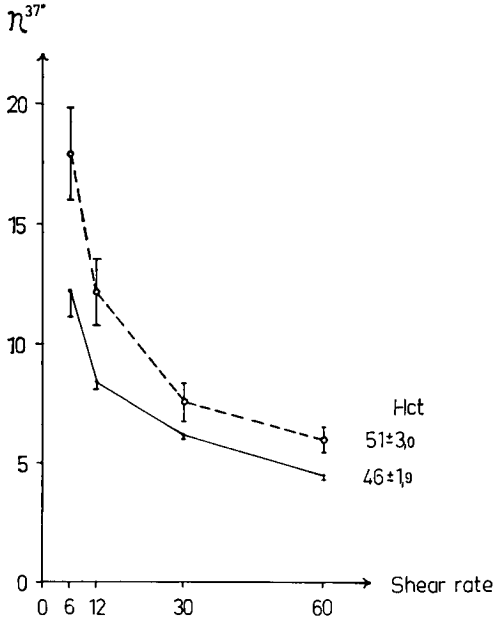

Fig. 2. Influence of contusion injury (400 blows) on viscosity of whole blood: (—) normal dogs, (--) contused dogs.

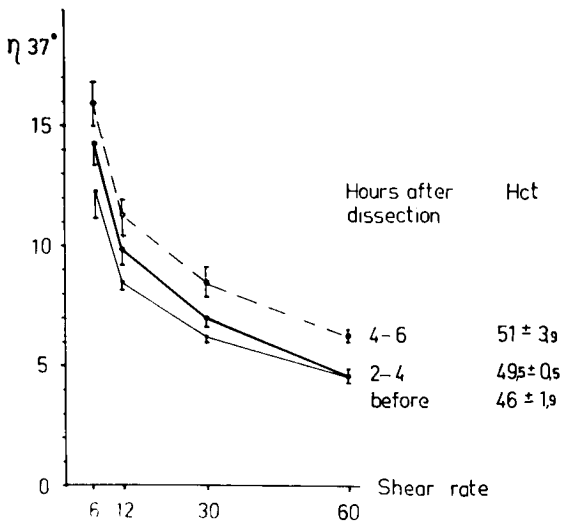

Fig. 3. Influence of neck dissection on viscosity of whole blood in dogs.

followed by an increased viscosity of whole blood, especially at lower rates of shear.

Figure 3 gives mean values and error of the mean from determinations of whole blood viscosity in the dogs subjected to neck dissection. It is evident that the viscosity of whole blood increased first at the lower rates of shear and later at any rate of shear. Before 2 hr. duration of neck dissection no increase occurred.

Viscosity of Whole Blood and Plasma in Humans

Venous blood from 18 subjects was sampled in one dry-heparinized and one dry-oxalated plastic bottle.

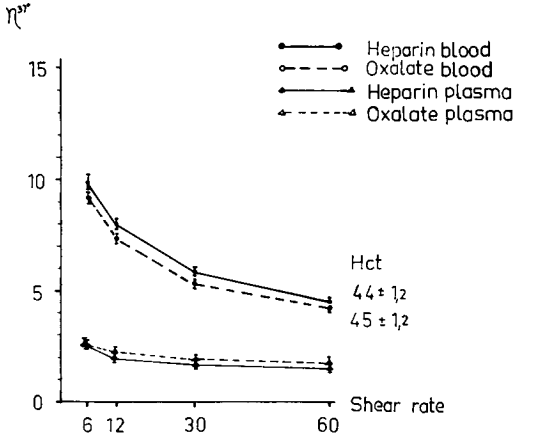

Fig. 4. Viscosity of whole blood in normal human beings.

The viscosity of whole blood and of plasma show increasing values on viscosity with decreasing rates of shear (Fig. 4). There was a slightly but significantly lower viscosity of the oxalated blood than of the heparinized blood. This difference was not seen in plasma.

Alterations in the Fluidity of Blood after Injury in Humans

Following tissue injury in man in principle the same alterations of the fluidity of blood were observed as in dog.

Figure 5 illustrates the plasma protein pattern in blood from two young men with fractures of the lower leg. They were only treated

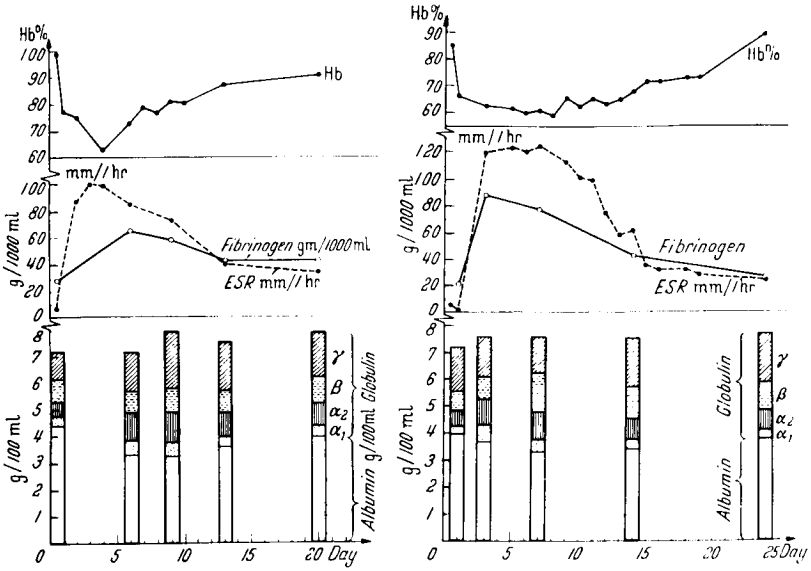

Fig. 5. Changes in hemoglobin, suspension stability, and plasma protein pattern in two patients with compound fractures of the lower leg.

for their local injuries and received no intravenous therapy. In both cases there was a decrease in the hematocrit, an increase in the sedimentation rate, a decrease in albumin, an increase in globulins, especially the α_2-fraction, and an increase in fibrinogen. This accumulation of large protein molecules at the expense of albumin leads both to an increase in the viscosity of the plasma and to a decrease in the suspension stability of the blood with consequent aggregation of cells. These changes vary in degree depending upon the severity of the injury.

Figure 6 gives viscosity values from a man with crush injury complicated with neurological signs of fat embolization on the third day of injury. The whole blood viscosity was at that time increased at all rates of shear but most marked at lower rates of shear. A drop in viscosity was obtained by hemodilution with Rheomacrodex, a low viscosity dextran preparation. Clinically this increased fluidity of blood was succeeded with disappearance of the neurological symptoms.

A patient with a 70% burned area treated in the classical way with whole blood, plasma, and electrolytes showed a very pronounced

elevation of hematocrit and increase of the whole blood viscosity, especially at low rates of shear as apparent from Figure 7.

Thus, the data hitherto presented show that tissue injury induces both changes in the concentration of particles and of the pattern of the vehicle—plasma. This led to marked alterations of the fluidity of blood especially at lower rates of shear and to an alteration of the

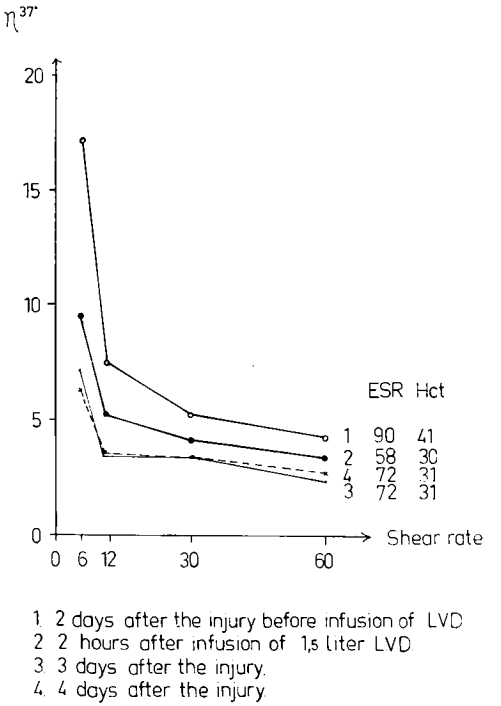

Fig. 6. Viscosity of whole blood in a patient with a crush injury.

microcirculatory flow pattern of blood, especially in the venules where there is a low pressure-head and a low rate of flow.

The fact that an increase of the whole blood viscosity is most marked at lower rates of shear has an important bearing for the flow of blood in vessels where the flow rate is low, i.e., venules, sinusoids, and veins. An increased viscosity at lower rates of shear must mean that the venous return of blood is impaired and in itself disposed to stagnation.

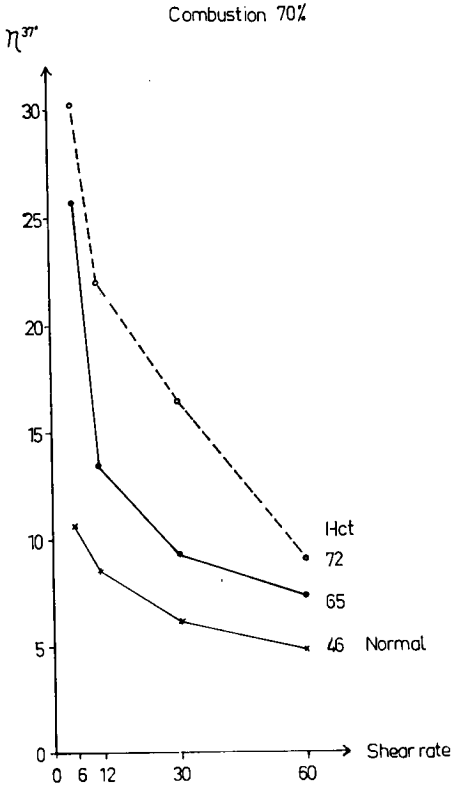

Fig. 7. Viscosity of whole blood from a patient with a burn injury of 70%.

Viscosity of Red Cell Suspensions

Since blood is a suspension its fluidity will depend both on concentration of particles and on the properties of the vehicle, which are both altered after tissue injury. The interrelationship between these two factors provoked the following investigation, the purpose of which was to study the influence of variations in particle concentration and in vehicle viscosity on the rheologic properties of red cell suspensions.

Procedure

Twice washed human red cells were suspended in different vehicles to give hematocrits varying from 0 to 70.

The following vehicles were used to make the suspensions: 0.9% saline, 4% solutions of three different dextran fractions in saline with average molecular weights of 40,000, 80,000, and 800,000, respectively, plasma, 4 and 6% albumin solutions, and 1 and 2% fibrinogen solutions. Hematocrits were determined on the prepared suspensions using Winthrobe's method.

Red Cells Suspended in Saline

Figure 8 gives data—mean from nine experiments—on suspension viscosity at different hematocrits and at different rates of shear. It appears that the suspension viscosity increased with increasing

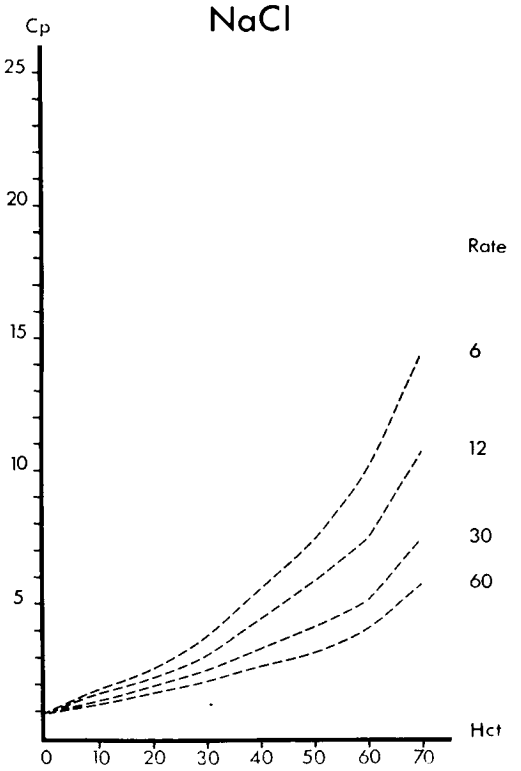

Fig. 8. Viscosity of red cell suspensions in saline at different hematocrits and different rates of shear.

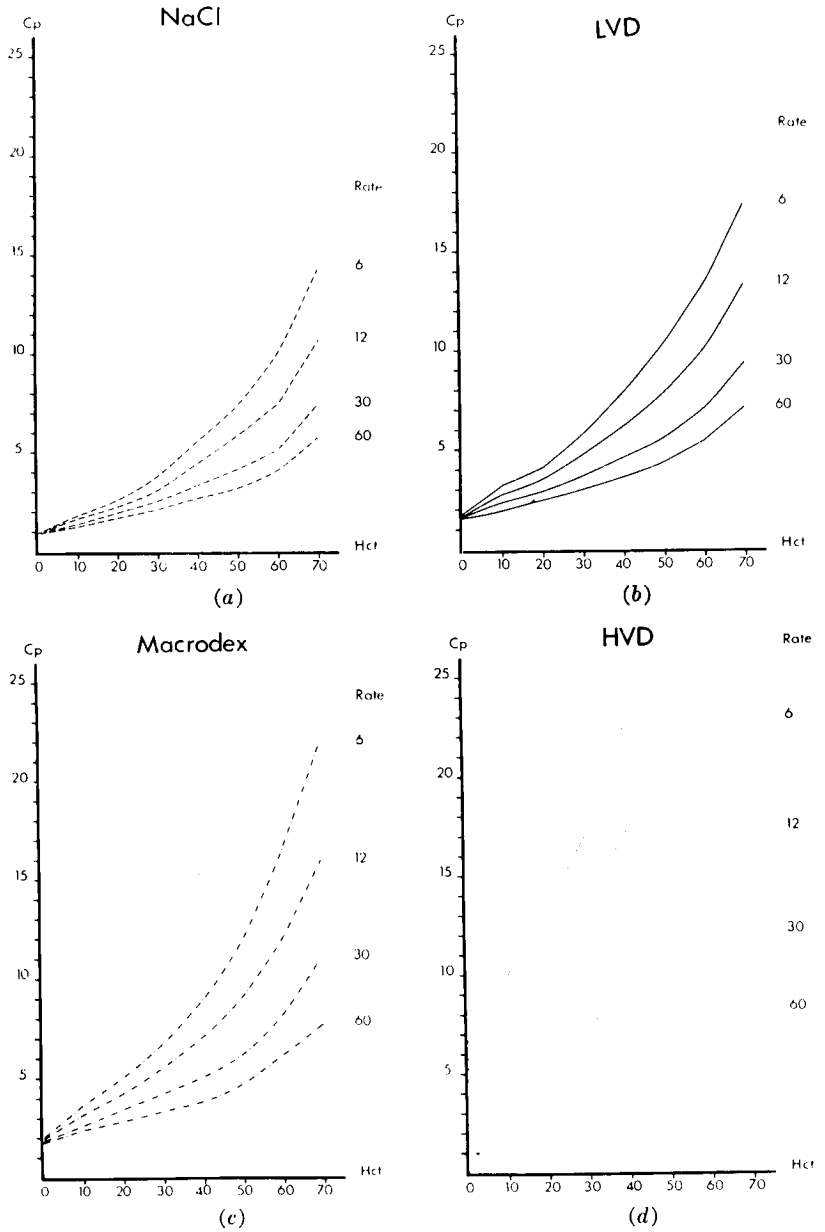

Fig. 9. Viscosity of red cell suspensions in different vehicles at different hematocrits and different rates of shear: (*a*) saline, (*b*) 4% solution of dextran in saline (average molecular weight 40,000 and intrinsic viscosity 0.18), (*c*) 4% solution of dextran in saline (average molecular weight 80,000 and intrinsic viscosity 0.26), and (*d*) 4% solution of dextran (average molecular weight 800,000 and intrinsic viscosity 0.70).

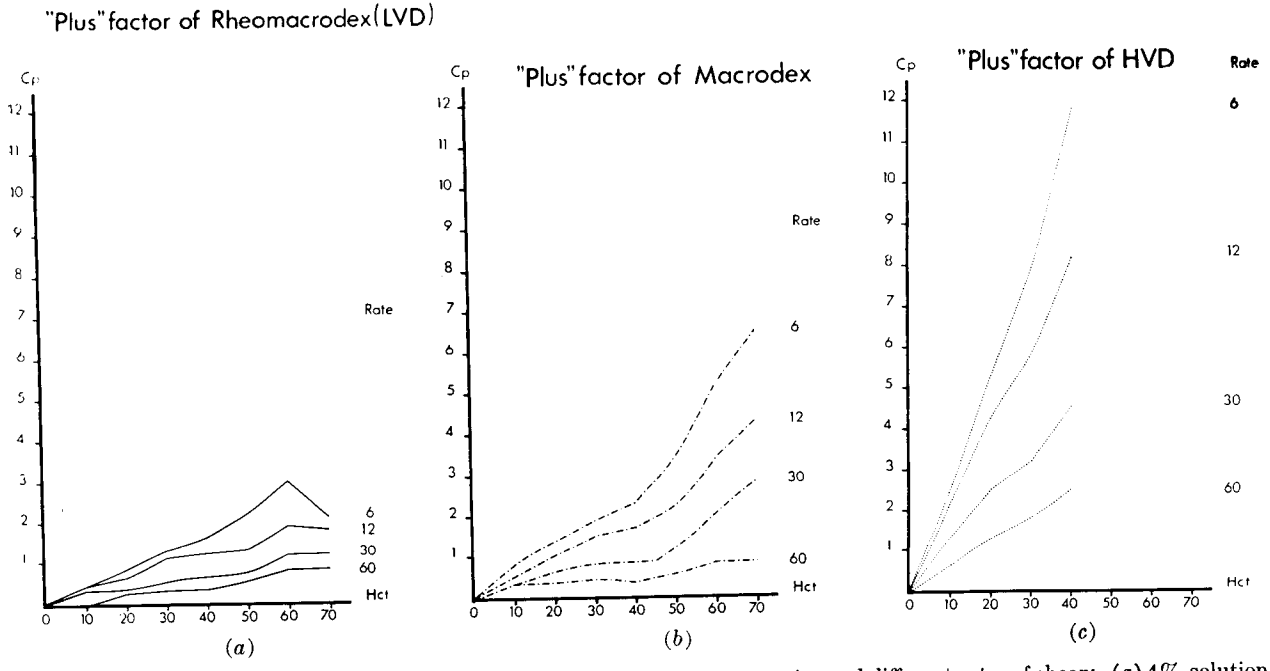

Fig. 11. Viscosity-plus factor for the different vehicles at different hematocrits and different rates of shear: (*a*) 4% solution of dextran in saline (average molecular weight 40,000 and intrinsic viscosity 0.18), (*b*) 4% solution of dextran (average molecular weight 80,000 and intrinsic viscosity 0.26), and (*c*) 4% solution of dextran (average molecular weight 800.000 and intrinsic viscosity 0.70).

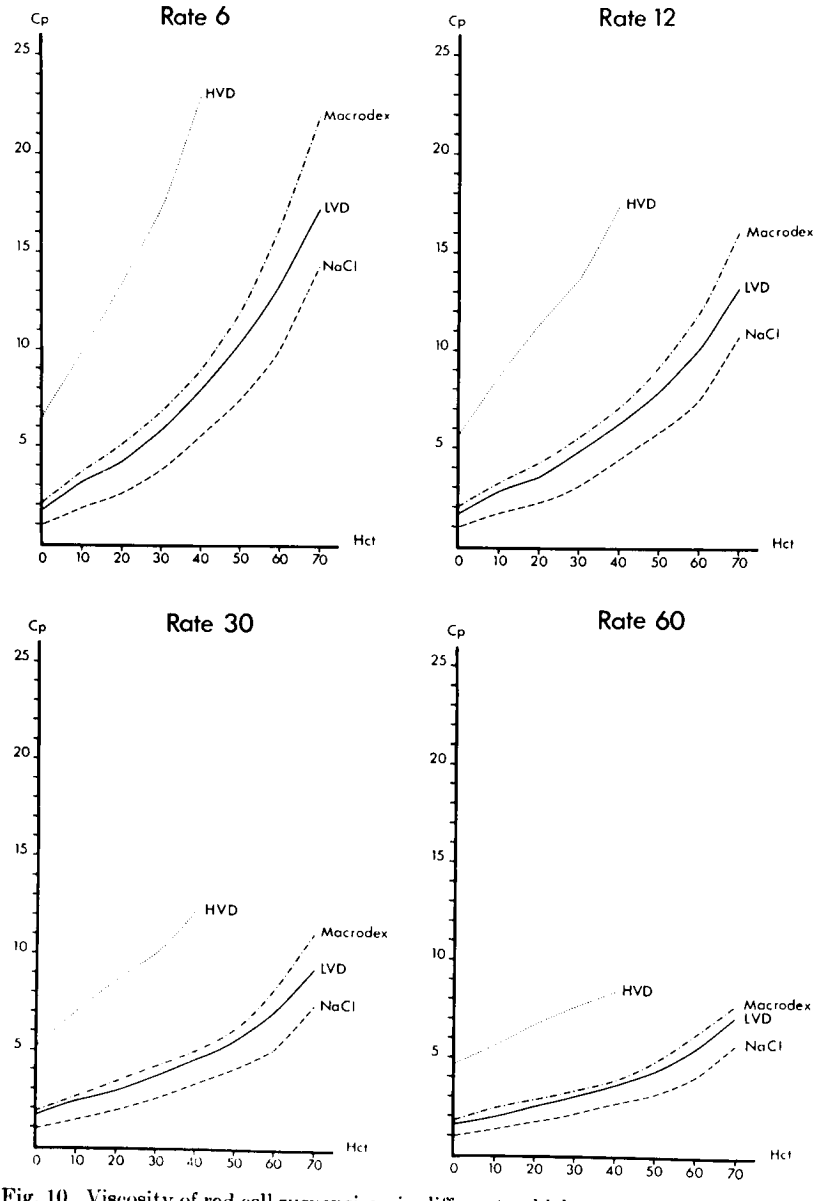

Fig. 10. Viscosity of red cell suspensions in different vehicles compared at different rates of shear.

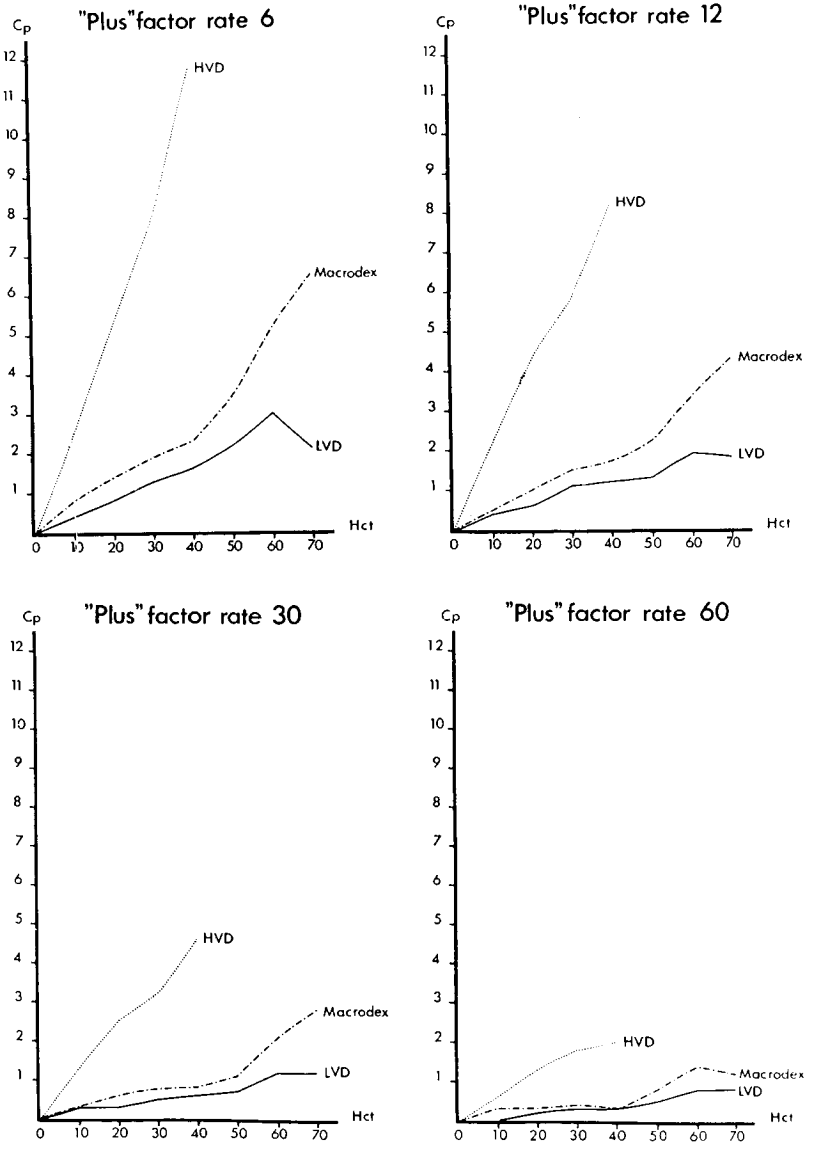

Fig. 12. Viscosity-plus factor for red cell suspensions in different vehicles at different hematocrits and different rates of shear.

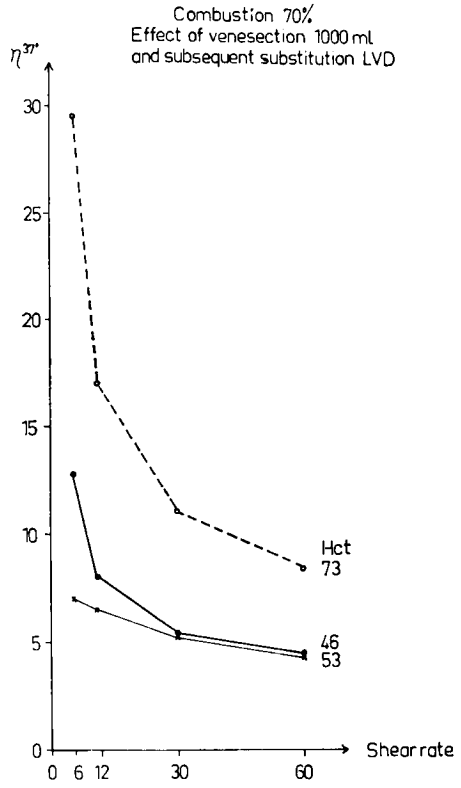

Fig. 13. Effect on whole blood viscosity of withdrawal of blood and substitution with Rheomacrodex in a 70% burned patient. Effect of venesection 1000 ml. and subsequent substitution LVD.

hematocrit and decreasing rate of shear. These data give the viscosity of the most simple red cell suspensions.

Red Cells Suspended in Different Dextran Solutions

The mean values of five experiments on each suspension are summarized in Figures 9 and 10.

Figure 9 gives the values on the suspension viscosity from each vehicle at different hematocrits and rates of shear. It appears that the suspension viscosity increased with increasing hematocrits, decreasing rate of shear, and increasing vehicle viscosity.

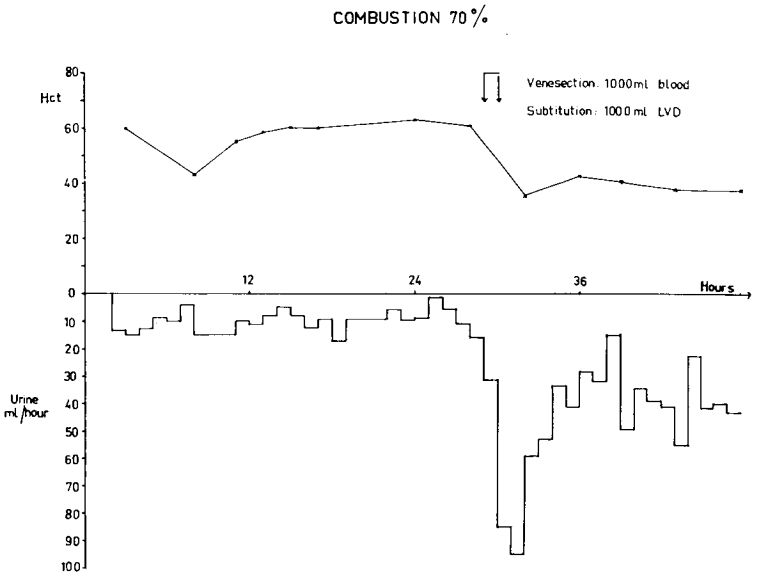

Fig. 14*a*. Effect on hematocrit and diuresis of withdrawal of 1000 ml. of blood and substitution of 1000 ml. of Rheomacrodex in the patient accounted for in the text and in Fig. 13.

Figure 10 illustrates the influence of the vehicle viscosity on suspension viscosity at different rates of shear. It is evident that an increasing vehicle viscosity influenced the suspension viscosity more at lower rates of shear, and also that there was a disproportionate increase in the suspension viscosity with increasing vehicle viscosity. The author has termed this disproportionate increase the "viscosity-plus factor." The values of this viscosity-plus factor for the different vehicles are given in Figure 11. It appears that the viscosity-plus factor increased with increasing vehicle viscosity, increasing hematocrit, and decreasing rate of shear.

The same kind of experiments was performed on normal plasma, pathologic plasma, 4 and 6% albumin solutions in saline, and 1 and 2% fibrinogen solutions in saline. The data from these experiments show that the viscosity of the red cell suspensions increased with increasing hematocrit, increasing vehicle viscosity, decreasing rate of shear, and the above-mentioned viscosity-plus factor.

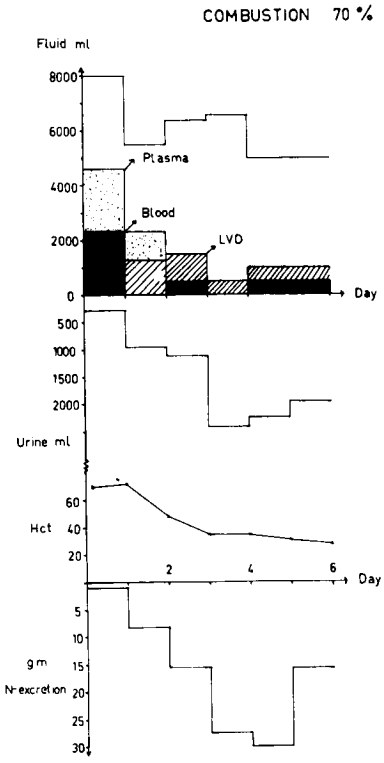

Fig. 14*b*. Transfusions, diuresis, hematocrit, and nitrogen excretion in the same patient.

Thus, the model experiments on red cell suspensions have shown that the viscosity of a suspension of red cells is influenced by the rate of shear, vehicle viscosity, concentration of red cells, and an additional factor termed viscosity-plus factor. This viscosity-plus factor accelerated with decreasing rate of shear, increasing hematocrit, and increasing vehicle viscosity (see Fig. 12).

Clinical Significance of Posttraumatic Rheologic Disorders

The clinical significance of the posttraumatic decrease of the fluidity of blood is illustrated by the following data from a severely burned patient.

Case Report

A 45-year old man was brought to the hospital with a 70% burned area 3 hr after the accident. He was treated according to generally accepted rules for burned patients. During this treatment the whole blood viscosity increased to the highest values in man ever recorded at this hospital (see Fig. 13). After 24 hr. his general condition turned into an irreversible shock with anuria. Then 1000 ml of blood was withdrawn and substituted with Rheomacrodex, a low-viscosity dextran preparation. In immediate response to this exchange-tranfusion, the whole blood viscosity decreased to normal values. His general condition improved rapidly and a large diuresis started immediately as seen from Figure 14. The diuresis showed a good nitrogen clearance effect in response to this rheologic treatment. This treatment thus improved the kidney function by improving the kidney perfusion. What was considered an irreversible shock was reversed. The patient survived 10 days but died from a foudroyant sepsis.

Further discussion of rheologic treatment of severe clinical conditions in surgery is given by Zederfeldt.[1]

Reference

1. Zederfeldt, in *Proc. 4th Intern. Congr. Rheology, Part 4*, A. L. Copley, ed., Interscience, New York, 1965, p. 397.

Synopsis

14585

Tissue injury induces a decreased fluidity of blood especially at lower rates of shear. The decreased fluidity is caused by (*a*) increased hematocrit, (*b*) increased viscosity of plasma, and (*c*) an additional factor called "viscosity-plus factor." The viscosity-plus factor accelerates with (*a*) decreasing rate of shear, (*b*) increasing hematocrit, and (*c*) increasing vehicle viscosity. Decreased fluidity of blood is of especial importance for the venous return and for the postcapillary flow where there is a low pressure head and a low flow rate. An increased viscosity of blood means by itself a threatening stagnation. Hemodilution with agents able to reduce viscosity, especially at low rates of shear, has resulted in remarkable improvements in severe clinical conditions.

Author

N67 14586

Streaming Birefringence Study of the Interaction of Submicroscopic Rods and Spheres*

H. WAYLAND* and MARCOS INTAGLIETTA, *Division of Engineering and Applied Science, California Institute of Technology, Pasadena, California*

INTRODUCTION

Many of the most important methods for the characterization of biological macromolecules depend on an application of hydrodynamics for interpretation of the results. Such methods include sedimentation, viscometry, streaming birefringence, and the transient Kerr effect. Since the natural medium for such macromolecules as proteins, nucleic acid, and various viruses is often an aqueous solution of salts, hydrodynamic methods can be applied to systems in which the natural environment of these macromolecules is closely simulated. Most of these methods depend on an extrapolation to zero concentration and zero flow rate to eliminate the effects of interactions—either chemical or hydrodynamic.

In flowing systems, such as blood and the sap of plants, the flow properties may be strongly influenced by the macromolecular makeup of the system. Large changes in flow properties of macromolecular systems are more likely due to chemical interactions than to hydrodynamic interactions, but a better understanding of the hydrodynamic interactions possible at the macromolecular level should be helpful in distinguishing between those phenomena of purely hydrodynamic origin and those in which other sources of interaction must be considered.

Theoretical studies on hydrodynamic interaction phenomena at the submicroscopic level have largely been confined to attempts to

* Work supported by grants A-2265 and GM 10844 from the National Institutes of Health of the U. S. Public Health Service.

PRECEDING PAGE BLANK NOT FILMED.

improve the Einstein theory for the viscosity of suspensions of spherical particles. Theoretical predictions range from no interaction effects to effects which should be readily observable at volume concentrations of a fraction of a per cent. Experimental evidence can be found which appears to be compatible with most of these theoretical treatments.

An experimental program has been undertaken at the California Institute of Technology to study interactions among particles of different shapes. A system with two particulate components, rods and spheres, was chosen to permit a variety of experimental techniques to be employed. Two experimental approaches are being used: precision viscometry and streaming birefringence. The change in viscosity due to addition of particulate matter to the matrix medium will be the sum of the effects due to all particles plus that due to their interactions with each other. Streaming birefringence (SBR), on the other hand, will detect only the orientation distribution of the elongated particles. By performing both viscometric and optical studies on the same systems it is hoped to gain further insight into the magnitude and nature of the hydrodynamic interactions for these heterogeneous systems.

Biological systems are usually obtainable in a much more nearly monodisperse state than are synthetic systems. For this reason, tobacco mosaic virus (TMV) was chosen for the rodlike particles. The TMV particles are rigid rods about 3000 A. long and 180 A. in diameter. The samples used were selected for monodispersity.

Viscometric studies[1] using 880 ± 80 A. polystyrene latex spheres for the spherical particles showed concentration effects of the mixtures of rods and spheres which seem best interpreted by assuming that the presence of the population of spheres interferes with the tendency of the rods to be oriented in shear flow, leading to a more rapid increase of viscosity with concentration than had been expected. There is some evidence that there may be some aggregation of the TMV particles at the lower shear rates, as suggested by Joly,[2] which is broken up by the presence of the spheres, particularly as the shear rate increases. Since SBR depends only on the properties of the elongated particles (including possible aggregation as well as orientation), SBR studies were undertaken on rod-sphere systems. Unfortunately, the polystyrene latex spheres were so large that they scattered so much light that SBR studies were impossible when they were present.

For the optical studies, southern bean mosaic virus (SBMV) was used for the spherical particles. The SBMV particles are regular polyhedra about 250 A. in diameter. Sedimentation velocity studies showed the SBMV population to be homogeneous, and electron micrographs of the mixtures showed no evidence of structuring of combinations of SBMV and TMV.

The Peterlin-Stuart[3] theory of streaming birefringence of a monodisperse population of noninteracting prolate ellipsoids of revolution gives the amount of retardation in simple shear flow in the form

$$\Delta n = [(2\pi\varphi)/\bar{n}]Gf(\Gamma/D, b) \tag{1}$$

where φ is the volume concentration, $\bar{n}$ the mean index of refraction of the solution, G an optical factor depending on the indices of refraction of the particle and that of the medium, Γ the velocity gradient, D the rotary diffusion constant of the ellipsoid about an axis normal to the axis of revolution, and $b = (a_1^2 - a_2^2)/(a_1^2 + a_2^2)$ where a_1 is the semiaxis of rotation and a_2 the semiminor axis of the ellipsoid. For small values of Γ/D.

$$f(\Gamma/D, b) \approx \Gamma/15D \tag{2}$$

This theory should be applicable to a rodlike particle if the corrected rotary diffusion constant is used. This has been calculated by Broersma[4] for a cylindrical particle to give

$$D = \{[3k\Gamma(\sigma - \gamma)]/(8\pi\eta a_1^3)\} \tag{3}$$

where

$$\sigma = \ln(2a_1/a_2)$$

$$\gamma = 1.57 - 7[(1/\sigma) - 0.28]^2$$

valid for

$$\sigma > 2 \text{ or } a_1/a_2 > 3.5$$

Perrin's[5] expression for the comparable rotary diffusion coefficient for an ellipsoid differs from this in that $\gamma = 1/2$ for his case. For the authors' case the important consideration is that the form of dependence on η is the same for the rod as it is for the ellipsoid. The actual value of η to be used in this expression, however, is the local viscosity felt by the particle and is believed to be somewhere between

the viscosity of the solvent and the bulk viscosity of the solution. The experiment has been designed to try to obtain a better understanding of the local viscosity felt by the elongated particles.

EXPERIMENTAL

Apparatus

The streaming birefringence measurements were made in a Couette-type cell with internal cylinder rotating, external cylinder diameter 5 cm., gap 2 mm., and length of rotor 5 cm. All measurements were made well below the Taylor transition velocity which occurred for a gradient of 35 sec.$^{-1}$. The equipment was housed in a room in which the temperature was kept at 70 ± 1°F. night and day, and all

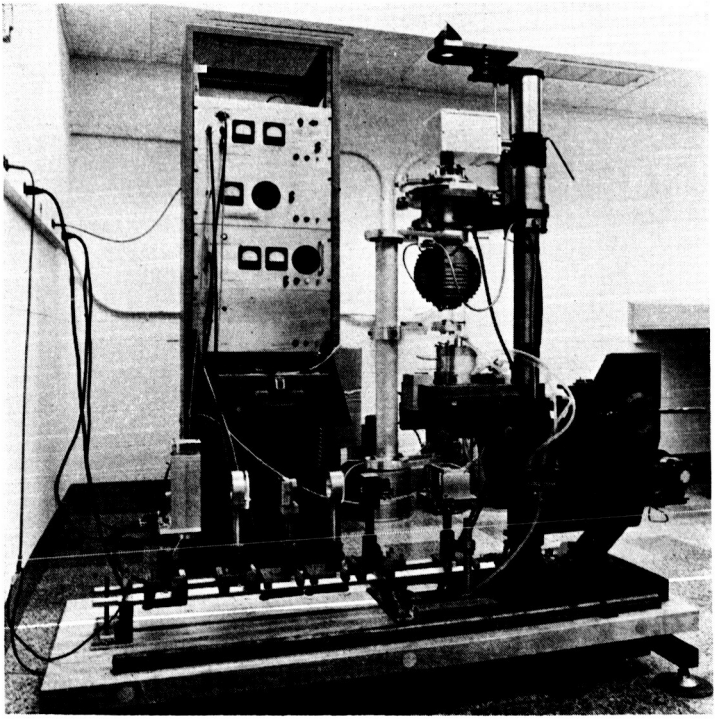

Fig. 1. Overall view of streaming birefringence apparatus.

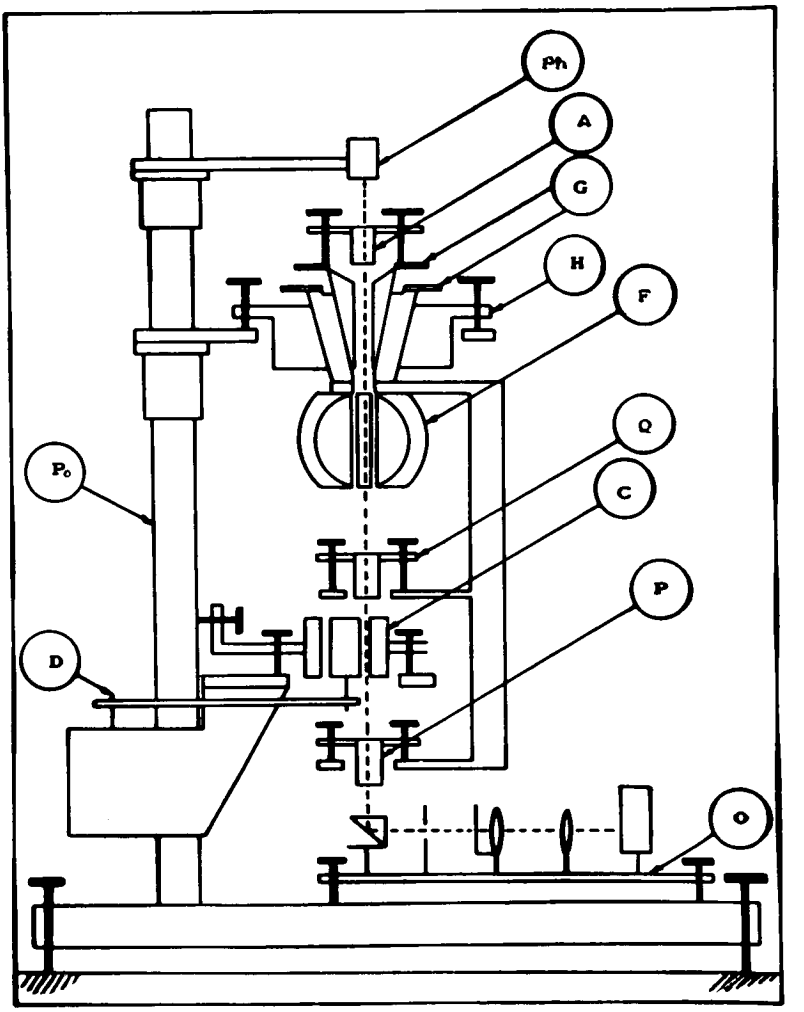

Fig. 2. Schematic diagram of streaming birefringence apparatus.

solutions were given adequate time to come to temperature equilibrium with the apparatus.

Detection of the SBR was done with a Faraday cell modulated photoelectric detecting device. A photograph of the equipment is shown in Figure 1, and a schematic diagram in Figure 2. Referring

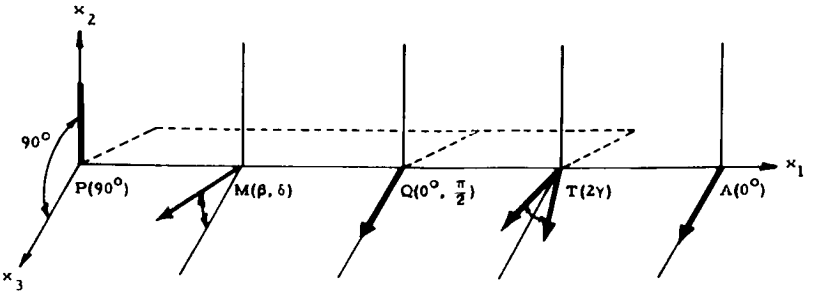

Fig. 3. Schematic of Faraday cell modulated polarimeter.

to the schematic, the optical bench O carries a high pressure mercury arc, a Wratten 77A filter to isolate the green line, and suitable lenses and stops to bring a pencil of light through the Couette cell C without grazing the walls The light is plane polarized by the Glan-Thomsen prism P, then passed through the cell to the quarter wave plate Q set with one axis parallel to the plane of polarization of P, through the Faraday modulator F to the analyzer A, crossed to P, and then to the photomultiplier Ph. The angle of isocline is first located, then the amount of birefringence is measured by rotating the entire assembly consisting of polarizer, $\lambda/4$ plate and analyzer to 45° with the isoclinics. (A precision stop was provided to permit rotation of this amount.) The analyzer is then uncoupled and rotated independently to give a minimum signal. The important relationships for these measurements are the following:[6,7] referring to Figure 3, P represents the polarizer giving plane polarized light parallel to the x_2 axis; M represents the unknown birefringence, with one of the isoclinic axes making an angle of β with the x_3 axis, and introducing a retardation δ; Q is a quarter wave plate; T the Faraday cell introducing a rotation $\gamma = \gamma_0 \sin \omega t$, and A the analyzer, crossed with P. If the light falling on the polarizer is of unit intensity, the intensity of light passing the analyzer is

$$I = \frac{1}{4}[1 - \cos 2\gamma(\cos^2 2\beta + \sin^2 2\beta \cos \delta) - \sin 2\gamma \sin 2\beta \sin \delta] \tag{4}$$

If the amplitude γ_0 of the angular rotation due to the Faraday cell is small, this expression can be broken down into a steady term, a term

at the driving frequency and a term at double the driving frequency. The amplifier in the photomultiplier circuit was sharply tuned to the fundamental so that the signal passing the amplifier is proportional to

$$\delta \approx \gamma_0 \sin \omega t \sin 2\beta \sin \delta \approx \delta\beta\gamma_0 \sin \omega t \tag{5}$$

This expression is linear in both the retardation and the angular displacement from the null point. By inserting a synchronous rectifier in the output of the amplifier, the signal was converted to d.c., and changed sign as the zero point was passed, making it possible to use a zero-centered meter as the indicator.

Rotating polarizer, quarter wave plate, and analyzer by 45° from the isoclinic (i.e., $\beta = 45°$ in Fig. 3), uncoupling the analyzer and rotating it an angle α from being crossed to P, the intensity of light passing the analyzer will be

$$I = \frac{1}{4}[1 - \cos 2\alpha(\cos 2\gamma \cos \delta - \sin 2\gamma \sin \delta) - \sin 2\alpha(\sin 2\gamma \cos \delta + \cos 2\gamma \sin \delta)] \tag{6}$$

Since only the fundamental is detected, the signal is proportional to

$$S \approx \gamma_0 \sin \omega t[\cos 2\alpha \sin \delta - \sin 2\alpha \cos \delta] = \gamma_0 \sin \omega t \sin (\delta - 2\alpha) \tag{7}$$

This vanishes when $\alpha = \delta/2$ and the change in signal intensity is linear in angular unbalance when near the zero point.

It has been possible to determine the angle of isocline to 1° for a relative retardation of 5×10^{-9} cm. with the mercury green line. The least count for the measurement of retardation was 0.3 A. These limitations are not due to the sensitivity or stability of the electronic equipment, but to limitations in the measurement of the angular position (±0.01°) and to extraneous birefringence in the windows. For extremely small birefringence, the precision was increased by measuring the retardation as a function of angular position over about 200° rotation and obtaining both the amount of birefringence and the isoclinic positions from a smooth curve drawn through these data points.

Experimental Data

Three basic mother solutions were prepared, with ratios of TMV to SBMV of 3:1, 1:1, and 1:3. All started with a nominal concentration of TMV of 0.3% by weight. Experiments were made with the basic solutions and with dilutions thereof. All solutions

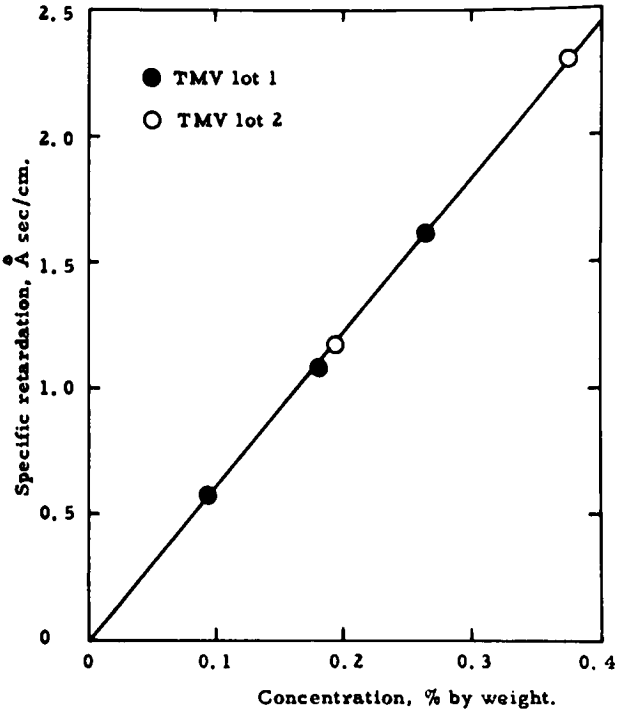

Fig. 4. Retardation per unit velocity gradient as a function of weight per cent concentration of tobacco mosaic virus (TMV).

were made in ultrafiltered distilled water containing 0.01*M* versene and had a pH of 7.4. Dilutions were made with the same versene solution. Concentrations were checked with a Zeiss PMQ II spectrophotometer.

Some anomalies appeared in the measurements of the angle of isocline at very low shear rates. These are being studied further and will be reported in another paper. They were not of a nature signif-

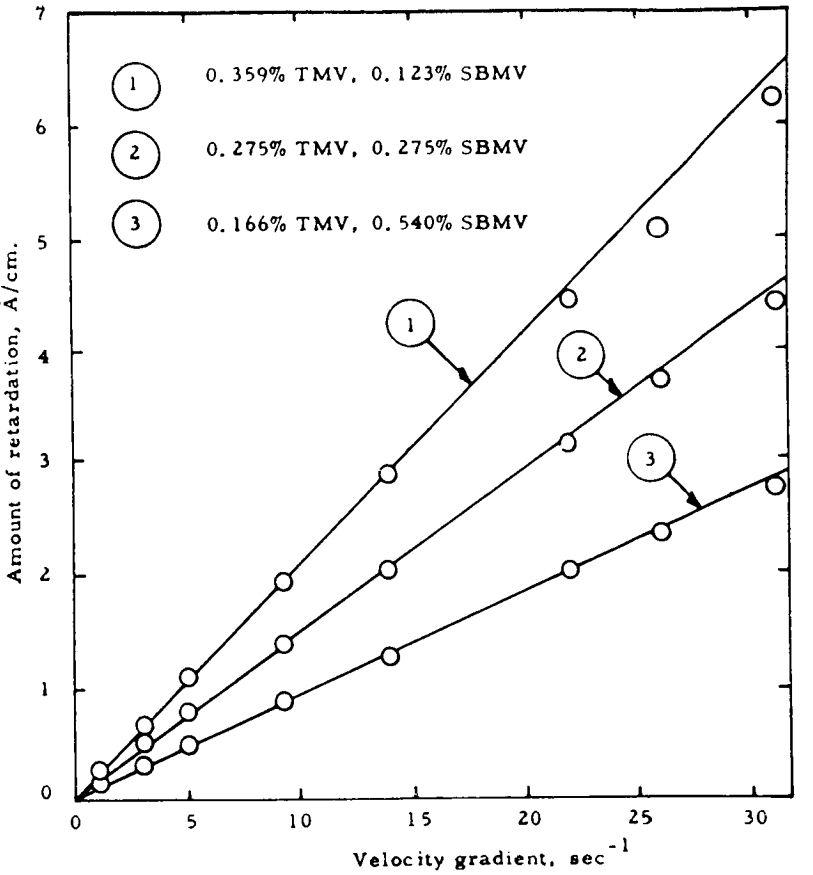

Fig. 5. Typical data on retardation of mixtures of TMV and SBMV as function of velocity gradient.

icantly to influence the measurements of the amount of birefringence which are reported here.

The amount of retardation per unit velocity gradient as a function of concentration for TMV alone is shown in Figure 4. The SBR is linear with concentration in the range of these studies, and the two different lots of TMV gave identical results. A typical set of data for the retardation of SBMV-TMV mixture as a function of velocity gradient is given in Figure 5. The specific retardation is obtained

from the slopes of these curves near the origin. The composite data for the specific retardation of seven different solutions as a function of concentration are given in Figure 6 compared with the data for

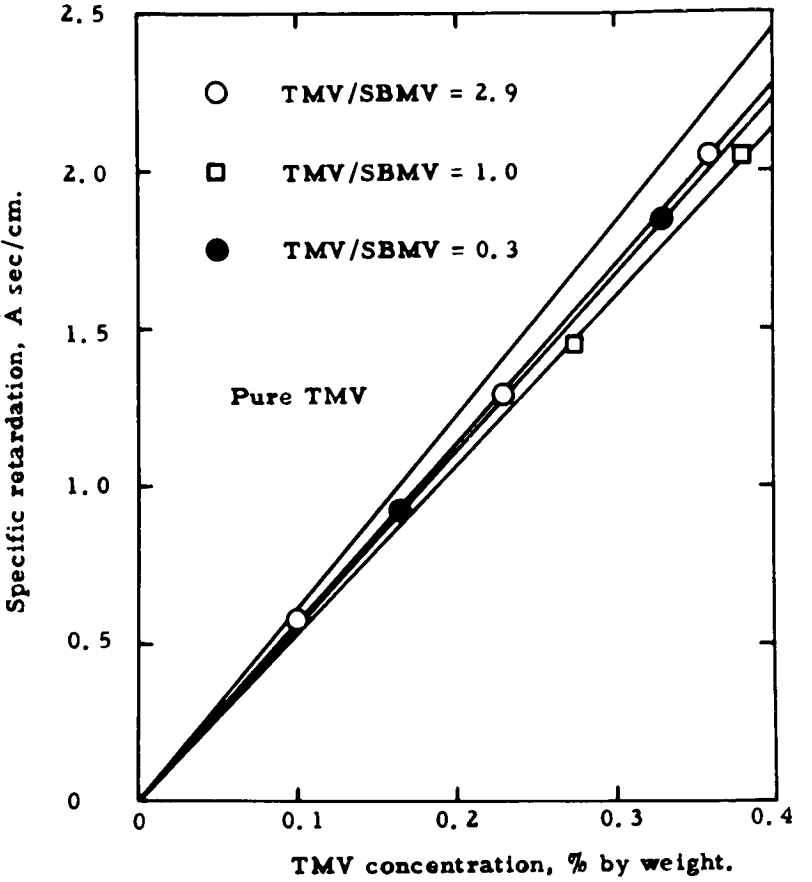

Fig. 6. Retardation per unit velocity gradient as a function of weight concentration for mixtures of TMV and SBMV.

TMV alone. The data for the specific retardation of a 0.3% solution of TMV with varying amounts of SBMV is plotted against SBMV concentration in Figure 7.

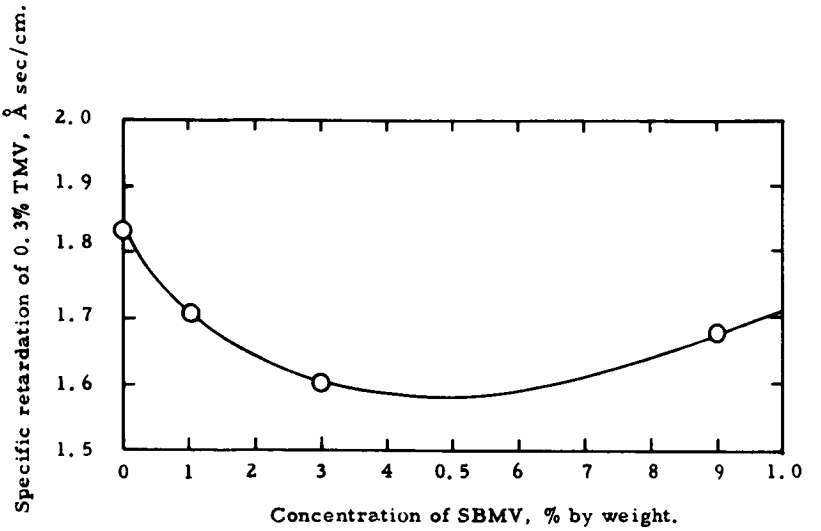

Fig. 7. Specific retardation of TMV-SBMV mixtures at TMV concentration of 0.3% as a function of concentration of SBMV.

DISCUSSION OF RESULTS

The initial drop in retardation as the amount of SBMV is increased, as seen in Figure 7, is quite opposite to what might be expected from viscosity considerations. Even accepting the fact that the local viscosity felt by the TMV in rotation may not rise so rapidly as the overall viscosity, the addition of the SBMV should be expected to increase the viscosity and not lower it. The bulk viscosity of the mixtures followed the expected trends, as can be seen from Figure 8. [The solutions were flown to the Massachusetts Institute of Technology by one of the authors (M. I.), and the measurements were made on the GDM viscometer named for Gilinson, Dauwalter, and Merrill who developed it.]

Examining other factors in eq. (3) which might increase D, we would need something which would decrease the length of particle a_1, or increase the factor $\sigma - \gamma$. Neither of these can be accounted for by effective increase in particle size by association, and electron micrograms taken after the experiments showed no evidence of average particle size being reduced by breakage of the TMV.

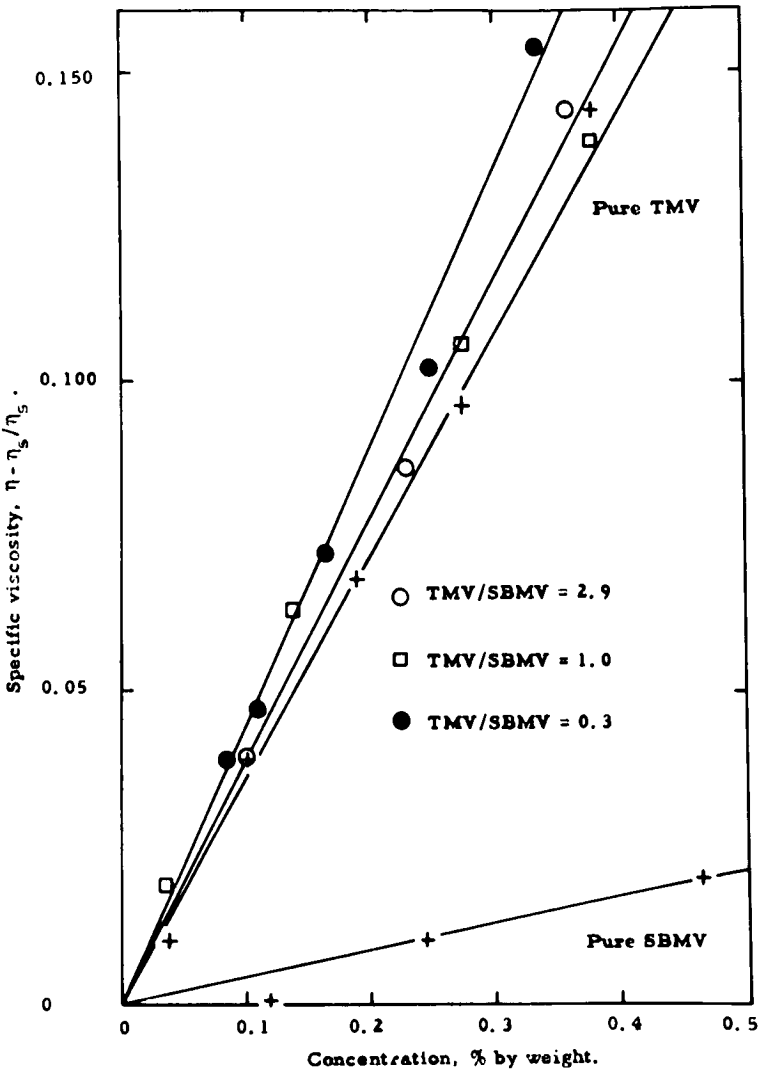

Fig. 8. Specific viscosity of TMV, SBMV, and mixtures as a function of concentration. (Specific viscosity of mixtures plotted as a function of concentration of TMV.)

Examining eq. (1), two other factors which might be responsible for the change in specific retardation are the mean index of refraction $\bar{n}$ and the optical factor for the TMV in its environment G. Addition of SBM to the TMV solution should increase $\bar{n}$ monotonically, with an overall change in the index of refraction of 0.002 for the addition of 1% SBMV. This would lead to a very small decrease in Δn, which would be linear with concentration. At 20°C. the index of refraction of water is 1.3330. The addition of 0.3% of TMV would raise this to 1.3335. With the maximum concentration of SBMV (1%) this would be raised to 1.3353, a change of 0.13%. The presence of versene would increase the reference index and reduce the percentage increment.

If we look at the optical factor G, we need to consider the difference between the index of refraction of the particle to that of the medium. Tobacco mosaic virus has an index of refraction of 1.6, so that the addition of 1% SBMV would decrease the increment (and hence Δn) by less than 1%, and would also be expected to be monotonic in the region studied.

A structuring of the TMV system at low velocity gradients, which might be disrupted at higher gradients, would be consistent with some of the ultracentrifuge data of Hearst and Vinograd.[8] The addition of the SBMV might be expected to break up this structure since these particles are more violently agitated by Brownian motion than is the TMV. This could be the explanation for the drop in specific retardation as SBMV is added, since the larger organized units may have a higher specific birefringence than the individual rods; this is consistent with the fact that many colloidal systems show an increase in birefringence which is faster than linear with concentration when the particles no longer act as individual units. This is difficult to reconcile with the linear increase in specific retardation with TMV alone shown in Figure 4, however. On this hypothesis one might explain the subsequent rise in the birefringence with further addition of SBMV to the fact that although the motion of the spherical particles tends to break up the aggregates, the addition of the spheres is also increasing the local viscosity which eventually reverses the trend to smaller birefringences.

Figure 9 gives a diagram of the relative proportions and size of the TMV and SBMV particles for the concentration used for the data of Figure 7. One possible explanation of the comportment of

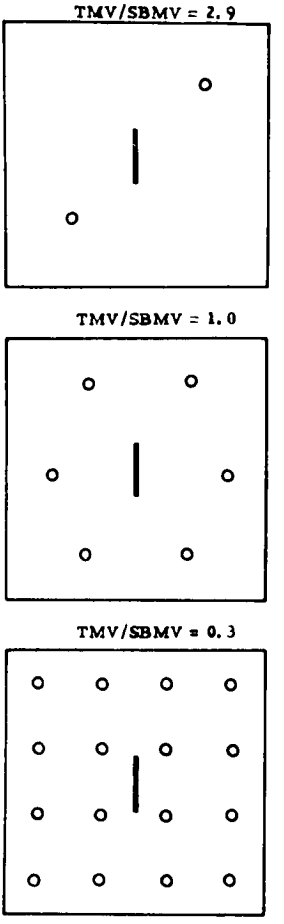

Fig. 9. Scale diagram of the relative proportions and sizes between particles in the TMV-SBMV mixtures for constant TMV concentration of 0.3% by weight.

Figure 7 is that for the lower concentrations of SBMV the interactions with the TMV occur relatively infrequently so that the usual statistical model employed in the theory of SBR is inadequate: one must appeal to fluctuation theory. As the concentration of SBMV increases, the system approaches more nearly to that on which the mathematical model is based and the presence of the SBMV manifests itself as an increase in local viscosity.

Experiments are planned on the transient Kerr effect for these mixtures to explore the type of interactions which occur when there is no transport due to flow superposed on the Brownian motion.

The authors wish to express their gratitude to Dr. N. Simmons of the Department of Nuclear Medicine of the University of California at Los Angeles for the samples of tobacco mosaic virus; to the Earhart and Campbell Laboratories of California Institute of Technology for facilities for growing the southern bean mosaic virus; to Mr. P. Knust-Graichen for isolation of the southern bean mosaic virus; to Professor E. W. Merrill of the Massachusetts Institute of Technology for making the GDM viscometer available; to Dr. J. Vinograd and Miss R. Kent for sedimentation velocity studies of the southern bean mosaic virus; and to the Applied Physics Corporation of Monrovia, California, for the use of the polarimeter amplifier.

References

1. Collins, D. J., and H. Wayland, *Trans. Soc. Rheology*, **7**, 275 (1963).
2. Joly, M., *Kolloid-Z.*, **145**, 65 (1956).
3. Peterlin, A., and H. A. Stuart, *Z. Physik*, **12**, 1, 129 (1939); *Hand- und Jahrbuch der Chemischen Physik*, Vol. 8, Becker u. Erler, Leipzig, 1943, Abt. 1B.
4. Broersma, S., *J. Chem. Phys.*, **32**, 1626 (1960).
5. Perrin, F., *J. Phys. Radium*, **5**, 497 (1934).
6. Wayland, H., and Badoz, J., *Comptes Rend.*, **250**, 688 (1960).
7. Intaglietta, M., "Streaming Birefringence Study of the Interactions of Submicroscopic Particles," doctoral dissertation, California Inst. of Technology, 1963.
8. Hearst, J. H., and J. Vinograd, *Arch. Biochem. Biophys.*, **92**, 206 (1961).

Synopsis

14586

A streaming birefringence apparatus using Faraday cell modulation and photoelectric detection is described. This apparatus was capable of angle of isocline measurement to $\pm 1°$ for a retardation of 0.5 A. and retardation measurements of 0.3 A. This apparatus was used to study the streaming birefringence of mixtures of rodlike particles 3000 by 180 A. (tobacco mosaic virus) and 250 A. diam. spherical particles (southern bean mosaic virus). With constant amounts of rods (0.3%) the specific retardation of the system first dropped and then increased with the addition of the spherical particles with a minimum at 0.5% spheres. Possible explanations are discussed.

author

HEMORHEOLOGY OF RED CELL SUSPENSIONS

Abstract

Rheology and Structure of Red Cell Suspensions†

S. CHARM* and W. McCOMIS, *Massachusetts Institute of Technology, Cambridge, Massachusetts,* and G. KURLAND, *Beth Israel Hospital, Brookline, Massachusetts*

A structural model developed for kaolin suspensions was applied to blood in order to determine the structure and strength of the red cell suspensions.

The yield stress of red cell suspensions determined in settling experiments agreed with the yield stress determined from shear stress-shear rate information employing Casson's equation.

Theoretical considerations indicate that the shear stress-shear rate curve for blood should approach a straight line. This was found to be true at shear rates above 40 sec.$^{-1}$. The slope of this line was predicted from calculations based on sedimentation experiments and a modified Einstein's equation.

The data suggest that the curvature of the shear stress-shear rate plot at low shear rates, is due to aggregates of cells which break down under increasing shear rate, resulting finally in individual flocs.

It is suggested that a floc consists of one to four cells with adhering plasma. The aggregate was calculated to have twice as much plasma associated with it as does a floc. However, the size of the aggregate could not be determined since the number of flocs associated with an aggregate could not be determined. Photographs clearly showing aggregate and floc formation in a small capillary tube were obtained.

† Published in the *J. Appl. Physiology,* **19** (Jan. 1964).

PRECEDING PAGE BLANK NOT FILMED.

N67 14587

The Influence of Electrokinetic Charge on the Rheological Properties of Red Blood Cell Suspensions

HAROLD A. COX, JR.† and GOUQ-JEN SU,
University of Rochester, Rochester, New York

INTRODUCTION

Considerable progress has been made in recent years in explaining some of the "anomalous" flow properties of blood, and in measuring, with sophistocated instrumentation, rheological properties which previously had not been determined. Complete explanations of all the rheological characteristics of a system as complicated as blood are still lacking, however. The present investigation was undertaken in the hope that it might contribute toward a more complete understanding of some of the phenomena which are manifested as rheological properties of blood.

The rheological behavior of a suspension is a quantitative indication of the response of the suspension to an applied force; that is, the amount of energy required to move the suspended particles relative to one another. In theory, the force between two suspended particles, which must be overcome by the force applied to the suspension, becomes quite strong when the particles attain a certain proximity to one another. Such an occurrence would result in an increase in the viscosity (and perhaps the yield point) of the suspension.

If the suspended particles bear like electrostatic or electrokinetic charges, these charges could keep the particles sufficiently far apart that the strong short-range forces could not come into play. Alterations of these charges could consequently have a profound effect on the strength of interparticle forces, and thus on the viscosity of the

† Present address: Pioneering Research Laboratory, Textile Fibers Dept., Experimental Station, E. I. du Pont de Nemours & Co. Inc., Wilmington, Delaware.

PRECEDING PAGE BLANK NOT FILMED.

suspension. This has been demonstrated in aqueous suspensions of glass frit[1] and a chlorinated polyether.[2]

The various suspended corpuscles and proteins responsible for the flow properties of blood all have electrokinetic charges, which have been investigated exhaustively. Their possible role in affecting blood's rheological characteristics has, until now, not been systematically investigated, to the best of the authors' knowledge.

One of the goals of the present research was to discover whether red cells normally exist at such distances from one another that a reduction in charge would bring them sufficiently close together for the strong short-range forces to produce a detectable change in the rheological properties of the suspension; or, on the other hand, if these forces predominate under normal conditions, in which case an increase in the cell charge would be expected to cause a viscosity decrease. It should be understood, however, that other forces between the cells, or between cells and plasma proteins, may be so strong that, so far as controlling the viscosity of the suspension, electrostatic effects would be relatively unimportant.

This preliminary study was concerned with red cell suspensions of 40% hematocrit in a shear rate region sufficiently high (from 400 to 1800 sec.$^{-1}$) that significant non-Newtonian properties were not exhibited. Ultimately, it is hoped that the approach could be extended to whole blood over a wide shear rate range, including rates less than 10 sec.$^{-1}$.

BACKGROUND

Attractive forces between red cells were noted as early as 1912 by Hess,[3] and the term "coherence resistance" came into being. Fåhraeus[4] observed the formation of rouleaux or *Geldrollen*, in which red cells agglomerate face to face like stacks of coins, and attributed the formation to four main factors: (*1*) properties of the fluid medium, (*2*) electrostatic attraction, (*3*) surface tension, and (*4*) hydration.

Knisely[5] and Shin et al.[6] also mention the possible importance of cell charge. Cokelet et al.[7] recently put forth the hypothesis that long rouleaux predominate in the creeping flow region (shear rates between 0 and 1 sec.$^{-1}$); they become shorter as the shear rate increases, and at shear rates above about 100 sec.$^{-1}$, the red cells exist as individuals.

Interassociation phenomena are also influenced by the presence of the plasma proteins. As discussed by Wells et al.,[8] the plasma pro-

teins have charges, as do the red cells, so that there is a possibility for association between red cells and their suspending medium, and between one red cell and another. The authors suspect that this association would be reversible under shear. The matter is discussed further by Merrill and Wells[9] and Shin et al.[6]

It should be evident from the above discussion that electrophoretic charges on red cells may be of considerable significance in affecting the rheological properties of blood, but these potential rheological implications seem not to have been considered by the many researchers who have investigated the electrokinetic properties of red cells. Most work has been directed toward studying the surface properties of the cells, alterations in which could control agglutination (here used in the sense of agglomeration or aggregation) and might be reflected in a change in erythrocyte charge. The "standard" book on the subject, that of Abramson,[10] is cited for most work prior to 1934, and for a general summary of electrophoretic techniques; the recent treatment of Brinton and Lauffer[11] is also an excellent general reference.

The electrokinetic charge on particles such as red cells arises primarily from (*1*) dissociation of ionizable groups on the surface (carboxyl in the case of red cells), leaving charged sites; and (*2*) adsorption of ions present in the suspending medium onto the particle surface, either at uncharged sites or at sites charged by dissociation.

Both dissociation and adsorption lead to a distribution of ions around the particle. In the case of the negatively charged red cell, cations are attracted much more strongly than anions, and thus on a time average the concentration of these cations (called counterions or *Gegenions*, since their charge is opposite to that of the particle) increases exponentially as the particle is approached. The particle charge is influenced by both the number and the valence of these counterions, so that changes in the pH or ionic strength of the suspending medium or the use of polyvalent cations (e.g., Al^{3+}, Th^{4+}) have quite a profound effect on the cell charge. Certain diseases[12–16] also have an effect.

PROCEDURE

The approach followed throughout this investigation was to study erythrocyte suspensions under conditions which were expected to change either the suspension viscosity or cell charge, and observe

the effect on the other. Human blood was obtained by venipuncture, using a 20-mm. glass syringe and 20 gage needle, and transferred immediately into a glass tube coated with sufficient ethylenediamine tetraacetic acid (EDTA) to prevent clotting. If the serum from this blood was desired, the whole blood was centrifuged at 4500 rpm for 15 min. or until the serum was free of formed elements. Immediately prior to experimentation, the red cells were washed twice in ten times their volume of physiological saline, centrifuging at 4500 rpm for 15 min. each time. It has been shown[10] that the amount of washing can have an effect on the cell charge, so the above washing procedure was never varied.

Preparation of Suspensions

Suspensions whose rheological behavior was to be studied were prepared by adding approximately 2.5 ml. of the appropriate solution to an equal volume of washed cells contained in a polyethylene test tube. The final hematocrit was adjusted by trial and error.

Much more dilute suspensions were necessary for electrophoresis measurements. These suspensions were prepared by adding a sufficient volume of washed, packed cells to approximately 50 ml. of solution to make a 0.1% suspension. This optimum suspension concentration was consistent with those of other investigators.

Rheological Measurements

After the hematocrit had been adjusted to 40 ± 1%, and the pH of the suspension measured with a Beckman model H-2 pH meter, approximately 4 ml. of suspension was introduced into the O-special measuring system of an Epprecht RM-15 viscometer.* This measuring system had a capacity of slightly less than 4 ml., and when used with the RM-15 viscometer, had a shear rate range of 28 to 1791 $sec.^{-1}$. It consisted of a hollow cylinder, attached to a driving head, and fitting coaxially inside a gap between two stationary concentric cylinders. As shown in Figure 1, this resulted in two concentric fluid-filled gaps, the hollow cylinder rotating in such a manner that it became simultaneously the outer cylinder of the inner gap, and the inner cylinder of the outer gap. Water at 25°C. surrounded

* Distributed by Drage Products Division of Torque Controls, Inc., Union City, New Jersey.

not only the outer cylinder but also the inner hollow core, maintaining very close temperature tolerances across both gaps. Both rheological and electrokinetic measurements were made at 25 °C.

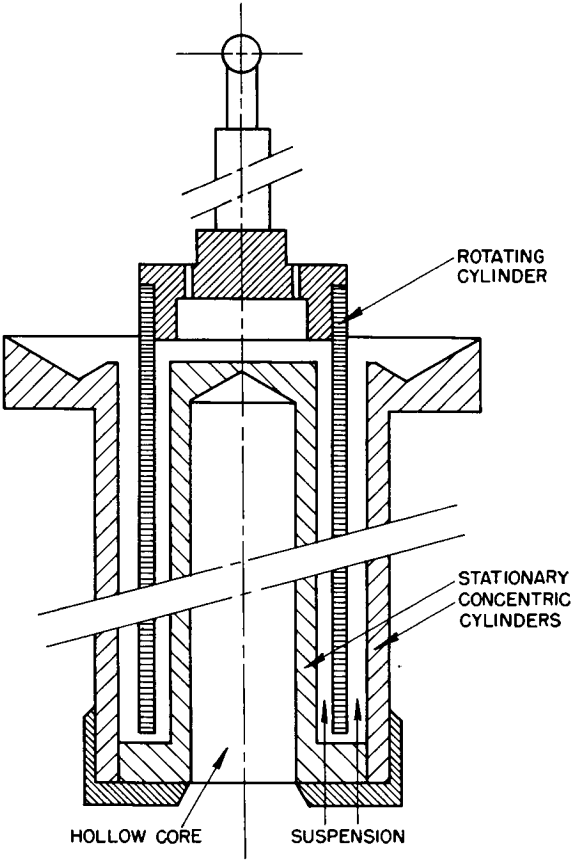

Fig. 1. O-spacial measuring system (not to scale).

Readings were then made at a series of shear rates, specifically 397, 576, 773, 1018, 1357, and 1791 sec.$^{-1}$. These were chosen because of the anticipation[17] that the differential viscosity (defined as $\eta_d = d\tau/d\dot{\gamma}$, where τ is the shear stress in dynes/cm.^{2} and $\dot{\gamma}$ is the shear rate in sec.$^{-1}$) would be constant in this range, and thus

could be used as a correlating variable. Ths linearity of the $\tau - \dot{\gamma}$ plot in this shear rate region was tested in each case.

Electrophoresis Measurements

The best method of determining the charge on red blood cells is that of microelectrophoresis, in which a dilute suspension of cells is placed in an electric field, and microscopic observations are made of the velocity with which individual cells move under the influence of this field. For a given field strength E, the velocity is proportional to the net charge on the particle, as long as the ionic strength of the suspending medium is essentially constant. The electrophoretic mobility U, defined as the ratio of the particle velocity (microns/second) to the field strength (volts/centimeter), is a convenient way of expressing the degree to which a particle is charged; by convention, the sign of the mobility indicates whether the particle bears a positive or negative charge.

Complete descriptions of the modified Northrop-Kunitz equipment used in this investigation are available in the literature.[1,2,18] The apparatus featured (*1*) a clutch timer, for accurate measurement of particle velocities, and (*2*) a Leeds & Northrup model K-3 potentiometer, for precise voltage measurement (used in obtaining the field strength). A magnification of 420× permitted the shape and orientation of individual cells to be observed at all times.

In general, ten individual cells were observed during each run, and their particle velocities averaged. Only a few minutes were required to determine the red cell mobility under a given set of conditions, and the mobility reported is accurate to about 5%.[19]

RESULTS

The effects, if any, on cell mobility and suspension viscosity produced by the following treatments were determined.

Bovine Albumin

Stephens[20] has suggested that there may exist an interaction between serum proteins and the red cell surface which could affect the cell mobility. Such an interaction could affect the rheological properties of the suspension as well, in the manner described by Wells et al.[8]

Inasmuch as albumin makes up approximately one-half of the total amount of proteins in the blood, a preliminary study of its effect on mobility and viscosity was undertaken. The albumin used was bovine, obtained as a 30% solution from Armour Pharmaceutical Co., Kankakee, Ill. It was added to unbuffered saline in such proportions as to yield solutions of 1.75, 3.5, and 7% albumin by volume. The 3.5% solution corresponded approximately to the albumin content of normal serum; the 7% solution, to the total protein content of normal serum. The pH of both electrophoretic suspensions and 40% cell suspensions was 7.15 ± 0.05. The results are shown in Table I.

TABLE I
Effect of Albumin on Mobility and Viscosity

Bovine albumin, %	Mobility, μ/sec./v./cm.	Differential viscosity η_d, cp.
0	−1.08	2.9
1.75	−0.54	3.1
3.5	−0.47	3.5
7	−0.34	4.0

Both the differential viscosity and the mobility are affected by the addition of merely a small quantity of albumin. Note in particular that the mobility is halved when the cells are suspended in a 1.75% albumin solution. Albumin addition increases the viscosity of the suspending medium, however, and this must be taken into account in the interpretation of mobility results. Since the frictional force on a particle moving through a fluid is proportional to the viscosity of that fluid, the mobility of a particle is inversely proportional to the viscosity of the suspending medium, other factors being equal. The observed mobilities may thus be made relative to mobilities in pure saline by the equation

$$U_c = U \cdot (\eta/\eta_s) \tag{1}$$

where U_c is the mobility corrected for the viscosity of the medium, U is the observed mobility, η is the viscosity of the suspending medium (albumin-saline in this case), and η_s is the viscosity of physiological saline. In this manner, the retardation of the red cell by more

viscous suspending medium may be eliminated from the total effect on mobility.

Similarly, the relative viscosity, and not the measured differential viscosity, must be used in evaluating the part played by the red cells in determining the viscosity of the cell suspensions. When these effects are taken into account, the mobility decrease produced by subsequent addition of albumin is considerably less than that originally observed, while the relative viscosity is not significantly increased by albumin addition, as shown in Table II.

TABLE II
Evaluation Using Corrected Mobility and Relative Viscosity

Bovine albumin, %	Corrected mobility, μ/sec./v./cm.	Relative viscosity, η_r
0	−1.08	2.9
1.75	−0.54	2.9
3.5	−0.52	3.1
7	−0.47	3.0

It must be concluded that, in the shear rate range used in this study, the charge reduction produced by albumin does not affect the rheological properties of the cell suspension.

Serum

Although albumin did not significantly alter the relative viscosity of red cell suspensions, it was believed that normal plasma—containing fibrinogen and globulin in addition to albumin—might offer a greater opportunity for interactions between cells. Abramson[10,21] reported a decrease in the mobility of red cells suspended in normal serum, while Wells et al.[8] showed that the viscosity of red cell suspensions increases as the saline-suspending medium is gradually replaced by serum. It was decided to determine whether or not these two effects were related. Accordingly, normal human serum was mixed with unbuffered saline in varying proportions between 0 and 100% serum by volume. Figures 2 and 3 illustrate the effect of serum on mobility and viscosity, respectively.

The decrease in observed mobility and corresponding increase in differential viscosity are consistent with the literature findings dis-

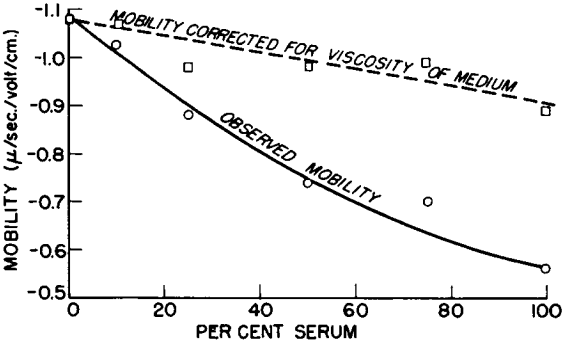

Fig. 2. Relation between cell mobility and serum content of saline-suspending medium.

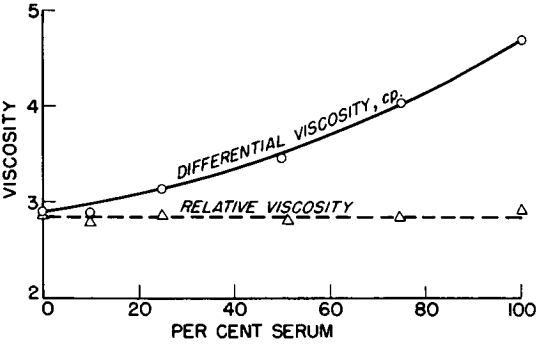

Fig. 3. Relation between suspension viscosity and serum content of saline-suspending medium.

cussed in the preceding paragraph. However, since the relative viscosity is independent of serum concentration, it is apparent that despite the decrease in both observed and "corrected" mobility with increasing serum concentration, the viscosity increase produced by serum is due not to charge effects but to the viscosity increase in the suspending medium. This conclusion may not apply to low shear rates, where interassociation phenomena such as rouleaux formation (for which electrostatic considerations can be important) predominate, while rouleaux have disintegrated into individual cells at the shear rates employed in the present study.

Antibody

Antibodies are well known for their ability to cause agglutination of erythrocytes, by a method involving an interaction between the antibody molecules and specific groups (agglutinogens) on the cell surface. Since it seemed plausible that these interactions might be promoted by a reduction in the cell charge, it was of interest to determine if the agglutination were accompanied by a mobility decrease and viscosity increase. The degree of agglutination should influence the suspension viscosity, but it was found that, for the antibody studied (anti-B, with type B cells), the mobility was not related to the degree of agglutination.

Trivalent Cation

A 0.0286M solution of $AlCl_3$ was added to a physiological saline solution, in amounts ranging from 0 to 10% by volume. Both the dilute suspensions used for electrophoresis, and the 40% suspensions used for rheological study, were buffered with $M/15$ Na_2HPO_4-KH_2PO_4 to pH 7.15 $\pm$0.05, to avoid any effect of pH. Care was taken to make electrokinetic measurements after the same elapsed time as was required to adjust the hematocrit and make rheological measurements, so that the observed mobility would indicate the particle charge at the exact time the relative viscosity was determined. The results are shown by Figures 4 and 5.

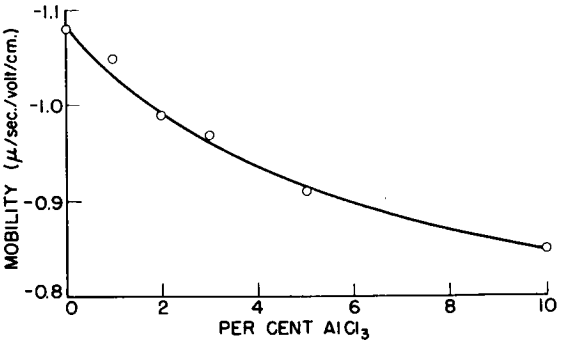

Fig. 4. Relation between cell mobility and $AlCl_3$ content of saline-suspending medium.

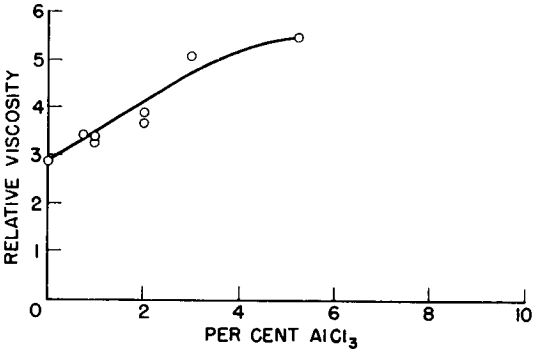

Fig. 5. Relation between suspension relative viscosity and $AlCl_3$ content of saline-suspending medium.

The first curve shows a definite decrease in cell mobility as the $AlCl_3$ concentration is increased, up to 10% $AlCl_3$ per total volume of suspending medium. Figure 5 shows a corresponding increase in relative viscosity, although measurements could be carried no further than 5% $AlCl_3$ per total volume of suspending medium, because larger amounts produced hemolysis. It is of course possible that the mobility decrease accompanies, rather than causes, the viscosity increase, but the effect of Al^{3+} (and probably other polyvalent cations) warrants further study.

Other Treatments

The ionic strength of the suspending medium (NaCl or $CaCl_2$ solutions) was varied over a three-decade range, isotonicity being maintained with a 10.4% sucrose solution. Because of leakage of electrolytes from the cell at these low salt concentrations, the mobility was never stable, but decreased as is shown in Figure 6. The fact that the relative viscosity was constant (Fig. 7), despite the rather pronounced decrease in mobility for cells in sucrose, indicates that the mobility is evidently not important in controlling suspension viscosity under these circumstances.

No conclusions regarding mobility-viscosity relationships can be drawn from experiments in which pH was varied, because the buffering action of the red cells too severely restricted the range of pH available for study.

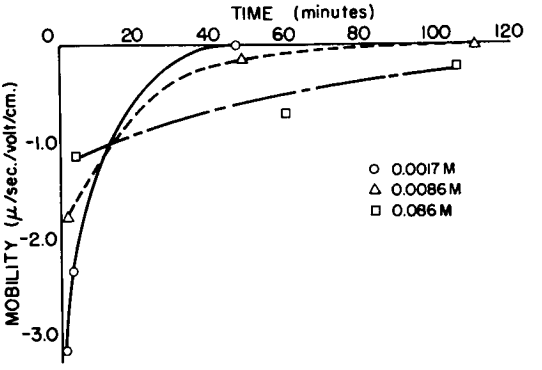

Fig. 6. Change of mobility with time (red cells in NaCl-sucrose solutions).

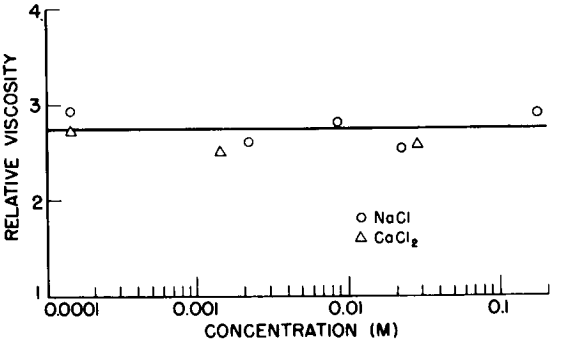

Fig. 7. Relation between relative viscosity of red cell suspensions and concentration of salt in sucrose-containing suspending media.

CONCLUSIONS

1. Under conditions such as might approximate those existing *in vivo,* electrical charge was found to have no significant effect on the rheological properties of erythrocyte suspensions in the shear rate range studied. The addition of albumin to saline up to a concentration twice that of normal plasma, and the replacement of saline by serum as a suspending medium both produced an increase in suspension viscosity and a decrease in cell mobility, but the viscosity increase was due not to charge effects but to the contribution of albumin and serum to the viscosity of the suspending media.

Studies of cells suspended in solutions of isotonic salts and sucrose also led to this conclusion.

2. A rather drastic treatment—adsorption of a polyvalent ion—did show a significant relationship between cell mobility and suspension viscosity. Further study of this relationship would be of interest.

3. The suspensions studied in this investigation, particularly those having serum proteins in the suspending media, might well show charge-flow relationships at low shear rates (e.g., less than 10 sec.$^{-1}$).

The authors express grateful appreciation to the following for their considerable assistance and cooperation during this investigation: Dr. Anthony J. Bowdler, senior instructor in medicine; Dr. Edwin L. Carstensen, associate professor of electrical engineering; Dr. Marylou Ingram, associate professor of radiation biology; and Dr. Stanley Middleman, assistant professor of chemical engineering; all of the University of Rochester.

References

1. DeClerck, D. H., and G.-J. Su, *J. Am. Ceram. Soc.*, to be published.
2. Cox, H. A., Jr., and G.-J. Su, to be published.
3. Hess, W. R., *Arch. Anat. Physiol. Abt.*, **1912,** 197.
4. Fåhraeus, R., *Physiol. Rev.*, **9,** 241 (1929).
5. Knisely, M. H., *Trans. Soc. Rheology*, **6,** 13 (1962).
6. Shin, H., G. Cokelet, E. W. Merrill, E. R. Gilliland, A. Britten, and R. E. Wells, Jr., *Biophys. J.*, **3,** 199 (1963).
7. Cokelet, G. R., E. W. Merrill, E. R. Gilliland, H. Shin, A. Britten, and R. E. Wells, Jr., *Trans. Soc. Rheology*, **7,** 303 (1963).
8. Wells, R. E., Jr., E. W. Merrill, and H. Gabelnick, *Trans. Soc. Rheology*, **6,** 19 (1962).
9. Merrill, E. W., and R. E. Wells, Jr., *Appl. Mech. Rev.*, **14,** 663 (1961).
10. Abramson, H. A., *Electrokinetic Phenomena*, Chemical Catalog Co., New York, 1934.
11. Brinton, C. C., Jr., and M. A. Lauffer, in *Electrophoresis*, M. Bier, ed., Academic Press, New York, 1959, ch. 10.
12. Ada, G. L., and J. D. Stone, *Brit. J. Exp. Pathol.*, **31,** 263 (1950).
13. Hanig, M., *Proc. Soc. Exp. Biol. Med.*, **68,** 385 (1948).
14. Rottino, A., and J. Angers, *Cancer Res.*, **21,** 1445 (1961).
15. Rottino, A., and J. Angers, *Clin. Chem.*, **8,** 579 (1962).
16. Woernley, D. L., C. Carruthers, J. M. Ohrt, and K. Lilga, *Exptl. Cell Res.*, **23,** 510 (1961).
17. Haynes, R. H., *Trans. Soc. Rheology*, **5,** 85 (1961).
18. DeClerck, D. H., Ph.D. thesis, Univ. of Rochester, New York, 1960.
19. Cox, H. A., Jr., Ph.D. thesis, Univ. of Rochester, New York, 1963.

20. Stephens, J. G., *J. Physiol.*, **95**, 92 (1939).
21. Abramson, H. A., *J. Gen. Physiol.*, **14**, 163 (1930).

Synopsis

14587

Suspensions of human erythrocytes in various isotonic media were studied by means of coaxial cylinder viscometry (from 400 to 1800 sec.$^{-1}$) and microelectrophoresis to determine whether or not a relationship existed between the electrokinetic charge on the cells and the rheological behavior of the suspensions. It is shown that the electrokinetic charge does not play a dominant role in controlling suspension flow behavior under normal conditions in this shear rate region. This was demonstrated through experiments using albumin solutions, normal serum, isotonic sucrose, and an isoantibody solution as suspending media. Reasons are given why a charge-flow relationship in these suspensions could be expected under other conditions, such as very low shear rates. The addition of a polyvalent cation to the system is capable of decreasing cell mobility to such an extent that the viscosity increases significantly, as was demonstrated with $AlCl_3$ in physiological saline.

author

N67 14588

The Profile Viscosity and Other Characteristics of Blood Flow in a Non-uniform Shear Field

GEORGE BUGLIARELLO,* CHANDRA KAPUR, and GEORGE HSIAO, *Civil Engineering Department, Carnegie Institute of Technology, Pittsburgh, Pennsylvania*

INTRODUCTION

The rheological properties of blood are usually determined either in a constant or nearly constant shear stress field (cone and plate or concentric cylinder viscometers) or in a variable shear stress field (capillary viscometers). The constant shear approach in virtue of its intrinsic simplicity is possibly the most convenient, from the diagnostic viewpoint, as a means of relating changes in the resistance to shear in blood to changes in the pathological or normal conditions of the organism, and from the rheological viewpoint, as a means of providing information on the effect of the various properties of blood (hematocrit, cell shape, plasma composition) on its resistance to shear. From the physological viewpoint, on the other hand, the nonuniform shear approach is more realistic, as it comes closer to the conditions prevailing *in vivo*. To become fully useful such an approach requires, however, a complete understanding of the essential characteristics of the flow in tubes and of their relationship to the flow under uniform shear conditions.

The scope of the present investigation will be confined to narrow channels because of their greater physiological significance in terms of the vascular resistance, and also because of the rheologically simpler and less interesting conditions approached in the physiological pressure range as the channels become wider.

One of the earlier known and most important characteristics distinguishing the flow of blood in the nonuniform shear stress field in the narrower channels is the existence of a peripheral cell-poor layer ascertained both through direct visual means and indirectly. (A

thin peripheral layer appears to be present also in a uniform shear field primarily under normal flow conditions as a result of geometrical interference of the walls with the cells.[1]) The few direct quantitative experimental determinations of the layer, both *in vitro* and *in vivo*, have shown that it fluctuates from instant to instant,[2–4] decreases as hematocrit increases,[2] and becomes relatively less important in the larger vessels (where the flow thus approaches that of a homogeneous fluid). In *in vivo* studies with whole blood, the layer was found usually to increase with flow rate[2,3] if sedimentation effects were absent. Similar determinations *in vitro* of the flow rate effect[4] were inconclusive because of the interference of settling. Indirect measurements of the peripheral layer based on light absorption techniques have been less reliable because of the difficulty in distinguishing between density and orientation effects.[5,6]

A second distinguishing characteristic of the nonuniform shear field is the shape of the velocity distribution in the cross section of the flow channel. The velocity has been shown to increase continuously from the wall toward the centerline[2–4,7,8] (except possibly at extremely low flow rates, where it may be nearly uniform across the diameter). The higher velocities in the core, in combination with the existence of a peripheral layer, lead to core concentrations which are lower than if the velocity were uniform over the cross section—an effect first demonstrated by Fåhraeus and Lindquist.[9] Such a "dynamic" effect is but one manifestation of the complex interaction of velocity and concentration distributions—as well as erythrocytes' orientation, rotation, and deformation phenomena—which governs the flow under nonuniform shear conditions[10–13] and which will be further investigated here.

Since, ultimately, the characteristics of the flow in a tube must be reflected in the overall relationship between driving force and flow rate, considerable information can also be derived—as last and comprehensively exemplified by Thomas[14]—from the pressure-flow curves, which are of much easier experimental determination that the details of the flow in the cross section. Such an approach must, however, proceed in concert with the experimental observations of the flow details, if the models used in the interpretation of the pressure-flow curves are to be realistic and of general physiological usefulness in understanding the characteristics of the *in vivo* flows. Thus, although it may be possible to interpret equally well a flow curve *in*

vitro as the result of a "sigma effect" or of a peripheral layer, as shown by Haynes,[15] certainly *in vivo* the occurrence of the one or the other phenomena would be no indifferent matter in regard to the exchange processes in the cross section and between the flow and the boundaries. Equally important to this effect is the possible occurrence of slip at the boundary,[3] not easily distinguishable analytically from the peripheral layer effect. Another aspect of considerable physiological importance in its bearing on the exchange processes in the flow is the relationship between the instantaneous flow picture and the long-range averages embodied in the pressure-flow curves. Finally, until the detailed flow picture is fully understood, attempts to predict nonuniform shear flow properties from uniform shear measurements are bound to be unsatisfactory, as observed, for instance, by Charm and Kurland.[16]

In a previous exploratory study of blood flowing through narrow horizontal glass capillaries, direct information was gained for a variety of flow conditions, on velocity profiles, peripheral layer dimensions, as well as the effect of sedimentation on these characteristics—an effect which, in turn, imposed approximations in the analysis of the observations. In the present study the same experiments have been repeated in vertical tubes, so as to eliminate the influence of sedimentation, and thus, hopefully, clarify those flow features (such as the effect of flow rate on the peripheral layer, the occurrence of off-centerline viscosity peaks, as well as the relation between instantaneous measurements and longer range averages) which could not be elucidated in the horizontal tubes, because of the possible interference of sedimentation. As in the previous study, the diameters of the tubes investigated were narrow enough (from 40 to 83 μ) to permit observation of the erythrocytes moving in the diametrical plane, and yet large enough to correspond to tube-to-cell size ratios exceeding by far the values at which a cell occupies most of the cross section and "bolus" conditions are approached.[2,17]

METHOD

The method is essentially the same as that of the study with the horizontal tubes,[3] where it is described in detail. The only changes in the apparatus have been in the orientation of the test section, in the light source, in the improved accuracy of the volumetric flow measurements at low rates, and in the use of a temperature probe downstream

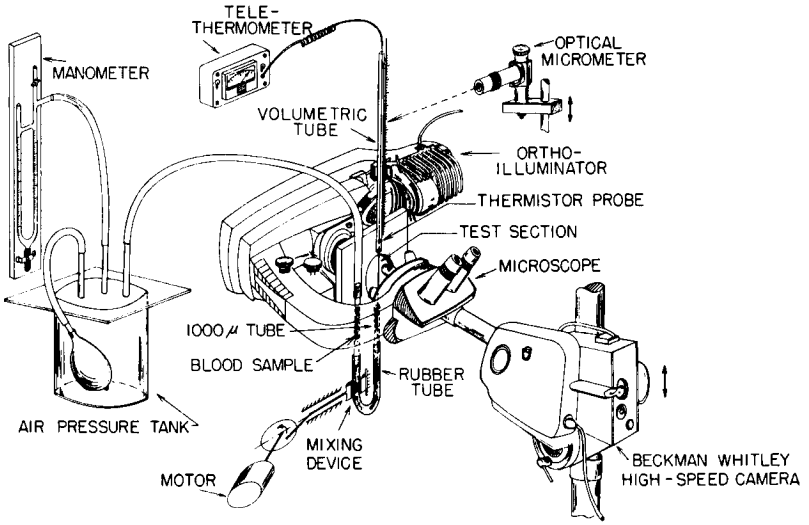

Fig. 1. Experimental apparatus.

of the test section to monitor optical heating. In brief, as shown in Figure 1, air pressure from an upstream reservoir caused the blood to flow upward into a vertical test section of precision glass tubing, 40, 66.6, or 83 μ in diameter and no less than 1000 diam. long. The upward flow arrangement was selected so as to facilitate the removal of cells settling on the upper end of the test section in the absence of flow. Mixing upstream of the test section was insured by compressing at a rate of 60 cycles/sec. (through a motor drive), the flexible plastic tube leading to the test section and containing the blood sample before the test. The device was disactivated a few instants before each test—a time sufficiently long for the waves set up by the compression to be dissipated, but too short for the concentration at the inlet of the test section (which reached for a distance of 10 mm. into the upstream glass tube 750 μ in diameter) to be affected by settling. Samples taken over long periods of time at different positions upstream of the test section showed no significant changes in hematocrit while the mixing device was in operation. The flow rate was measured volumetrically by observing through an optical micrometer the advance of the meniscus in precision tubings located downstream of the test section and ranging in diameter from 300 (for the lower flow

rates) to 550 μ. The maximum error did not exceed 4%. In the measure of the pressures (performed with a mercury manometer, and corrected for capillary effects in the volumetric tubes), the error never exceeded 3% at the lowest pressures and decreased as pressure increased.

At a distance of approximately 600 diam. from the inlet, the diametrical plane of the test section, illuminated from an oil-immersion condenser of NA 1.25, was observed through a phase-contrast microscope, connected to a Beckman-Whitley Magnifax camera running at speeds of approximately 3000 frames/sec. The microscope magnified the test section 970 times; the magnification on the film depended on the position of the camera. In order to reduce heating from the light source, the 1400-w.a.c. carbon arc of the previous experiments was replaced by a 300-w. tungsten bulb in the condenser of the microscope; this also eliminated the large fluctuations in the light intensity characterizing the a.c. carbon arc. The intensity of illumination was, however, somewhat reduced, making the observation of the core of the 83-μ tubes more difficult. During a series of preliminary tests, a 520 Yellow Spring Instrument (YSI) thermistor probe positioned (as shown in Fig. 1) directly across the outlet of the test section, and connected to a 43TC YSI telethermometer having a sensitivity of 0.4°, did not indicate any increase in temperature caused by the light source. There continued to be, however, no way of ascertaining the occurrence of local increases in temperature in the test section in correspondence of the microscope.

Blood from healthy human subjects treated with acid citrate dextrose in the standard doses was used in all tests. In order to eliminate as much as possible aging effects, the tests were performed usually within 6 to 10 hr., and never later than 24 hr. from the taking of a sample. Different samples had thus to be used for different series of tests, which was rheologically a disadvantage since the viscosity of both whole blood and plasma (measured with a Brookfield concentric cylinder viscometer) varied from sample to sample, making comparisons between different tests more difficult. All the tests were performed at room temperature (from 25 to 32°C.), and so were the viscosity measurements on the same samples.

In the range of shear rates for which reliable measurements could be obtained with the viscometer (from 12.8 to 335 sec.$^{-1}$ for plasma, and narrower for the higher concentrations), the results of the viscom-

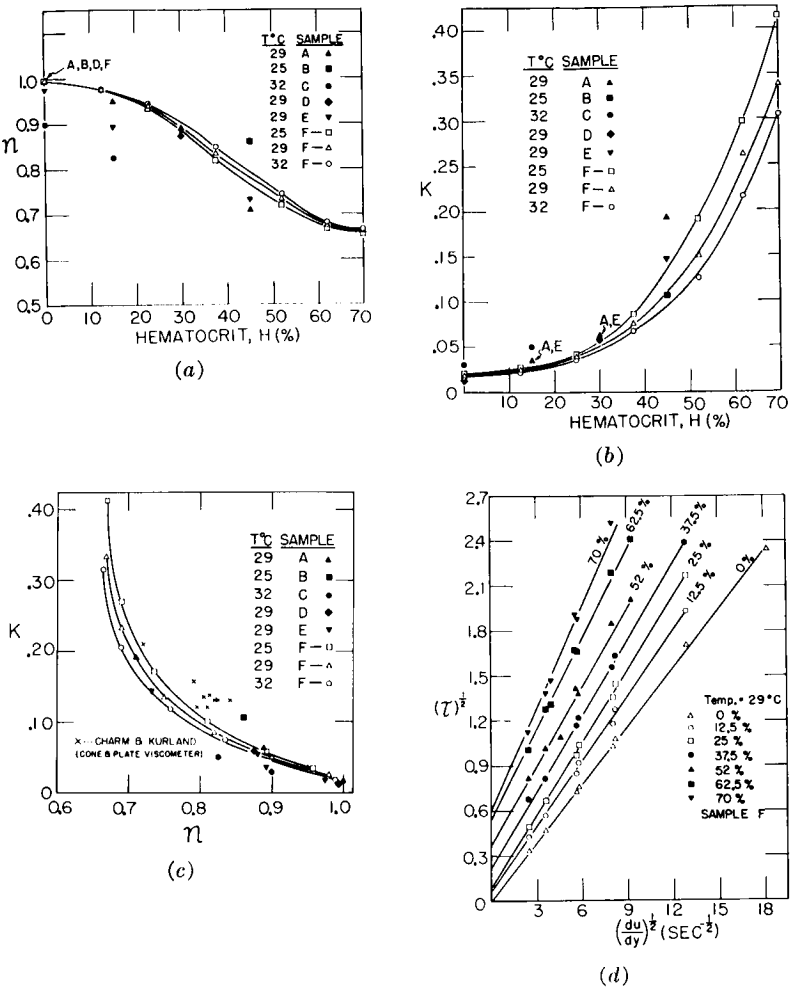

Fig. 2. Constant-shear viscosity characteristics of the blood samples. [Units of $\tau^{1/2}$ in d: $(\text{dynes/cm.}^2)^{1/2}$.]

eter measurements could be well represented by a power-law relation between the shear stress τ and the rate of shear du/dy: $\tau = K(du/dy)^n$.

The values of the two rheological indexes n and K for all the samples used in the tests are plotted respectively in Figures 2*a* and 2*b* as a

function of hematocrit and in Figure 2*c* as a function of each other. Also shown in Figure 2*c* are results for dog blood obtained by Charm and Kurland[16] with a cone and plate viscometer. The more extensive data for sample *F*—a sample actually not used in the microscopic studies—were gathered as a guide for extrapolation of the results for the other samples. A plot of $\tau^{1/2}$ vs. $(du/dy)^{1/2}$ for sample *F* at 29°C. (Fig. 2*d*) would indicate, if extrapolated to zero shear rate, yield shear stresses ranging from 0.005 dyne/cm.^{2} at $H = 12.5\%$ to 0.38 dyne/cm.^{2} at $H = 70\%$, values which are of the same order of magnitude as other published results.[16,18]

Meaning of Measurements

Since, for analysis purposes, the useful length of the films was limited (~0.3 sec. or ~1000 frames), the question arises as to what extent an average of the observations over such a limited time range is representative of long-range averages, such as those normally embodied in viscometric measurements.

In Figure 3 the ratio $d(N)/d$ of the value $d(N)$ of the peripheral layer averaged over N frames to the value d averaged over the total number of frames that could be analyzed ($N = 1000$) is plotted as a function of N for three different tests in the 40-μ tubes. The ratio is seen to vary with N, but to fall within ~10% of the final value already

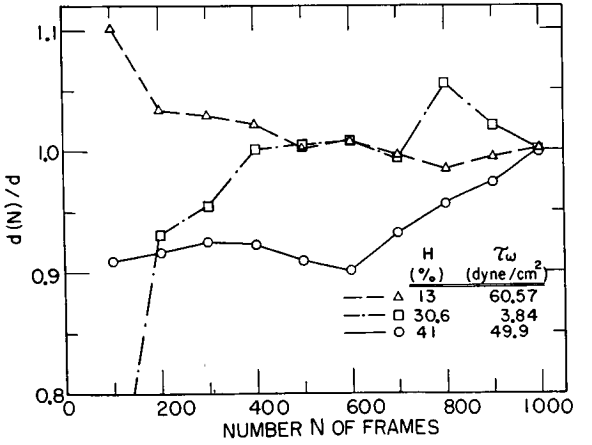

Fig. 3. Variation of average peripheral layer dimensions with length of film analyzed.

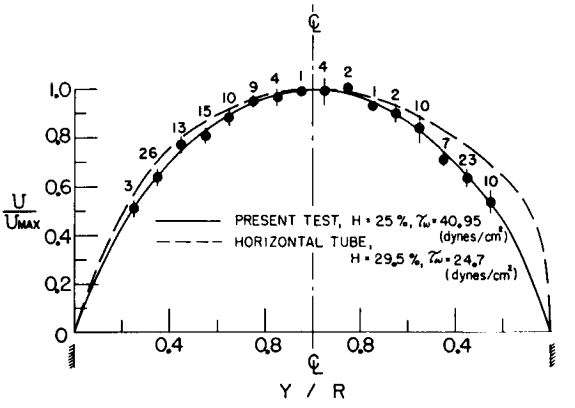

Fig. 4. Influence of settling on the shape of the velocity profiles: comparison between profiles in a vertical tube (present test) and in a horizontal tube. Tube diameter: 40 μ.

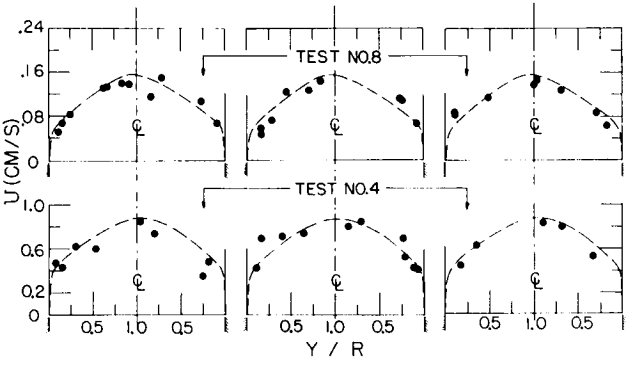

Fig. 5. Comparisons between instantaneous velocity measurements (black dots) and average velocity profiles (dashed curves).

after $N = 200$. Thus it can be expected that d will not vary much with further increases in N, and that, consequently, the results of the film analysis are close to the long-term averages for $N \rightarrow \infty$. This is confirmed by the good agreement existing in most tests between the flow rates Q_c computed by integration of the average velocity profiles for the useful film length ($N = 1000$) and the flow rates Q_M measured volumetrically over several seconds; for each of the representative

tests in Figures 7 to 9, the value of the ratio Q_M/Q_c is indicated below the velocity profile. In the case of the horizontal tubes, the agreement between Q_c and Q_M had not been as satisfactory, partially because of the poorer precision of the measurements particularly at low flow rates but also because of the approximations involved in calculating flow rates from velocity profiles made asymmetric by sedimentation effects.

The axial symmetry of the average velocity profiles is a consistent feature in all the tests in the vertical tubes and a further confirmation that long-range average conditions were approached. The symmetry is exemplified in Figure 4 which shows a typical velocity profile for the vertical tubes, and compares it to a profile for a horizontal tube[4] exhibiting a pronounced asymmetry caused by settling. Measurements of the erythrocytes' velocities over a very small number of frames could, however, be markedly asymmetric and vary considerably from the average velocity profiles, as shown in Figure 5.

PERIPHERAL LAYER CHARACTERISTICS

Among the observations with the technique used in this study, those of the peripheral layer are the most reliable, since the smaller optical density in the region near the wall makes the outer cells always clearly visible. The characteristics of the layer for selected experiments are summarized in the five plots of Figure 6.

Figures 6*a* and 6*b* show the variation of the ratio d/R of the average peripheral layer thickness d to the tube radius R, with the reciprocal of the wall shear stress τ_w for two nominal concentrations (the actual concentration varying somewhat in each case from test to test). The thickness d was computed as the average, over the useful length of the film, of the distances from the wall to the outer boundary of the nearest cell, measured at an arbitrarily fixed station. Here, unlike the case of the horizontal tubes, d was always nearly equal at either wall. The instantaneous values were different, however.

At the higher concentration (hematocrit $H = 40\%$, Fig. 6*a*), d/R tends to increase with shear stress. In the 40-μ tubes the increase is pronounced; in the 66.6- and 83-μ tubes, where the data extend to lower shear stresses, d/R is nearly constant at low τ_w, but increases at the higher shear stresses. The values of d/R are larger for the 40-μ tubes than for the 66.6- and 83-μ tubes, where they are practically

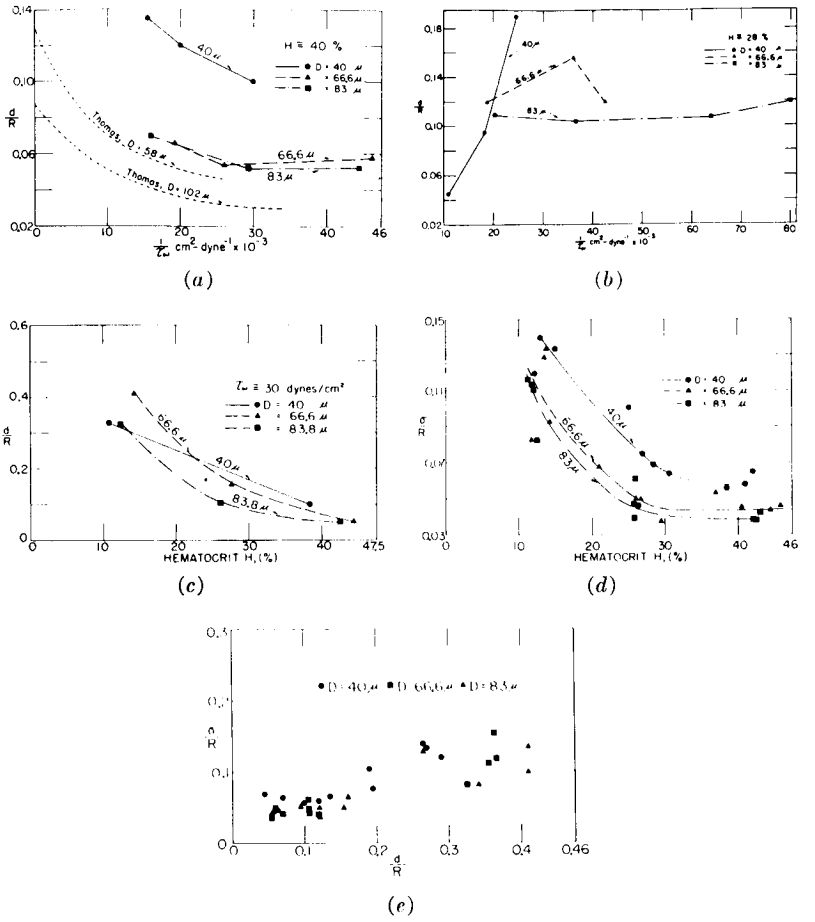

Fig. 6. Peripheral layer characteristics. Here d/R is the ratio of peripheral layer thickness to tube radius and σ/R is the corresponding ratio for the standard deviation of d.

identical (but the difference in the dimensions of these two tubes may be too small to have an appreciable effect within the precision of the measurements).

The effect of shear stress on the peripheral layer was not manifest in similar data for the horizontal tubes. Except for the insensitivity of d/R to tube size in the larger tubes, the shape of the d/R vs. τ_w

relation for the 40% concentration is essentially in agreement with Thomas' predictions[14] based on an analysis of Kümin pressure-flow data for ox blood. Two of Thomas' curves for two different tube diameters are replotted in Figure 6*a;* given the different blood types used in the two sets of experiments not much significance should, however, be attributed to comparisons of numerical values.

At a lower concentration ($H \simeq 28\%$, Fig. 6*b*), the influence of shear stress on d/R is less uniform. In the 40-μ tubes d/R decreases rapidly with increases in τ_w, whereas in the two wider tubes it remains practically constant. Lower reliance must be placed on these data than on those of Figure 6*a* because of the greater fluctuations of the peripheral layer at the lower concentrations and also because of the limited shear stress range of the 40-μ observations. However, the intimation of a trend at lower hematocrits different from that at the higher ones cannot be overlooked. A decrease in the peripheral layer thickness with increasing flow rate would actually be in agreement with the observations of Segré and Silberberg, in dilute suspensions of inert spheres.[19]

The strong dependence on hematocrit of the peripheral layer dimensions, already observed in the horizontal tubes, is confirmed by the data of Figure 6*c* for an arbitrarily selected but approximately constant value of τ_w. The predominance of the concentration effects over the shear stress effects is accentuated by the smaller scale used for the ordinates in this plot. The anomalous d/R value for the 40-μ tubes at low hematocrit was also observed in the horizontal tubes[4] but is of dubious significance; as pointed out before, the boundary of the peripheral layer becomes a progressively less meaningful concept when concentration decreases. This is emphasized by Figure 6*d* where the standard deviation σ of the peripheral layer thickness d is plotted (as a fraction of R) versus hematocrit for a number of tests. The ratio σ/R increases rapidly in all tubes as concentration decreases, decreases with tube size, and is relatively unaffected by wall shear stress, at least within the range of values in the diagram.

The data of Figure 6*d* give a quantitative measure of the degree of idealization involved in the concept of a peripheral layer as a clear-cut region with a well-defined margin. At the larger hematocrits ($H \sim 40\%$) the peripheral layer has a standard deviation equal to approximately one-half its thickness. As the hematocrit decreases, σ becomes a progressively less important fraction of d, so that, para-

doxically, at the lower concentration the errors involved in the idealized picture of the peripheral layer may actually be smaller. The relationship between σ and d is summarized in Figure 6*e*.

VELOCITY PROFILES AND PROFILE VISCOSITIES

In Figures 7 to 9 the velocity profiles and the corresponding profile viscosity distributions are shown for a series of tests at high hematocrit (~40%) in the 40- and 66.6-μ tubes and for some representative tests at lower hematocrit in the same tubes. Data for the 83-μ tubes

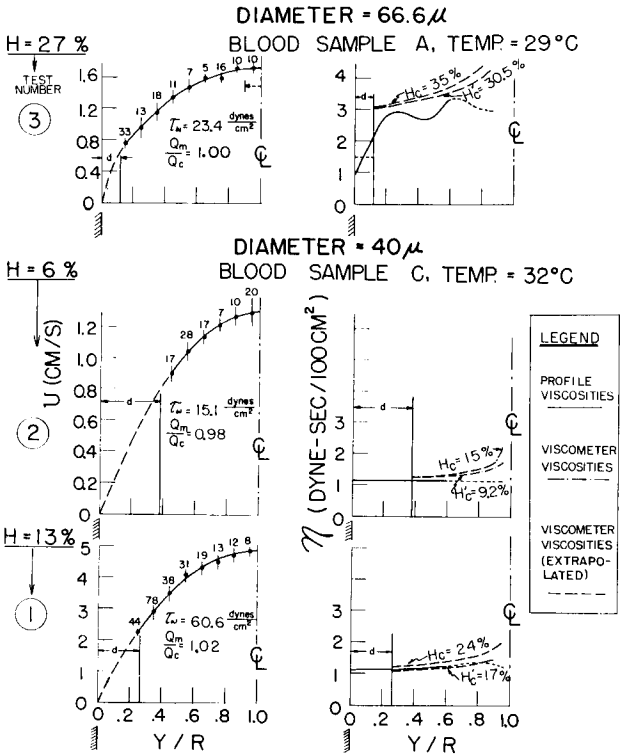

Fig. 7. Velocity and viscosity profiles for representative tests at low and medium concentration. Here U is the average velocity at a radial station y/R, η the viscosity, d the peripheral layer thickness, Q_M the volumetrically measured flow rate, Q_c the flow rate computed by integrating the velocity profile; other details in the text.

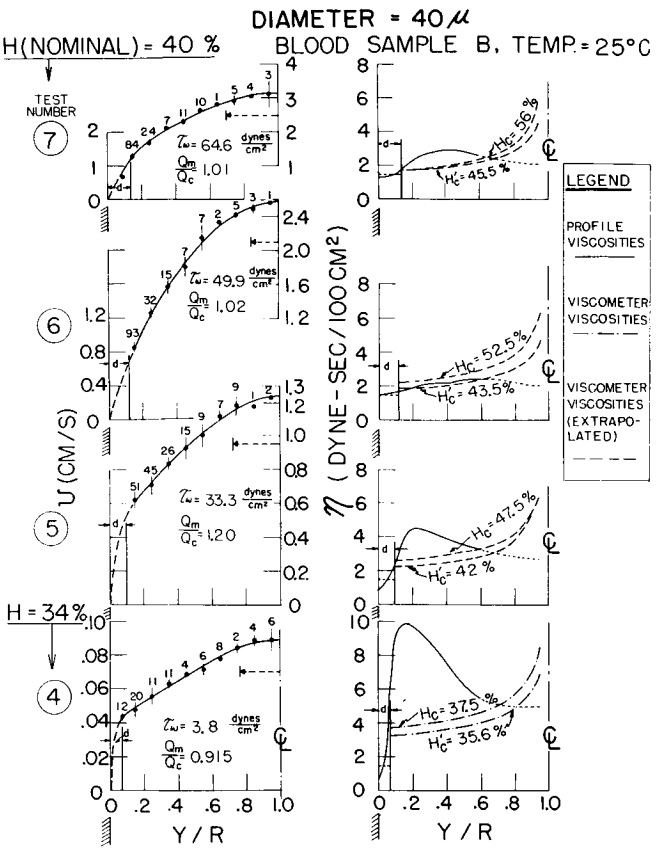

Fig. 8. Velocity and viscosity profiles for representative tests at higher concentration in the 40-μ tube.

are not shown, as at higher concentrations the cells could be distinguished only in the region close to the wall.

The velocity profiles were obtained by averaging the velocities of individual cells within laminae $0.1y/R$ wide, as previously described;[4] the results, given the axial symmetry of the flow, have been plotted over half the diameter only. The number and the segment associated with each point give respectively the number of measurements of which the point is the average and their standard deviation; the region near the centerline where the greater optical density makes the

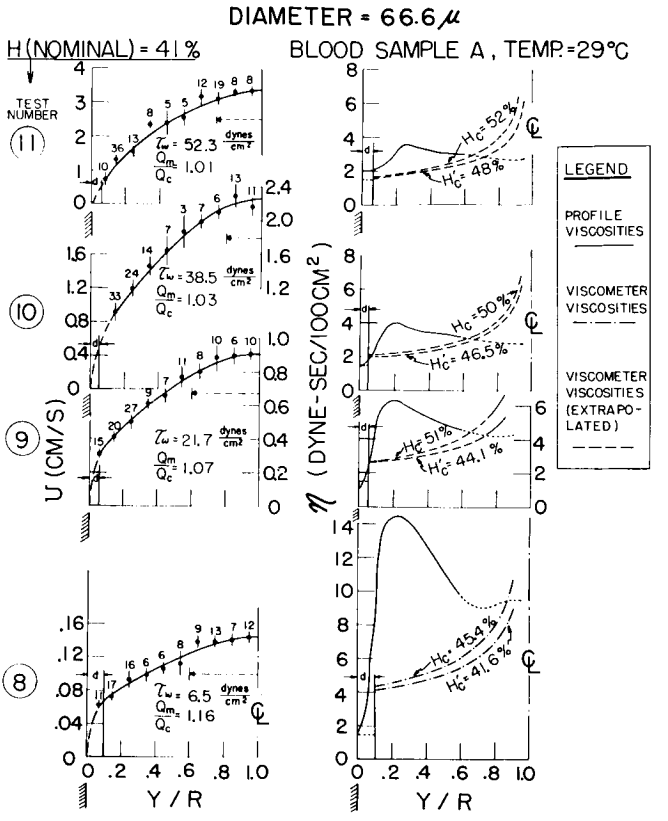

Fig. 9. Velocity and viscosity profiles for representative tests at higher concentration in the 66.6-μ tube.

measurements more difficult and prone to error is indicated by the dashed segment issuing from the centerline, and the region near the wall where there were no cells to define the profiles is shown dashed. Comparisons of the profiles on a dimensionless basis confirm and strengthen the observations with the horizontal tubes of a tendency toward Newtonian conditions with increases in flow rate and decreases in concentration. In particular the effect of flow rate is more marked, at least at the higher concentrations, than for the horizontal tubes. The effect of tube size appears to be more complex, but in general none of these effects can be satisfactorily described in terms

of a single shape factor such as the degree of bluntness (a fact not clearly evident from the analyses for the horizontal tubes).

The shape of the velocity profiles for the two tests at very low flow rate in Figures 8 and 9 (tests 4 and 8) suggests strongly the possibility of slip at the wall (an occurrence, it should be noted, which would not affect the shape of the viscosity profiles discussed next, except in the immediate neighborhood of the boundary).

The profile viscosities were computed for points $0.05y/R$ apart, as the ratios of the shear stress τ to the slope du/dy of the velocity profile. The symmetry of the average velocity profiles makes rigorously true, for steady flow conditions, the assumption of a linear variation of τ from the value τ_w at the wall to zero at the centerline, which was only an approximation for the asymmetric profiles in the horizontal tubes. Instantaneously, of course, given the microscopic unsteadiness of the flow, exemplified by Figure 5, τ will vary, and so will du/dy and the viscosity.

The meaning of the profile viscosities in the narrow tubes of the sizes studied here has been discussed before,[4] but will be briefly elaborated. Since each cell moves with the velocity of its center of gravity, the velocity is constant across the cell; however, the assumption of a stepwise average velocity profile for the whole flow (the sigma phenomenon approach[20]) would be unrealistic because the cells do not proceed in orderly columns.[2,4] (Such a profile would be almost as unrealistic as the assumption of a stepwise profile for turbulent flow on the ground that at each given instant portions of the fluid involved in an "eddy" have essentially a common translatory motion.) A stepwise profile would be even less realistic if flow were to occur inside a cell. Thus, except when a cell occupies a very large portion of the cross section, a continuous average velocity profile appears to be justified, and consequently so does the concept that the ratios of the shear stress to the slope of the average profile are a measure of the effectiveness of momentum transfer across the radius.

Comparisons of the profile viscosities with viscosities based on the assumption of a sharply defined plasma peripheral layer and on the results of constant shear viscometer measurements, as shown in the plots at right in Figures 7 to 9, become therefore meaningful as an indication of the limitations of an idealized picture of the flow. Equally meaningful are comparisons between profile viscosities in a given tube for different flow conditions, since limitations in the con-

cept of profile viscosity are likely to be primarily a function of tube size rather than flow rate.

In the figures, the viscometer viscosities for the core have been computed both for the nominal core concentration $H_c = H \cdot R^2/(R - d)^2$, (where H is the reservoir concentration) and for a core concentration corrected for the dynamic effect, $H_c' = H \cdot Q_c/Q_c'$ (where Q_c is the flow rate for the whole cross section and Q_c' the flow rate for the core, both computed by integration of the velocity profiles). The core viscosities were computed by interpolating to the required concentrations the n and K indexes of Figure 2, and by assuming the power-law rheological equation to be valid also outside the range of shear stresses investigated in the viscometer; the plasma viscosities were assumed to remain constant at all shear stresses.

Because of the errors and uncertainties inherent in the determination of the profile viscosities (stemming both from the limitations of the average velocity profiles and from the large possible error in the determination of their slopes in the region near the axis where the profile viscosities are shown dashed), significance can be attributed only to the most pronounced features of the profiles, namely: (*1*) at low concentrations (e.g., tests 1 and 2), the absence of any pronounced change at the nominal boundary of the peripheral layer; (*2*) at the higher concentrations, a gradual increase in viscosity from the periphery to the core; and (*3*) also, at the higher concentrations, the occurrence of viscosity peaks in the core close to the nominal boundary of the peripheral layer, peaks of increasing magnitude as the shear stress in a given tube decreases. The occurrence of the peaks appears to be strongly affected by concentration (as indicated, e.g., by a comparison of test 3, which at a hematocrit $H \sim 30\%$ shows essentially no peak, and test 10 ($H \sim 40\%$), which shows a peak).

DISCUSSION OF THE PROFILE VISCOSITIES

The absence of an abrupt demarcation between the nominal boundary of the peripheral layer and the core in the profile viscosity distributions is in agreement with visual observations of the peripheral layer and with the large standard deviations of its dimensions (Fig. 6*d*), confirming the oversimplification involved in two-fluid rheological models which postulate a clear-cut plasma region and a core containing all the cells. In addition to causing the gradual increase in viscosity (i.e., in momentum exchange) from the layer to the core, the presence

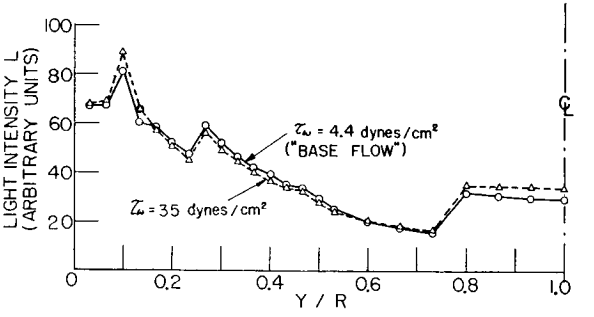

Fig. 10. Taylor's light intensity measurements (190-μ tube).

of cells in the peripheral layer must also be physiologically significant, as already noted, in promoting the exchange of heat and matter within the layer.

The most striking feature of the profile viscosity plots is the occurrence of the off-centerline peaks at high hematocrits, a feature that cannot be predicted from a two-region rheological model and the results of uniform shear viscometry (which, as shown in Figs. 7 to 9, would always lead one to expect a monotonic increase in viscosity from the wall to the centerline). In the flow of blood, the only previous indication of this phenomenon appears to have occurred in studies with horizontal tubes, where, however, the occurrence of sedimentation made the results open to doubt.[4]

An indirect study which may suggest the phenomenon but is of difficult interpretation, is Taylor's measurement of the light transmitted by suspensions of red cells in isotonic saline flowing through a capillary 190 μ in diameter (see Fig. 10).[5] Optical density changes were found to be induced by progressive increases in flow rate above a very small reference value. Near the wall and the centerline the density decreased, while in an intermediate region it increased less or even decreased, a pattern attributed by Taylor to the combined effects of inward accumulation of cells from the peripheral layer and of increased cell orientation in the centerline region. The pattern of optical density changes is supported by similar findings of Bayliss[6] in tubes comparable in size to those of the present study.

Vejlens, in 1959,[21] on the strength of much earlier (1938) experimental results with isolated spheres in laminar flow, proposed a differ-

ent interpretation of the flow-induced changes in optical density, suggesting that they could be the result of a concentration gradient caused by drift of the cells not only from the periphery but also from the core of the flow toward the intermediate radial region (a phenomenon recently investigated in greater detail by Segré and Silberberg[19]).

A feature on which Taylor did not elaborate is the abrupt increase in light intensity L exhibited near the centerline by his data for a 24% concentration (the only concentration for which actual values of the light intensity were presented). If the light intensity measurements were to lend themselves to a straightforward interpretation, such a feature could indicate the occurrence of lower concentrations near the centerline even at the very low flow used as a reference condition ($\tau_w = 4.4$ dynes/cm.^{2}).

The combination of centripetal and centrifugal drift of the erythrocytes suggested by Vejlens offers also the most immediate explanation of the viscosity peaks observed in the present experiments. If such were indeed the cause of the peaks, their decrease in magnitude at the higher flow rates and their tendency to occur much closer to the wall than to the centerline would be in qualitative agreement with the observations of Segré and Silberberg of concentration effects in the flow of dilute suspensions of inert spheres.[19]

The increase with shear stress of the peripheral layer in blood at high hematocrits (Fig. 6*a*) would, however, indicate that unlike the case of the sphere suspensions where the layer decreases, the decrease in magnitude of the peaks is caused by a spreading of the cells only inward toward the centerline rather than toward the wall.

In the absence of direct confirmation through concentration measurements, and in view of the uncertainties associated with the determination as well as to a certain extent with the precise meaning of the viscosity distributions, the deduction of the occurrence of an off-center concentration peak must still be considered only tentative. It is doubtful whether any further and more precise information on the characteristics of the flow in the core can be achieved without recourse to novel methods, because with the determination of the broad characteristics of the profile viscosity distributions the present experimental technique appears to have reached the limit of its potential.

Investigation supported by Research Grant He-05557 of the National Heart Institute, National Institutes of Health, U. S. Public Health Service.

References

1. Merrill, E. W., E. R. Gilliland, G. Cokelet, H. Hsin, and R. E. Wells, Jr., *J. Appl. Physiol.*, **18**, 255 (1963).
2. Bloch, E. H., *Am. J. Anat.*, **110**, 125 (1962).
3. Copley, A. L., and P. H. Staple, *Biorheol.*, **1**, 3 (1962).
4. Bugliarello, G., and J. W. Hayden, *Trans. Soc. Rheology*, **7**, 209 (1963).
5. Taylor, M., *Australian J. Exptl. Biol. Med. Sci.*, **33**, 1 (1955).
6. Bayliss, L. E., *J. Physiol.*, **149**, 593 (1959).
7. Vejlens, G., *Acta Pathol. Microbiol. Scand.*, Suppl. 33 (1938).
8. Bugliarello, G., and J. W. Hayden, *Science*, **138**, 981 (1962).
9. Fåhraeus, R., and T. Lindquist, *Am. J. Physiol.*, **96**, 562 (1931).
10. Bloch, E. H., *Trans. Soc. Rheology*, **7**, 9 (1963).
11. Harding, F., and M. H. Knisely, *Angiology*, **9**, 317 (1958).
12. Knisely, N. H., *Trans. Soc. Rheology*, **6**, 13 (1962).
13. Haynes, R. H., *Trans. Soc. Rheology*, **7**, 19 (1963).
14. Thomas, H. W., *Biorheol.*, **1**, 41 (1962).
15. Haynes, R. H., *Am. J. Physiol.*, **198**, 1193 (1960).
16. Charm, S., and G. S. Kurland, *Am. J. Physiol.*, **203**, 417 (1962).
17. Prothero, J., and A. C. Burton, *Biophys. J.*, **1**, 565 (1961).
18. Cokelet, G. R., E. W. Merrill, E. R. Gilliland, H. Shin, A. Britten, and R. E. Wells, *Trans. Soc. Rheology*, **7**, 303 (1963).
19. Segré, G., and A. Silberberg, *J. Fluid Mech.*, **14**, 136 (1962).
20. Dix, F. J., and G. W. Scott Blair, *J. Appl. Phys.*, **11**, 574 (1940).
21. Vejlens, G., in *Flow Properties of Blood and Other Biological Systems*, A. L. Copley and G. Stainsby, eds., Pergamon Press, New York–Oxford, 1960, p. 61.

Synopsis

14588

In a previous exploratory study of the detailed characteristics of blood flow in small horizontal glass capillaries, viscosity profiles obtained from experimentally determined velocity profiles for the cross section frequently exhibited a peak at an intermediate position between the centerline and the wall. In the present study, the phenomenon as well as the other detailed features of the flow are investigated in greater detail, with capillaries in the vertical position (so as to eliminate the asymmetries in the flow pattern caused by sedimentation, which had been shown to affect significantly the results in the horizontal layout). The flow of human blood of varying hematocrits in capillaries 40 to 83 μ in diameter, was observed over a range of flow rates by high-speed microcinematography at 3000 frames/sec. and a magnification of approximately 970×. Velocity profiles determined by averaging over the whole useful duration of the film the velocities of erythrocytes observed at fixed radial stations were nearly axisymmetrical in all cases, as expected from the absence of settling effects. Almost instantaneous velocity profiles corresponding to observation periods of a few milliseconds were, however, asymmetric and could deviate appreciably from the average profiles. The axial symmetry of the average flow permitted the more accurate measurement of the peripheral layer characteristics (thickness, standard deviation), and, from

cont. on next page

them, the determination of the average concentration in the cell-rich core of the flow. From such concentration and from the results of uniform shear viscometric measurements, viscosity profiles were computed for the cross section of the flow and compared with experimental viscosity profiles obtained directly by differentiation of the average velocity profiles. The experimental viscosity profiles concur with the peripheral layer measurements in indicating the gradual nature of the transition from the peripheral layer to the core—a characteristic that may have physiological significance also in terms of other exchange processes in the peripheral layer. Although the determination of the experimental viscosity profiles is subject to a considerable degree of uncertainty, the occurrence of off-center viscosity peaks at the higher hematocrits, particularly at the lower flow rates, may be suggestive of a concentration effect caused by a concurrent drift of the erythrocytes from the walls and the centerline toward an intermediate radial position.

Author

N67 14589

The Difference in Circulation Times Between Erythrocytes and Plasma *in vivo*

S. ROWLANDS* and A. C. GROOM, *St. Mary's Hospital Medical School, London, England,* and H. W. THOMAS, *National Institute for Research in Dairying, Shinfield, Reading, England*

A now well-established method of measuring the output of blood from the heart in man or in animals consists of injecting a dye or a radioactive substance into a vein and then, over the course of the next minute or so, measuring its concentration in arterial blood as a function of time after it has passed through and become mixed in the heart.[1] The usual shape of the arterial dilution curve, as it is called, is shown in Figure 1. The flow of blood is determined from the integrated area of this curve. It was in the course of measurements of this type that the difference in circulation times between red cells and plasma first became evident to us—as a by-product of the experiments. The curve shown was produced as follows: Arterial blood flowed by a tube from the carotid artery of an anaesthetized cat through a scintillation counter and back into the animal so that none was lost.[2] The output of the counter went to a rate meter and then to a recorder. In Figure 1 the deflection in the lower trace indicates the instant at which red cells labeled with P^{32} were injected into the superior vena cava, the middle trace marks off seconds and the upper trace is the output of the rate meter. Seven years ago we were using this method for measuring the cardiac output in cats and for reasons which are irrelevant to the present paper we were giving, alternately, injections of red cells labeled with radioactive phosphorus and of serum albumin labeled with radioactive iodine. Now when the traces of one particular experiment were examined it was obvious, without any measurement, that the time between the injection and the beginning of the record was varying alternately with the type of injection.

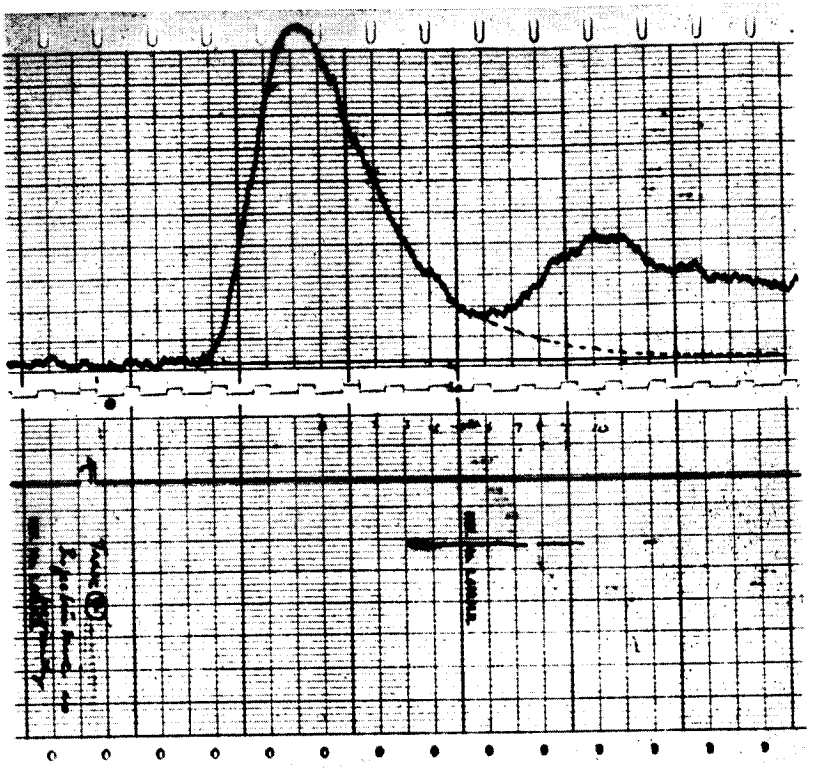

Fig. 1. Usual shape of the arterial dilution curve.

In Figure 2 traces 7 and 8 out of a series of 10 in one experiment are superimposed with the injection points and base lines coincident. Curve 7 is subsequent to an injection of albumin and curve 8 of red cells. Note that the two curves intersect twice. We examined all our curves and noted the elapsed time between injection and the start of the curve (minimum pulmonary circulation times), between injection and the peak of the curve (modal pulmonary circulation time), and between start of the curve and the point of onset of recirculation (minimum total circulation time). The results derived from six experiments[3] are as follows.

The overall mean of the ratios of circulation times (albumin/corpuscles) derived from six experiments:

1. Minimum pulmonary circulation time 1.060 ± 0.016 (S.E. mean) ($t = 3.75$; $P < 0.001$).

2. Modal pulmonary circulation time 1.092 ± 0.010 (S.E. mean) ($t = 9.0$; $P < 0.001$).

3. Total circulation time 1.162 ± 0.018 (S.E. mean) ($t = 8.9$; $P < 0.001$).

It can be seen that the overall mean ratios of the circulation times of minimum pulmonary, modal pulmonary, and minimum total all differ significantly from unity. The probability of the effect being due to chance is less than one in a thousand. These results were published six years ago and they have not to the authors' knowledge been called in question. They have aroused interest but the subject remained a sideline to the authors who did not attempt a serious study until the last twelve months.

In the meantime we redesigned our apparatus to record arterial dilution curves of radiophosphorus and radioiodine simultaneously.[4] Instead of the arterial blood passing through one scintillation counter as previously, there were now two scintillation counters side by side and the blood passed between them. The two counters and the associated electrical circuits were so designed that one detected radiophosphorus-labeled cells only and the other radioiodine-labeled albumin only. The two traces shown in Figure 3 were recorded simultaneously on the two channels of one recorder after

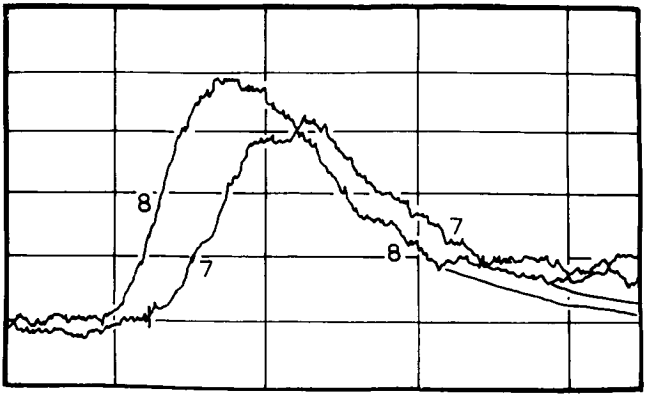

Fig. 2. Recordings 7 (radioactive albumin) and 8 (radioactive red cells) out of a series of 10, superimposed with their injection points and base lines coincident.

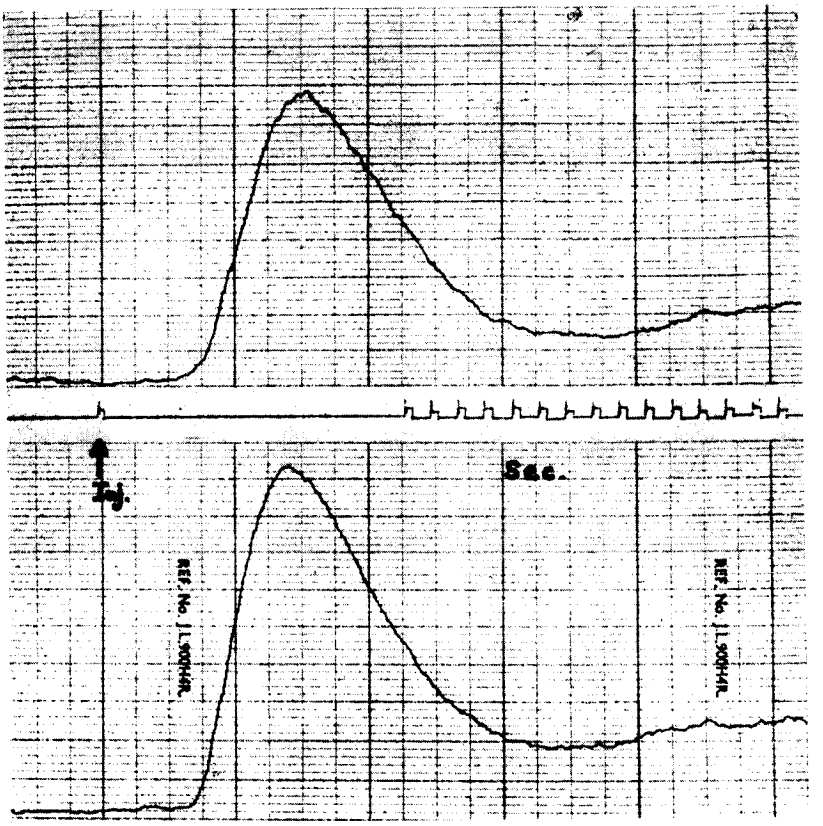

Fig. 3. Showing two traces recorded simultaneously on the two channels of one recorder after labeled cells and labeled albumin had been injected together.

labeled cells and labeled albumin had been injected together. The red cell curve is the lower of the two traces. The displacement in time of the two curves is more obvious when they are superimposed (Fig. 4). Many scores of traces of this sort were recorded, and in all the red cells were ahead.

Before we discuss the figures derived from these new traces it would be well to consider possible causes of this phenomenon. Of course, instrumental errors have been eliminated; all the radioactivity subsequent to its injection can be accounted for, and ancillary measurements during the experiments on arterial and venous pressure, heart

Fig. 4. Superimposed curves.

rate, pulse shape, blood volume and hematocrit show that the procedures did not alter the circulation in any relevant way. A separate series of experiments[5] in which P^{32} and I^{131} were injected in the form of inorganic ions as well as bound to red cells and to albumin suggests that the cells were getting ahead of all the molecular constituents of blood and not just the protein, so the phenomenon is unlikely to result from a delay in protein with respect to the other constituents of blood.

How then did cells and fluid become separated in time? The most likely explanation is the axial streaming of corpuscles. Fåhraeus,[6] more than thirty years ago, published evidence of a reduction in the value of the hematocrit when blood flowed through tubes of bore less than 1 mm. His interpretation was that in such circumstances the corpuscles congregated along the axis of the tube where the fluid velocity is greatest.

This concept of axial streaming has had a ready acceptance among physiologists; more so, perhaps, than past evidence would seem to justify. To our knowledge the original experiments have not been repeated by other workers but now one of us has been able to confirm them in another way.[7] How can this axial streaming come about? Whitmore[8] has pointed out that for a flowing suspension of spheres the center of a sphere cannot approach the boundary wall closer than a distance equal to its radius. He goes on to prove that, in consequence, the concentration of the suspension is reduced close to the boundary wall. Hence, the concentration will be higher in the faster moving central stream of flow in a tube. Simi-

lar considerations probably apply to a suspension of red cells but analysis of the problem is complicated by their nonspherical shape and the fact that they are easily deformable. Goldsmith and Mason[9] have shown that flexible fibers and globules of oil migrate centrally in tube flow but that rigid bodies do not, or at least to a much lesser extent. This radially directed hydrodynamic force may also be experienced by the flexible red cell but it must be remembered that Goldsmith and Mason's experiments were done at slow rates with very dilute suspensions.

If axial streaming occurs then a relatively cell-free layer of plasma ought to be seen near the wall in transparent tubes. Many workers claim to have seen this and to have measured its width. Others with seemingly valid techniques have been disappointed. Quite recently Bloch[10] has reported experiments in which he photographs the flow of blood in small vessels *in vivo* through a microscope with a ciné camera at normal and at ultra-high frame speeds. At ultra-high speed the paths of the individual cells can be followed on his films and he has shown that the flow, far from being laminar, as was widely accepted, is highly complex; one could describe it as turbulent from the microscopic point of view although the Reynolds number is far below the critical value. Red cells were seen in close proximity to the wall of the vessels, apparently touching the wall or 1 to 2 μ from it. When Bloch took motion pictures at a normal frame speed the peripheral plasma layer was, in his words, a sharply defined clear zone; but at high frame speed the layer was seen in detail and found to extend in an irregular manner toward the center of the vessel, its configuration changing every few milliseconds. Such spaces were interspersed by red cells which slid against the wall and a few milliseconds later another irregular plasma layer recurred. Bloch goes on to suggest that the peripheral layer, as usually seen, is an optical artefact and this is supported to a large extent by Bayliss' recent work.[11]

Nevertheless we are compelled to accept the existence of some form of axial streaming. It is difficult to see how else, apart from slip at the wall, one can explain the readily observed decrease in viscosity of blood when measured in smaller and smaller tubes. Another consequence of axial streaming is a reduction of concentration of the cells when blood flows through small tubes[6] and Thomas has verified that this does occur.[7] There is no likely explanation of this finding apart from axial migration of cells.

in circulation times or even whether another explanation ought to be sought? The answer is "no." Turning back to consider the results of the new experiments where the traces were recorded simultaneously, the most accurate measurement is the position of the peaks of the distributions. From 50 measurements we find a mean ratio of circulation times of 1.074 when P^{32} is in the cells and a value which does not differ significantly from unity when P^{32} is in the suspending fluid. But from the point of view of deciding between the contributions of axial streaming and molecular diffusion the *mean* circulation times are of much more value. This is difficult to measure *in vivo* because the indicators begin to come round again before they have completely cleared from the first circulation. A correction can be made, but in fact the errors of measuring mean circulation times *in vivo* are greater than the differences in times. Moreover in the animal we are dealing with a complex system of branching elastic tubes of varying diameter and differing lengths. The shapes of our arterial dilution curves depend much more on the distribution in length of the branching tubes than on the dispersion of the fluid within them. Unpublished work by Thomas indicates that by whatever mechanism red cells get ahead, the shapes of our arterial dilution curves will always be similar and only the displacement of the curves is of significance. Moreover the complex paths of red cells demonstrated by Bloch's high speed photography[10] complicate the application of Taylor's mathematical analysis[12] which assumes laminar flow.

For these reasons we have left our *in vivo* studies temporarily and gone on to study the same phenomenon in rigid tubes, a report of which will be given later.[14] There is a good precedent for doing this. Poiseuille, the father of biorheology, was forced to abandon the animal for the rigid tube.

References

1. Kinsman, J. M., J. W. Moore, and W. F. Hamilton, *Am. J. Physiol.*, **89**, 322 (1929).
2. Groom, A. C., and S. Rowlands, *Phys. Med. Biol.*, **3**, 138 (1958).
3. Groom, A. C., W. B. Morris, and S. Rowlands, *J. Physiol.*, **136**, 218 (1957).
4. Groom, A. C., P. W. Roberts, S. Rowlands, and H. W. Thomas, *J. Physiol.*, **146**, 17P (1959).
5. Rowlands, S., *J. Exptl. Med. Sci., Calcutta*, **3**, 77 (1959).
6. Fåhraeus, R., *Physiol. Rev.*, **9**, 241 (1929).

There is however the possibility that some of the apparent difference in circulation times between cells and plasma might be merely a manifestation of molecular diffusion. Taylor[12] has presented a theoretical analysis and some confirmatory data has been supplied by Bourdillon[13] of the distribution downstream of a diffusible substance initially at a uniform concentration in a short length of a tube carrying a slowly flowing liquid. In the absence of diffusion the substance would subsequently lie between two parallel elongating paraboloids[13] which represent the variation of longitudinal displacement over the cross section of the tube. But diffusion across the surfaces of the paraboloids reduces the longitudinal dispersion of the diffusible substance expected purely on the basis of laminar flow. Moreover the greater the diffusion coefficient the less will be the longitudinal dispersion of the dissolved substance. Taylor also showed that in certain circumstances the distribution along the axis of the tube would be symmetrical and that the mean of the distribution would move with the mean flow of fluid. A consequence of this effect is that if two substances of differing diffusion constants were introduced together into a liquid flowing slowly down a tube then at a sampling point downstream (*a*) the substance which diffused more slowly would begin to be detected first, (*b*) the maximum concentrations of the two substances would be achieved simultaneously, (*c*) the substance which diffused more slowly would clear more slowly than the other, and (*d*) the mean of the distributions along the tube of both substances would move together at the mean flow of the fluid.

Now from the point of view of the animal experiments presented earlier in this paper the diffusion rate of albumin will be much greater than that of red cells (but this distinction may be obscured by the complex irregular movement of red cells observed by Bloch[10]). The effects of diffusion alone would therefore be that labeled red cells should arrive first, the peaks of the labeled red cell and labeled albumin curves should coincide, and the albumin should disappear first. Irrespective of diffusion constants, the mean velocities of the two moieties should be identical. This is not what we find in our animals. Certainly the red cells arrive first, but their peak is before that of albumin and they clear first (Figs. 2–4).

Can one decide, on the basis of these experiments, the relative contribution of axial streaming and molecular diffusion to differences

7. Thomas, H. W., *Lab. Pract.*, **10**, 771 (1961).
8. Maude, A. D., and R. L. Whitmore, *Brit. J. Appl. Phys.*, **7**, 98 (1956).
9. Goldsmith, H. L., and S. G. Mason, *Nature*, **190**, 1095 (1961).
10. Bloch, E. H., *Am. J. Anat.*, **110**, 125 (1962).
11. Bayliss, L. E., *J. Physiol.*, **149**, 593 (1959).
12. Taylor, Sir G. I., *Proc. Roy. Soc. (London)*, **A219**, 186 (1953).
13. Bourdillon, J., *Experientia*, **18**, 530 (1962).
14. Thomas, H. W., R. J. French, A. C. Groom, and S. Rowlands, in *Proc. 4th Intern. Congr. Rheology, Part 4*, A. L. Copley, ed., Interscience, New York, 1965.

Synopsis

14589

Evidence is presented that *in vivo* the red cells have a shorter circulation time than the fluid constituents of blood. A mechanism which would explain the shorter circulation time of cells is discussed.

Author

N67 14590

The Flow of Red Cell Suspensions through Narrow Tubes: The (Extracorporeal) Determination of the Difference in Mean Velocities of Red Cells and Their Suspending Phase

H. W. THOMAS,* *National Institute for Research in Dairying, Shinfield, Reading, England, and* R. J. FRENCH, A. C. GROOM, and S. ROWLANDS, *Physics Department, St. Mary's Hospital Medical School, London, England*

It is now well established that if red cell suspensions are observed flowing through fine glass capillary tubes of diameters decreasing from about 500 to 25 μ, one obtains increasing values of apparent fluidity[1-4] and decreasing values for the "dynamic concentration" (i.e., the mean concentration of red cells within the tube).[5,6] Similar results have been obtained with other particulate suspensions.[7]

From observations on man and on experimental animals we know that there are significant apparent differences in the concentration of red cells in various parts of the circulatory bed[8] and that there are significant differences in the mean circulating velocities of the red cells and of the plasma.[9-15]

A number of mechanisms have been cited in explanation of one or more of these various phenomena. The presence of slip at the tube wall could lead to an increased apparent fluidity, but not to a reduced dynamic concentration or to a difference in circulation times of red cells and their suspending phase. The presence, *in vivo*, of an extravascular space into which labeled proteins can, but labeled red cells cannot, penetrate[8] could account for a variation of the red cell concentration within the circulatory bed, and even for a difference in circulation times, provided one may assume in addition

PRECEDING PAGE BLANK NOT FILMED.

that the labeled protein moves, not only out of the circulation but also returns in an interval of time comparable to that of the observation of the clearance curve. A difference in the diffusion constants of two labeled components should not lead to a difference in the mean velocities but because of the difference in the shape of the clearance curves[16,17] there could result an apparent difference in cases where the clearance of the labeled material is incompletely observed.

There remains however one mechanism that can account for all phenomena, at least on a qualitative basis. It is known that particles of a suspension flowing through a cylindrical tube are subject to radial migrations. Particle centers are in any case excluded mechanically from the surface of the tube, and this leads to an effective reduced concentration of particles at the tube wall.[18] In addition there are centripetal forces of hydrodynamic origin which lead to further radial migrations of particles.[19,20] Particles move therefore from regions of lower fluid velocity to regions of higher velocity. From continuity considerations this must result in both a difference in mean velocities of the particles and the suspending phase, and in a reduction in the dynamic concentration.[21,22] A reduction in concentration of particles at the wall where the shear stress is greatest must also result in an increase in apparent fluidity.[21,22]

It has been shown that in the case of a dilute suspension with negligible particle interactions, particles in the neighborhood of the axis of flow are subject to centrifugal forces.[19] Since it is desired here to consider concentrated suspensions of red cells, the effects of these forces are probably severely attenuated by particle interactions. Furthermore, due to the peculiar geometry of flow through a tube, changes in concentration at the tube wall are expected to cause much greater changes in the apparent fluidity, dynamic concentration, and in the difference in circulating velocities of cells and their suspending phase, than would similar changes at the tube axis. When wall effects are observed, the change in apparent fluidity is almost invariably an increase, the change in dynamic concentration a decrease, and the cells invariably lead the suspending phase. Hence the centripetal effects are dominant and for the purpose of the present discussion, we are effectively neglecting any centrifugal effects.

Although the radial migration of red cells could account for all observations qualitatively, it must be stressed that this does not

necessarily mean that none of the other cited mechanisms is also involved. The quantitative data available is still too sparse, and insufficiently precise to decide the relative contributions. However, the radial migrations of red cells must be a very significant, if not the most important, mechanism involved. It alone can account for the *in vitro* observation of the reduced dynamic concentration of red cells, and it provides the most plausible explanation of the differential circulation observed *in vivo*.

In the light of these considerations, it is therefore important to know whether the red cells have a higher mean velocity than their suspending phase when a red cell suspension flows through a rigid tube under laboratory conditions. The present contribution describes an experiment in which such an effect seems to have been demonstrated.

One must recognize here that such a demonstration may be implicit in the recently published work of Bourdillon.[17] His flow

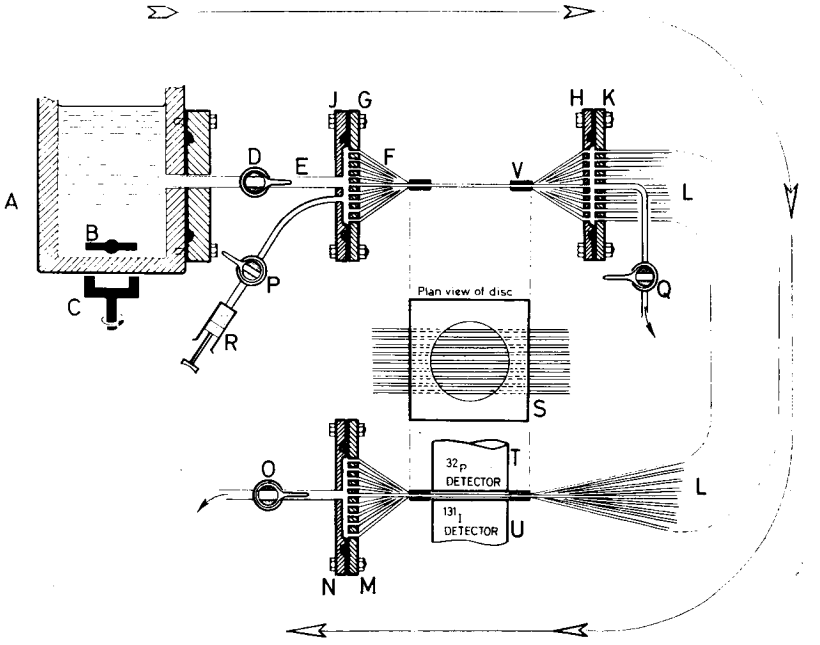

Fig. 1. Simplified diagram of apparatus (not to scale).

conditions were certainly different from the authors', and since he did not observe the complete clearance of his labeled material, it is extremely difficult to distinguish an apparent separation of cells and their suspending phase due to diffusion effects, from a real separation. The authors also feel that their method is much more convenient and accurate than the effluent sampling followed by chemical analysis which Bourdillon had to employ.

Preliminary work has been confined to artificial circulatory beds constructed by connecting in parallel several lengths of nylon tubing of about 200 μ bore. Figure 1 is a schematic diagram of the most satisfactory system the authors have been able to evolve to the present date. The perspex reservoir A contains a suspension of bovine red cells in physiologically normal saline containing 1% weight/volume of crystallized bovine albumin. This is maintained in a thoroughly mixed condition by a magnetic stirring index B. A suitable air pressure is applied to the reservoir in order to drive the suspension through the normally open stopcock D, the flexible connection E, the two sections F and L of the fine bore tubing and the normally open stopcock O, either to waste, or to a graduated pipette for a flow measurement. Section F consists of 26 pieces of the 200-μ bore nylon tubing of length 15 cm., and section L has the same number of pieces each 150 cm. long. These tubes are cemented into perspex discs G, H, K, M which are then bolted together against O-ring rubber seals.

For an experimental determination of the differential circulation of the cells and their suspending phase, the suspension contained within the initial short section F of the fine tubes is replaced by a similar suspension containing radioactive isotope tracers. Red cells are labeled with radioactive phosphorus, ^{32}P, and the suspending phase either with ^{32}P in the form of inorganic phosphate ion, or radioactive iodine, ^{131}I, in the form of inorganic iodide ion or human serum albumin. For this step, stopcocks D and O are closed, and stopcocks P and Q are opened. The inactive material in the section F is washed out by the labeled material injected from the tuberculin syringe R. The radioactivity in the section F (volume 0.14 ml.) has actually been monitored during this procedure, and the injection of 0.5 ml. is sufficient to ensure that the inactive material is effectively washed out. Stopcocks P and Q are then closed, O opened, and the flow of suspension from the reservoir restored by opening the stop-

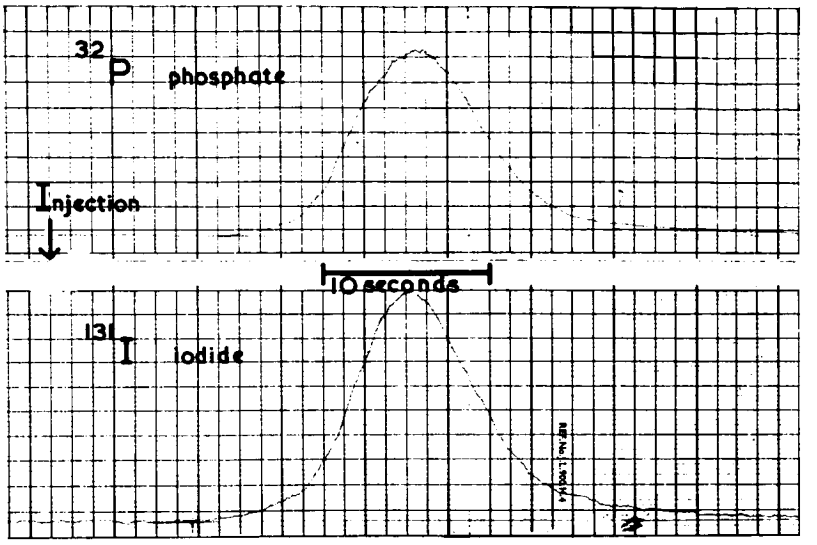

Fig. 2. Clearance curves obtained when injected suspension contained unlabeled red cells + ^{32}P phosphate + ^{131}I iodide. Stress at tube wall τ is 50 dynes cm.$^{-2}$, concentration c is 0.31 $\pm$ 0.08.

cock D. The labeled suspension is cleared from the initial section F, and is detected at the point S, a mean distance of 129 cm. downstream, by means of two scintillation crystal detectors T and U, one sensitive to the β-radiation of the ^{32}P isotope and one sensitive to the γ-radiation of the ^{131}I isotope. The detectors and their associated electronic equipment have been described elsewhere[23] and are essentially the same as those used in the *in vivo* experiments described by Rowlands et al.[15] Preliminary injections with dye have been used to insure that the point S is one of equal transit time for all tubes. It was necessary to make considerable longitudinal adjustments to the tubes with respect to the disc S. This disc not only retains these adjustments, but also acts as a spacer between the two detectors. A similar disc V is used when the counters are placed at that point in order to determine the initial activity of the injected material.

Figures 2 to 4 show the three kinds of clearance curves that have been obtained, depending on the nature of the labeling of the injected suspension.

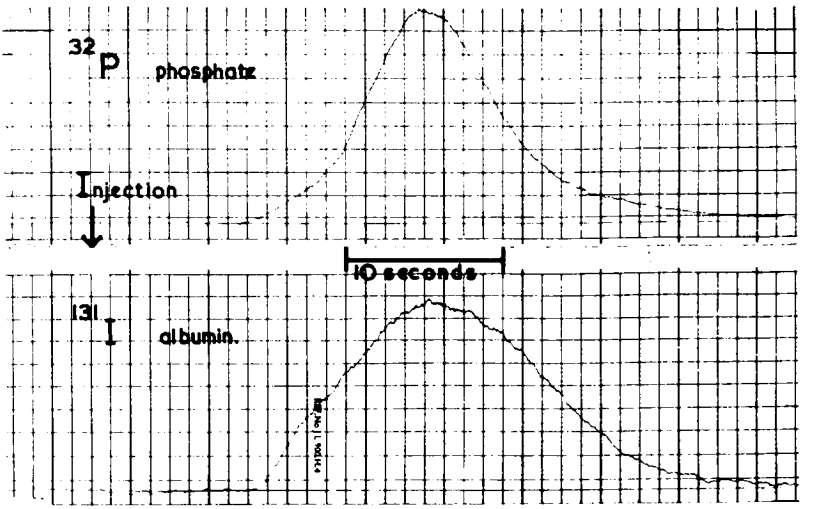

Fig. 3. Clearance curves obtained when injected suspension contained unlabeled red cells + ^{32}P + ^{131}I albumin. Stress at tube wall τ is 50 dynes cm.$^{-2}$, concentration c is 0.36 ± 0.04.

In the case of Figure 2 the suspension contained both the ^{32}P and the ^{131}I label in the form of inorganic ion. The iodide peak seems to be slightly ahead but there is no obvious difference in the mean circulation times, both curves being fairly symmetrical about the same point in time. The phosphate curve is noticeably broader than the iodide curve, but this is perfectly consistent with a difference in diffusion constants of the two ions and the theoretical solution given by Taylor for the dispersion of diffusing solutes in a fluid flowing through a cylindrical vessel.[16]

Figure 3 shows the clearance curves obtained when the injected suspension is labeled with ^{32}P isotope in the form of inorganic phosphate, and ^{131}I isotope as human serum albumin. The curves are again fairly symmetric, with no obvious difference in mean circulation times. The phosphate curve, in contrast to the result of Figure 2, is now noticeably narrower than the albumin curve, again consistent with the difference in diffusion constants and Taylor's theory.[16]

Now when the ^{32}P label is included within the red cells and the ^{131}I label as albumin, curves as shown in Figure 4 are obtained. There are marked differences. The red cell curve rises much more

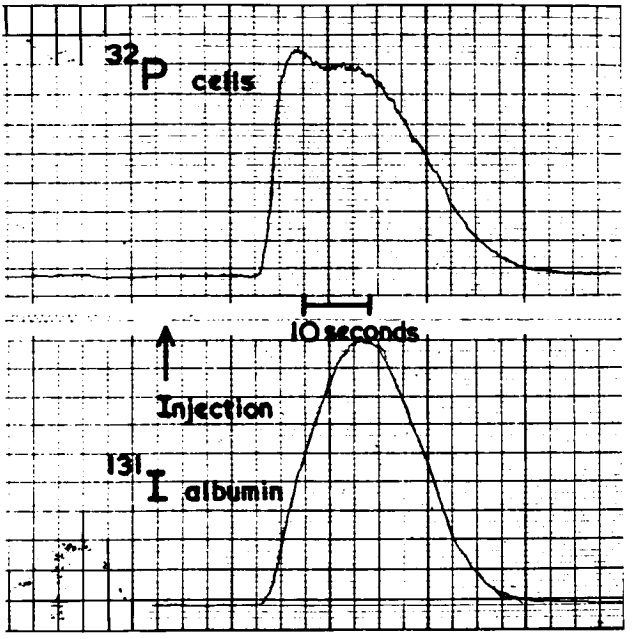

Fig. 4. Clearance curves obtained when injected suspension contained ^{32}P labeled cells + ^{131}I albumin. Stress at tube wall τ is 50 dynes cm.$^{-1}$, concentration c is 0.38 ± 0.02.

rapidly to a peak value which is appreciably ahead of the peak in the albumin curve. There is a suggestion of a secondary peak in the red cell curve coincident in time with the albumin peak. This could be accounted for by the slight interference (1 to 2%) between the two detector channels, and the possible slight loss of radioactive phosphorus from the cells. In other experiments this secondary peak has been hardly noticeable, and sometimes a little more exaggerated.

One should note that there is a mechanism in addition to molecular diffusion to be considered in any discussion of the shapes of the clearance curves. As the annuli of the fluid are sheared with respect to one another, red cells come into frequent collisions, they tumble and roll and follow paths which are not parallel to the tube walls. This is clear from ciné-film data on the flow of blood.[24–26] Since the volume vacated by a red cell is partially replaced by the suspending

TABLE I
Results for Measured Ratios of Mean Circulation Times

Nature of radioactive labeling of injected suspension	Red cell sample	Red cell concn.	Shear stress at tube wall, dynes cm.$^{-2}$	Ratio mean circulation times $^{131}I/^{32}P$		
				Mean value	No. of observations	Standard deviation
Control Runs						
^{32}P phosphate + ^{131}I iodide (soln. in saline injected into saline)	—	—	20	0.99_3	5	0.00_9
^{32}P phosphate + ^{131}I albumin	A	0.36 ± 0.04	50	1.01_6	9	0.00_7
^{32}P phosphate + ^{131}I iodide	A	0.31 ± 0.08	50	0.98_9	8	0.00_8
Experimental Runs						
^{32}P cells + ^{131}I albumin	A	0.38 ± 0.02	50	1.08_7	6	0.00_5
^{32}P cells + ^{131}I albumin	B	0.40 ± 0.03	25–100	1.04_6	5	0.00_3
^{32}P cells + ^{131}I albumin	B	0.19 ± 0.02	12.5–100	1.04_0	8	0.01_2
Calculated Values						
	—	0.40	50	1.07_6	—	—

phase, small elements of the latter will also follow irregular paths. The net result is an additional effective diffusion of any radioactive label, be it enclosed within red cells or not. It is anticipated that this effective diffusion is a function of the shear rate. It may also be a function of the radial position, since the shear annuli become less convex as one moves out from the center toward the wall. The authors know of no satisfying term for this phenomenon. The term "shear-induced collision diffusion" is descriptive but rather cumbersome.

The clearance curves, such as those of Figures 2 to 4 have been analyzed further by means of a mechanical integrator in order to determine accurate values of the mean circulation times. These times are taken as the distances from the points of injection to the centers of moment of the areas under the curves. Some results for the ratio (mean circulation time ^{131}I)/(mean circulation time ^{32}P) are presented in Table I.

The first row shows the results of a preliminary test of the instrumentation when ^{32}P labeled phosphate and ^{131}I labeled iodide contained in a saline solution was injected into a saline solution. The ratio of circulation times was insignificantly different from zero.

The control measurement where inorganic phosphate and albumin were used to label the injected suspension gave a mean value for the ratio of 1.01_6, slightly but significantly higher than unity. The take-up of appreciable phosphate by the red cells could give such a result, but it is not felt that the nature of the take-up mechanism allows this explanation. For the other type of control measurement, a mean value for the ratio slightly but significantly below unity was obtained. This is understandable since it is known that appreciable concentrations of iodide can be taken up rapidly by red cells. The experimental runs indicate a large difference in mean circulation times of red cells and their suspending phase. The source of the discrepancy between the results of the two experiments at approximately 0.4 concentration is as yet untraced, but the authors nurse the suspicion that variations in deformability of various samples of red cells could be a serious factor. The last row in Table I gives a theoretical result based on the experimental results of Kümin[2] and calculation according to the methods and equations given in refs. 21 and 22. With all the uncertainties involved, both experimental

and theoretical, the figure does not warrant too serious a comment, but is included for interest. The few preliminary results at the present level of precision do not indicate any significant changes in the ratio of circulation times with the variation of shear stress at the tube wall over the range of 12.5 to 100 dynes cm.$^{-2}$, or with variation of concentration of red cells within the range 0.2 to 0.4. More experimental results are required before reliable quantitative conclusions can be drawn.

Differences in diffusion constants can be ruled out as a cause of this difference in circulation times. The control runs, obtained under similar hydrodynamic conditions to the experimental runs, are in qualitative accord with Taylor's theory.[16] One must also note that at the end of a recorded curve, the clearance of the active material is virtually complete so that one obtains a measure of the true mean circulation time, which Taylor predicts should be independent of the diffusion constant, and which fact is essentially confirmed by our control runs. It is presumed that electrical effects due to a charge being built up on the nylon wall of the tube can be ignored, since the cells are suspended in a strongly ionized solution.

The authors believe therefore that a difference in mean circulation times of red cells and their suspending phase has been established, and that the effect probably can only be explained by radial migrations of red cells. An interesting possibility would be to deduce the true concentration profile of red cells from the shape of the clearance curves such as those of Figure 4. The present data are of course inadequate, and there are forbidding problems of analysis to be overcome.

This work was assisted by a grant from the St. Mary's Hospital Endowment Fund. One of us (H. W. T.) is supported by a U.S. Public Health Service Grant HE 05732 from the National Heart Institute. We are grateful to Professor Holder and Mr. Bialokoz of the Engineering Laboratory, Oxford University, for the loan of a mechanical integrator.

References

1. Fåhraeus, R., and T. Lindqvist, *Am. J. Physiol.*, **96**, 562 (1931).
2. Kümin, K., Inaugural dissertation, Univ. of Bern, 1949.
3. Bayliss, L. E., in *Deformation and Flow in Biological Systems*, A. Frey-Wyssling, ed., North Holland, Amsterdam, 1952.
4. Haynes, R. H., and A. C. Burton, *Am. J. Physiol.*, **197**, 943 (1959).
5. Fåhraeus, R., *Klin. Wochschr.*, **7**, 100 (1928); *Physiol. Rev.*, **9**, 241 (1929).

6. Thomas, H. W., *J. Lab. Practice*, **10**, 771 (1961).
7. Scott Blair, G. W., *Rheol. Acta.*, **1**, 123 (1958).
8. Lawson, H. C., in *Handbook of Physiology*, Vol. 1, Sec. 2, Am. Physiological Soc., Washington, 1962.
9. Dow, P., P. F. Hahn, and W. F. Hamilton, *Am. J. Physiol.*, **147**, 493 (1946).
10. Freis, E. D., J. R. Stanton, and C. P. Emerson, *Am. J. Physiol.*, **157**, 153 (1949).
11. Groom, A. C., W. B. Morris, and S. Rowlands, *J. Physiol.*, **136**, 218 (1957).
12. Lilienfield, L. S., J. C. Rose, and F. A. Porfido, *Circulation Res.*, **5**, 64 (1957).
13. Ochwadt, O., *Arch. Ges. Physiol.*, **256**, 112 (1957).
14. Crane, G. C., J. E. Holloway, R. Adams, and I. C. Woodward, *Intern. J. Appl. Radiation Isotopes*, **7**, 23 (1959).
15. Rowlands, S., A. C. Groom, and H. W. Thomas, in *Proc. 4th Intern. Congr. Rheology, Part 4*, A. L. Copley, ed., Interscience, New York, 1965, p. 371.
16. Taylor, G. I., *Proc. Roy. Soc. (London)*, **A219**, 186 (1953).
17. Bourdillon, J., *Experientia*, **18**, 530 (1962); **19**, 250 (1963).
18. Maude, A. D., and R. L. Whitmore, *Brit. J. Appl. Phys.*, **7**, 98 (1956).
19. Segré, G., and A. Silberberg, *Nature*, **189**, 209 (1961); *J. Fluid Mech.*, **14**, 115, 136 (1962).
20. Goldsmith, H. L., and S. G. Mason, *Nature*, **190**, 1095 (1961); *J. Colloid Sci.*, **17**, 448 (1962).
21. Bayliss, L. E., in *Handbook of Physiology*, Vol. 1, Sec. 2, Am. Physiological Soc., Washington, 1962.
22. Thomas, H. W., *J. Biorheol.*, **1**, 41 (1962).
23. Groom, A. C., P. W. Roberts, S. Rowlands, and H. W. Thomas, *J. Physiol.*, **146**, 17–18P (1959).
24. Bugliarello, G., and J. W. Hayden, *Trans. Soc. Rheology*, **7**, 209 (1963).
25. Bloch, E. H., *Am. J. Anatomy*, **110**, 125 (1962).
26. Lutz, B. R., and G. P. Fulton, *Med. Biol. Illustration*, **7**, 26 (1957).

Synopsis

14590

A small but significant difference in the mean circulation times of red cells and plasma flowing through various circulatory beds in experimental animals and in human subjects has been frequently reported in the scientific literature. In order to try and elucidate the mechanism of this phenomenon, simultaneous measurements have been made of the circulation times of radioactive labeled red cells and albumin injected into a red cell suspension flowing through an artificial bed of 26 nylon tubes of 200 μ bore connected in parallel. The observed clearance curves for the labeled red cells and albumin were markedly different, and there was a significant difference in mean circulation times.

author

MEDICAL BIORHEOLOGY

PRECEDING PAGE BLANK NOT FILMED.

Abstract

The Effect of Dietary Fat on Whole Blood and Plasma Viscosity†

S. E. CHARM, *Massachusetts Institute of Technology, Cambridge, Massachusetts,* G. S. KURLAND, *Beth Israel Hospital, Brookline, Massachusetts,* C. TEJADA, *Institute of Nutrition of Central America, Guatemala City, Guatemala,* and W. McCOMIS, *Massachusetts Institute of Technology, Cambridge, Massachusetts*

An examination with a cone and plate viscometer of the viscosity at 230 sec.$^{-1}$ of the blood of 40 medical students before and 3$^1/_2$ hr. after a fatty meal showed no change in blood viscosity although the serum lipids increased.

In 7 separate experiments, no change was found in plasma viscosity as determined by the capillary tube technique although the plasma lipids increased.

From theoretical considerations, it was suggested that in order to detect changes in plasma and whole blood viscosities after a fatty meal, it would be necessary to employ methods of determining viscosity within a 2% error.

Employing the GDM narrow gap viscometer with shear rates as low as 0.1 sec.$^{-1}$, no differences were observed in either plasma or whole blood viscosities even though the plasma lipids increased. The data with the GDM viscometer compared well with that obtained with the cone and plate type.

In 2 cases it was observed with both the Brookfield cone and plate as well as the GDM viscometers that whole blood viscosities *decreased* with an increase in plasma lipids. The plasma viscosities were unchanged. This decrease in whole blood viscosities may have been caused by the effect of the plasma lipids on the cell aggregate forces. In one study, an increase in whole blood viscosity was noted 3$^1/_2$ hr. after ingestion of 500 ml. of cream. Theoretical analysis of this case

†Published in the *J. Appl. Physiology,* **18** (Nov. 1963).

PRECEDING PAGE BLANK NOT FILMED.

indicates that the increase in suspended bodies may not account for the entire increase in viscosity. Sedimentation data were used to evaluate the structure of blood according to a model described for kaolin suspensions by Michaels and Bolger. No difference in sedimentation was noted in this case $3^1/_2$ hr. after the fatty meal. The calculated "pore size" of the suspension was 57 μ before and after the meal.

The effect of long term nutritional status on blood viscosity was studied in Guatemala on 3 different socio-economic groups with different nutritional environments. No significant difference in blood viscosity adjusted for hematocrit was noted in the 3 groups in spite of a wide range of fat intake.

N67 14591

Rheological Disturbances and Their Treatment in Clinical Surgery

BENGT ZEDERFELDT,* *Department of Surgery, University of Göteborg, Göteborg, Sweden*

In his communication, Gelin[1] has shown that the viscosity of red cell suspensions is dependent on the rate of flow, hematocrit, vehicle viscosity, and further on a "viscosity plus factor," which is dynamically dependent on the other factors.

This means, that already in normal conditions blood streaming in venules and veins has a higher viscosity than the same blood streaming in arteries and arterioles.

Following tissue injury, changes occur in the blood and plasma with an increase of large and asymmetrical protein molecules in the plasma and with aggregation of formed elements. These changes in plasma composition will markedly influence the viscosity of whole blood and plasma at all rates of flow but most markedly at slow flow rates. A vicious circle will occur with increased suspension viscosity, decreased rate of flow, and thereby further increase of the viscosity. This results in stagnation of cells in postcapillary venules and in a decreased venous return to the heart, which will all impair the nutritional blood flow through the tissues. Figure 1 shows the microcirculatory pattern in the bulbar conjunctiva of a patient with a femoral fracture. Note the aggregation of cells and the stasis of cells in the postcapillary venules. The effects of changes in the physical properties of blood can be studied experimentally on animals.[2] Critical experiments designed to demonstrate the pathophysiological significance of such flow disturbances must meet the requirements of reversibility. For that reason increase of whole blood viscosity with intravascular aggregation has been induced experimentally by infusion of solutions with large and viscidizing molecules, such as fibrinogen, gelatin, and high viscous dextran. Low viscous dextran has been

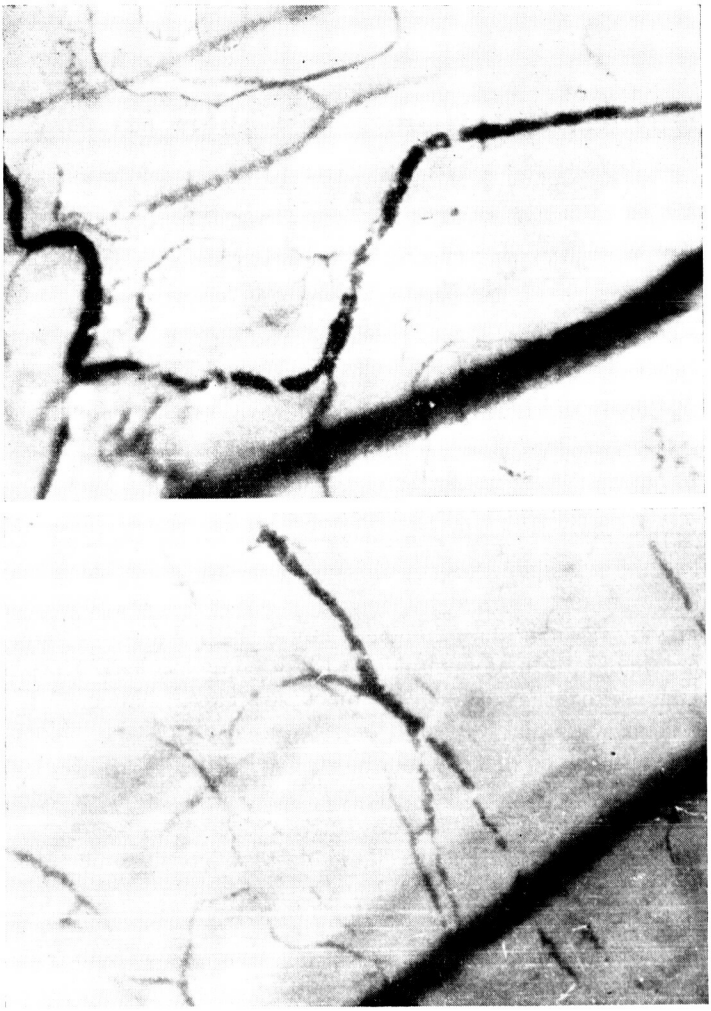

Fig. 1. Microcirculatory pattern in the bulbar conjunctiva in a patient with femoral fracture.

shown to be able to reverse such disturbances. Thus, one and the same substance can be used both to produce and to reverse aggregation only by varying its molecular properties.

The influence of induced changes in the physical properties of blood

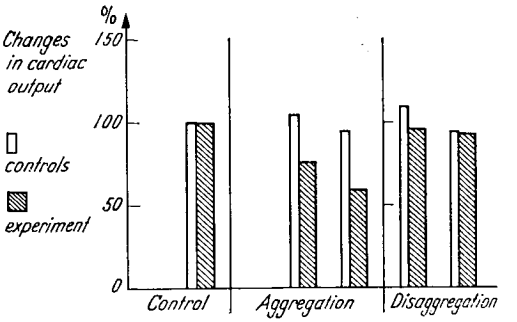

Fig. 2. Changes in cardiac output during induced intravascular aggregation and subsequent disaggregation.

with intravascular aggregation of blood cells has been investigated by determinations of cardiac output, peripheral resistance, hind limb blood flow, renal and hepatic blood flow. These experiments demonstrate that despite a slight increase in blood pressure and in blood volume the administration of high viscous dextran is followed by a decrease in flow whereas subsequent infusion of low viscous dextran is followed by an increase in flow to pre-experimental values without any further rise in blood pressure. Figure 2 shows cardiac output during a period of induced intravascular aggregation and during disaggregation.

The influence of such flow disturbances on tissue nutrition has been studied in experiments concerning gas exchange and metabolic response[3] and further on the rate of wound healing[4] and on microscopic examinations of organs from animals subjected to standardized trauma or to administration of high viscous dextran. It has been found that during a period of induced aggregation the oxygen consumption as well as the carbon dioxide elimination decrease, while no significant metabolic disturbances appeared in the arterial blood (Fig. 3). When low viscous dextran is infused to reverse this aggregation oxygen consumption and carbon dioxide elimination increase again, a transient acidosis appears with lowering of pH and increase in pCO_2 and lactic acid. This indicates that during the period of aggregation an accumulation of acid material in the tissues occurs and that the acid material cannot be released until the flow is improved. Further it was found that changes in the capillary flow due to changes in the physical properties of blood cause a decrease of the

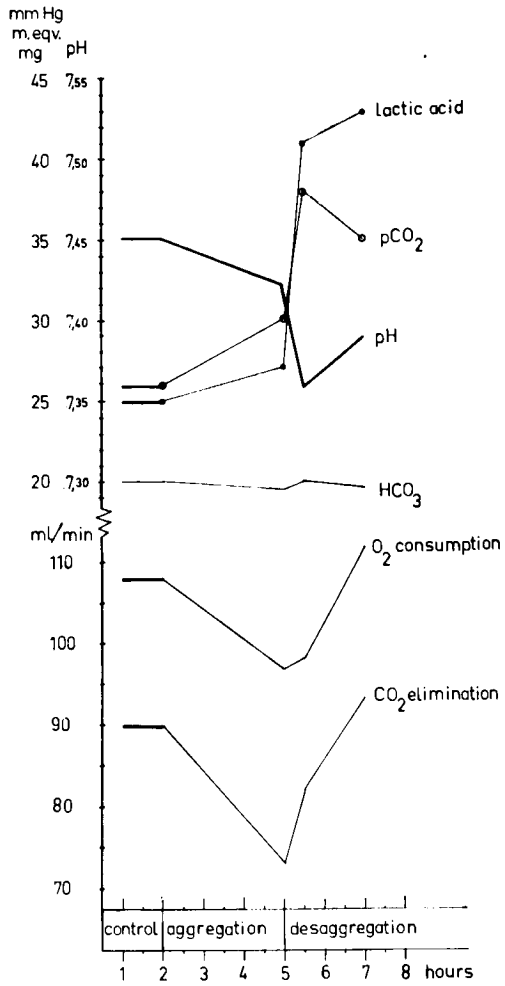

Fig. 3. Metabolic changes in response to induced aggregation and subsequent disaggregation. Mean values from five dogs.

rate of wound healing (Fig. 4) and cause microscopic changes in parenchymatous organs, especially the liver, the kidney, and the myocardium.

It is thus obvious that changes in the microcirculation due to altered physical properties of the blood have a pronounced pathophys-

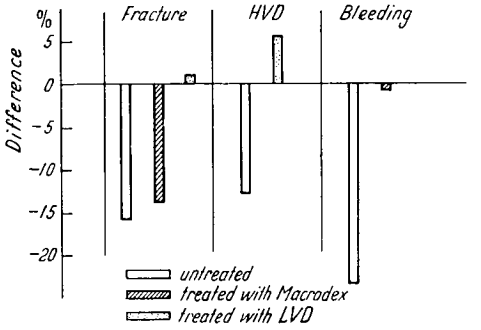

Fig. 4. Changes in the rate of wound healing after induced intravascular aggregation and subsequent disaggregation.

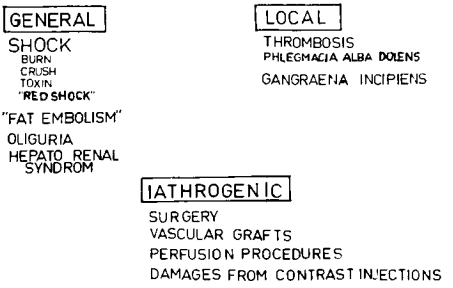

Fig. 5. Diagram showing indications for the clinical use of low viscous dextran.

iological significance. Therefore these changes call for an effective counteraction. Experimental and clinical studies have shown that this can be afforded by infusion of low viscous dextran which lowers the viscosity of whole blood, especially at low rates of shear. The indications for treatment with low viscous dextran in the clinic are shortly to increase the perfusion of tissues with blood when this perfusion is decreased by rheological causes. Figure 5 shows the indications for the use of low viscous dextran in the clinic. Some of these indications will be illustrated with case reports. Figure 6 shows a case of burn injury where a man had a 40% burned area. To the right are viscosity data of whole blood and to the left are determinations of perfusion pressure, flow through the leg, and calculated peripheral resistance. Curve *A* to the right represents the blood viscosity four hours after the injury. It is evident that the viscosity

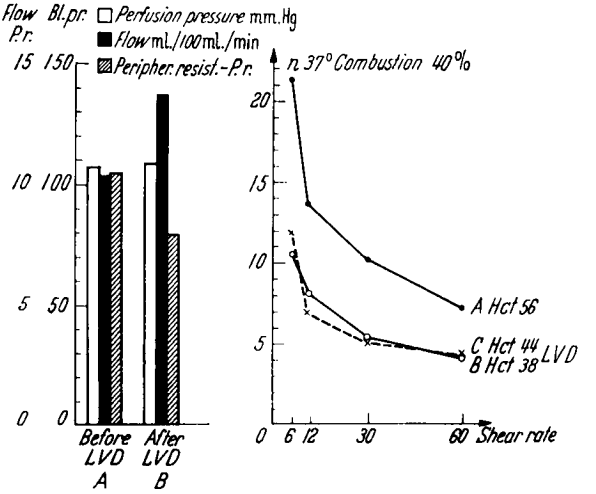

Fig. 6. Viscosity and flow data from a patient with 40% burned area before and after treatment with low viscous dextran.

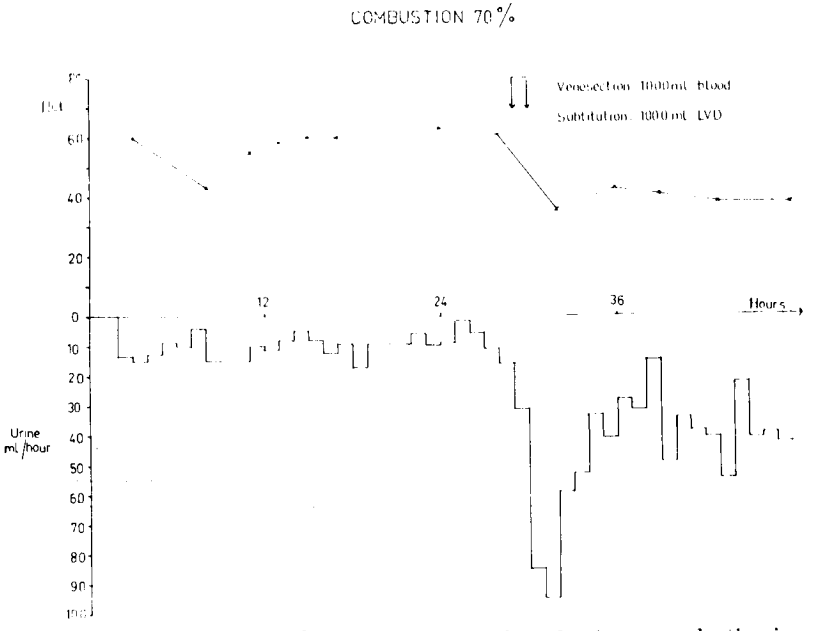

Fig. 7. Effect of low viscous dextran on hemotocrit and urinary production in a patient with 70% burned area.

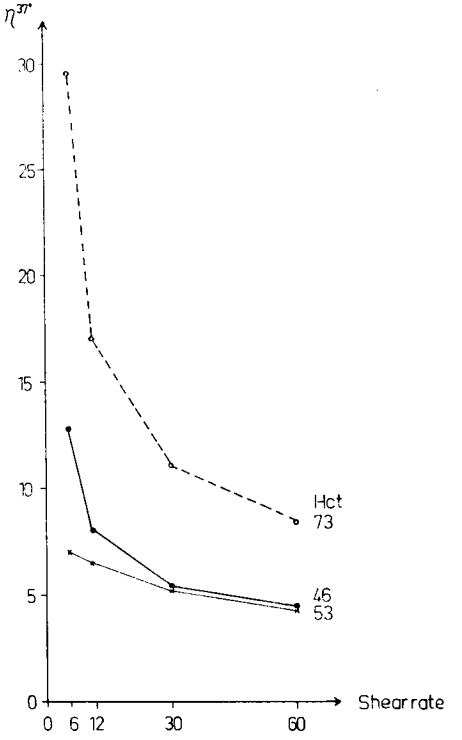

Fig. 8. Viscosity data from same patient as Fig. 7.

of whole blood is significantly elevated at all rates of shear, but most markedly at low shear rate. The viscosity values are about double that of normal blood. To the left is seen that with a perfusion pressure of 100 mm. of mercury the flow was about 10 ml./100 ml. tissue/minute. After this the patient was given 1000 ml. of low viscous dextran intravenously. Curve *B* represents the viscosity of whole blood one hour after the end of the infusion. At this time the viscosity of whole blood is about normal and it can be seen to the left that with unchanged perfusion pressure flow has increased by 40% up to 14 ml./100 ml. tissue/minute and that at the same time the calculated peripheral resistance has decreased by about 40%. Lastly, curve *C* represents whole blood viscosity 24 hr. later during continuous infusion of Rheomacrodex. It is obvious that the infusion of low viscous dextran increases the peripheral circulation by decreasing

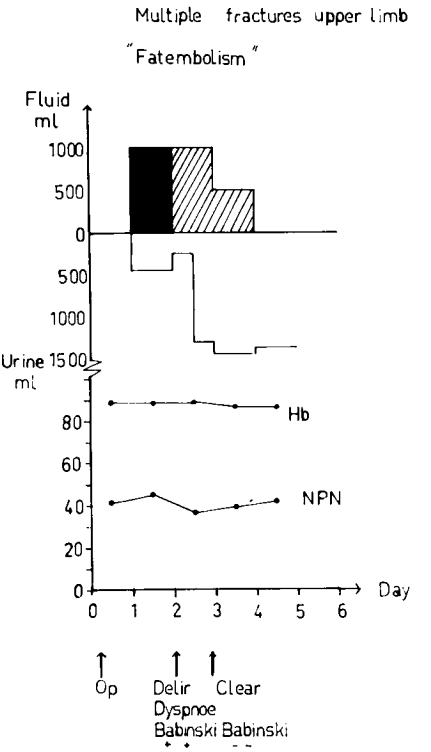

Fig. 9. Case of "fat embolism." Results of treatment with low viscous dextran.

the peripheral resistance. To illustrate these changes in a more pronounced case, the following two figures give data from a man with a 70% burned area.

He was first treated with blood and plasma and during this treatment became anuric (Fig. 7). At this time he had the highest viscosity of whole blood the author has seen (Fig. 8). He was subjected to venesection of 1000 ml. of blood and substitution of this volume by low viscous dextran. The viscosity of whole blood normalized and the patient immediately responded with a large urine excretion.

Fat emboli are a regular finding following crush injuries even if the neurologic signs are infrequent. Recent studies[5] have shown that the process of fat embolization is due to changes in the physical state of

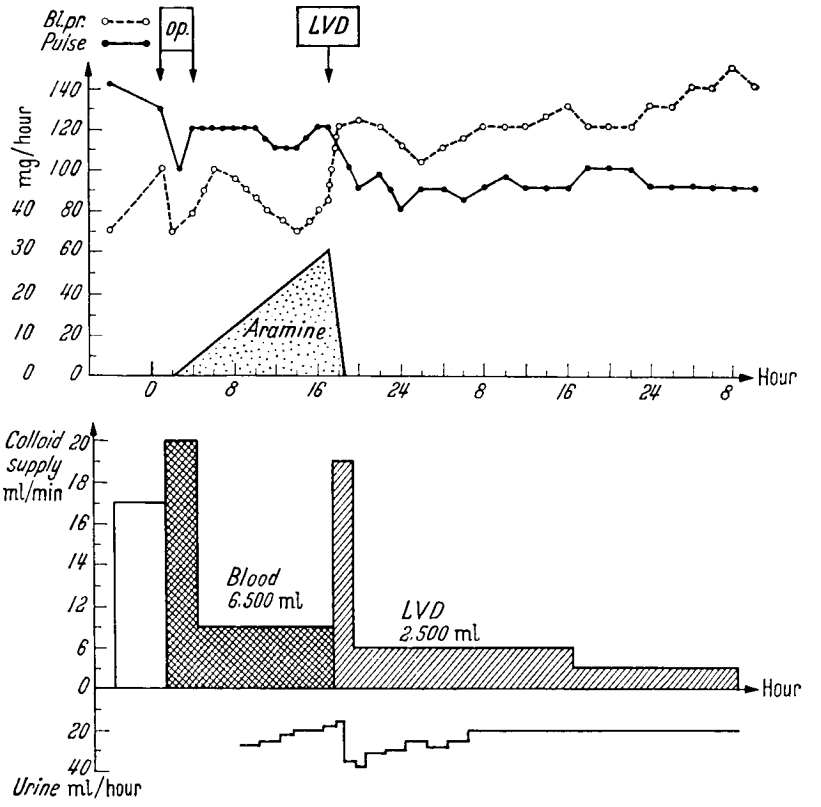

Fig. 10. Case of toxic shock. Result of treatment with low viscous dextran.

blood fat and is initiated by the injured tissue. The period for formation of fat emboli seems to end during the first day of injury. The clinical symptoms of fat embolism, however, usually do not appear until two or more days after injury, thus when further embolization of fat no more occurs. At this time, however, there is marked stagnation of aggregated blood cells in the venules. In patients with clinical symptoms of fat embolism the treatment with low viscous dextran was found to reverse aggregation and venular stasis of blood cells, improve respiration, and reverse the neurological sign, which is illustrated in Figure 9. The effect of low viscous dextran should not be ascribed to anact ion on the fat emboli *per se* but to an improvement of the circulation in vessels not occluded by fat emboli.

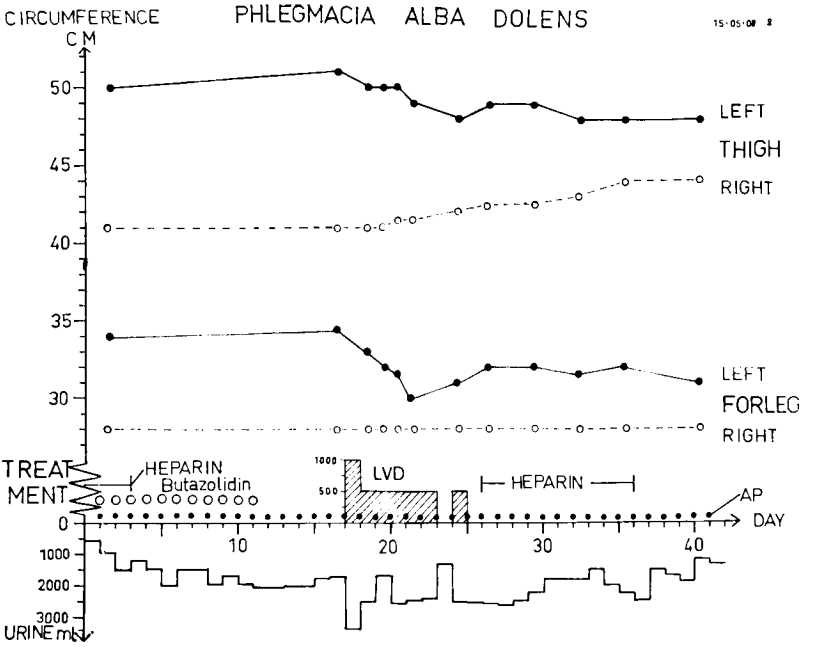

Fig. 11. Case of phlegmasia alba dolens. Result of treatment with low viscous dextran.

Toxic shock from pancreatitis, peritonitis, and intestinal obstruction is followed by marked changes in the flow properties of blood and stagnation of aggregated blood cells. In patients with advanced toxic shock in whom the prognosis was considered poor and in whom transfusion of whole blood, plasma, and Macrodex and the use of vaso pressor agent failed to restore peripheral circulation low viscous dextran was found to reverse shock. Such a case is exemplified in Figure 10. A 52-year-old woman weighing 121 lb. was admitted to the hospital in poor condition with profound shock due to advanced peritonitis from a perforated intestinal tumor. Blood pressure was 70 mm. of mercury and the pulse rate 140. She was treated pre-operatively with Macrodex and blood. During the operation large hemorrhage occurred and the operative and postoperative shock was combatted with whole blood and with Aramine as a vaso pressor agent. Despite massive transfusions of whole blood, increasing doses of Aramine were necessary to maintain blood pressure. During this

period blood volume was determined and showed normal values with plasma volume of 2.7 liters and red cell volume of 1.7 liters with a hematocrit of 44. Microscopy of the bulbar conjunctiva showed the capillary flow to be very poor with standstill of aggregated blood cells in the venules, arteriolo-venular shunting, and marked constriction of the arterioles. The patient was considered to be in irreversible shock. At that time 1000 ml. of low viscous dextran was rapidly infused and was followed by continuous infusion of 2000 ml. of low viscous dextran during two days. Within one hour after the start of low viscous dextran infusion the Aramine administration could be stopped. The response of blood pressure, pulse rate, and urine flow is apparent from the figure. The general condition improved rapidly and the skin changed from cold and cyanotic to warm and red. The capillary flow in the bulbar conjunctiva became faster and the stagnation of cells disappeared. The shock was reversed.

Oliguria with kidney and liver damages, so-called "hepatorenal syndrome," are consequences of shock, injury, transfusions of incompatible blood, and also extracorporeal circulation, hypothermia, and after the use of large doses of intravascular contrast media for angiografic studies. Because of experimental data low viscous dextran has been widely used to prevent and to treat patients with so-called "hepatorenal syndrome" and with lower nephron nephrosis. Figure 11 shows data from a patient with venous thrombosis and phlegmasia alba dolens. This case did not respond at all to the ordinary treatment with heparin, dicumarol, and butazolidin. Infusion of low viscous dextran immediately resulted in better circulation with decrease of the leg circumference.

These case reports illustrate some of the indications for flow promoting therapy[6] with low viscous dextran is the clinic.

References

1. Gelin, L.-E., in *Proc. Intern. 4th Congr. Rheology, Part 4,* A. L. Copley, ed., Interscience, New York, 1965, p. 299.

2. Gelin, L.-E., and B. Zederfeldt, *Acta Chir. Scand.*, **122,** 336 (1961).

3. Bergentz, S.-E., A. Carlsten, L.-E. Gelin, M. Litwin, C. M. Rudenstam, B. Söderholm, and O. Thulesius, *Nord. Med.*, **66,** 1515 (1961).

4. Zederfeldt, B., *Acta Chir. Scand.*, Suppl. 224 (1957).

5. Bergentz, S.-E., *Acta Chir. Scand.*, Suppl. 282 (1961).

6. Bergentz, S.-E., L.-E. Gelin, C. M. Rudenstam, and B Zederfeldt, *Acta Chir. Scand.*, **122,** 343 (1961).

Synopsis

1459 /

It has been shown that tissue injury of different kinds is followed by changes in the physical properties of blood with increased viscosity, especially at low rates of flow, marked changes in the capillary circulation with stagnation in postcapillary vessels as a dominant finding. This leads to decreased venous return and metabolic disturbances. Low viscous dextran is one agent able to improve the capillary blood flow when this flow is decreased by changes in the physical properties of blood and thereby improves the tissue nutrition.

author

Abstract

Rheologic Disturbances and Tumor Spread

CARL-MAGNUS RUDENSTAM, **University of Gothenberg, Gothenberg, Sweden*

Surgery, still the most effective therapy for malignant tumors, runs the risk of tumor spread increases. This spread can be explained by increased liberation of tumor cells into the blood stream because of the manipulation of the tumor during operation. The surgical trauma as such may in itself increase the risk of development of metastases. Earlier experimental investigations have shown an increased take of subcutaneously injected tumor cells in relation to trauma. This increased take has been thought to depend on hormonal effects in connection with the stress reaction induced by the trauma.

Injury is followed by changes in the flow properties of blood with increased blood viscosity and aggregation of the formed elements leading to stagnation of cells in post-capillary venules. After trauma, there is also an increased tendency to thrombus formation and during the first 2–3 hours after a tissue injury, a consumption of coagulation factors occurs in the blood, indicating an intravital coagulation process.

If tumor cells are circulating in the blood, it is probable that the post-traumatic changes in the rheology of blood will influence the distribution of tumor cells and the formation of metastases.

The purpose of this study was to investigate whether changes in the microcirculation influence the frequency of take and the number of metastases in the lungs after intravenous injection of tumor cells. Three different tumor-host systems have been used: (*1*) 20-methylcholantrene induced sarcoma in rats, (*2*) Rous-rat sarcoma, and (*3*) spontaneous mammary carcinoma in C_3H-mice.

It was found that changes in the microcirculation induced by injury or by injection of high viscosity dextran increases the take frequency, especially when a comparatively small number of tumor cells are given, and the number of metastases in the animals with take. The effect of disturbed microcirculation on these two factors is different for different tumors.

In Vivo HEMORHEOLOGY IN MAN AND ANIMALS

N67 14592

Hemorheological Investigations in the "Arterial Spiders" of the Human Skin

HARALD HARDERS,* *First Medical Clinic, University of Hamburg, Hamburg, West Germany*

INTRODUCTION

Intravital hemorheological investigations in the terminal vascular bed of healthy and diseased humans are facing a series of fundamental limitations. In many areas of the body the vessels are covered by the surfaces of skin and mucous membranes and therefore obscured. The areas in which a microvascular system is visible are either highly sensitive to outer influences as the anterior segments of the eye or inaccessible as the fundus oculi. Hemorheological conclusions therefore often had to be drawn from observations with limited experimental interaction. Furthermore, the pressure values encountered in the accessible surfaces are low and the diameter of vessels is small. These circumstances induce technical difficulties and errors of measurement.

It is the purpose of this paper to call attention to certain frequent pathological vascular formations, which from the point of view of hemorheology, present unique features by which they are characterized as a suitable model for the study of blood flow in the terminal vascular bed of man.

The vascular structure in question consists of a star- or spider-shaped arterial branching originating from a central artery which reaches the skin in a right angle from the deeper layer, then surpassing the skin level in its center where it enters peculiar formations, the so-called "subepidermal ampulla." From here the arterial branches in their first portion dive into deeper layers, later emerging as radiary arteries which form a round vascularized area of some millimeters up to some centimeters diameter. In the periphery the branches pass

PRECEDING PAGE BLANK NOT FILMED.

over into capillaries which in turn are connected to an anastomosing venous network. The peculiarities distinguishing the "arterial spiders" from other similar looking vascular formations are: the almost exclusive limitation to the upper part of the body and especially to the exposed areas, the arterial character, the centrifugal flow, the high pressure within the branchings and pulsatory phenomena, and finally the occurrence in a certain group of clinical conditions and the combination with other vascular transformations.[1–3,8]

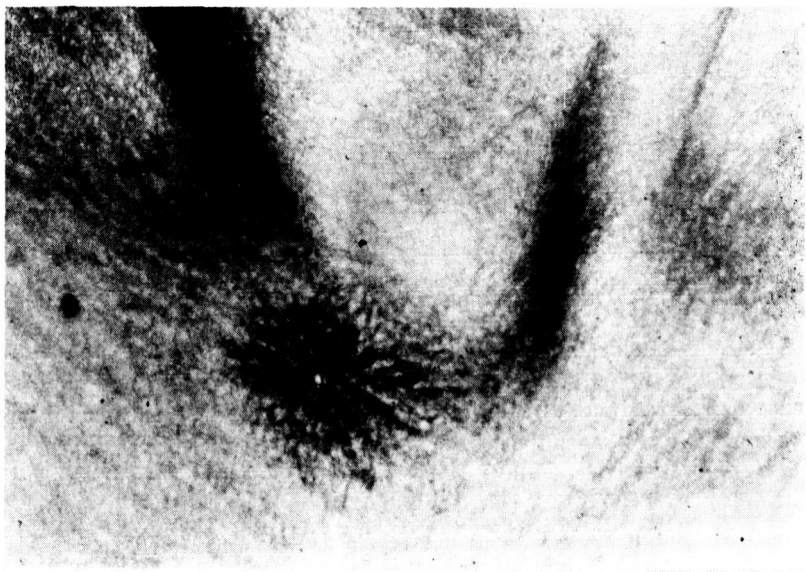

Fig. 1. Great arterial spider in a case of cirrhosis of the liver over the sternoclavicular joint. Diameter almost 4 cm. Approximately two-thirds of the original size.

In experiments with the arterial spiders of the human skin we have tried to improve the visibility of the vascular tree and to gain direct access for measurements, because the overlying skin has turned out as an obstacle for detailed and exact procedures. Clearing up of the skin by application of oil has proved unsatisfactory. Both purposes have then been attained by the cantharide-blister method, which has previously been used for other microscopical studies in dermatology and for investigations into capillary permeability.

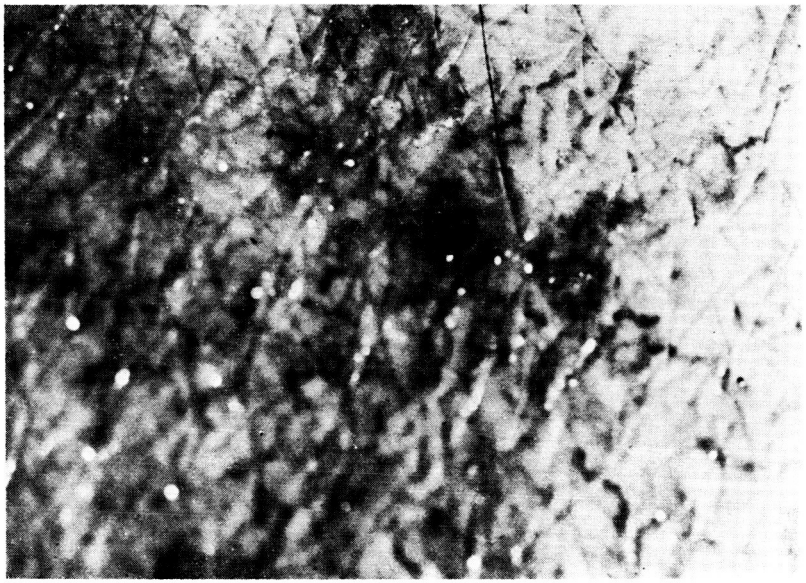

Fig. 2. Arterial spider of the skin in incident light. The vascular branchings are covered by the skin and hardly visible. 10×.

METHODS

After attaching 0.2% Cantharoplast (Madaŭs) to the area of the spider a blister is developed within 12 to 24 hr. By careful removal of the blister surface the vascular ramifications are exposed in their whole extent. It goes without saying that a certain amount of inflammatory artifact has to be taken into account. The blister ground is strongly hyperemic, but extravasates can be prevented by limitation of the plaster application.

Now the arterial walls are directly exposed to vital microscopic study under high magnifications and to micromanipulation. The following aspects of the experiments will be dealt with: vascular anatomy, pressure recordings by microcapsule methods, microvascular pulsation, and micromanipulation.

VASCULAR ANATOMY

Martini and Staubesand[7,8] in their excellent histological study of excised material have reconstructed the morphology of the arterial

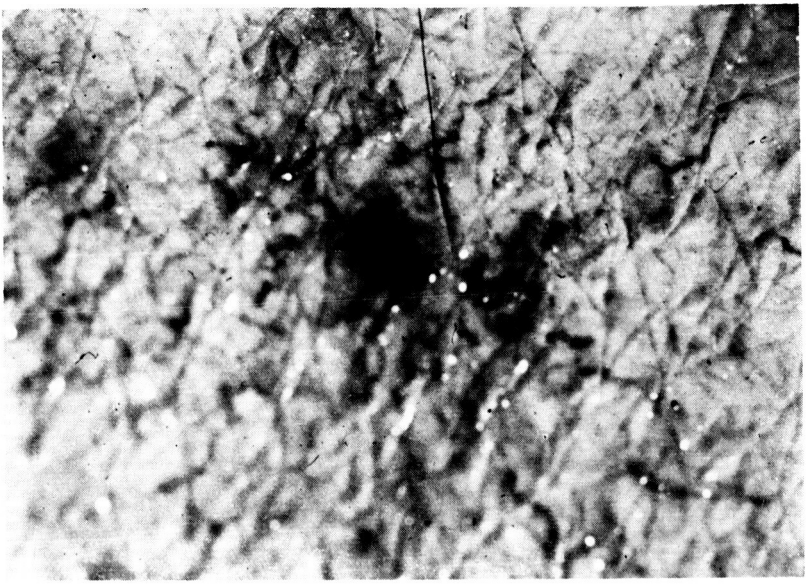

Fig. 3. The same arterial spider after clearing up of the skin by application of immersion oil. The visibility of the vascular tree is still insufficient for detailed study. 10×.

spider. Vital microscopy now shows complete agreement with their findings. Especially the following details have been established: the circumscribed and limited appearance of the area in which the central artery perforates the skin level; the irregularity and cushion-like deformation of the vascular lumen in this area; the bizarre coiling of the central artery and its branches, sometimes with spiral course; and the dipping of the arterial branchings below skin level and reappearance in the periphery of the lesion.

PRESSURE RECORDINGS

It has been known from clinical observations and previous experiments that the central parts of the arterial spiders do not blanch unless under high outer pressure, for instance, with a cover glass. In occasional injury of spiders arterial bleeding has been noted and by application of a macroscopic transparent plastic capsule Bean has estimated pressure values up to 100 mm. Hg.[2]

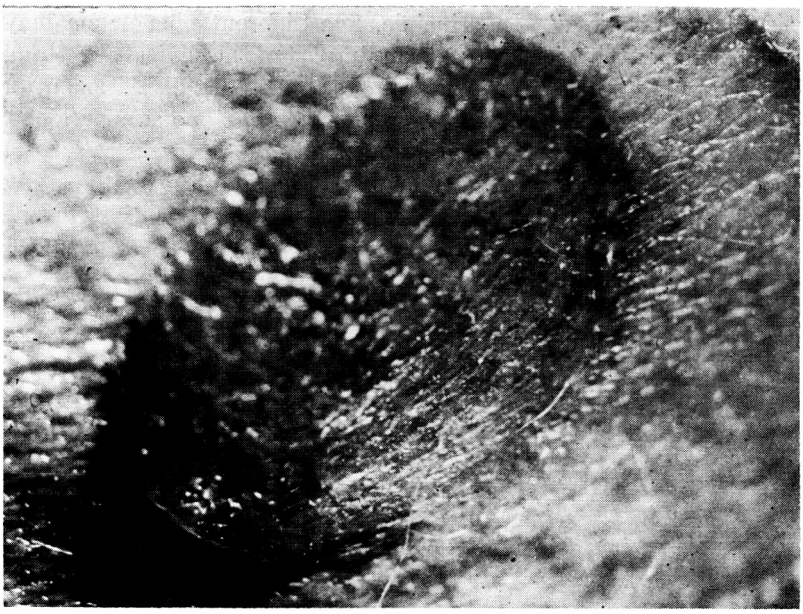

Fig. 4. Cantharide blister after 22 hr. application of 0.2% Cantharoplast (Madaŭs) above an arterial spider. 5×.

Using a personal design of a transparent microcapsule attached to an Ultropak microscope we have tried to obtain better differentiated pressure recordings in detailed areas.[6,9] In a series of ten measurements in cirrhotic patients with normal arterial blood pressure the following systolic pressure values have been obtained: in the central part from 90 to 100 mm. Hg; in the central third from 30 to 60 mm. Hg; and in the outer third, 30 mm. Hg and below. The highest value at which total blanching of the subepidermal ampulla has been noted was 105 mm. Hg. This considerable pressure loss in a course of a few millimeters of irregularly formed and coiled arteries is a challenging feature of the arterial spiders.

MICROVASCULAR PULSE

For this type of measurement of blood pressure with transparent microcapsules, pulsatory phenomena are used as criteria. This gives the occasion to mention briefly the microscopical appearance of

"capillary pulsation." In principle, five different phenomena may be discussed as the microscopical counterpart of the clinical symptom, namely, pulsatory variations of diameter, pulsatory displacement of a vessel or vascular tree, pulsatory deformation of vascular loops, pulsatory variations of flow rate, and finally pulsatory variations of vascular filling. The arterial spiders are a good object for the study of micropulsatory phenomena, and it must be noted that in the

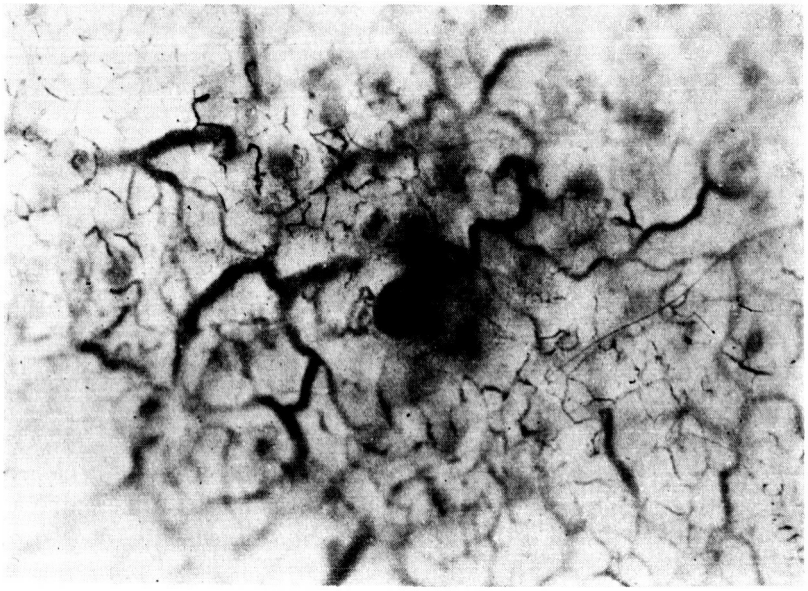

Fig. 5. The central part of an arterial spider exposed by drawing a cantharide blister and removal of the blister surface. The subepidermal ampulla, the coiled course of the central artery and its branches, and the finer arterial-capillary network are clearly visible. During microscopical observation cellular details of the streaming blood and flow characteristics can be differentiated. 20×.

exposed arterial spider usually none of these features are observable if interaction with the structure is avoided. It can be shown that more or less all of the described phenomena may appear after application of outer pressure in the range of the pressure amplitude. As already shown in previous investigations in aortic insufficiency,[4] the phenomenon which before all deserves denomination as microvascular pulse is the diastolic collapse of the vessels provoked by

outer pressure in the range of the pressure amplitude as used here for our measurements.

MICROMANIPULATION

In order to obtain direct intravascular pressure recordings for purposes of comparison with the values of the transparent microcapsule method a Leitz micromanipulator was used.[5,11,12] So far,

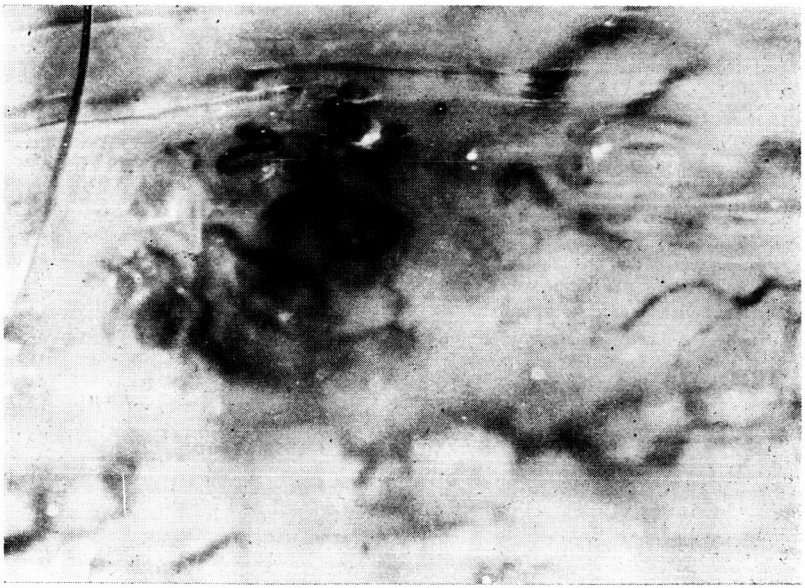

Fig. 6. Higher magnification of the central part of another arterial spider. Spiral-shaped and coiled arteries originating from the central artery. 35×.

exact data have not been obtained, but a preliminary study has shown that micropuncture and aspiration of blood is an easy procedure due to the total exposure of the vessel under study and the large inner diameter of the central artery up to a maximum of 200 or 300 μ and its relatively thin walls.

It may be expected, that forthcoming studies will soon give results of pressure recordings with different methods in the same object.

CLINICAL ASPECTS

From the clinical point of view it is important to note that the arterial spiders are sometimes observed in apparently healthy persons, in small children, in puberty, more frequently in pregnancy and before all in chronic liver disease.[1–3,8] The frequency of their occurrence in progressive cirrhoses together with their specific features make the spider a valuable clinical stigma. It therefore serves for

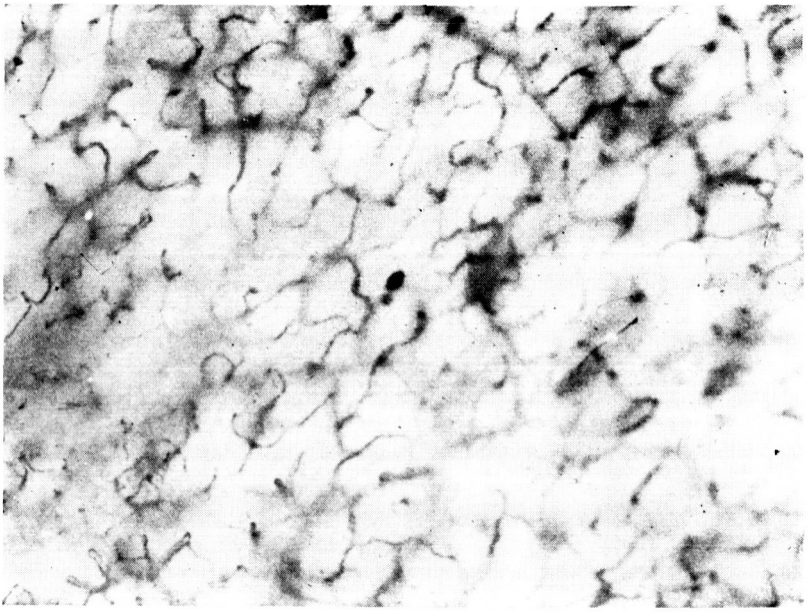

Fig. 7. Apparently normal skin area in a patient, who has spiders in other localizations, suffering from cirrhosis of the liver. Removal of the epidermis revealed the presence of micropools. 40×.

diagnostic as well as prognostic purposes because rapid enlargement and appearance of new spiders suggest progress of the disease and short survival. Differentiation from other similar looking vascular formations is therefore necessary.

So-called "venous stars" can be distinguished easily by the absence of pulsation and the lack of centrifugal flow. They do not have the predilection sites as described above.

The angiomata of Osler's disease may in some instances be confused with spiders but the bleeding episodes, the affection of mucous membranes of lip and tongue, the lack of pulsation and the characteristic morphology with clear-cut capillary aneurysm formation permit the distinction. It must, however, be noted that about 20% of Osler patients develop cirrhosis of the liver and that the blood pressure within the Osler angiomata due to extensive opening of arterio-venous communications may occasionally rise up to 50 mm. Hg, even leading to some degree of pulsation.

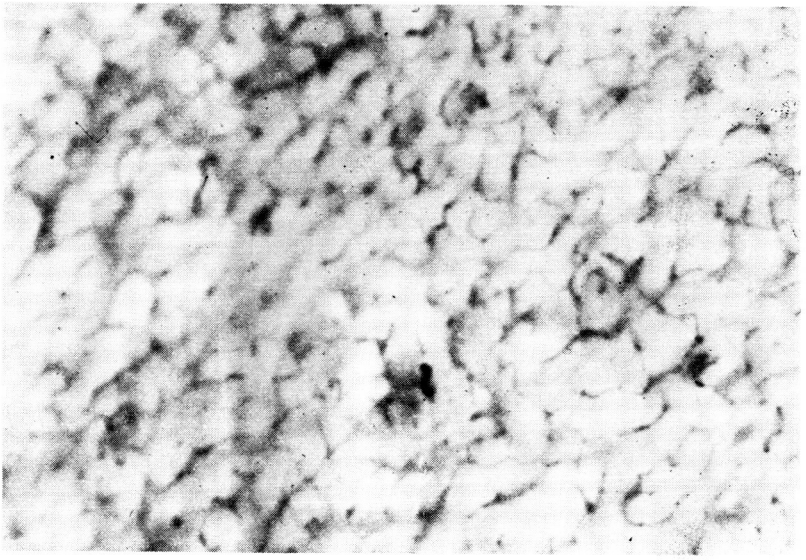

Fig. 8. Cantharide blister ground in another skin area of the same patient. Antlerlike branching of vascular sprouts assuming the shape of a microspider. 40×.

"Cherry angiomata" are too different in shape, predilection, and color to be mixed up with spiders.

A study of all accessible parts of the terminal vascular bed in cirrhotic patients shows that the spiders do not constitute an isolated vascular abnormality, but one of several expressions of a widespread dynamic transformation process of the whole terminal vascular bed. Red palms (palmar erythema), red tongue, warm red skin, "dollar-paper skin," vascularized appearance, teleangiectatic "mats,"

clubbed fingers and other symptoms, of which the spiders are just one, show that the function and morphology of the microvascular system are profoundly changed.

Experiments in which we exposed skin areas macroscopically free of spiders or other vascular changes have shown that after removal of the epidermis by a cantharide blister all transitions from normal skin

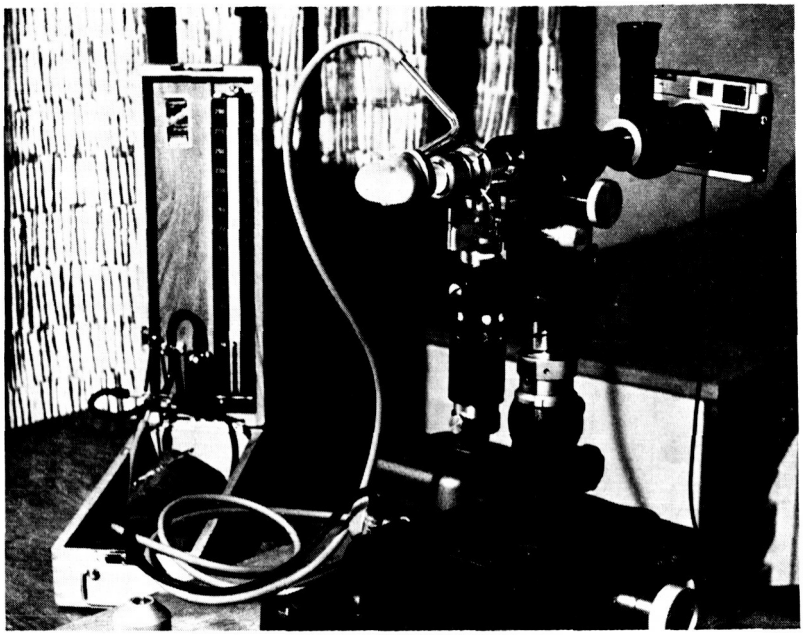

Fig. 9. Equipment for measurement of microvascular pressure. A transparent capsule is attached to an Ultropak microscope (Leitz). The pressure chamber is connected to a sphygmomanometer, the cuff is ligated. The pressure inside the capsule can easily be seen at the mercury column. Photography or cinephotomicrography of pulsatory phenomena during measurement is possible.

capillaries to "microspiders" can be revealed. In the mucous membrane of the tongue, vital microscopical studies have revealed extensive dilatation of capillary loops in the fungiform papillae as the cause of its red macroscopical appearance, further indications of the generalized nature of the microvascular transformation.

What is the meaning of these changes whose cause is not known? Does this widespread rearrangement of the microvascular system

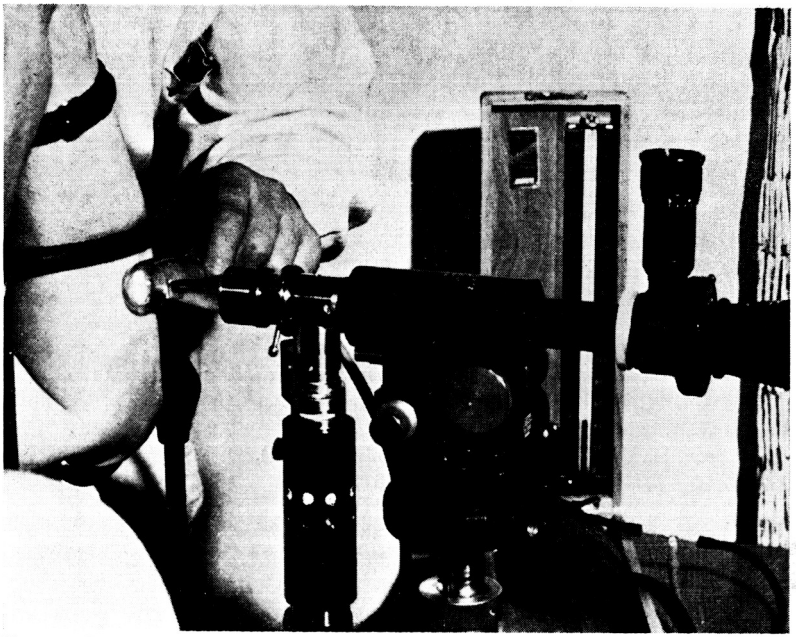

Fig. 10. Pressure recording in an arterial spider in the forearm of a patient.

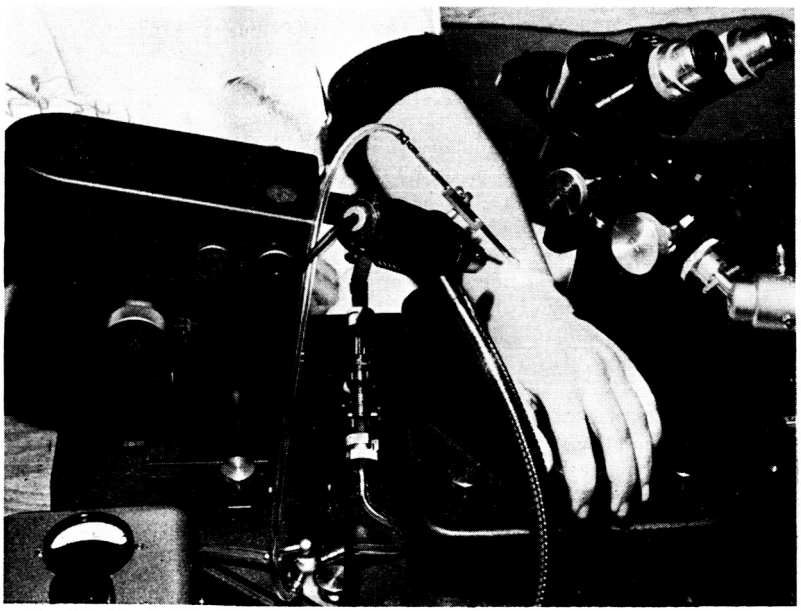

Fig. 11. Equipment for direct micromanipulation and pressure recording consisting of a Leitz micromanipulator with microneedle, tube system, and a stereobinocular microscope with illumination.

have any hemodynamic influence? Circulation analysis so far has failed to disclose evidence for constant changes in the general circulation.[10] The question is if the summation of all these microvascular changes may influence the general circulation at all. In any case, relations to clinical features in cirrhosis patients such as rarity of disturbances of peripheral circulation and the almost absolute absence of arterial hypertension deserve further investigation.

References

1. Bean, W. B., *Quart. Bull. Northwestern Univ. Med. School*, **27**, 98 (1953).
2. Bean, W. B., *Vascular Spiders and Related Lesions of the Skin*, Charles C Thomas, Springfield, Ill., 1958.
3. Bean, W. B., *Arch. Internal Med.*, **106**, 35 (1960).
4. Harders, H., *Bibliotheca Anat.*, **4**, 566 (1964).
5. Irwin, J. W., *Bibliotheca Anat.*, **1**, 50 (1961).
6. Linnér, E., *Am. J. Opthalmol.*, **41**, 646 (1956).
7. Martini, G. A., and J. Staubesand, *Virchows Arch. Path. Anat. Physiol. Klin. Med.*, **324**, 147 (1953).
8. Martini, G. A., *Z. Klin. Med.*, **153**, 470 (1955).
9. Stepanik, J., *Ophthalmologia*, **132**, 98 (1956).
10. Tsakiris, A., and A. Bühlmann, *Schweiz. Med. Wochschr.*, **93**, 325 (1963).
11. Ullrich, J., and K. Thurau, *Leitz Mitt. Wiss. Techn.*, **2**, 85 (1962).
12. Wirz, H., *Helv. Phys. Acta*, **13**, 42 (1955).

Synopsis

14597

The "arterial spider" of the human skin is a suitable model for hemorheological studies in man by immediate accessibility of a terminal arterial vascular tree under unusually high pressure by the use of cantharide blisters. The central arteries may have inner diameters up to several hundred microns and are visible in their connections with the arterial branches, the capillary network, and collecting venous net. Direct microscopical observation under high magnification of flow characteristics and behavior of streaming cells, micromanipulation, and pressure recordings are possible. The morphology of the vascular spiders is described with emphasis on unusual vascular formations as spiral arteries and abrupt changes of inner vascular diameter. Functional and rheological findings and pressure recordings are discussed, which show systolic arterial pressures exceeding 100 mm. Hg and dropping abruptly within the course of few millimeters. Under clinical conditions the arterial spiders are a valuable sign in chronic liver disease. They do not constitute a localized vascular abnormality but are part of a widespread structural and functional transformation of the whole peripheral vascular bed. This transformation is, e.g., expressed by palmar erythema and changes in the terminal vascular bed of mucous membranes, skin, and finger tips. The origin and the purpose of such universal microvascular rearrangement in liver diseases are still unknown.

author

N67 14593

Biological Reactions Interfering with Flow through the Microcirculation†

JOHN W. IRWIN* and DOLORES C. ALCAIDE, *Microcirculatory Laboratory, Massachusetts Eye and Ear Infirmary, Boston, Massachusetts*

INTRODUCTION

Poiseuille[1] was one of the modern pioneers in the field of rheology. It is of interest that although he was a physician, he devised his law after a series of observations made on the flow of water through a set of glass capillary tubes. A century later, Landis[2] made cinematographic records of the flow of blood through the mesenteric vessels of the frog. He also studied the flow of a filtered mixture of acacia and graphite, which had been introduced into an arteriole of the mesentery, through the following capillary bed. From these records certain calculations were made which suggested that Poiseuille's law could apply to capillary blood flow in only a very restricted sense.

Blood is a mixture of complex materials. In the microcirculation, it flows through multiple channels which are capable of changing their diameters either individually or collectively. The study of rheology of blood in the microcirculation, therefore, is most difficult. To date, adequate mathematical formulas have not been devised. Fortunately, mathematicians, physicists, engineers, and biologists realize that they must unite in order to achieve desired progress. Certain groups of biologists have studied microscopically the blood flow of the microcirculation, and through the years certain concepts have evolved.

In this laboratory the pulmonary microcirculation of living mammals has been studied for over a decade. It is now evident that the

† This work supported in part by a grant from the Vick Chemical Co. and a grant from the Mary Dexter Fund.

rheology of the pulmonary circuit is quite flexible and that various biological agents have marked effects upon it.

It is the purpose of this paper to discuss certain phenomena characteristic of the changes in the rheology of blood in the rabbit lung during certain biological reactions.

METHODS

The lungs of all rabbits were prepared for microscopical observation by methods described in detail by Irwin and Macdonald[3] and Irwin et al.[4] The anesthetic agent was intravenous sodium pentobarbital, 0.45 g./kg. of body weight. Additional smaller doses were administered as required. A tracheotomy was performed. A polyethylene tube was then inserted into the trachea and tied securely. A cannula was placed in this tube, filling approximately two-thirds of its lumen. Inflation of the lung was accomplished with the use of intratracheal oxygen. This insufflation of oxygen, in addition to the anesthesia, suppressed respiratory movements. A thoracotomy on the right side between the fourth and fifth ribs enabled the middle lobe of the right lung to be exposed. This lobe was delivered so that it could rest on a constant flow of mammalian Ringer's solution issuing from the tip of a quartz rod. Light from a 1000-w. projection bulb was transmitted down the rod to transilluminate the lung. Observations of the pulmonary microcirculation were made with various microscopes, with magnifications ranging from 40× to 900× and were recorded on 16 mm. motion picture film.

Changes in the pulmonary microcirculation were studied during both active and passive anaphylaxis and following the injection of histamine, 5-hydroxytryptamine (serotonin), and epinephrine. Some of these changes have been previously discussed.[5–7]

Active sensitization of rabbits was accomplished by injecting each of two toe pads with 0.5 ml. of an emulsion containing Freund's adjuvant,[8] saline, and 25 mg. of bovine serum albumin (BSA). At weekly intervals thereafter 10 mg. of BSA was injected intravenously. Rabbits received from 1 to 3 of these booster injections. Five to ten days after the last injection the rabbit was anesthetized and prepared for observation. A shocking dose of 50 mg. of BSA was injected intravenously. Immediately prior to anesthesia, 15 ml. of blood was drawn from each rabbit. A quantitative determination

of the amount of circulating antibody-nitrogen per milliliter was done, using a precipitin method as described by Kabat and Mayer.[9] The specific precipitates were dissolved in biuret reagent and analyzed on the Beckman D.U. spectrophotometer.

In passive anaphylaxis, rabbits which had been sensitized to BSA over a 4 to 12 week period were bled. The pooled serum was analyzed quantitatively as previously described. Known amounts of antibody-nitrogen were injected intraperitoneally into untreated rabbits. Twenty-four hours later, these rabbits were shocked intravenously with varying amounts of BSA, such that the total antigen-antibody ratio ranged from 1:20 to 2.5:1.

When histamine shock was to be studied, 5 to 50 mg. of histamine phosphate per kilogram of body weight was rapidly injected intravenously while the microcirculation of the rabbit's lung was under observation. The effects of serotonin and epinephrine were studied under the same experimental conditions. The serotonin dose was 25 mg./kg. of body weight. The serotonin preparation used was serotonin creatinine sulfate H_2O. Epinephrine 1–1000 was given in dosages of 0.01 ml. to 0.1 ml./kg. of body wt.

RESULTS

During active anaphylaxis, the pulmonary microcirculation is markedly affected. In certain highly sensitized rabbits the intravenous shocking dose of antigen will result in such constriction of pulmonary arterioles and venules that the lung becomes very pale and almost free of blood. In less sensitive rabbits the constriction is less marked, but changes in the intravascular elements can be pronounced. These changes are multiple. White blood cells begin to stick to vascular walls, particularly on the venous side. Red cells tend to aggregate. Most striking, in all sensitized animals, are the multiple amorphous "hyaline" masses which appear in the arterioles and venules of the lung only seconds after the shocking dose has been administered. These masses are quite rigid. Within minutes they may become lodged in the pulmonary vessels, thereby occluding blood flow. Such obstruction is almost invariably followed by death.

The changes in the pulmonary microcirculation during passive anaphylaxis are similar to those observed during active anaphylaxis. Here again hyaline emboli appear frequently and can cause occlusion

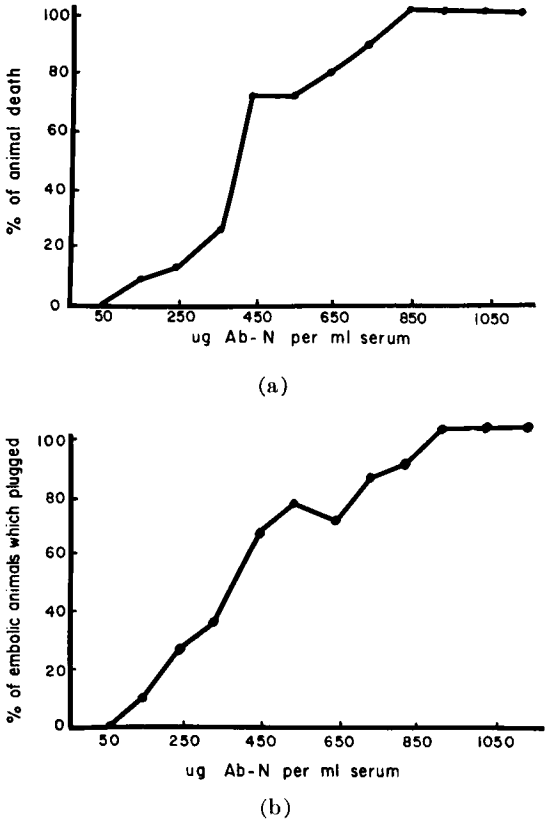

Fig. 1. Graph of serum antibody-nitrogen concentration (*a*) in active anaphylaxis against the per cent of rabbits which died, and (*b*) against per cent of animals with plugging pulmonary emboli at shock.

of blood flow. However, constriction of pulmonary arterioles and venules is often the major change.

The composition of these hyaline emboli is of interest. The possibility that they are predominantly precipitated antigen-antibody complexes is great. Figure 1*a* graphs the serum antibody-nitrogen concentration in active anaphylaxis against the per cent of rabbits which died and Figure 1*b* graphs antibody-nitrogen concentration against per cent of animals with plugging pulmonary emboli at shock. It can be seen that there is a definite relationship between antibody-

nitrogen concentration and death due to embolization and occlusion. In the passive anaphylactic experiment, the circulating antibody concentration was uniformaly low and therefore could not be related to death and embolization. Death, however, could be correlated with antigen-antibody ratio. Of the rabbits that died, 85% had ratios between 2.5:1 and 1:1. Considerable more work is indicated in passive anaphylaxis so that these preliminary results may be confirmed or refuted.

At various periods histamine and serotonin have been considered to be important chemical factors in anaphylaxis. In the rabbit, lethal doses of histamine cause marked changes in the pulmonary microcirculation. The opening and the dilation of pulmonary capillaries are characteristic reactions. Pulmonary arterioles and venules at first constrict, but frequently dilate immediately before the heart beat ceases. Red blood cell aggregates, sticking of white blood cells, and hyaline emboli are observed, but these phenomena occur much less frequently in histamine shock than they do in anaphylactic shock.

Serotonin (5-hydroxytryptamine) also causes marked changes in the pulmonary microcirculation. As with histamine shock, the most prominent reaction is the rapid constriction of the pulmonary arterioles and venules. Red blood cell aggregates, white blood cell sticking, and hyaline emboli are again observable, although relatively infrequently. Epinephrine is not involved in anaphylaxis. Indeed, it can often aid a rabbit in overcoming the effects of anaphylactic shock. As a sympathomimetic, it causes conspicuous change in the circulatory system. Its effects on the pulmonary microcirculation are fairly consistent. For the first minute there is marked constriction of the pulmonary arterioles. During this phase, linear blood flow in the arterioles is slowed and occasionally stopped. Within a minute, the arterioles dilate and linear blood flow greatly increases. Venules dilate and the capillary beds become most active. The rate of linear blood flow distinctly increases in both capillaries and venules.

DISCUSSION

Data have been presented to show that the linear flow of blood through the pulmonary microcirculation of living rabbits can be markedly affected by certain biological reactions such as anaphylaxis,

histamine shock, serotonin shock, and doses of epinephrine. For instance, aggregates of cells can obstruct a few or many of the microscopic vessels. It would also appear that substances usually held in solution in plasma can be brought out of solution to form masses which can block or impede the flow of blood through these vessels. Finally, the microscopic blood vessels can constrict or dilate so as to affect the linear flow of blood. This can occur in a local area or can be more generalized.

Admittedly, anaphylaxis, histamine shock, serotonin shock, and pharmacological doses of epinephrine are not stresses which biological organs must face routinely. These experiments, however, do point out that the pulmonary microcirculation can change rapidly. It is, therefore, imperative that any mathematical formulation of pulmonary blood flow take into consideration the flexibility of the pulmonary vascular system. Such a task is a formidable one but with more accurate methods of measurement and with the use of computer facilities the possibility of success is increased.

References

1. Poiseuille, J. L. M., *Recherches sur la force du coeur aortique*, Vol. 1, Paris, 1828, p. 1.

2. Landis, E. M., *Am. J. Physiol.*, **103**, 432 (1933).

3. Irwin, J. W., and J. Macdonald, *Anat. Record*, **117**, 1 (1953).

4. Irwin, J. W., W. S. Burrage, C. E. Aimar, R. W. Chestnut, *Anat. Record*, **119**, 391 (1954).

5. Burrage, W. S., and J. W. Irwin, *J. Allergy*, **24**, 289 (1953).

6. Burrage, W. S., J. W. Irwin, J. I. Gallemore, D. M. K. Wang, *J. Allergy*, **25**, 293 (1954).

7. Walter, J. B., J. A. Frank, and J. W. Irwin, *Brit. J. Exptl. Pathol.*, **42**, 603 (1961).

8. Freund, J., and K. McDermott, *Proc. Soc. Exptl. Biol. Med.*, **49**, 548 (1942).

9. Kabat, E. A., and M. M. Mayer, *Experimental Immunochemistry*, C. C Thomas, Springfield, Ill., 1948.

Synopsis

14593

Methods to study the pulmonary microcirculation of living rabbits have been presented. Changes in both the caliber of these vessels and in the fluidity of the blood flowing through them have been noted during anaphylaxis, histamine shock, and serotonin shock. Pharmacological doses of epinephrine also markedly affect the flow of blood through the pulmonary microcirculation. It is suggested that studies in rheology must take into account the capacity of the microscopic pulmonary blood vessels to change their calibers rapidly and the fact that the consistency of blood is not necessarily constant.

author

N67 14594

The Effects of Plasma Proteins upon the Rheology of Blood in the Microcirculation

ROE E. WELLS, JR.,* *Departments of Medicine, Harvard Medical School and Peter Bent Brigham Hospital, Boston, Massachusetts*

INTRODUCTION

Present studies would suggest that the shear rate dependence of blood is most pertinent to the conditions of flow within the microvascular system. Arbitrarily this vascular network involves the smallest arteries (arterioles) of 0.1 mm. i.d., proceeds to the capillary vessels to 7 to 10 μ diam., and the postcapillary venous system (venules) up to 100 μ i.d. Viscometric studies have shown that above 10 inverse seconds the viscosity of normal blood ranges between 6 and 4 cp. Below 1 or 2 inverse seconds the viscosity of blood rises in an exponential-like fashion and at 0.1 sec.$^{-1}$ may be between 20 and 30 cp.[1] The quantitation of rates of shear within the vessels of the microcirculation is not a simple matter. First, the arteriolar inflow side may change its caliber by as much as 10-fold, ranging from complete closure as in shock or frostbite to maximal dilation as in heat stroke; secondly, the cinemicrophotography of Fulton and Lutz[2] and Bloch[3] reveal that in animal studies capillary flow may be intermittent and for periods reverse itself; and thirdly, the peripheral vascular system is not under voluntary control, so that any procedure designed to examine the system may cause a response that changes the character of the flow or vessel size dramatically. Consider the subtle stimuli that produce blushing. The venous or outflow side of the capillary system has a relatively slower flow than its anatomical counterpart on the arterial side. This is to say that at an equal distance from either end of the capillary, the venous system is wider and operates at a considerably lower pressure than its arteriolar equivalent. It is in this venous side that the earliest changes in fluid

structure and vessel character are observed in a variety of diseases. Rates of shear within the microvascular system then may vary widely, from 0 to 100 sec.$^{-1}$ or more.

Over the past years the author has been examining the effects of the individual protein fractions of the plasma upon the viscosity characteristics of whole blood and of red cell suspensions. During these studies in a hospital environment he also had occasion to see a significant number of patients with profound alterations in their plasma protein values. Many of these patients suffered from disturbances of their circulation which appeared to be directly related to changes in the character or concentration of their plasma proteins. Since intravascular aggregation was often a feature of these problems a study was conducted of the effects of plasma proteins upon viscosity, suspension stability, and cell aggregate formation *in vivo* and *in vitro*. It was possible to photograph the microvascular system of man and compare these observations with the changes in the plasma proteins and fluid structure of the blood *in vitro*.

TECHNIQUES

Red cell suspensions were made up by using red cells from type O donors twice washed in buffered saline and then resuspended in saline or protein solutions. Albumin was obtained as concentrated (pooled) American Red Cross albumin 25 g./liter, diluted to a final solution of 3.5 g.-%. Globulin was made up of a solution of α, β, and γ fractions in ratios of 4/9, 3/9, and 2/9, respectively, the final concentration being 2.2 g.-%. These fractions were obtained through the generous assistance of the Protein Foundation, Jamaica Plain, Massachusetts. Fibrinogen was made up in concentrations ranging from 0.3 to 2 g.-% in distilled water with resulting osmotic equivalence to whole plasma of 280 milliosmoles. Protein analyses were done by the biuret method and by paper electrophoresis. Fibrinogen was analyzed by the method of Quick. Viscosity was measured by means of a Couette-type viscometer (GDM) over a shear rate range of 0.1 to 20 sec.$^{-1}$. Sedimentation rates were measured every 15 min. in a Wintrobe hematocrit tube. Photomicrographs of the conjunctival vessels were made with a 35-mm. single lens reflex camera using a Zeiss 25-mm. lens and extension tubes ranging from 20 to 25 in. Patients were comfortably seated with the chin resting on a foam

rubber base. A xenon flash tube was synchronized to 1/1000 of a second. Film used was fine grain positive black and white or Ektachrome color.

Photomicrographs of the conjunctival vessels were made at the same time blood was drawn for analysis of hematocrit, albumin, globulin, fibrinogen, sedimentation rate, and electrophoretic separation of serum proteins.

DISCUSSION AND RESULTS

Normal erythrocytes have a weakly negative charge in the slightly alkaline pH of the blood (7.4). Albumin, with a molecular weight of 66,000 and an axial length:width ratio of 3:1, has a relatively strong negative charge. Although repulsion on the basis of similar charges may not be the entire explanation, red cells in solutions of albumin did not aggregate, settled with extreme slowness (1 mm. in $2^1/_2$ hr.), and of the three protein fractions, had the least effect upon viscosity. Viscosity-shear rate curves were quite similar to those of red cells in saline. Fibrinogen, a far heavier molecule (330,000 mw.) and longer (ratio 12:1), has almost a neutral charge. Although red cells aggregate easily into rouleaux forms in solutions of fibrinogen, the sedimentation of these aggregates is not rapid until the normal physiological concentration (0.2 to 0.4 g.-%) is exceeded. At these normal concentrations sedimentation of 5 to 10 mm./hr. is observed. At 0.9 g.-% aggregates are large (from 6 to 12 cells) and settle with extreme rapidity, 60 mm./hr. This protein molecule appears to be the principal one accounting for the small but distinct yield value reported by Dintenfass[4] and by Merrill et al.[5] Dintenfass has considered the reversibility of the fluid structure of blood between low and high shear as a possible factor in the origin of thrombosis *in situ;* i.e., the formation of a clot in veins under conditions of stagnant circulations. Clinically, fibrinogen is measured infrequently in comparison to the third component, globulin. The majority of diseases which are associated with aggregated red cells relate to alterations in the make up and concentration of globulin. This fraction is a mixture of proteins ranging in molecular weight from 35,000 to 1,000,000. Its net charge is negative but less so than albumin. It separates into a variety of subfractions which are classified variously. The old classification utilized α, β, and γ as the

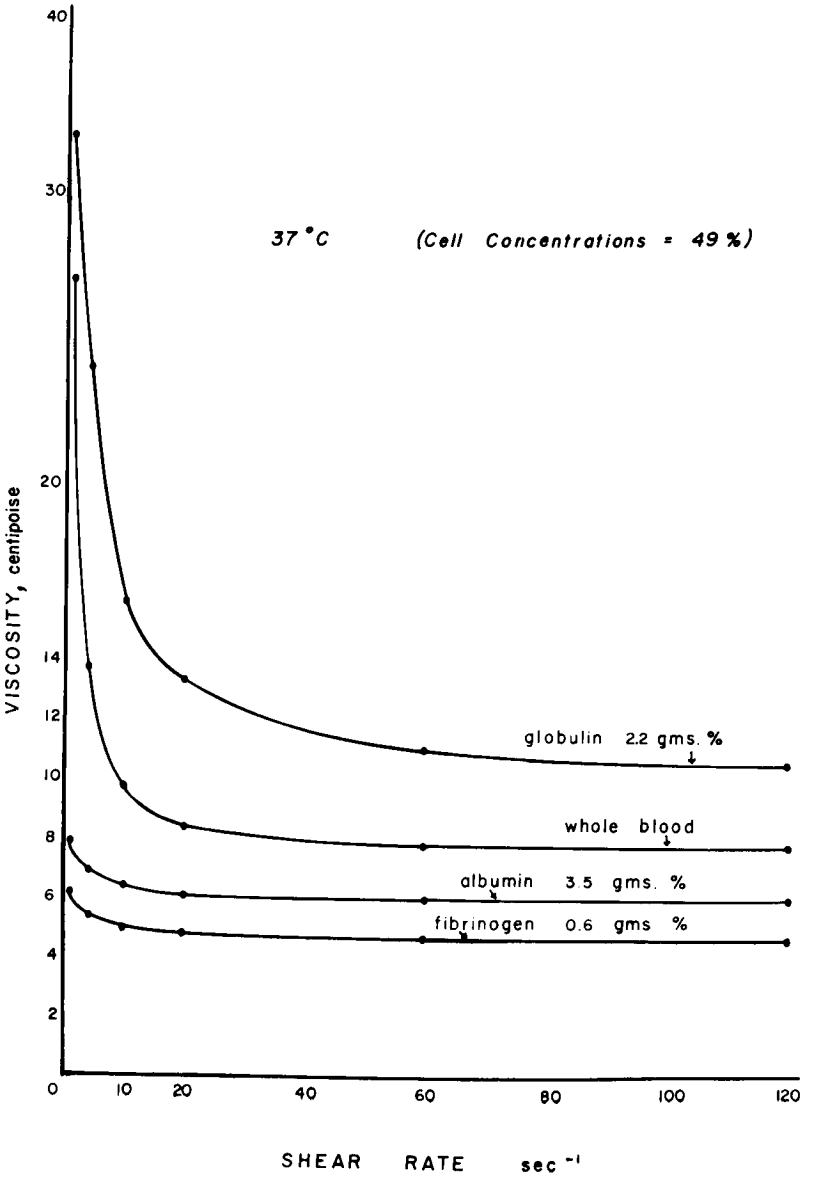

Fig. 1. Comparison of effects of protein fractions upon viscosity of red cell suspensions.

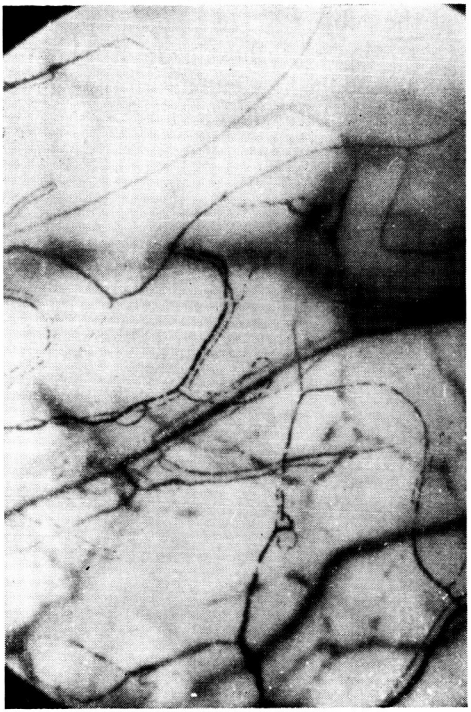

Fig. 2. Photomicrograph conjunctive normal man. (12× on 35 mm. film.)

major subgroups. These subfractions mixed in the ratio found in normal blood produce irregular aggregates, fewer rouleaux than fibrinogen, and only slight sedimentation. The effect of globulin upon the viscosity of red cell suspensions is the most profound of the three major fractions (Fig. 1). Although albumin was studied at 3.5 g.-%, it is, as noted, the lowest of the three viscosity values. Fibrinogen, at 0.6 g.-%, is intermediate, and globulin, at 2.2 g.-%, has the highest viscosity values. If fibrinogen and globulin are compared on an equal weight-volume basis, then fibrinogen has the slightly greater effect upon viscosity.

The correlation between plasma protein levels and cell aggregation *in vivo* is considerably less predictable than that of red cell suspensions *in vitro*. The use of the conjunctiva of the eye as a representation of the rest of the microvascular system has been considered by various authors.[6] It has the main advantage of not requiring any handling

or preparation of the subject. The photographic process is of such short duration that response to heat or light stimuli is precluded by the short duration of the flash. The use of unusually long extension tubes was a result of requiring flat field lenses and the need for long working distances to avoid threatening the subject.

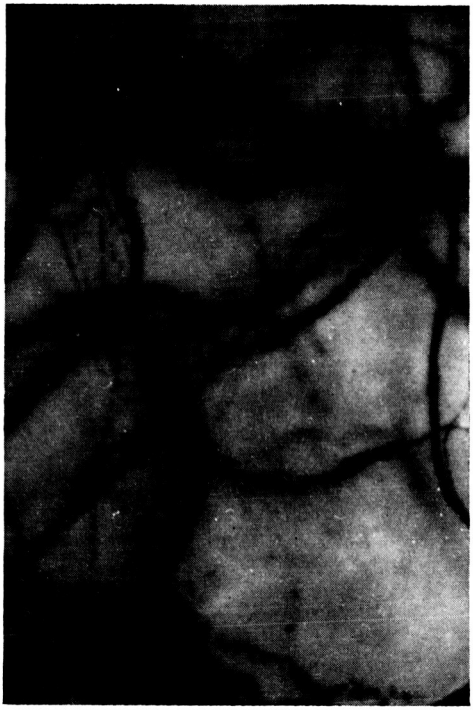

Fig. 3. Conjunctival vessels in patient with multiple myeloma. (20× on 35 mm. film.)

The smallest vessels of the normal subject are seen as relatively straight systems while some aggregation is apparent in the post-capillary venules (Fig. 2). Viscosity, plasma proteins, and sedimentation rate were all normal. One of the most common diseases associated with a high sedimentation rate and cell aggregation is multiple myeloma. The vascular pattern is shown in Figure 3. Here there is venular dilatation, increased tortuosity, neovasculari-

zation, and severe clumping. In this subject (C. B.) the hematocrit was 39, and the sedimentation rate 64 mm./hr. which, corrected for the volume decrease in cells was 51 mm./hr. The fibrinogen level was normal 274 mg.-%, globulin was elevated at 4 g.-%, and the albumin was normal.

The viscosity shear rate curves in this case revealed a slight increase in overall values above those predicted for a hematocrit of 40. Importantly at the low shear rates 0.1, 0.2, and 0.5 sec.$^{-1}$, values were considerably elevated attaining a viscosity of 130 cp. at 0.1 sec.$^{-1}$. Since anemia is a common pattern in these patients there may be some rheologic advantage in reducing viscosity values at low shear.

Elevated fibrinogen levels are usually more transient than the globulin levels. The most marked elevations have been observed in acute injury without hemorrhage. The elevation may last from only 12 to 36 hr. In the case of a major burn (42% of third degree) 7 hr. after injury, marked aggregation was seen *in vitro* but the high hematocrit (48) reduced its apparency *in vivo*. Dilatation was noted and very sluggish flow was described by the photographer. Sedimentation rate was 34 mm./hr. Total protein, 7 g.-%; albumin, 4.1 g.-%; and globulin 2.9 g.-%. Fibrinogen was 884 mg.-%. The viscosity shear rate curves revealed high viscosity values. Most striking were the shear stress-shear rate curves which plotted by the Casson system (shear stress$^{1/2}$ vs shear rate$^{1/2}$) revealed an intercept at zero shear (by extrapolation) of (0.21 dyne/cm.^{2})$^{1/2}$ shear stress. This is taken as evidence of a significant yield value. The patient's subsequent course was complicated, as it is in many burn cases, by vasodilatation which remained so marked that the patient felt "cold" in an ambient temperature of 94°F.

Other patient studies have revealed the greatest cell aggregation is observed in patients with macroglobulinemia (Waldenstrom). In these cases marked dilatation of all vessels is seen and stagnant flow is apparent in most cases. Although anemia in this disease is common, viscosity values are virtually double their predicted values on the basis of hematocrit. Of the three cases of macroglobulinemia studied thus far photomicrographs of the vertical tubes used in sedimentation rate analysis reveal very large aggregates while sedimentation was negligible. This is attributed to the high plasma viscosity (2 cp. at 10 sec.$^{-1}$) and its ability to support these cell masses.

The author is deeply indebted to Professor H. Edgerton, Mr. S. Teicher, and Mr. E. R. Schildkraut of the Stroboscopic Laboratory, Massachusetts Institute of Technology, for their guidance and assistance in the photomicrographical studies. The advice of Dr. R. Pennell, and Mr. M. Melin of the Protein Foundation and their generous supply of protein fractions is also gratefully acknowledged.

References

1. Wells, R. E., Jr., and E. W. Merrill, *J. Clin. Invest.*, **41**, 1591 (1962).
2. Fulton, G. P., and B. R. Lutz, *Med. Biol. Illustr.*, **7**, 26 (1957).
3. Bloch, E. H., *Am. J. Anat.*, **110**, 125 (1962).
4. Dintenfass, L., *Kolloid-Z.*, **180**, 160 (1962).
5. Merrill, E. W., G. R. Cokelet, A. Britten, and R. E. Wells, Jr., *Circulation Res.*, **8**, 48 (1963).
6. Ditzel, J., *Acta Med. Scand.*, Suppl. 343, **164**, 11 (1959).

Synopsis

14594

Each of the three major fractions of the plasma proteins has a different effect upon suspension stability and viscosity. The changes observed *in vitro* do not always correlate with those observed *in vivo*. Both globulin and fibrinogen cause cell aggregation but as globulin exists at 3 to 4 times the concentrations of fibrinogen it accounts for the major viscosity effects of the two fractions. Albumin inhibits cell aggregation and reduces viscosity. Cell aggregation *in vivo* may lead to reduced or stagnant flow, and conversely, stagnant flow in the presence of increased fibrinogen or globulin may lead to profound cell aggregation. The integrity of cell aggregates increases with increasing fibrinogen or globulin levels which may withstand the excursion from the venous system through the larger vessels to eventually occlude the arteriolar system.

author

N67 14595

Visual Particle Velocity Measurement in Fluid Streams

P. A. G. MONRO,* *Anatomy School, University of Cambridge, England*

INTRODUCTION

The technique to be described here was developed primarily for studying the flow of blood in live tissue; it was later modified for the measurement of the flow of blood in fine glass tubes, and parallel studies were also made with fluids containing small fluorescent particles. Photographic records of streak images of amphibian blood flow were made by Basler[1] in 1918 and this technique was further developed by Hugues[2] for experiments on blood flow in the vessels of the rabbit's mesentery. Although the velocities measured by Hugues ranged up to 80 mm./sec. and the vessels measured up to 200 μ bore, it was not possible to make immediate readings and the apparatus was cumbersome as the camera had to be rotated about the optical axis of the microscope in order to bring the movement of the film into a plane at right angles to that of the blood vessel. These disadvantages are only relative and the same principle for the study of high speed events is incorporated in the streak camera. High speed framing cameras have more recently been used by Bloch[3] for studies of flowing blood in both amphibian and mammalian vessels. The behavior of individual red cells can be followed by this method, but at 5000 frames/sec. 100 ft. of 16 mm. film will be exposed in less than one second and the camera will take about four-fifths of this time to reach full speed. It is therefore not a very convenient method for studying transient events whose occurrence is unpredictable.

Direct measurement of moving blood cells has usually been confined to relatively slow velocities such as those of cells in a small vein whose image may be observed to move across the graticule (reticle) of a microscope eyepiece and timed with a stop watch. Another

method used by Knisely[4] is to fit a small gear wheel in the position of the graticule and arrange this to be driven by an electric motor at such a speed that the blood cells appear to move tangentially to the rotating wheel in the spaces between the gear teeth. A better method is to place a semireflecting optical surface somewhere between the objective and the eyepiece of the microscope. By this means the image of a moving illuminated spot may be seen in the eyepiece. The spot, or better a series of spots, is caused to move with the blood cells at the same velocity and in the same direction. Brånemark[5] has used a cathode-ray tube to move a spot slowly at a known velocity. By this method it is possible to make relatively accurate measurements of blood cells moving at velocities slightly exceeding 1 mm./sec.

METHOD

(a) Double Purpose Instrument

The prototype apparatus, illustrated in Figure 1, utilizes in one instrument both the principle of the moving spot for relatively slow velocities and the directly observed streak image for much higher velocities. The principle of the latter depends on the fact that for most individuals a moving image such as that of a spot of light or of a moving blood cell cannot be perceived as such if its angular velocity across the eye exceeds about 100°/sec. Instead the spot or particle is seen as a streak. It is impossible to gain any idea of the velocity of such a streak and often not even of its direction. If a glass block or mirror is caused to displace this image in a plane at right angles to the original movement of the streak, the streak image will be displaced so that it is inclined at an angle depending on the original velocity of the image and the velocity imparted by the glass block or mirror. If these two velocities are relatively the same, the streak image or images will be inclined at 45°: the eye can measure the angle accurately by means of a graticule line preset in the eyepiece. In the photograph (Fig. 1) the covers to some parts of the apparatus have been omitted for clarity. A fine glass tube lies between two capillary tubes connected by flexible tubing to the air supply. The water bath for maintaining a constant temperature of 37°C. is also omitted.

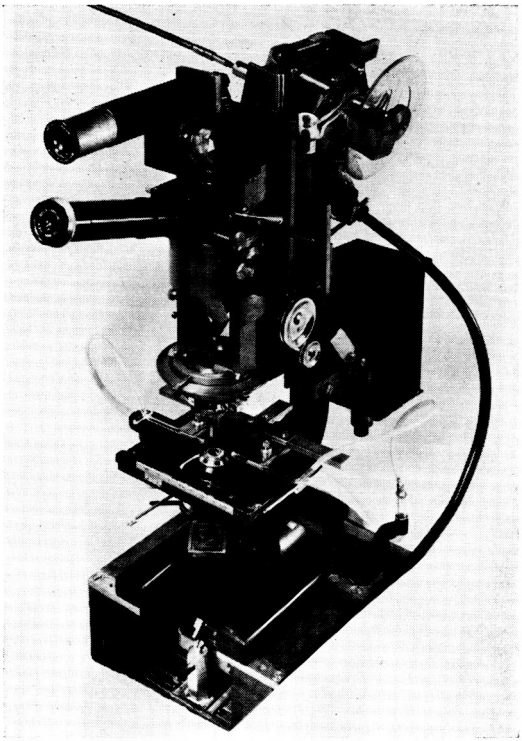

Fig. 1. Prototype instrument. Covers have been removed from some parts to show the components.

In the three-dimensional line diagram—Figure 2, which is not to scale—the optical pathways are drawn to indicate how the images are seen in the two eyepieces. A glass tube or blood vessel (*1*) contains moving particles or blood cells which are primarily imaged by the microscope objective (*2*) into the plane of the optical slit (*6*). Since the blood vessel which is to be observed may not lie in the same vertical plane as the optical slit, a K-mirror/system (*3,4*) is rotated about a vertical axis until the image of the required blood vessel is brought into the correct plane. The field lens of the eyepiece (*5*) assists in the formation of the image which is seen in the lower eyepiece (*10*) after the rays of light from the primary image are partially (20%) reflected from the parallelogram-shaped beam-splitting prism (*7*) and then pass through the erecting lens (*8*) and the graticule (*9*)

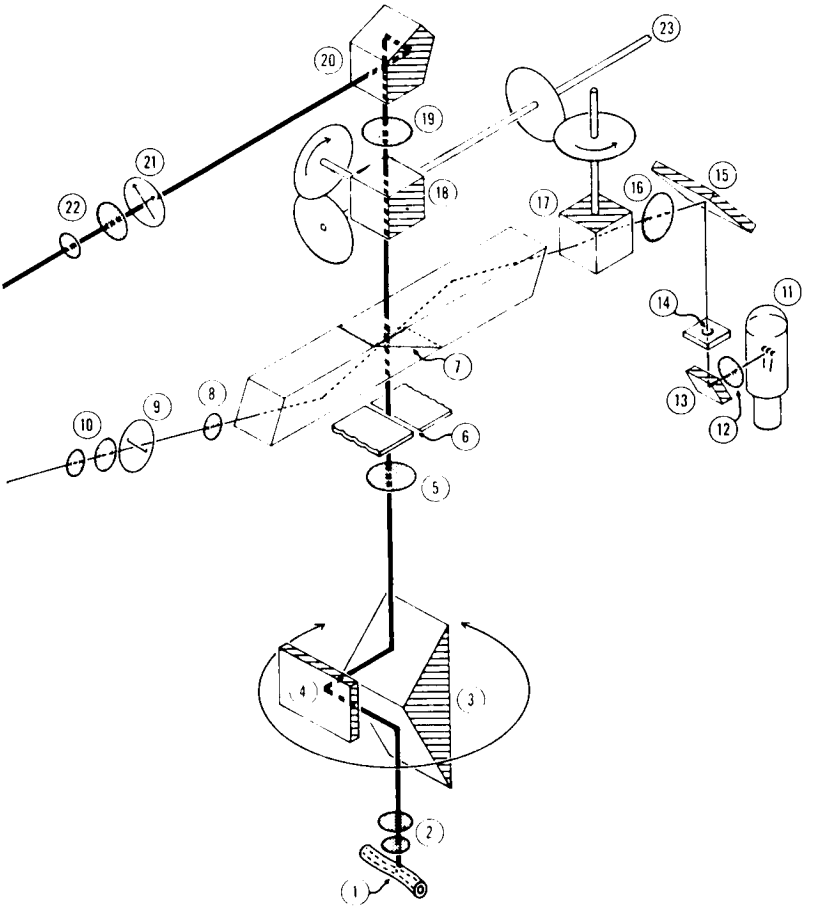

Fig. 2. Three-dimensional drawing of prototype instrument.

with a horizontal scale. The particles or blood cells thus appear to move along this scale. In order to measure their velocity the image of a spot of light is caused to appear to move along the scale with the same velocity. The low voltage lamp (*11*) illuminates the pinhole (*14*)—or series of holes—by means of the condenser (*12*) which forms an image of the lamp filament in the anastigmat lens (*16*). The two front-surfaced mirrors (*13,15*) facilitate the alignment. The anastigmat lens (*16*) forms an image of the pinhole in

the plane of the graticule (*9*) after the rays of light have been displaced first in a horizontal plane by the rotation of the glass block (*17*) and then transmitted through the beam-splitting prism (*7*). The glass block (*17*) is rotated about a vertical axis by means of helical gearing from a shaft (*23*) driven by an infinitely variable calibrated ball and plate gear and synchronous motor (not shown). The gearing is adjusted until the spot of light appears to move along the image of the glass tube or blood vessel with the same velocity as the particles or blood cells and the gearing ratio is indicated on a circular scale. If the magnification of the objective is known the velocity may easily be calculated or, for convenience, read off a graph along straight lines drawn for each objective used.

If the image is moving across the graticule of the eyepiece at a velocity which is too fast to be measured in this way, the principle of the streak is employed. The lower eyepiece (*10*) is observed as before while the optical slit (*6*) is slid into position and adjustments made to the microscope so that the image of the blood vessel or glass tube is located along the slit which is narrowed to the correct width of the fluid stream. The greater part (80%) of the light from the slit will be transmitted by the beam-splitting prism (*7*) and be displaced in a plane at right angles to the slit by the rotation of the second glass block (*18*) which is driven about a horizontal axis in the plane of the slit by helical gearing coupled 1:1 to the first glass block (*17*). Thus streak images of the moving particles or blood cells and of the spot of light are seen in the second eyepiece (*22*) after inversion by the lens (*19*) and after having been turned through 90° by the pentagonal prism (*20*). The streak image of the spot of light will always move along one or other of the two crossed graticule lines (*21*) which are each at 45° to the vertical. The variable gearing is adjusted until the streak images of the moving particles or blood cells are also seen parallel to one or other of these graticule lines. A fuller description of this apparatus with constructional data is given elsewhere.[6,7]

It will be appreciated that whereas glass tubes should have no optical imperfections to detract from the information content of the image, observations of blood vessels in live tissue necessitate the passage of light through the endothelial cells of the wall of the vessel and these will form images which are not moving and are therefore seen as vertical streaks. Also, the light may have to pass through a

considerable thickness of tissue, which even though it is not in focus, will still produce some scattering of the light. It is often an advantage to reduce the aperture of the substage condenser in these circumstances and to diminish the circumambient room lighting.

A number of observations have been made in class experiments on rabbit ear chambers and hamster everted cheek pouches by students who have learned this technique very quickly.

This prototype apparatus was designed to measure blood cell velocities in live tissue at up to 8 mm./sec. with a 4-mm. objective. In practice, velocities so far observed have not exceeded 5 mm./sec. in a rabbit ear arteriole of 12 μ bore. In vessels of this size and up to 20 μ bore there is no evidence of arterial pulsation although in vessels of 30 μ bore and larger this pulsation has been observed by Hugues.[2] Very much faster blood flow rates may be observed in fine glass tubes. The prototype apparatus is not entirely suitable for measuring these high particle velocities: the helical gearing was not intented to be driven at fast speeds and the construction is unnecessarily elaborate.

(b) Eyepiece Instrument

This instrument utilizes only the streak image principle but has been made in a more compact form so that it can be exchanged for the eyepiece of an ordinary monocular microscope (see Fig. 3). The control box, containing the meter and batteries, lies in the foreground but it is an advantage to use extra dry batteries to supply the motor when in continuous use. On the stage of the microscope is the calibrator consisting of a circular ground glass plate which may be rotated at a known speed by a flexible drive from a synchronous electric motor. If this rotates at 1 rps the tangential velocity near the edge of the plate is 30 cm./sec. If the plate is moved by the mechanical stage so that the objective lies almost over the center of the plate the velocity is almost zero.

The three-dimensional line diagram (Fig. 4) shows the arrangement of the components as in Figure 2 but also shows an elevation drawn in two planes combined. The key numbers (*1–6*) refer to the same components as in Figure 2 but the K-mirror system may be omitted since the eyepiece instrument can be rotated in the draw tube of the microscope to bring the optical slit (*6*) into the same plane as the blood vessel or glass tube. Only one glass block (*7*) is required which

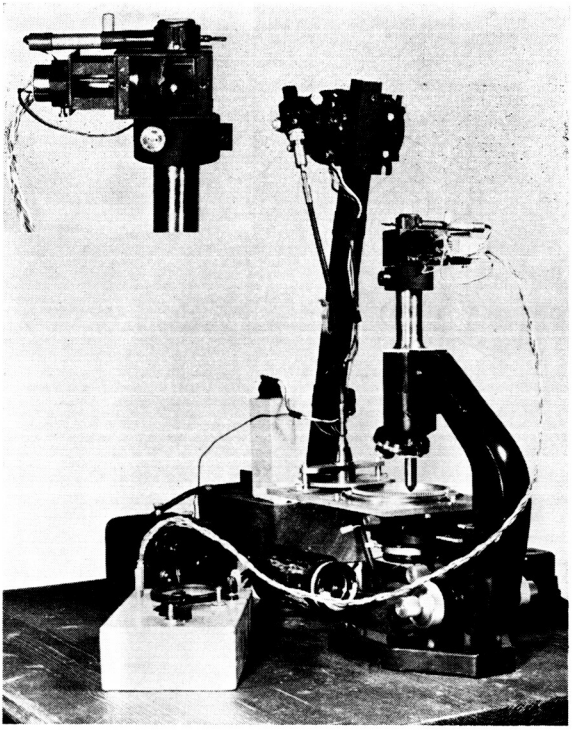

Fig. 3. Eyepiece instrument showing (inset) the glass block and auriscope lamp to illuminate the phototransistor.

is mounted on two sets of ball bearings (*12*) and is driven directly by a flexible sleeve from a small reduction-geared precision electric motor (*13*) working effectively in the range of 20 to 2000 rpm. In order to provide a reference line at 45° to the plane of the slit, a glass slip (*8*) is positioned at 45° to the optical axis immediately below the eye lens (*9*) of the eyepiece. This glass slip is transparent but will reflect a proportion of the light from a slit (*10*) illuminated by the auriscope lamp (*11*). The slit is fixed to the plane surface of a planoconvex lens and is so positioned that its image is seen in focus by the eye lens. In aligning the slit, the planoconvex lens (*10*) is rotated so that the image of the slit lies in the plane of the streak images of stationary objects as seen when the glass block is rotated; the planoconvex lens is then rotated 45°, indicated by lines engraved on its

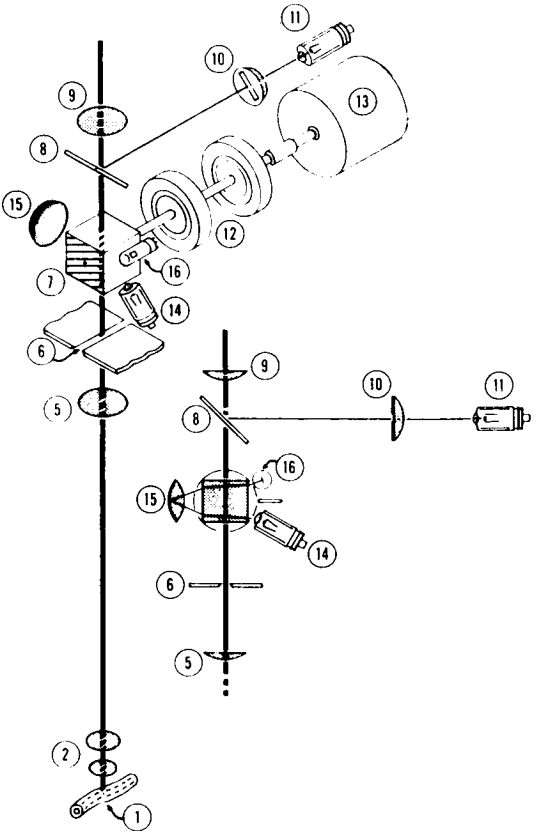

Fig. 4. Three-dimensional drawing of eyepiece instrument with (inset) a combined elevation of components for alignment of illuminated slit and tachometer.

mount. It will be appreciated that the optical axis of this optical system (*8,10,11*) does not have to be in the same vertical plane as that of the axis of rotation of the glass block (*7,12,13*), but the eyepiece velocity meter is more compact if constructed in this fashion.

Although the speed of the precision motor can be controlled by a rheostat and the speed is proportional to the current over a wide range, more accurate measurement of the speed of rotation of the glass block is provided by a photoelectric tachometer. This is shown better in the elevation drawing (Fig. 4). Four times, for each revolu-

tion of the glass block, light from another auriscope lamp (*14*) passes through two parallel faces of the block and is reflected by a lensed mirror (*15*) and back through the same two faces of the glass block onto a OCP71 phototransistor (*16*), all contained within the housing of the glass block. The output frequency of the phototransistor may be measured by an oscilloscope or by an integrating transistor circuit supplying a milliammeter directly in two ranges. Two microswitches for the auriscope lamps are mounted on the instrument which is connected to the control and velocity indicator box by 7-way connectors and thin cable. Owing to the present mechanical limitations of the calibrator, it has not been possible with this instrument to measure velocities greater than 30 cm./sec. (corresponding to particle velocities of 10^5 times their diameter), but the image quality appears to be equal to that at lower velocities and therefore it is probable that much faster velocities can be measured under conditions of good optical contrast. It will be appreciated that if the microscope objective is replaced by that of a telescope, the movement of large objects may be measured in a similar manner.

OBSERVATIONS

It is not proposed at the present stage of investigations of the behavior of flowing blood to consider in detail the observations made with these instruments. Tentative conclusions, which in part support those of previous workers,[8,9] are that in rigid glass tubes:

1. Relative blood cell velocity is greatly dependent on the concentration of cells.

2. There seems to be a marked species difference, e.g., the behavior of dog blood is more predictable that that of human blood.

3. Presumed "normal" specimens of human blood show wide variations in behavior.

4. The apparent relative viscosity of whole blood (using Sequestrene as an anticoagulent) is reduced and cell velocity is increased in glass tubes whose bore is diminished in the range of 100 to 40 μ.

5. In the smaller glass tubes, when observing across the diameter of the tube, the blood cells appear to move more at the same velocity since the streak images are all almost parallel, i.e., there is less evidence of axial streaming. At lower velocities in wide tubes axial streaming is more evident since the streak images show greater variation in obliquity.

6. Dilute suspensions of fluorescent particles of 2 to 10 μ in size show great variation in the range of obliquity of the streak images. Those particles nearer the axis are of course moving much faster than those nearer the wall. The range of variation of particle velocities as seen across the diameter of the tube is very much greater than is seen in whole blood of approximately the same viscosity by measured volume flow under similar conditions.

When observations are made on live tissue, axial streaming is seen in veins containing relatively slow moving blood cells (approximately 0.1 mm./sec.). In arterioles in the range of 12 to 20 μ bore (measured between the innermost edges of the endothelial walls, variable and irregular) the blood cells are all seen to be moving at the same velocity (1 to 5 mm./sec.) in a relatively narrow column surrounded by a relatively wide zone of cell free plasma. The appearance of blood flowing in arterioles of relatively narrow bore is strikingly different from that of whole blood passing through much wider glass tubes. In conscious rabbits it is evident also that the concentration of cells in the blood is very variable: at one moment there will be a short column of relatively concentrated cells and this will be followed by a column of plasma that is relatively cell free. This may be seen with the aid of a microscope and may be recorded on ciné film at ordinary rates of 25 frames/sec. and exposed for 20 msec. This intermittent concentration of cells may be recognized more easily with the aid of the visual particle velocity meter, and it appears that the velocities of the more concentrated cell columns are the same despite the lengths of the columns. There is of course a rhythmical change in the velocity of blood in an arteriole but this has a much longer periodicity than the pulse wave and is of the order of 10 to 30 sec. depending on the level of general autonomic tone. Under anaesthesia, the arterioles are more dilated as has been described previously,[10] and this periodicity of corpuscular concentration is less evident; it may still be observed, however. If in a conscious rabbit, showing this phenomenon of intermittent concentration of blood cells followed by cell-free columns of plasma, the arteriole is followed back to its larger vessels of origin, it will be appreciated that the cell-free areas, which are the more easily observed, are still apparent in these larger vessels, but this phenomenon is seen less frequently.

The significance of these observations and their analysis will be discussed more fully elsewhere.[11]

The author gratefully acknowledges the advice and encouragement he received from Professor J. D. Boyd as well as a grant from the Royal Society for some of the original apparatus used in this research.

References

1. Basler, A., *Pflügers Arch. Ges. Physiol.*, **171**, 134 (1918).
2. Hugues, J., *Arch. Intern. Physiol.*, **16**, 565 (1953).
3. Bloch, E. H., *Am. J. Anat.*, **110**, 125 (1962).
4. Knisely, M. H., *Anat. Rec.*, **58**, 73 (1934), abstract.
5. Brånemark, P-I., *Scand. J. Clin. Lab. Invest.*, **11**, Suppl. 38, (1959).
6. Monro, P. A. G., *Res. Develop. Ind.*, **15**, 34 (1962).
7. Monro, P. A. G., *Bibliotheca Anat.*, **4**, 34 (1964).
8. Fåhraeus, R., *Physiol. Rev.*, **9**, 241 (1929).
9. Kümin, K., Inaugural Dissertation, Universität Bern. Freiburg in der Schweiz: Palusdruckerei, 1949.
10. Monro, P. A. G., *Bibliotheca Anat.*, **1**, 110 (1961).
11. Monro, P. A. G., *Biorheol.*, in press.

Synopsis

14595

The principles of methods for measuring the velocities of flowing blood cells are discussed. A description is given of a prototype instrument designed to measure directly very slow blood cell velocities seen in small veins as well as the much faster velocities (up to 5 mm./sec.) seen in arterioles in the rabbit ear chamber and in the everted hamster cheek pouch. A more compact eyepiece visual velocity measuring instrument is also described. This may be exchanged for the eyepiece of an ordinary monocular microscope and is more convenient for measuring the very much higher velocities (up to 10^5 times their diameter per second) of blood cells or other particles caused to flow in fine glass tubes. The appearances of blood flowing at high velocities in fine blood vessels are discussed. These indicate that flowing blood in the larger arterioles contains loose aggregates of red cells separated by zones of relatively cell-free plasma.

Author

N67 14596

Flow Pattern Pertaining to Vascular Permeability as Observed by Fluorescence Vital Microscopy

SIEGFRIED WITTE,* *Medizinische Klinik, University of Erlangen, Erlangen, Germany*

Biorheological research has been mainly concerned with the intravascular behavior of the streaming blood.[1] However, one of the main functions of blood vessels is normal permeability allowing an exchange of fluid and substances between intra- and extravascular compartments. Vascular permeability is connected with rheological phenomena. Normal permeability depends on undisturbed intravascular blood flow.[2,3,8,10] When the author started vital microscopic studies of these exchange processes, he found a well-suited untoxic fluorescent dye, brillantsulfoflavin, which is bound to plasma protein fractions.[5] The rheological behavior of these fluorescent-tagged proteins may be observed easily in the rat mesenteric vessels.[6]

The extravascular phenomena connected with permeability will be discussed now in detail. During the author's studies, he found that fluorescence is not restricted to the streaming blood plasma, but will spread from the terminal vascular bed to the surrounding perivascular tissue, as was described some time ago.[6,7,9] With the present techniques of vital microscopy it cannot be decided if the dye in the extravascular space is still bound to proteins or not. However, different forms of dye spreading in the perivascular tissues seem to favor the idea of a dye-protein complex at least during permeation itself.

Under normal experimental conditions, a fine network of tiny capilliform fluorescent streaks will develop. Figure 1 shows the first phase after injection of the dye demonstrating its appearance at the arterial part of the terminal vascular bed, with a filling of the arteriole and several capillaries. In the second phase (Fig. 2) the fluorescent material has reached the venous vessels. Besides, several vessels

PRECEDING PAGE BLANK NOT FILMED.

are surrounded by small fibrous or meshy fluorescent seams, for instance, the arteriole and its capillary branches. Slightly later (Fig. 3) fluorescence has spread in streaks around the venule and its branches.

Fig. 1. Terminal vessels in rat mesentery after intravenous injection of brillant-sulfoflavin. Fluorescent microscopy. 40×. From 5 to 10 sec. interval between Figs. 1–3.

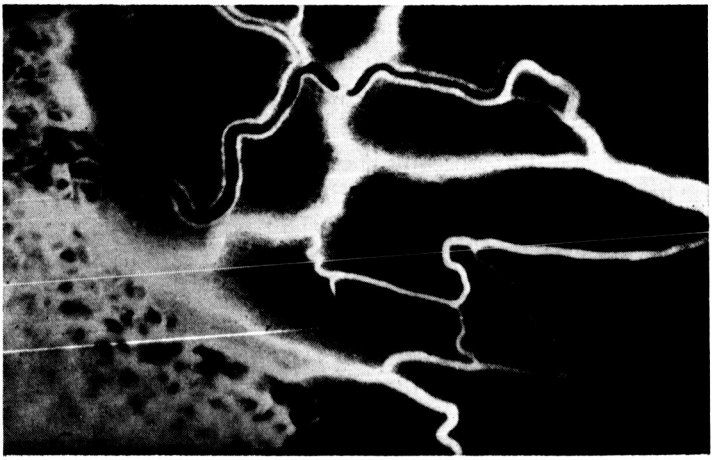

Fig. 2. Same as Fig. 1.

The following figures show another example of the formation of a rather tight perivascular network within the interstitial space. At first (Fig. 4) the nutritive arteriole and the capillaries are labeled brightly by their fluorescent content. The perivascular tissue re-

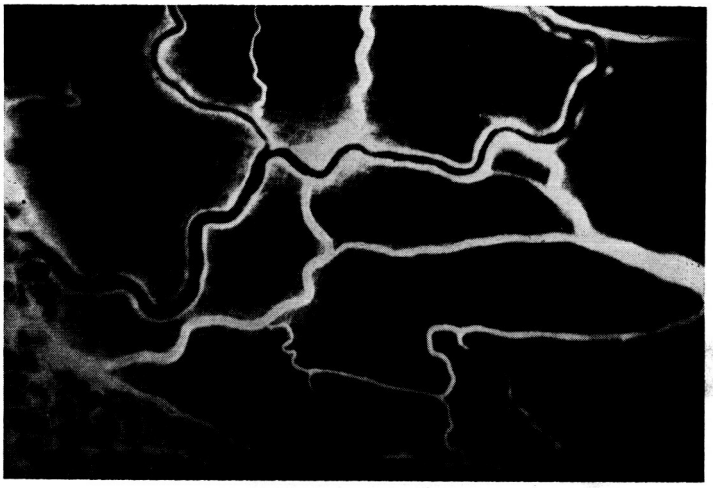

Fig. 3. Same as Fig. 1.

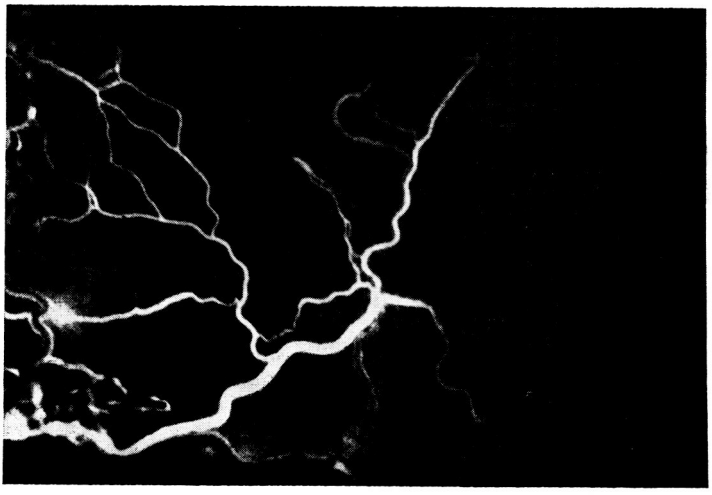

Fig. 4. Additional experiment with same conditions as Fig. 1. From 5 to 10 sec. interval between Figs. 4–7.

mains practically dark. Some seconds later (Fig. 5), a fibrous network which surrounds the capillaries can be seen. Then (Fig. 6) it becomes more pronounced while the intravascular fluorescence decreases and finally (Fig. 7) one can observe an evenly labeled, brightly fluorescent network in the connective tissue.

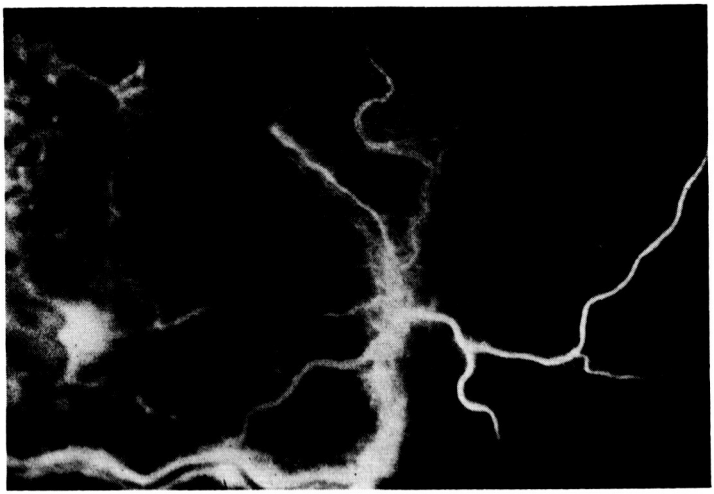

Fig. 5. Additional experiment with same conditions as Fig. 1.

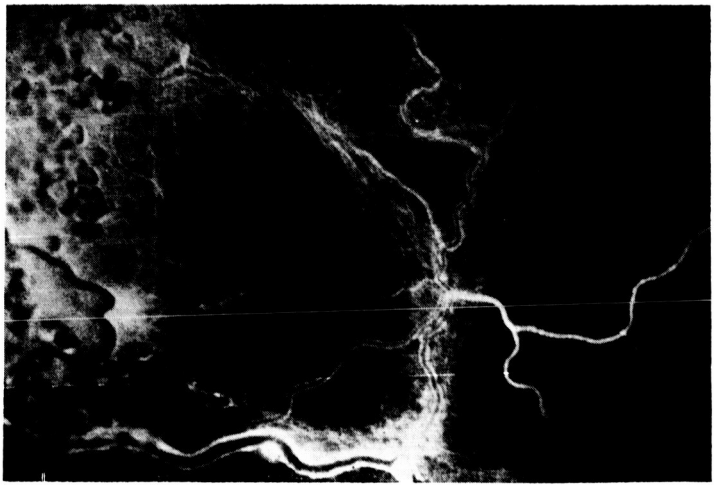

Fig. 6. Additional experiment with same conditions as Fig. 1.

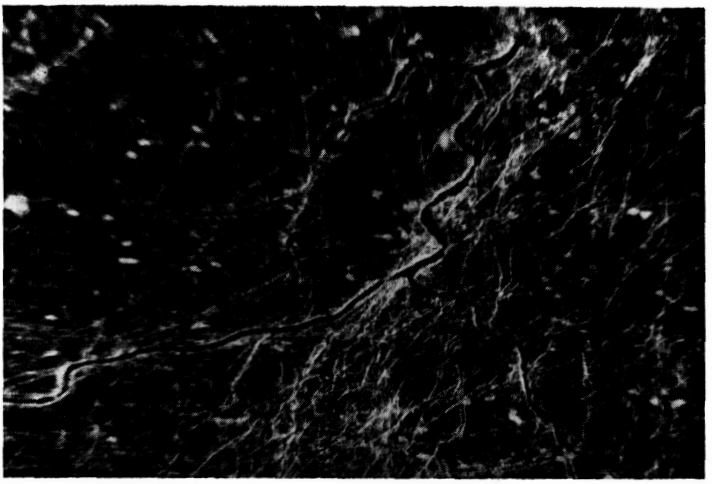

Fig. 9. Capillary network in rat mesentery. Dark-field illumination demonstrating the connective tissue fibers. 40×.

as well as in the already demonstrated network system. The last preparation (Fig. 8) shows distinctly these diffuse clouds of the dye around some capillaries.

One can compare these phenomena with the effect obtained by drawing a fountain pen across blotting paper. The microscopic observations seem to favor the opinion that extravascular fluid transport follows pre-formed routes. They follow the fibrils of the connective tissue as may be seen in the preparations under dark-field illumination (Fig. 9).

By microscopic observation, an attempt was made to estimate the time of dye spreading across the perivascular tissue. With the help of an ocular scale the transit time was measured from the wall of the terminal vessels into the surrounding area at a right angle to the vessel itself. This time was calculated from the first appearance in the vessel under observation until a distance of five marks on the ocular scale, corresponding to 76 μ using a 150-fold magnification, was traversed. Measurements were performed in arterioles, capillaries, and venules as well.

From these results a rough estimation of the medium speed of spreading of fluorescent material was made; of course, there were no exact quantitative times. Preliminary results are summarized in

A completely different form of dye spreading may be observed in cases of pathologically increased vascular permeability. Here, the permeating labeled material spreads in a diffuse and cloudy way

Fig. 7. Same conditions as Fig. 4.

Fig. 8. Terminal vessels in rat mesentery after intravenous injection of brillant-sulfoflavin. Increased vascular permeability after intravenous infusion of thrombin. Fluorescent microscopy. 40×.

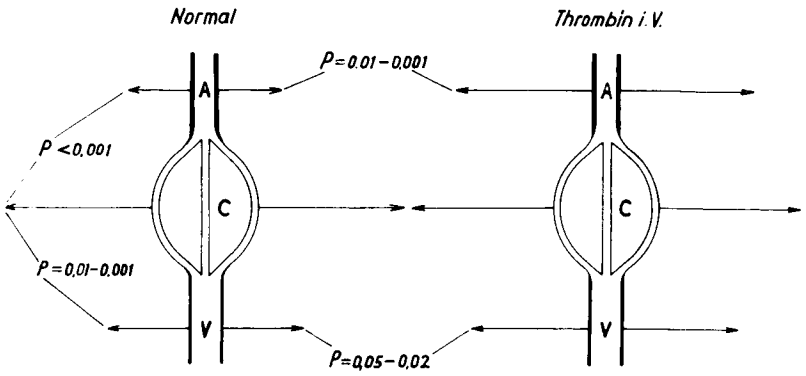

Fig. 10. Schematic presentation of the results of dye transport from the terminal vessels (where *A* is arteriole; *C*, capillary; and *V*, venule) into the surrounding connective tissue. The length of the marks represents the flow rate (total 160 determinations). Left: normal experimental conditions; right: increased vascular permeability after thrombin infusion.

Figure 10. On the left, normal values are tabulated. The drawing is supposed to symbolize the terminal vascular bed with arteriole, capillaries, and venule. The length of the marks corresponds to the medium spreading velocity of the fluorescent material, i.e., the distance covered by the material per second. These are averages of a total of 160 determinations. In spite of the technical imperfections one can see that the dye migrates with different velocity. Maximal speed has been observed for the dye penetrating from the true capillaries. The lowest values are found around arterial vessels whereas the perivenous spreading follows a middle course. The differences between the means are significant. The results may be explained by varying permeability of the different sections of the terminal vascular bed. On the right, the results from model experiments with pathologically increased vascular permeability are shown for comparison. Formerly, it was found that the permeability will be increased regularly after slow intravenous infusion of carefully calculated doses of thrombin, resulting from the disturbed coagulation caused by this coagulation enzyme.[4,7] In this experimental model, an increased spreading velocity of the dye from the arterioles and venules can be seen. The differences between these values and the controls are significant. The pericapillary spreading remains unchanged however, indicating that this speed corresponds to the maximum which

may be attained by the dye transport from the small muscular vessels in pathological state only. This maximal flow rate in the perivascular tissue averaged about 3 μ/sec. in the experiments. In perivascular spreading, the fluid seems to follow fibrous elements of the connective tissue.

It is hoped that these experiments on the rheological behavior of interstitial fluid will contribute to further studies in a new field in biorheology.

Thanks are due Dr. K. Th. Schricker and Mrs. A. Weber for their valuable technical assistance.

References

1. Copley, A. L., and G. Stainsby, eds., *Flow Properties of Blood and Other Biological Systems*, Pergamon, New York-Oxford, 1960.
2. Edlund, T., and L. Juhlin, *Acta Pharmacol. Toxicol.*, **11**, 37 (1955).
3. Szabó, G., and S. Magyar, *Acta Med. Acad. Sci. Hung.*, **16**, 377 (1960).
4. Witte, S., *Folia haematol.*, **1**, 320 (1957).
5. Witte, S., *Z. Ges. Exptl. Med.*, **129**, 181 (1957).
6. Witte, S., *Z. Ges. Exptl. Med.*, **129**, 358 (1957).
7. Witte, S., *Thromb. Diath. Haemorrhag.*, **2**, 146 (1958).
8. Witte, S., *Bibliotheca Anat.*, **1**, 56 (1961).
9. Witte, S., and K. Schricker, *Verhandl. deut. Ges. Inn. Med.*, **66**, 572 (1960).
10. Zweifach, B. W., *Functional Behavior of the Microcirculation*, C. C Thomas, Springfield, Ill., 1961.

Synopsis

14596

The intravascular blood flow forms the basis of an undisturbed vascular permeability. Of special interest is the behavior of macromolecular material especially of the plasma proteins. Visibility of these proteins may be achieved by fluorescent labeling and observation by fluorescent microscopy (rat mesentery). The spreading of the labeled material after passing the wall of the terminal vessels was demonstrated. Two different forms of spreading in the perivascular tissues may be distinguished. Normally, tiny capilliform fluorescent streaks arranged in a network will develop. This phenomenon would be compatible with a flow along a pre-formed system. If permeability is increased pathologically, the extra vascular fluid will spread in a diffuse cloudy manner. The velocity of spreading of fluorescent material was determined. Maximal flow rate occurs for the dye penetrating from capillaries (3 μ/sec.). The lowest values are found around arterioles. In cases of increased vascular permeability, spreading velocity reaches maximal values around all sections of the terminal vascular bed. These investigations of the streaming interstitial fluid will give access to a new field of biorheology.

author

N67 14597

Intracapillary Rheological Phenomena

P-I. BRÅNEMARK,* *Department of Anatomy, University of Gothenburg, Sweden*

The behavior of corpuscles and plasma of the blood in tissue capillaries is of prime importance to the body since it is by an interaction and exchange of material from capillaries to tissue cells and vice versa that these more or less differentiated cells are enabled to survive and function. This is a well-known and well-established fact and so far there are no arguments. However, as soon as we try to analyze what really happens to the blood in the capillaries—how the corpuscles flow, how they change in shape, how the flow properties of the blood suspension change when it is forced through these minute tubes, and how the transfer of particulate and nonparticulate matters through the endothelium occurs—there appears to be as much disagreement as there is agreement on the first statement: the functional interaction and interdependence of capillaries and tissue. Obviously our ignorance in this respect is a serious drawback in our attempts to understand the functions of the body as a biological mechanism.

There are many ways to attack the problem: the flow conditions and properties of blood or other similar suspensions in narrow tubes can be calculated as a purely mathematical, physical problem and the resulting formulas can be tested in model experiments where the flow can be evaluated in different types of tubes and tubular branching. A rapidly increasing amount of information as a result of such attempts is accumulating.[1] Many new facts and ideas of this kind have been presented during the symposium. They help to form a basis for our thinking in terms of rheology and they demonstrate very clearly how complicated things are in capillary tubes.

Unfortunately, however, the biologic situation is even worse because the living tissue capillaries exhibit much more complex,

ever-changing circulatory conditions than any capillary model has ever provided.

How can we try to clear things up? It might be worthwhile starting from scratch, initially avoiding desk calculations and deductions, just carefully watching what really happens in the tissue capillaries of the living body. Here improved vital microscopic techniques may be of assistance by supplying the information required,[2,3] Once we have the correct information then it is time for analysis, simplifications, etc. Probably no single method will definitely tell us what really happens in the capillaries, we shall learn only through a combination of theoretic calculations, model experiments and *in vitro* tests, biochemistry, and vital microscopy.

With these considerations in mind some common intracapillary phenomena will be described which were observed by direct microscopy in living animals and man,[4] but no attempt will be made to give detailed rheologic analysis.

The particulate elements of the blood suspension—erythrocytes, granulocytes, and platelets—indicate intracapillary rheology. However, prerequisite for an evaluation of flow phenomena is detailed information on size, form, and rigidity of the corpuscles.

ERYTHROCYTES

The classical symmetric biconcave disc form,[5] the "rest form," is seldom observed in capillaries (Fig. 1).[6] The red blood cells are characterized by a high degree of plasticity. This means that they are continuously changing in shape as they are exposed to the varying hemodynamic forces when passing the capillaries. It does not however mean that they lack characteristic form. A detailed analysis of their behavior clearly demonstrates that when deviating from the rest form they follow certain regular patterns.

Under *in vivo* conditions the red cell behaves more or less like a rubber membrane stretched within an elastic flexible ring. The different types of deformation (see Fig. 2) can be referred to this model.

A capillary lumen of less than 8 μ, the diameter of a red blood cell, does not definitely constitute a hindrance for the passage of the erythrocyte.[7] By elongation, often in combination with more or less pronounced deformation, it can, without apparent difficulties,

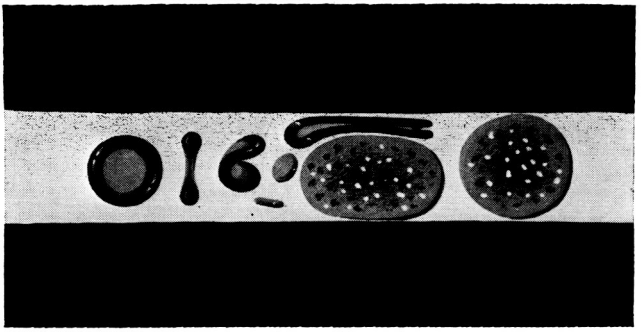

Fig. 1. Schematic illustration of corpuscular shape. The vital microscopic observations have been performed in a modified Leitz Intravital microscope. Microphotographic registration on 35 mm. Gewaert Scientia 39 C 56 film using a modified Arriflex camera with synchronized flash equipment (1/10,000 sec.) and on 16 mm. Kodachrome II using a Paillard-Bolex camera with microadaptor.

The magnification in Figs. 2, 3, 7, and 8 is represented by red cells having a diameter of 7 to 8 μ and a thickness of 1 to 2 μ.

pass a lumen of 2 μ or even less. The elongation is often combined with flection around an axis sometimes situated near the margin of the cell or sometimes close to the center.

Flection is another type of deviation from the original disc form. It may by symmetric or more or less asymmetric depending on the situation of the axis in relation to the center of the cell.

The changes in shape can, however, be further complicated by influence from still another force. Thus the cell may rotate around an axis which forms an angle with the two aforementioned axes. Moreover the picture may be further obscured by a rotation of the cell around the axis of elongation. The resulting shape of the red cell after these various deformations is so complicated that it can hardly be mathematically represented or expressed. This is an example of the difficulties encountered in attempts to reproduce the intracapillary behavior of the blood corpuscles in model experiments.

The most common types of deviation from the original biconcave disc form are crenated cells and spheroid cells. They occur even in normal, healthy subjects but in small numbers. These cells probably represent old erythrocytes just about to be broken down. At changes in osmotic conditions, local or general, these forms appear in increasing number.

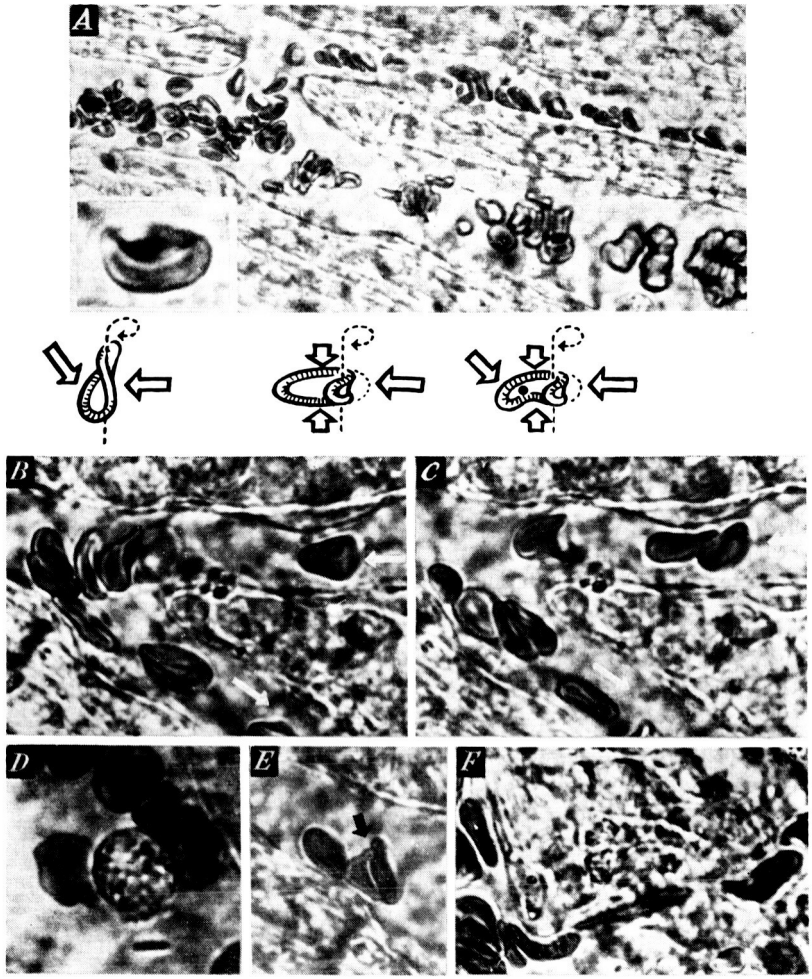

Fig. 2. Human blood cells in capillaries, observed by vital microscopy in a titanium chamber installed in a twin-pedicled skin tube (Brånemark et al., ref. 10). *D*, Rabbits ear chamber (Brånemark and Lindström, ref. 11). (*A*) Different shapes of erythrocytes including rouleaux formation in characteristic wide venules in human granulation tissue. Inset at lower left shows basket-like erythrocyte as observed in a slow flow venule. (*B*) (*C*) Some characteristic types of erythrocyte deformation. The forces acting upon the red cell and the axes of rotation are represented schematically. Observe the protrusion of the nucleus of the endothelial cell into the lumen. (*D*) Granulocyte with processes pointing toward neighboring platelet, suggestive of possible adhesion. (*E*) To the right symmetrically bent and slightly elongated red cell with indentation caused by the marginal zone of the neighboring erythrocyte. Observe the clear plasma layer between the red cell and the endothelium in *B* and *C* as contrasted to *E*. (*F*) Characteristic elongation, irregular deformation, and bending of red cells when passing narrow capillary.

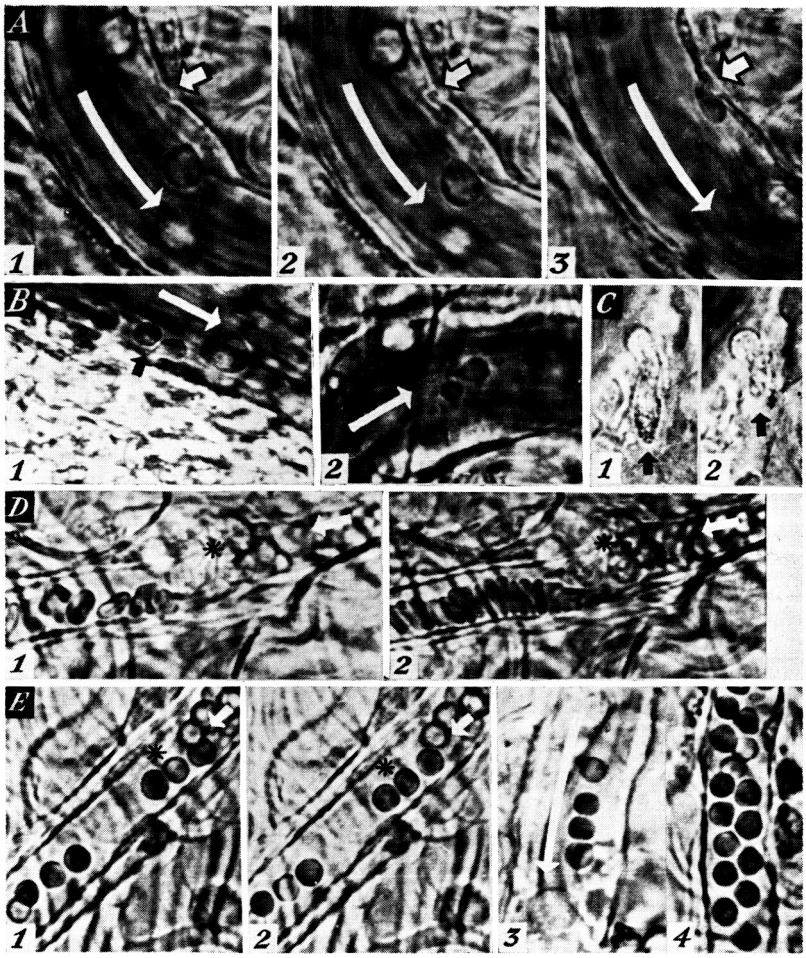

Fig. 3. (*A*)*1–3*: Adhesion of erythrocyte to endothelium (at arrow). Observe granular process at the point of endothelial fixation. Flow velocity is approximately 1 to 1.2 mm./sec. and time interval between the pictures is 0.07 sec. (rabbit's mesentery). (*B*)*1,2*: Point and broad area fixation of erythrocytes to endothelium (*1.* human connective tissue, and 2. rabbit's mesentery). (*C*)*1,2*: Deformation of granulocytes when passing a narrow capillary. Observe regained spheroid form of the granulocyte when entering the wider vessel in 2 (rabbit's ear chamber). (*D*)*1,2*: White cell at * is intermittently blocking corpuscular flow. Observe cardlike arrangement of erythrocytes after passage (rabbit's mesentery). (*E*)*1,2*: Spheroid forms of erythrocytes after local application of hypotone saline. Observe suspect linkage between the two erythrocytes at *. *3*: Spheroid erythrocytes with broad endothelial fixation. Observe intercorpuscular deformation. Flow velocity approximately 1.2 mm./sec. *4*: Characteristic hexagonal deformation of spheroid erythrocytes (rabbit's mesentery).

The static picture of crenated cells might give the impression that they are less deformable than the normal discoid erythrocyte. They might then get stuck in the capillaries by simple mechanical fixation, thereby causing partial or total blockage of flow. This is, however, not the case. On the contrary, the crenated cells are deformable, which enables them to pass even narrow capillaries (see Fig. 7*D6*). Moreover they do not appear to exhibit increased adhesion to one another by their form.

When a number of spheroid cells are subjected to compression, they deform into more or less polygonal shape.[8] They appear to be more form resistant (Fig. 3*E4*) than the disc form and are as a rule only peripherally flattened (Fig. 3*E1,2,3*).

GRANULOCYTES

These cells occur under normal conditions in the circulation as more or less regular spheres, often with varying sizes of processes on the surface (Fig. 1 and Fig. 2*D*). The plasticity is usually much less than that characterizing the red cells. Especially when they pass in the marginal plasma zone, rolling alongside the endothelium, they are slightly flattened in a characteristic way, as if being pressed against the wall.

The granulocytes may, however, also exhibit a high degree of plasticity. This enables their passage through even very narrow capillaries, during which they perform snakelike movements and the granulae are characteristically displaced (Fig. 3*C*). In contrast to the red cell, the granulocyte immediately regains its original form as soon as it enters a vessel of wider caliber (Fig. 2*F* and Fig. 3*C*).

Granulocytes can, however, also be resistant to deformation. They may then constitute a much more common temporary or constant, partial or total, corpuscular and/or plasma hindrance than has been hitherto suspected (Fig. 3*D*).

PLATELETS

As a rule platelets are more or less distinctly disc-formed. They have low contrast *in vivo* but sometimes appear more distinct in plasma possibly after phagocytosis. The shape of the platelet should be analyzed in detail with the aid of methods for high resolution vital microscopy now available.

RELATION OF CORPUSCLES TO ENDOTHELIUM

During certain conditions the blood corpuscles may adhere to the endothelium (Fig. 4). The area of fixation is often only point-sized, sometimes, however, covering a considerable part of the surface of the cell (Fig. 3*B*). The latter type is especially characteristic for granulocytes, forming an endothelial pavement. The mechanism behind this phenomenon was hitherto mainly unknown.

It should be emphasized that the fixation of a corpuscle to the endothelial wall can be established instantaneously even in a rapid flow (Fig. 3*A*). This results in considerable retardation and the fact that adhesion persists even in a rapid flow of 1 mm./sec. or more is at least an indirect measure of its mechanical capacity. It is noteworthy that these wall-adherent corpuscles even after 20 min. or more of exposure to the forces of flow may suddenly be released and join the circulation, apparently regaining their original form and behavior.

When there is a more or less complete microvascular pavement with granulocytes, this may in a histological section simulate complete blockage of the lumen. Before an evaluation of the nutritive

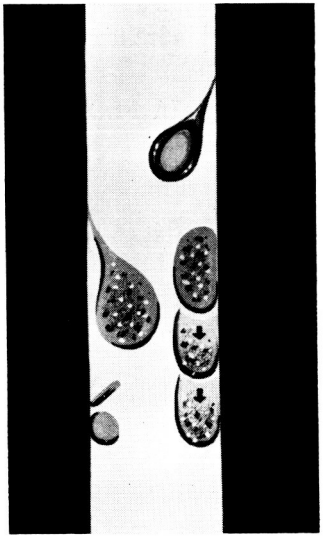

Fig 4. Adhesion of blood cells to endothelium (see comments Fig. 1 caption).

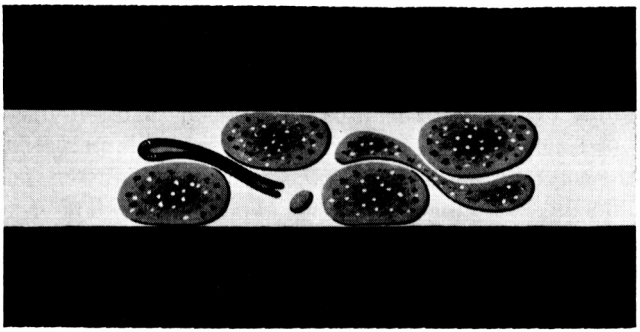

Fig. 5. Granulocyte, platelet, and erythrocyte passing a capillary with white cell pavement (see comments Fig. 1 caption).

status of the tissue is considered and attempted, it should be emphasized that even under these conditions the flow of erythrocytes and platelets often continues remarkably uninfluenced with flow velocities of 1 mm./sec. or even more. The corpuscles then wind their way in the free spaces between the wall-adherent cells (Fig. 5). The red cells pass because of their plasticity, the platelets because of their small size. Even granulocytes pass, but often with some difficulty because of their higher degree of rigidity. They may thereby cause temporary or permanent hindrance to flow.

PLASMA FLOW

The flow patterns of plasma are indicated by the behavior and movements of the erythrocytes and platelets: the erythrocyte by its plasticity and the platelet by its small size. The "turbulence" phenomena (Fig. 6), which are very common in the capillaries and especially at their branching, can thereby be observed (Figs. 7*A* and 7*C*). This enables simultaneous observation of the corpuscular flow and the behavior of the marginal plasma layer. The intermittent flow in capillary short circuits (e.g., in the joint capsule[9]), which occurs under varying physiological conditions, is probably related to the marginal plasma flow in the shunted vessels.

These platelet indicators also demonstrate the various layers of plasma, which in such a whirlpool rotate with different radius and different velocity.

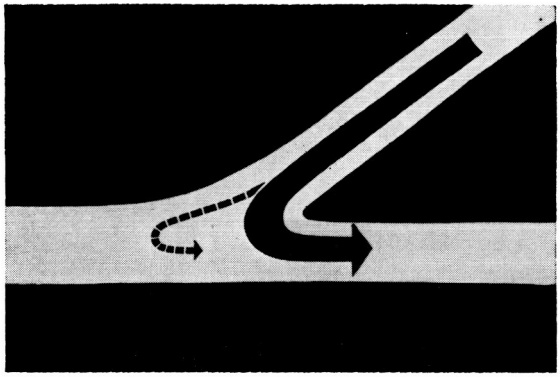

Fig. 6. Direction of plasma flow at arteriolocapillary branching with a distant hindrance in the left branch (see comments Fig. 1 caption).

An interesting phenomenon in relation to turbulence is illustrated in Figure 7*B1–5*. Single erythrocytes very slowly approach a major vessel with high corpuscular velocity (more than 1 mm./sec.). Before being incorporated by this rapid flow, the shape of the red cell fluctuates in a characteristic, periodic manner (Fig. 7*B1–3*) with a length of each cycle of approximately 0.25 sec. This phenomenon appears to elucidate some characteristics of the internal structure of the red cell as well as the rheologic forces in a junction between a slow and a fast flow vessel.

The flow in capillaries is usually not continuous but more or less regularly periodic with varying intervals. Phases of slow flow or stagnation are usually shorter than phases of fast flow (Fig. 8*A*). The transition between slow and fast phases often occurs instantaneously.

A capillary hindrance (relative or complete) influences flow conditions even at a great distance, thus interfering with considerable parts of the capillary system. This is illustrated by the irregular release of corpuscles when one branch of a capillary is distantly blocked, as in Figure 8*B*.

CAPILLARY WALL

The flow conditions in capillaries are influenced not only by variations in intravascular pressure but also by fluctuations in capillary

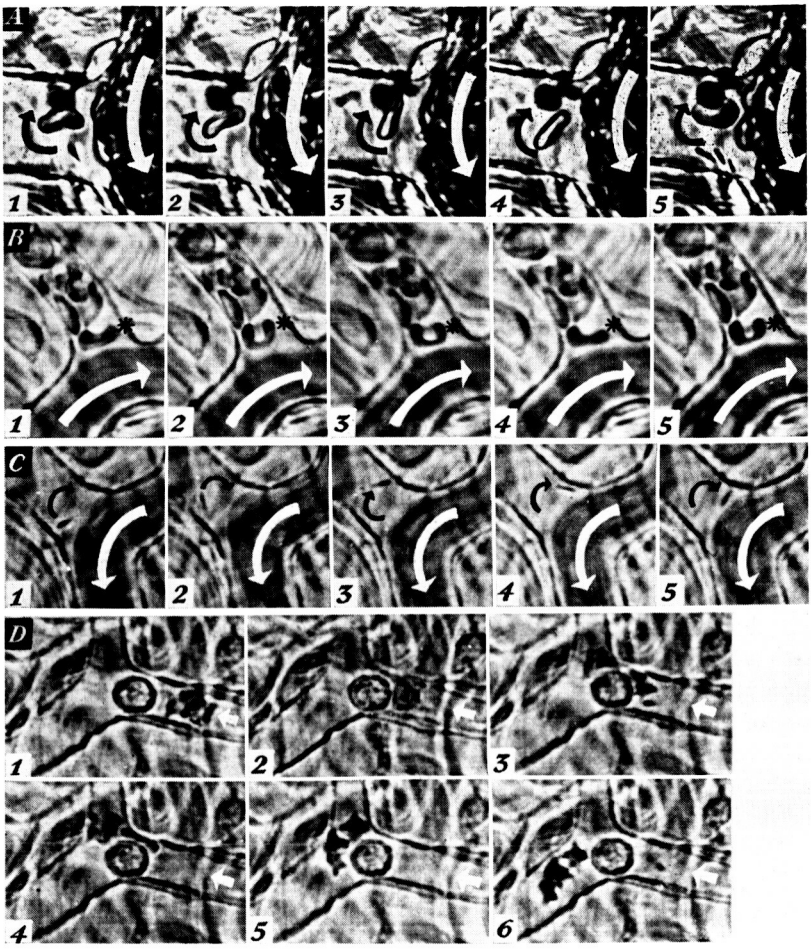

Fig. 7(*A*)*1–5*: Plasma turbulence as indicated by rotating erythrocyte (rabbit's mesentery). (*B*)*1–5*: Periodic deformation of erythrocyte before entering fast flow vessel from almost stagnant vessel. Time interval between pictures, 0.07 sec. Length of cycle (1–3) approximately 0.25 sec. (rabbit's mesentery). (*C*) *1–5*: Plasma turbulence indicated by rotating platelet (rabbit's mesentery). (*D*)*1–6*: Crenated erythrocytes passing between wall-adherent granulocyte and endothelium, space being approximately 2 μ. Observe characteristic deformation in *4* and regained crenated form in *5* and *6*. Note that the granulocyte has changed slightly in position by rotation during the passage of the erythrocytes.

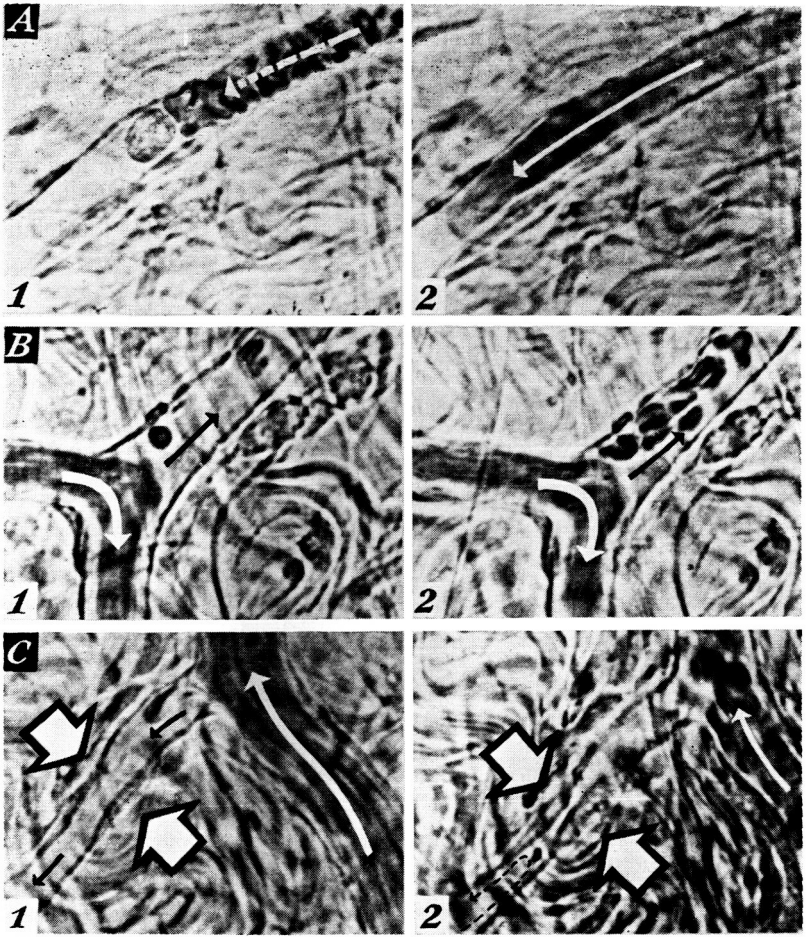

Fig. 8(*A*)*1*, *2*: Different flow phases in a capillary, stagnant in *1* and fast flow (1 mm./sec.) in *2*. Time interval, 0.07 sec. (rabbit's mesentery). (*B*)*1*, *2*: Different flow phases at arteriolar branching, upper vessel being distantly partially blocked. Observe clear plasma layer (rabbit's mesentery). (*C*) *1*, *2*: illustrates interference of capillary flow by structural complex (between arrows) consisting of endothelial plasma layer, nuclear region of endothelial cell and periendothelial mast cell. In *2* a platelet is attempting passage in retrograde direction but failing, indicated by thin dotted arrow (rabbit's mesentery).

caliber and by the endothelial surface. These remarkably often occur at those parts of the capillary where a structural complex consisting of the endothelial plasma layer, the nuclear region of the endothelial cell, and a periendothelial mast cell is situated (Fig. 9 and Fig. 8*C*). The phenomenon, which can be more or less pronounced, causing from slight interference on corpuscular flow to complete blockage, can be initiated by, e.g., changes in local fluid balance.

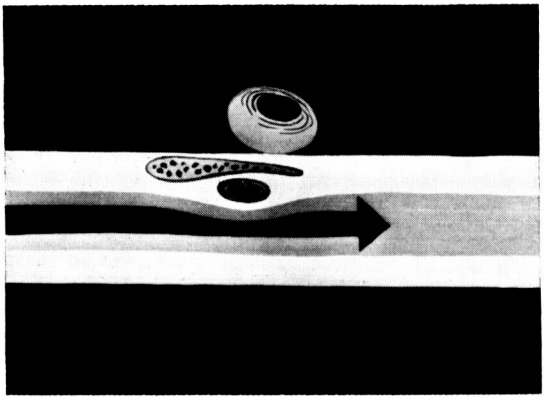

Fig. 9. Structural complex in capillary wall affecting flow (see comments Fig. 1 caption).

Ultra-structure analysis* of corpuscular and internal capillary structure (Figs. 10 and 11) supplies further evidence to vital microscopic information suggesting highly irregular endothelial lining and noncylindrical shape of capillaries.

The agreement in this respect between vital microscopic and electron microscopic information, contradict methodological artefacts. Such errors might, however, influence the distance between corpuscle and endothelium (equals plasma layer) by optical phenomena and by shrinkage, respectively. Thus exact measures on the depth of this layer cannot be given. The unusual case represented in Figure 11*b* in contrast to the ordinary appearance as in Figure 11*a* however indicates that appreciable variation occurs in the depth of the free

* This information was kindly provided by Dr. T. Zelander, University of Gothenburg.

Fig. 10. Survey electron micrograph of a blood capillary in the exocrine rat pancreas: *E*, erythrocyte; *L*, capillary lumen; *N*, endothelial cell nucleus; *EN*, endothelium; *PE*, periendothelial space; and *P*, pancreatic epithelium. 2160×.

plasma layer. This is in good agreement with vital microscopic observations also demonstrating variations in this layer, in one and the same vessel, even at relatively small changes in flow velocity.

The author gratefully acknowledges the cooperation of J. Lindström, U. Breine, K. Aspegren, and I. Jonsson, as well as research assistance by Miss M. Dunér, A.-Chr. Lundgren, and Y. Winsnes. The investigations reported here were supported by grants from The National Heart Institute of USPHS (H-5724), Swedish Association of Heart and Chest Diseases. Antirheum, League, King Gustaf V's Fund, Swedish Cancer Society and Swedish Medical Research Council.

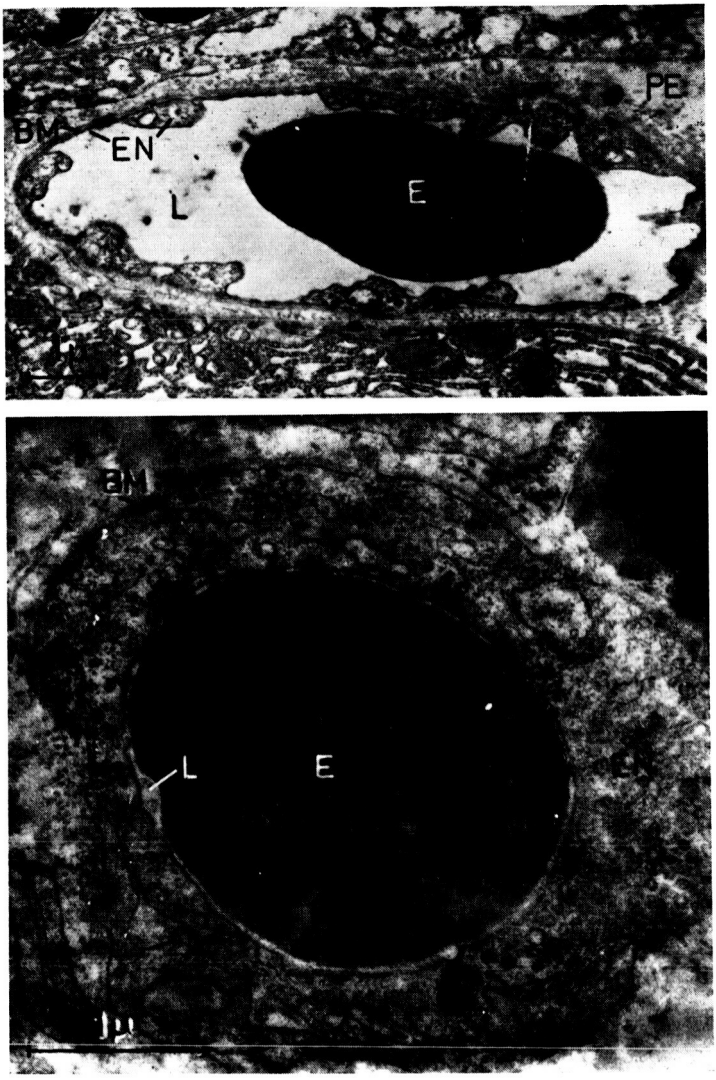

Fig. 11. (*a*) Electron micrograph of obliquely sectioned blood capillary showing the basement membrane and the variable thickness of the endothelium: *E*, erythrocyte; *L*, capillary lumen; *EN*, endothelium; *BM*, basement membrane; and *PE*, periendothelial space. 10,010×. (*b*) Cross section of exceptionally narrow blood capillary. 22,330×. These electron micrographs were kindly provided by Dr. Zelander, University of Gothenburg.

References

1. Whitmore, R. L., *Biorheol.*, **1**, 201 (1963).
2. Brånemark, P-I., *Leitz-Mitteilungen*, **2**, 73 (1962).
3. Brånemark, P-I., *J. Roy. Microscop. Soc.*, **83**, 29 (1964).
4. Brånemark, P-I., *Proc. 3rd Europ. Conf. Microcirc.*, Jerusalem 1964, Bibl. anat., S. Karger, Basel-New York, in press.
5. Prankerd, T. A. J., *The Red Cell*, Blackwell, Oxford, 1961.
6. Brånemark, P-I., and J. Lindström, *Biorheol*, **1**, 139 (1963).
7. Lehmann, H., and R. G. Huntsman, in *Functions of the Blood*, R. G. MacFarlaine and A. H. T. Robb Smith, eds., Academic Press, New York-London, 1961, p. 73.
8. D'Arcy, W. T., in *On Growth and Form*, J. T. Bonner, ed., University Press, Cambridge, 1961.
9. Lindström, J., and P-I. Brånemark, *Arthritis Rheumat.*, **5**, 226 (1962).
10. Brånemark, P-I., K. Aspegren, and U. Breine, *Angiology*, in press.
11. Brånemark, P-I., and J. Lindström, *Anat. Rec.*, **145**, 533 (1963).

Synopsis

14597

Intracapillary flow phenomena, the shape and behavior of the blood corpuscles when passing the capillary system, their relation to one another and to the endothelial wall are described and illustrated microphotographically on the basis of direct microscopic observations of living tissue capillaries in animals and man. The complexity of capillary structure and function is demonstrated. The examples of capillary rheology described and illustrated might form a basis for further calculations and analysis in attempts to understand capillary function.

author

BIORHEOLOGY OF TISSUE MATERIALS

PRECEDING PAGE BLANK NOT FILMED.

N67 14598

Some Mechanical Properties of Collagenous Frameworks and Their Functional Significance

R. D. HARKNESS* and MARGARET L. R. HARKNESS,*
Department of Physiology, University College, London, England

The object of this paper is to consider briefly a number of problems concerning mechanical properties of mammalian connective tissue, in which the authors have been interested.

STRUCTURE OF CONNECTIVE TISSUE

Cells in general have little mechanical strength and are supported by an extracellular connective tissue framework, in which the component of major importance mechanically is the fibrous protein collagen which forms about a quarter of the total body protein or about 5% of body weight.[1,2] The molecules of this protein are collected into *fibrils*, cylindrical structures of approximately uniform diameter along their length which is large (probably $^1/_{10}$ mm. or more) compared to their diameter (usually of the order of 500 to 1000 A.). They are collected into bundles or sheets, but remain separated from one another, being apparently held together by some cementing material which has not been identified with certainty, but is presumed to be a protein polysaccharide gel. Similar or related material is found in the spaces between the bundles of fibrils, blending into a distinct thin (500 A.) surface layer, on which the cells of epithelial surfaces rest.

The evidence that the ultimate resistance of tissues to mechanical deformation depends largely on the extracellular collagenous framework is indirect and based on a general correlation between the presence of this material and mechanical strength. For example, collagen makes up about 90% of the dry material of tendon, a tissue whose only function is mechanical.

PRECEDING PAGE BLANK NOT FILMED.

MECHANICAL PROPERTIES OF THE REPRODUCTIVE TRACT

The first problems examined concerned the tissues of the female reproductive tract.[1,3] The fetuses develop in the uterus in the upper part of the reproductive tract. The passage to the exterior through which they are eventually born is, in effect, a pocket in the skin with skinlike tough inextensible highly collagenous walls (up to 10% of wet weight). The narrowest part of this passage is at the lower end of the uterus, the cervix, which is normally much too small in diameter to allow an object as large as the mature fetus to pass through, and has inextensible collagenous walls. How then is the mature fetus enabled to pass through? The authors examined the effect of tension on the excised cervix of the rat by pulling its walls out between two parallel rods inserted through the central canal, and found evidence of two changes at the end of pregnancy.[4,5] First the cervix behaved as if the passage through it had become wider, i.e., the circumference of the limiting collagenous framework had increased as if it were anticipating the passage of the fetus. The evidence was, in brief, that length-tension curves taken to the point of rupture were similar in the nonpregnant condition and at the end of pregnancy. The central part of the length-tension curve was approximately linear and could be described by the equation $l = l_z\,(1 + kf/f_b)$, where l is the circumference, l_z the circumference obtained by extrapolation of the line to zero tension, f is the tension, f_b is the breaking tension, and k is a constant. The principal change in pregnancy was an increase in l_z.

The circumference did not, however, increase quite to that of the fetus, and in addition another change was found. When the tissue was put under constant load, it extended more readily at the end of pregnancy, a change in its properties which presumably allows expulsive forces at parturition to stretch it to the required size. Evidence was obtained as follows. It was found that in time, after application of a load, the rate of extension became constant. This rate K was measured and expressed as a ratio to the length (which is close to l_z above) l_0 obtained by extrapolation to zero time. The effect of load on this ratio was examined and measurements corrected to constant tension per unit cross-sectional area of collagen (estimated chemically) to enable variations in the state of the tissue under different physiological conditions to be examined. The measurement

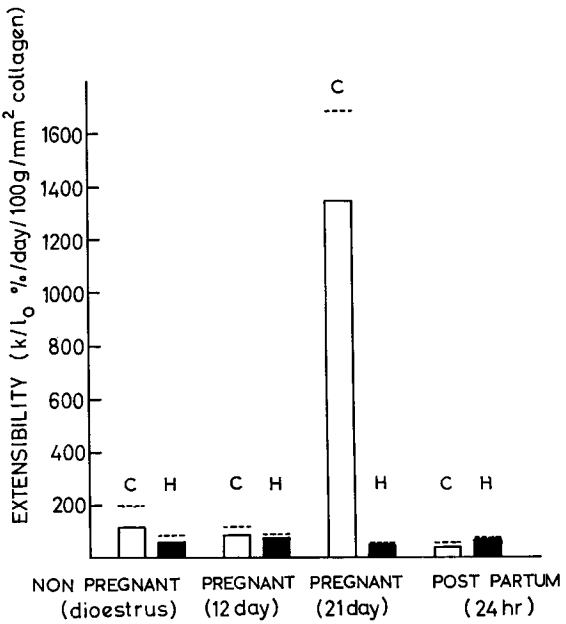

Fig. 1. Comparison between changes in extensibility of the cervix *C* and the uterine horn *H* in pregnancy in the rat. The distance between the dotted line and the top of the column represents the standard error of the mean.

so obtained will be referred to as "extensibility." The ratio (K/l_0) was found to be approximately proportional to the square root of tension (l_0 was little affected by variations in tension).

Examination of the cervix at different times of pregnancy showed that extensibility rose about 10 to 20 times during pregnancy in the rat, and that this change was completely reversed within 24 hr. of parturition.[4,6]

This work was extended in two directions: first to the examination of other parts of the reproductive tract, which showed that the uterus itself was much less extensible than the cervix at the end of pregnancy (Table I and Fig. 1). This is of interest as it suggests a possible cause of difficulty in parturition, namely, an extension of the uterine type of tissue into the cervix. Secondly, an attempt was made to obtain evidence about the nature of the linkages in the tissue which determined extensibility by examining the effect of enzymes.[3,7]

This subject will not be discussed further. It led the authors to look at other tissues primarily in search of a more convenient one on which to examine the effects of enzymes, but also because it was of

TABLE I
Comparison Between Extensibility of Pregnant and Nonpregnant Uterine Horn and Cervix in the Rat[a]

	Uterine horn	Cervix
Nonpregnant (dioestrus)	63 ± 16(5)	115 ± 70(10)
12 day pregnant	68 ± 14(4)	85 ± 30(5)
End of pregnancy (21 days)	39 ± 5(12)	1340 ± 330(8)

[a] Measurements were made on rings of horn or on whole excised cervix at 37°C. The measurements of extensibility is the ratio of rate of extension K under constant load to length l_0 at zero time, obtained by extrapolation, with units $100 \times \text{day}^{-1}$ (per cent per day). All measurements are corrected to tension of 100 g./mm.^{2} cross-sectional area of collagen, calculated for length l_0 from the total collagen content of the sample (measured chemically) assuming it to be evenly distributed. This is from 5 to 10% of the breaking tension. The estimate of variation is the standard error of the mean. The figures in brackets give the number of animals. Figures for uterine horn unpublished; cervix from ref. 6.

interest to compare the specialized tissue they had been examining with what one might describe as more ordinary ones.

MECHANICAL PROPERTIES OF SKIN

The tissue to which the authors paid most attention was skin, a highly collagenous one whose natural function is to a considerable extent mechanical, and which was obtainable in rings which were usable on the same apparatus as used for the cervix.

To begin with, an examination was made of the effect of load on the ratio k/l_0 mentioned above, using rings of skin cut from the rat's ankle, and it was found to be approximately linear. The results, therefore, could not be directly compared with those obtained on the reproductive tract. However, in young animals they were of the same order as in the nonpregnant cervix when corrected to 100 g./mm.^{2} collagen as above, which was from 5 to 10% of breaking tension.[8]

EFFECT OF AGE

Next, the effect of age was examined, since there is evidence that growth of skin involves plastic extension of the collagenous framework in addition to new formation and probably reabsorption of collagen.

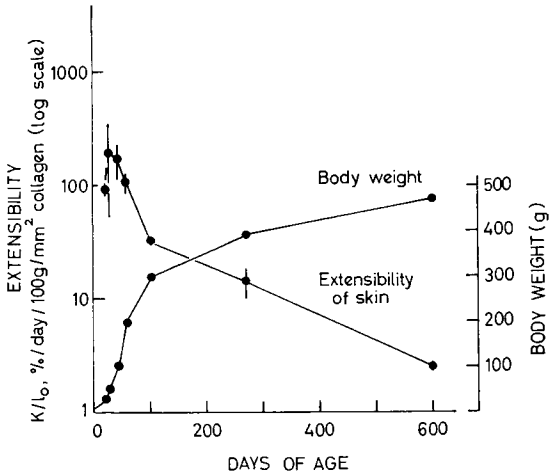

Fig. 2. Extensibility of skin and body weight of rats of different ages. Measurements of extensibility were made on rings of skin from the ankles of male rats, and are corrected to tension of 100 g./mm.^{2} collagen (ref. 8).

Extensibility was found to diminish with age by a factor of about 80 times (Fig. 2), and to be roughly correlated with the specific rate of growth [$(1/l)\ dl/dt$, where l is length and t time] though not enough information was collected to examine the relation in detail. It was found that as extensibility fell with age, tensile strength rose, though the extent of the change was much smaller (3 times).

RELATION BETWEEN EXTENSIBILITY AND TENSILE STRENGTH

An inverse relation between extensibility and tensile strength was found also in experiments with enzymes and on tissues of rats and chicks suffering from lathyrism,[8,9] a condition characterized by weakening of connective tissues and brought about by ingestion of certain leguminous seeds, and a number of pure substances, for example, β-

aminopropionitrile, probably an active factor in these seeds. The relation was approximately $[K/l_0] = af_b^{-3}$, where f_b is breaking tension per unit cross-sectional area of collagen, a is a constant, and $[K/l_0]$ is extensibility (corrected to constant tension per unit cross-sectional area of collagen).

THE SKIN OF THE RAT'S TAIL*

As a consequence of the relation between extensibility and tensile strength, this was measured first instead of extensibility in experiments on enzymes, since the tests are much quicker to do. This led

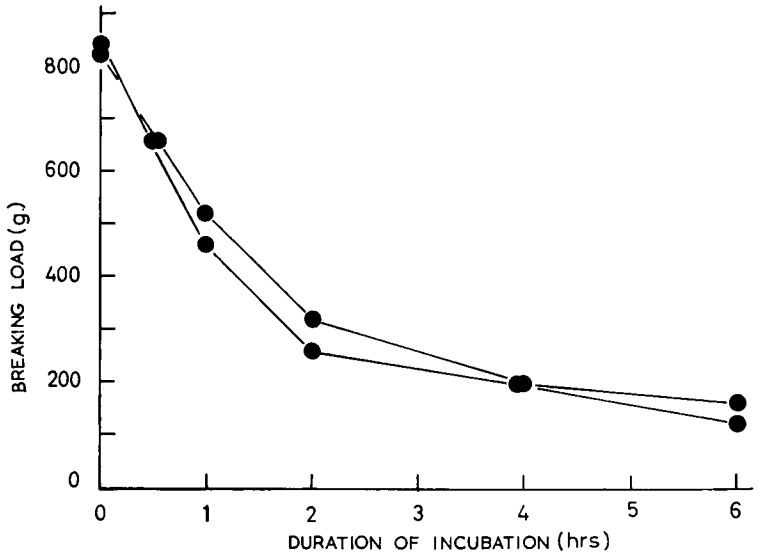

Fig. 3. Effect of incubation in Locke's solution of rings of skin from rat's tail on breaking load. Rings of skin 3 mm. wide, from single rats, were incubated at 37°C. Figures for two sets of such rings are shown in separate curves.

into a digression which is interesting enough to merit a short description. One of the test tissues used was the skin of the rat's tail. This can very easily be cut into rings of standard size and similar properties in an individual tail. These seemed excellent test objects

* This work was done in conjunction with Mrs. P. Fry.

until it was found that by simply incubating them, at 37°C. but also lower temperatures, in physiological salt solutions caused a very large drop in tensile strength in a matter of hours (Fig. 3). Other tissues and skin from other places so far as were tried are not affected in this way.

At first it was supposed that this was an enzymic effect and attempts were made to prove this. The results, however, eventually

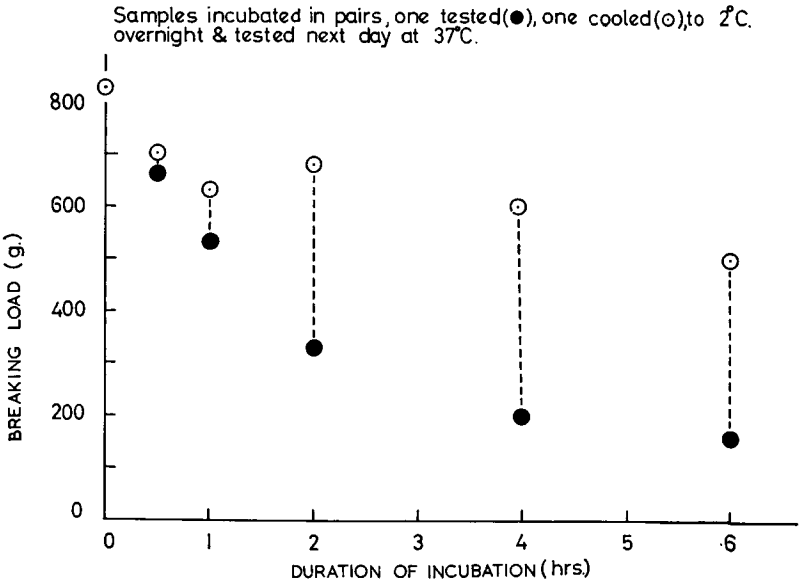

Fig. 4. Effect of incubation followed by cooling to 2°C. overnight on breaking load of rings of skin from tail of rat. Conditions as in Fig. 2.

showed fairly clearly that it was not, the strongest piece of evidence being that the effect was reversed by cooling the sample (Fig. 4).

This effect is still not understood. Its interest is that it suggests the possibility that much smaller changes in the environment of the collagenous framework, than would have been previously expected, might be involved in alterations in mechanical properties under different physiological circumstances, for example, in the rapid change in the cervix in the first day after parturition.

SURFACE MECHANICAL RESISTANCE

The increase in tensile strength with age drew attention to the function of skin as a protective barrier against mechanical assault. As the animal grows older it appears there is a change in the nature of the collagenous framework, such that whatever quantity of collagen is present has more mechanical strength. The total effectiveness of the skin, however, will depend also on the quantity of collagen present, and this, per unit area, is found to increase with age. These two factors, increase in quantity and change in quality (Fig. 5), combine to increase what might be called the "surface mechanical resistance" more than either would alone. A figure has been derived for it by multiplying the quantity of collagen per unit area of skin by the tensile strength. The result is in fact the breaking load per unit length of skin, and the reason for deriving it in this roundabout way is to separate the two factors involved. The value rises with age from about 10 to 150 g./mm. The combination of these two factors, of quantity and of the particular quality measured by tensile strength, obviously give a very imperfect description of surface mechanical resistance, and the value of the term is principally to draw attention

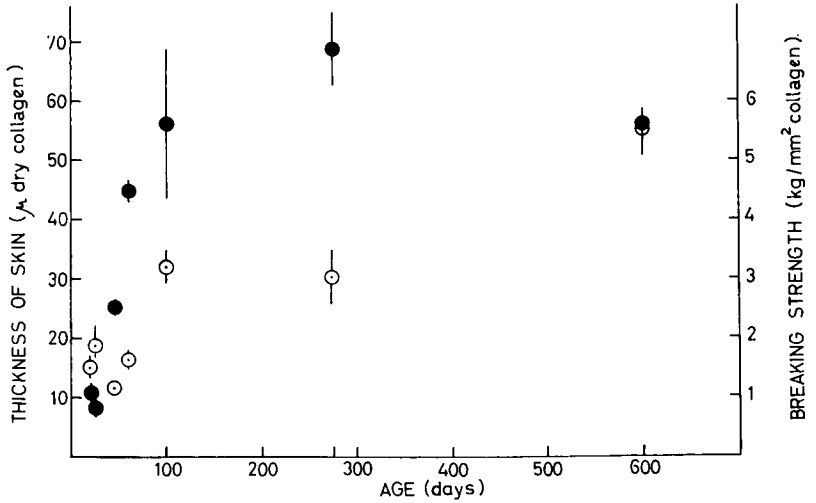

Fig. 5. Breaking strength (○) and thickness (●) of skin collagen in male rats of different ages. There were 45 rats in each group. The length of the vertical lines is twice the standard area of the mean.

to something about which very little is known. It was at least partly the realization of this ignorance that led to the last subject—the skin of an animal with a different order of surface mechanical resistance, namely, the hippopotamus.

THE SKIN OF THE HIPPOPOTAMUS

The hippopotamus has a skin which is strikingly different from that of the majority of animals. First, it is much thicker than usual, particularly on the back and flanks. This is well shown by comparison with the skin of a much larger animal, the elephant (Fig. 6). Secondly, that on the back and flanks is of an unusual consistency being stiffer and less flexible, though no physical examination of these properties has been made. This skin contracts very little in area after removal, unlike that of other animals and of the animal's own abdominal wall, i.e., it contains only a small or no elastic element under tension in life. Some measurements of its tensile strength have been made in collaboration with Professor C. P. Luck (Depart-

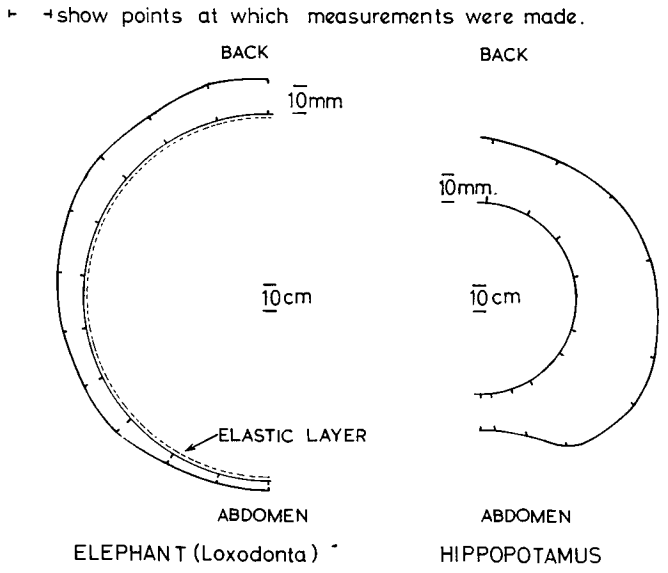

Fig. 6. Diagram of cross section of abdomen in elephant and hippopotamus to show variations in thickness of skin. Both animals were adult females. The scale for thickness of skin is 10 times that for diameter of abdomen.

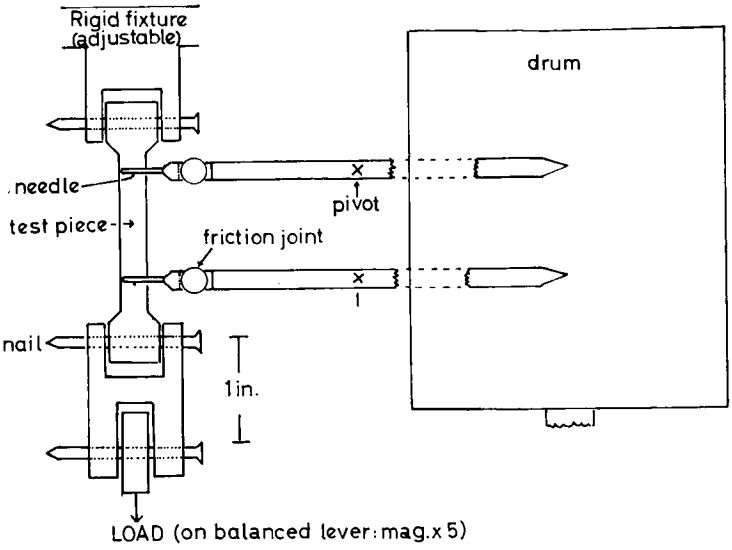

Fig. 7. Diagram to show method of measuring tensile strength of test pieces of hippopotamus skin. The central part of each test piece was cut with scalpel blades fixed parallel to one another 3 mm. apart, the ends shaped with a knife. The effect of load on the distance between the needles was recorded on a drum. Load was increased stepwise by 2 lb. every 15 sec. until the sample broke, rupture occurring at some point between the needles. All material between the needles was subsequently removed and its total hydroxyproline content estimated after acid hydrolysis.

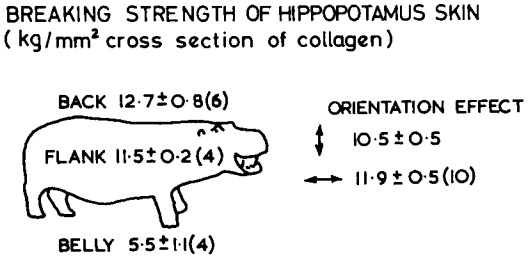

Fig. 8. Diagram showing position from which samples of hippopotamus skin were taken and their properties. The estimate of variation is the standard error of the mean. The number of samples is given in parentheses.

ment of Physiology, Makerere College, Kampala, Uganda). The method is shown diagramatically in Figure 7. Test pieces of square section cut with knives held 3 mm. apart were used. Tensile strength was expressed per unit cross-sectional area of collagen calculated for breaking length from chemical measurements. The measurements gave rather higher figures for back and flanks than in the oldest rats examined (Fig. 8). Figures for belly skin were lower.

The functional significance of the hippopotamus' unusual type of skin is not established, but it seems probable that it is related to the fact that these animals fight vigorously and frequently with their teeth. Their skins are heavily scarred, and appear to have a remarkable power of healing, in spite of being for most of the time immersed in water which must frequently be contaminated heavily with intestinal flora. It is obvious that a much more thorough investigation of this and other types of skin would be of great interest.

CONCLUSIONS

In this article the authors have set out deliberately to consider a number of problems even if superficially and somewhat speculatively. The object has been to show that there is a wide field of biological interest in the study of the rheological properties of connective tissues, in which knowledge is still rudimentary. One might add finally that some of these problems, for example, the properties of the connective tissues of the reproductive tract, or the surface mechanical resistance of the skin in relation to automobile accidents, are also of practical importance in medicine.

The authors are very grateful to the Empire Rheumatism Council of Great Britain for a grant for this work, to the Wellcome Trust for a grant to visit Uganda, and to Dr. R. Laws and to Capt. F. Poppleton for providing facilities for obtaining and examining material from hippopotamus.

References

1. Harkness, R. D., *Biol. Rev.*, **36**, 399 (1961).
2. Harrington, W. F., and P. H. V. Hippel, *Advanc. Protein Chem.*, **16**, 1 (1961).
3. Harkness, M. L. R., and R. D. Harkness, in *Flow Properties of Blood and other Biological Systems*, A. L. Copley and G. Stainsby, eds., Pergamon Press, New York-Oxford, 1960, p. 207.
4. Harkness, M. L. R., and R. D. Harkness, *J. Physiol.*, **148**, 524 (1959).
5. Harkness, R. D., and M. A. Nightingale, *J. Physiol.*, **160**, 214 (1962).
6. Harkness, M. L. R., and R. D. Harkness, *J. Physiol.*, **156**, 112 (1961).

7. Harkness, M. L. R., and R. D. Harkness, *Nature*, **183**, 1821 (1959).
8. Harkness, M. L. R., and R. D. Harkness, *Am. J. Physiol.*, in press.
9. Fry, P., M. L. R. Harkness, R. D. Harkness, and M. Nightingale, *J. Physiol.*, **164**, 77 (1962).

Synopsis

14598

(*1*) Examination of the mechanical properties of the uterine cervix, the narrowest part of the birth canal in the rat, gave evidence that two factors are involved in the change which takes place in pregnancy to allow the birth of the mature fetus; an increase in the natural circumference of the collagenous framework, and an increase in its "extensibility" under tension. This property was measured by the ratio of the rate K of extension, when this had become constant under constant load, to length l_0 at zero time obtained by extrapolation, the figures so obtained being corrected to a standard tension per unit cross-sectional area of collagen, calculated for length l_0 from the total collagen content of the sample. No increase in pregnancy was found in the extensibility of the uterus itself. (*2*) A similar examination of rat's skin showed a marked drop (80 times) in extensibility with age associated with a rise in tensile strength. Thus there appears to be a change in the properties of the collagenous framework of the skin increasing the "surface mechanical resistance" more than would be expected from change in collagen content, which, per unit area, also increases with age. (*3*) Some properties of the skin of an animal with peculiarly high surface mechanical resistance, the hippopotamus, are discussed.

author

N67 14599

Rheology of Synovial Fluid and Its Role in Joint Lubrication

LEOPOLD DINTENFASS,* *Sydney Hospital and the Department of Medicine, University of Sydney, Sydney, Australia*

INTRODUCTION

A review of studies by Barnett, Davies, MacConaill, Charnley, Ogston, Sundblad, and others indicates that there exists a tendency to explain the lubricating mechanism existing in synovial joints by either the lubricating properties of synovial fluid or the lubricating properties of the articular surfaces. The proponents of the respective hypothesis attempted to apply either the theory of hydrodynamic lubrication or the theory of boundary lubrication. Neither of these theories, however, can represent the lubrication mechanism in joints; both theories are too crude for this purpose. The nearest approach to reality appears to be represented by more recent elastohydrodynamic theories. It is the aim of this paper to show that both the synovial fluid and the articular cartilage play an important role in the joint lubrication, and that thixotropy of synovial fluid is the key parameter in the lubricating performance of the synovial fluid itself, and of the cartilage whose pores it fills. It will be suggested also that any pathological changes in either the synovial fluid or the articular cartilage, lead to a breakdown of joint lubrication.

PHYSIOLOGICAL ASPECTS OF SYNOVIAL JOINTS

Diarthrodial joints are comprised of two or more opposing cartilage-covered bone ends, joined by a flexible tube of dense connective tissue, the articular capsule,[1] which is lined with the synovial membrane. Within this enclosure is a small quantity (from 0.1 to 1 ml.) of clear and viscous fluid, the synovial fluid. Adjacent to the joints are tissue components such as fluid. Adjacent to the joints are tis-

sue components such as ligaments, fascial layers, tendons, tendon sheaths, and bursae. Not only are these structures of great importance in the normal mechanical functions of the joint but in the majority of articular diseases they are either primarily or secondarily affected. Since articular cartilage, an elastic and avascular tissue, is the recipient of most of the mechanical shocks and stresses that are exerted upon the skeleton, it is apparent that the smooth cartilagenous surface, so essential in normal joint function, is constantly endangered.

Movements of joints are of the following types: sliding, rotation, and rolling. The proportions of these components of joint movement vary with the type of joint and with the type of movement. Under all conditions, various degrees of pressure are exerted. Pressure in the hip joint may be as high as 450 lb. psi according to Osborne and Fahrni.[2] As the femoral head acts as a fulcrum of a lever, moments of 700 kg. cm. and the vertical reacting force of 200 kg. may be observed.[3] The effects produced by these pressures may be even larger than it would appear from the static measurements due to the fact that the movements of joints are not unidirectional but reciprocal.[4]

A REVIEW OF SOME PRESENT IDEAS ON LUBRICATION IN JOINTS

The excellent lubricating properties and low-friction performance of synovial joints are well known, but the actual reasons for these phenomena and their mechanics are obscure. The frictional properties of synovial joints are 10-fold and 100-fold better than those of engineering designs working under comparable conditions. The coefficient of friction for synovial joints was reported to be[5] only 0.0075, and even as low[6] as 0.002.

Sundblad[7] suggested that the lubrication is achieved mainly by a wedgelike fluid film which undergoes continuous displacement. Ogston and Stanier[8] stated that synovial fluid is well suited for the lubrication of a bearing required to carry a load at varying rates of movements. At higher rates of movement the viscosity falls and the drag on the joint is relatively lessened, while the load which it can bear is not reduced because the greater rate of movement more than offsets the decrease in viscosity. The elasticity[9] of synovial fluid may be significant, because under stress rapidly applied an elastic fluid yields

less than a viscous fluid; the latter deforms irreversibly, the energy of deformation dissipating as heat. Elastic fluid would protect synovial membranes when a sudden stress is applied. The thixotropic properties of synovial fluid and the resulting ability of the fluid to support high loads at low rates of shear were appreciated by Barnett et al.[10] The theory of a wedgelike film, that is, the theory of the hydrodynamic lubrication, was promoted by MacConaill[11] who suggested also that a convergent viscous film is set up in the region of the load-line of the joint by the action of the intra-articular cartilages which set themselves at a slight inclination to the flattened moving surface. While the theory of hydrodynamic lubrication in joints was supported by Barnett et al., it was strongly opposed by Charnley[12–14] who suggested the existence of boundary lubrication conditions in joints. Charnley argued that the resiliency of articular permits an intimate contact between opposing surfaces, thus negating the concept of a wedgelike lubricant. He considered also that hydrodynamic lubrication is unsuitable in a reciprocating motion, and even impossible in the case of slow-moving surfaces under heavy loads. Charnley believed that the synovial fluid is not essential for lubrication and that only the surfaces themselves play a part in the joint lubrication.

Articular cartilage was found to be a sponge by Lewis and McCutchen who suggested that lubrication in joints is due to the synovial fluid being squeezed out from the porous cartilage under pressure.[6,15]

THEORIES OF LUBRICATION IN ENGINEERING SYSTEMS

In order to appreciate the lubrication mechanism of synovial joints it is considered necessary to review some of the present theories of lubrication. Evaluation of these theories, carried out in the following section, will serve as a basis for discussion of joint lubrication.

Theories of lubrication[16–19] are concerned with frictional and deformation phenomena of and between two solid bodies which slide, rotate, or roll one over the other. Under coefficient of sliding friction we understand a coefficient of proportionality f between load W and the force F required to slide this load. If we place a block of metal on a metal plate, the force required to slide this block may be quite large. The sliding does not take place over the whole surface of the block but only over a restricted number of contact points.

Even on highly polished metals the surface irregularities are large in relation to molecular size and may be compared in shape to alpine peaks and valleys. When two surfaces are brought together the area of contact is determined by a number of these asperities. At such points intense pressures are generated by very small loads, thus causing plastic deformation of the softer surfaces. When one metal surface is moved over another, the work of friction, related to the very small contact area, results in generation of high surface temperatures, even of the order of 1000°C. Much of the work necessary to slide one metal surface over another is due to shearing of microwelds which are constantly being broken and reformed.

Friction of rubber or rubberlike materials over metal is due to two main causes:[20] (*1*) the adhesion of rubber to the surface, and (*2*) to deformation occurring in the rubber when it slides on surfaces.

Boundary Lubrication

Boundary lubrication[17] involves simultaneous deformation of the surface and of the lubricant. The coefficient of friction is independent of the viscosity of the lubricant and of the sliding velocity. The fluid film reduces friction by two mechanisms: (*1*) by reducing the proneness of surfaces for local welding, and (*2*) by carrying part of the load.

If one surface is metal and the other is rubber, the elasticity of rubber will influence the friction. The area of contact no longer will be proportional to the load W but will be proportional to the term $(W/E)^{2/3}$, where E is the elastic modulus of the rubbery surface.

Hydrodynamic Lubrication

Under the conditions of hydrodynamic lubrication, a fluid pressure is generated in a wedge of lubricant that forms as a result of motion of two surfaces, and this pressure supports the load and keeps the sliding surfaces completely separated. The thickness of this film depends entirely upon the viscosity of the lubricant η, the sliding velocity V, the load W, and the dimensions of the bearing. The following equation[17] relates the load-carrying capacity to other parameters.

$$W/\eta V = 1.23D^2/Ch \tag{1}$$

where C is the diametrical bearing clearance, H the minimum film thickness, and D the diameter of the journal (inner component of the rotating system).

The frictional drag is given by

$$f = K(\eta V/W)^{0.5} \tag{2}$$

where K is a numerical constant of the order of unity.

The above equations are valid only at very low loads or at very high speeds.

Quasihydrodynamic Lubrication

Larsen and Perry[21] suggested that, as the value of $\eta V/W$ increases, the friction decreases to a minimum and then rises slightly in the region described as quasihydrodynamic lubrication The film thickness is supposed to be low, but its wedge-forming capability depends on the presence of polar compounds (such as carboxylic acids). These compounds, by being adsorbed onto the surfaces, promote the wedging effect. Polar films may exist under conditions of load and speed which would not be permitted by the classical hydrodynamic theory; the latter would expect such film to be squeezed out.

Contact Lubrication

Experimental studies of Archard and Kirk[22] indicated that the viscosity of lubricants is pressure dependent That is, the viscosity of lubricant increases with the pressure applied. Consequently, higher loads can be supported than expected from the classical theory of hydrodynamic lubrication.

$$h = 0.67(\alpha\eta V)^{2/3}R^{1/3} \tag{3}$$

where α is the coefficient of pressure-induced changes in viscosity; this is equal to 3×10^{-9} cm.^{2}/dyne for many commercial lubricants; R is the relative radius of the curvature, defined as $1/R = 1/R' + 1/R''$, where R' and R'' are radii of the inner and the outer component, respectively.

Elastohydrodynamic Lubrication

The elastohydrodynamic lubrication represents the third departure from the classical hydrodynamic theory, this one being due to the

elastic deformation of surfaces. Crook[23] found appreciable elastic deformations under heavy loads. As, simultaneously, the viscosity of lubricant increased, the film thickness remained independent of load, slightly dependent on speed, and greatly dependent on temperature. In other words, the film thickness depended primarily on the viscosity of the lubricant. The film thickness was of the order of one micron.[24] Blok[25] stressed that the elastohydrodynamic theory permits the film thickness to be hundredfold higher than that obtained from the classical hydrodynamic theory. Blok suggested two following expressions:[25,26]

$$h = 1.18R(W/ER)^{-1/11} \cdot [\eta\alpha(V' + V'')/R]^{8/11} \quad (4)$$

where E is the reduced Young's modulus: $1/E = 0.5(1 - v_1^2)/E' + (1 - v_2^2)/E''$ where E' and E'' are moduli for the two surfaces, while v_1 and v_2 are their respective Poisson's ratios; V' and V'' are the sliding and the rolling velocities.

$$f = 1.33(P/\alpha)^{1/2} \cdot (P/E)^{-5/8} \cdot (\eta V_r/RE)^{3/8} \cdot (V_s'/V'') \cdot (\lambda/\beta\eta V'^2) \cdot [1 + 2(\alpha/P) \cdot \ln(8\lambda/\beta\eta V'^2)^{-1}] \quad (5)$$

where β is the coefficient relating viscosity of lubricant to temperature, P the maximum pressure in film, and λ the heat conductivity of lubricant.

The film thickness may be quite small when compared with the local elastic deformations.[27] Notwithstanding this fact, the film will exist under very intense pressures.[28]

ELUCIDATION OF INFORMATION ON JOINT LUBRICATION THROUGH APPLICATION OF LUBRICATION EQUATIONS TO SYNOVIAL JOINTS

In evaluation of lubrication equations and in elucidation of information by means of these equations it is important to know the viscosity of synovial fluid. As illustrated by Figure 1, the viscosity of healthy synovial fluid is at least about 100 poises at the rate of shear of about 0.1 sec.$^{-1}$ and about 1 poise at the rate of shear of 100 sec.$^{-1}$.

Evaluation of the Classical Hydrodynamic Equation (1)

In order to assume easy working conditions in joint, the load of only 30 kg. will be substituted into equation; the corresponding di-

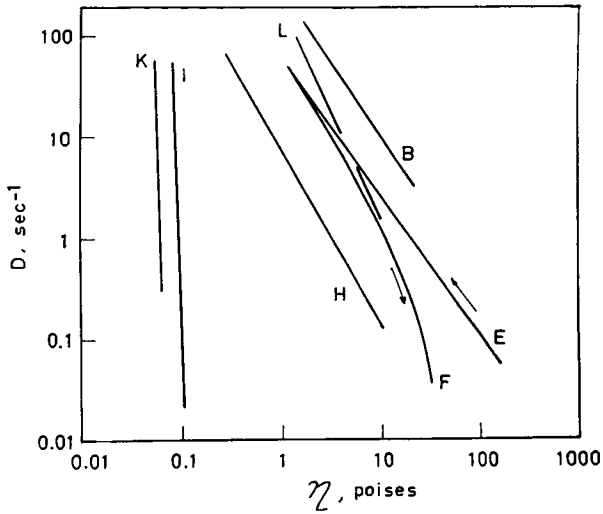

Fig. 1. Flow curves of human and animal synovial fluid. Viscosity η is plotted against the rate of shear D on a log-log scale. Flow curves of human synovial fluid are after Bloch and Dintenfass (ref. 29); K and I represent synovial fluid from rheumatoid arthritis cases; B, E, and F represent synovial fluid from traumatic arthritis cases. Please note that viscosity of the fluid depends on the rheological history, as illustrated by curves E and F, determined consecutively and in the opposing direction of rates of shear. Curve H is after Ogston and Stanier (refs. 8 and 35) and represents ox synovial fluid. Curve L is after Sundblad (ref. 7) and represents a 0.24% solution of hyaluronic acid.

ameter D of the spherical part of the joint is assumed to be 2 cm., and the diametrical clearance to be 0.2 cm. while the film thickness in the working region is assumed to be one micron. After substitution we obtain $\eta V = 100$. If we substitute for the velocity of movement 1 cm./sec., the corresponding viscosity of the synovial fluid should be 100 poises. The rate of shear developed in a gap of one micron and relative velocity of surfaces of 1 cm./sec. would be 10,000 sec.$^{-1}$. This is incompatible with the experimental results: if the viscosity of synovial fluid is to be equal 100 poises, the rate of shear cannot be 10,000 sec.$^{-1}$; at such high rate of shear the actual viscosity of synovial fluid will be well below 0.1 poise. Viscosity of synovial fluid will be about 100 poises if the rate of shear will be no more than 0.1 sec.$^{-1}$. Discrepancy between the theory and the experimental findings is about 100,000-fold. This discrepancy will not be affected if different

values are assumed for the film thickness. Any increase in the film thickness will bring about a simultaneous decrease in the rate of shear. For instance, if the film thickness were 0.01 cm., the term ηV will be equal 10,000. At velocity of movements of 1 cm./sec., the viscosity of synovial fluid would be 10,000 poises, while the rate of shear calculated will be 100 sec.$^{-1}$. As the viscosity of 10,000 poises corresponds in reality to the rate of shear of 0.001 sec.$^{-1}$, the discrepancy between the theory and experiment will remain 100,000-fold. An increased load will cause this discrepancy to be magnified.

Evaluation of Blok's Equation (4)

In the elastohydrodynamic equations it is necessary to substitute a value for the modulus of elasticity of cartilage. Using the deformation curves for bone and cartilage, and for bone alone, obtained recently by Camosso and Marotti,[30] one can calculate the elastic modulus to be from 500 to 2500 kg./cm.^{1}. Elastic modulus given by McCutchen[6] for articular cartilage soaked in water is only from 5 to 110 kg./cm.^{2}. If any of these values will be substituted to eq. (4), the load being assumed to be about 200 kg., the calculated viscosity of synovial fluid will be between 100 and 500 poises, at sliding velocity of 1 cm./sec. While the discrepancy is large again, an uncertainty is introduced through assumed values for the elastic modulus of the cartilage. As cartilage appears to be time and rate of shear dependent, the Blok's equation should be perhaps modified to accommodate such parameters.

The main discrepancy of the cited and other equations lies in the extraordinary high values for viscosity calculated through them, these values not corresponding to the experimental data. Calculated and experimental values of viscosity of synovial fluid cannot be reconciled unless it is postulated that the rate of shear developed in a joint is much less than that developed between two rigid surfaces, the gap and the velocity being equal.

It is quite likely that an elastic deformation of cartilage takes place not only in the plane normal to the plane of surfaces but also in the plane parallel to the plane of surfaces. If, as a result of the latter deformation during joint movements, one of the articular surfaces lags behind by only one millimeter, the rate of shear across one micron gap will be decreased by a factor of 1000. Another cause of a decrease in the effective rates of shear might be the nonequilibrium con-

dition prevailing in the gap between articular surfaces, due to the intermittent and reciprocating type of movement. Thixotropic breakdown of synovial fluid might be less than the one corresponding to the nominal rate of shear under equilibrium conditions.[31] This mechanism may be responsible for a 100-fold discrepancy between the calculated and actual viscosity of synovial fluid or may be responsible for a 100-fold discrepancy between the nominal and the effective rate of shear.

The above may be specially true for elastohydrodynamic theories of lubrication. Tanner[32] suggested recently that the criterion of application of the elastohydrodynamic theory to joint lubrication is a question if the elastic deformation (in axial direction) results in an area of contact comparable in dimension with the area of articular cartilage. As the preliminary calculations gave an affirmative answer, it appears that elastohydrodynamic theory, and elaborations of this theory, should be of value in considerations of joint lubrications.

SYNOVIAL FLUID IN JOINT LUBRICATION

It is the author's belief that the key to the solution of lubricating mechanism in joints rests in the rheology of synovial fluid. Unless a clear picture is obtained of the rheological properties of this fluid, in health and in disease, an application of engineering solutions is not feasible.

The fact that synovial fluid exhibits non-Newtonian characteristics has not been appreciated for a long time, and it is quite recently that Barnett,[33] Davies and Barnett,[34] and Ogston and Stanier[8,35] determined the viscosity of synovial fluid as a function of the velocity gradient. The data obtained by some of these investigators, and by Bloch and Dintenfass,[29] are illustrated by Figure 1. Synovial fluid obtained from healthy humans and animals shows thixotropy, while synovial fluid obtained from rheumatoid arthritis cases exhibits Newtonian flow.

It has been shown conclusively[7] that viscosity and thixotropy of synovial fluid is chiefly due to its content of hyaluronic acid. A breakdown of the polysaccharide with hyaluronidase or its removal by acetic acid precipitation reduced the viscosity of synovial fluid to viscosity of water, whereas protein splitting enzymes did not show such

pronounced effect.[7] However, Blomberg and Ogston[36] observed that papain-treated hyaluronic acid shows Newtonian properties. They suggested that removal of protein from the hyaluronic acid-protein complex leads to important changes in the physicochemical properties of the synovial fluid.

It should be noted that Newtonian flow is exhibited by fluid obtained from rheumatoid arthritis cases, whereas fluid obtained from the traumatic arthritis shows thixotropic behavior. It might appear at first sight that such difference in rheological behavior may be due to a reduction in the concentration of hyaluronic acid or changes in protein or lipid content That this is not the case has been shown by Sundblad[7] who found that while in traumatic arthritis the content of hyaluronic acid varies from 0.10 to 0.17 g. per 100 ml., in rheumatoid arthritis this content is about 0.15 g. per 100 ml. Also, Nettelbladt and Sundblad[37] showed in an electrophoretic study that there is no difference in the albumin and gamma globulin content between fluid from rheumatoid arthritis and osteoarthritis cases.

It appears that the rheological changes in synovial fluid are not due primarily to some variations in the chemical composition of the fluid, but are due to some physicochemical changes. The presence of thixotropy may be expected to be due to aggregation and coiling of hyaluronic acid molecules and to formation of intermolecular bonds. In Newtonian systems such aggregation and intermolecular bonds would be absent.

Ogston and Stanier[8] rightly stated that synovial fluid is very well suited for the lubrication of a bearing required to carry a load at varying rates of movement. At higher rates of movement the viscosity falls and the drag of the joint is relatively lessened, while the load which it can bear is not reduced because the greater rate of movement more than offsets the decrease in viscosity.

Synovial fluid was observed to show some degree of elasticity.[8,38] On repeated shearing the flow times may increase.[7,38] These phenomena suggest that synovial fluid might behave as an elastic gel, especially under conditions of rapid or transient stresses. A formation of an instantaneous gel might be perhaps related to the so-called "normal stress" in which a pressure normal to the plane of surfaces is exerted during rotation or sliding. The elasticity of synovial fluid[9] may be significant because, under stress rapidly applied, an elastic gel will yield less than a viscous fluid. Such action would

protect the synovial membranes when a sudden stress is applied. Also, the fluid cannot be squeezed out from the space between the articular surfaces under conditions of sudden stresses.

Synovial fluid shows the following attributes: (*1*) thixotropy, which permits constant load-bearing property; (*2*) wetting of surfaces, which is due to affinity of hyaluronic acid and articular cartilage; (*3*) elasticity and/or normal stress, which prevent the fluid to be squeezed out from the gap; and (*4*) good heat conductivity, which permits a rapid heat transfer away from the sliding surfaces.

That the synovial fluid is indeed required for proper lubrication and functioning of joints may be judged from the effect caused by a fall in temperature. As shown by Hunter et al.[39] and Horwath and Hollander,[40] a drop in temperature causes an increased resistance of joints to movement and causes a decrease in the exertable external force. Both phenomena are due to an increase in the viscosity of synovial fluid and, to some degree, to changes in the elasticity of the cartilage.

ARTICULAR CARTILAGE IN JOINT LUBRICATION

Camosso and Marotti[30] found that articular cartilage shows an elastic response under low stresses of short duration and plastic deformation under higher stresses. These data can be explained on the basis of observations made by McCutchen and on the basis of the fact that synovial fluid is thixotropic. McCutchen[6] found that articular cartilage is a porous, spongelike body, the solid matrix representing only 59% of the total volume. Short-time deformations indicated that cartilage soaked in water has a modulus of about 110 kg./cm.^{2}, while long-time deformations resulted in an elastic modulus of only 5 kg./cm.^{2}. As the synovial fluid is a thixotropic fluid, and as it fills the pores of the spongelike cartilage, it may be expected that the elastic modulus of the cartilage varies over a thousandfold range as a function of time and stress.

A sponge filled with thixotropic fluid would be expected to show a high elastic modulus at instantaneous stresses. Instantaneous plastic properties of synovial fluid and high viscosity at low rates of shear or at very short stresses will help to reinforce the articular cartilage for the event of sudden high load. Such behavior will coincide with the elastohydrodynamic considerations which require

a set ratio of load and elastic modulus. It may be noted that elastic deformations of bone and cartilage were less in older animals as against younger and lighter animals.[30]

The presence of synovial fluid in cartilage pores explains the affinity of synovial fluid to cartilage. While McCutchen believes that such structure should permit a lubrication through "weeping," that is, through the film being formed by a fluid squeezed out from the cartilage under pressure,[6,41] it could be rather expected that a sponge, filled with a liquid, will be capable not only of extruding this fluid under pressure but also of sucking-in this fluid and preventing cavitation.[42]

It should be easy to appreciate that elastic deformations of cartilage will cause a decrease in pressure existing in the lubricating fluid through an increase of the contact area. This mechanism will promote also an existence of a film or nearly constant thickness. Similar effect would be caused by synovial fat pads,[10] which reduce the film thickness while not taking part in the actual load-bearing mechanism. A film of synovial fluid[43] will be always interposed between surfaces and no direct contact will take place in a healthy joint (note the quasihydrodynamic lubrication).

Elastic deformations of cartilage may occur not only in the normal but also in a plane parallel to the plane of articular surfaces. The resulting lateral movements may be expected to decrease the effective velocity gradient across the gap.

PATHORHEOLOGY OF JOINT LUBRICATION

It has been suggested[44] that as long as the synovial fluid is normal and healthy, that is, it is thixotropic, elastic, and surface-active, and as long as the articular cartilage remains resilient, the articular surfaces are never in immediate contact and, consequently, boundary lubrication does not take place. If however pathological changes in synovial fluid cause changes in the intermolecular bondings of hyaluronic acid molecules, or if they deprive the synovial fluid of its content of hyaluronic acid, the resulting decrease in viscosity and flow type will impair lubrication. In the absence of a thixotropic and elastic fluid, most likely only a boundary-type of lubrication exists.

If the synovial fluid is normal but there is a decrease in the degree of smoothness and resiliency of the articular surfaces lubrication will

be also impaired. A decrease in the normal and lateral deformations of cartilage will cause a large increase in the local pressures and in the velocity gradient across the gap between the opposing surfaces. Synovial fluid will be forced to perform under much higher rates of shear than usual. Both phenomena, increase in pressure and in rates of shear, might be expected to lead to a degradation of hyaluronic acid-protein aggregates in a way analogous to the mechanically induced degradation of polymers.[45,46] A degradation of synovial fluid will decrease its lubricating properties and allow this fluid to be squeezed out from the gap between the surfaces. A decrease in the lubricating action of synovial fluid will lead to wear of the cartilage[47] and to an increase of the intra-articular temperature.[40] Both these actions will cause, in their turn, a further deterioration of joint structure and functions.

As rightly stated by Davies and Barnett,[34] a *circulus vitiosis* may exist: on the one hand, trauma or infection causes a decrease in the viscosity of synovial fluid, and this in turn causes pathological changes in the articular surfaces; on the other hand, an increase in the hardness of the joint surfaces may lead to a mechanical degradation of the synovial fluid, and to consequent and further damage to the articular cartilage. In such a way the circle is completed.

The author gratefully acknowledges assistance from a grant from the National Health and Medical Research Council of Australia during the tenure of which this paper was prepared.

References

1. Bennet, G. A., in *Pathology*, W. A. D. Anderson, ed., C. V. Mosby Co., St. Louis, Mo., 1957, p. 1251.
2. Osborne, G. V., and W. H. Fahrni, *J. Bone Joint Surg.*, **32B**, 148 (1950).
3. Scales, J. T., and J. M. Zarek, *Brit. Med. J.*, **1954**, 1007.
4. Evans, F. G., H. R. Lissner, and H. E. Pedersen, *Anat. Record*, **101**, 225 (1948).
5. Barnett, C. H., and A. F. Cobbold, *J. Bone Joint Surg.*, **44**, 662 (1962).
6. McCutchen, C. W., *Wear*, **5**, 1 (1962).
7. Sundblad, L., *Acta Soc. Med. Upsalien*, **58**, 115 (1953).
8. Ogston, A. G., and J. E. Stanier, *J. Physiol.*, **119**, 244 (1953).
9. Ogston, A. G., and J. E. Stanier, *Biochem. J.*, **52**, 149 (1952).
10. Barnett, C. H., D. V. Davies, and M. A. MacConnaill, *Synovial Joints, Their Structure and Mechanics*, Longman's Green, New York, 1961.
11. MacConaill, M. A., *J. Bone Joint Surg.*, **32B**, 244 (1950).

12. Charnley, J., in *Proceedings of the Symposium on Biomechanics*, Inst. Mechanical Engineers, London, 1959, p. 12.

13. Charnley, J., *Triangle*, **4**, 175 (1960).

14. Young, H. H., *1960–61 Yearbook of Orthopedic and Traumatic Surgery*, Year Book Medical Publ., Chicago, 1961, p. 310.

15. Lewis, P. R., and C. W. McCutchen, *Nature*, **184**, 1285 (1959).

16. Archard, J. F., *Research*, **9**, S27 (1956).

17. Bondi, A., in *Rheology*, Vol. 3, F. H. Eirich, ed., Academic Press, New York, 1960, p. 444.

18. Bowden, F. P., *Endeavour*, **16**, No. 61, 5 (1957).

19. Bowden, F. P., *J. Colloid Sci.*, **11**, 555 (1956).

20. Grosch, K. A., *Nature*, **197**, 858 (1963).

21. Larsen, R. G., and G. L. Perry, *Trans. Am. Soc. Mech. Engrs.*, **67**, 45 (1945).

22. Archard, J. F., and M. T. Kirk, *Proc. Roy. Soc. (London)*, **261**, 532 (1961).

23. Crook, A. W., *Phil. Trans. Roy. Soc.*, **250**, 287 (1958).

24. Crook, A. W., *Nature*, **190**, 1182 (1961).

25. Blok, H., in *Proceedings on the Proc. International Conference on Gearing*, Inst. Mechanical Engineers, London, 1958, p. 144.

26. Blok, H., in *Proceedings of the International Conference on Gearing*, Inst. Mechanical Engineers, London, 1958, p. 464.

27. Dowson, D., and G. R. Higginson, *J. Mech. Eng. Sci.*, **1**, 6 (1959).

28. Barwell, F. T., in *Proceedings of the International Conference on Gearing*, Inst. Mechanical Engineers, London, 1958, p. 117.

29. Bloch, B., and L. Dintenfass, *Australian-New Zealand J. Surgery*, **33**, 108 (1963).

30. Camosso, M. E., and G. Marotti, *J. Bone Joint Surg.*, **44A**, 699 (1962).

31. Dintenfass, L., *Rheol. Acta*, **2**, 187 (1962).

32. Tanner, R., private communication, 1962.

33. Barnett, C. H., *Ann. Rheum. Diseases*, **17**, 229 (1958).

34. Davies, D. V., and C. H. Barnett, *Med. Grundlagenforsch.*, **3**, 625 (1960).

35. Ogston, A. G., and J. E. Stanier, *J. Physiol.*, **119**, 253 (1953).

36. Blomberg, B. S., and A. G. Ogston, *Biochem. J.*, **66**, 342 (1957).

37. Nettelbladt, E., and L. Sundblad, *Arthritis Rheumat.*, **2**, 144 (1959).

38. Scott Blair, G. W., P. O. Williams, E. T. Fletcher, and R. L. Markham, *Biochem. J.*, **56**, 504 (1954).

39. Hunter, J., E. H. Kerr, and M. G. Whillans, *Can. J. Med. Sci.*, **30**, 367 (1952).

40. Horwath, S. M., and J. L. Hollander, *J. Clin. Invest.*, **28**, 469 (1949).

41. McCutchen, M. A., *Nature*, **184**, 1284 (1959).

42. Taylor, G. I., and J. C. P. Miller, *Quart. J. Mech. Appl. Math.*, **9**, 129 (1956).

43. Barnett, C. H., D. V. Davies, and M. A. MacConaill, *Brit. Med. J.*, **1961**, 47.

44. Dintenfass, L., *Nature*, **197**, 496 (1963).

45. Basu, S., and P. R. Chaufhury, *J. Colloid Sci.*, **12**, 19 (1957).

46. Kuhn, W., *Makromol. Chem.*, **35**, 200 (1960).

47. Barnett, C. H., *J. Bone Joint Surg.*, **38B**, 567 (1956).

Synopsis

14599

The theories of lubrication were reviewed, and it was concluded that neither the classical hydrodynamic theory nor the boundary theory permits an adequate description and explanation of lubrication in synovial joints. It is suggested that the key factor is the thixotropic behavior of synovial fluid which enables preserving constant load-bearing capacity at various rates of movement. The elastic properties of the articular cartilage might depend on the presence of synovial fluid in its pores. The pressure exerted in the fluid will depend on the elasticity of the cartilage and on the area of contact. The velocity gradient in the gap will depend on the normal and lateral deformations in the articular cartilage. Pathorheology (rheological pathology) of the synovial joints is discussed and related to physicochemical and morphological changes in both synovial fluid and cartilage. The proposed outline of lubrication in synovial joints explains the interdependence of synovial fluid and articular surfaces. Both synovial fluid and articular cartilage are necessary components of joint lubrication.

Author

N67 14600

Factors Affecting the Rheological Behavior of Hyaluronic Acid†

WARD PIGMAN,* G. MATSUMURA, and A. HERP, *Department of Biochemistry, New York Medical College, New York, New York*

INTRODUCTION

Hyaluronic acid is a component of the extracellular fluids of connective tissue. It is probably formed by the fibroblasts and is the component of these fluids responsible for their viscosity and semi-gel character. Much of the research on the rheology of hyaluronic acid has been carried out on synovial fluids and purified materials from this source. In the present paper, the viewpoint will be adopted that synovial fluid represents a diluted form of the ground substance which separates connective tissue cells and through which metabolites move to and from the cells.

Hyaluronic acid was first isolated by Karl Meyer, who with his associates, was responsible for much of the information leading to the current concepts of its structure.[1] Its molecular weight has been reported as 2 to 8 $\times$ 10^6 for preparations from a number of sources, except that preparations from vitreous humor were definitely of lower molecular weight.[2–5] It is composed of long chains of alternating units of D-glucuronic acid and *N*-acetyl-D-glucosamine connected as shown in Figure 1. The chains exist as expanded highly hydrated random coils. Since at neutral pH the carboxyl groups are highly ionized, the chains carry negative charges at approximately 10 to 12 A. intervals. The existence of this network of closely spaced negative charges is the principal basis for the expanded structure and the marked influence of salt concentration on the viscosity of hyaluronic acid solutions.[6–8] At isotonic salt concentrations, changes in salt concentrations are only a minor influence, however.

† This work supported by the U. S. Public Health Service, National Institute of Arthritis and Metabolic Diseases, AM-04619.

PRECEDING PAGE BLANK NOT FILMED.

Numerous studies have been made of the viscosity of hyaluronic acid solutions and synovial fluids. Ragan and Meyer,[9] Ogston and Stanier[10] found an approximately linear relation between log viscosity and concentration, whereas Ropes et al.[7] reported a better linearity for log viscosity vs. the square root of the hexosamine concentration.

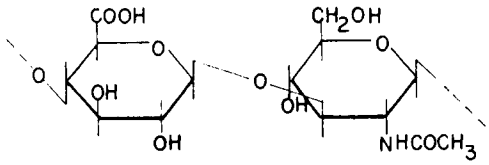

Fig. 1. Repeating unit of hyaluronic acid.

However, the viscosities of hyaluronic acid solutions are non-Newtonian and depend upon the shear rate.[10–19] Numerous schemes have been proposed to express the anomalous viscosity of hyaluronic acid solutions and synovial fluids and to use this property as an indirect measure of the degree of polymerization of the hyaluronic acid.[10,11,13–15] By these criteria, synovial fluids from patients with connective tissue diseases have been shown in several investigations[12,13,18,19] to have reduced anomalous viscosities, although Scott Blair et al,[14] found no clinical significance for the differences.

HYALURONIC ACID PROTEIN COMPLEXES

Ogston and Stanier[10] gave a different interpretation to the cause of the anomalous viscosity of synovial fluids and ascribed it to the presence of a complex of hyaluronic acid with a protein component. But hyaluronic acid virtually free of protein could be isolated from synovial fluids by mild methods.[17,20] This purified hyaluronic acid exhibited high anomalous viscosity and had an intrinsic viscosity similar to that of synovial fluids. Also the addition of serum proteins to the hyaluronic acid had a negligible effect on the viscosity.[32] This work makes it evident that the anomalous viscosity is a property of the undegraded hyaluronic acid molecule. However, some of the hyaluronic acid of synovial fluid seems to be firmly attached to a small amount of protein, but no evidence exists that it has any influence on the viscosity.[21]

INTRINSIC VISCOSITY

The complex nature of anomalous viscosity would seem to suggest the use of a more direct measure of degree of polymerization such as the intrinsic viscosity. When plotted in the usual way as η_{sp}/c vs. concentration, hyaluronic acid solutions gave nonlinear plots. As shown by Sundblad,[11] linear relations over a range of η_{sp} between 0.5 and 15 are obtained by plots of η_{sp}/c vs. η_{sp} as suggested earlier by

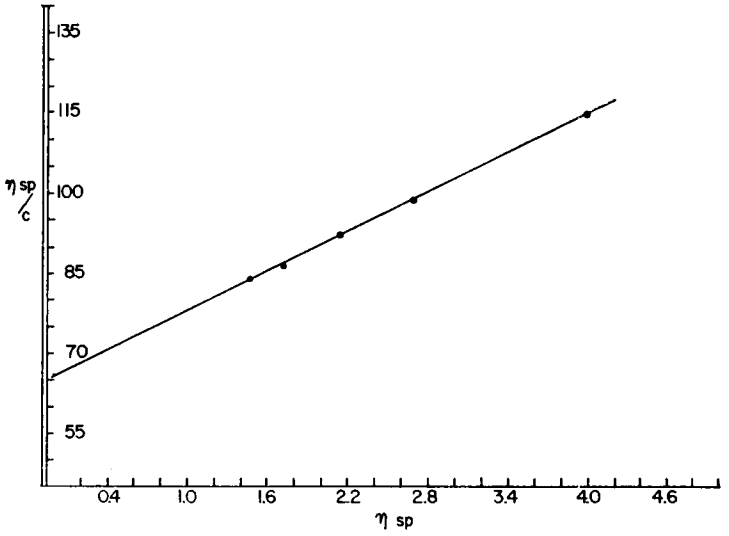

Fig. 2. Plot of intrinsic viscosity of human post-mortem synovial fluid. Viscosity was measured at 30°C., and the synovial fluid was dialyzed and diluted with 0.2*M* sodium phosphate, pH 7.3. The concentration *c* is gram of hyaluronic acid estimated from carbazole reaction per 100 ml.

Huggins.[22] When used for synovial fluids directly, however, the measurement of intrinsic viscosity is complicated by the necessity of determining the concentration of hyaluronic acid. Sundblad[11] showed that hexosamine determinations could be used after hyaluronidase action and precipitation of most of the proteins. However, an easier method is to precipitate an aliquot as the mucin clot by addition of acetic acid, dissolve the clot with dilute alkali, and determine uronic acid by the Dische method.[23,24] The intrinsic viscosity of purified hyaluronic acid solutions was shown to be the same when measured in

capillary viscometers of widely different rates of flow and to be only slightly affected by differences in temperature and buffer composition.[17] The intrinsic viscosity of hyaluronic acid in normal human synovial fluids varied[23,25] in the range of about 60 to 100 dl./g., although Sundblad[11] gave lower values. A typical result for a human synovial fluid is shown in Figure 2. For synovial fluids from patients with connective tissue diseases, the intrinsic viscosity seemed to be markedly decreased from normal fluids.[11,12,23,25]

In our laboratory, the highest intrinsic viscosity observed for human synovial fluids has been about 100 dl./g. and that of isolated hyaluronic acid[26] about 80 dl./g. When these results are converted to molecular weights using the relationship $[\eta] = 0.036M^{0.78}$, established by Laurent et al.,[27] the molecular weights are 1×10^7 for the hyaluronic acid in the synovial fluid and $6\text{–}7 \times 10^6$ for the isolated material. (Concentrations in the formula are grams per milliliter.)

Degradation of hyaluronic acid during isolation is probably a frequent cause of the low viscosities and molecular weights of purified hyaluronic acids. The rapid depolymerization of hyaluronic acid by auto-oxidants and by serum fractions under acid conditions (discussed below) probably explain the low molecular weights (from 34,000 to 82,000) reported for hyaluronic acid isolated from human myometrium and aortic tissue.[28,29]

Since many properties of hyaluronic acid are profoundly affected by changes in its degree of polymerization, the intrinsic viscosities should always be recorded.

POLYDISPERSITY

The homogeneity of the hyaluronic acid in tissue fluids is another characteristic of fundamental importance, especially since the degree of polymerization seems to be reduced in some connective tissue diseases. Unfortunately very little information is available. Laurent et al.[27] fractionated bovine vitreous body with cetylpyridinium chloride and recovered hyaluronic acid fractions varying in molecular weight (ultracentrifuge) between 1×10^5 and 1.5×10^6. Berman[30] obtained very similar results using chromatographic procedures.

An attempt[31] was made to carry out a similar study of the polydispersity of the hyaluronic acid in human rheumatoid synovial fluids. Although a high degree of polydispersity was shown, the

results are of questionable significance. The hyaluronate was isolated as the "mucin clot," the formation of which is known to cause extensive degradation.[32]

GEL STRUCTURE AND BINDING CAPACITY

Ogston and Phelps[33] have calculated that at concentrations down to 0.01%, extensive interlocking of hyaluronic acid molecules will occur, and for concentrations above 0.1%, the solutions consist of a uniform three-dimensional network.* Equilibrium dialysis experi-

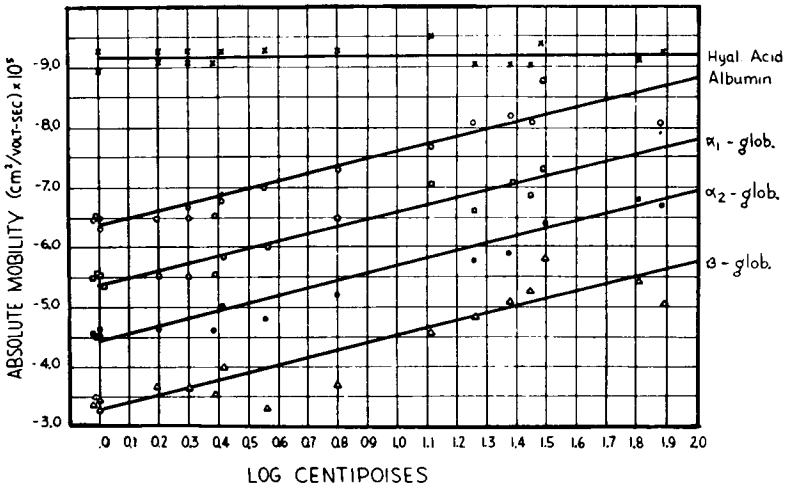

Fig. 3. Effect of apparent absolute viscosity on the electrophoretic mobility of serum and synovial fluid components (ref. 16). Veronal buffer pH 8.6, μ = 0.1.

ments showed that hyaluronic acid solutions in contact with solutions of substances such as inulin or serum albumin did not attain the same concentration of these substances on both sides of the membrane. This result indicates that much of the water surrounding the hyaluronic acid is not available as a solvent. Ogston and Phelps calculate that each gram of hyaluronic acid immobilizes about 300 ml. of

* Although the work was done with the hyaluronic acid protein complex, the results probably hold generally for purified hyaluronic acid solutions.

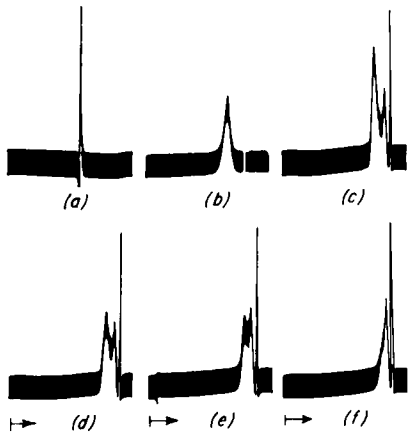

Fig. 4. The pi peak: A complex of hyaluronic acid with albumin (ref. 40). (*A*) Hyaluronic acid (HA) 160 mg./100 ml.; (*B*) bovine plasma albumin (BPA) 250 mg./100 ml.; (*C*) HA and BPA 480 mg./100 ml.; (*D*) HA and BPA 280 mg./100 ml.; (*E*) HA and BPA 280 mg./100 ml.; (*F*) HA and BPA 250 mg./100 ml. Time: (*A*) 195 min.; (*BCDE*) 225 min.; HA in (*CDEF*) *ca.* 150 mg./100 mg.; veronal buffer pH 8.6, $\mu = 0.1$.

solvent. This effect may explain the low concentrations of serum proteins in normal synovial fluids.

The behavior of hyaluronic acid solutions and synovial fluids in the ultracentrifuge also suggests a gel-like structure.[34] Hyaluronic acid sedimented very slowly unless the solutions were highly diluted, and the sedimentation of some protein components of synovial fluid was slower than for blood serums or hyaluronidase-treated synovial fluids.[35–37] With particles of different sizes, the rates of sedimentation were shown to be a function of the particle size and to increase with decrease of the molecular weight of the hyaluronic acid.[37]

Under the conditions of Tiselius electrophoresis, hyaluronic acid was the component of synovial fluids with the highest mobility. In the ascending limb, the hyaluronic acid moved as a single component into the buffer. The protein components moved more slowly and moved in the environment of the hyaluronic acid "gel" network. Two effects of the moving network of hyaluronic acid chains were observed. As shown in Figure 3, the albumin and α- and β-globulins moved more rapidly than in the absence of hyaluronic acid, and the mobilities were proportional to the logarithm of the viscosity of the solu-

tion. When the hyaluronic acid had not been depolymerized, synovial fluids and synthetic mixtures of hyaluronic acid and albumin in veronal buffers at pH 8.6 showed a new component in the electrophoretic patterns. This component was called the pi component.[34,38–40] An electrophoretic pattern showing a pi peak formed in a solution of hyaluronic acid and serum albumin is shown in Figure 4. It was formed poorly or usually not at all in solutions containing depolymerized hyaluronic acid, in rheumatoid synovial fluids, and in synovial fluids treated with hyaluronidase.

When synovial fluids were filtered on membranes retaining the hyaluronic acid, some proteins were retained with the hyaluronic acid.[7,10,41] This behavior was ascribed by Ogston and Stanier to the presence of a hyaluronic acid-protein complex, the composition of which was shown by Curtain to be dependent on the pH. The complex must be easily dissociable since hyaluronic acid could be freed[17,20,42] from the proteins of synovial fluid by repeated electrophoresis at pH 7, and by absorption methods combined with ultrafiltration.[21]

These experiments involving equilibrium dialysis, ultrafiltration, ultracentrifugation, and electrophoresis show that hyaluronic acid solutions probably consists of three-dimensional networks which influence the movement of proteins probably both sterically and through the influence of the numerous negative charges. The electrophoresis and ultracentrifugal work also showed that this characteristic is dependent upon the degree of polymerization.

Although all this work implies that hyaluronic acid solutions have a gel character, few direct measurements have been made.[43] The behavior in the ultracentrifuge is not that of a rigid gel but one for which cross-bonds are re-established during the period of centrifugation.

DEPOLYMERIZATION OF HYALURONIC ACID

Hyaluronic acid solutions and even lyophilized sodium salts are easily depolymerized. From the practical viewpoint of storage, hyaluronic acid solutions can be stabilized by the use of veronal buffers or 5 to 10% ethanol.[17]

The best known agents causing depolymerization of hyaluronic acid are the hyaluronidases of which the most studied are from micro-

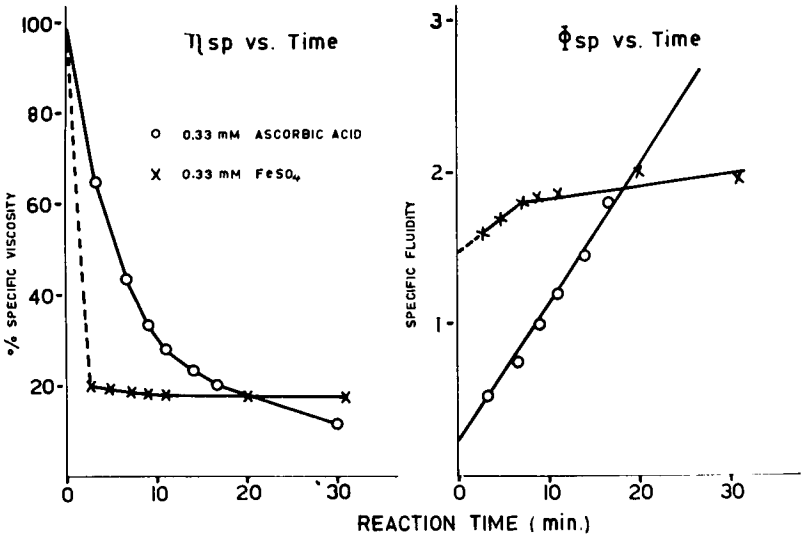

Fig. 5. Effect of auto-oxidants on the viscosity of hyaluronic acid. Reactions were carried with 0.4 mg. of hyaluronic acid/milliliter of 0.2*M* sodium phosphate, pH 7.3, at 30°C. The hyaluronic acid had intrinsic viscosity (ref. 17) of about 40 dl./g. The same conditions were used for following figures.

organisms, testes, and leeches. This work has been reviewed adequately and will not be considered here.[44]

Hyaluronic acid is rapidly depolymerized by oxygen in the presence of auto-oxidants, also called reducing substances. The reaction, which may be general for many types of polymers, has been called oxidative-reductive depolymerization (ORD reaction).[45,46] Auto-oxidants of particular biological interest are ascorbic acid, cysteine, and cuprous and ferrous ions. However, auto-oxidant activity is shown by many enediols, thiols, and quinones. Anti-oxidant activity, i.e., inhibition of the auto-oxidants, is shown by a number of substances, especially sulfur compounds, although many substances such as alcohols and albumin inhibit when at high concentrations.

In Figure 5 the reduction in viscosity of hyaluronic acid solutions by several auto-oxidants is shown. Ferrous ions had a rapid action, whereas ascorbic acid was the most active of the organic compounds. Since the viscosity curves are not linear, comparisons of rates of reduction of viscosity cannot be made quantitatively. However,

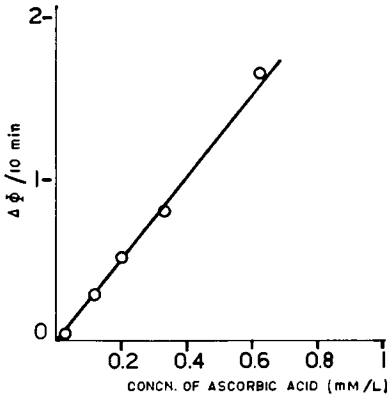

Fig. 6. Effect of ascorbic acid concentration on rate of change of fluidity of hyaluronic acid. Ordinate shows the increase of specific fluidity in first 10 min.

fluidity*-time plots are linear in the early part of the reaction, as shown for the same data plotted as fluidity vs. time in Figure 5.

The effect of various concentrations of ascorbic acid is shown in Figure 6. The rate expressed as the increase of fluidity in 10 min. was proportional to the ascorbic acid concentration up to a concentration of 1 mM/liter.

The dependence of the reaction on oxygen is shown in Figure 7 for ferrous ions and ascorbic acid as auto-oxidants. The reactions were carried out in the presence of nitrogen which had been freed from oxygen by passage over red-hot copper, previously reduced with hydrogen. The effect could only be clearly demonstrated when the oxygen concentration was very low, probably less than 2 to 3 ppm. "Prepurified" nitrogen, with about 20 ppm of oxygen, caused extensive degradation. As shown in the figure, in the presence of nitrogen, the fluidity remained constant with ascorbic acid and ferrous ions as reducing agents, but the fluidity increased rapidly on admission of air into the system. Ferrous ions showed a modified effect in that in air an initial increase of fluidity occurred before the viscosity could be measured. The ferrous ions in air thus caused an initially rapid reaction followed by a slower secondary reaction.

The auto-oxidation of ascorbic acid, ferrous or cuprous ions is generally considered to be a free-radical reaction. The necessity

* Fluidity is the reciprocal of specific viscosity.

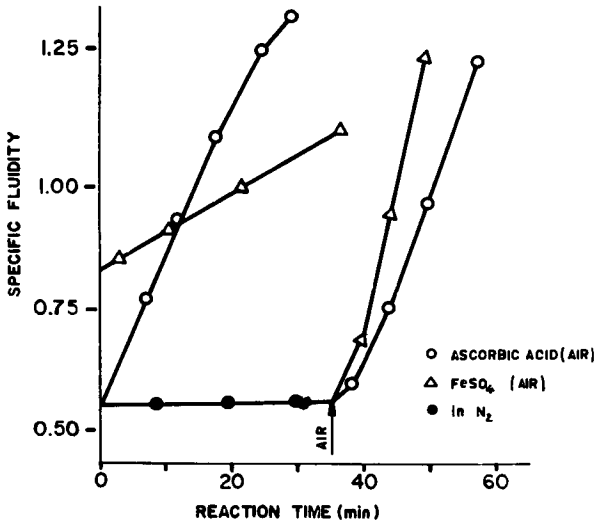

Fig. 7. Effect of removal of oxygen on depolymerization of hyaluronic acid by ferrous ions and ascorbic acid. For anaerobic experiments shown with solid circles, the gas phase was oxygen-free nitrogen. At the point indicated by an arrow, air was introduced into the reaction vessel.

of oxygen for the degradation of hyaluronic acid further supports this mechanism. Another support is the halide effect. In the halide series, the ability to quench free radicals (probably OH· radicals) has been shown to increase markedly with the atomic number.[47] In Figure 8, the effect of halide and phosphate ions (0.2*M* solutions as sodium salts) on the reduction of viscosity of hyaluronic acid solutions is shown with ascorbic acid as the auto-oxidant. In the presence of iodide ions or bromide ions, the effect of ascorbic acid was completely abolished. With fluoride ions, the increase of fluidity was the same as for phosphate ions (the usual buffer). Chloride ions showed a partial inhibition. When viscosity-time curves were used for comparison, the decrease of viscosity on a percentage basis was the same for water (without salts), phosphate buffer, and fluoride ions. This similarity may have been fortuitous since in the absence of salts, hyaluronic acid solutions have a high viscosity.

Further evidence for a free-radical mechanism for the ORD reaction was shown by the nature of inhibitors of the reaction. Alcohols,

sugars, and proteins in high concentrations were inhibitory. Inhibitors active in low concentrations (3 mM/liter) were sodium diethyldithiocarbamate, thiourea, 1,3-diethylthiourea, 2-amino-ethylisothiouronium bromide (AET), many thiol compounds, and toluene.[45] Such compounds also are protective against ionizing radiations, reactions generally considered to involve free-radical intermediates.

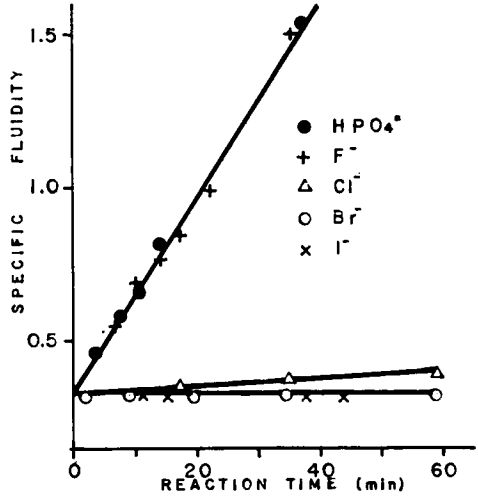

Fig. 8. Effect of halogen ions on depolymerization of hyaluronic acid by ascorbic acid. 0.2*M* solutions of the sodium salts were used, otherwise same as Fig. 5.

Recently alizarin (the formula for which is shown in Fig. 9) has been found to be the most active inhibitor of the degradation of hyaluronic acid by ascorbic acid and ferrous ions. Its structure resembles more that of the enediols and quinones which are autooxidants, but it was found to be a powerful anti-oxidant of the ORD reaction at a concentration 0.3 mM/liter.

It has also been demonstrated recently that catalytic amounts of iron and copper ions (from 3 to 10 μM/liter) enhance the activity of ascorbic acid solutions (330 μM/liter) in the ORD reaction.

These features of the ORD reaction suggest that the mechanism might be based on that given below when both metal and ascorbic acid are present.[48] The hyaluronic acid free radical (R′·) could react

in

$$O_2 + Fe^2 \rightleftharpoons (Fe^3O_2^-)$$
$$(Fe^3O_2^-) + RH \rightarrow Fe^3O_2H + R\cdot$$
$$\rightarrow Fe^2 + HO_2\cdot + R\cdot$$
$$R\cdot + HO_2\cdot \rightarrow ROOH$$
$$ROOH + Fe^2 \rightarrow RO\cdot + Fe^3 + OH^-$$
$$R'H + RO\cdot \rightarrow R'\cdot + ROH$$

(where RH is ascorbic acid and R'H is hyaluronic acid)

numerous ways with oxygen or other free radicals, including those generated from hydrogen peroxide. Since the polysaccharide chain is cleaved, it seems probable that an atom attached to one of the carbon atoms connecting adjacent hexosamine and uronic acid residues may be the site of attack. Preliminary results have indicated that the uronic glycosidic linkage may be the most susceptible, and the above considerations suggest that an atom at C-4 may be the primary site.

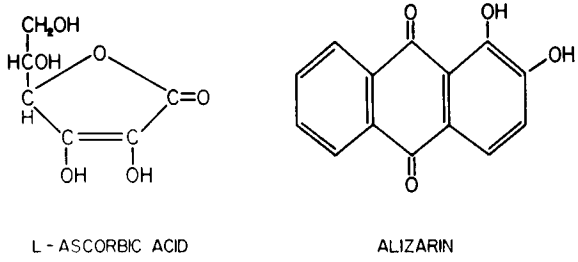

Fig. 9. Structures of L-ascorbic acid and alizarin.

It has also been found that human serums and synovial fluids contain an inhibitor of the action of ascorbic acid.[46,49] Thus, the reduction of the viscosity of synovial fluid with auto-oxidants required a tenfold greater concentration of these substances than for solutions of purified hyaluronic acid.

The stoichiometry of the ORD reaction is analyzed in Table I for various concentrations of ferrous ions and ascorbic acid from the data given earlier.[45] By the use of the formula relating intrinsic viscosity and molecular weight given by Laurent et al.,[27] the number of linkages cleaved could be calculated for different amounts of auto-oxidant. Only 8 to 13 linkages per molecule were cleaved at

TABLE I
Stoichiometry of ORD Reaction

Intrinsic viscosity,[a] dl./g.	Molecular weight,[b] $\times 10^{-6}$	No. linkages broken/ molecule	Concn. auto-oxidant, mM/liter	No. auto-oxidant molecules present/ linkage broken[c]
		Ascorbic Acid as Auto-oxidant		
46	3.54	—	0	—
32	2.21	0.60	0.025	370
18	1.06	2.34	0.038	145
15	0.83	3.26	0.077	210
12	0.63	4.62	0.145	360
6	0.26	12.60	0.290	205
Average				260
		$FeSO_4$ as Auto-oxidant		
32	2.21	0.60	0.025	370
22	1.37	1.58	0.038	210
17	0.98	2.62	0.077	260
11	0.56	5.32	0.145	240
8	0.37	8.57	0.290	335
Average				280

[a] Calculated from the data of Pigman et al. (ref. 45).

[b] $[\eta] = 36\ MW^{0.78} \times 10^{-5}$.

[c] Initial concentration of hyaluronic acid was 0.113 μM/liter with MW of 3.54×10^6.

the usual concentrations of auto-oxidant (*ca.* 0.3 mM/liter). A large excess of auto-oxidant was required for each cleavage, the average being 260 to 280 molecules of auto-oxidant per linkage cleaved.

Several other types of depolymerizations of hyaluronic acid are also known. Thus, neutral solutions of hyaluronic acid rapidly lose their viscosity at elevated temperatures.[45] Since the reaction was inhibited by ethanol and by veronal buffer, it may involve an oxidative depolymerization, but without added auto-oxidant. Solutions at pH 11 also lose their viscosity rapidly at room temperature,[7] but this reaction has not been studied further.

Synovial fluids when made weakly acidic (pH 2.5 to 3.5) rapidly lost their viscosity irreversibly, although purified hyaluronic acid was shown to be relatively stable under these conditions.[32] Numerous

reports have also been made of the existence in animal tissues of substances of low activity which degrade hyaluronic acid under weakly acidic conditions (pH *ca.* 3) but not under neutral conditions.[50] At present, the nature of these degradations by tissues and tissue fluids is highly uncertain. Although called hyaluronidases, the agents could be protein auto-oxidants or be associated with proteins. Further work on this problem is badly needed before any clarification is possible.

References

1. Weissmann, B., and K. Meyer, *J. Am. Chem. Soc.*, **76,** 1753 (1954).
2. Balazs, E. A., *Federation Proc.*, **17,** 1086 (1958).
3. Fessler, J. H., A. G. Ogston, and J. E. Stanier, *Biochem. J.*, **58,** 656 (1954).
4. Blumberg, B. S., and G. Oster, *Science*, **120,** 432 (1954).
5. Fessler, J. H., *Biochem. J.*, **76,** 124 (1960).
6. Madinaveitia, J., and T. H. H. Quibell, *Biochem. J.*, **34,** 625 (1940).
7. Ropes, M. W., W. v. B. Robertson, E. C. Rossmeisl, R. B. Peabody, and W. Bauer, *Acta Med. Scand.*, Suppl. **196,** 700, (1947).
8. Hadidian, Z., and N. W. Pirie, *Biochem. J.*, **42,** 260 (1948).
9. Ragan, C., and K. Meyer, *J. Clin. Invest.*, **28,** 56 (1949).
10. Ogston, A. G., and J. E. Stanier, *Biochem. J.*, **46,** 364 (1950); **52,** 149 (1952).
11. Sundblad, L., *Acta Soc. Med. Upsaliensis*, **58,** 115 (1953).
12. Levine, M. G., and D. H. Kling, *J. Clin. Invest.*, **35,** 1419 (1956).
13. Barnett, C. H., *Ann. Rheum. Dis.*, **17,** 229 (1958).
14. Scott Blair, G. W., P. O. Williams, E. T. D. Fletcher, and R. L. Markham, *Biochem. J.*, **56,** 504 (1954).
15. Johnston, J. P., *Biochem. J.*, **59,** 633 (1955).
16. Pigman, W., F. M. Patton, and D. Platt, *Arch. Biochem. Biophys.*, **69,** 334 (1957).
17. Pigman, W., S. Rizvi, and H. Holley, *Biochim. Biophys. Acta*, **53,** 254 (1961).
18. Jebens, E. H., and M. E. Monk-Jones, *J. Bone Joint Surg.*, **41B,** 388 (1959).
19. Morisaki, N., T. Kageyama, N. Tajima, and G. Matsumura, *Comm. X Congr. Lega Intern. contro Reumatismo, Roma* **2,** 927 (1961).
20. Balazs, E. A., and L. Sundblad, *Acta Soc. Med. Upsaliensis*, **64,** 137 (1959).
21. Sandson, J., and D. Hamerman, *J. Clin. Invest.*, **41,** 1817 (1962).
22. Huggins, M. L., *J. Am. Chem. Soc.*, **64,** 2716 (1942).
23. Stafford, C., W. Niedermeier, H. Holley, and W. Pigman, unpublished results.
24. Dische, A., *J. Biol. Chem.*, **167,** 189 (1947).
25. Bollet, A. J., *J. Lab. Clin. Med.*, **48,** 721 (1956).
26. Matsumura, G., M. de Salegui, A. Herp, and W. Pigman, *Biochim. Biophys. Acta*, **69,** 574 (1963).
27. Laurent, T. C., M. Ryan, and A. Pietruszkiewicz, *Biochim. Biophys. Acta*, **42,** 476 (1960).

28. Iversen, O. H., and K. Marcker, *Acta Pharm. Toxicol.*, **18**, 101 (1961).
29. Bertelsen, Sv., and K. Marcker, *Nature*, **191**, 386 (1961).
30. Berman, E. R., *Exptl. Eye Res.*, **2**, 1 (1963).
31. Näntö, V., P. Seppälä, and E. Kulonen, *Clin. Chim. Acta*, **7**, 794 (1962).
32. Pigman, W., W. Hawkins, E. Gramling, S. Rizvi, and H. L. Holley, *Arch. Biochem. Biophys.*, **89**, 184 (1960).
33. Ogston, A. G., and C. F. Phelps, *Biochem. J.*, **78**, 827 (1960).
34. Platt, D., W. Pigman, H. L. Holley, and F. M. Patton, *Arch. Biochem. Biophys.*, **64**, 152 (1956).
35. Johnston, J. P., *Biochem. J.*, **59**, 620 (1955).
36. Platt, D., W. Pigman, and H. L. Holley, *Arch. Biochem. Biophys.*, **79**, 224 (1959).
37. Laurent, T. C., and A. Pietruszkiewicz, *Biochim. Biophys. Acta*, **49**, 258 (1961).
38. Platt, D., W. Pigman, and H. L. Holley, *Biochem. J.*, **79**, 605 (1961).
39. Pigman, W., E. Gramling, and H. L. Holley, *Biochim. Biophys. Acta*, **46**, 100 (1961).
40. Gramling, E., W. Niedermeier, H. L. Holley, and W. Pigman, *Biochim. Biophys. Acta*, **69**, 552 (1963).
41. Curtain, C. C., *Biochem. J.*, **61**, 688 (1955).
42. Roseman, S., and D. Watson, *IX Intern. Congr. Rheumatic Diseases*, Canada, 1957, June 24.
43. Jensen, C. E., and J. Koefoed, *J. Colloid Sci.*, **9**, 460 (1954).
44. Meyer, K., and M. M. Rapport, *Adv. Enzymology*, **13**, 199 (1952).
45. Pigman, W., S. Rizvi, and H. L. Holley, *Arthritis Rheumat.*, **4**, 240 (1961).
46. Pigman, W., and S. Rizvi, *Biochem. Biophys. Res. Comm.*, **1**, 39 (1959).
47. Allen, A. O., *Radiation Chemistry of Water and Aqueous Solutions*, Van Nostrand, New York, 1961, pp. 60–65.
48. Ingold, K. U., *Chem. Rev.*, **61**, 563 (1961).
49. de Salegui, M., S. Rizvi, H. Holley, and W. Pigman, *Federation Proc.*, **21**, 171 (1962).
50. Gibian, H., *Mucopolysaccharide und Mucopolysaccharidasen*, Franz Deuticke, Wien, 1959, p. 132.
51. Pigman, W., *Bull. Soc. Chim. Biol.*, **45**, 185 (1963).

Synopsis

14600

The rheological characteristics of hyaluronic acid are markedly dependent upon many substances found in tissues and fluid. They are markedly affected by the presence of salts, pH, natural autooxidants, anti-oxidants, and oxygen. Three-dimensional networks (semigels) are formed which, considerable evidence shows, could affect the movement of large molecules including the diffusion of proteins.

The gel structure of the intracellular ground substance of connective tissue is probably provided by hyaluronic acid and seems to be highly dependent upon the degree of polymerization. Since the gel structure influences the mobility, variations in gel structure may provide a mechanism of control of permeability of metabolites moving to and from cells and capillaries.[51]

author

It is denoted generally by T_D, to indicate the "denaturation temperature."

TRANSITIONS IN THE NATIVE STATE

In the native state the collagen molecules are more tightly packed; the density is approximately 1.3 g./cu. cm. and the material is highly crystalline. If a specimen of collagen taken directly from an animal is slowly heated, there is little evident change before 60°C. when the specimen shrinks to a fraction of its original length, approximately one-fifth of the collagen fibers were axially aligned as in tendon. This is the most obvious and well known of the transitions in bulk collagen, and is denoted by T_s, signifying shrinkage temperature. For mammalian collagen, T_s is usually in the vicinity of 60°C. However, some confusion has occasionally arisen from apparently higher values obtained by using excessive heating rates or insensitive methods of detection. Figure 1 therefore indicates schematically a generally acceptable method of determining T_s. A strip of the fibrous collagen is clamped at its ends. One clamp is attached to the

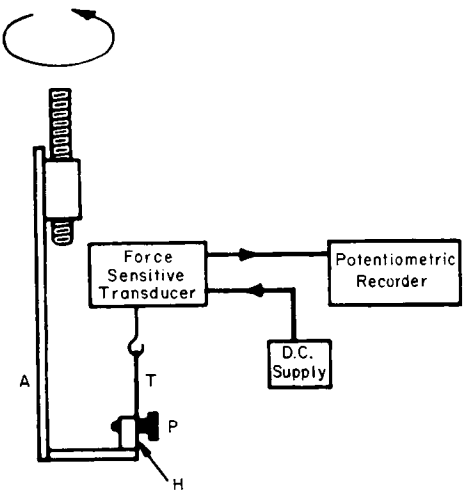

Fig. 1. Schematic apparatus used for controlling the length of tendon T and for measuring the force developed when it contracts. Here A is a movable arm and H a metal holder into which the two free ends of the looped tendon are held by the plug P.

N67 14601

Structural Transitions in Native Collagen and Their Physiological Significance

B. J. RIGBY* and P. MASON, *Division of Textile Physics, C.S.I.R.O. Wool Research Laboratories, Ryde, Sydney, Australia*

INTRODUCTION

Collagen occurs in the native state as a fibrous protein with a high degree of crystallinity. The physicochemical properties of this material, particularly those governing the dramatic phenomena associated with its melting, have been studied extensively for many years and have now been related to the basic structure of the collagen molecule.[1] At the same time, collagen forms the main fibrous protein of the connecting and supporting tissues of the body, and its structure and mechanical properties are thus of considerable biological importance. In this paper we shall consider some of the transitions which take place in collagen and indicate how they may relate to pathological conditions in man.

TRANSITIONS IN DILUTE SOLUTION

Collagen is readily solubilized by treatment in weak acids, and studies of such properties as light scattering, viscosity, and optical rotation of the resulting solutions have been used to obtain information about the basic molecular unit in collagen.[2–4] Together with observations by x-ray and electron microscope techniques, these studies have revealed that the elementary unit is a three-stranded rope some 2600 A. long, normally held in a rigid, fully extended state by hydrogen bonding between the strands. When the temperature of a *neutral* solution is raised, a transition occurs between 35 and 40°C. from the rigid rodlike form to the randomly coiled form. This is thus the transition temperature for collagen where the molecules are effectively isolated from interaction with their neighbors.

PRECEDING PAGE BLANK NOT FILMED.

moving head of an extensometer, and the other is attached to a very stiff force transducer. At the start of a test the extensometer is adjusted so that the specimen is just taut and the transducer output indicates a slight force. The liquid in which the specimen is immersed is then heated at a constant rate, usually of the order of one degree in 5 min. Figure 2 shows the result obtained for kangaroo-tail tendon in saline solution. The shrinkage at 58°C. is very evident, and there is also an inflection in the curve at about 48°C. which will be discussed further below.

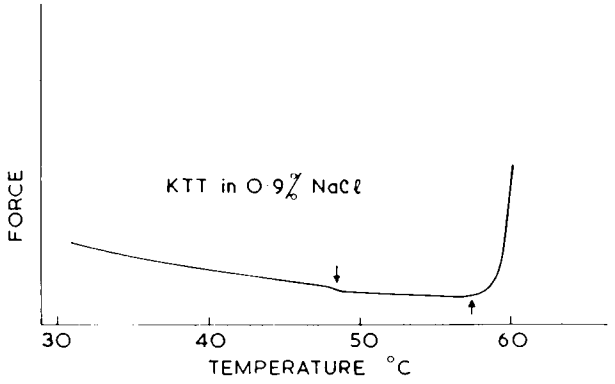

Fig. 2. A force-temperature curve for kangaroo-tail tendon immersed in 0.9% saline. The tendon is mounted in the apparatus of Fig. 1. The arrow pointing down indicates a glass transition, and that pointing up indicates the shrinkage temperature T_s (after Mason and Rigby, ref. 8).

This phenomenon of shrinkage has been shown to be simply a manifestation of a first-order phase change in the collagen;[5] that is, it is the macroscopic result of individual crystalline aggregates of rodlike molecules melting and retracting into random coils. However, it cannot therefore be assumed that T_s represents the thermodynamic melting point of the collagen crystals. On the contrary, the work of Oth et al.,[6] based on well-established principles of polymer science, has shown that the true reversible melting point T_m is obtained only when crystalline and melted regions coexist in the specimen, and is thus not measured in the specimen outlined above. An extensive series of measurements[7] on the system collagen-ethylene glycol showed that T_m obeyed the relation for the variation in melting

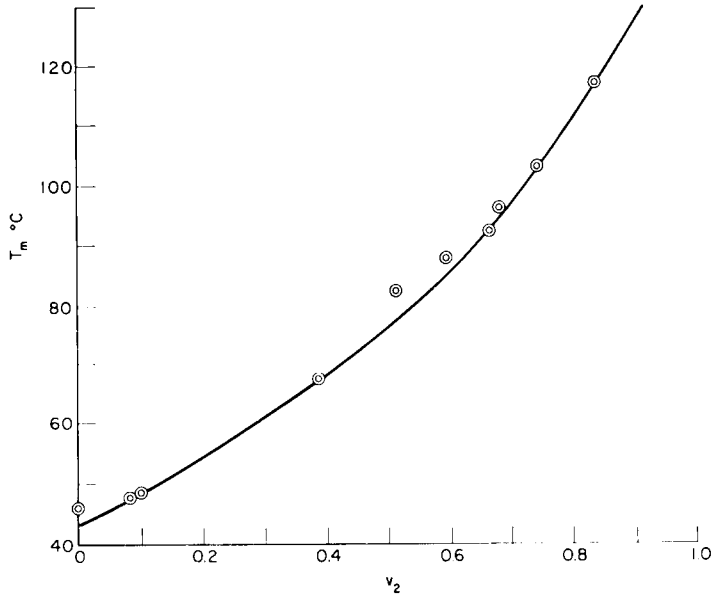

Fig. 3. The melting temperature T_m plotted as a function of volume fraction of collagen v_2 for collagen-ethylene glycol mixtures. The solid line is calculated from theory (after Flory and Garrett, ref. 7).

point of a polymer with a volume fraction v_1 of added diluent, viz.,

$$1/T_m - 1/T_m^\circ = [(R/\rho_2 V_1 \Delta h)](v_1 - \chi v_1^2) \qquad (1)$$

where T_m° is the melting point of the undiluted polymer, ρ_2 the density of the amorphous polymer, V_1 the molar volume of the diluent, χ the interaction constant, and Δh the specific heat of fusion of crystalline polymer.

The experiments were conducted over a wide range of concentration extending right down to dilute solutions, and the relation between T_m and the volume proportion of collagen, v_2, is shown in Figure 3. It is evident from this that there is a single melting process involved, and that the actual value obtained for T_m depends solely upon v_2. In this figure, the occurrence of T_s some 10°C. above T_m is an artefact produced by "superheating." None the less, the reproducibility of T_s even for collagens of quite different macro-

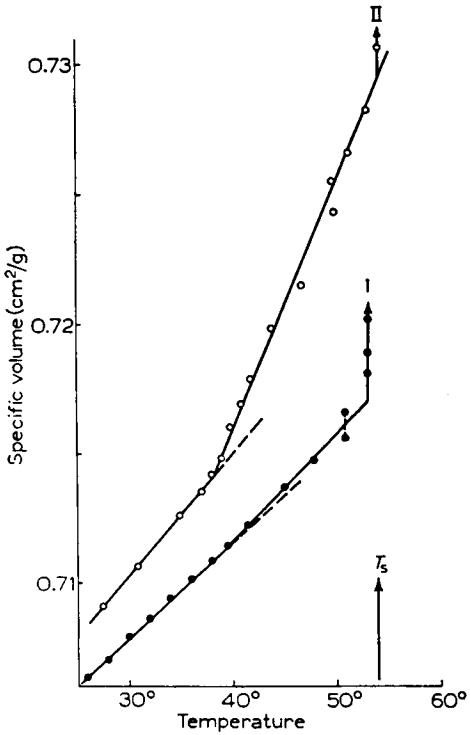

Fig. 4. Thermal expansion of beef collagen in 0.9% saline. (I) native material and (II) partially melted material (after Mason and Rigby, ref. 8).

structure (e.g., skin, tendon, cartilage taken from the same animal) is remarkable, and this consistency is a feature deserving elucidation.

We now return to the small inflexion in the force-temperature curve which was noted in Figure 2. This would appear to arise from a glass transition (at a temperature denoted by T_g) in the less ordered regions of the specimen. Flory and Garrett[7] observed reversible glass transition behavior between 40 and 45°C. for collagen in water, and ascribed this to rotational motion in side groups. It would seem, however, that the main backbone motions are directly involved, from the magnitude of the effect obtained when the specimen is partly melted. Figure 4 shows the result of one of the authors experiments[8] on the thermal expansion of a beef-collagen specimen first in the native state (black circles) and then after partially melting (open

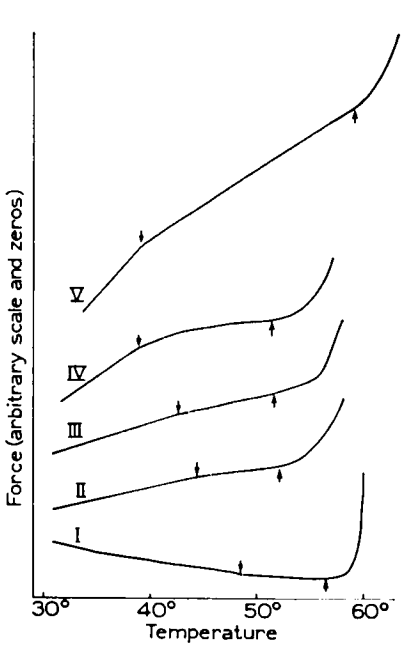

Fig. 5. Force-temperature relations for partially melted tendon in 0.9% saline. Arrow pointing down indicates location of T_p and arrow pointing up indicates location of T_s (after Mason and Rigby, ref. 8).

circles). The main melting is clearly seen on both curves. On the initial curve a small increase in expansivity occurs at about 40°C., but after the melting has taken place and the experiment is repeated, a much larger increase occurs at the same temperature.

The authors have been able to show these transitions in a simpler way by noting the changes in force with temperature,[8] in a sample which is held at its natural length in an extensometer as described above. Figure 5 shows a series of runs taken with one sample. Curve I is for the native material and the slight kink in the curve at 48°C. represents T_p, while T_s is represented by the sudden large increase in force at about 57°C. When the sample is partially melted by heating it beyond T_s for a few minutes and then returning it to room temperature, the subsequent behavior takes on a new pattern. Curves II, III, and IV show this. Now it can be seen that the major melting takes place at a lower value (about 51°C., which

is an estimate of T_m for a native collagen in 0.9% saline[8]) while T_g is lowered progressively to a stable value of about 39°C. In curve V the sample has been allowed to rest for a long period at 20°C. There has been much recrystallization as evidenced by the fact that the large-scale melting now takes place at the original value 58°C. Note, however, that the glass transition temperature has remained fixed at 39°C.

INFLUENCE OF THE LIQUID MEDIUM ON TRANSITION TEMPERATURES

It is well known that the thermal stability of collagen can be greatly affected by the nature of the liquid in which it is placed. Lennox[9] has tabulated the effects of a large number of reagents, some of which elevate the shrinkage temperature while others depress it; in extreme cases the depression may even be to a value below room temperature so that the material actually dissolves, for instance, in cold formic acid or concentrated sodium thio cyanate. In these latter cases it seems likely that the action is one of hydrogen bond breaking, so that the stability of the individual molecule is reduced, and T_D falls well below room temperature.

From the considerations in the preceding section, however, it will be seen that it is not necessary to change the individual molecular stability in order to affect melting; it is sufficient to produce a change in swelling. To illustrate this some effects will be discussed which sometimes, though not invariably, result from washing the collagen quite free from its original saline solution and allowing it to come to equilibrium in distilled water.[10]

In this experiment the most obvious result is that the sample swells. Figure 6 shows the effect with kangaroo-tail tendon. In most cases the authors noted that there are two general levels of swelling. The first stage is reversible when the sample is replaced in 0.9% saline, while the second (larger) stage is not. The authors have shown that it is the reticular sheath which limits the swelling to the first stage, for if this is slit, swelling will proceed to the second stage (see Fig. 6). If force-temperature curves (as in Fig. 2) are now made with these swollen samples the interesting fact is discovered that the shrinkage temperature T_s of the material in the first stage of swelling is about 51°C., while that of the second stage is much lower,

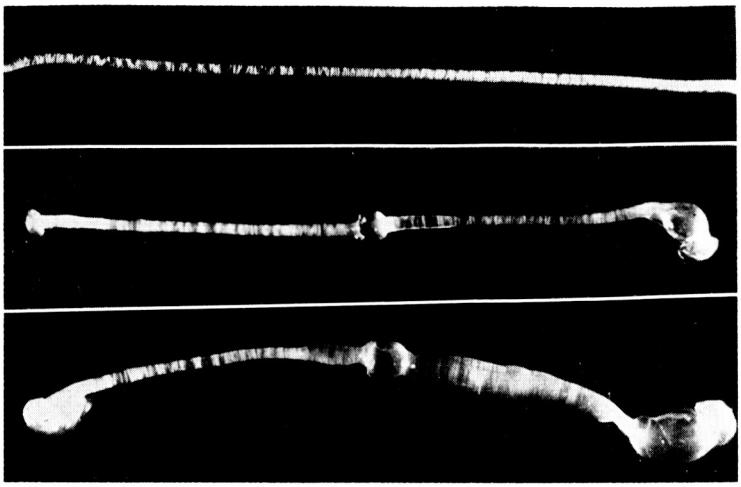

Fig. 6. Swelling of kangaroo-tail tendon (*A*) in 0.9% saline, (*B*) in water, and (*C*) after slitting right-hand side [as (*B*)] (after Kwon et al., ref. 10).

and in many cases as low as 39 to 40°C. Thus in the highly swollen second stage there is evidently little molecular interaction remaining, and although the specimen retains its cohesion it has approximately the same thermal stability as a dilute solution. Under these conditions T_m and T_g are no longer distinguishable from T_D.

INFLUENCE OF PROLONGED STRAIN ON TRANSITION TEMPERATURES

Under this heading the action of mechanical strain at room temperature and in 0.9% saline is considered. There are many parameters which can be varied in a mechanical experiment, and for the purposes of this paper only the effect of static strain and at two levels is considered. These were chosen to be 1 and 10%. One per cent was chosen because it would be encountered in the normal functioning of tendon, and 10% was chosen as a convenient level representing an extreme situation. The samples were extended to 1 or 10% and then held for varying periods of time. They were then released and force-temperature measurements made as described above. The behavior at 10% strain may be summarized as follows:[11]

(*1*) After short times of extension (up to 15 hr.) the structure is

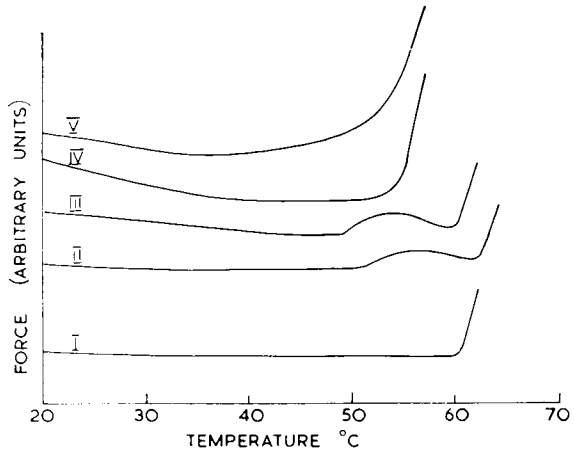

Fig. 7. Force-temperature relations for rat-tail tendon in 0.9% saline. The tendons were mechanically conditioned as follows: (I) native tendon, (II) 1% extension held for 22 hr., (III) 10% extension held for 4 hr., (IV) 10% extension held for 17 hr., and (V) 10% extension held for 69 hr. (after Rigby, ref. 11).

changed so that it begins to break down at about 51°C., although the final gross breakdown still occurs at the normal value 60°C. (*2*) After long times the structural damage is such that it begins to fail at about 35°C., although the final rupture occurs at 51°C., i.e., at the temperature of onset in the first series.

At 1% strain only the first type of behavior is observed, and is generally reversible upon resting the tendon for 12 hr. or more. Figure 7 summarizes the experiments. Again it can be noted that two major transitions are apparent, one at 51°C. and the other at 35°C.; and it seems likely that they may be interpreted as resulting from structural damage leading to successive increases in swelling.

At this point it should be emphasized that the samples were subjected to only a very small force when they were tested in the force-temperature experiment. Thus it can be said that damage already exists in the structure under no force. However, if an external force is applied while the sample is heated then the situation is different. In concluding the experimental section of this article an illustration of this is given. If a tendon is loaded with a mass appropriate to an extension of about 1% it is found that the creep (gradual extension

with time) is very small compared to 1%, for temperatures of from 20 to nearly 40°C. At 40°C. there is a sudden large increase in the extension and if the load is not removed, or if the temperature is not reduced, the sample will break. Again there is evidence of a structural change at about 40°C.

DISCUSSION

In considering the biological significance of these different transitions it will first be noticed that the two most destructive transitions are T_m and T_s which involve large irreversible changes in the collagen. However, the transitions at T_D and T_g, though apparently reversible under laboratory conditions, are probably the more important because they occur very close to normal body temperatures.

Strictly speaking, T_D is relevant only to dilute solutions, and it may be that the significance of this transition is in determining the configuration of the molecules during the processes of metabolism.

The transition of greatest relevance to the state of native collagen would seem to be that which has been identified above as the glass transition T_g. This is reversible under conditions where the material is not subject to mechanical loading, but, as indicated by the last experiment described above, irreversible damage may be done when the specimen is under tension.

To suggest a direct connection between, on the one hand, irreversible deformations occurring when T_g is exceeded, and, on the other, the various pathological conditions in body tissues classified as collagenous diseases would, at the moment, be purely speculative. However, the importance of such a connection clearly merits further investigation. The gaps in present knowledge are twofold; in the first place we need to know the detailed mechanical conditions under which collagenous tissue may be damaged, e.g., critical limits for stresses and strains applied singly or cyclically. In the second place we have little information concerning the variation in T_g with the relevant parameters, particularly swelling, pH, electrolyte concentration, amino acid composition, and mechanical loading. Many of these relations are known for the higher transition temperatures T_m and T_s as discussed in part above. In one instance the direct correlation between T_s and amino acid content (proline and hydroxyproline) has been shown[3,12] to extend also to transitions observed in

acid conditions close to 40°C. It is suggested that more attention of this kind should now be devoted to the transitions occurring in the neighborhood of the actual temperatures existing *in vivo*.

References

1. Harrington, W. F., and P. H. Von Hippel, *Advan. Protein Chem.*, **16**, (1961).
2. Boedtker, H., and P. Doty, *J. Am. Chem. Soc.*, **78**, 4267 (1956).
3. Doty, P., and T. Nishihara, in *Recent Advances in Gelatine and Glue Research*, G. Stainsby, ed., Pergamon Press, New York, 1958, p. 92.
4. Rich, A., and F. H. C. Crick, *J. Mol. Biol.*, **3**, 483 (1961).
5. Garrett, R. R., and P. J. Flory, *Nature*, **177**, 176 (1956).
6. Oth, J. F. M., E. T. Dumitru, O. K. Spurr, Jr., and P. J. Flory, *J. Am. Chem. Soc.*, **79**, 3288 (1957); see also L. Mandelkern, *Rubber Chem. Tech.*, **32**, 1392 (1959).
7. Flory, P. J., and R. R. Garrett, *J. Am. Chem. Soc.*, **80**, 4836 (1958).
8. Mason, P., and B. J. Rigby, *Biochim. Biophys. Acta*, **66**, 448 (1963).
9. Lennox, F. G., *Biochim. Biophys. Acta*, **3**, 170 (1949).
10. Kwon, D. S., P. Mason, and B. J. Rigby, *Nature*, in press.
11. Rigby, B. J., *Biochim. Biophys. Acta*, in press.
12. Rigby, B. J., *Biochim. Biophys. Acta*, **62**, 183 (1962).

Synopsis

1460/

Four structural transitions in collagen are considered, viz., the shrinkage temperature T_s at which a specimen shrinks abruptly to about one-quarter of its original length; the melting temperature T_m, which is the true thermodynamic melting point of the crystalline system and may be 10°C. or more below T_s; the glass transition temperature T_g, which is lower than T_m and which marks an abrupt increase in the thermal expansion coefficient; and finally the denaturation temperature T_D, which is the temperature at which collagen molecules in dilute solution undergo the transition from helices to random coils. Measurements of T_s and T_g are described and discussed in relation to (*a*) partial premelting of the specimens, (*b*) the effects of swelling in water, and (*c*) the influence of prolonged mechanical strain. T_g is the only one of the bulk transitions which occurs in the vicinity of normal body temperature and may be closely involved in the pathology of collagenous structures. It is suggested that the effects of such factors as swelling, pH, amino acid composition, and mechanical loading, which have already been studied in relation to T_s, should now be examined in relation to T_g.

Author

Abstract

The Subsidence of Muscle Fiber Dispersions

H. COREY, *T. J. Lipton, Inc., Hoboken, New Jersey*

The settling behavior of meat dispersions was investigated as a possible objective method for the evaluation of texture.

Samples of cooked, freeze-dried chicken meat were dispersed in a Waring blendor with deionized water and the resulting slurries deaerated and "aged" before experiments were begun. Prior to the onset of settling, these dispersions form large flocculated structures which apparently undergo syneresis. The distance-time data give curves that are invariably S-shaped and can also in part be fitted to the La Mer subsidence expression $t/(h_0 - h_t) = \alpha + \beta t$ whereby the expected linearity is observed.

The several variables of the system including particle size, percentage solids, salt (NaCl) concentration, "aging" time, shearing time in blendor, and vessel geometry were examined for their effect on the linear region of the La Mer plot. Of particular interest is the observation that under conditions where floc formation is the dominant initial phase, the magnitude and relative displacement of the slopes are hyperbolic functions of the initial height and the percentage solids in the dispersion. For any given percentage solids the slopes *increase* in magnitude with *decreasing* column height. When the height is kept constant the slopes *decrease* in magnitude with *increasing* percentage solids.

The subsidence velocity of these muscle fiber dispersions exhibits a marked dependence on the starting height of the system. This remarkable phenomenon leads to the conclusion that the mechanism of settling can be considered an overdamped elastic recoil. On this basis a modified form of the well known vibration equation was derived: $h = C_1 \exp\{-u_1 t\} + C_2 \exp\{-u_2 t\} + f(t)$. This proves adequate to describe completely the general form of all the settling

PRECEDING PAGE BLANK NOT FILMED.

curves obtained. In a particular case, with proper choice of spring constant and damping factor, the calculated time–distance curve closely matches that drawn from experimental data. Since the ma or exponential terms diminish rapidly with time, the vibration equation also predicts a linear decay of velocity as does the La Mer expression. Thus the physical picture of homogeneous density during compression required by the La Mer treatment may very well represent the limiting mode of behavior for the elastic recoil model.

N67 14602

Polarisationsoptik aus dem Glaskörper tierischer Augen gesponnener Fäden als Ausdruck ihres biorheologischen Verhaltens

HANS H. PFEIFFER*, *Laboratorium für Polarisationsmikroskopie, Bremen, Bundesrepublik Deutschland*

1. MECHANISCHE UND LICHTOPTISCHE ANISOTROPIE

Das corpus vitreus der Augen von Säugern und andern Vertebraten, dessen Isolierung aus dem Auge mehrfach[1,2] angegeben wurde, zeigt nach leichtem Verletzen ein Abtropfen und dabei das Phänomen des Fadenziehens (Spinnbarkeit, Fibrogenesis). Diese Deformation der im wesentlichen aus dem sauren Mucopolysaccharid der Hyaluronsäure aufgebauten Substanz[3] ist mit einer Orientierung der Leptonen assoziiert, wie sich an vielerlei Auswirkungen anisodiametrischer Struktur erkennen lässt. Kündet schon die Fadenförmigkeit des Gebildes die *Länge als ausgezeichnete Richtung* an, so ist nach Beobachtungen der Zugfestigkeit, Längsspaltbarkeit und quer gerichteten Quellungsmaximums die Kohäsion nach der Länge am grössten, vertikal dazu am kleinsten. Von der Kohäsion des Fadens hängt auch der Effekt der Orientierungsviscosität ab, welcher mit wachsender Zugspannung zu einer Zunahme der Viscosität pro Einheit des Querschnittes führt und nach *Nitschmann* und *Schrade*[4] mit der von ihnen entwickelten Spinnwaage (Fig. 1) zu messen ist, indem an einem beim Ausziehen fliessenden Faden aus der Zugkraft **P**(dyn), dem Querschnitt **q** (cm²) und der Länge **l**(cm) des Fadens zur Ermittlung der Viscosität η die von *F. Trouton* angegebene Beziehung:

$$\eta = \frac{1}{3} \frac{\mathbf{P}}{\mathbf{q}} \frac{\mathbf{l}}{\Delta \mathbf{l}} \Delta \mathbf{t} \qquad (1)$$

angewandt wird. Zu erwarten ist ferner beschleunigte Wärmeleitung in der Längsrichtung und eine entsprechende Ausrichtung elektrischer und magnetischer Kraftfelder. Vor allem aber kann vertikal zur Fadenachse *transmittiertes Licht* nur nach den ausgezeichneten Richtungen längs und quer zur Achse des Fadens schwingen, und die beiden Schwingungsrichtungen sind unterschiedlichen Brechungskoeffizienten $n_{\parallel}$, $n_{\perp}$ zugeordnet, d.h. das Licht wird beim Passieren des Fadens in zwei linear polarisierte Anteile n_0, n_e zerlegt, deren

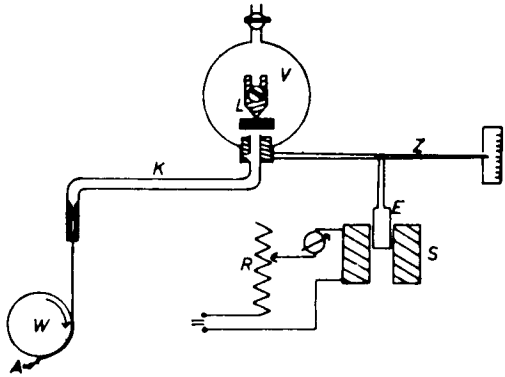

Fig. 1. Schema der Spinnwaage nach *Nitschmann* und *Schrade*[4] mit als Waage ausgebildetem Vorratsgefäss *V*, welches mittels zweier Stahlschneiden *L* auf flach geschliffenen Lagern ruht und auf einer Seite die rechtwinklig gebogene Ausflusscapillare *K*, auf der andern den Zeiger *Z* gegenüber der Scala zeigt. Der ausgepresste Faden legt sich tangential an den Umfang einer motor-getriebenen Walze *W* und wird durch den Schaber *A* abgezogen. Die Stromstärke wird durch den Wilderstand *R* reguliert. Der Versuch wird mit wachsender Zuggeschwindigkeit bis zum Reissen fortgeführt; *S* Solenoid, *E* Eisenhern.

Schwingungsrichtungen senkrecht aufeinander stehen. Den beiden Schwingungsrichtungen dieser Orientierungsdoppelbrechung kommt teils ohne Vorbehandlung, teils nach Anfärben, manchmal auch nur ausserhalb des sichtbaren Wellenbereiches im Ultraviolett, eine in gleicher Weise unterschiedliche Absorption parallel und vertikal zur Fadenachse mit den Koeffizienten $k_{\parallel}$, $k_{\perp}$ zu, sogen. Dichroismus. Schliesslich erfolgt auch die Beugung des Lichtes durch gesponnene Fäden anisotrop, indem Intensität der Beugung und Polarisationsgrad des abgebeugten Lichtes in der Längsrichtung und senkrecht dazu verschieden sind (Doppelbeugung, Beugungspolarisation).

Alle *drei Effekte* des polarisierten Lichtes sind an den vom corpus vitreus ausgezogenen Fäden nachgewiesen worden, am häufigsten die den geringsten Aufwand bei Durchführung der Experimente verlangende Doppelbrechung. Alle diese polarisations-optischen Arbeitsweisen können qualitativ angewandt werden und nur auf das Vorkommen einer irgendwie orientierten Ultrastruktur gerichtet sein. Wertvoller wegen der grösseren Summe an Information aber ist natürlich eine quantitative Durchführung der Versuche.[5]

2. STRÖMUNGSDOPPELBRECHUNG GESPONNENER FÄDEN

Ohne die Morphologie der aus dem Glaskörper ausgezogenen Fäden[2] nochmals zu schildern, seien grundlegende Bemerkungen zu allen jenen polarisationsoptischen Methoden und zuerst zur Doppelbrechung hierhergerückt.

Quantitativ wird der Effekt der Strömungsdoppelbrechung

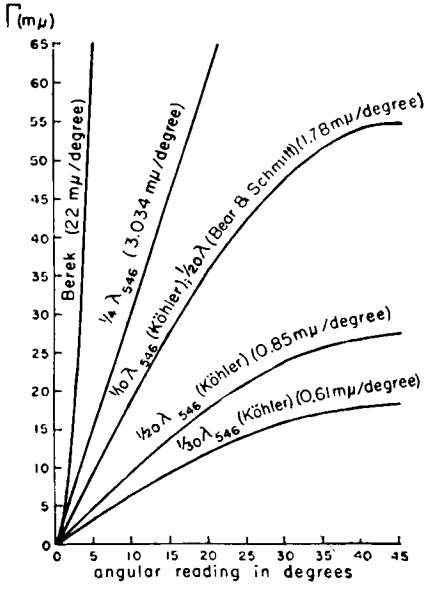

Fig. 2. Charakeristiken verschiedener Kompensatoren mit Retardation ($m\mu$) als Ordinate, den Winkelgrössen (Grade) als Abscisse. Die Brüche der Wellenlängen beziehen sich auf die grüne Hg-Bande 5460 Å.

zunächst an dem Auslöschwinkel χ (im englischen Schrifttum: angle of isocline) gemessen. Er kann mittels eines durch regulierbaren Präzisionsspalt seitlich ausgeblendeten Areals des Fadens bei $\pm 15°C$ aus der Orthogonalstellung der gekreuzten Nicols je nach Viscosität und Fliessgefälle zu $\chi = 65$ bis $72°$ ermittelt werden. Nachdem dann die Nicols in Diagonalstellung gebracht worden sind, wird mit Gipsplättchen Rot I oder Quarzkeil oder auch Kompensator nach Sénarmont[5] der im vorliegenden Falle positive *Charakter* ($n_e > n_0$) der

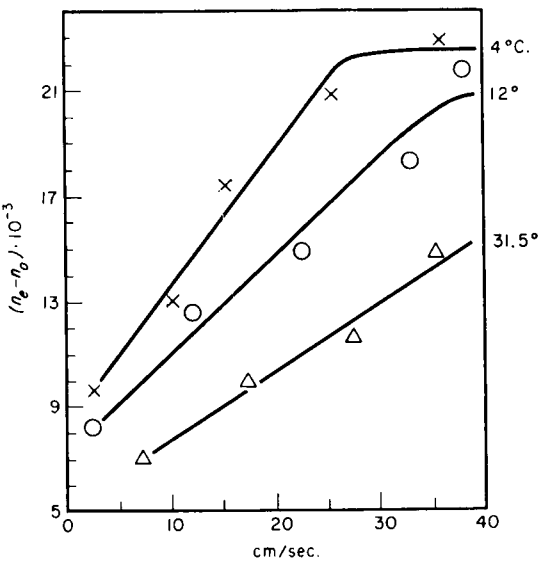

Fig. 3. Abhängigkeit der Strömungsdoppelbrechung ($n_e - n_0$) von der Geschwindigkeit des Fadenziehens (cm/s) bei verschiedenen Temperaturen.

Doppelbrechung ermittelt. Durch eine densitometrische Anordung[6] oder auch kompensatorisch wird schiesslich die *Intensität* der Strömungsdoppelbrechung bestimmt. Wegen der niedrigen Grössenordnung der bei den Glaskörperfäden zu ermittelnden Werte empfiehlt sich dazu der Gebrauch eines $\lambda/30$-Kompensators nach *Brace* in Kombination mit der Halbschattenvorrichtung nach *Macé de Lepinay*.[5] (Vgl.über die unterschiedliche Empfindlichkeit gebräuchlicher Kompensatoren Fig. 2). Exakte Messungen der Intensität der Doppelbrechung sollten auf die Einheit der Fadendicke, des

Fliessgefälles und der Viscosität reduziert werden, mindestens Übereinstimmung in diesen Parametern verlangen.

Im allgemeinen wächst die *Strömungs-Doppelbrechung* anfangs linear, dann langsamer mit den Fliessgeschwindigkeiten und erreicht bald eine Sättigung (Fig. 3). So wird ihre Zunahme auch bei Versuchen der Streckhärtung mit der Spinnwaage[4] bei schnellerer Bewegung der Walze **W** beobachtet. Plötzliches Abbremsen der Fliessbewegung der Fäden führt zu inverser Massenbewegung; solche Fliess-Elastizität[2] kann bei höheren oder niedrigeren Werten der Doppelbrechung vorkommen. Eine schnelle Reduktion ihrer Intensität bei konstanter Temperatur konnte in solchen Fällen nicht gefunden werden. Daraus folgt, dass beim Fliessen der Fadenmasse weder ein deutlicher photo-elastischer, Effekt eintritt, noch die Leptonen des corpus vitreus kolloiden Assoziaten vergleichbar sind, welche bei Zunahme des Fliessgradienten in weniger anisotrope oder gar isotrope Mikro-Leptonen zerfallen. Mit zunehmender Temperatur sinkt die optische Anisotropie wegen der Kompensation des ausrichtenden Effekts des Fadenspinnens durch zunehmende Lebhaftigkeit der *Brown'*schen Bewegung (Fig. 3). Sehr wahrscheinlich ist die Stärke der Doppelbrechung der Glaskörperfäden auch konzentrationsabhängig. Darauf scheint der gelegentliiche Befund langsamen Abklingens des Effekts hinzuweisen, eine Erscheinung, welche wohl eher auf Schwerbeweglichkeit der Leptonen oder eine hohe Viscosität als auf einen früher im Sinne einer Stetigkeitstheorie gedeuteten Rückgang elastischer Verzerrung zurückzuführen ist. In einigen Fällen vorgekommene Trübung des Glaskörpers, vielleicht hervorgerufen durch eine Synchisis scintillans, ergab neben erhöhter Viscosität eine gegen die Norm gesenkte Doppelbrechung. Rheologisch von Bedeutung ist schliesslich, dass die ausrichtende Wirkung des Fadenziehens an zentral gelegenen Partien der Fäden eine geringere Intensität der Strömungsdoppelbrechung als an peripheren Stellen hervorruft, was sicher mit schwächerer Orientierung innerhalb der mittleren Partien zu interpretieren ist.

3. DICHROISMUS UND BEUGUNGSPOLARISATION BEIM FADENSPINNEN

(*a*) Da die spinnend deformierte Glaskörpersubstanz neben der Strömungsdoppelbrechung lichtoptisch auch *anisotrope Absorption* (Dichroismus) zeigt, sind Versuche und Messungen auch an diesem

Phänomen angestellt worden. Ganz allgemein handelt es sich bei der Erscheinung darum, dass die Strukturen der Fäden chemische Gruppen enthalten, welche bei Untersuchung in polarisiertem Lichte dieses anisotrop absorbieren. Bei den Glaskörperfäden muss die Erscheinung im Wellenbereich sichtbaren Lichtes allerdings erst durch Färben mit organischen Farbstoffen, wie Congorot, Thioninblau, Jodviolett und anderen, experimentell induziert werden. Kenntlich wird dieser stets mit Doppelbrechung assoziierte Färbungsdichroismus beim Einstellen nacheinander auf beide Schwingungsrichtungen des hindurchgeschickten linear polarisierten Lichtes durch die unterschiedliche Färbung, in andern Fällen auch durch Differenz in der Nuance oder der Helligkeit. Vom Dichroismus im Wesen verschieden, wie freilich sicher nur durch spektrophotometrische Analyse erkannt werden kann,[7] ist die *Metachromasie*. Bei dieser tritt mit steigender Farbstoffkonzentration eine deutliche Verschiebung der Absorptionsbande nach geringeren Wellenlängen hin ein, die beim Dichroismus ausbleibt. Beim Spinnen von Fäden aus den mit Congorot gefärbten Glaskörpern wird Grün stark absorbiert, wenn die Schwingungsebene des Lichtes parallel zur Fadenachse gerichtet ist; hingegen entfällt die Grünabsorption fast vollständig, wenn die Schwingungsebene vertikal zur Fadenrichtung steht

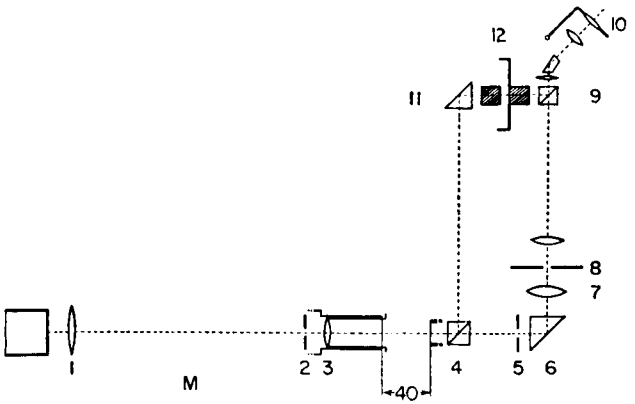

Fig. 4. Schema des Strahlenganges im Mikroskop-Photometer *Leitz*. Es bezeichnen: *M* Monochromator, 1 und 2 dessen Kollimator und Spalt, 3 Projektionsobjektiv, 4 und 9 Verteilprismen, 6 und 11 reflektierende Prismen, 5 Diaphragma für den Vergleichsstrahl und 8 seine Abbildungsebene, 7 Kondensor, 10 Lupe vor dem Okular, 12 Messschraube.

(*"wahrer Dichroismus"*). Maximal ist der färbungsdichroitische Effekt übrigens bei Behandlung mit niedrigen Farbstoffkonzentrationen.

Färbungsdichroismus wird allgemein mit orientierter Anlagerung der Farbstoffpartikel oder (?) lokaler chemischer Bindung der Farbstoffe in den Interstitien des Fadengefüges gedeutet. Beim *Metalldichroismus* hingegen, wie er beispielsweise durch Behandlung mit Goldchlorid oder Silbersalzen vorkommt, kann diese Deutung nach Röntgenbeugungs-Diagrammen nicht zutreffen, und es wird angenommen, dass die Metallteilchen durch photo-elastische Spannungen dichroitisch werden oder nicht Eigendichroismus, sondern Formdichroismus vorliegt, d.h. in regelmässigem Wechsel farblose Balken und metallerfüllte Interstitien die Spinnfäden aufbauen.

Die *quantitative Bestimmung* des Dichroismus besteht in der Ermittlung der Differenz der beiden zueinander gehörenden, nach spektrophotometrischer Technik zu ermittelnden Absorptionskoeffizienten $k_{\parallel}$, $k_{\perp}$.[5,7,9] Indem bei senkrechter Inzidenz vom einfallenden Licht der Anteil $\nu = (n-1)^2/(n+1)^2$ reflektiert wird, so resultiert als Durchlässigkeit **D**:

$$\mathbf{D} = \left\{4n/[n+1)^2\right\}^2 e^{-(4\pi k/\lambda_0)d} \tag{2}$$

und nach Austausch des natürlichen gegen den dekadischen Logarithmus für jeden der beiden Absorptionskoeffizienten die Beziehung (3):

$$k = \frac{\left[2\log\frac{4n}{(n+1)^2} - \log \mathbf{D}\right]\cdot\lambda_0}{4\pi d\cdot\log e} \tag{3}$$

Bei den Messungen hat sich das zuletzt von *Boguth*[8] beschriebene Mikroskop-Photometer von Leitz wegen seiner relativen Einfachheit gut bewährt (Fig. 4). Den bei dieser Apparatur durch den konvergenten Strahlengang entstehenden Fehler am Messergebnis kann man aus der approximativen Lösung der von *Boguth*[8] mitgeteilten Integralgleichung vermeiden.*)

* In der Textilindustrie und bei Fadenuntersuchungen weithin gebräuchlich ist statt der Ermittlung der Differenz der Absorptionskoeffizienten die Bestimmung eines dichroitischen Koeffizienten als Quotienten: $\mathbf{D}^* = k_{\parallel}/k_{\perp}$; vgl. *Preston*[10]. Die damit erkennbaren Gesetzmässigkeiten stimmen aber mit den hier vorgezogenen Bestimmungen völlig überein.

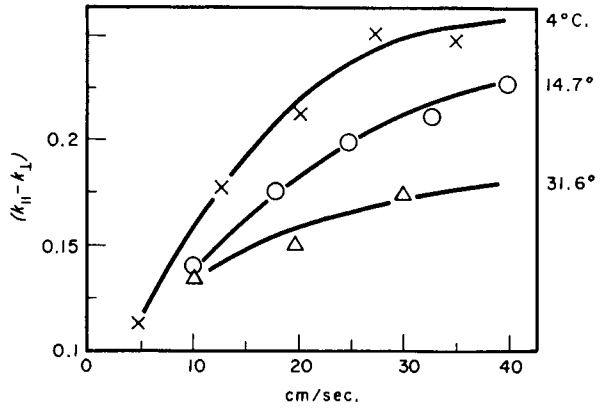

Fig. 5. Abhängigkeit des Färbungsdichroismus $k_{\parallel} - k_{\perp}$ von der Geschwindigkeit des Fadenziehens(cm/s) bei abgeänderten Temperaturen.

Im *gesetzmässigen Verhalten* gleicht der Färbungsdichroismus der Fäden des corpus vitreus lückenlos der Strömungsdoppelbrechung. Die mit zunehmender Ausziehgeschwindigheit der Fäden verknüpfte Verbesserung der leptonischen Orientierung äussert sich dementsprechend in einer durch eine Sättigungskurve zu beschreibenden Steigerung auch des Dichroismus (Fig. 5), wie z. Bsp. Spinnwaage-Versuche mit beschleunigter Walzendrehung belegen können. Umgekehrt proportional verhält sich der Dichroismus hingegegen mit wachsender Temperatur.

(*b*) Das Phänomen der *Beugungspolarisation*[5] besteht im Wesen darin, dass der elektrische Vektor, welcher parallel zu den beim Fadenziehen ausgerichteten Leptonen schwingt, weniger leicht als der vertikal zu dieser Hauptdimension schwingende hindurchgeht, jener also im Vergleich zu letzterem bevorzugt abgebeugt wird. Ein messbarer Anteil des transmittierten Lichtes wird dann bei dem Prozess geradlinig polarisiert. Eine qualitative Prüfung einer ziemlich monochromatischen Strahlung nach ihrem Passieren der Glaskörperfäden wird am besten mit drehbarem Analysator and $\lambda/4$-Platte vorgenommen.[11] Stets wenn sich beim Drehen des Analysators Helligkeitsschwankungen zeigen und ausserdem bei einer bestimmten Stellung die Lichtintensität bis auf null sinkt, kommt linear polarisiertes Licht als Anteil eines bestimmten Polarisationsgrades vor. Aber auch, wenn nach Einstellen des Analysators

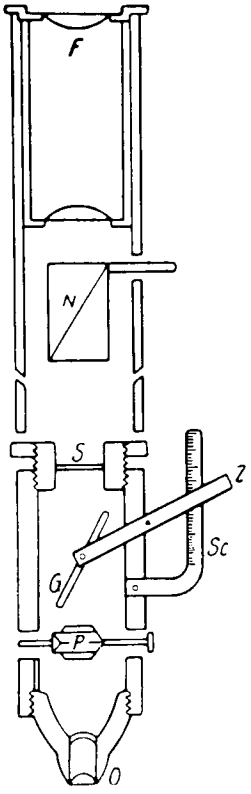

Fig. 6. Schema der Vorrichtung zur beugungspolarisatorischen Messung nach *J. Koenigsberger* mittels *Savart*'scher Platte S. Ferner bedeuten: *F* auf ∞ eingestelltes Fernrohr, *N* Innennicol mit weiter Apertur, *O* Objektiv, *P* ein ein wenig exzentrisches, total reflektierendes, rechtwinkliges Prisma, *G* Glasplatte, deren gegen die Instrumentenachse variierbare Neigung mit dem System aus Zeiger *Z* und Scala *Sc* gemessen wird.

auf das Helligkeitsminimum dessen Lage mit einer früheren Minimumstellung ohne $\lambda/4$ ohne weiteren Eingriff oder aber nach Drehen der $\lambda/4$-Platte um 180° zusammenfällt, so enthält die Strahlung einen überwiegenden Anteil linear polarisierten Lichtes und nur eine begrenzte Beimengung von natürlichem, elliptischem oder zirkularem Lichte.

Indessen ist das Kriterium der Helligkeitsschwankungen infolge

nur sehr geringer Polarisation nicht immer leicht und sicher festzustellen. Besser empfindlich wird die Versuchsanordnung erst bei *quantitativer Erfassung* des Polarisationsgrades $\Delta\Gamma = \text{II}/(N + \text{II})$, wenn wie in der Messanordnung nach *J. Koenigsberger* (Fig. 6) eine *Savart*'sche Platte zu Hilfe genommen wird.[5] Da der beugungspolarisatorische Effekt direkt proportional der durchstrahlten Schichtdicke und der Differenz der Lichtbrechungs- und der Absorptions-Koeffizienten, umgekehrt proportional der Gitterkonstante des Objekts ist, lässt sich die Empfindlichkeit der Messmethode durch ein Filter zur Reduktion der Wellenlänge, etwa ein Ultraviolettschwarzglas 366 mμ (Schott & Gen.) noch erheblich steigern. Indem nach Deduktionen theoretischer Physiker[5] unter sonst konstanten Bedingungen allgemein bei Zunahme einer Aggregation der Leptonen der Grad des Beugungspolarisation wächst, darf vielleicht aus einer Verstärhung des Phänomens beim rheologischen Versuch des Fadenziehens auf eine solche Folgewirkung geschlossen werden.

4. SCHLUSSFOLGERUNGEN

(*a*) Durch die Befunde beim Studium der Phänomene der Strömungsdoppelbrechung, des Färbungsdichroismus und der Beugungspolarisation der aus dem corpus vitreus gesponnenen Fäden kann kein Zweifel darüber herrschen, dass durch die experimentelle Deformation des Objekts rheologisch eine auf leptonischer Ebene bestehende *ultrastrukturelle Orientierung* hervorgerufen wird, auch wenn der elektronenmikroskopische Nachweis geordneter Fibrillen noch aussteht.

(*b*) Nach der *Orientierungstheorie*[12] kommen die polarisationsoptischen Effekte übereinstimmend so zustande, dass suspendierte Leptonen der beim Ausspinnen der Fäden laminar strömenden Glaskörpersubstanz in eine solche Rotation versetzt werden, dass das Substrat eine Vorzugsachse erhält, nämlich die Richtung, in welcher sich die Leptonen statistisch am längsten befinden. Diese Kinematik wird dann überlagert durch die desorientierende *Brown*'sche Bewegung (Fig. 7), so dass, wie vor allem Versuche mit veränderter Temperatur zeigen, das Mass der polarisatorischen Effekte und die spezielle Lokalisierung der Vorzugsrichtung wesentlich beeinflusst werden.

(*c*) Nach diesen Vorstellungen[12] führen zu Anfang (zur Zeit $t = 0$) isotrope Verteilungen der Leptonen bei allen Richtungen zu einem

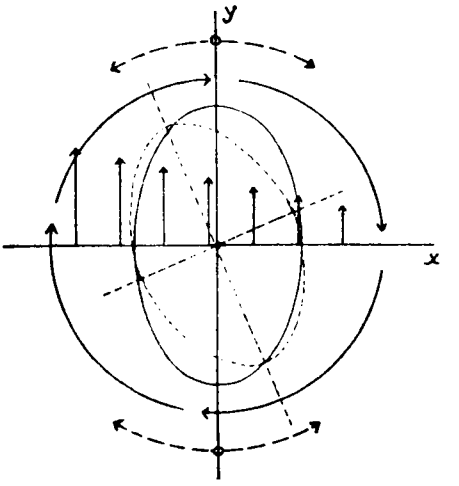

Fig. 7. Schema der Orientierung stabförmiger Leptonen nach der Orientierungstheorie. Es bezeichnet x das Strömungsgefälle (abnehmend von links nach rechts), y die Strömungsrichtung. Die ausgezogenen Pfeile beim Umfang der Figur deuten die einsinnig nach rechts gerichtete Rotation der Leptonen im Strömungsgefälle an, die gestrichelten Pfeile den Einfluss der *Brown*'schen Teilchenbewegung. Die ausgezogene Ellipse gibt ein Masz der Richtungsdichte in Polarkoordinaten (maximale Akkumulation in Richtung y), die gestrichelte ein Masz der *resultierenden* Richtungsdichte.

Pendeln der Amplitude der Verteilungsfunktion der Periode $\tau/2$. Dabei verteilen sie sich zu Beginn des *Orientierungsprozesses* ($t = 0$) gleichmässig auf alle Richtungen in der Ebene, und durch ungleichmässige Rotation werden die Teilchenachsen schrittweise in der Strömungsrichtung angehäuft. Während die initiale, isotrope Einstellung der Leptonen für die halbe Periode der Umlaufbewegung ($t = \tau/2$) charakteristisch ist, wird die extreme Verteilung mit der halben Periode der Teilchenverteilung, d.i. ein viertel Periode der Umlaufbewegung des Systems ($t = \tau/4$) erreicht. Dabei dürfte letztere Einstellung nur von sehr langen Leptonen in sehr langer Zeit in asymptotischer Annäherung erfolgen.

(*d*) Indessen gilt es zu berücksichtigen, dass der Effekt der leptonischen Orientierung eigentlich *nur im statistischen Sinne* strenge Gültigkeit beanspruchen kann. Sicherlich ist ein Denken in Termini leptonischer Orientierung nur mit erheblicher Simplifizierung der Verhältnisse möglich, auch wenn sehr viel feinere Fibrillen biolo-

gischer Materialien elektronenmikroskopisch in der Tat die postulierte leptonische Anordnung gezeigt haben. Auch mag die polarisationsmikroskopisch erschlossene Orientierung im einzelnen mit statistischen Eigenschaften der orientierten Strukturen beträchtlich ultramikroskopischer Komplexität in Korrelation stehen, vermutlich aber wohl weniger in Form linearer, mit Proteinen assoziierter Mucopolysaccharide als vielleicht eher polymerer, kompakter, *granulosen Makromolekeln*—eine durch die biorheologischen Versuche gestützte Auffassung, welche durch das Phänomen der Fliess-Elastizität der Fäden[2] noch beträchtlich kompliziert werden dürfte.

References

1. Pfeiffer, H. H., *Naturwissenschaften*, **48**, 133 (1961).
2. Pfeiffer, H. H., *Biorheol.*, **1**, 111 (1963).
3. Pfeiffer, H. H., *Acta Histochem.*, **13**, 360 (1962).
4. Nitschmann, H., und J. Schrade, *Helv. Chim. Acta*, **31**, 297 (1948).
5. Pfeiffer, H. H., *Das Polarisationsmikroskop als Messinstrument in Biologie und Medizin*, Friedr. Vieweg & Sohn, Braunschweig, 1949.
6. Swann, M. M., und J. M. Mitchison, *J. Exptl. Biol.*, **23**, 226 (1950).
7. Pfeiffer, H. H., *Ann. Histochim.*, Suppl. **2**, 165 (1962).
8. Boguth, W., in *Handbuch der Mikroskopie in der Technik*, Vol. 1, H. Freund, ed., Umschau Verlag, Frankfurt, 1957, p. 469.
9. Pfeiffer, H. H., in *Flow Properties of Blood and other Biological Systems*, A. L. Copley und G. Stainsby, eds., 1960, Pergamon Press, New York-Oxford, p. 145.
10. Preston, J. M., *Modern Textile Microscopy*, Emmott & Co., London, 1933.
11. Schönrock, O., in *Praktische Physik*, Vol. 1, Fr. Kohlrausch, ed., B. G. Teubner, Berlin, 1944, p. 499.
12. Peterlin, A., und H. A. Stuart, in *Hand- und Jahrbuch der chemischen Physik*, Vol. 8, A. Eucken, ed., Becker & Erler Kom.-Ges., Leipzig, 1943.

Synopsis

14602

Three effects of thread-shaped deformation of the vitreous humour of animal eyes were qualitatively and quantitatively studied in polarized light: the flow birefringence, the double absorption or dichroism, and the double diffraction (Doppelbeugung, Beugungspolarisation). For each case, an attempt was made to interpret the behavior of the spinning threads by assuming the orientation theory of Peterlin and Stuart (in *Hand- und Jahrbuch der chemischen Physik*, Vol. 8, A. Eucken, ed., Becker & Erler Kom.-Ges., Leipzig, 1943) within its limitations.

author

BLOOD CLOTTING AND LOW SHEAR HEMORHEOLOGY

N67 14603

La Propriété Thrombodynamique du Caillot: Propriété Hémorhéologique Spécifique Explorée par le Thrombélastographe (La fonction thrombodynamique des plaquettes, de la fibrine et de certains facteurs du plasma et du sérum)

MAURICE E. LEROUX,*† *Laboratoire d'hématologie, Faculté de médecine de Tours, Tours, Indre et Loire, France*

En 1948 la thrombélastographie de Hartert[13] a ouvert des horizons entièrement nouveaux dans l'étude de la coagulation. Elle en donne une représentation chronométrique, fonction de la vitesse des réactions enzymatiques, et surtout une représentation hémorhéologique originale, fonction de l évolution d'une certaine propriété physique du caillot mesurée par l'appareil et que nous appellerons tout à l'heure la *propriété thrombodynamique*. Ses applications cliniques sont des plus intéressantes. D'une pratique très courante en Europe continentale, elles sont aujour-d'hui parfaitement codifiées[3,10,26,39,40,43,49] notamment grâce aux travaux princeps de Hartert puis à nos nombreuses contributions, faites avec le Professeur Marchal, Samama et al. Nous n'en parlerons ici qu'incidemment, pour illustrer l'exposé de nos travaux sur la nature de la propriété hémorhéologique explorée par le thrombélastographe et sur les *facteurs* biologiques qui la conditionnent.

† *Adresse professionnelle:* Département d'hématologie de la Faculté de médecine et Centre régional de Transfusion sanguine, 2, Boulevard Tonnellé, Tours, Indre et Loire, France.

PRECEDING PAGE BLANK NOT FILMED.

I. LA COAGULATION DANS LE THROMBÉLASTOGRAPHE

Le thrombélastographe de Hartert se compose schématiquement d'une cuve oscillante et d'un système de torsion[13–15,26,28,40] (voir figure 1).

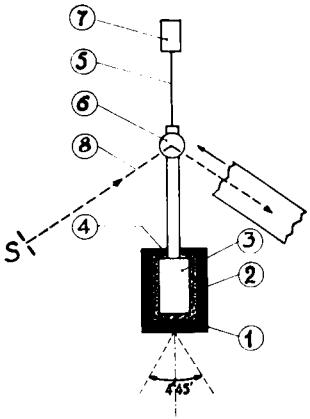

Fig. 1. Schéma de fonctionnement du thrombélastographe. (1) Cuve en acier V2A. (2) Caillot. (3) Cylindre en acier V2A, relié au fil de torsion. (4) Couche d'huile de vaseline protégeant le caillot de la déssiccation. (5) Fil de torsion. (6) Miroir solidaire du système de torsion. (7) Potence de fixation du fil de torsion. (8) Faisceau lumineux d'une lampe à fente.

La *cuve cylindrique* en acier poli V2A est animée autour de son axe vertical d'une *oscillation périodique* dont l'amplitude est de 4° 45′ et la durée de 9 secondes, y compris un arrêt d'une seconde à chaque extrêmité du déplacement.

Le *système de torsion* se compose d'une corde en acier de 0.2mm de diamètre et de 20mm de long, soudée en haut à une potence, aboutissant en bas à un dispositif d'amortissement hydraulique apériodique porteur d'un *miroir*, puis à un *cylindre* en acier V2A qui pend librement dans la cuve.

Le *faisceau lumineux* d'une lampe à fente est réfléchi par le miroir et, par un dispositif optique convenable, renvoyé dans les mêmes conditions à une *échelle visuelle* graduée en millimètres et à un *kymographe* dont le papier se déplace à la vitesse de 2mm par minute.

La coagulation du sang total ou du plasma se produit à 37°C dans l'espace annulaire de 1mm de large limité par les parois d'acier

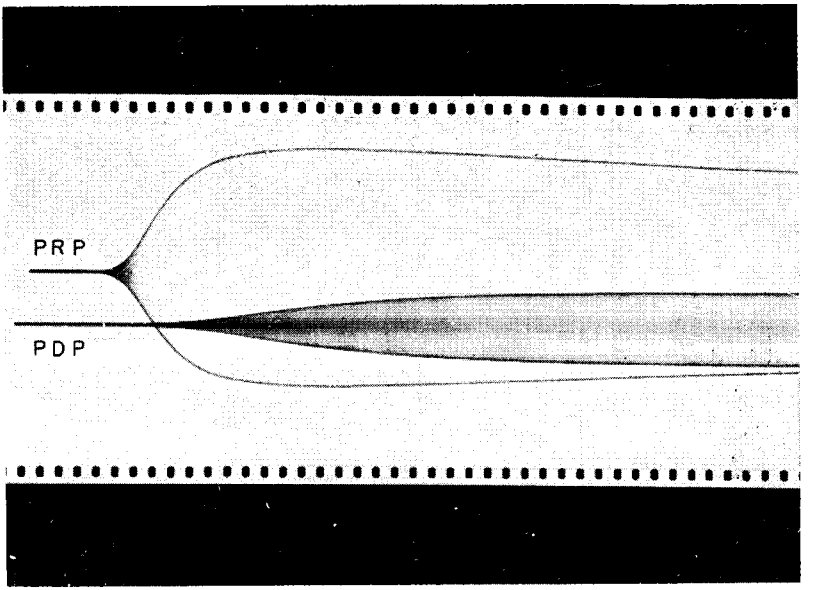

Fig. 2. Le diagramme normal de la coagulation du plasma, en présence (PRP) et en l'absence (PDP) des plaquettes.

de la cuve et du cylindre. Tant que le milieu coagulable reste fluide, les oscillations de la cuve ne sont pas transmises au cylindre: le spot lumineux de l'échelle reste immobile et le kymographe enregistre un trait rectiligne, la constante r qui représente en dernière analyse la vitesse de la thromboplastino-formation, Dès que de la fibrine se forme, une structure, le caillot, est élaborée et adhère aux parois de la cuve et du cylindre, les rendant solidaires. Les oscillations de la cuve sont dès lors transmises au cylindre, donc au système de torsion et au miroir, en fonction de la propriété rhéologique examinée. L'intensité du phénomène se mesure, à chaque oscillation de la cuve, par la longueur du déplacement du spot lumineux sur l'échelle graduée et surtout par l'emplitude A du diagramme à deux branches enregistré.

Ce diagramme a l'aspect général d'un diapason pour la coagulation du *sang total* ou du *plasma riche en plaquettes* (PRP). Il perd cette silhouette caractéristique quand la coagulation est enregistrée après une conservation de plusieurs heures et pour les *plasmas dépourvus de plaquettes* (PDP), (voir figure 2).

II. L'ÉVOLUTION DE LA PROPRIÉTÉ HÉMORHÉOLOGIQUE DU CAILLOT ÉTUDIÉE

Ces deux aspects graphiques correspondent à des fifférences frappantes de l'intensité et de l'évolution de la propriété hémorhéologique étudiée[13,15,26,28,34,40] (voir figure 3).

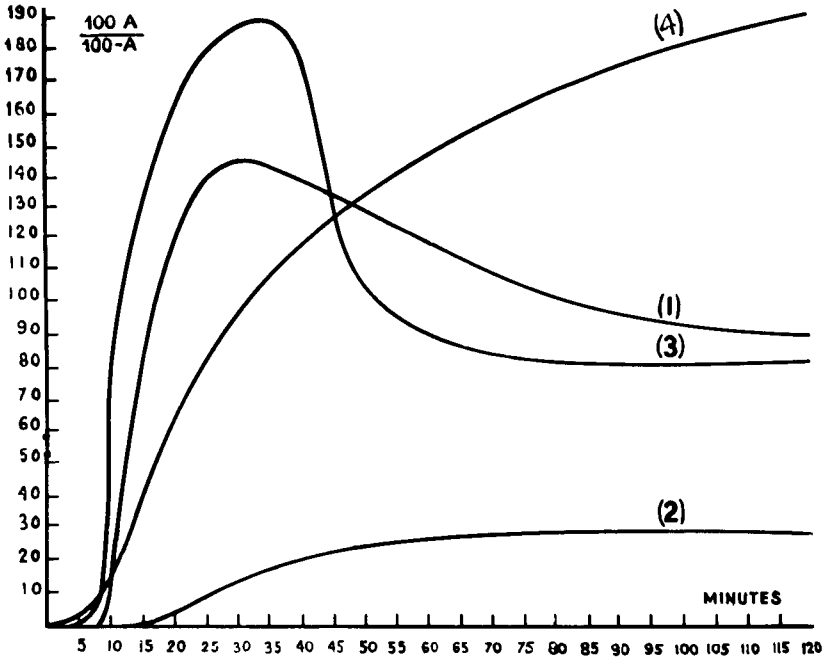

Fig. 3. Evolution en fonction du temps de la propiété hémorhéologique enregistrée par le thrombélastographe dans les caillots: (1) des plasmas normalement riches en plaquettes (PRP), (2) des plasmas pauvres en plaquettes, (3) des plasmas trop riches en plaquettes, (4) des PRP hyperfibrinogénémiques.

Dans le cas du PRP elle commence à se manifester 8 à 10 minutes après la recalcification. Elle a une croissance sigmoïde régulière et passe par un maximum 20 à 30 minutes plus tard, l'amplitude du diagramme étant alors voisine de 55mm. Ensuite, elle décroit lentement en une courbe d'allure hyperbolique qui devient asymptotique au bout de 2 à 3 heures.

Dans le cas du PDP, elle commence à se manifester plus tard après la recalcification. Sa croissance sigmoïde initiale est plus tôt terminée mais l'intensité qu'elle atteint finalement est bien moins grande puisque l'amplitude maxima du diagramme est voisine de 20mm à l'état normal. Enfin, la phase hyperbolique de décroissance terminale n'existe plus: les deux branches du diagramme restent parallèles après avoir atteint leur écartement maximum.

La figure 3 montre en outre que cette phase de décroissance terminale, caractéristique du caillot normal, absente du caillot aplaquettaire, est anormalement rapide et intense au cours des hyperplaquettoses[1,26,28,29,34–36,38,40,44] et au contraire supprimée de la coagulation des PRP fortement hyperfibrinémiques,[22,23,26,28,34,40] ceci aussi bien expérimentalement qu'en clinique.

Au total, la propriété hémo-rhéologique étudiée par le thrombélastographe est évolutive et passe normalement par un maximum. Elle apparait fondamentalement conditionnée par les *plaquettes* et à un moindre degré par la *fibrine* et l'examen des courbes de la figure 3 semble indiquer qu'à partir d'un certain moment au moins, les plaquettes et la fibrine ont sur elle un effet antagoniste.

III. LA NOTION DE PROPRIÉTÉ THROMBODYNAMIQUE DU CAILLOT: SON IMPORTANCE PHYSIOLOGIQUE

Il est aujourd'hui démontré que la propriété du caillot explorée par le thrombélastographe n'est pas la viscosité.[12,13,26,28] Expérimentalement, les systèmes les plus visqueux sont quasi inertes dans l'appareil. Par contre, la *thixotropie* peut intervenir dans certaines conditions.[12] Son influence est minime à l'état physiologique.

La force motrice horizontale du caillot qui entraine le cylindre et tord le fil d'acier n'est pas un couple de frottement comme dans le viscosimètre de torsion mais un couple de traction. Le caillot tire sur le cylindre et, puisqu'il ne lui transmet pas intégralement le mouvement de la cuve, on peut en déduire qu'il se déforme aussi par allongement réversible. Hartert en a conclu que la propriété hémo-rhéologique considérée est l'*élasticité*.[13–15] Dans certaines conditions expérimentales particulières, il a pu mettre en évidence un comportement élastique du caillot au thrombélastographe.[18] Scott Blair a montré par ailleurs[6,45] que le caillot du sang natif de boeuf, coagulé par la géloplastine plasmatique de Copley, réagit dans le gélomètre à tube en U comme une structure visco-élastique du type Maxwell.

Sans nier que des phénomènes visco-élastiques interviennent, nous avons montré en 1957[26] que, dans les conditions particulières de l'expérience, les facteurs physiques en cause sont complexes et ne peuvent pas être réduits convenablement à un seul paramètre. Par exemple, la courbe biphasique caractéristique de l'évolution thrombélastographique des caillots obtenus à partir du sang total ou du plasma riche en plaquettes (PRP), qui ont un haut degré de rigidité, est entièrement différente des diagrammes univoques de visco-élasticité établis par Scott Blair dans les conditions que nous venons de dire. Des courbes d'évolution comparable à celle de Scott Blair ne peuvent être obtenues au thrombélastographe qu'avec les caillots des sangs ou des plasmas fortement hyperfibrinogénémiques, érythrémiques ou thrombopéniques. Or l'examen de tels caillots anormaux par les procédés de l'histologie,[2,24] au microscope à contraste de phases[25,46,47] ou au microscope électronique,[11,25] montre que leur réticulum fibrineux est si hétérogène qu'il est difficile de leur appliquer les lois de l'élasticité. D'ailleurs certains d'entre eux, les caillots aplaquettaires, ne sont pas sous tension pendant l'examen, comme en témoigne la trace sombre qu'ils laissent tout le long de l'axe longitudinal de leurs diagrammes, correspondant à un arrêt momentané de la torsion chaque fois que le système passe par sa position de repos.[26]

Tout récemment, le Professeur Guillot, titulaire de la chaire de physique de la Faculté de pharmacie de Paris, a construit un dispositif mécanique macroscopique fonctionnant d'une manière identique au thrombélastographe.[12] Il a pu étudier ainsi le comportement de systèmes parfaitement ou imparfaitement élastiques: aucun ne donne de diagrammes diphasiques comparables au thrombélastogramme normal. Par le même dispositif expérimental et par des modifications convenables des parois de la cuve et du cylindre du thrombélastographe (remplacement par d'autres métaux ou revêtement par divers agents), il a pu confirmer le rôle considérable de l'adhésivité du caillot aux parois, sur lesquel nous insistons depuis 1957.[26]

En effet, ce qui est examiné en fin de compte par le thrombélastographe est l'*aptitude du caillot à effectuer un travail mécanique:* exercer un couple de traction sur un système de torsion. Cette propriété de l'ordre dynamique, le caillot l'exerce principalement grâce à sa *rigidité* et à son *adhérence pariétale,* toutes deux fonctions des condi-

tions normales ou anormales de sa *structuration*. On voit qu'il s'agit d'une propriété entièrement spécifique des caillots de la coagulation sanguine. Elle a une signification hautement physiologique puisque le caillot n'a d'aptitude normale à l'hémostase que s'il est capable de faire obstacle à la pression intra-vasculaire *in situ* grâce à son adhérence et à sa rigidité. Elle peut être gravement perturbée au cours de syndromes hémorragiques ne s'accompagnant pas d'anomalies chronométriques de la coagulation. Elle ne peut être normale que si le caillot a été édifié avec le concours des plaquettes comme l'est, *in vivo*, le thrombus rouge physiologique. Pour toutes ces raisons, nous avons proposé en 1957[26,28,34] de l'appeler la *propriété thrombodynamique* et de substituer le terme de *thrombodynamographie* à celui de thrombélastographie: nous utiliserons ces dénominations dans la suite de cet exposé.

IV. LES FACTEURS BIOLOGIQUES DU COMPORTEMENT THROMBODYNAMIQUE DU CAILLOT

Par les travaux inauguraux que Hartert a publiés entre 1948 et 1957,[13–16,19] par nos premières recherches personnelles de 1957[26,28,34] et par celles de Vreeken (1957)[49] et de Sokal (1957–1960),[46,47] il a été démontré que le caillot acquiert progressivement sa propriété thrombodynamique physiologique au cours de la *structuration* de son *réticulum fibrineux* par les *plaquettes* et certains *facteurs plasmatiques et sériques accessoires*. Les diagrammes atteignent leur amplitude maxima quand s'achève cette structuration. Toute anomalie thrombodynamique, en plus ou en moins, indique qu'elle est défectueuse et selon sa nature et son aspect graphique, cette défectuosité peut n'avoir aucune conséquence hémostatique ou être hémorragipare, thrombogène ou les deux à la fois.[26,39,40]

Ceci étant établi dès 1957, nous avons ensuite poursuivi nos recherches initiales sur le rôle respectif de la fibrine, des facteurs plasmatiques et sériques de la structuration et des plaquettes. Nos résultats successifs[3,22,23,29-32,35,36,38,40,41] ont été publiés en équipe avec le Professeur Marchal, Samama, Jamain et deux de nos collaboratrices, R. J. Prost et Y. Beaslay qui ont fait leur thèse de doctorat en médecine sur le sujet dans notre laboratoire.[1,14]

Nous avons beaucoup progressé dans ces études par la pratique de l'*enregistrement simultané de la coagulation du plasma riche en plaquettes* (*PRP*) *et du plasma dépourvu de plaquettes* (PDP)[32] (voir

figure 2). Le PRP est le plasma de sédimentation spontanée de la deuxième heure du sang veineux, prélevé sur citrate en matériel non mouillable. Il a approximativement la même richesse en plaquettes que le sang d'origine. Le PDP est le surnageant congelé et décongelé 3 fois de la centrifugation du PRP en matériel non mouillable, à 4°C., à 3000 G, pendant 30 minutes.[1] L'amplitude maxima Am_2 du diagramme du PDP, normalement voisine de 20mm, dépend de la fibrine (donc du fibrinogène) et de divers facteurs plasmatiques et sériques. L'amplitude maxima Am_1 du diagramme du PRP, normalement voisine de 55mm, dépend en outre des plaquettes. La valeur de $Am_1 - Am_2 = A_p$, peu différente à l'état normal de 35mm, représente donc spécifiquement l'activité thrombodynamique des plaquettes.[32,41]

A. Le role quantitatif basal de la fibrine

On peut le préciser en faisant varier la quantité de fibrinogène dans le PDP et en analysant les variations correspondantes de l'amplitude maxima Am_2.[1,30,31,44]

Dans des expériences d appauvrissement, des PDP hyperfibrinagénémiques sont dilués par des PDP normaux débarrassés de leur fibrinogène par le thrombine ou par la bentonite. Dans une autre série d'expériences, le PDP normal défibrinogéné ou le PDP d'un sujet atteint d'afibrinogénémie congénitale sont progressivement enrichis en fibrinogène par diverses préparations de fraction I ou de fibrinogène purifié du plasma humain.

Dans tous les cas, les courbes de variations obtenues sont comparables. Leur pente ne diffère que par la pureté et la qualité despréparations de fibrinogène utilisées, ce qui permet éventuellement de tester leur activité thérapeutique.[1,31]

La figure 4 montre comment l'amplitude maxima Am_2 des diagrammes des caillots aplaquettaires augmente régulièrement en fonction de la masse de fibrine qu'ils contiennent. La relation est pratiquement linéaire de 0 à 15 g. de fibrignogène par litre de plasma. Elle ne tend à devenir asymptotique que pour des chiffres très élevés, jamais rencontrés *in vivo*.

Au fur et à mesure qu'augmente la masse de fibrine dans ces expériences, elle développe un effet anticoagulant déjà trouvé par Copley[4,5,7] et par Triantaphyllopoulos[48] grâce à d'autres procédés d'étude. Il est particulièrement net aux très fortes concentrations

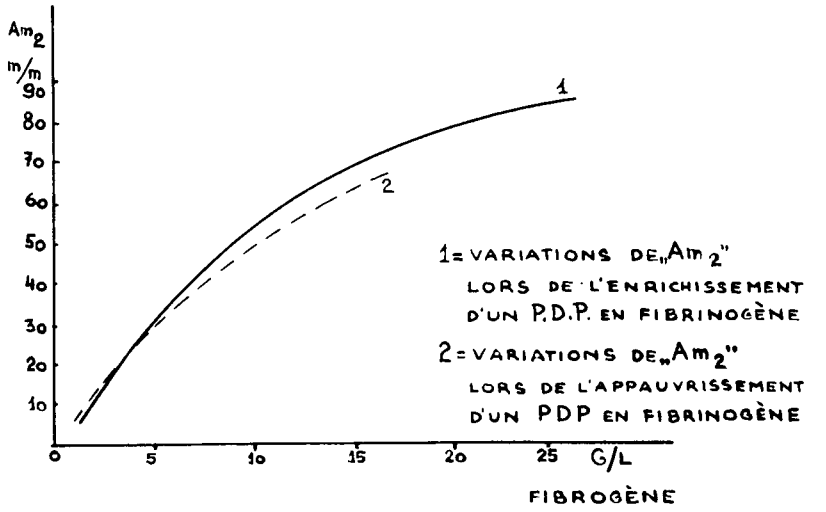

Fig. 4. Variations de la propiété thombodynamique des caillots aplaquettaires en fonction de la masse de leur fibrine.

expérimentales de fibrine. Le sérum qui exsude de ces caillots transporte un effet antithrombine dans les plasmas normaux. Des expériences en cours diront s'il s'agit d'une antithrombine VI, résultat de l'action de plasmine néoformée sur la fibrine.

B. Le rôle adjuvant d'autres facteurs plasmatiques et sériques

Par l'étude statistique de l'amplitude maxima Am_2 des diagrammes de 800 PDP normaux ou pathologiques dont le taux de fibrinogène était connu, nous avons démontré que la fibrine n'est pas la seule variable de la propriété thrombodynamique en dehors des plaquettes.[1,30,31]

La *thrombine* détermine la vitesse d'apparition et d'évolution des propriétés hémo-rhéologiques de la fibrine mais n'influence pas leur intensité terminale.

En bloquant les groupes —SH du milieu et par l'étude de déficits acquis, nous avions mis en évidence en 1957[26] l'action du facteur de stabilisation de la fibrine de Laki et Lorand (fibrinase de Loewi, nouveau *facteur XIII* de la nomenclature internationale des facteurs de coagulation). En enchainant les monomères de fibrine par des liaisons fortes (—S—S—), le facteur XIII confère aux fibres une

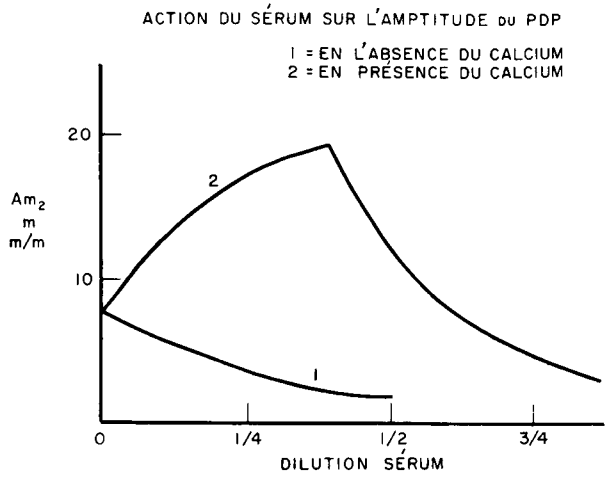

Fig. 5. Graphiques expérimentaux montrant l'activité dans le sérum du facteur XIII et d'un inhibiteur sur la propriété thrombodynamique des caillots aplaquettaires provenant du fibrinogène purifié, coagulé par la thrombine.

solidité normale. Plusieurs auteurs ont montré depuis qu'un défaut thrombodynamique du caillot semblable à celui que produit l' absence presque complète de fibrine est la seule anomalie apparente de la coagulation des sujets ayant une absence congénitale de facteur XIII.

Récemment, nous avons repris son étude [*in* 1] en précisant les actions du PDP défibrinogéné et du sérum sur le comportement thrombodynamique des caillots, solubles dans l'urée 5M, du fibrinogène purifié dépourvu de facteur XIII et coagulé par la thrombine. Deux activités antagonistes apparaissent dans ces conditions. L'une, le facteur XIII, ne se manifeste qu'en présence de *calcium*. Elle rend les caillots aplaquettaires insolubles dans l'urée, augmente l'amplitude maxima de leurs diagrammes et la pente de la courbe d'accroissement de l'amplitude maxima au cours de l'enrichissement en fibrinogène purifié des PDP défibrinogénés. Elle est thermostable, non adsorbable et partiellement consommée par la coagulation. En l'absence de calcium, c'est une *activité inhibitrice de la propriété thrombodynamique* qui se manifeste. Elle a les effets inverses du facteur XIII sur l'amplitude maxima. Elle est thermostable, non adsorbable et partiellement activée par la coagulation.

La figure 5 montre l'effet de ces deux facteurs antagonistes dans le sérum.

Avec des fractions VI hautement purifiées, nous n'avons pas retrouvé l'action des albumines, rapportée par Sokal en 1960.[47] Par contre, nous avons mis en évidence [*in* 1] une activité positive de la *céruloplasmine* sur l'amplitude maxima du PDP.

Enfin, certaines mucoprotéines dont le taux s'élève ou qui apparaissent au cours des états inflammatoires augmentent pour leur propre compte l'amplitude maxima des diagrammes de thrombodynamographie.[30-32] Elles ne sont pas encore identifiées avec certitude mais nos premiers résultats paraissent mettre en cause une *alpha-2-macroglobuline.*

C. Le role déterminant des plaquettes : la fonction thrombodynamique des plaquettes

La thrombine, le fibrinogène, le facteur XIII, le calcium et probablement d'autres facteurs concourent à former une fibrine normale

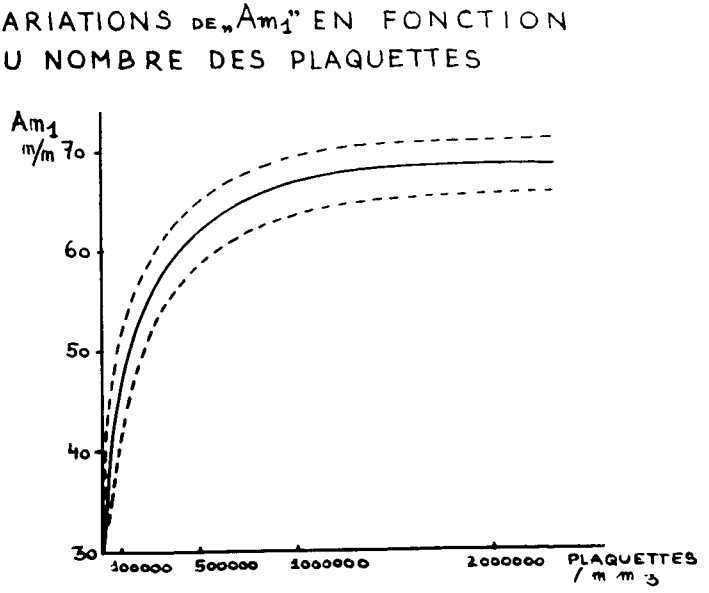

Fig. 6. Variations de la propriété thombodynamique des caillots en fonction du nombre des plaquettes qui les structurent.

Les *plaquettes* gouvernent la structuration de cette fibrine en un caillot normal et lui confèrent ses propriétés rhéologiques physiologiques. Elles ont une *fonction thrombodynamique* d'importance fondamentale. Tout phénomène lié à cette activité thrombodynamique des plaquettes s'enregistre sur les diagrammes de coagulation du sang total ou du PRP et est, par définition, absent du PDP.

On peut étudier l'effet des plaquettes thrombodynamiques sur l'amplitude maxima en appauvrissant un PRP en plaquettes, par centrifugation ou dilution avec le PDP homologue. On peut aussi enrichir progressivement un PDP normal avec des plaquettes séparées du sang homologue prélevé sur EDTA en matériel non mouillable, grâce à une technique permettant de les obtenir sans altérations.[1,26,40,41,44] La courbe des variations correspondantes est hyperbolique (voir figure 6). Le gradient de l'augmentation de Am_1 sous l'effet des plaquettes décroit avec leur nombre, surtout à partir de 100.000 plaquettes par mm3, mais il ne s'annule jamais avant des concentrations supérieures à 1.000.000 par mm3. Cependant, si l'on poursuit l'enrichissement expérimental au-delà de 3.000.000 par mm3, l'activité thrombodynamique globale des plaquettes diminue rapidement puis finit par s'annuler complètement.

A l'effet du nombre s'ajoute une notion fondamentale d'*aptitude fonctionnelle*. Nos recherches ont montré comment la fonction thrombodynamique des plaquettes est une fonction vitale d'éléments figurés.

Elle n'est exercée que par des plaquettes entières, sous leur forme spiculaire, apte aux activités biologiques. Elle est, avec la fonction de rétraction, la première à disparaitre au cours de la conservation.[26] Toute altération morphologique l'annule irréversiblement.[1,26] Les lysats de plaquettes et les granules plaquettaires n'ont plus qu'une activité prothromboplastique dans la coagulation mais sont totalement inertes sur le caillot.[26,37] Les immun-thrombolysines[8,9] et tous les immun-sérums expérimentaux préparés avec une fraction plaquettaire[42] l'abolissent.

Le revêtement de la cuve et du cylindre de l'appareil par la fibrine native la rend inopérante, ce qui prouve que l'adhérence pariétale des caillots normaux dépend principalement de l'*adhésivité* des plaquettes. Leur fonction thrombodynamique est bloquée par les dextranes dans les conditions de nos expériences d'incubation, qui prouvent la participation active de l'*atmosphère plasmatique péri-*

plaquettaire.[31] Nos recherches sur l'activation des plaquettes par le facteur Hageman activé(facteur XII) et par la céruplasmine [*in* 1] et les données du microscope à contraste de phases[1,46,47] démontrent qu'elle implique une *métamorphose visqueuse.* Son défaut spécifique

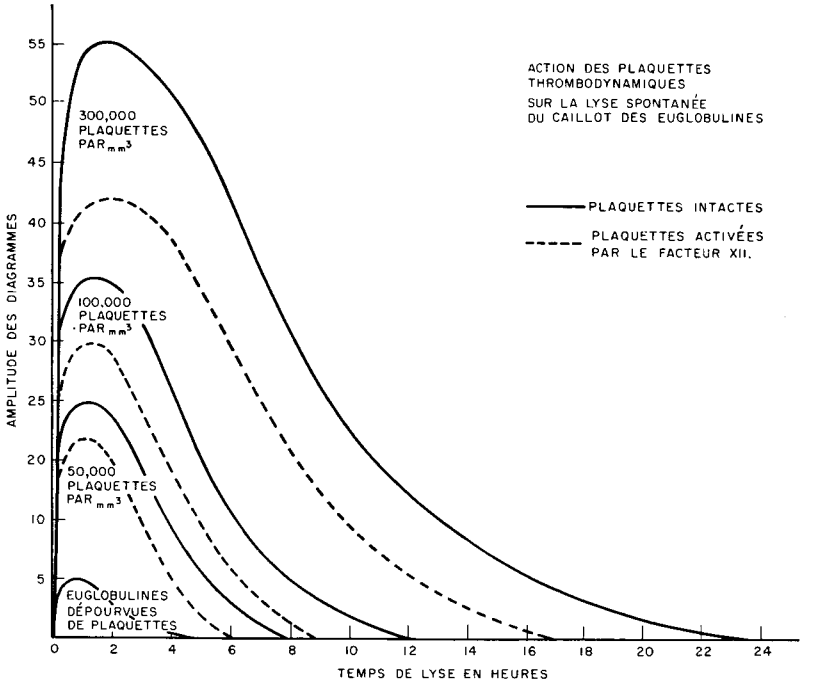

Fig. 7. Expériences montrant que les plaquettes retardent la lyse spontanée des caillots d'euglobulines au prorata de leur activité thrombodynamique globale. Les plaquettes préalablement activées par le facteur XII ont perdu irréversiblement une partie de cette activité.

et les conditions de sa correction *in vitro* au cours de la thrombasthénie héréditaire de Glanzmann-Naegeli[26,40] achève de prouver qu'elle concerne des plaquettes aptes à la *rétraction.*

Etant donnés ces caractères, la fonction thrombodynamique des plaquettes utilise la *thrombosthénine* de Lüscher et le *magnésium* et emprunte son énergie aux enzymes et substrats plaquettaires et plasmatiques de la *glycolyse,*[33] dont l'un ou plusieurs pourraient équivaloir au cofacteur sérique de la rétraction décrit par Hartert.[16,19]

Beaucoup plus significative que la fonction prothromboplastique, et d'autres qui ne concernent que la coagulation,[26,37] *elle est l'archétype des fonctions plaquettaires vitales de l'hémostase* qu'elle résume toutes, d'autant plus que nous venons de découvrir [*in* 1] que les plaquettes protègent le caillot contre la lyse par la plasmine au prorata de leur activité thrombodynamique. La figure 7 illustre cette propriété protectrice sur la lyse spontanée du caillot des euglobulines.

Tout ceci explique l'intérêt primordial de son exploration en clinique, notamment pour le diagnostic et le traitement des purpuras thrombopéniques et des thrombopathies[9,26,27,37,39,40] par les tests simples, global et unitaire, que nous avons mis au point avec Marchal, Samama et Prost.[30,31,40,41]

V. LES ASPECTS THROMBODYNAMOGRAPHIQUES DE LA STRUCTURATION DU CAILLOT: LA SYNÉRESE ET LA RÉTRACTION

La fibrino-formation s'accomplit en trois étapes [*in* 26]. La thrombine transforme les molécules de fibrinogène en molécules de fibrine. Elles se polymérisent avec le concours du facteur XIII et du calcium pour former les *fibres primaires*, transparentes. Celles-ci se rassemblent en faisceaux de *fibres secondaires* opaques, définitives, par un processus comparable sinon identique à une *synérèse*, mettant en oeuvre d'importantes forces interstructurales d'attraction qui deviennent en fin de compte des forces intrastructurales de cohésion. Ses principaux paramètres étant le pH et la force ionique, nous les avons fait varier dans des PDP normaux et pathologiques.[26] Nous avons ainsi prouvé que le thrombodynamogramme n'est sensible qu'aux fibres secondaires du caillot et que le degré de leur synérèse conditionne jusqu'à un certain point l'intensité de leur aptitude thrombodynamique.

Cependant la thrombodynamographie,[26,28,34,40] confirmant les observations de microscopie électronique de De Robertis,[11] Köppel,[25] et Hovig,[21] prouve que la *structuration du caillot normal est gouvernée par les plaquettes thrombodynamiques*, qui sont les centres de la coagulation, les points de départ de la fibrino-formation et finalement les noeuds du réticulum fibrineux.[2,11,24–26] Selon Lüscher[33] et Sokal,[47] il peut s'agir de plaquettes isolées ou agrégées par amas et formant

entre elles un réseau autonome par fusion de leurs spicules, riches en thrombosthénine. Les caillots aplaquettaires ont un réticulum anarchique et lâche de fibres longues, épaisses et irrégulières. Au contraire, les caillots plaquettaires normaux sont faits d'un réseau

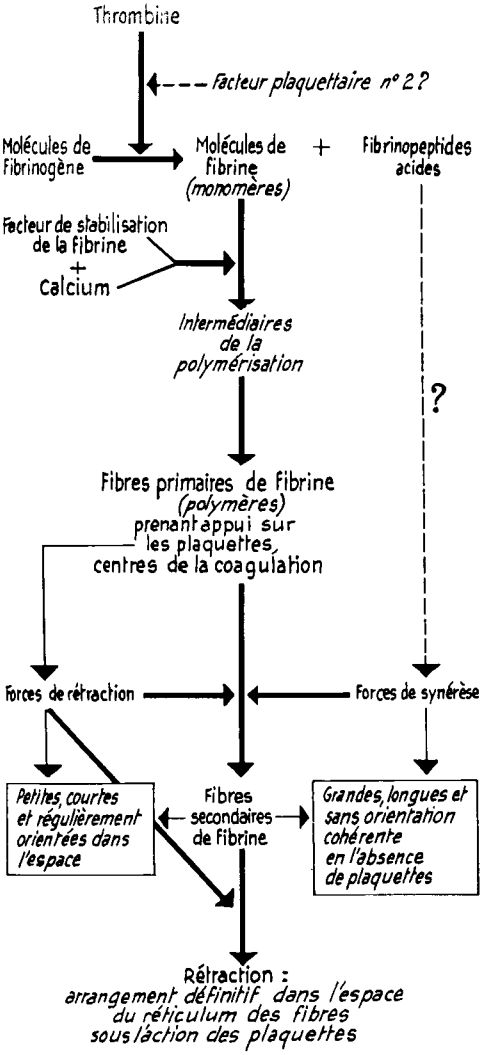

Fig . 8. Schéma de la structuration du caillot, selon M. E. Leroux.

serré et rigide de fibres courtes et fines, régulièrement distribuées dans l'espace.

Comme nous le savions déjà, les plaquettes qui structurent le caillot sont celles qui, finalement le rétractent en resserrant son réticulum fibrineux par l'exercice d'une force centripète de faible intensité, spécifique et par conséquent présente dès le début de la fibrino-formation. *L'activité thrombodynamique des plaquettes est, selon nous*[26,28,35] *une expression particulière de leur force de rétraction.*

Nous venons de voir que les plaquettes thrombodynamiques confèrent au caillot sa solidité en orientant ses fibres et en limitant et régularisant leur épaisseur, c'est-à-dire leur synérèse. L'évolution comparée de la propriété thrombodynamique en fonction des quantités respectives de fibrine et de plaquettes (voir figure 3) achève de montrer qu'à tout moment la structuration du caillot est gouvernée par deux forces antagonistes d'arrangement interne: une *force de synérèse* liée aux fibres de fibrine et une *force de rétraction* liée aux plaquettes thrombodynamiques.[26,28,35] Les faibles forces de rétraction l'emportent sur les forces initialement plus importantes de synérèse dès qu'assez d'entre elles, d'interstructurales qu'elles étaient, deviennent intrastructurales. Les plaquettes, déformées par la synérèse des fibres qui leur adhèrent, reprennent alors leur forme initiale et réduisent ou non le volume du caillot selon qu'elles parviennent ou non à vaincre les forces par lesquelles elle le font adhérer à la paroi. Le résultat final est aussi fonction de la proportion respective de fibrine et de plaquettes. Tous ces faits sont résumés dans la figure 8.

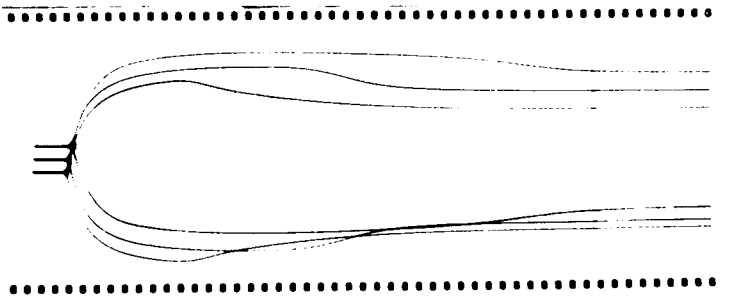

Fig. 9. Hyper-rétractilité en "goulot" enregistrée sur un PRP de leucémie myéloïde (600.000 plaquettes par mm3). Les concentrations en leucocytes ont été amenées à 20.000 (en haut), 50.000 (au milieu) et 75.000 (en bas) pour montrer que la leucocytose sensibilise le phénoméne lié à l'hyperplaquettose.

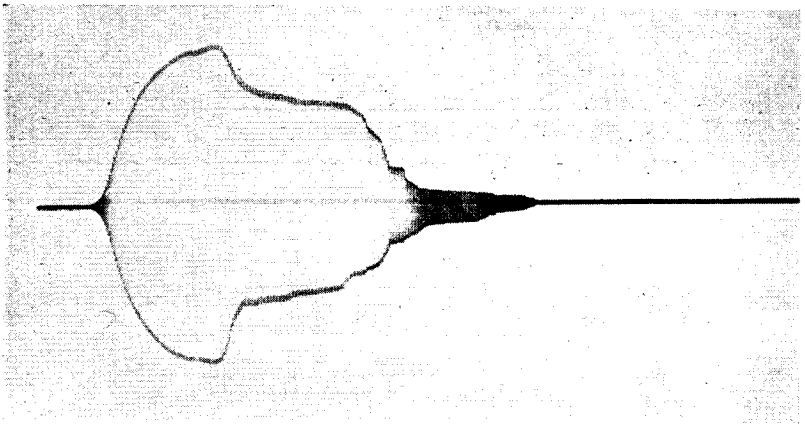

Fig. 10. Hyper-rétractilté pseudo-fibrinolytique en "troupie" au cours d'une néphropathie. Le PDP homologue était normal. L'image pathologique du PRP était supprimée par un immun-sérum de lapin anti plaquettes humaines. Elle étrait transportée dans les PRP normaux par le sérum du malade.

Ainsi pensons-nous que les thrombodynamogrammes de la coagulation du sang total et du PRP sont porteurs d'une *image de rétraction.* Chacune de leurs branches a un aspect comparable aux diagrammes du rétractographe de Hartert.[17] Leur rapprochement terminal est le témoin d'une amorce progressive d'arrachement du caillot de la cuve sous l'effet de la force de rétraction.

Ce rapprochement terminal ne se produit pas dans les thrombopénies,[2,30,37,39,40] les thrombopathies thrombo-adynamiques[26,27,40] et les hyperfibrinémies intenses.[23,26,32,40] Au contraire, dans les hyperplaquettoses expérimentales[1,26,30,31,40,44] et les thrombocythémies des syndromes myélo-prolifératifs et post-splénectomiques, il est anormalement accentué en une image en *"goulot"*[26,35,38,40] favorisée par l'hyperleucocytose[36,40] mais non déterminée par elle comme le pensait Hörder[20,50] (voir figure 9). Enfin, dans certaines thrombopathies hyperthrombodynamiques[27] c'est une image d'arrachement en *"marches d'escalier"* ou en *"toupie"* qui est produite à cause de l'hyperplaquettose et (ou) d'un facteur sérique modificateur de l'adhésivité des plaquettes[26,29,40] (voir figure 10). Ces aspects pseudo-fibrinolytiques de l'hyper-rétractilité sont annulés par les immun-sérums antiplaquettaires et absents des diagrammes de PDP.

Ils se distinguent ainsi des images de fibrinolyse, plus accentuées sur les diagrammes de PDP que sur ceux de PRP. En clinique, ils sont le signe hématologique le plus constant d'états thrombogènes en même temps qu'hémorragipares. On comprend qu'il en soit ainsi puisque l'hyper-rétractilité contribue à propager la coagulation de proche en proche mais s'avère capable, *in vitro* (et probablement *in vivo*), d'arracher brutalement le caillot de ses insertions pariétales.

VI. CONCLUSION

Il apparait au total que le thrombélastographe de Hartert enregistre une propriété spécifique des caillots, conditionnée surtout par leur rigidité et leur adhérence pariétale, représentant leur aptitude à l'hémostase.

Les facteurs biologiques qui la déterminent sont précisés par l'examen de la coagulation en présence et en l'absence des plaquettes. Ce sont les facteurs qui structurent le caillot: fibrine, facteur XIII et calcium d'une part, plaquettes vivantes et actives d'autre part. Ces deux groupes d'agents règlent l'équilibre entre la synérèse des fibres de fibrine et la rétraction du caillot par les plaquettes, dont dépend le type de diagramme enregistré.

L'auteur exprime toute sa gratitude à son maitre, le Professeur Georges Marchal, à Monsieur Samana et aux docteurs Bernard Maupin, Gérard Lambert, Jacques Muselet, Renée Prost et Yvonne Beaslay, qui ont collaboré à ses travaux, et à Madame Andrée Bapicot-Valère pour son assistance technique dévouée. Il remercie Monsieur Françis Myard, professeur honoraire de mécanique à l'école centrale des Arts et Manufactures de Paris, ancien président de la société mathématique de France, qui a bien voulu examiner avec lui les implications physiques de ses résultats expérimentaux.

Cet article fait le point actuel de recherches commencées par l'auteur en 1954 et poursuivies successivement:

—au laboratoire d'hémostase du centre d'études biologiques de l'hopital Tenon et de la chaire de pharmacologie de la faculté de médecine de Paris (Professeur J. Cheymol),

—au laboratoire d'hémostase de la clinique des maladies du sang de l'hopital Broussais et de la chaire d'hématologie de la faculté de médecine de Paris (Professeur G. Marchal),

au laboratoire d'hémostase de la maternité des hopitaux Tenon et Bichat, Paris (Docteur B. Jamain),

—et actuellement au laboratoire d'hématologie de la faculté de médecine (Professeur agrégé M. E. Leroux) et du centre régional de transfusion sanguine (Professeur R. Arnaud) de Tours.

Bibliographie

1. Beaslay, Y., "Nouvelles études expérimentales sur le rôle des plaquettes, du fibrinogène et de divers facteurs du plasma dans le déterminisme des propriétés thrombodynamiques du caillot," Thèse doct. méd., Paris (1963), 109p.

2. Champy, C., A. Fiehrer, et M. Demay, *Presse Med.*, **60**, 1107 (1952).

3. *Sang*, **31**, 65 (1960).

4. Copley, A. L., *Hémostase*, **3**, 13 (1963).

5. Copley, A. L., et B. Becher, *Nature*, **192**, 568 (1961).

6. Copley, A. L., et G. W. Scott Blair, *Proc. 8th Congr. Int. Soc. Blood Transf., Tokyo 1960*, Karger édit. Basel, 1962, 66p.

7. Copley, A. L., D. Steichele, M. Spradau, et R. S. Thorley, *Nature*, **183**, 1683 (1959).

8. Dausset, J., M. Samama, M. E. Leroux, B. Maupin, et G. Marchal, *Atti del 7imo Congr. int. della Int. Soc. Haematol., Roma 1958*, Il Pensiero Sc., édit., Roma, Vol. 2, No. 1, 693.

9. Dausset, J., M. Samama, M. E. Leroux, R. J. Prost, et G. Marchal, *Rev. Hématol.*, **14**, 129 (1959).

10. De Nicola, P., *Thromboelastography*, C. C Thomas, Springfield, Illinois, 1957, 110 (1957).

11. De Robertis, E., *Blood*, **10**, 528 (1955).

12. Guillot, M., et M. Samama, *Hémostase*, **3**, 67 (1963).

13. Hartert, H., *Klin. Wochschr.*, **26**, 577 (1948).

14. Hartert, H., *Z. exp. med.*, **117**, 189 (1951).

15. Hartert, H., *Deut. Arch. Klin. Med.*, **199**, 234 (1952).

16. Hartert, H., *Klin. Wochschr.*, **32**, 139 (1954).

17. Hartert, H., *Klin. Wochschr.*, **36**, 1084 (1958).

18. Hartert, H., in *Flow Properties of Blood and Other Biological Systems*, A. L. Copley and G. Stainsby, eds., Pergamon Press, New York-Oxford, 1960, p. 186.

19. Hartert, H., H. G. Lasch, et I. Pfisterer, *Thromb. Diath. Haemorrhag.*, **1**, 446 (1957).

20. Hörder, M. H., et J. Pileggi, *Acta Haematol.*, **17**, 111 (1957).

21. Hovig, T., *Thromb. Diath. Haemorrhag.*, **8**, 455 (1962).

22. Jamain, B., M. E. Leroux, G. Lambert, et J. Cheymol, *Rev. Franc. Gynecol. Obstet.*, **53**, 741 (1958).

23. Jamain, B., M. E. Leroux, A. Letessier, et J. Muselet, *Semaine Hôp. Paris*, **35**, 1378 (1959).

24. James, T. N., H. Johnson, R. W. Munto, G. Diab, et J. Caldwell, *Blood*, **19**, 751 (1962).

25. Köppel, G., *Proc. 7th. Congr. europ. Soc. Haematol. London, 1959*. Vol. 2, Karger, Basel, 1960, 808 p.

26. Leroux, M. E., "La thrombélastographie (thrombodynamographie). Etudes théoriques, techniques, expérimentales et cliniques sur la thrombélastographie et sur quelques problèmes connexes liés à la biologie de la coagulation sanguine," Thèse doct. méd., Paris, 1957, 407p.

27. Leroux, M. E., J. R. Leroy, et Y. Beaslay, *9ème Congr. Soc. europ. Hématol., Lisbonne 1963*, S. Karger, Basel-New York, sous presse.

28. Leroux, M. E., B. Jamain, et J. Cheymol, *Rev. Franc. Gynecol. Obstet.*, **53,** 25 (1958).

29. Leroux, M. E., G. Marchal, B. Jamain, et M. Samama, *Proc. 7th Congr. Europ. Soc. Haematol., London, 1959,* Vol. 2, Karger, Basel-New York, 1960, 737.

30. Leroux, M. E., M. Samama, Y. Beaslay, et R. J. Prost, *Transfusion,* **5,** 169 (1962).

31. Leroux, M. E., M. Samama, Y. Beaslay, R. J. Prost, et G. Marchal, *Proc. 8th. Congr. Europ. Soc. Haematol., Wien 1961,* S. Karger, Basel-New York, 1962, Comm. 371.

32. Leroux, M. E., M. Semama, B. Jamain, et G. Marchal, *Pathol. Biol. (Semaine Hop).*, **9,** 341 (1961).

33. Lüscher, E. F., et M. Bettex-Galland, *J. Physiol.*, **53,** 145 (1961).

34. Marchal, G., et M. E. Leroux, *Transac. 6th. Congr. europ. Soc. Haematol., Copenhague, 1957,* S. Karger, Basel-New York, 1957, 478p.

35. Marchal, G., M. E. Leroux, G. Duhamel, J. Chenderovitch, et G. Goglin, *Sang,* **28,** 245 (1957).

36. Marchal, G., M. E. Leroux, G. Duhamel, et M. Samama, *Sang,* **29,** 666 (1958).

37. Marchal, G., M. E. Leroux, B. Maupin, et M. Samama, *Proc. 7th. Congr. int. Soc. Blood Transf., Rome, 1958,* S. Karger, Basel-New York, 1959, 946p.

38. Marchal, G., M. E. Leroux, et M. Samama, *Sang,* **29,** 265 (1958).

39. Marchal, G., M. E. Leroux, et M. Samama, *Presse Med.*, **68,** 1333 (1960).

40. Marchal, G., M. E. Leroux, et M. Samama, *Atlas de thrombodynamographie,* SPEI., Paris, 1962, 186p.

41. Marchal, G., M. Samama, M. E. Leroux, et R. J. Prost, *Rev. Franc. Etudes Clin. Biol.*, **6,** 68 (1961).

42. Maupin, B., M. E. Leroux, R. Dechamboux, et G. Lambert, *Atti del 7mo Congr. int. della Int. Soc. Haematol. Roma, 1958,* Vol. 2, Il Pensiero Sc., Roma, 1960, 689 p.

43. Parreira, F., *Trombelastografia. Analise experimental e semiologica,* Gazet Med. Portug., Lisbonne, 1961, 240 p.

44. Prost, R. J., L'amplitude maxima du thrombodynamogramme. Influence des plaquettes et du fibrinogène. Application à l'étude des anticorps antiplaquettaires," Thèse doct. méd., Lyon, 1959, 92p.

45. Scott Blair, G. W., in *Flow Properties of Blood and Other Biological Systems,* A. L. Copley and G. Stainsby, eds., Pergamon Press, New York-Oxford, 1960, 172 p.

46. Sokal, G., *Rev. Belge Pathol. Med. Exptl.*, **26,** 220 (1957).

47. Sokal, G., *Plaquettes sanguines et structure du caillot. Etude morphologique et thrombélastographique,* ASCIA, Bruxelles, 1960, 234p.

48. Triantaphyllopoulos, D. C., *Can. J. Biochem. Physiol.*, **36,** 250 (1958).

49. Vreeken, J., "Thrombelastografie," Thèse doct. méd., Amsterdam, 1957.

50. Winckelmann, G., et M. H. Hörder, *Acta Haematol.*, **18,** 261 (1957).

Résumé

14603

La propriété hémo-rhéologique spécifique des caillots explorée par le thromb-élastographe de Hartert mérite d'être appelée *propriété thrombodynamique* car elle exprime leur aptitude physiologique à faire équilibre, *in situ*, à la pression intravasculaire au cours de l'hémostase, notamment grâce à leur *rigidité* et à leur *adhérence pariétale*. Elle se développe progressivement au cours de la *structuration* du caillot par la fibrine, le facteur XIII, le calcium, d'autres facteurs sériques et les plaquettes. La *fonction thrombodynamique des plaquettes* est essentielle: elle résume toutes leurs activités vitales dans l'hémostase. L'évolution structurale du caillot, enregistrée par l'appareil, dépend de la résultante de forces antagonistes de *synérèse*, liées à la fibrine, et de *rétraction*, liées aux plaquettes.

author

N67 14604

Clot Retraction. Kinetics and Correlation with the Clotting Process

H. HARTERT,* *University of Heidelberg, Heidelberg, West Germany*

Clotting *in vitro* is the solidification of fluid blood or plasma by the clotting process. Clot retraction is the decrease of clot volume and the increase of a deposit which is pressed out from the shrinking clot. A clot free from red cells may decrease to 10% or less of its original volume by retraction. The final product will resemble a piece of India rubber rather than a blood clot.

This striking change of a clot in a glass tube, which seems to occur with a distinct interval of rest after the clotting process, received many explanations regarding its physiological purpose as well as biochemical causes.

On the other hand, it was apparent that progress in biochemical explanation of the very complicated clotting process did not bring about enough evidence to explain the retraction mechanism. This phenomenon seemed to be something outside the clotting biochemistry, perhaps related to fibrinolysis.

Lastly, explanations for the physiological usefulness of retraction were very poor in contrast to fibrinolysis. Recanalization of thrombotic vessels or contraction of the wound bed were the only noteworthy clues.

Retraction in a glass tube does not reflect the conditions *in vivo*. Especially in normal vessels the limiting walls will, for example, never be as rigid and as wettable as a glass tube. Retraction cannot simply be looked upon as a phenomenon per se, as its action depends upon the surface in contact with the blood clot.

To learn further details of the retraction process, the author tried to eliminate adherence of the clot to the container's surface, which may delay retraction to an unknown extent. Yet it proved rather difficult to get rid of the surface. Hirschboeck[1] and Budtz-Olsen[2] may have

PRECEDING PAGE BLANK NOT FILMED.

had the same thought, when they suspended a drop of clotting blood in an oil mixture without contact to any solid surface. But as was demonstrated recently,[3] the retraction of this drop after clotting is subject to interference with a thin layer of an impermeable skinlike texture of fibrinoid and perhaps phospholipid[4] molecules. Retraction can only occur if this skin has been torn by the increasing inside pressure caused by the increased strain of the fibrin clot by its retraction activity.

But without regard to the influence of surface on retraction there is another obstacle in getting a pure retraction without mechanical impediments. This obstacle is the comparably high viscosity of the serum in the meshes of the contracting fibrin network, not to mention the blood cells obstructing the pathways. Since the meshes narrow with the progress of retraction, the viscosity effect becomes the more important, the more retraction comes to the point, where the last holes in the network will close. Mathematically as well as practically an important part is also played by the original diameter of the clot: retraction is slowed down by Poiseuille's law in the case of increasing clot volume, since although the pathways for the serum become longer, their width is still the same as in smaller clots.

A retraction experiment without these two important impediments must take advantage of a clot which does not adhere to any solid surface and which has a minimal diameter, at least in one dimension. Figure 1 shows the container of an apparatus which will be described below. A standard clotting mixture of 1 mm. thickness, a recalcified fresh plasma platelet-rich (*b* in Fig. 1) which has been citrated immediately after withdrawal from the antecubital vein and then slowly centrifuged, is put into the container. It is carefully overlayed by saline (*a* in Fig. 1) containing the same concentration of calcium

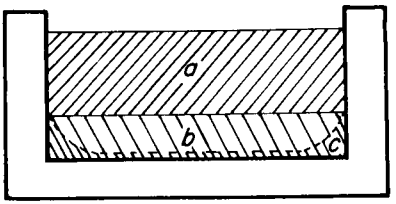

Fig. 1. Container of the retractograph showing *a*, saline; *b*, plasma; and *c*, retracted clot (see text for explanation).

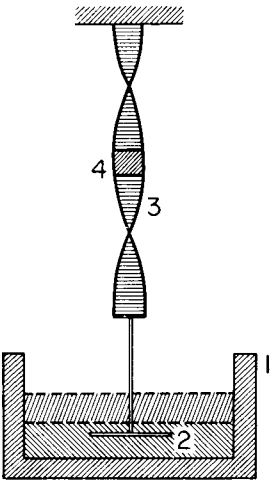

Fig. 2. Principle of the retractograph. 1, container; 2, feeler platelet; 3, Abramson spring; and 4, mirror.

ions as normal serum or by Ringer solution, both of which have less specific gravity than plasma. After clotting and retraction, three layers will be found instead of two. Below the former interface between Ringer solution and the plasma serum is now found, whereas the boundary of the clot has moved very near the bottom of the siliconed glass container.

If the clotting mixture were overlayed, for example, by oil or some other fluidity chemically not closely related to the solution of the plasma, something very different would occur. As mentioned above a skin would arise which would prevent the clot from retracting as long as it were not torn In any case, retraction could only commence after a hole appeared in the skin and this retraction would be somewhat irregular. Figure 2 is a diagram of the retractograph.[5a] This version was demonstrated in 1959 before the British Society of Rheology.[6] It is nothing other than the aforementioned container with a feeler platelet to control the movement of the upper boundary of the retracting clot. The feeler adheres safely to the clot in the middle of its circular surface. The movement of the feeler is transmitted to an Abramson spring and to a small mirror which reflects a beam of light to a photokymographic recorder. Figure 3 shows a normal retractogram. With an earlier version of this method the

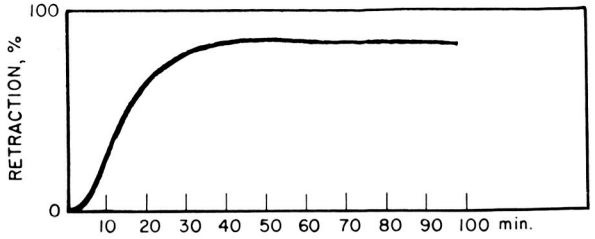

Fig. 3. Normal retractogram.

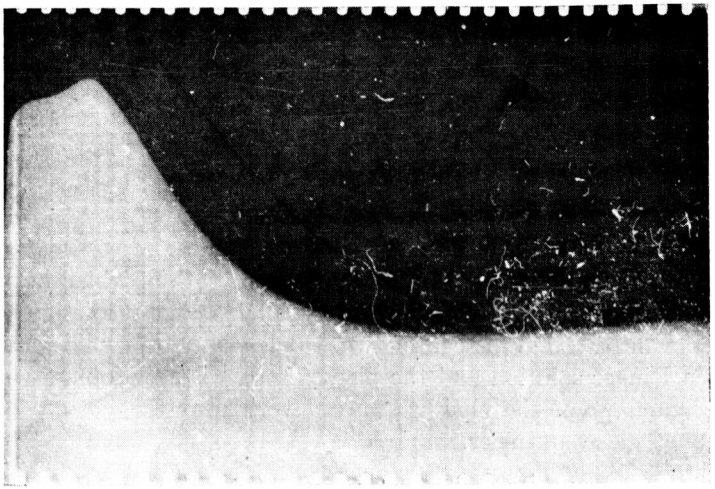

Fig. 4. Special retractogram which shows the decreasing surface tension of the fluid plasma before it clots and retracts at the same time.

author could prove in 1957 that retraction starts simultaneously with the development of the first continuous fibrin strands in connection with viable platelets.[7] This experiment will not be gone into detail here, but roughly speaking, it involved the competition between the decrease of surface tension in a hanging drop of clotting plasma before proper clotting and the increase of retractive tension in this drop after clotting. In this experimental arrangement the decrease of surface tension enlarged the surface of the fluid drop, whereas retraction of the clotted drop tended to reduce it. Figure 4 shows the resulting retractogram. The decline represents a decrease of surface tension, actually, a recording of the increasing surface of

the fluid plasma. This can only happen as long as the plasma remains in a fluid state. The process comes gradually to an end some minutes after recalcification, which took place at the starting point of the curve. On the other hand, retraction is marked by an ascent of the curve. As can be seen this ascent develops gradually from the lower vertex of the curve, and, interestingly enough, there is no horizontal interval between the descending and ascending parts of the curve. This means that the moment of clotting is also the moment in which retraction begins. Controls in a test tube on the average showed clotting 20 sec. later than retraction began in the retractograph.

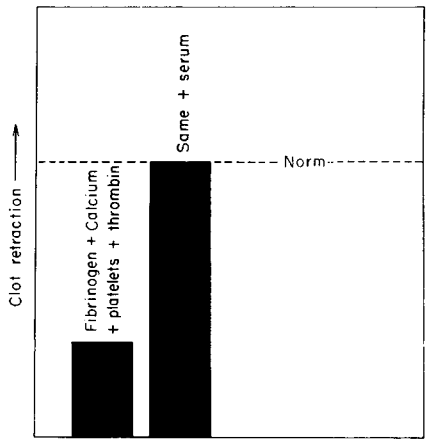

Fig. 5. Role of retraction cofactor for normal clot retraction.

By following the normal curve upward an increase in steepness is found, which means an increase in reaction of the retraction process. The highest speed of retraction is usually found about 15 min. after recalcification. Then it decreases gradually and terminates after about 45 min. This end point represents the maximum tension of the clot, after which there is usually a slight but prolonged relaxation of the tension, probably due to a relaxing substance from the platelets as mentioned by Lüscher.[8]

To characterize the retraction process one may speak of a tension which is produced by it and is measureable. This presumes that the

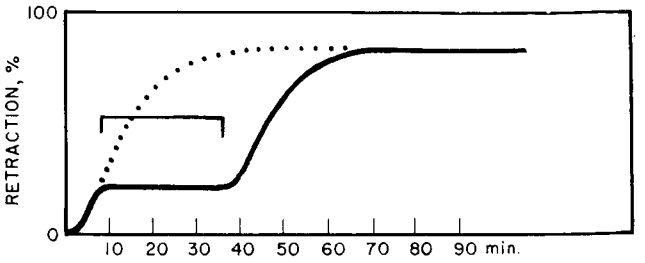

Fig. 6. Influence of cold on the chemical phase of clot retraction. The scale is 4°C.

measuring device performs the measurement in an isometric way. The other method is to measure retraction isotonically. In most instances in this paper retraction was measured almost isotonically if not otherwise mentioned. The retraction apparatus can be adjusted to both extremes, that is, to every proportion between isotonic and isometric measurement. Most retractograms shown represent the actual movement of retraction, which means they are isotonic recordings.

As is well known, fibrinogen dissolved in saline is clottable by thrombin. Such a clotting mixture does not show any retraction, of course. Yet, similarly, if platelets are added it does not retract. Even on the addition of calcium, which is necessary to make the fibrin insoluble in urea and to give it the proper structure, retraction does not occur. Only with the addition of serum is there normal retraction (Fig. 5). Up to now there is still controversy about what kind of substance in serum is necessary for the retraction process. In collaboration with Lasch and Pfisterer some properties of this hypothetical factor were found,[5b,9] which seem not to be related with a known clotting factor. This was called a retraction cofactor, but it could not be isolated. Much work has been done on this interesting problem by Lüscher,[10,11] who is a well-known expert in this field. The author regrets that he is unable to go into this matter in this paper since it involves not only the biochemistry of platelets and of fibrin formation but also that of contractive proteins as in physiology of the muscle. Also the author does not intend to go into the correlation between single clotting factors and retraction in this paper which would be entering into another domain.

In order to understand the following experiments it is necessary to know the influence of cold on retraction. At a lower temperature (e.g., 22°C.), the retraction process is about four times longer, whereas the maximum contraction is only 8% less than that at 37°C.[12] At 4°C. retraction is absolutely zero. Of course, this behavior is to a great extent the effect of cold on the clotting process itself, since there cannot be retraction if there is no clotting.

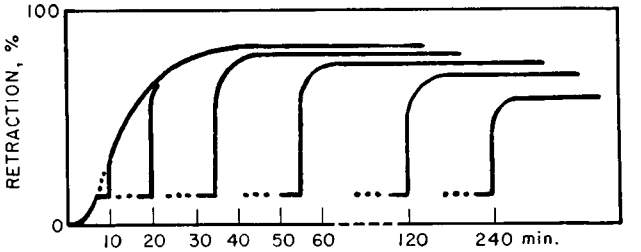

Fig. 7. Influence of mechanical arrest and its release on the physical phase of clot retraction.

The next problem is: Why is retraction delayed if it seems to be one and the same as the clotting process? To answer this question attempts were made to artificially delay retraction in the retractograph by blocking it as follows:

1. The first method of blocking was by rapid cooling to +4°C. in different stages of the proceeding retraction and again rapidly warming to 37°C. after certain intervals. In Figure 6 the plasma was cooled for 20 min. to 4°C. after retraction had already begun. When it was warmed again, retraction went on nearly in the same way of the normal curve. That means that the basic biochemical process of retraction was interrupted by cold, which simultaneously stopped its mechanical action.

2. The other way to block retraction is a mechanical one. This was done by arresting the feeler plate in the retractograph for certain amounts of time. Figure 7 shows the effect of arresting retraction 5 min. after its onset from 5 min. to 4 hr. It is apparent that the arrest did not alter the yield of retraction if the artificial delay did not exceed 15 min. Arrests of longer duration produced a gradual increase but not a great deterioration of retraction. Immediately after retraction, recovery took place in a comparatively

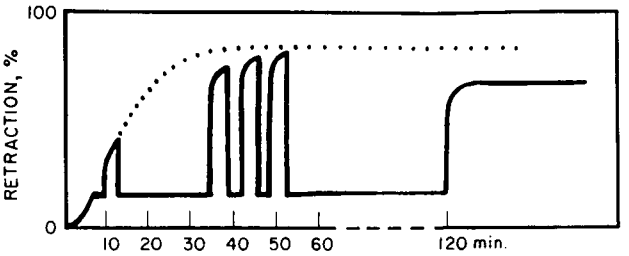

Fig. 8. Influence of alternating retraction and release.

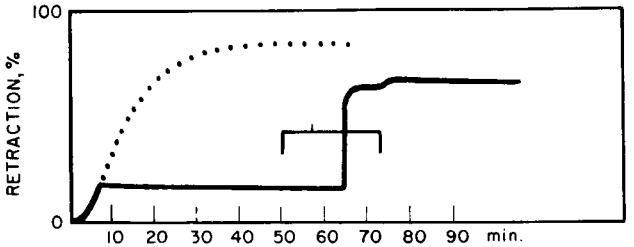

Fig. 9. Influence of arrest during chemical phase and cold during physical phase of retraction. The scale is 4°C.

short time. If release took place before the expected maximum retraction, the curve followed, after a somewhat short acceleration, the trail of the control retractogram. This behavior of the clot resembled very much a spring tightened by mechanical strain. This is proved by Figure 8, which shows the effect on retraction when it is repeatedly taken back by simply reverting the feeler plate to its previous position. Here the clot shows the quality of an elastic body, rather than the Maxwell body,[13] which can be put under strain as well as relaxed.

If retraction is blocked in an early stage as shown, and then released (e.g., after 1 hr.), the whole process of retraction has already passed on isometrically. This means that the clot does not change in shape but by a molecular process tightens like a spring, which may set free its strain at the time when it is released.

The normal retractogram (Fig. 3) shows the retraction process 40 min. after its onset. With regard to the above experiments this seems to represent the time of chemical activity producing the

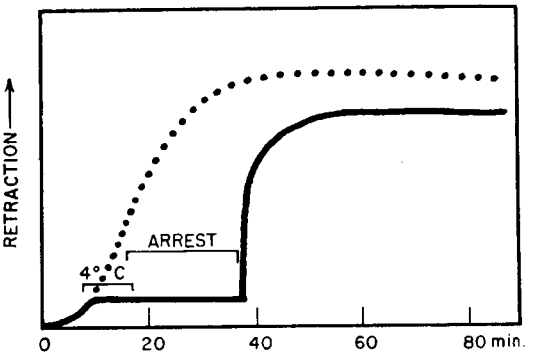

Fig. 10. Influence of limited cooling on chemical phase and arrest with release on physical phase of clot retraction.

contractive strain. Some experiments performed by Gross[14] and Born[4] in connection with the author's work proved that the time of the highest release of ATP from platelets corresponds with the time of highest retraction activity, that is, with the steepest ascent of the retractogram.

As was seen above, cold is able to stop the biochemical phase of retraction. If the theory regarding the linkage of biochemical and physical retraction proves right, cooling of an isometrically tightened clot after the chemical phase is over should not hinder the purely physical phase. Thus retraction should now appear during the cool phase if released, provided cooling did not begin earlier than about 45 min. after clotting. Figure 9 shows a schematic retractogram of this experiment. After 5 min. of retraction it was mechanically blocked, the temperature being 37°C. Forty-five minutes later the still blocked clot was cooled to +4°C., and 20 min. later the cooled clot was released. The result was a good retraction in spite of the low temperature. Subsequent warming to 37°C. did not bring about any great increase of retraction. While the experiments were performed additional measurements were made. In the last retractogram (Fig. 10), retraction was first interrupted by cooling to 4°C. and then after 10 min. blocked in a standstill position. Five minutes later the clot was warmed to 37°C. and 15 min. later released again. Until this moment the clot had had only about 25 min. for biochemical retraction activity. Because

the normal activity lasts approximately 40 to 45 min., it was expected that a rest of about 15 min. in chemical activity could be observed. This proved to be correct.

References

1. Hirschboeck, J. S., *J. Lab. Clin. Med.*, **33,** 347 (1948).
2. Budtz-Olsen, O. E., *Clot Retraction*, Oxford Univ. Press, London, 1951.
3. Hartert, H., unpublished data.
4. Born, G. V. H., private communication.
5. Hartert, H., (*a*) *Klin. Wochschr.*, **36,** 1084 (1958); (*b*) *Klin. Wochschr.*, 139 (1954).
6. Hartert, H., in *Flow Properties of Blood and Other Biological Systems*, A. L. Copley and G. Stainsby, eds., Pergamon Press, New York-Oxford, 1960, p. 375.
7. Hartert, H., *Proceedings of the Fourth International Congress in Biochemistry, Vienna*, Vol. 10, E. Deutsch, ed., Pergamon Press, London, 1958, p. 239.
8. Lüscher, E., private communication.
9. Hartert, H., H. G. Lasch, and I. Pfisterer, *Thromb. Diath. Haemorrhag.*, **1,** 445 (1957).
10. Lüscher, E., *Thromb. Diath. Haemorrhag.*, **4,** 178 (1960).
11. Lüscher, E., *Ergeb. Physiol. Biol. Chem. Exptl. Pharmakol.*, **50,** 1 (1959).
12. Kriessmann, A., dissertation, Heidelberg, 1962.
13. Scott Blair, G. W., in *Flow Properties of Blood and Other Biological Systems*, A. L. Copley and G. Stainsby, eds., Pergamon Press, New York-Oxford, 1960, p. 172.
14. Gross, R., private communication.

Synopsis

14604

Retraction of the blood clot consists apparently of a chemical phase, which brings about a strain in the clot. Retraction (i.e., the physical phase of retraction) takes place after chemical tightening of the clot. The moment when it begins depends upon the process of detachment at the interface between clot and surface of the container. The speed of retraction depends on the volume of the clot and on the number of blood cells, provided a normal amount and quality of fibrinogen as well as platelets is present. Roughly speaking, the yield is determined by the same factors. The physical potency of retraction remains active for several hours after clotting, yet decreases progressively. After 4 hours, e.g., it still has two-thirds of its initial value. The chemical phase of retraction seems to be identical with that phase of the clotting process in which the fibrin and platelets containing clot structure is established.

Author

Fat Embolism—a Hemorheologic Disturbance

N67 14605

SVEN-ERIK BERGENTZ,* *University of Gothenburg, Gothenburg, Sweden*

Trauma of various kind causes alterations in the rheologic properties of blood. These can be demonstrated as an increased viscosity, aggregation of the formed elements such as platelets and red cells, and increased erythrocyte sedimentation rate (ESR). Blood contains, however, also fat, which cannot exist in the blood as a solution but is treated as a formed body. The largest of these formed bodies can be seen in a microscope in dark-field illumination as dancing refractile particles with a size of about one micron (so-called chylomicra). These chylomicra have their own anatomy, being built up by a nucleus of triglycerides and a very thin shell of cholesterol, phospholipides, and protein. It is the purpose of this paper to analyze the role played by blood fat for the formation of fat emboli.

The term fat embolism is used to define both a pathoanatomical and a clinical condition. Used as a *pathoanatomic* term it indicates the appearance in the capillary bed of fat droplets which can be visualized by fat stains. These fat droplets differ from chylomicra by their size, which usually is 10 to 50 μ, and by the fact that they are free and not surrounded by a membrane. This pathoanatomic condition is very common after various types of trauma, but it also occurs in intoxications and infections. It appears early after trauma, within minutes or hours. Used as a *clinical* term, fat embolism defines a syndrome appearing after massive trauma, and only after trauma, especially fractures, and is indicated by impaired circulation, particularly in the lungs, brain, and kidneys. The clinical picture is relatively rare, and it does not appear until one or a few days after the injury. The relationship between the pathoanatomical phenomenon of fat embolism and the clinical syndrome with the same name is therefore far from clear. In this paper the term is primarily used

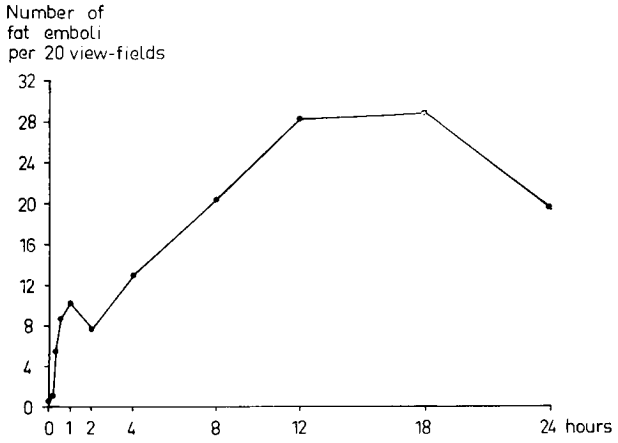

Fig. 1. Number of fat emboli in lungs of rabbits at different intervals after fractures. Mean values from 83 animals.

in a pathoanatomic sense, and later on its relationship to the clinical syndrome will be discussed.

The explanation for the genesis of fat embolism, generally accepted since almost 100 years, is that fat droplets from the bone marrow after a fracture are transported to the lung where they lodge in the capillaries and eventually go over to the systemic vessels. This theory might possibly explain the fat emboli after fractures but not after infections, intoxications, extracorporeal circulation, and various types of metabolic disturbances. The theory cannot explain the clinical phenomenon of fat embolism, as it has been shown that remarkably large amounts of fat can be tolerated intravenously, probably more than the whole fat content in a femur, while no significant amount of fat actually leaves a fractured bone. It is therefore obvious that there must be some other source of the fat emboli. It was suggested as early as 1863 by a German, Grohe,[1] that the fat particles normally occurring in blood might form fat droplets by some changes in their physical state. In 1927, Lehman and Moore[2] demonstrated that this actually did occur *in vitro* when ether was added to lipemic blood and *in vivo* when ether was given intravenously or inhaled for a couple of hours. The author's main interest has been to find if a similar change in the blood fat also occurs after injury.[3]

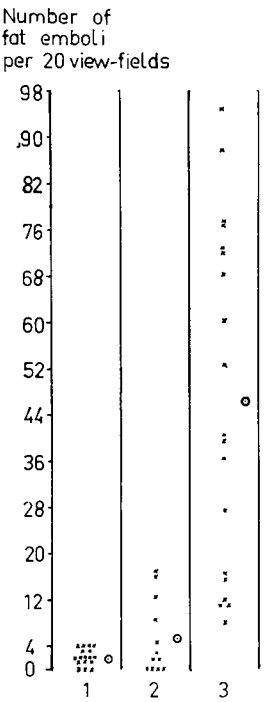

Fig. 2. Number of pulmonary fat emboli in rabbits subjected to the following procedures: (*1*) injection of fat emulsion, (*2*) fractures, and (*3*) injection of fat emulsion + fractures.

Before any work is done on the genesis of the posttraumatic fat embolism it is necessary to know exactly when after an injury the fat droplets are formed. This has been analyzed by production of bilateral femoral fractures and soft tissue injuries in rabbits and dogs. The rabbits were killed at various time intervals after the trauma, and pieces of lung tissue taken post-mortem. The amount of fat embolism was estimated by counting the number of intravascular fat droplets in standardized osmium-stained lung specimens. The results of these experiments are shown in Figure 1. From this is apparent that fat emboli appear in the lung as early as 15 min. after the trauma, that they increase in number particularly for the first 2 to 3 hr., that the increase then is slower, and that there is no further increase after about 18 hr. In dogs repeated lung biopsies

Fig. 3. Fat droplets, 3 and 9 μ in diameter, included in and attached to an aggregate of chylomicra. The specimen was taken from the surface of the plasma from a rabbit 1 hr. after multiple fractures. Dark-field illumination.

were taken, in one group during the first 12 hr. after fracture, and in another group between 12 and 24 hr. after fracture. The results in the dog show the same main features as in the rabbit. The number of fat emboli in animals subjected to soft tissue injury with 200 blows with a padded hammer on each thigh is about 50% less than in animals subjected to bilateral femoral fractures.

Thus, the formation of fat emboli is obviously a very early phenomenon after injury. If blood changes are responsible for formation of fat emboli, then an increased amount of blood fat, i.e., a state of hyperlipemia, during this time might result in an increased number of fat emboli. We have studied the influence of hyperlipemia in rabbits by injection of 3 g./kg. bwt (body weight) of a fat emulsion for intravenous use (Lipomul) and produced fractures 1/2 hr. later. As seen in Figure 2 this produced within 1/2 hr. a very pronounced fat embolism compared to the very slight degree of fat embolism produced at this time by the same tissue injury alone, or by the same degree of hyperlipemia alone. The conclusion from this experiment is that trauma must have produced such changes in the physical state of the injected fat that it can no longer stay in a completely emulsified state but forms fat droplets, which can be visualized in the tissue specimens as fat emboli. It is not known, however, whether trauma has the same effect on alimentary hyperlipemia as it has on this "artificial" hyperlipemia. This has been studied in dogs given a heavy fat meal such as cream, and 3 hr. later subjected to nembutal

anesthesia, lung biopsy, and then to fractures and repeated biopsies. It was found the hyperlipemia as such does not produce a significant fat embolism, but the fractures do. The degree of this fat embolism is higher in the hyperlipemic than in the nonhyperlipemic dogs 1/2 and 1 hr. after the fracture, but after 12 hr. there is no difference.

Thus, this observation supports the idea that blood fat is of importance for the formation of fat emboli. To study the appearance of the visible part of the blood fat after injury we have used both dark-field microscopy and microscopy in ultraviolet light after staining with phosphine, a water soluble fat stain, which gives the fat a very marked fluorescence. In these studies it was found that fat droplets appear on the surface of the plasma after injury when blood is taken in citrate and spun at 1.900 g. for 20 min. These fat droplets have a size of 2 to 3 μ, but some go up to 15 μ. They occur often isolated though it is not unusual to find them in groups of various numbers. Occasionally they are attached to an aggregate of chylomicra as seen in Figure 3, where there are two fat droplets, 3 and 9 μ in diameter, the smaller included in and the bigger attached to an aggregate of chylomicra. Even more interesting, however, is the finding of fat droplets in the buffy coat at the top of the red cell column in this blood after fracture. The gray-white material in the buffy coat contains large aggregates of platelets with white blood cells and varying numbers of chylomicra, either as free dancing particles or as aggregates connected in particular to the aggregates of platelets. In these aggregates of chylomicra but also free from them are seen fat droplets, mostly quite small, with a size of 2 to 5 μ. It should be noted that such fat droplets can be found even in normal blood, but there is a significant increase in blood from traumatized animals during the time when fat droplets appear not only in blood from the traumatized tissue but also in venous blood from other parts of the body and in arterial blood. The finding of aggregated chylomicra and fat droplets in these aggregates seem to support the idea that fat droplets can form from the blood by changes in the physical state of the blood fat.

To find out if such posttraumatic changes in the physical state of blood could be demonstrated also *in vivo* we have investigated the capillary flow during the time after injury when fat emboli appear in the lung. Figure 4 shows what happens within a few seconds after a local contusion injury of a hamster's cheek pouch, which has

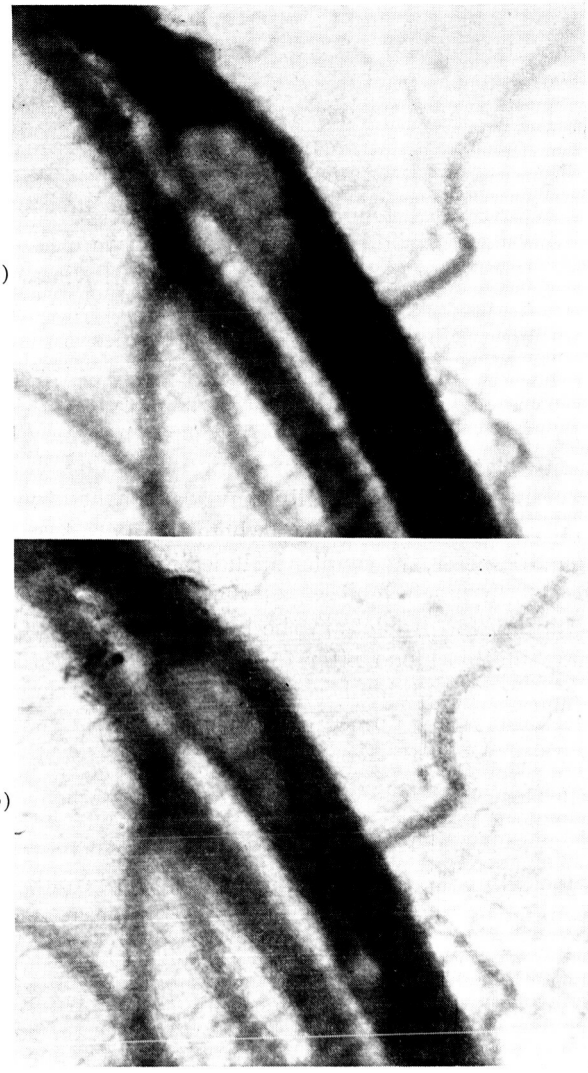

Fig. 4. Venule and arteriole in a hamster's cheek pouch close to a crush injury, a few minutes after performing the injury. (*a*) A white mass has stopped in the venule, adherent to the wall. (*b*) A "white embolus" is being swept away by the blood stream (at the bottom of the picture). This embolus comes from the white mass, which has decreased in size.

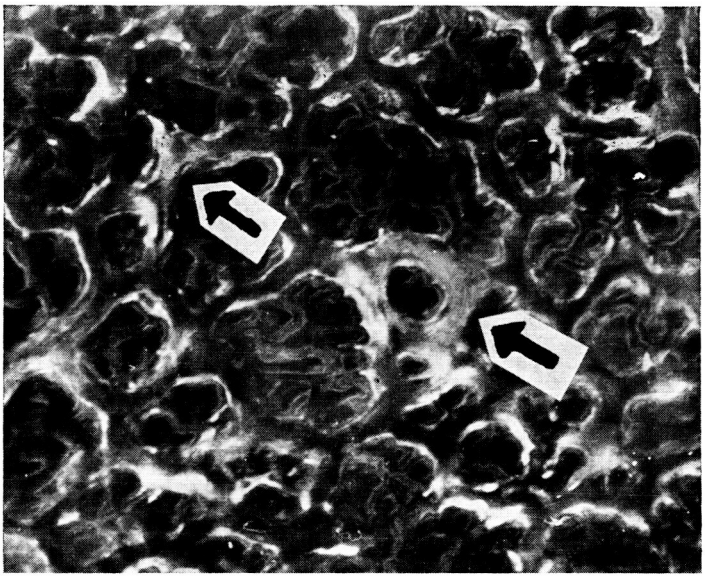

Fig. 5. The vascular bed in the lung in a rabbit 12 hr. after multiple fractures. The arrows indicate white masses which have been arrested in the lung capillaries.

been studied in a microscope by transillumination. White masses are seen close to the traumatized tissue. These masses often stick to the endothelium of the vessels and then increase in size obviously by taking elements from the streaming blood. These growing masses now and then disrupt giving rise to so-called "white emboli." In the lung a similar phenomenon is found as seen in Figure 5 taken a few hours after femoral fracture in a rabbit. A thoracotomy was performed, the lung was kept expanded with a continuous stream of oxygen through a catheter in trachea, and is observed in vital microscope. These white emboli do not seem to impair the flow, and there is no aggregation of red cells at this time. The aggregation of the red cells starts within 2 to 4 hr. and increases during the time of observation.

It is well known from numerous studies that the white platelet-aggregates appearing after injury represent the first part of the hemostatic process, the formation of a white thrombus.

The results of this investigation, therefore, made it necessary to study the effect of injury on the various coagulation factors during

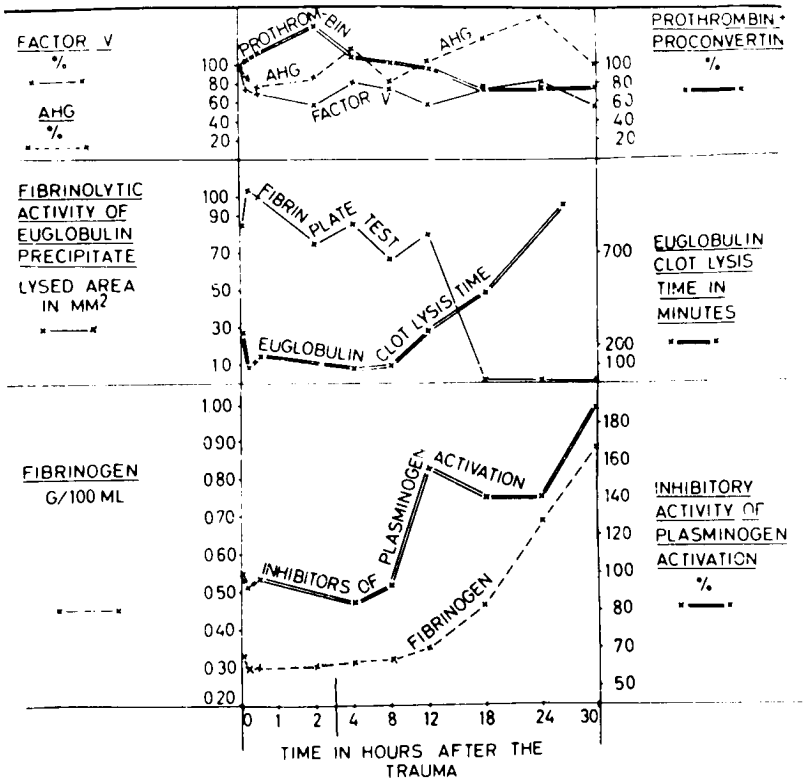

Fig. 6. Effects of bilateral femoral fractures on coagulation and fibrinolysis in a dog. Results of a typical experiment.

this time. This has been done in dogs subjected to femoral fractures and repeated blood sampling, the first after 10 min. Figure 6 summarizes the results. Antihemoglobin (AHG) and factor V decrease as early as 10 min. after injury and they are still down 40 min. and 2 hr. after fracture. Following this no further decrease takes place but rather a tendency to increase is seen. Fibrinogen also shows a decrease as early as 10 to 30 min. after trauma; the decrease is still present after 2 hr. but then there is a marked increase in the fibrinogen. These three factors, AHG, factor V, and fibrinogen are consumed in the coagulation process. Experiments in dogs which have been heparinized immediately before fracture were repeated,

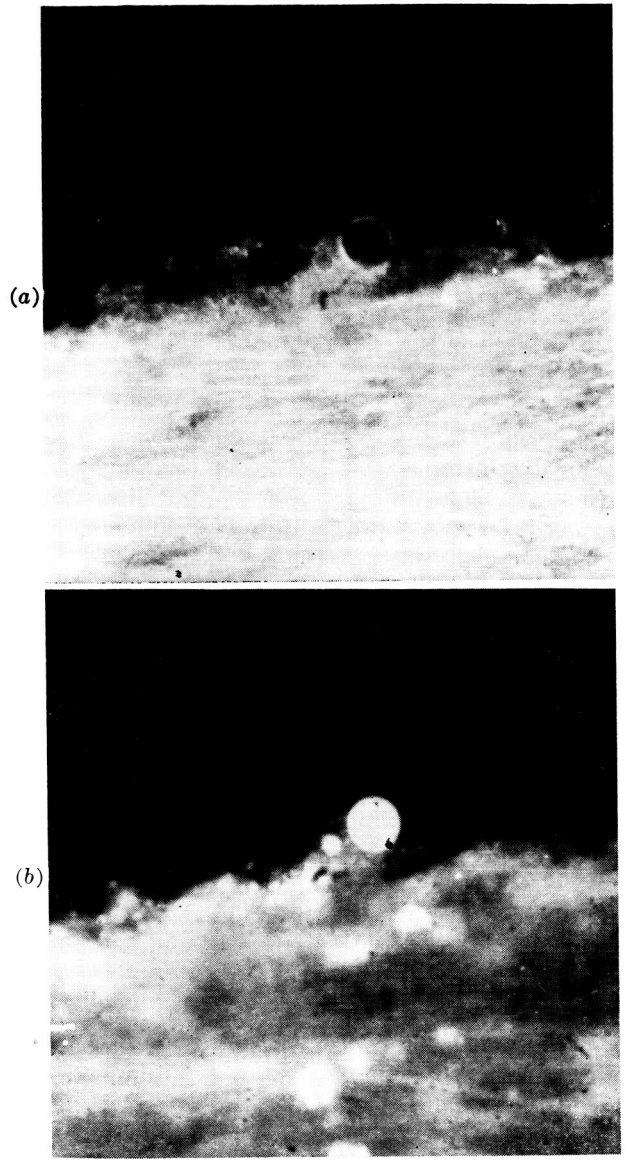

Fig. 7. Fat droplets, 10 and 3.5 μ in diameter, at the edge of an experimental thrombus in a ligated femoral vein in a nonhyperlipemic rabbit. This thrombus was removed 20 hr. after soft tissue injury on the contralateral leg. Phosphine staining. (*a*) Taken in visible light with dark-field illumination. (*b*) Taken in ultraviolet light.

and in those cases there was no decrease whatsoever in these factors. The results show that trauma initiates a coagulation.

To recapitulate, fat emboli in the lung appear within the very first hours after injury. During this time fat droplets appear in the blood both free and incorporated in aggregates of platelets and chylomicra. White aggregates appear in the capillary bed *in vivo;* they contain platelets and are the first morphological sign of the coagulation process. This coagulation process can also be demonstrated in a decrease in the coagulation factors which are consumed in a coagulation process.

Thus it was necessary to see if there was any connection between the coagulation process and the formation of fat emboli. To study this a technique described by Borgström et al.[4] was used. The femoral veins were ligated on both sides in a rabbit. This normally does not cause thrombi to appear. If the animal is traumatized with a padded hammer on one side, thrombi will appear within 3 hr. on the traumatized side and within 6 hr. on the nontraumatized side. These thrombi consist, as all real thrombi, of a small white head and a longer red tail. The white head which must have the same composition as white emboli, is dissected free, stained with phosphine, and studied both in dark-field microscopy and ultraviolet light. The white thrombi consist of large masses of aggregated platelets. There are also some red and white blood cells and fibrin. Interestingly enough there are large masses of chylomicra and also fat droplets of various sizes especially at the margins of the thrombi as seen in Figure 7. Most droplets are 2 to 5 μ, but there are also droplets up to 15 μ. Around the thrombus there are large amounts of chylomicra, quite different from the very small number of chylomicra present in the peripheral blood. There are also aggregates of chylomicra and in these and also free from them are fat droplets of 2 to 15 μ. This experiment makes it seem probable that fat droplets are formed in an intravascular coagulation process from the fat which normally is present in the blood.

It should then be possible to produce fat emboli without trauma by initiating a massive intravascular coagulation. This was done by injection of thromboplastic substances of various types, and was in fact found to give rise to fat emboli of exactly the same type as seen after trauma. Such a coagulation process can also be initiated by a traumatization of the blood produced, e.g., in artificial oxygen-

ators. This is known to result in disruption of platelets and to some extent also red blood cells. When such blood goes back into the patient it has thromboplastic properties, which give rise to an intravascular coagulation process. However, heparin does not prevent the very first phase of the coagulation, that is, aggregation of platelets and disruption of these aggregated platelets, nor does it prevent the formation of fat emboli. It is, therefore, not surprising to find that extracorporeal circulation is followed by the appearance of fat emboli, probably as a regular phenomenon.

From the results just reviewed it is concluded that injury produces such changes in the physical state of blood that fat droplets are formed from blood fat. These blood changes are probably related to the intravascular coagulation process which is initiated by injury.

How can we interpret the clinical syndrome of fat embolism generally ascribed to the fat droplets found in the capillary bed? To understand this it is important to shortly recapitulate the microcirculatory changes which appear after injury. During the very first hours after injury white emboli appear in the small vessels. At the same time fat droplets are found in the blood and in the capillary bed. There is a decrease in the number of platelets and in the various coagulation factors. No red cell aggregation is seen until about 4 hr. after injury, increasing in severity with time up to two to three days. For the first 24 hr. this aggregation is accompanied by a *reduced* ESR, but later the ESR is markedly increased reaching a maximum after 5 to 7 days. During all this time there is a tendency for vein thrombi to form in stagnated veins. Colloids with low viscosity such as low viscosity dextran counteract this tendency in the later phase of red cell aggregation (later than 24 hr.). Before that time, however, low viscosity dextran has no such effect while heparin has.

The significance of the flow changes produced by red cell aggregation has been evaluated in various experimental studies. From these it is evident that the flow disturbances cause an impaired peripheral nutritive blood flow indicated by appearance of acidosis, decreased rate of wound healing, decreased oxygen consumption, and necroses in parenchymatous organs.[5] The stasis of aggregated cells in venules can explain the anemia of injury.

The clinical fat emboli syndrome can be understood as a consequence of decreased nutritive blood flow in the lungs (dyspnoe,

cyanosis), brain (confusion, coma, paresis), or kidneys (decreased urinary output, uremia). These symptoms appear as a rule after 1 to 4 days, at a time when the intravascular red cell aggregation is most marked. Fat emboli will always be found in the lungs and often in other organs at that time. These have been formed earlier, however, and the formation of new fat emboli may have ceased when symptoms appear. The pathophysiological significance of fat emboli as such is doubtful, at least in the lungs. It is therefore reasonable to assume that the decreased nutritive blood flow responsible for the appearance of the fat emboli syndrome is caused not primarily by the fat emboli as such but by other posttraumatic alterations in the rheology of the blood, especially the aggregation of red cells.

The impaired blood flow after injury, caused by intravascular red cell aggregation, can be improved by infusion of substances that increase the fluidity and the suspension stability of the blood. Colloids with low viscous properties such as low viscosity dextran is known to have such effect. This agent was used in a few clinical cases of fat embolism with encouraging results.

References

1. Grohe, F., in Canstatt's *Jahresbericht über die Fortschritte der gesamten Medicin in allen Ländern im Jahre 1862*, Vol. 1, Würzburg, 1863, p. 45.

2. Lehman, E. P., and R. M. Moore, *A.M.A. Arch. Surg.*, **14**, 621 (1927).

3. Bergentz, S.-E., *Acta Chir. Scand.*, Suppl. **282** (1961).

4. Borgström, S., L. E. Gelin, and B. Zederfeldt, *Acta Chir. Scand.*, Suppl. **247** (1959).

5. Gelin, L.-E., and B. Zederfeldt, *Acta Chir. Scand.*, **122**, 336 (1961).

Synopsis

14 605

Posttraumatic fat embolism is generally assumed to be caused by intravasation of major fat droplets from traumatized fat tissue, particularly the bone marrow. Fat embolism is, however, a relatively common phenomenon even without a mechanical injury. In experimental animals fat embolism can be produced in different ways, including the initiation of an intravascular coagulation process, for instance by injection of thromboplastic substances. Evidence is given to show that the posttraumatic fat embolism can be caused by a hemorheologic disturbance with a change in the physical state of the fat normally occurring in the blood. This change is probably due to an intravascular coagulation process initiated by the trauma.

author

N67 14606

A Study in Rheology of Blood Clotting in Human Subjects

LEOPOLD DINTENFASS, *Department of Medicine, University of Sydney, Sydney, Australia*

INTRODUCTION

Although the clotting of blood involves a transformation of a fluid into a gel, the field of rheology of clotting has been neglected up till the most recent times. Some insight into the complexity of rheology of blood coagulation has been obtained through the pioneering effects of Hartert[1] and de Nicola,[2] who developed the thromboelastograph, and of Scott Blair,[3] and Copley and Scott Blair,[4] who applied a gelometer in order to study viscoelasticity of clotting.

In contradistinction to the above, biochemistry of blood coagulation is covered by enormous literature. It may be thought feasible, that a key to the clotting mechanism might be elucidated through the microrheological studies.

In the present investigation a cone-in-cone viscometer was used in order to follow viscosity changes during clotting. It is for the first time that a study of clotting was carried at different, but homogeneous, rates of shear. It will be shown that the rate of clotting depends not only on the intrinsic properties of the particular blood sample but also on the velocity gradient at which such clotting takes place.

INSTRUMENTATION

The instrument applied in this study was a cone-in-cone rotational viscometer constructed by Dintenfass[5,6] (Fig. 1). This viscometer permits a determination of blood viscosity over the region of rates of shear from 0.006 to 200 sec.$^{-1}$.

The instrument consists essentially of two coaxial cones, the

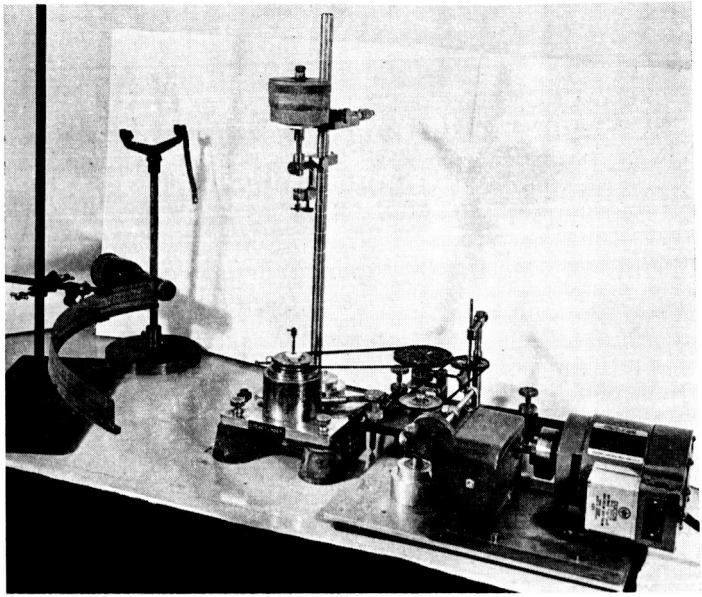

Fig. 1. The rorational cone-in-cone viscometer.

internal cone being suspended on a torsion strip, with the external cone being rotated by means of a gear box and a drive. The cones are centered by means of two micrometers. The internal cones are made from Teflon and have angles of 35 and 37° toward the vertical axis of the instrument. The external cone is made from brass and has an angle of 40° toward the vertical axis of the instrument. Cones are thermostated. The viscometer was calibrated using standard oils obtained from the National Standards Laboratories, Sydney. The rates of shear were calculated according to equation by Oka, as elaborated in an earlier paper.[6] The coefficient of proportionality between the rate of shear D and the number of revolutions per minute f is equal to 1.254 and 0.732 for the internal cones of the half-angle 37 and 35°, respectively.

METHODS

Samples of blood were obtained from patients and healthy persons in the laboratory. Blood was extracted by means of untreated needles and untreated syringes, but in the absence of anticoagulants.

A stop watch was started at the moment of blood extraction and the time intervals of the subsequent events were noted. A sample of 1 to 2 ml. was required to fill the gap between cones.

RESULTS

The clotting of blood was studied by means of a cone-in-cone viscometer, the samples of blood being obtained from healthy persons and from patients suffering from anaemia, coronary infarction, venous thrombosis, leukemia, polycythemia, rheumatoid arthritis, and cancer. Observations were made on one sample at one particular rate of shear, and the results were plotted as viscosity against the time which had elapsed from the moment of extraction of the blood. The onset of clotting was made evident by a more or less rapid increase in viscosity.

A series of clotting curves is illustrated by Figures 2, 3, and 4. It may be observed that the onset of clotting takes place after various time periods, depending not only on the origin of the particular blood sample but also on the velocity gradient and temperature.

When clotting is studied at 36 to 37°C., a consistently more rapid clotting takes place at higher rates of shear (from 20 to 100 sec.$^{-1}$). The latent period, before the onset of clotting, may be twice or even threefold longer at low rates of shear (below 1 sec.$^{-1}$).

It may be observed, however, that the above pattern becomes reversed when the clotting takes place at decreased temperatures (from 20 to 29°C.).

The general aspects of clotting appear to be the same in sheep.

DISCUSSION

Copley and Scott Blair[4] divided the process of blood coagulation into the following phases: first, when only changes in viscosity but not rigidity are observed; second, when the rigidity is low and the coagulum shows delayed elasticity; and third, when the gel structure is fully established. The present work deals only with the first stage of the process. In terms of thromboelastography, the present work deals with the stages r and k.

A perusal of Figures 2, 3, and 4 will suggest that a general pattern of clotting exists, coagulation of blood proceeding much more rapidly at high velocity gradient at body temperature. When, however, the

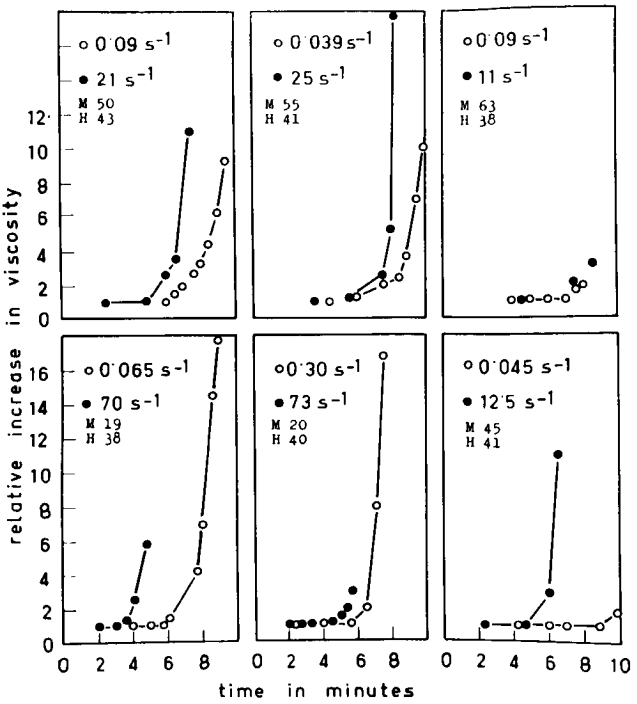

Fig. 2. Clotting curves of healthy persons. Clotting was followed by means of the cone-in-cone viscometer at low and at high rates of shear. Time is measured from the moment of blood extraction. Relative viscosity increase is the ratio of viscosity measured during clotting to the viscosity of unclotted blood at the same rate of shear. Tests were carried out at 37 °C. Here *M* indicates male; *H*, hematocrit; and s^{-1}, rate of shear in reciprocal seconds.

temperature of blood coagulation is decreased, a reversal of the above pattern appears to follow.

It might be considered that when the chemical reaction of plasma clotting is delayed due to decrease in temperature, a pronounced aggregation of red cells takes place in the time period during which the plasma clotting itself is not yet evident. One can envisage that some, yet undefined process goes on during the initial stages of clotting involving a rapid aggregation of red cells and, thus, a rapid increase in the structural viscosity. It might be of interest to note that Scott Blair[7] observed that blood clots are thixotropic. While it

is already proved[5,6,8] that fresh human blood is thixotropic, thixotropy being due to aggregation of red cells, the role of red cells in the clotting process is not yet clear.

A concept that red cells participate in clotting is not new. Gregoire[9] found that blood coagulation in insects proceeds mainly through

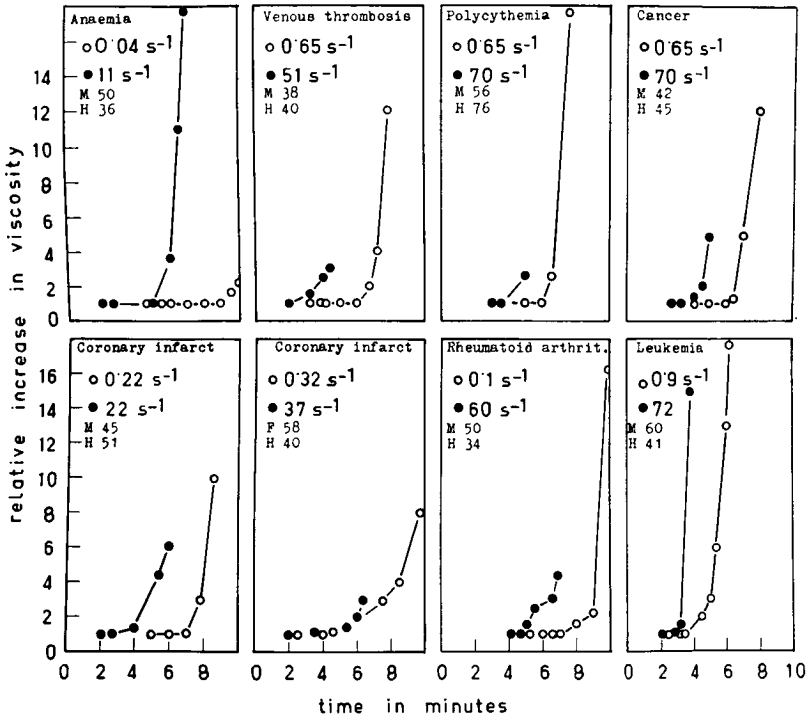

Fig. 3. Clotting curves for patients suffering from anemia, venous thrombosis, polycythemia, cancer, coronary infarction, rheumatoid arthritis, and leukemia. Clotting was followed by means of the cone-in-cone viscometer at low and at high rates of shear. Time is measured from the moment of blood extraction. Here *M* indicates male; *F*, female; *H*, hematocrit; and a^{-1} rate of shear in reciprocal seconds. All tests carried out at 37°C.

cellular clotting. Heilbrunn[10] stated that it should be recognized that a clot can be formed by an aggregation of blood cells alone. While many authors might consider that clotting does not occur if a formation of fibrin or fibrin like substance does not take place,

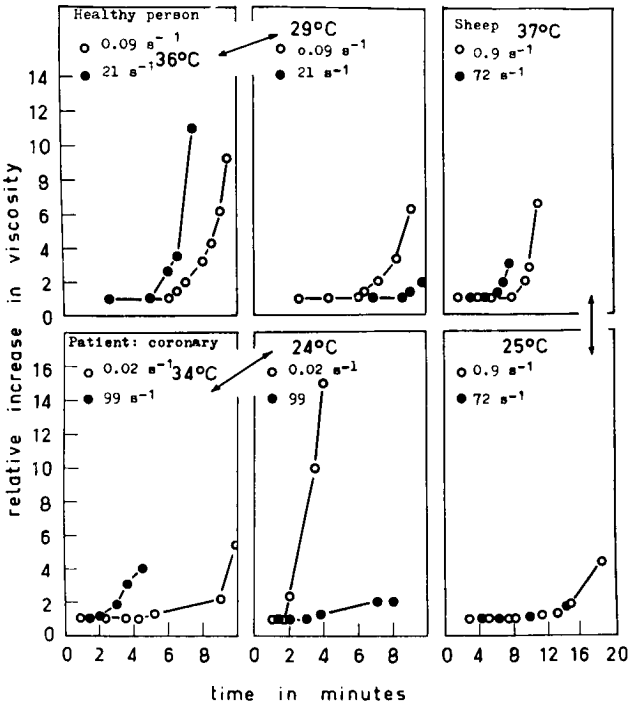

Fig. 4. Clotting curves at different temperatures. Clotting was followed by means of the cone-in-cone viscometer at low and at high rates of shear. A reversal of clotting pattern is indicated by both human subjects; similar trend may be observed in the case of a sheep. While at body temperature the rate of clotting is much more rapid at high rates of shear, at decreased temperatures the reverse is true. Here s^{-1} indicates rate of shear in reciprocal seconds.

Copley—among a few others—appreciated the importance of cellular aggregation.[11]

It should be stressed that the red cell itself might contain and extrude clotting initiators.[12–14]

A recent morphological and rheological study carried out at low and at high velocity gradients, showed[15] that a white thrombus (that is, a thrombus containing aggregates of platelets) takes place at high velocity gradients while a red thrombus (in which red cells are enmeshed in fibrin) is typical for low velocity gradients. Intermediate structures were obtained *in vitro* at intermediate rates of shear.

It appears that, from rheological standpoint, there might be two typical modes of clotting. The first one, taking place at slow or negligible flow rates, would involve aggregation of red cells. The second one, corresponding to high velocity gradients, would not contain in its body any appreciable number of red cells.

While no quantitative study was carried out on final clots, it was easy to observe that tensile strength of plasma clots was very high. The clot strength decreased as the concentration of red cells increased, at hematocrits of 70 and 75 the clots become very fragile. It could be that red cells act as "holes" in the plasma clot, if reviewed from the strength rheology standpoint. It is likely, however, that the concentration of red cells in a clot is not the most important factor in its strength rheology. Macfarlane and Tomlinson[16] observed that clots formed by thrombotic patients are significantly stronger than clots formed from blood of healthy persons.

CONCLUSIONS

The latent period before the onset of clotting depends not only on the origin of blood but also on the velocity gradient at which the process is taking place. At body temperature clotting proceeds more rapidly at high velocity gradients. This pattern is reversed at decreased temperatures.

There is scope for further study of rheology of clotting which might bring about an insight into the processes of clotting and thrombosis. It well may be that biochemical studies alone, unless assisted by biorheological theories and techniques, might lead to an impasse.

The author gratefully acknowledges assistance of a grant from the National Health and Medical Research Council of Australia.

References

1. Hartert, H., *Flow Properties of Blood and Other Biological Systems*, A. L. Copley and G. Stainsby, eds., Pergamon Press, New York-Oxford, 1960, p. 186.

2. De Nicola, P., *Thromboelastography*, C. C Thomas, Springfield, Ill., 1957.

3. Scott Blair, G. W., *Flow Properties of Blood and Other Biological Systems*, A. L. Copley and G. Stainsby, eds., Pergamon Press, New York-Oxford, 1960, p. 172.

4. Copley, A. L., and G. W. Scott Blair, *Flow Properties of Blood and Other Biological Systems*, A. L. Copley and G. Stainsby, eds., Pergamon Press, New York-Oxford, 1960, p. 412.

5. Dintenfass, L., *Circulation Res.*, **11**, 233 (1962).
6. Dintenfass, L., *Biorheol.*, **1**, 91 (1963).
7. Scott Blair, G. W., *Lab. Pract.*, **8**, 220 (1959).
8. Dintenfass, L., *Med. J. Australia*, **1**, 575 (1963).
9. Gregoire, C., *Arch. Biol.*, **66**, 103 (1955).
10. Heilbrunn, L. V., *Functions of the Blood*, R. G. Macfarlane and A. H. T. Robb-Smith, eds., Blackwell Scientific Pub., Oxford, 1961, p. 283.
11. Copley, A. L., *Ärztliche Forsch.*, **11**, I/114 (1957).
12. Bradlow, B. A., *Brit. J. Haematol.*, **7**, 476 (1961).
13. Quick, A. J., *Nature*, **192**, 882 (1961).
14. Imglis, J. A., and J. W. Halliday, *Nature*, **192**, 882 (1961).
15. Rozenberg, M. C., and L. Dintenfass, *Australian J. Exptl. Biol. Med. Sci.*, in press.
16. Macfarlane, R. G., and A. H. Tomlinson, *J. Clin. Pathol.*, **14**, 320 (1961).

Synopsis

14606

A study of blood clotting was carried out by means of a cone-in-cone rotational viscometer. Blood samples were obtained from healthy persons and from patients suffering from anaemia, coronary infarction, venous thrombosis, leukemia, rheumatoid arthritis, polycythemia, and cancer. Also blood from a sheep was employed. Clotting of blood was made apparent by a viscosity increase. The rate of clotting depended not only on the origin of the sample but also on the velocity gradient at which such clotting took place. At body temperature, clotting proceeds more rapidly at higher velocity gradients.

Author

N67 14607

Influence of Plasma Proteins on the Rheology of Human Blood

E. W. MERRILL,* W. G. MARGETTS, and G. R. COKELET, *Department of Chemical Engineering, Massachusetts Institute of Technology;* A. BRITTEN and E. W. SALZMAN, *Massachusetts General Hospital, Boston, Massachusetts;* and ROBERT B. PENNELL and MARSHALL MELIN, *Protein Foundation, Boston, Massachusetts*

INTRODUCTION

Samples of blood from normal human donors were studied with a Couette viscometer[3] capable of measuring torques in the range of 100 to 0.01 dyne cm. With reference to Figure 1, which is a cross-sectional diagram of the Couette viscometer, in order to determine the rheological properties of the sample being tested, the sample of blood is contained between a rotor of coin silver and a polymethyl methacrylate stator. The mean radial clearance is 1465 μ. The rotor is caused to rotate by means of a hollow shaft through which water at 37°C. is pumped. The rotor is driven by a synchronous motor and gear trains both clockwise and counterclockwise at rotational speeds of 20 to 0.01 rpm, corresponding to shear rates in the liquid annulus of 20.5 to 0.0103 $(\text{sec.})^{-1}$.

In the experiments described immediately following, the red blood cells were resuspended at various levels of hematocrit in their respective plasmas. In other experiments described subsequently in this paper red cells from type O blood (normal human donors) were suspended in various wet protein fractions, identified below, as prepared from whole plasma by the Protein Foundation. Rheological testing was completed within 48 hr. from the time of the original fractionation.

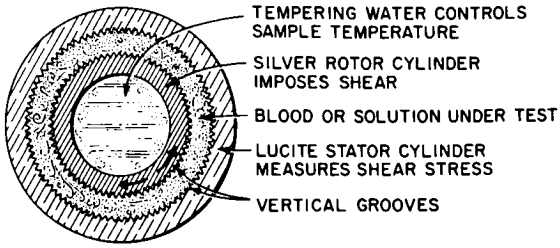

Fig. 1. Cross-sectional diagram of the Couette viscometer.

EFFECT OF FIBRINOGEN ON RHEOLOGICAL PROPERTIES

The dominant role of fibrogen in producing a yield shear stress in blood, earlier noted,[4] was more extensively examined by determining the relation between the concentration of fibrinogen as it occurred naturally (innately) in the blood of several normal donors, and the yield shear stress. Use was made of certain of the equations proposed by Casson[1] in a manner elsewhere described.[2] This includes plotting the experimental data as square root of shear stress vs. square root of shear rate (Figs. 3–6).

The method of determining fibrinogen concentration was that of Cullen,[6] and the values noted in Table I and Figure 2 refer to the concentration found after the blood had been drawn into ACD solu-

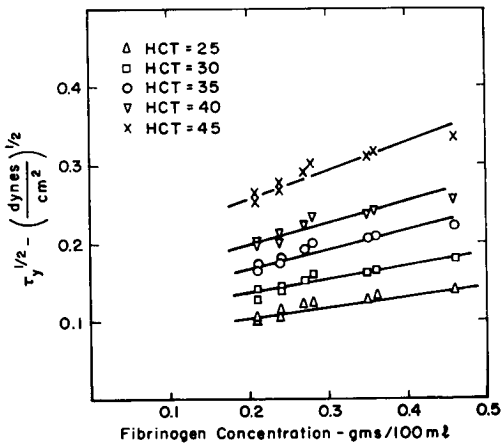

Fig. 2. Yield shear stress vs. innate fibrinogen concentration.

tion sufficient in quantity to produce an approximate dilution of 10% of the original plasma.

From the results shown in Table I, and plotted in Figure 2, the

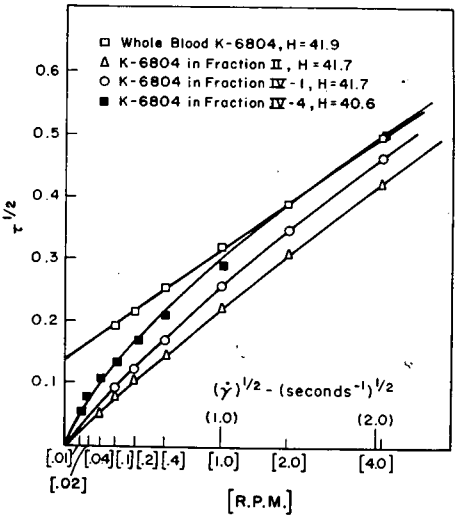

Fig. 3. Red cells suspended in protein fractions. Ordinate in $(\text{dynes/cm.}^2)^{1/2}$.

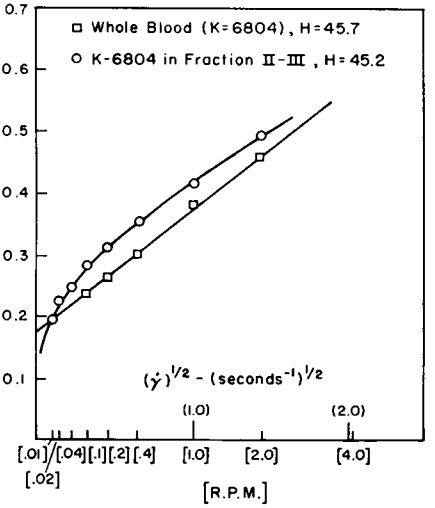

Fig. 4. Red cells suspended in fraction II-III. Ordinate: $\tau^{1/2}$ $(\text{dynes/cm.}^2)^{1/2}$.

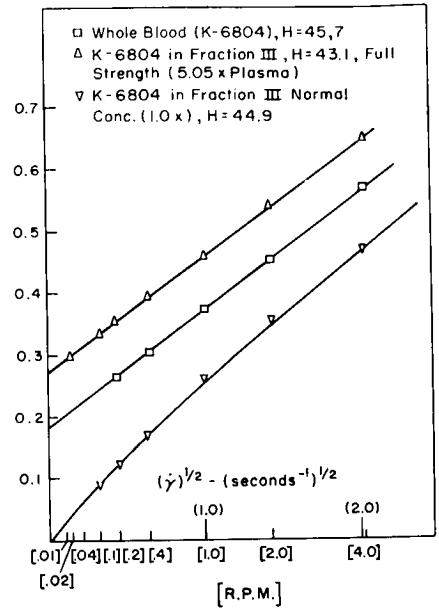

Fig. 5. Red cells suspended in fraction III (β-globulin). Ordinate: $\tau^{1/2}$ (dynes/cm.^{2})$^{1/2}$.

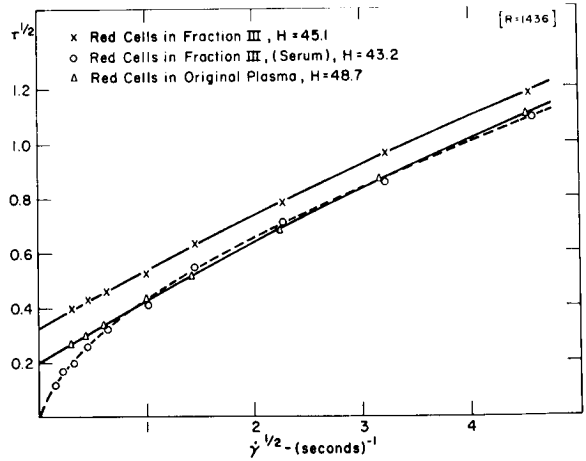

Fig. 6. Red cells suspended in fraction III.

TABLE I
Rheological Properties of Normal Blood, Yield Shear Stress vs. Fibrinogen Concentration and Hematocrit H

Sample No.	Fibrinogen concn., g./100 ml.	(Yield shear stress)$^{1/2}$ − $\tau_y^{1/2}$, [dynes/cm.^{2}]$^{1/2}$ H = 25	H = 30	H = 35	H = 40	H = 45
K-6005	0.21	0.106	0.141	0.172	0.201	0.264
K-6804	0.21	0.103	0.131	0.165	0.204	0.252
K-4782	0.24	0.113	0.148	0.182	0.212	0.278
N-1265	0.24	0.109	0.141	0.175	0.204	0.266
N-2380	0.27	0.120	0.153	0.191	0.223	0.291
N-8492	0.28	0.123	0.160	0.198	0.233	0.303
N-6273	0.36	0.131	0.165	0.207	0.241	0.316
K-5834	0.35	0.128	0.164	0.206	0.238	0.321
K-4370	0.46	0.138	0.177	0.221	0.256	0.334

following correlation was obtained between the yield shear stress τ_y and the concentration of fibrinogen C_F in grams/100 ml.:

$$\tau_y^{1/2} = (H - 0.07)^{1/2} (1.55\ [C_F] + 0.76)$$

This correlation is applicable *only* over the range of innate fibrinogen concentration studied, viz. 0.21 to 0.46 g./100 ml. Over this range it was found to hold with a mean error of 9% for 37 different samples from normal donors. Below fibrinogen concentrations of about 0.2 g./100 ml., the yield shear stress relation is unknown since few normal donors have blood fibrinogen concentrations less than this value. It is established that in the total absence of fibrinogen there is usually zero yield stress. Cokelet[4] showed that suspensions of washed red cells in well-defibrinated serum totally lacked yield shear stress, and more recently blood drawn from a patient with afibrinogenemia was found by analysis[6] to contain no fibrinogen and by viscometry to have no yield shear stress. It therefore seems clear that, in Figure 2, the yield shear stress must somehow go to zero as the fibrinogen concentration is decreased to zero.

RED CELLS SUSPENDED IN PROTEIN FRACTIONS

Purified protein fractions were prepared by the Protein Foundation, Boston, Massachusetts. Normal red cells were separated from their plasma, rinsed twice in the protein fraction, and then finally suspended

TABLE II
Composition of Different Protein Fractions

Sample	Total protein, g./100 ml.	Albumin g./100 ml. plasma	Globulin g./100 ml. plasma	Fibrinogen g./100 ml. plasma	% of Total Protein by Electrophoresis, Albumin	α	Globulin, β	γ	Fibrinogen
Fraction II	1.5	0.2	1.3	0.04			3	97	
Fraction II-III	4.3	0.5	3.7	0.11	6	6	48	37	3
Fraction III	3.6	0.3	3.2	0.12	10	15	67[a]		9
Fraction IV-I	1.3	0.9	0.4	No clot		89	10		
Fraction IV-4	3.3	2.2	1.1	No clot	30	41	29		

[a] Poorly resolved slow-moving components, probably mostly β.

in a fresh sample of the same fraction. These samples were then tested with the GDM viscometer.

The composition of the different protein fractions used is listed in Table II. From the Casson plots of the fractions tested (see Figs. 3 and 4) it appears that the suspensions tested did not have a yield shear stress value. These results are similar to those found for protein solutions made from dried protein fractions.[4]

Fraction II, which was predominantly γ-globulin did not exhibit a yield shear stress. There was a detectable amount of fibrinogen in this sample (0.04 grams/100 ml. plasma), but the concentration was not large enough to induce any detectable red cell aggregation and rouleaux formation. Fraction IV-1, which was mainly composed of α_1- and α_2-globulin, also did not show a yield shear stress. The protein fraction which contained albumin, α_1-, α_2-, and β-globulin, fraction IV-4, did not exhibit a yield value.

Red cells combined with fraction II-III, which is predominantly β- and γ-globulin, had a higher viscosity than the other fractions tested. However, the fraction did not appear to have a yield shear stress as shown in Figure 4, when combined with red cells, and the higher viscosity could have resulted from the fibrinogen present inducing limited red cell aggregation and the increased concentration of proteins in the sample used.

EFFECT OF β-GLOBULIN ON RHEOLOGICAL PROPERTIES

Investigators have determined that an increase in the concentration of β-globulin phase increases the ability of red cells to form rouleaux.[7] A purified fraction of β-globulin was obtained from the Protein Foundation. The fraction also had a detectable amount of fibrinogen in the concentrated solution.

Normal red cells were washed twice in the protein fraction (fraction III) and finally suspended in the fraction. As shown in Figure 5, the red cells suspended in the β-globulin-rich plasma exhibited a much higher yield shear stress than the red cells in their own plasma. As type O cells were used no antigenic reaction is suspected. In addition, as stated previously, red cells from the same whole blood were added to other protein fractions and no yield shear stress values were determined. When fraction III was diluted (one volume of fraction III to four volumes saline) and combined with red cells in a similar

manner, no yield shear stress was detected. The concentration of the plasma proteins are listed in Table III for the plasma samples rich in β-globulin. The protein fraction combined with the red cells was determined to have a lower concentration of globulin[8] than the uncombined material. It is possible that some of the protein fraction was adsorbed on the surface of the red cells. However, considering that the cells were first washed with a portion of fraction III and that there are inaccuracies in the analytical protein determination, no conclusions can be drawn.

TABLE III
Protein Content of Normal Plasma and Fraction III

	Normal K-6804	Full strength uncombined	Fraction III combined	Diluted fraction III
	Protein Composition, g./100 ml. Plasma			
Total protein	6.8	3.5	3.4	0.9
Albumin	3.3	0.3	0.4	0.2
Globulin	3.5	3.2	3.0	0.7
Fibrinogen	0.21	0.12	0.13	0.05
	Electrophoretic Analyses, % of Total Protein			
Albumin	60			
α_1-globulin	3			
α_2-globulin	8			
β-globulin	11	67[a]		
γ-globulin	12			
Fibrinogen	6			

[a] See Table II footnote.

If the β-globulin molecules are acting as bridging agents, the actual mechanism by which this takes place has not been determined. If we accept the Bangham et al.[9] theory that the major charged group on the surface of the red cell is a phosphate group from one of the phospholipids, it could be hypothesized that Ca^{2+} or other divalent cations effect a bridge between phospholipids on the surface of the red cell and in the lipoprotein complexes (β-globulin). Ethylenediamine tetraacetic acid was used as an anticoagulant. Therefore, the existence of unchelated cations in the plasma is doubtful. However, it is possible that the divalent cations are not removed from the red cell membrane, as the Ca^{2+} ions hold the membrane together and removal of the Ca^{2+} from the membrane would result in cell breakdown.

TABLE IV
Rheological Properties of Red Cells Suspended in Fraction III

Sample	Hematocrit	(Yield shear stress)$^{1/2}$ $-$(dynes/cm.^{2})$^{1/2}$
Normal, K-6804	45.7	0.180
Full strength fraction III	43.1	0.275
Diluted fraction III	44.9	0

Due to the fact that hemolysis is not noticeable on addition of the Ca^{2+} complexing anticoagulants, it appears that very little, if any, of the Ca^{2+} associated with the red cell membrane is removed.

The yield shear stresses for the normal sample and for red cells suspended in fraction III are listed in Table IV.

It should be noted that there was fibrinogen present in the sample of fraction III obtained. The large increase in the yield value is partially due to the fibrinogen present. However, by comparing the fibrinogen concentrations in the purified fraction and in the normal plasma (Table III), it is obvious that the β-globulin molecules present in the purified fraction are contributing significantly to the increased yield shear stress.

Due to the fact that there was an appreciable amount of fibrinogen (0.12 g./100 ml.) in the fraction III sample, red cells were suspended in serum rich in β-globulin which was prepared from the original fraction III plasma. Red cells were washed twice in saline and then suspended in the serum and in the plasma phases which had a high concentration of β-globulin. The red cells suspended in the fraction

TABLE V
Red Cells Suspended in Fraction III

Sample	Hematocrit	Fibrinogen concn., g./100 ml.	$\tau_y^{1/2}$ $-$ [dynes/cm.^{2}]$^{1/2}$
Red cells in original plasma	48.7	0.28	0.200
Red cells in fraction III-plasma	45.1	0.12	0.330
Red cells in fraction III-serum	43.2	0	0

III sample which contained fibrinogen again exhibited a higher yield value than the normal blood from which the red cells were obtained. Red cells suspended in the fraction III serum did not exhibit a yield shear stress. The data are presented in Figure 6 and Table V.

Of the protein fractions, β-globulin had the largest effect on the rheological properties of blood except for fibrinogen. Even though a high concentration of β-globulin did not produce a yield value in the absence of fibrinogen, a significant increase occurred in the viscosity and in the yield shear stress for the sample of red blood cells suspended in a β-globulin fraction in the presence of fibrinogen.

PHYSIOLOGICAL SIGNIFICANCE

It has been shown that, of the plasma proteins, fibrinogen is singularly important in bringing about a yield shear stress. This yield shear stress, being that stress required to initiate flow and break up the three dimensional network in stationary blood may have physiological significance. For if blood flow in a particular network of small vessels has been stopped by any one of a number of causes—temporary compression of tissue, extreme exposure to cold, profound vasconstriction—the flow cannot recommence until the arteriolar pressure becomes sufficiently great to overcome the yield shear stress in all parts of the microvascular system in which the flow is stopped.

It should be noted that the development of a plasma layer at the walls of the smaller arteriols, capillaries, and venules decreases the resistance to flow.[10] This plasma layer is formed more easily in bloods which show a more pronounced ability to aggregate, the effect of which would be to cause the blood to flow more easily once flow became re-established. Clearly, more studies are needed to establish unequivocally the physiological significance of the peculiar rheological properties of blood caused by fibrinogen.

This study was supported in major part by Public Health Service Grant HE-06423 from the National Heart Institute, U. S. Public Health Service. The support of the MIT Instrumentation Laboratory, its director, Dr. C. Stark Draper, and P. J. Gilinson, Jr., and C. R. Dauwalter of the Laboratory staff are acknowledged with gratitude.

References

1. Casson, N., *Rheology of Disperse Systems*, C. C. Mill, ed., Pergamon Press, New York-London, 1959, chap. 5.

2. Merrill, E. W., W. G. Margetts, G. R. Cokelet, and E. R. Gilliland, in *Proc. 4th Intern. Congr. Rheology, Part 4*, A. L. Copley, ed., Interscience, New York, 1965, p. 135.

3. Gilinson, P. J., Jr., C. R. Dauwalter, and E. W. Merrill, *Trans. Soc. Rheology*, **7**, 319 (1963).

4. Cokelet, G. R., Sc.D. thesis, MIT, 1963.

5. Curtis, A. S. G., *Biol. Rev.*, **37**, 82 (1962).

6. Cullen, G. E., and D. D. Van Slyke, *J. Biol. Chem.*, **41**, 587 (1920).

7. Edsall, J. H., *Advances in Protein Chemistry*, Vol. 3, Academic Press, New York, 1947.

8. Hunter, F. F., and M. Grove-Rasmussen, *Am. J. Clin. Pathol.*, **20**, 5 (1950).

9. Bangham, A. D., B. A. Pethuca, and G. V. A. Seam, *Biochem. J.*, **69**,12 (1958).

10. Fåhraeus, R., *Acta Med. Scand.*, **161**, 151 (1958).

Synopsis

14607

By means of a Couette GDM viscometer described by Gilinson, Dauwalter, and Merrill [*Trans. Soc. Rheology*, **7**, 319 (1963)] and in continuation of experimental procedures and correlation methods described by Cokelet, Merrill, et al. [*Trans. Soc. Rheology*, **7**, 303 (1963)] further studies were made on the role of fibrinogen and the other plasma proteins in the rheology of blood measured near and at zero shear. These studies include (*1*) correlation of the rheological parameters (including yield stress) with the measured fibrinogen content of numerous samples of normal human blood and blood from a patient with afibrinogenemia, and (*2*) comparison of the rheological properties of suspensions of red cells in the Cohn fractions.

author

N67 14608

Viscosity of Blood at Low Shear Rates: Observations on Its Relation to Volume Concentration and Size of the Red Cells

MAGNUS I. GREGERSEN,* BRANKO PERIC† SHU CHIEN, DUNCAN SINCLAIR,‡ CHEN CHANG,* and HARRY TAYLOR,
Columbia University College of Physicians and Surgeons, New York, New York

INTRODUCTION

Many of the papers appearing in this Symposium are clearly the product of the recent successful development of suitable instrumentation for studying viscosity at low rates of shear, approximating conditions at near zero flow. Without these tools the authors, among others, could not effectively explore the functional significance of pseudo-plastic properties of blood, body fluids, cells, and tissues.

In working out the experimental design for testing the effects of plasma expanders on blood viscosity it was noted that in general there was a straight-line relation between the log of the viscosity and red cell percentage which greatly simplified the problem of correcting data for unexpected osmotic changes in red cell volume.[1,2] It may be noted that the results of Haynes and Burton[3] and Wells and Merrill[4] also fall on a straight line on a semilog plot. The authors have since examined this relation in the blood of certain mammals selected because of the differences in the size of their red cells. Thanks to the generous cooperation of Dr. Henderson and Hugo Schmidt of The Ringling Brothers, Barnum and Bailey Circus, and of Dr. Gandal of The Bronx Zoo the authors were able to run a limited number of tests on elephant blood in which the mean corpuscular volume (MCV) of the red cell was 120 μ^3 and on goat blood in which the

† International postdoctoral Fellow, National Institutes of Health.
‡ Supported by National Institutes of Health Training Grant.

PRECEDING PAGE BLANK NOT FILMED.

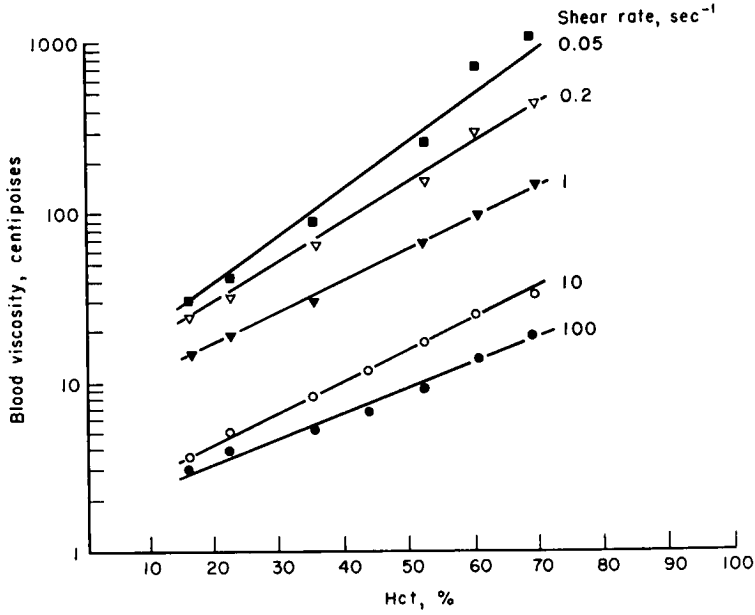

Fig. 1. Heparinized dog blood taken November 21, 1962. This shows a typical test of the relation between viscosity (at 25°C.) and the hematocrit value (corrected for plasma trapping) at shear rates ranging from 100 sec.$^{-1}$ to 0.05 sec.$^{-1}$. Note that extrapolation of the curves to zero cell concentration would give intercepts that vary with the shear rate.

MCV was 18.2 μ^3 to compare with similar tests on human blood in which the MCV was 92 μ^3 and dog blood in which the MCV was 66 μ^3. In all instances the MCV was determined from measurements of the erythrocyte count with the Coulter counter, and from centrifuge hematocrit value corrected for plasma trapping to give the true volume per cent cells H.

According to Einstein (1906), the relative viscosity of a suspension is linearly related to the volume concentration of the particles and independent of their size. However, his equation applies to dilute suspensions in which there is no interaction between the particles, a system scarcely comparable to blood. As Bayliss points out:[5] "Arrhenius modified and extended the Einstein equation, and arrived at the expression $\log \eta_s = \beta C$, where C is the mole fraction of the suspended particles."

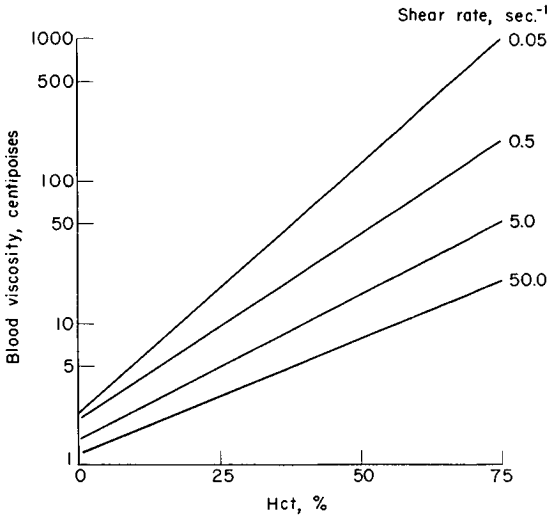

Fig. 2. Heparinized dog blood. Viscosity measured at 37°C. Average results from 5 experiments. Curves as fitted by the method of least squares extrapolated to zero cell concentration show the shear-rate dependence of the intercept at zero cell concentration.

The authors' results on blood are in accord with this form of relationship between viscosity and volume concentration of suspended erythrocytes, with the exception of some of their data on goat blood.

Another problem that comes up in relation to particle size is its possible effect on the so-called yield stress τ_y which has recently been examined in human blood by Merrill and associates.[6,7] When the present data from heparinized blood were analyzed on a Casson plot, there appeared to be a definite influence of particle size on the yield value.

It may also be noted that in testing the relation of log of viscosity versus red cell concentration in heparinized blood, defibrinated blood, and washed red cells in Ringer's solution, useful clues were found from the intercepts of the curves obtained at widely different shear rates. In heparinized blood the intercepts at zero cell concentration seem to vary with the shear rate, being significantly higher at 0.05 sec.$^{-1}$ than at 0.5, 5, and 50 sec.$^{-1}$, indicating the non-Newtonian character of plasma. However, in defibrinated blood which presumably differs from heparinized blood only in the absence of fibrinogen, the inter-

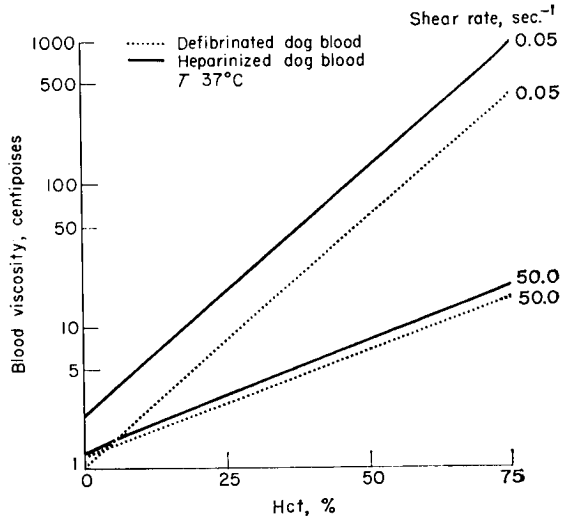

Fig. 3. Comparison of viscosity of heparinized and defibrinated dog blood at 50 and 0.05 sec.$^{-1}$ through a wide range of cell concentrations showing that removal of fibrinogen lowers the viscosity and abolishes the shear-rate dependence of the intercept.

cepts of the curves at all shear rates were, within experimental error, the same, indicating that serum is Newtonian. The same applies to washed red cells in Ringer's solution where, as expected, the intercepts are lower than in defibrinated blood. Direct measurements of viscosity versus shear rate of cell-free plasma, serum, and Ringer's solution seemed to support these inferences, although it must be conceded that difficulties were encountered in measuring the small torques with the authors' model of the GDM viscometer at the lowest shear rates in these suspending media.

METHODS AND MATERIALS

The tests were made on freshly drawn blood. A portion was heparinized (50 mg./100 ml.) and another portion defibrinated immediately. Additional small samples were allowed to clot to obtain serum for electrophoretic studies. Washed cells were prepared from the heparinized blood.

The desired ranges of cell concentrations (from 10–15% up to

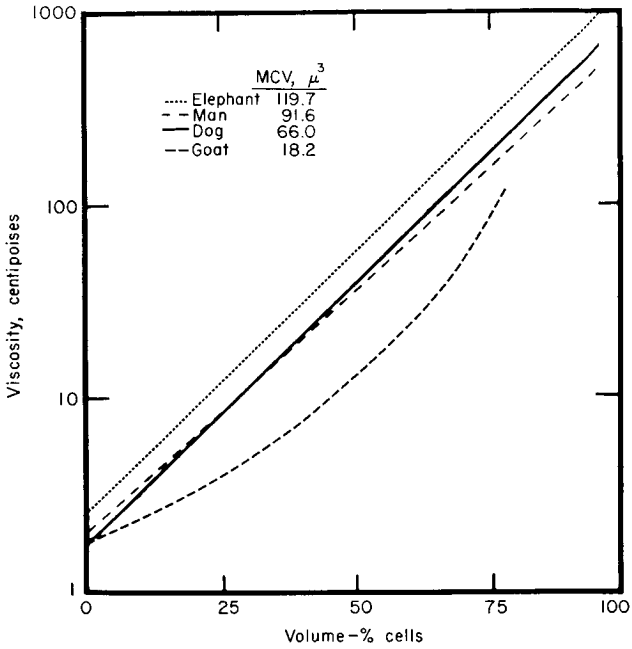

Fig. 4. Showing the relation of viscosity at 0.5 sec.$^{-1}$ to volume per cent cells in elephant, man, dog, and goat blood.

80–90% and in some instances 96–98%) were prepared by filling 5 or 6 tubes with heparinized blood, and after brief centrifugation transferring suitable amounts of the supernatant plasma from one tube to another to dilute or concentrate the red cells as required. The same procedure was used with defibrinated blood and washed red cells in Ringer's solution. After thorough mixing, a small sample was then taken from each tube for hematocrit determinations to establish the final cell concentration, and for the erythrocyte count and the cell size distribution with the Coulter counter and distribution plotter. Plasma proteins were measured by the refractometric method, with Kjeldahl determinations and with paper electrophoresis (Beckman), the strips being scanned with the Beckman Analytrol apparatus.

Viscosities were measured at shear rates from 50 down to 0.05 sec.$^{-1}$ with the GDM viscometer.[8] Measurements were made at 37°C. unless otherwise indicated. In all instances samples were thor-

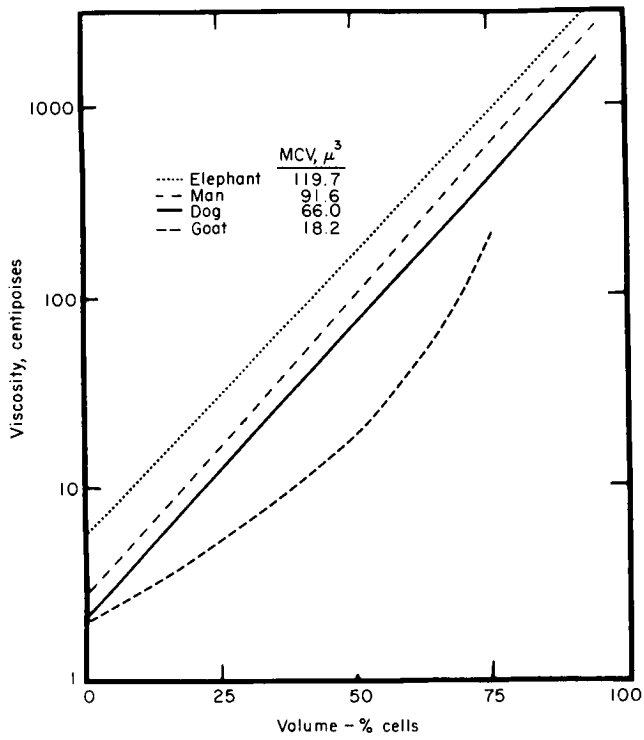

Fig. 5. The same as Fig. 4 but at a shear rate of 0.05 sec.$^{-1}$. See text for discussion.

oughly mixed immediately before determining the torque to avoid, so far as possible, errors from the settling of cells.

RESULTS

The straight-line relation between log of viscosity and hematocrit (corrected for plasma trapping) is illustrated by the typical results in Figure 1, taken from one of the early tests on heparinized dog blood at room temperature (25°C.). This graph also shows the influence of shear rate on the intercept at zero cell concentration. Figure 2 represents average curves from several experiments on heparinized dog blood as fitted by the method of least squares. All subsequent graphs represent least squares lines unless otherwise noted. Again,

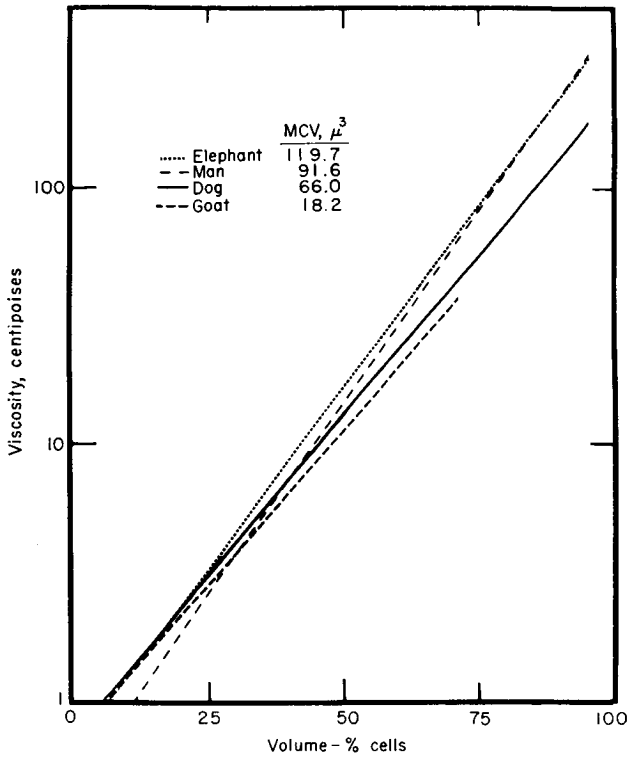

Fig. 6. Showing the relation of viscosity at 0.5 sec.$^{-1}$ to the volume per cent cells of washed red cells suspended in Ringer's solution. For discussion see text.

there is a consistent linear relation between log of viscosity and red cell concentration. Also the shear-rate dependence of the intercept at zero cell concentration is clearly apparent.

Figure 3 compares the results on heparinized and defibrinated dog blood. As seen here, removal of fibrinogen (dotted line) consistently lowers the viscosity at all shear rates. Furthermore, the shear-rate dependence of the intercepts at zero cell concentration has disappeared which, as mentioned earlier, indicates that serum, in contrast to plasma, is Newtonian in its behavior. Similar tests on washed red cells suspended in Ringer's solution also show that the intercepts are no longer shear-rate dependent. Hence, fibrinogen appears to be responsible for the non-Newtonian behavior of plasma.

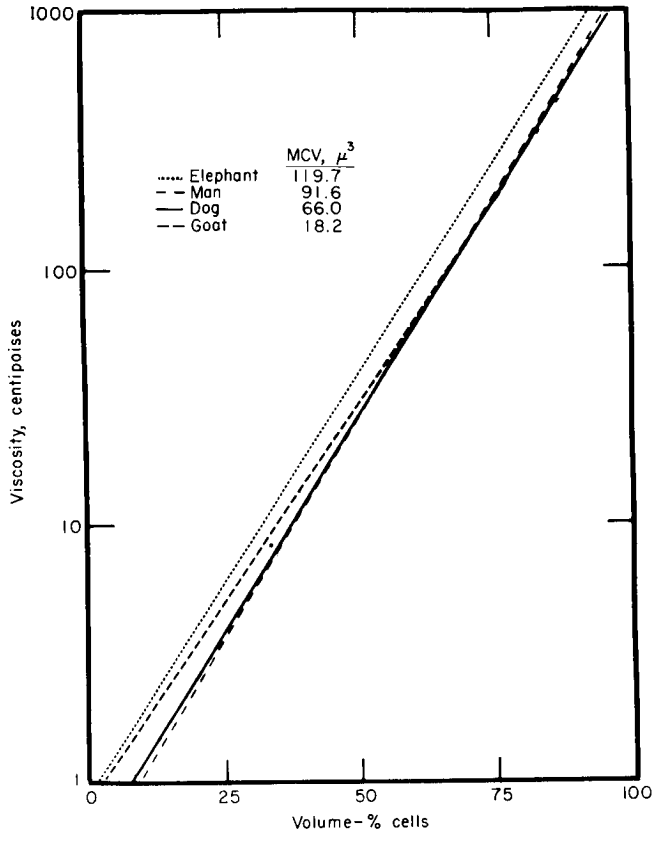

Fig. 7. Same as Fig. 6 with viscosity at 0.05 sec.$^{-1}$.

The relation of viscosity to volume per cent cells in heparinized blood from elephant, man, dog, and goat may be seen in Figures 4 and 5 at shear rates of 0.5 and 0.05 sec.$^{-1}$, respectively. In both graphs the straight-line relation is seen to hold for the results on elephant, human, and dog blood, but not for goat blood.

The curvilinear relation for goat blood was at first interpreted as an artifact and ascribed to technical errors. Later results have driven the authors to revise their interpretation and to accept at least tentatively the curved relation shown here. For some reason not clear, goat blood appears to be an exception. Nevertheless, it is

TABLE I

Results of Regression Analysis of the Relation $\ln \eta = a + bH$[a] for Heparinized Blood

Species	Shear rate, sec.$^{-1}$	a	b
Human	50	0.415 ± 0.073	0.0369 ± 0.0014
Human	5	0.460 ± 0.066	0.0477 ± 0.0012
Human	0.5	0.718 ± 0.072	0.0580 ± 0.0013
Human	0.05	1.052 ± 0.141	0.0717 ± 0.0025
Dog	50	0.277 ± 0.042	0.0357 ± 0.0009
Dog	5	0.413 ± 0.052	0.0462 ± 0.0011
Dog	0.5	0.576 ± 0.090	0.0627 ± 0.0020
Dog	0.05	0.805 ± 0.175	0.0781 ± 0.0038
Elephant	50	0.454 ± 0.030	0.0366 ± 0.0008
Elephant	5	0.548 ± 0.031	0.0509 ± 0.0008
Elephant	0.5	0.964 ± 0.092	0.0621 ± 0.0023
Elephant	0.05	1.828 ± 0.154	0.0678 ± 0.0037

[a] Here η is in centipoise and H in per cent.

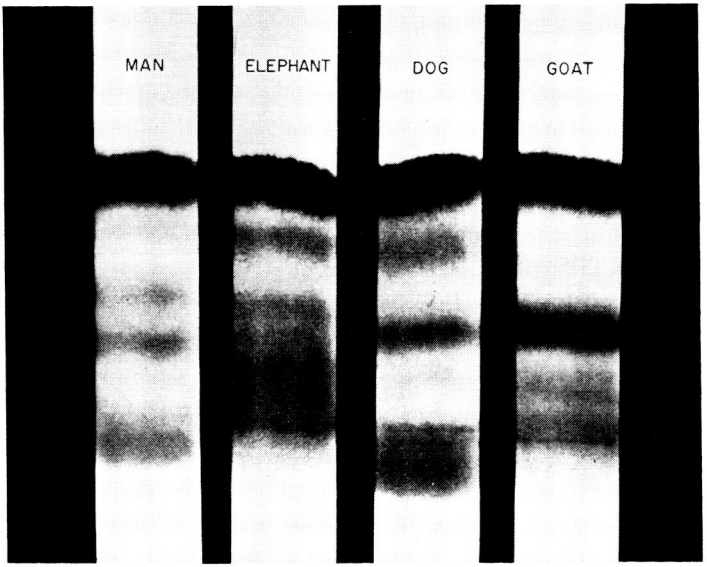

Fig. 8. Typical paper strips from electrophoresis on elephant, man, dog, and goat serum juxtaposed for comparison.

	%	GRAMS %
γ	16.3	1.20
β	13.0	0.96
α^2	8.7	0.64
α^1	4.3	0.32
Albumin	57.7	4.26
Globulin	42.3	3.12
Total Protein	100.0	7.38

A/G Ratio 1.36: 1

MAN

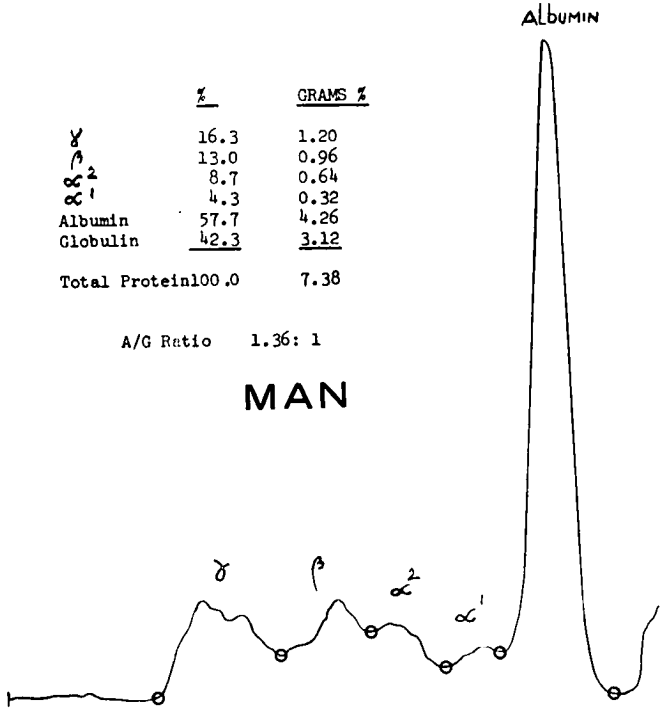

	%	GRAMS %
γ	18.7	1.34
β	5.6	0.40
α^2	12.6	0.90
α^1	8.4	0.60
Albumin	54.7	3.91
Globulin	45.3	3.24
Total Protein	100.0	7.15

A/G Ratio 1.21: 1

GOAT

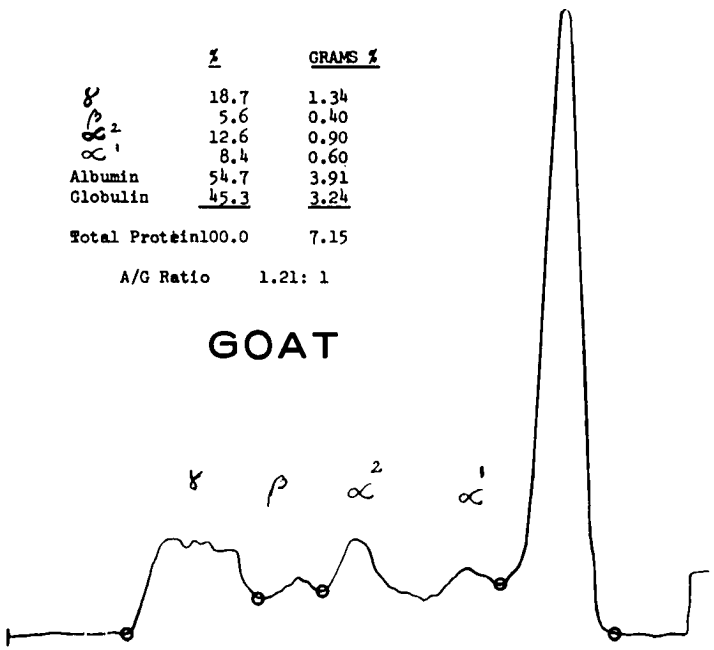

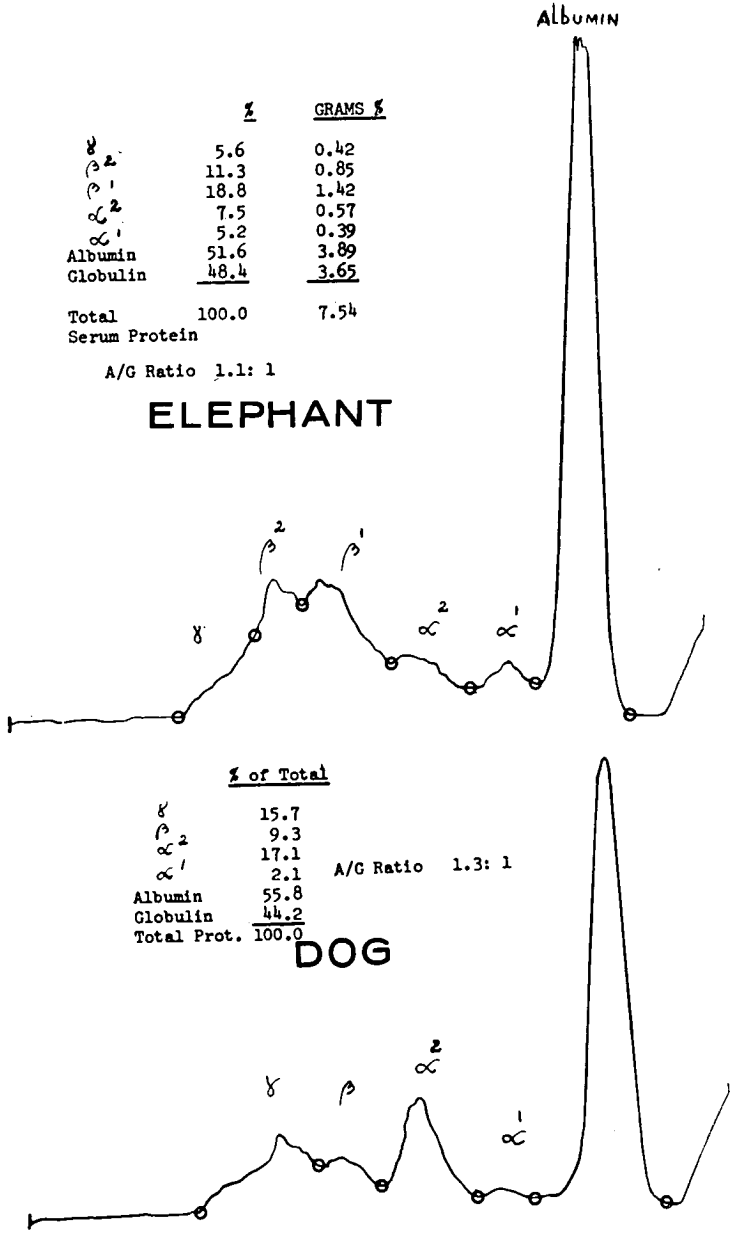

Fig. 9. Densitometer records of the stained paper strips shown in Fig. 8. Note the differences in the protein fractions in the four species as tabulated above the densitometer curves. See text for discussion.

TABLE II

Results of Regression Analysis of the Relation $\ln \eta = a + bH^a$ for Red Cells Suspended in Ringer's Solution

Species	Shear rate, sec.$^{-1}$	a	b
Human	50	-0.144 ± 0.048	0.0382 ± 0.0010
Human	5	-0.474 ± 0.127	0.0529 ± 0.0024
Human	0.5	-0.770 ± 0.121	0.0688 ± 0.0022
Human	0.05	-0.701 ± 0.255	0.0792 ± 0.0055
Dog	50	-0.250 ± 0.081	0.0386 ± 0.0015
Dog	5	-0.149 ± 0.093	0.0443 ± 0.0018
Dog	0.5	-0.310 ± 0.208	0.0575 ± 0.0040
Dog	0.05	-0.624 ± 0.283	0.0778 ± 0.0051
Elephant	50	-0.191 ± 0.042	0.0421 ± 0.0009
Elephant	5	-0.273 ± 0.044	0.0511 ± 0.0010
Elephant	0.5	-0.409 ± 0.104	0.0646 ± 0.0024
Elephant	0.05	-0.181 ± 0.179	0.0759 ± 0.0045
Goat	50	-0.31 ± 0.12	0.041 ± 0.011
Goat	5	-0.29 ± 0.09	0.046 ± 0.018
Goat	0.5	-0.36 ± 0.14	0.056 ± 0.009
Goat	0.05	-0.13 ± 0.07	0.070 ± 0.022

[a] Here η is in centipoise and H in per cent.

apparent, for example (Fig. 5), at 0.05 sec.$^{-1}$ that the viscosity at the same volume per cent cells is very much lower in goat blood than in that of the other species. For example, at 50% cell concentration the viscosities are 19, 60, 100, and 170 centipoises for goat, dog, man, and elephant, respectively. Hence, cell size appears to have a marked effect on viscosity, at least in heparinized blood. Also the viscosities obviously fall in the order of cell size. The authors succeeded in measuring viscosity of packed cells (96–98% cells) in human blood. The values were approximately 3600 centipoises at 0.05 sec.$^{-1}$.

The results obtained with washed cells suspended in Ringer's solution at shear rate 0.5 sec.$^{-1}$ are plotted in Figure 6; those at shear rate 0.05 sec.$^{-1}$ in Figure 7. It will be seen at once that the striking relation of cell size to viscosity noted in the tests with heparinized blood samples has been markedly changed. Also the results with goat blood no longer fall on a curve but on a straight line, and at the lowest shear rate (Fig. 7) the viscosity of goat cells at 50% concentration is now higher (30 centipoises), whereas the viscosities of elephant (40 centipoises), human (26 centipoises), and dog cells (27 centipoises)

are all lower than in heparinized plasma. Not visible on the graph is the viscosity of packed human red cells which now falls at about 2500 centipoises as compared to 3600 centipoises in heparinized blood.

Tables I and II list respectively the results of regression analysis of the data from all tests on heparinized blood and on washed red cells suspended in Ringer's solution.

DISCUSSION

The difference in behavior of goat red cells in heparinized blood as compared with those from elephant, man, and dog remains unexplained. This, and the absence of any observable sedimentation in goat blood, may be a matter of size, but could also be related to species differences in the plasma. With this in mind, the electrophoretic patterns in the four species were examined. It may be seen in Figure 8 that there are visible differences in the stained paper strips which show up more clearly on the densitometer records in Figure 9.

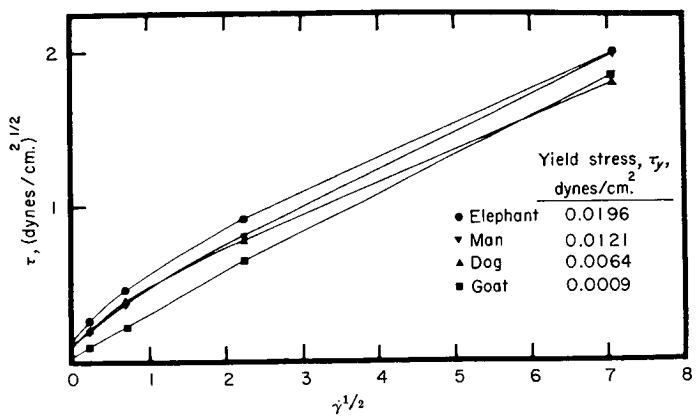

Fig. 10. Casson plot for heparinized blood from elephant, man, dog, and goat. Volume-% red cells = 45. Abscissa values in $1/sec.^{1/2}$.

The gamma globulin fraction prominent in goat serum (18.7%) seems to be low in elephant serum (5.6%); and although this globulin fraction in the goat is similar in magnitude in man (16.3%) and dog (15.7%), the distribution curves are somewhat different. Furthermore, it may be noted that the α^1-fraction is percentage-wise

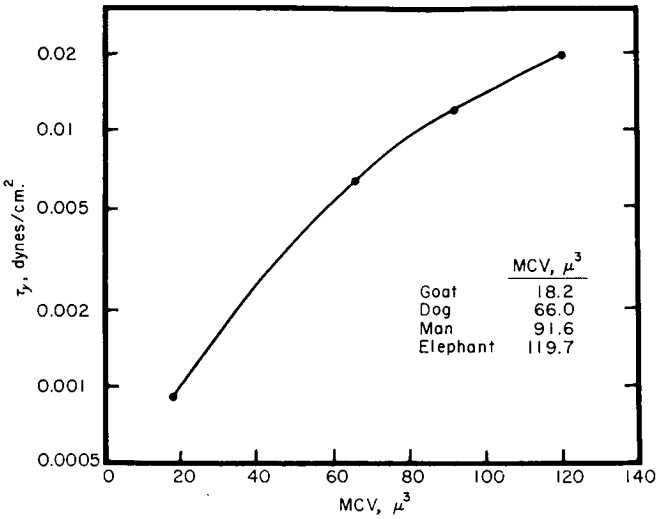

Fig. 11. Graph of data from the Casson plots in Fig. 10 showing the relation between the estimates of yield stress τ_y and the mean corpuscular volume (MCV). Volume-% red cells = 45.

higher in the goat (8.4) as compared with either elephant (5.2), man (4.3), or dog (2.1).

With the evidence presented it would appear that more questions may have been raised than answered. While the tests on heparinized blood apparently show a striking effect of cell size on viscosity, the results with washed cells suspended in Ringer's solution do not justify the same conclusion. In the final analysis, it may turn out that the nature of the suspending medium rather than cell size plays a major role in the observed differences.

The points on the Casson plot shown in Figure 10 were calculated from the least squares curves derived for heparinized blood at 45 vol.% cells. It is apparent here, as also noted by Merrill et al.[6] that the Casson equation does not yield a straight line for blood. Extrapolation of the curves to zero shear rate gives the values of the yield stress τ_y tabulated below the curves. The curve obtained by plotting these values for τ_y as a function of MCV is shown in Figure 11. The spread of the data for the washed cells experiments does not justify a similar analysis.

SUMMARY

In blood, the log of the viscosity η is, in general, linearly related to the volume per cent concentration of red cells H at any given shear rate from 50 down to 0.05 sec.$^{-1}$ In heparinized blood the intercept at zero cell concentration is shear-rate dependent. In defibrinated blood the viscosity is somewhat lower and the intercept is no longer shear-rate dependent but identical for the curves at all shear rates. The same holds for washed red cells suspended in Ringer's solution except that the viscosity is again reduced below that of defibrinated blood.

The effect of red cell size on the relation of viscosity to red cell concentration was investigated in tests with blood from the elephant, man, dog, and goat in which the mean corpuscular volumes (MCV) are 120, 92, 66, and 18 μ^3, respectively.

In experiments with heparinized blood there were striking differences in the viscosity at the same volume per cent cell concentration which appeared to be clearly correlated with the differences in MCV. In contrast to the results on elephant, human, and dog blood, the log of viscosity versus volume per cent cells in heparinized goat blood follows a curve and not a straight line, but when the tests were made on washed red cells in Ringer's solution, the results with goat cells fell on a straight line. Furthermore, in the tests with washed cells the relation of red cell size to viscosity seemed to be quite different, suggesting that species differences in the plasma may account for the results obtained with heparinized blood. The marked differences observed in the electrophoretic patterns tend to strengthen this possibility.

Casson plots of the data from tests on heparinized blood indicate significant species differences in the yield values τ_y which appear to be related to differences in the MCV.

The work reported here was done under U. S. Army contract DA-49-193-MD-2272 with generous financial support from several private donors including The Mary Evelyn Townsend Fund, The Brook Foundation, Mrs. George W. Perkins, and Mrs. Alan M. Scaife. The authors received technical assistance from Mrs. C. Fialk, Mr. A. Peraino, and Mr. M. Lubic. They also wish to express their appreciation to Prof. E. W. Merrill who kindly helped in arranging for the construction of the GDM viscometer. Their sincere thanks also go to Dr. John Lundberg and several of his associates at the Murray Hill Laboratories of The Bell Telephone Co. who gave generously of their time and technical knowledge as

did Prof. Edward Leonard of the Department of Chemical Engineering, Columbia University, to help the authors surmount many technical difficulties. Their constant interest and advice in the course of the investigations has been of inestimable value to the authors. However, they are not in any sense to be held accountable for any shortcomings in experimental data or for the inferences drawn, and the conclusions expressed in this report.

References

1. Gregersen, M. I., B. Peric, S. Usami, S. Chien, C. Chang, and D. G. Sinclair, *Fed. Proc.*, **22,** 641 (1963), abstract.

2. Gregersen M. I., S. Usami, B. Peric, C. Chang, D. Sinclair, and S. Chien, *Biorheol.*, **1,** 247 (1963).

3. Haynes, R. H., and A. C. Burton, *Am. J. Physiol.*, **197,** 943 (1959).

4. Wells, R. E., and E. W. Merrill, *J. Clin. Invest.*, **41,** 1591 (1962).

5. Bayliss, L., in *Handbook of Physiology*, Sec. 2, Vol. I., Williams & Wilkins, Baltimore, Md., 1962, p. 137.

6. Merrill, E. W., E. R. Gilliland, G. Cokelet, H. Shin, A. Britten, and R. E. Wells, *J. Appl. Physiol.*, **18,** 255 (1963).

7. Merrill, E. W., G. R. Cokelet, A. Britten, and R. E. Wells, Jr., *Circulation Res.*, **13,** No. 1, 48 (1963).

8. Gillinson, P. J., C. R. Dauwalter, and E. W. Merrill, *Trans. Soc. Rheology*, **7,** 319 (1963).

Synopsis

In vitro tests on heparinized blood from elephant, man, dog, and goat revealed species differences in the blood viscosity at low rates of shear. These differences may be related to the mean corpuscular volume of the red cell, although species differences in the plasma may also play a role. Similar, though less pronounced, results were obtained for red cells suspended in Ringer's solution.

Author Index

Abe, S., 147
Alcaide, D. C., 425
Allen, R. D., 173

Bergentz, S-E., 581
Brånemark, P-I., 459
Britten, A., 601
Bugliarello, G., 351
Burnell, J. A., 215

Chang, C., 613
Charm, S., 231, 255, 335, 395
Chien, S., 613
Cokelet, G. R., 135, 601
Copley, A. L., 3
Corey, H., 533
Cox, H. A., Jr., 337

Dintenfass, L., 489, 593

Fåhraeus, R., 11
Fox, E. A., 125
Frasher, W. G., Jr., 257
French, R. J., 381
Fukada, E., 281

Gelin, L-E., 299
Gilliland, E. R., 135
Goldsmith, H. L., 85
Gregersen, M. I., 613
Groom, A. C., 371, 381

Harders, H., 413
Harkness, J., 267
Harkness, M. L. R., 477
Harkness, R. D., 477
Hartert, H., 571
Herp, A., 505
Hsiao, G., 351

Ibe, T., 281
Intaglietta, M., 317
Irwin, J. W., 425

Joly, M., 45

Kamiya, N., 157
Kapur, C., 351
Kawai, H., 281
Kochen, J. A., 193
Kurland, G., 231, 255, 335, 395
Kuroda, K., 157

Leroux, M. E., 549

Margetts, W. G., 135, 601
Mason, P., 521
Mason, S. G., 85
Matsumura, G., 505
McComis, W., 231, 335, 395
McDonald, D. A., 205
Melin, M., 601
Merrill, E. W., 135, 601
Monro, P. A. G., 439

Oka, S., 89

Palmer, A. A., 245
Pennell, R. B., 601
Peric, B., 613
Pfeiffer, H. H., 535
Pigman, W., 505

Raman, K. R., 215
Rigby, B. J., 521
Rowlands, S., 371, 381
Rudenstam, C-M., 409

Sacks, A. H., 215
Saibel, E., 125

Salzman, E. W., 601
Scott Blair, G. W., 35
Segré, G., 103
Shono, H., 281
Silberberg, A., 119
Sinclair, D., 613
Sobin, S. S., 257
Song, C., 255
Su, G.-J., 337

Taylor, E. W., 175
Taylor, H., 613
Tejada, C., 395
Thomas, H. W., 371, 381

Wayland, H., 257, 317
Weissenberg, K., 19, 261
Wells, R. E., Jr., 431
Whitmore, R. L., 69
Whittington, R. B., 267
Witte, S., 451

Zederfeldt, B., 397
Zimmermann, M. H., 201

Subject Index

Acid, hyaluronic, rheology of, 505
Aggregation, of biological polymers, 45
Anaphase chromosomes, movement of, 175
Animal eye, vitreous humor, 535
Arterial spiders, of the human skin, 413
Artery,
  simulated, auscultatory blood pressure in, 215
  viscoelasticity of the main pulmonary segment, 257

Biological materials, instrumentation for testing deformation in, 261
Biological reactions, and microcirculation flow, 425
Biological suspensions, flow through tubes, 85
Biological systems, rheological theory of, 35
Birefringence, streaming, of submicroscopic rods and spheres, 317
Blood, auscultatory pressure in simulated arteries, 215
Blood,
  human,
    flow through branching glass capillary channels, 245
    influence of plasma proteins on rheology of, 601
    plasma skimming in, 245
Blood, red cell suspensions, and electrokinetic charge, 337
Blood, whole, effect of dietary fat on viscosity of, 395
Blood clotting, rheology in humans, 593
Blood flow,
  dimensional analysis of, 231
  energy losses in tubes, 255
  in a capillary, 89
  properties of, 205
  viscosity in a non-uniform shear field, 351
Blood in the microcirculation, and plasma proteins, 431
Blood near zero shear, Casson equation and rheology of, 135
Blood sedimentation, historical significance of, 11
Blood viscosity, at low shear rates, 613
  new viscometer for, 281
Brownian movement, of cytoplasmic granules, 175

Capillary channels, branching glass, 245
Capillary viscometer, 267, 281
Casson equation, and rheology of blood near zero shear, 135
Cells, red,
  and their suspending phase, mean velocities of, 381
  flow of hemoglobin in hemolysing, 193
  flow of suspensions in narrow tubes, 381
  rheology and structure of suspensions, 335
  volume concentration and size in blood viscosity, 613
Cell suspensions, red blood, and electrokinetic charge, 337
Charge, electrokinetic, and red blood cell suspensions, 337
Chromosomes, anaphase, movement of 175
Circulation times, for erythrocytes and plasma *in vivo*, 371
Clot, thrombodynamic property of, 549
Clot retraction, kinetics of, 571

Clotting process, correlation with clot retraction, 571
Clotting, rheology in humans, 593
Collagen, frameworks, mechanical properties of, 477
native, structural transitions in, 521
Cytoplasmic granules, Brownian and saltatory movements of, 175

Deformation of biological materials, instrumentation for the testing of, 261
Dimensional analysis, of pulsating blood flow, 231
Dispersions, muscle fiber, subsidence of, 533

Electrokinetic charge, and red blood cell suspensions, 337
Embolism, fat, as hemorheologic disturbance, 581
Endoplasm, in *Nitella*, 157
slime mold, 173
Energy losses, for blood flow through tubes, 255
Erythrocytes, circulation time, *in vivo*, 371
Extracorporeal flow, instrumentation for the testing of, 261
Eye, animal, vitreous humor, 535

Fat, dietary, effect on whole blood and plasma viscosity, 395
Fat embolism, as hemorheologic disturbance, 581
Fiber dispersions, muscle, subsidence of, 533
Fibrin, thrombodynamic function of, 549
Filaments, spun, of animal eye vitreous humor, 535
Flow, blood, dimensional analysis of, 231
energy losses in tubes, 255
fluid mechanics of, 69
in a capillary, 89
viscosity in a non-uniform shear field, 351
Flow, extracorporeal, instrumentation for the testing of, 261
Flow, of biological suspensions through tubes, 85
Flow, of hemoglobin in the hemolysing red cell, 193
Flow, of red cell suspensions in narrow tubes, 381
Flow, Poiseuille, of a suspension of spheres, 103
Flow, pulsatile, stability of, 205
Flow, through microcirculation, and biological reactions, 425
Flow, through tubes, 125
Flow pattern, for vascular permeability, by fluorescent vital microscopy, 451
Fluid, synovial, role in joint lubrication, 489
Fluid mechanics, in biorheology, 3
of blood flow, 69
Fluid streams, visual particle velocity measurement in, 439
Fluorescent vital microscopy, flow pattern for vascular permeability by, 451

Hemoglobin, flow in the hemolysing red cell, 193
Hemorheologic disturbance, fat embolism as, 581
Hemorheology, research in, 19
Hyaluronic acid, rheology of, 505
Hydrodynamic interaction, between particles in suspension, 119

Joint lubrication, role of synovial fluid in, 489

Kinetics, of clot retraction, 571

Lubrication, joint, role of synovial fluid in, 489

Microcirculation, biological reactions and flow through, 425
plasma proteins and blood in, 431

Microscopy, fluorescent vital, flow pattern for vascular permeability by, 451
Muscle fiber dispersions, subsidence of, 533

Nitella, rotational protoplasmic streaming in, 157

Optics, polarization, in determining biorheologic behavior, 535

Particle, visual, velocity measurement in fluid streams, 439
Permeability, vascular, flow pattern by fluorescent vital microscopy, 451
Plasma, circulation time, *in vivo*, 371
thrombodynamic function of, 549
viscosity, effect of dietary fat on, 395
Plasma proteins, and blood in the microcirculation, 431
and human blood rheology, 601
Plasma skimming, in human blood, 245
Platelets, thrombodynamic function of, 549
Polarization optics, in determining biorheologic behavior, 535
Polymers, of biological origin, aggregation of, 45
Pressure, auscultatory blood, in simulated arteries, 215
Proteins, plasma, and blood in the microcirculation, 431
and human blood rheology, 601
Protoplasm, slime mold, viscoelasticity of, 147
Protoplasmic streaming, rotational, in *Nitella*, 157
Pulmonary artery, viscoelasticity of the main segment, 257
Pulsatile flow, stability of, 205

Rheologic disturbances, and tumor spread, 409
following tissue injury, 299
treatment in clinical surgery, 397
Rheological phenomena, intracapillary, 459
Rods, submicroscopic, streaming birefringence study of, 317
Rotational protoplasmic streaming, in *Nitella*, 157

Saltatory movement, of cytoplasmic granules, 175
Sap, movements in trees, 201
Serum, thrombodynamic function of, 549
Shear field, non-uniform, viscosity of blood flow in, 351
Shear rates, low, viscosity of blood at, 613
Skin, human, arterial spiders of, 413
Slime mold endoplasm, properties of, 173
Slime mold protoplasm, viscoelasticity of, 147
Spheres, submicroscopic, streaming birefringence study of, 317
Spun filaments, of animal eye vitreous humor, 535
Streaming birefringence, of submicroscopic rods and spheres, 317
Streams, fluid, visual particle velocity measurement in, 439
Surgery, clinical, for rheological disturbances, 397
Suspensions, red cell, and electrokinetic charge, 337
flow through narrow tubes, 381
rheology and structure of, 335
Synovial fluid, role in joint lubrication, 489

Thromboelastograph, in measuring the thrombodynamic functions of blood, 549
Thrombodynamic property of clot, 549
Tissue injury, rheologic disturbances following, 299
Tubes, energy losses for blood flow through, 255

Tumor spread, and rheologic disturbances, 409

Vascular permeability, flow pattern by fluorescent vital microscopy, 451
Viscoelasticity, of slime mold protoplasm, 147
of the main pulmonary artery segment, 257
Viscometer, for measurement of small amounts of blood, 281
new capillary-type, 267, 281
Viscosity, blood, at low shear rates, 613
flow in a non-uniform shear field, 351
new viscometer for, 267, 281
Viscosity, relation to volume concentration and size of red cells, 613
Visual particle velocity, measurement in fluid streams, 439
Vitreous humor, animal eye, 535